AN EVALUATION OF PETROLEUM SYSTEMS WITHIN THE BILLILUNA SUB-BASIN AND ADJACENT STRUCTURAL REGIONS, NORTHEASTERN CANNING BASIN

by

PETER JAMES HAWKE

A thesis submitted to the University of Adelaide in partial fulfilment for the Degree of
MASTER OF PHILOSOPHY (PETROLEUM GEOSCIENCE)

Australian School of Petroleum
The University of Adelaide
Australia

September, 2017

Abstract

The intracratonic Canning Basin, Western Australia, contains three Palaeozoic petroleum systems (The Larapintine L2, Ordovician – Silurian; The Larapintine L3 and L4, Devonian – early Carboniferous; and the Gondwannan G1 and G2, late Carboniferous – Permian). The NW-SE oriented Fitzroy Trough and Gregory Sub-basin (separated only by the Jones Arch) are the regional source kitchens, and shelfal positions updip from the Fitzroy Trough are oil productive from the Larapintine L3 and L4 petroleum system in fields such as Blina and Sundown, and more recently the Ungani field. A lack of exploration drilling in comparable shelfal positions updip from the Gregory Sub-basin is perceived to account for the absence of similar hydrocarbon discoveries. Through the use of a newly reprocessed regional 2D seismic grid and an enhanced stratigraphic framework produced from well correlations and palaeogeographic reconstructions, it is demonstrated that elements of all of the three petroleum systems are present on the Betty Terrace, Balgo Terrace and within the Billiluna Sub-basin of the northeast Canning Basin. Good quality reservoirs such as the late Devonian Knobby Sandstone (averaging 20.6% porosity and 567 mD permeability), the Tournaisian Laurel Formation (featuring up to 22% porosity), members of Visean-Sakmarian Grant Group (up to 18.5% porosity and 1015 mD permeability), and the Sakmarian Poole Sandstone (in excess of 20% porosity) were intersected in well bores, tied to 2D seismic data and mapped throughout the study area. Stratigraphy with regional seal potential (including Laurel Formation shales, the Grant Group B member, shales of the mid-Carboniferous Anderson Formation and the Permian Noonkanbah Formation) are determined from exploration wells to be present across the project area. A regional geochemical source rock assessment indicates that the Permian Noonkanbah Formation is organically rich (2.17% TOC), and that the pre-Carboniferous stratigraphy (members of Anderson Formation, 0.14% TOC; Laurel Formation, 0.56% TOC; Devonian Gogo Formation, 0.14% TOC; and the Silurian Carribuddy Group Bongabinni Member, 0.13% TOC) are organically lean. The Llanvirn Goldwyer Formation (1.5% TOC) is regionally organically rich, though is unlikely to be found in a basinal palaeogeographic setting within the study area. Thermal maturity was investigated using 1D and 2D petroleum systems models, which determined that (1) the Noonkanbah Formation is immature, and (2) that the pre-Carboniferous source rocks are mature for hydrocarbon generation, reaching peak thermal maturity in the Triassic (200 Ma). 4-way dip closures, 3-way fault bound dip closures, and horst block trapping configurations were identified on 2D seismic, but an analysis of

exploratory dry holes indicates that structural closures that developed in the Carboniferous were likely reconfigured during the Triassic Fitzroy Movement, where hydrocarbons leaked out of traps. Modelling indicates that the timing of hydrocarbon generation occurred over two main periods; the Siluro-Devonian (436 Ma – 350 Ma) and in the Triassic (220 Ma – 192 Ma). It is designated that exploration within all three petroleum systems in the project area is considered to be high-risk. It is concluded from this study that the Larapintine L3 and L4 petroleum system represents the best prospectivity in positions nearest the Gregory Sub-basin.

Statement of Confidentiality

A confidentiality agreement, between Pangaea Resources Pty Ltd and The University of Adelaide, embargos the public inspection or borrowing of this thesis until the expiry of a three year confidentiality period, effective from the date on which this project is approved by The University of Adelaide.

Statement by the Author

I certify that this work contains no material which has been accepted for the award of any other degree or diploma in my name in any university or tertiary institution and, to the best of my knowledge and belief, contains no material previously published or written by another person, except where due reference has been made in the text. In addition, I certify that no part of this work will, in the future, be used in a submission in my name for any other degree or diploma in any university or other tertiary institution without the prior approval of the University of Adelaide and where applicable, any partner institution responsible for the joint award of this degree.

Subject to a two year confidentiality period, as stated on page iii, I give consent to the following:

- That this copy of my thesis, when deposited in the University Library, be made available for loan and photocopying, subject to the provisions of the Copyright Act 1968.
- That the digital version of my thesis may be made available on the internet, via the University's digital research repository, the Library Search and also through internet search engines, unless permission has been granted by the University to restrict access for a period of time.

Peter J. Hawke

Acknowledgements

An enormous amount of thanks goes to my primary supervisor Dr. Simon Holford. Amongst his extremely busy schedule he guided the project through the ups-and-downs of supervisor changes and numerous years of work towards the finish line. I thank him for his direction and guidance, support, encouragement, and for putting up with me as a remote candidate.

Secondly, a huge amount of thanks goes to my external supervisor Dr. Douglas Hamilton at Pangaea. Doug stepped up through his demanding calendar to guide me through to the culmination of this study. I thank him graciously for his time, particularly as I neared end of the journey, for his efforts and attention to detail, and providing valuable direction.

There are numerous other key individuals to whom I owe thanks. Firstly, to Mr. Andrew R. Scott at Altuda Energy Corporation, who was a key person that helped me get this project off the ground. His support and encouragement is greatly appreciated. It not for Andrew Scott's efforts and initial supervisory role in the early stages of this study, this project would likely not have commenced. Dr. Mark Tingay also played a significant initial supervisory role, and for that I say thanks, especially for taking me on as a remote student. Mr. Andy Mitchell and Dr. Kathryn Amos were key players in the establishment of my candidature at the ASP, and I thank Andy for his guidance as the ASP Postgraduate Research Coordinator. The ASP family is a great team to work with, and I thank them for being so accommodating.

Secondly, I owe an enormous amount of thanks to Pangaea and its past and current executive team members. Without their approval, support, encouragement and guidance this project would be non-existent. This project owes an enormous amount of gratitude to Pangaea for the provision of newly reprocessed 2D seismic data – a key ingredient in this study. Many people at Pangaea helped contribute to this thesis, either directly in research guidance or indirectly through support, and for that I say thanks. Special recognition go to Ms. Lisa Miller for her guidance at various stages of the project.

Many thanks to my fellow students at the ASP for providing support during my initial candidature period in Adelaide. Thanks to the staff and fellow postgrads at Kathleen Lumley College who settled me into Adelaide life during my early living-in period. Thanks to Professor Steve Begg for accommodating me in his excellent Decision Making and Risk Analysis course (perhaps one of the best courses at the ASP!). And generally, thanks to the

city of Adelaide for being an awesome place in which to study. The ASP is set apart by having an excellent home ground!

I cannot forget to mention my friends and family in Sydney. I apologise for my unavailability at various social gatherings. My parents and brother were instrumental in pushing me on this journey. A very special thanks goes to Ms. Jesamina Barbaro, whom without her understanding, support, patience and delicious Italian cooking I would not have reached the finish line.

Now to those who will likely never see this. Thanks to Spotify and their endless list of musicians who encouraged me through the endless Friday and Saturday evenings when approaching the end of this project. So here's to Daft Punk, Artic Monkeys, Cold Play, Deadmau5, Empire of the Sun, Fleetwood Mac, Galantis and many other excellent producers for their contribution. Thanks also goes to my coffee percolator for the late night encouragement.

List of Contents

List of Figures

List of Tables

1. Introduction

1.1 Definition of the Problem

The intracratonic Canning Basin contains sediments belonging to three major Palaeozoic petroleum super systems: Ordovician – Silurian (Larapintine L2), Devonian – early Carboniferous (Larapintine L3 and L4) and late Carboniferous – Permian (Gondwannan G1 and G2) (Bradshaw et al, 1994). Carlsen and Ghori, (2005) state that Palaeozoic aged petroleum systems account for 25% of recoverable global hydrocarbons. In 2013, the U.S. Energy Information Administration evaluated that the Canning Basin may contain 235 Tcf of recoverable gas in Goldwyer Formation shales and 9.8 billion barrels of oil (EIA, 2013). Thus, there is an anticipation amongst petroleum explorers that the Canning Basin should contain significant recoverable petroleum resources.

Contrary to the above proposition, the Canning Basin mainly produces oil from six small fields (Table 2.3), the largest of which – the Blina Field, is located on the Lennard Shelf nearby to other producing areas (Figure 1.1). Exploration activity currently accounts for approximately 300 wells drilled in the basin, and approximately 90,000 line kilometres of 2D seismic acquisition (Figure 1.1). Carlsen and Ghori (2005) recognise that the Canning Basin is significantly under-explored; where other global Palaeozoic petroleum basins contain significantly higher well densities of 500 wells per 10,000 km^2.

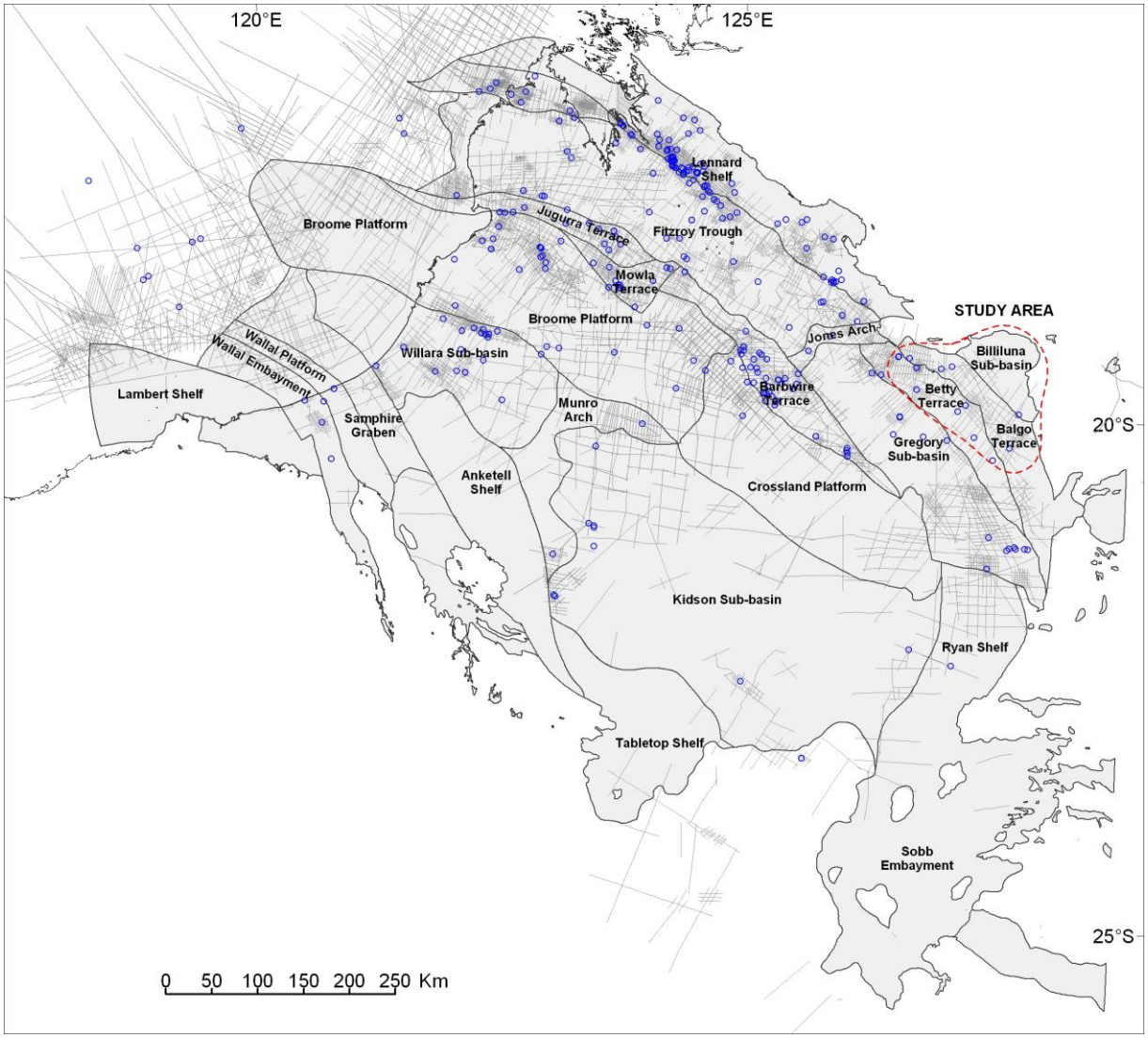

Figure 1.1. The Canning Basin. Tectonic elements with regional well coverage (blue), and 2D seismic coverage (light grey).

Presently, exploration in the basin has a regional focus for conventional and unconventional hydrocarbons (Chapter 2.6), though there is a sustained exploration effort on the Lennard Shelf and neighbouring shelfal positions surrounding the Fitzroy Trough – a large northwest-southeast trending graben that contains in excess of 10 kilometres of sediment – a regional source kitchen.

The problem to be addressed in this study is to determine whether active petroleum systems exist within the project area that have likely generated and expelled hydrocarbons. The study area for this project is located in a shelfal position along strike from the Lennard Shelf; in a

northeastern portion of the Canning Basin known as the Betty Terrace, Balgo Terrace and Billiluna Sub-basin (Figure 1.1).

1.2 Geography

The Canning Basin (approximately 595,000 km^2) is a sedimentary basin occupying approximately one quarter of Western Australia (Purcell, 1984). The basin is comparable in size to other onshore and offshore Australian sedimentary basins, such as the Bonaparte Basin, Officer Basin and the Georgina Basin (Figure 1.2). The Canning Basin is situated along the north-western Australian coastline to the north of Port Headland, stretching north of Derby and east out to Lake Mackay at its' most southeastern point. Large parts of the basin lie within the Great Sandy and Gibson Deserts, and the geographical region is largely uninhabited (Yeates, Gibson, Towner, and Crowe, 1984).

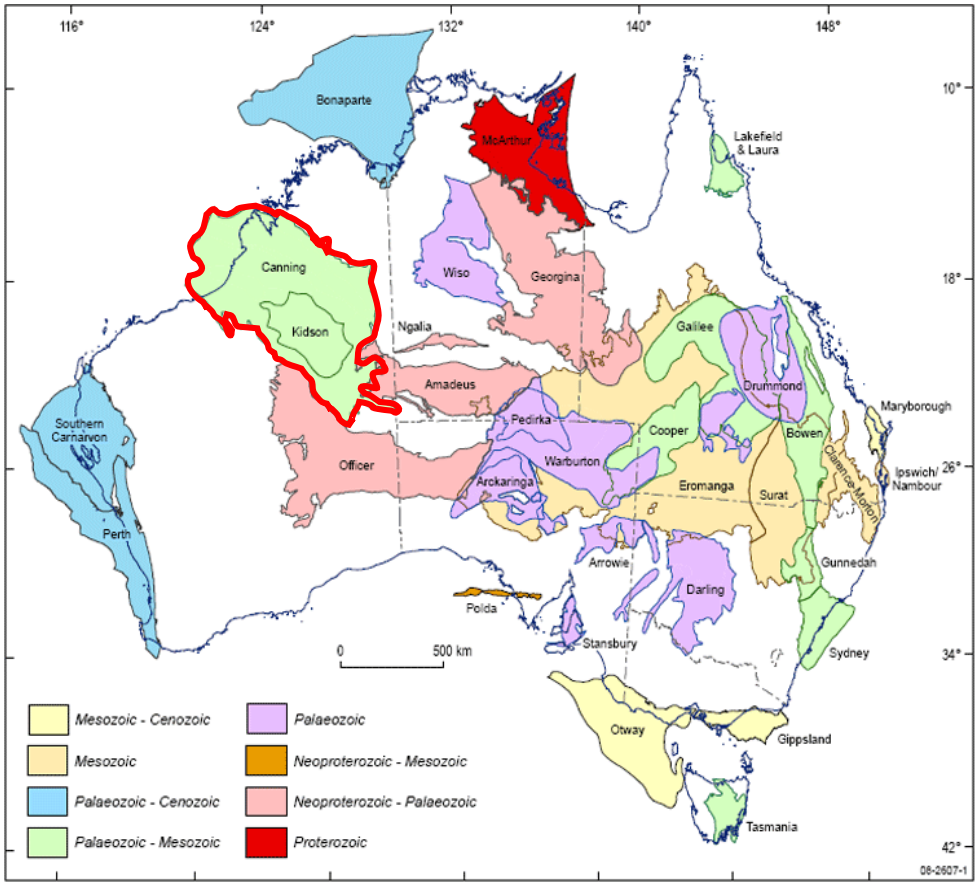

Figure 1.2. Australian continent with prominent sedimentary basins. Canning Basin highlighted in red (modified after GA, 2015).

1.3 Geological Overview

The Canning Basin consists of numerous tectonic provinces that trend in a northwest-southeast direction inland from the WA coast. The basin has a long, multi-stage depositional history extending from the Ordovician to the Cretaceous, and can be divided into several distinct structural and sedimentological phases (Chapter 2.3), which relate to the development of petroleum systems. Rifting in the Ordovician created northwest-southeast trending graben systems accommodating the Larapintine L2 petroleum system. Stratigraphy belonging to this system includes the highly proclaimed Goldwyer Formation shales, understood to be mature and organically rich (Wulff, 1987; Chapter 2.5) in various positions within the basin.

Early Devonian to Carboniferous aged sediments comprising the Larapintine L3 and L4 petroleum systems were deposited following Early Devonian exhumation. Notable sequences include the Devonian aged Gogo Formation; a marine shale sequence understood to actively charge hydrocarbons into Late Devonian reservoirs (Yellow Drum Formation) at the Blina oil field (Table 2.2). Further, the Carboniferous Fairfield Group comprises the Laurel Formation which features a marginal marine carbonate platform developed in shelfal regions (including this study area; Chapter 6); a regionally mappable reservoir and organically rich source rock (Wulff, 1987; Chapter 2.5).

Late Carboniferous to Cretaceous sediments belonging to the Gondwannan G1 and G2 petroleum systems were deposited following uplift and erosion due to a period of exhumation in the middle Carboniferous (Edwards et.al, 1997). A marginal marine Grant Group comprises interbedded sandstone and shale couplets potentially harbouring petroleum. The Grant Group underlies the Permian marine Noonkanbah Formation, representative of a marine transgression in the basin, which is a regionally mappable seal (Chapter 4).

Exhumation in the Triassic, Cretaceous and Tertiary removed large tracts of sediment from across the Canning Basin. Apatite Fission Track Analysis (AFTA) (Duddy, et al, 2003) demonstrates that sediments within the Canning Basin petroleum systems reached their maximum paleo-temperatures during the Triassic.

1.4 Key Project Contributions

Several geological contributions that evolved from undertaking this study are:

1. Previous regional petroleum geology studies (for example: Brown, et al., (1984); Smith, (1984); and Yeates, et al., (1984); Apak and Backhouse (1999); Carlson and Ghori (2005); Haines and Ghori, (2010)) involved mapping 1980's vintage 2D seismic data. Reprocessing the vintage data within the project area greatly enhanced its clarity and therefore its interpretability (Chapter 5 and 6). The tectonic framework is enhanced in this thesis by a slight revision to the tectonic elements map (Chapter 6.2.1).
2. Triassic exhumation is not visible on seismic data, so work by Duddy et al (2003) is a significant contribution to geological knowledge. Although petroleum prospectivity assessments have been undertaken in the past, exhumation in Triassic and younger times have never been applied to the project area principally because they haven't been detected. This thesis encompasses Duddy's work to assess the petroleum systems in light of this data.
3. Wulff (1987) produced the most comprehensive source rock geochemical and thermal maturation study of the project area. 1D modelling was undertaken by Wulff, however 2D petroleum systems modelling has never before been produced within the study area, which this project delivers (Chapter 8).
4. By reviewing previous petroleum systems studies, producing a comprehensive source rock geochemical analysis, producing a stratigraphic framework, utilising recent AFTA derived Triassic exhumation (Duddy et al 2003), interpreting reprocessed 2D seismic data, and producing 2D petroleum systems modelling; this thesis becomes the most comprehensive petroleum systems analysis of the northeast Canning Basin.

1.5 The Study Area

The study area for this project is located in a northeastern portion of the Canning Basin, across three major tectonic regions – the Billiluna Sub-basin, the Balgo Terrace and the Betty Terrace. The size of the study area is approximately 38,000 km^2 (Figure 1.3).

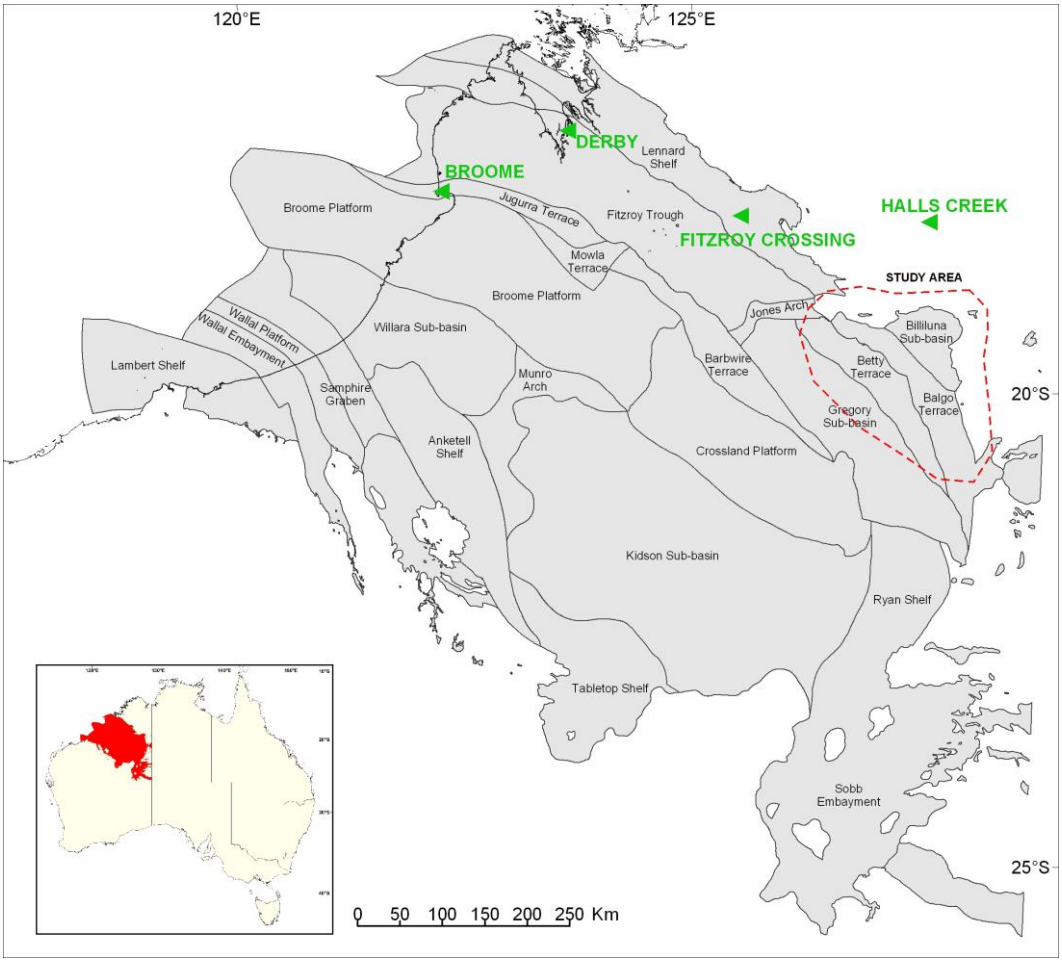

Figure 1.3. The Canning Basin. Regional towns labelled and study area identified (red)

1.6 Research Questions

The key questions addressed in this project are:

- Are organically rich and thermally mature source rocks present within the project area? Did these source rocks generate and expel hydrocarbons?
- Are good quality reservoir rocks and seals present in the study area?
- Are favourable trapping mechanisms and sealing rocks present in the study area?

- Do trapping geometries develop prior to the generation and migration of hydrocarbons?
- Do all petroleum system elements and processes occur together with suitable timing to promote the accumulation and preservation of hydrocarbons?

1.7 Project Aim, Objectives and Methodology

This study ultimately aims to evaluate the petroleum systems within the Billiluna Sub-basin, Betty Terrace and Balgo Terrace structural regions of the northeastern Canning Basin in Western Australia, to identify and determine if the petroleum systems within the study area are likely to have generated hydrocarbons, and if accumulations of petroleum are likely to exist within the region.

This project has eight objectives:

1. Review the existing exploration results and publications pertinent to the study area, and collate all existing data from exploration to produce an updated, relevant poro-perm, TOC, Rock Eval Pyrolysis and petrophysical log database.
2. Produce well correlations in a stratigraphic framework to highlight petrophysical characteristics, correlative properties, reservoir properties, and seal potential of stratigraphy within the project area.
3. Interpret the reprocessed 2D seismic grid to map the key formations across the study area. Map geophysical structure and stratigraphy whilst defining trapping geometries. Perform a simple depth conversion of key regional seismic lines to enable 2D petroleum systems modelling of the project area.
4. Analyse the geochemical database to characterise organic richness, thermal maturation and generation potential of candidate source rock intervals.
5. Model the existing well locations in petroleum systems modelling software and calibrate the models with existing Vitrinite Reflectance (thermal maturity) measurements.
6. Produce 2D models across the Betty Terrace, Balgo Terrace and Billiluna Sub-basin to understand the evolution of petroleum systems in regions without well penetration.

7. Assess prospectivity of the study area for petroleum potential by integrating the results of the source rock study, structural and stratigraphic framework and petroleum systems modelling.
8. Recommend key steps to further reduce exploration risk within the study area.

The methodology is outlined in Figure 1.4.

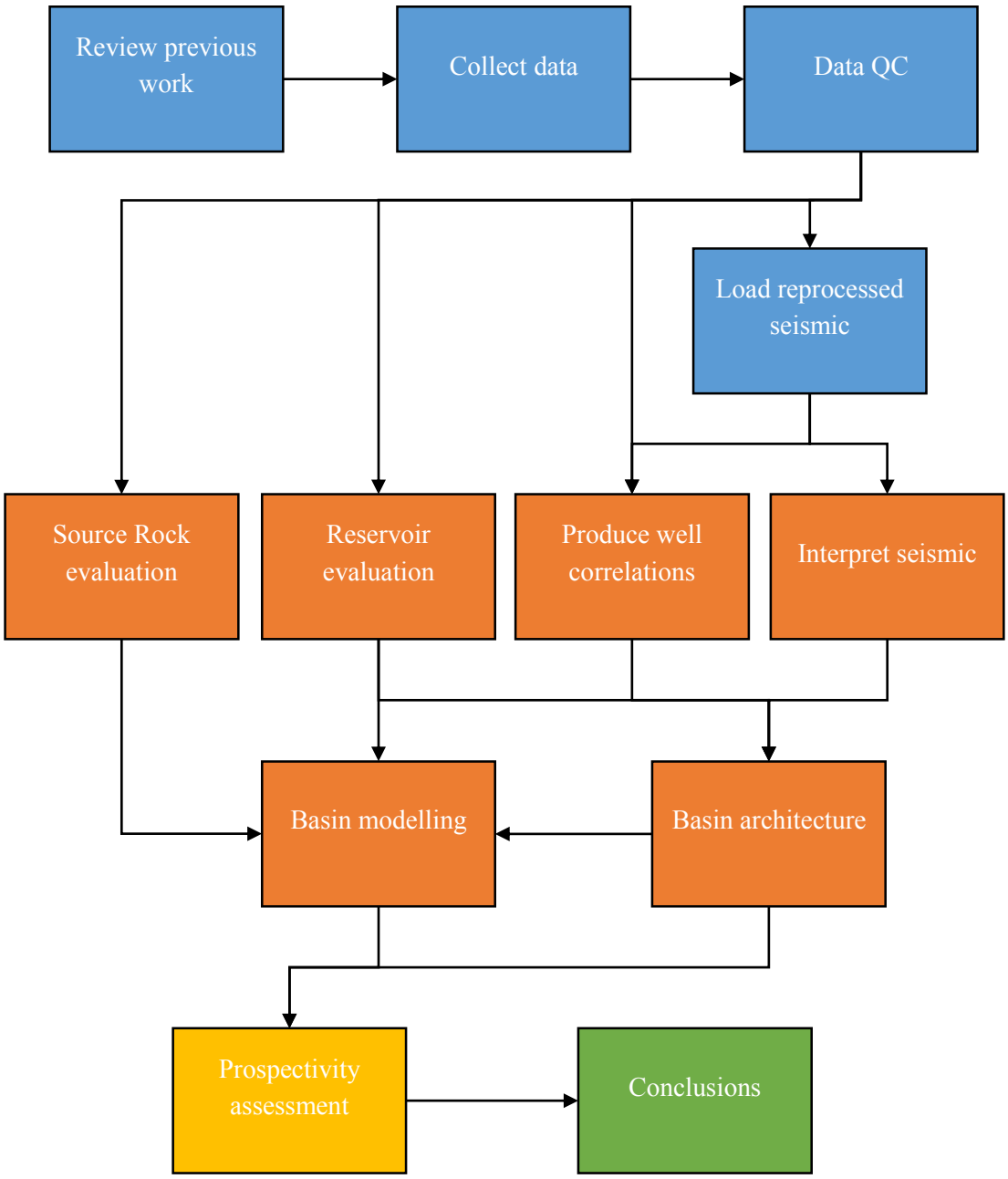

Figure 1.4. Overview of methodology

2. Geological Overview

2.1 Regional Geology

The geology of the Canning Basin has been documented by a number of authors including Brown, et al., (1984); Smith, (1984); and Yeates, et al., (1984). A recent review of the north eastern Canning Basin has been conducted by authors Apak and Backhouse (1999) and Carlson and Ghori (2005). The following review of the regional geology will include reference to features pertinent to the study area – The Betty Terrace, Balgo Terrace and Billiluna Sub-basin.

The Canning Basin has a long, multi-stage depositional history extending from the Ordovician to the Cretaceous, and can be divided into several distinct structural and sedimentological phases. More than 10km of sediments lie within the Fitzroy Trough, and up to 18km of strata may be present in the Gregory Sub-basin – the basin's deepest depocentre (Yeates, Gibson, Towner, and Crowe, 1984).

The Canning Basin is subdivided into various structural provinces (Figure 2.1). The expansive Kidson Sub-basin and Willara Sub-basin are situated in the centre, and the Anketell Shelf and Wallal Embayment truss the basin to the southwest; where the stratigraphy is mostly horizontal to sub-horizontal (Yeates, Gibson, Towner, and Crowe, 1984). The north and north-eastern areas of the Canning Basin have experienced a more intense multi-phase deformational history. The centrally located Kidson Sub-basin and neighbouring Broome and Crossland Platforms transition in the northeast. The northwest-southeast oriented Fitzroy Trough and Gregory Sub-basin are located on the north eastern side of the basin. The northern most structural provinces of the Canning Basin are the Lennard Shelf, Billiluna Sub-basin and Balgo and Betty Terrace areas (Figure 2.2).

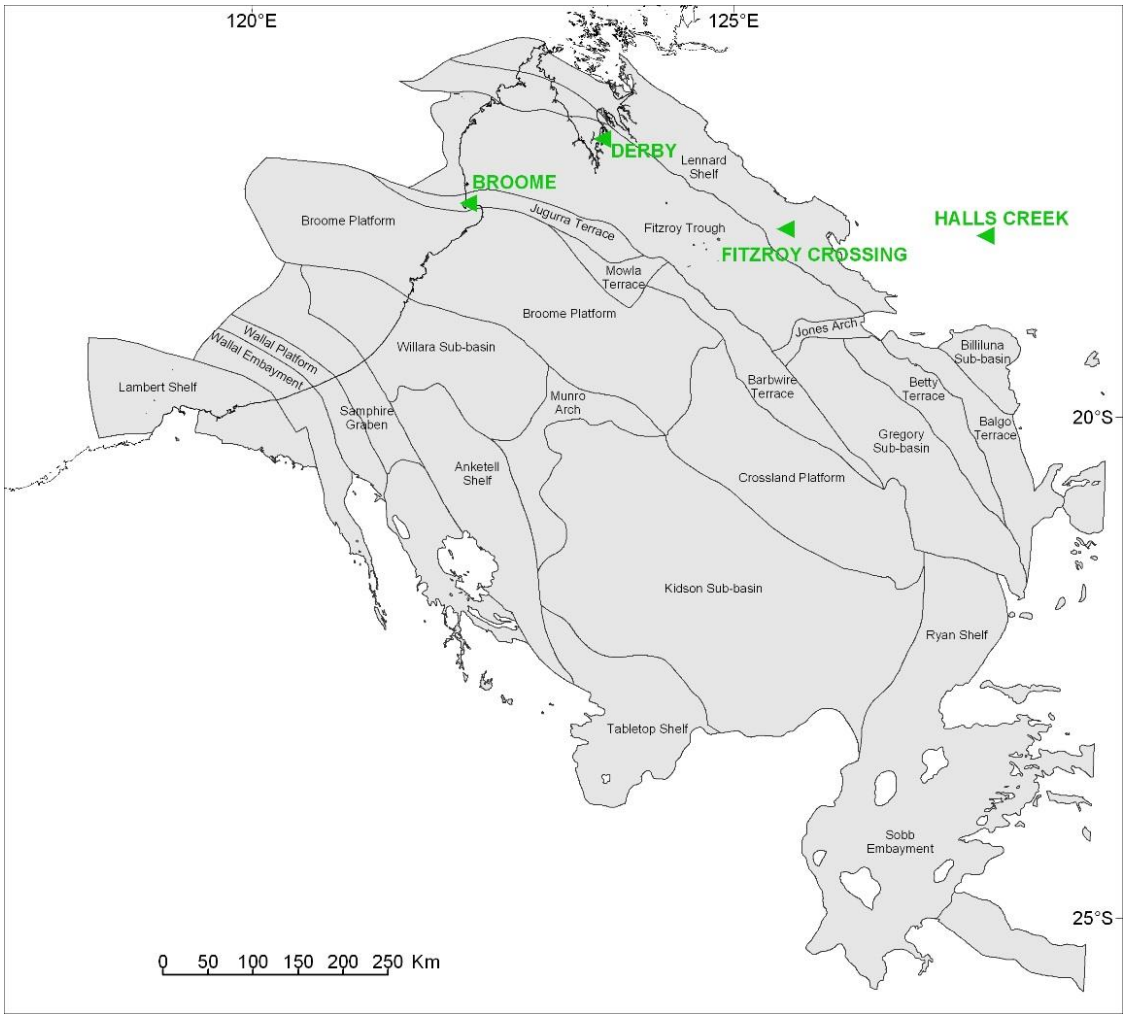

Figure 2.1. The regional Canning Basin. Tectonic elements and regional locations labelled.

2.2 Geological Division of the Study Area

The study area includes the Billiluna Sub-basin, the Balgo Terrace and the Betty Terrace; each of which are separated by major fault systems (Figure 2.2); a north-northeast trending Halls Creek fault system active during the Pre-Cambrian and possibly the Palaeozoic; a Palaeozoic north-south trending marginal basin fault system on the eastern boundary; and a major northwest-southeast trending fault system largely controlling the Gregory Sub-basin (Smith, 1984). The Billiluna Shelf area comprises the north-eastern-most structural region of the Canning Basin. It is bounded by the northwest-southeast trending Mueller Fault and intersected by the Halls Creek fault blocks on the northern basin margin. The Balgo Terrace lies southwest of the Billiluna Shelf, situated between and controlled by the Mueller Fault

and the Stansmore Fault. The Betty Terrace is located south-westward and is influenced by similar northwest-southeast trending structural regimes (Smith, 1984).

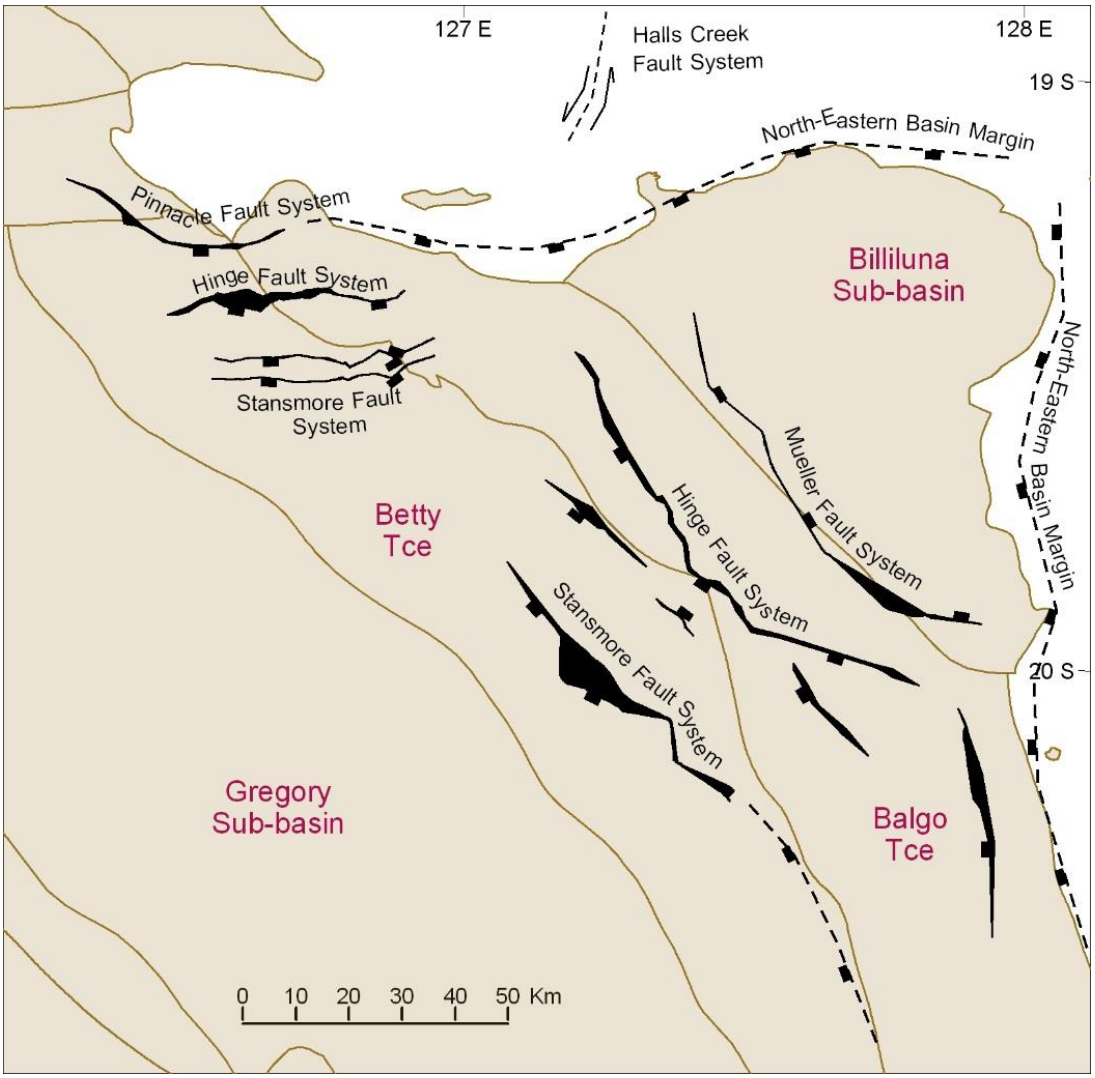

Figure 2.2. Structural features within the Study Area. Inferred faults are dashed (Modified after Tyler 2000), Solid faults are derived from Seismic interpretation, brown lines show tectonic elements provided by the WA Geological Survey.

2.3 Geological History

2.3.1 *Archean*

The Canning Basin unconformably lies above Archean basement. Archean east-west compressional events imprint a visible steep westerly dipping fabric to Archean rocks. These north-south oriented compressional tectonic movements facilitated east-west trending folds in

the southern region of the basin (Irwin 1998), and show a clear unconformity that is commonly visible on regional seismic lines (Chapter 5.3.8).

2.3.2 *Ordovician to Silurian*

Deposition in the Canning Basin commenced in the Early Ordovician after a period of extension (Samphire Marsh Movement, Figure 2.3 and Figure 2.4) (Haines and Ghori, 2010). An important feature of Ordovician time is the development of the Larapintine Seaway (Figure 4.6, Cook and Totterdell, 1990) connecting the Canning, Amadeus and Georgina Basins. Together with northwest-southeast trending troughs that developed due to extensional tectonics, it accommodated shallow marine sandstones, carbonates and conglomerates (Carranya Beds). These rocks crop out on the northern basin margin and are locally hundreds of metres thick in basin depocentres (Nambeet Formation equivalent) (Smith, 1984). A depositional hiatus and extensive erosion preceded uneven subsidence in the Late Silurian and Early Devonian resulting in the waning of the Kidson sub-basin and down-to-the-basin faulting in the Fitzroy Graben (Yeates, et al., 1984). The Siluro-Devonian marginal marine Carribuddy Formation disconformably overlies the Carranya Beds. These evaporites (anhydrites) are extensive and provide a regional seal in most areas of the Canning Basin (Yeates, et al., 1984). The Carribuddy Formation may also contain local reservoir facies north of the Gregory Sub-basin, equivalent of the Nambeet and Willara units to the south, though possibly eroded by Devonian regional events (Haines and Ghori, 2010).

2.3.3 *Devonian to Mid-Carboniferous*

The Early Devonian Prices Creek Movement resulted in uplift, folding and erosion (Figure 2.3, Edwards, et al., 1997), prior to deposition of Devonian – lower-mid Carboniferous strata (Figure 2.4). A terrestrial sandstone (Tandalgoo Formation) is generally widespread (Haines and Ghori, 2010), although is believed to not cross the Fenton Fault hinge into the Gregory sub-basin or adjacent areas (Smith, 1984). During this time the Fitzroy and Gregory sub-basins obtained graben style properties, and secondary faulting generated parallel to the elongate axis forming terrace and shelf structuration near the eastern basin margin (Yeates, et al., 1984). Following subsidence of the Fitzroy Trough and Gregory Sub-basin, a Late Devonian Lennard River Group of shallow marine carbonates, evaporites, sandstones and

shales were deposited. Carbonate sequences were commonly built up on shelfal areas, where as the Fitzroy and Gregory sub-basins – now the major basin depocentres – received a predominantly clastic influx. The fluvial Knobby Sandstone disconformably overlies the Lennard River Group (Smith, 1984). The unit transitions into a shale, siltstone and sandstone progression of the Luluigui Formation in the central depocentres. As subsidence slowed, lagoonal limestones of the Early Carboniferous Fairfield Group filled the depressions (Figure 2.3. This sequence combined with the Laurel Formation and merged into the shallow marine clastic sequences of the Anderson Formation (Edwards, et al., 1997).

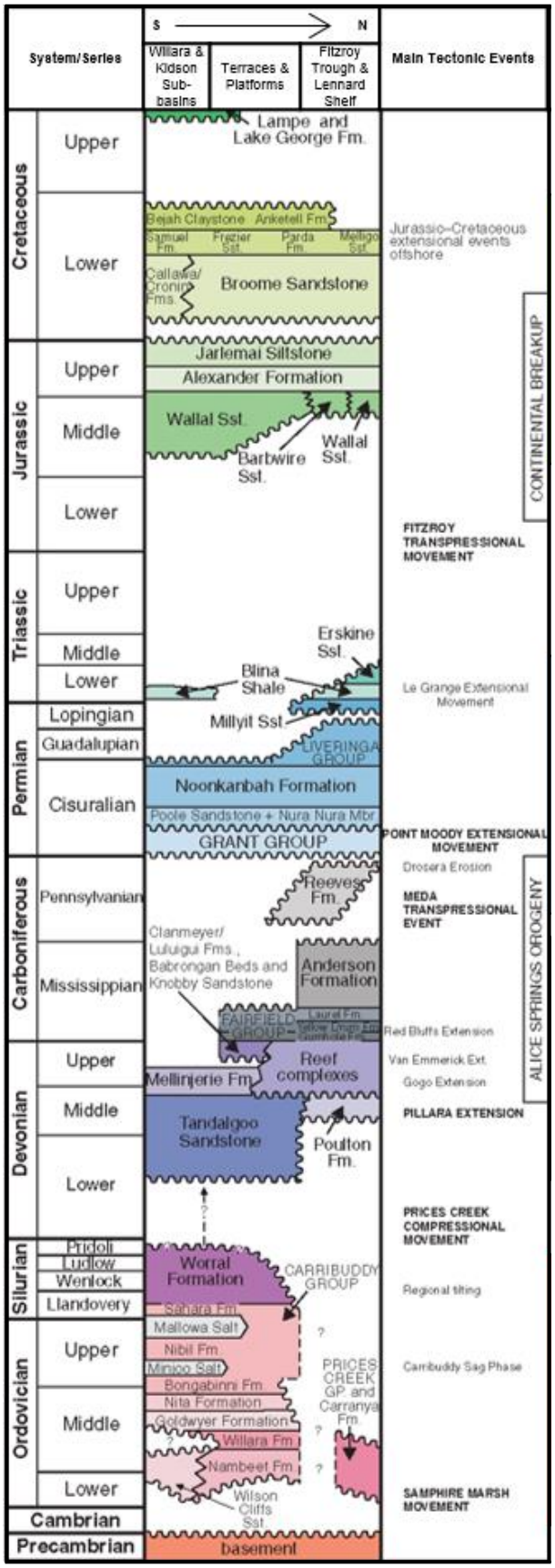

Figure 2.3. Stratigraphic column of the Canning Basin (Haines, 2009)

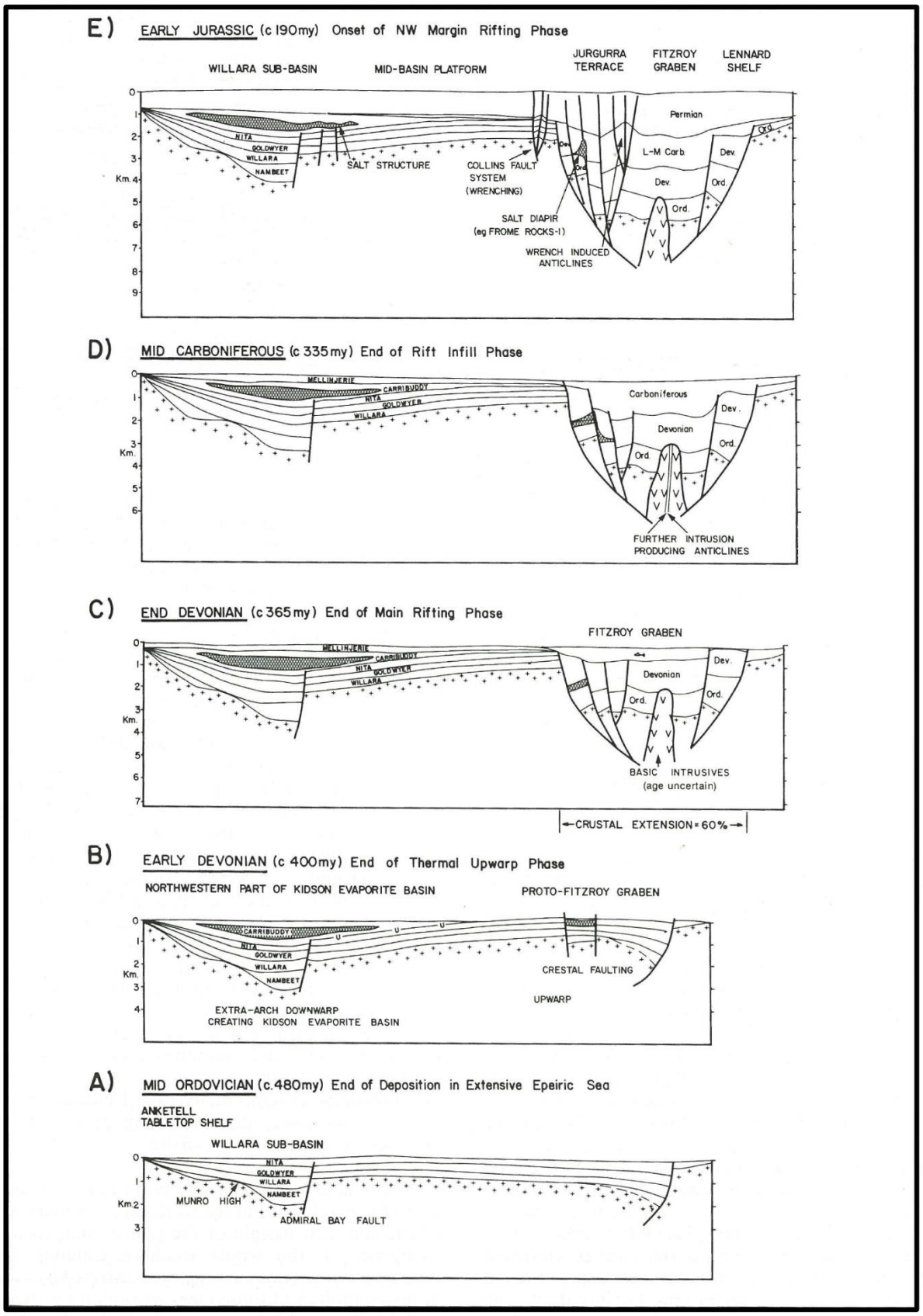

Figure 2.4. Tectonic development of the main Canning Basin elements. (Brown et al, 1984)

2.3.4 *Late Carboniferous to Permian*

The compression, uplift and erosion of the middle Carboniferous Meda Transpression was prior to deposition of Upper Carboniferous – Permian strata (Figure 2.3 and Figure 2.4, Edwards, et al., 1997). The Late Carboniferous – Early Permian Grant Group is glacigene in parts (Pre-Grant Group) (Edwards, et al., 1997), mixing with marginal marine well-sorted medium-grained sandstones, deposited extensively, though thinly (Casey and Wells, 1960). Stratigraphic relations within the Grant Group are complex, featuring porous sandstone and shale interbedded successions, potentially both reservoir and seal units (Haines and Ghori, 2010). A post-glacial transgression resulted in the deposition of the Early-Mid Permian fluviatile Poole Sandstone; inferred to be present in deeper trough areas and noted to not crop out in the eastern regions (Casey and Wells, 1960). The Mid-Permian Noonkanbah Formation conformably overlies the Poole Sandstone (Figure 2.3), featuring fossiliferous and calcareous fine sandstone and shale sequences (Yeates, et al., 1984). The Liveringa Formation's three members all appear in the eastern provinces (Balgo, Condren Sandstone and Hardman members) with sharp conformable boundaries (Guppy, Lindner, Rattigan, and Casey, 1958). The Late Permian Mylit Sandstone is inferred to extend into, and overly Mid-Permian rocks in southern parts of the basin, though likely not well preserved in outcrop (Smith, 1984).

2.3.5 *Triassic*

The Early Triassic Blina Shale is likely to be undifferentiated in areas where it unconformably overlies the fluvial Mylit Sandstone (Casey and Wells, 1960). The Early-Mid Triassic fluvial (siltstone, sandstone) Culvida Sandstone (equivalent of the Erskine Sandstone in the Fitzroy Trough) overlies the Mylit Sandstone, and comprises flora-rich, fossiliferous, massive, current-banded sandstones (Casey and Wells, 1960). The post-glacial transgression ceased in the Mid-Triassic during the Fitzroy Movement (Figure 2.3 and Figure 2.4), where anticlinal structures formed, and several kilometres of sediments (up to 2.9 km) were eroded from within the Fitzroy Trough (Edwards et al., 1997; Duddy et al., 2003).

2.3.6 *Jurassic and Younger*

Younger sequences, as noted by Casey and Wells (1960), are observed in locales within the eastern Canning Basin. A restricted deposit of Late Cretaceous massive, partly shaley

sandstone with occasional conglomerate interbeds are observed in the Godfreys Tank area, west of Lake Gregory (Figure 2.5). These Godfrey Beds are noted by Casey and Wells (1960) to be 60 metres thick. Tertiary laterite and pisolitic ironstones are observed up to 15 metres thick in confined areas near Christmas Creek (Figure 2.5) close the north-eastern basin margin. Massive marl and carbonate beds (Lawford Beds) are noted to overly the Godfrey Beds near Christmas Creek. Recent Quaternary deposits include evaporites, gravels and alluvial soils, as well as widespread medium to coarse grained aeolian sands that cover large areas as dunes in the Great Sandy and Gibson Deserts (Casey and Wells, 1960).

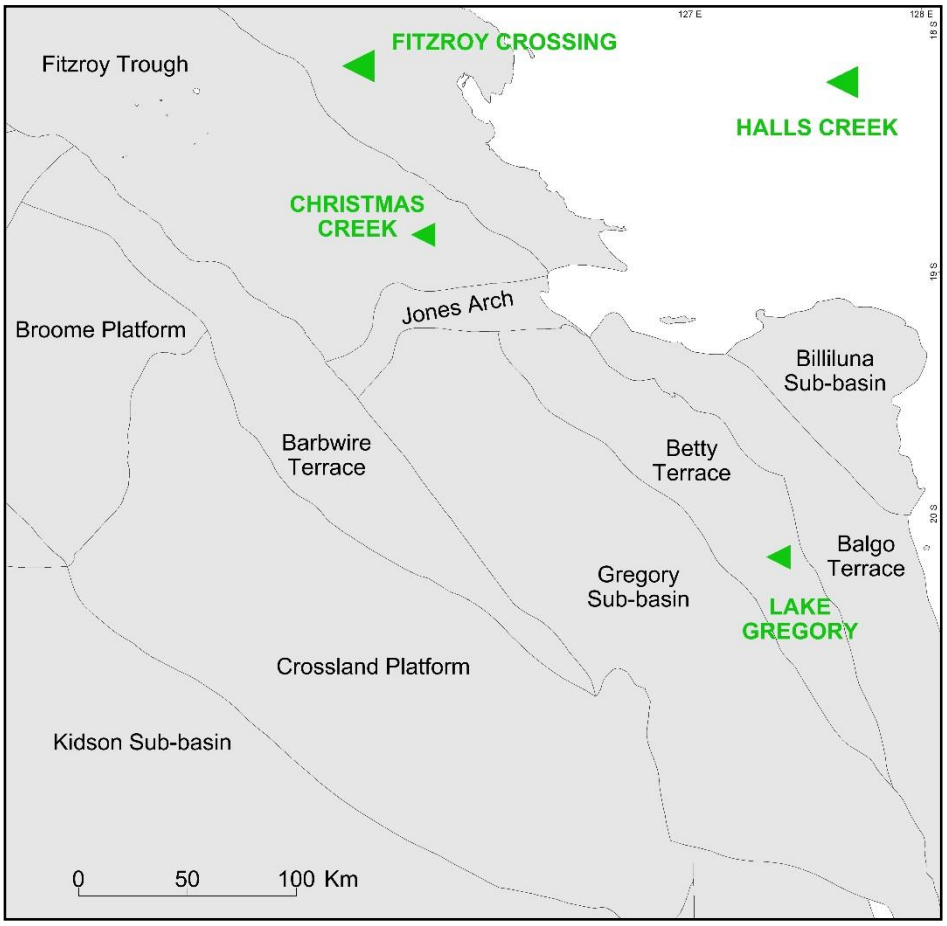

Figure 2.5. Late Cretaceous sediments are preserved west of Lake Gregory. Tertiary laterites are preserved near the north-eastern basin margin near Christmas Creek.

2.4 Petroleum Systems

A 'Petroleum System' is a geologic system that encompasses the hydrocarbon source rocks and all related oil and gas, and which includes all of the geologic elements and processes that are essential if a hydrocarbon accumulation is to exist (Magoon and Dow, 1994). A petroleum system requires a (1) source rock of sufficient organic richness and thermal maturity to generate and expel hydrocarbons, a (2) reservoir or carrier bed with suitable porosity and permeability characteristics to allow hydrocarbons to migrate and accumulate in a definable (3) trapping geometry, a (4) sealing lithology or geologic configuration to contain accumulated hydrocarbons, and an (5) optimal timing of the occurrence of these elements and processes (including migration) to allow the hydrocarbon products to be preserved over geologic time to the present day.

2.4.1 *Petroleum Systems in the Canning Basin*

Palaeozoic petroleum systems provide approximately 25% of recoverable hydrocarbons globally (Carlsen and Ghori, 2005). Bradshaw et al (1994) and Carlsen and Ghori (2005) recognize that the Canning Basin hosts three major Palaeozoic petroleum super systems based on isotopic and biomarker studies: Ordovician – Silurian (Larapintine L2), Devonian – early Carboniferous (Larapintine L3 and L4) and late Carboniferous – Permian (Gondwannan G1 and G2). Stratigraphic sequences of the Canning Basin can be treated according to these divisions (Figure 2.6).

Three main structural and stratigraphic phases have influenced the establishment of petroleum systems in the research area. Figure 2.6 relates these petroleum systems to stratigraphy. Early Ordovician extension (Samphire Marsh Movement) created northwest-southeast trending troughs accommodating Ordovician to Silurian aged rocks of the Larapintine L2 petroleum system (Haines and Ghori, 2010). The Early Devonian Prices Creek Movement resulted in uplift, folding and erosion that facilitated the Larapintine L3 and L4 petroleum system (Edwards, et al., 1997) with deposition of Devonian to Early-Mid Carboniferous strata. The compression, uplift and erosion of the Mid Carboniferous Meda Transpression was responsible for the deposition of Upper Carboniferous to Permian rocks representing the Gondwannan G1 and G2 petroleum system (Edwards, et al., 1997).

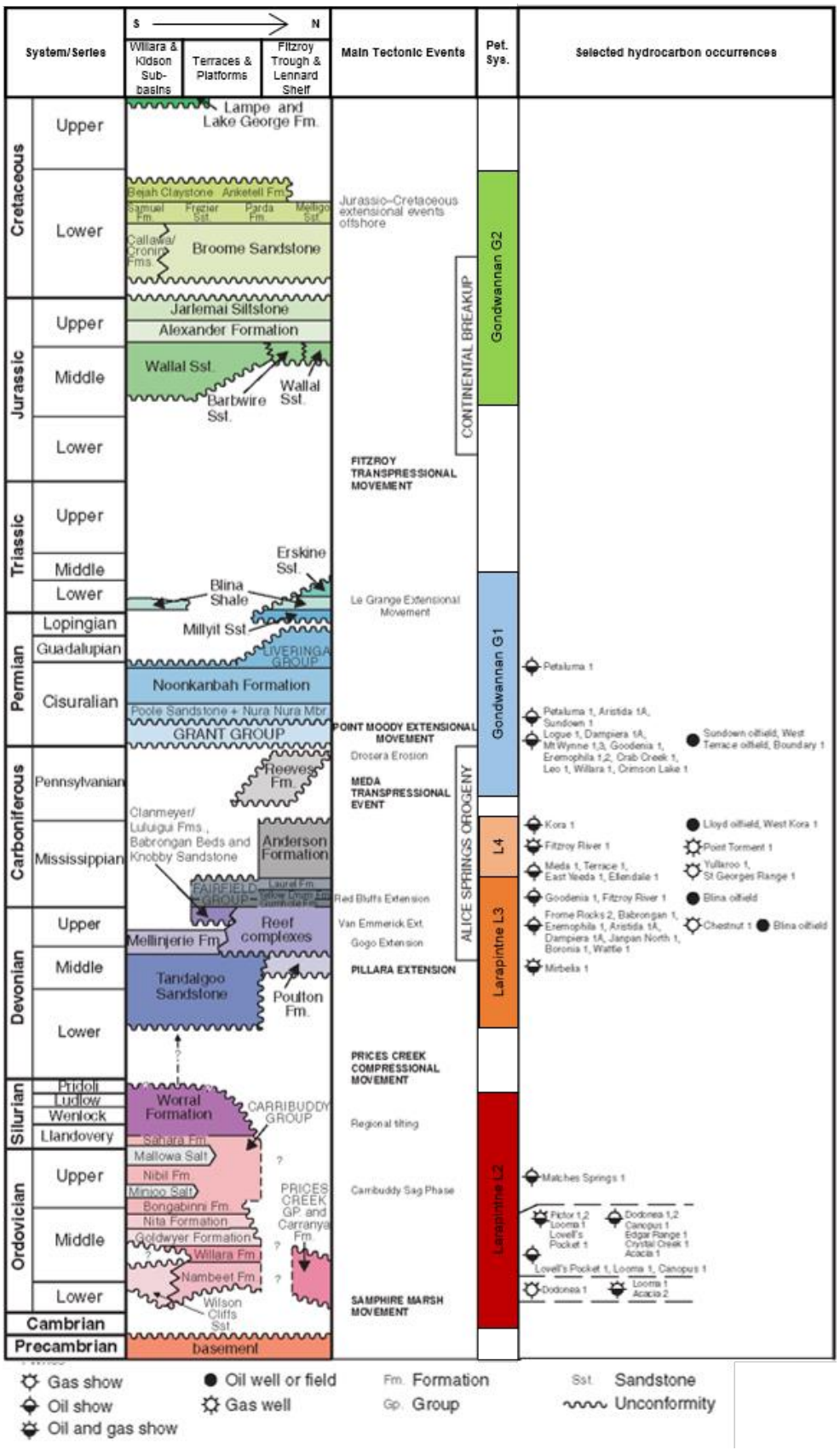

Figure 2.6. Stratigraphic chart with relations to tectonic events, petroleum systems and selected hydrocarbon occurrences (Modified after Haines 2009)

2.5 Source Rock Potential - Review of Wulff (1987)

Wulff (1987) has provided the most comprehensive study of source rock potential to the study area. Their study examines five source rock intervals that are anticipated to contain suitable organic richness and optimal thermal maturity to generate hydrocarbons within the Canning Basin. The intervals tested by Wulff (1987) are the Permian aged Noonkanbah Formation (belonging to the Gondwannan G1 petroleum system), Carboniferous Laurel Formation (Larapintine L3 petroleum system) Devonian Gogo Formation and Pillara Formation (Larapintine L3) and the Ordovician Goldwyer Formation (Larapintine L2). Wulff (1987) accessed well data from twenty-one exploration wells. Importantly, Atrax 1, Bindi 1, Kilang Kilang 1, Lake Betty 1, Ngalti 1, Olios 1 and Selenops 1 are utilised in their work, thus providing a good point for discussion in this research project. It is worth noting here that two wells have been drilled since Wulff's 1987 report; Lanagan 1 (drilled in 2008) and Lawford 1 (drilled in 2008 and re-entered in 2011).

Wulff concluded that the Devonian and Ordovician sequences are the most likely to have the ability to generate significant quantities of hydrocarbons. This was because the Gogo Formation experienced a transitional marine to marine depositional environment, similar to that of the shallowest unit of the Goldwyer Formation (unit 4). Their interpretation comes after determining a predominately type II to type III kerogen (Algal marine or terrestrial organic matter) for the Devonian and Ordovician aged sections. They recommend that exploration targets for these units should be focused on preserved thicknesses expected to be found in the hanging wall section (down thrown block) of large listric faults commonly observed in the area. Wulff's work concluded that the Permian and Carboniferous aged stratigraphy is unlikely to be able to source significant quantities of hydrocarbons; Wulff (1987) explains that the lower section of the Permian Noonkanbah Formation is composed principally of type III kerogen due to its terrestrial deposition, and that the upper marine unit of the Noonkanbah Formation, although containing up to 2% Total Organic Carbon (TOC) is predominantly comprised of oxidised and reworked material (type IV kerogen). According to their maturation study the interval is likely not buried deep enough to enter the oil window. Wulff (1987) concludes that the Carboniferous Laurel Formation, though is mature for oil generation, is comprised mostly of Inertinite (with TOC less than 1%), and is unlikely to generate significant quantities of hydrocarbons.

Horstman (1984), Wulff (1987) and Duddy et al. (2003) have completed thermal history reconstructions using Canning Basin wells. Horstman (1984) utilised the projection of Vitrinite Reflectance data to determine that 500 metres to 1000 metres of sediment was removed from the Canning Basin during a Triassic exhumation event. Wulff (1987) goes further with Apatite Fission Track Analysis (AFTA) revealing that the basin has been affected by at least two significant thermal events in the Carboniferous (the Meda Transpression event) and the Triassic (Fitzroy Movement event). Duddy et al. (2003) have advanced the use of AFTA to postulate that four events impacted the thermal histories of the Canning Basin (Carboniferous, Triassic/Jurassic, Cretaceous and Tertiary). The work by Duddy et al. (2003) is significant as it demonstrates that sediments attained maximum maturity in the Triassic before significant exhumation in the Triassic and Jurassic.

2.6 Previous Exploration

Exploration in the Canning Basin began in 1922 when Freney Oil Company drilled four wells after seeing encouraging signs of oil in a water bore near Pillara Range (Cadman et al. 1993). Exploration accelerated in 1952 with the Bureau of Mineral Resources (BMR) Reconnaissance Gravity Program. The first seismic survey was shot in 1963 by Hackathorn to verify leads identified by photo interpretation and geological mapping (Jacobson, 1984). Early data acquisition within the study area was generally regional in nature due to the remote location (~350 km inland), particularly because early acquisition methodology involved mobilizing masses of equipment through desolate areas. Exploration in the basin ceased during the petroleum industry recession of the 1970's and resumed in the early 1980's. Today, available seismic data is generally evenly spaced across the study area. Data is mostly mid-1980's vintage, however a few smaller survey lines date back to the 1960's and 70's. Larger seismic surveys within the research area include the Billiluna 1981, Bloodwood 1982, Mt Bannerman 1982 and Sturt 1985 seismic surveys. The importance of data quality to prospect identification and evaluation is discussed by Jacobson (1984). The variable surface conditions in the region have a significant impact on the quality of seismic, with data collected in zones of sandy plains, variable surface weathering, and high rainfall. Modern day data processing techniques aim to overcome poorer seismic quality and was utilised to improve the clarity of data used in this project.

Early drilling efforts have generally been lean and thus only sparse well coverage exists in the study area. Petroleum exploration wells in the area include Atrax 1, Selenops 1, Olios 1, Ngalti 1, BMR Lucas 13 and 14, BMR Billiluna 1 and BMR Mount Bannerman 4. Most of these wells target shallower Permian objectives, while Olios 1, Ngalti 1, Strax 1 and Selenops 1 penetrate to the deeper Devonian rocks. A number of mineral exploration holes are located near the northern study area margin, though these are very shallow.

Table 2.1 summarises the occurrences of oil and gas within shelfal and depocentre regions of the basin. Most historic oil and gas encounters are from the Ordovician, or Devonian to Carboniferous sections of the stratigraphy; that is, the Larapintine L2 and Larapintine L3 and L4 petroleum systems. The reader is referred to Cadman et al. (1993) for further information on the accumulations that are not mentioned here.

Cadman et al. (1993) summarize hydrocarbon play types within the Canning Basin and their associated discoveries. Table 2.2 summarises this detail with reference to Palaeozoic petroleum systems.

PET. SYS.	FM	LENNARD SHELF								FITZROY TROUGH		BARBWIRE TCE		DAMPIER TCE	
		Janpam North	Kora	Terrace	Meda	Ellendale	Boronia	Crimson Lake	Point Torment	Yulleroo	St George Range	Mirbelia	Dodonea	Pictor	
G2	Liveringa														
G2	Noonkanbah														
G2	Poole														
G2	Grant							Oil							
L4	Anderson		Oil						Gas						
L3	Laurel			Oil	Oil	Oil	Gas			Gas	Gas				
L3	Nullara	Oil			Gas										
L3	Napier														
L3	Pillara/Gogo						Oil								
L3	Mellinjerrie											Oil			
L3	Poulton														
L3	Tandalgoo														
L3	Carribuddy														
L2	Nita													Oil	Gas
L2	Goldwyer												Oil		
L2	Willara														
L2	Nambeet												Gas		

Table 2.1. Hydrocarbon occurrences in the Canning Basin, modified after Cadman et al., (1993).

RESERVOIR	SEAL	TRAP / OBJECTIVE	SOURCE	'DISCOVERY' WELL	PET. SYS.
		LATE CARBONIFEROUS to PERMIAN			
Grant Fm sandstone	Grant Fm shales/siltst	Compressional culmination with internal stratigraphic traps	Laurel Fm shales	Sundown No. 1 Oil	Gondwannan GI
Grant Fm sandstone	Grant Fm shales/siltst	Unfaulted four-way dip closure within palaeo-monadnock	Laurel Fm shales	West Terrace No.1, Oil	
Grant Fm sandstone	Grant Fm shales/siltst	?	Laurel Fm shales	Boundary No. 1 Oil	
Grant Fm sandstone	Grant Fm shales/siltst	Faulted, four-way dip closure on Laurel Fm carbonate horizon	Laurel Fm shales	Crimson Lake No.1, Oil	
		CARBONIFEROUS			
Anderson Fm sandstone	Anderson Fm shales	Faulted four-way dip closure	Laurel Fm shales	Lloyd No. 1 Oil	Larapintine L4
Anderson Fm sandstone	Anderson Fm shales	?	?	Point Torment No.1, Gas	
Anderson Fm sandstone	Anderson Fm shales	Unfaulted four-way dip closure	Laurel Fm shales	Kora No. 1 Oil	
Laurel Fm carbonates	Laurel Fm shales	Four-way dip closure	Laurel Fm shales	Terrace No.1 Oil	Larapintine L3
Anderson Fm sandstone	Anderson Fm shales	Four-way dip closure	Laurel Fm shales	West Kora No. 1 Oil	
Anderson Fm sandstone	Anderson Fm shales	Compressional culmination with internal stratigraphic traps	Laurel Fm shales	Sundown No. 1 Oil	
Laurel Fm sandstone	Laurel Fm shales	Reef-like seismic anomaly	Laurel Fm shales	Meda No. 1 Oil	
Laurel Fm clastics	Fairfield Group shales	Faulted, four-way dip closure on Intra-Fairfield Group	Gogo Fm shales	Ellendale No. 1 Oil and Gas	
Laurel Fm limestone	Laurel Fm shales	Anticline	Laurel Fm shales	St George Range No. 1 Gas	
Laurel Fm sandstone	Laurel Fm shales	Anticline	Laurel Fm shales	Yulleroo No. 1 Gas	
		DEVONIAN			
Yellow Drum Fm, leached dolostones	Fairfield Group shales	Compaction drape closure over Devonian reef	Gogo Fm shales	Blina No. 1 Oil	Larapintine L3
Nullara Fm carbonates	Nullara Fm shales	Reef-like seismic anomaly	Gogo Fm shales	Janpam North No.1, Oil	
Nullara Fm calcarenite	Nullara Fm shales	Reef-like seismic anomaly	Gogo Fm shales	Meda No. 1 Gas	
Nullara Fm leached dolostones	May River Member shales	Unfaulted shale draped biohermal and biostromal mound	Gogo Fm shales	Blina No. 1 Oil	
Gogo Fm clastics	Gogo Fm shales	?	Gogo Fm shales	Boronia No. 1 Oil	
Mellinjerie Lst dolostones	Lower Pillara Fm shales	Fault dependent closure at top Nita Fm level.	?	Mirbelia No. 1 Oil	
		ORDOVICIAN			
Nita Fm dolostones	Nita Fm shales	Tilted fault block with internal four- way dip closure	Goldwyer Fm shales	Pictor No. 1 Oil	Larapintine L2
Goldwyer Fm carbonates	Goldwyer Fm shales	Fault dependent closure at top Nita Fm level.	Goldwyer Fm shales	Dodonea No. 1 Oil	
Nambeet Fm dolomitic ss	Upper Nambeet Fm ?	Fault dependent closure at top Nita Fm level.	Upper Nambeet Fm ?	Dodonea No. 1 Gas	

Table 2.2. Hydrocarbon plays in the Canning Basin (modified after Cadman et al., 1993)

Currently, the entirety of the Canning Basin is under exploration lease. There are at present twenty-two exploration companies present in the basin (Figure 2.7). The largest proportion of exploration leases are held by Buru Energy Ltd, New Standard Energy Ltd (NSE)/Conoco Phillips (in Joint Venture), Hess Corporation and Backreef Oil Pty Limited. Buru Energy and the Conoco Phillips/NSE joint venture are the parties that have most recently completed work programs. Buru Energy Ltd is currently the largest explorer in the basin (by acreage position and perseverant work programs), and has had the most recent exploration success with their Valhalla (2007) prospect, Yulleroo (discovered in 1967 and tested in 2008) and most recent Ungani well discoveries (2011 and 2012, Figure 2.8). Buru's Ungani play recently completed Extended Production Testing (EPT) producing 1,025 barrels of oil per day during the EPT (Buru Energy, 2015).

In 2012 Hess Corporation acquired unlisted Kingsway Oil, instantly making Hess Corporation the then largest tenement holder in the basin (by acreage position), with interest in permits covering large parts of the Kidson Sub-basin. In 2013 Apache Energy Ltd. entered into a Joint Venture agreement with Buru Energy to explore the potential of the Ordovician Goldwyer Formation on the Broome Platform and Dampier Terrace (western Canning Basin) valued at $25 Million, and Fitzroy Graben (central-north Canning Basin) valued at approximately $7.2 Million (plus the majority of work program costs), to earn approximately 40% interest in the permits. Other recent activities to note include the Goldwyer Shale Gas exploration program undertaken by New Standard Energy Ltd. together with ConocoPhillips, as part of a $73 Million four-year work program to evaluate the unconventional potential of the Ordovician Goldwyer Formation across the Kidson Sub-basin (funded by ConocoPhillips to earn a 75% interest in the project). The joint venture drilled a three-well program in 2012 and 2013. ConocoPhillips exited the joint venture in 2014.

One take away message from these investments is a heightened interest in large acreage positions containing regional unconventional prospects, where recent shale exploration joint ventures coupled with encouraging drilling results have led to new exploration in the Canning Basin.

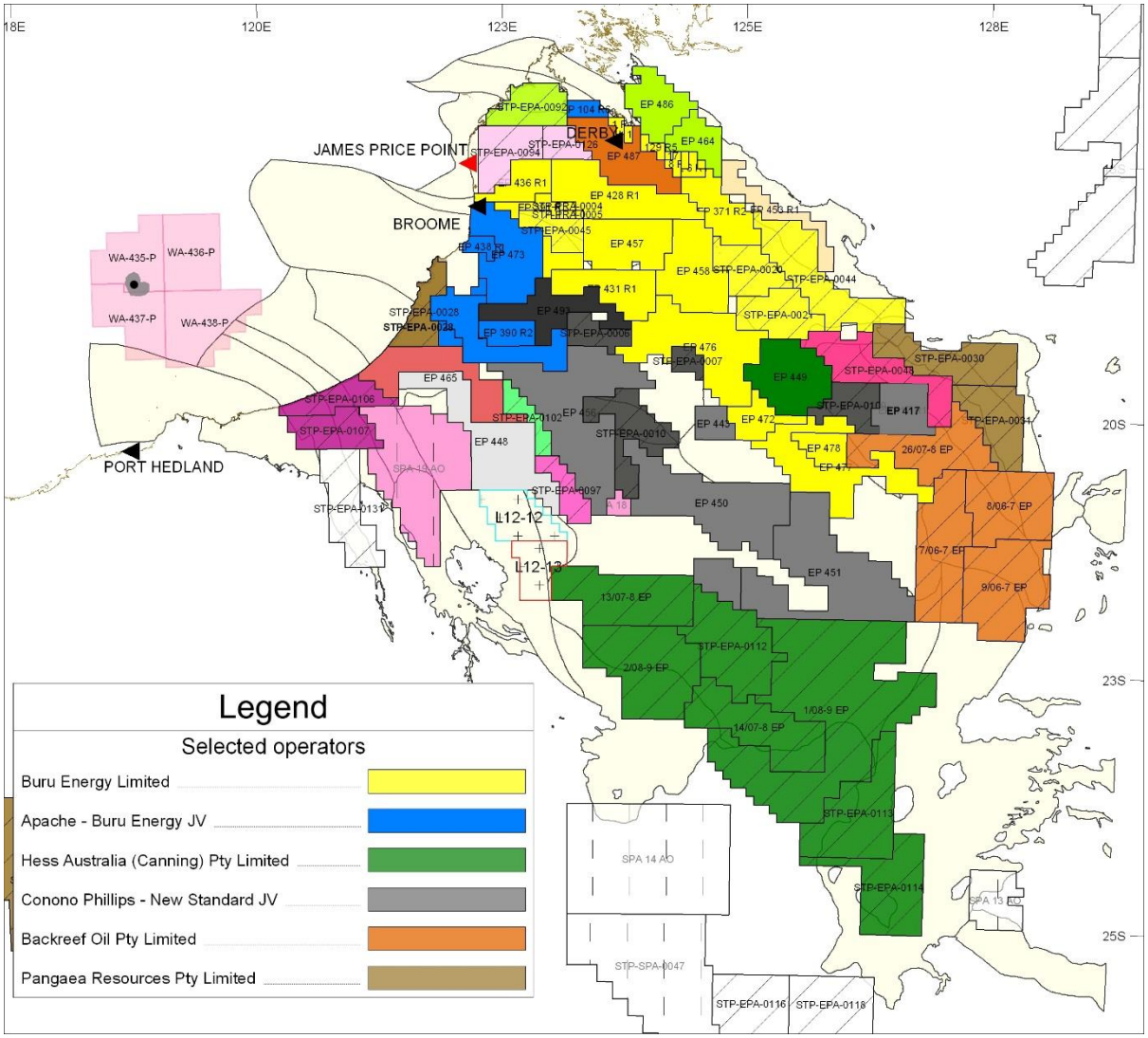

Figure 2.7. Current population of explorers in the Canning Basin

2.7 Production

The first commercial oil was found by Home Energy Company at Blina 1 on the Lennard Shelf, recovered from within the Fairfield Group (Cadman et al 1993). The Blina field (Figure 2.8) is one of the small fields still in production, currently operated by Buru Energy Ltd.

Another small neighbouring producing area, the West Kora field (Figure 2.8), was discovered by Esso Australia in 1984 and produced 20,000 barrels of oil at 350 barrels per day, but was eventually shut-in due to increased water cut from 35% to 85%. Now operated by Buru Energy, there are plans for a workover program to bring the field back into production. Both of these oil fields are located on shelf structures nearer to the Western Australia coast.

Geological characteristics similar to those hosting producible oil may be present in neighbouring shelf regions, including this project research area.

Table 2.3 summarises Canning Basin commercial production as of 1993. A common feature is that all the producing fields are relatively small; remarkable given the large size of the basin. This leads to questions such as; (1) is the relatively small commercial production related to a deficiency in exploration, or; (2) is this an indication that one (or some) of the basin petroleum systems (i.e. either the Larapintine L2, L3 and L4 or Gondwannan G1 or G2 systems) have properties that are not optimally performing to enable the generation, migration or preservation of hydrocarbons?

Refer to Cadman et al. (1993) for a compilation of production data on the fields shown in Table 2.3.

Field	Initial Recoverable Reserves (P90) MMSTB	Remaining Recoverable Reserves (P90) MMSTB
Blina	2.059	0.673
Boundary	0.017	0.006
Lloyd	0.143	0.006
Sundown	0.303	0.101
West Terrace	0.154	0.006
West Kora	0.024	(TSTM)

Table 2.3. Production within the Canning Basin as of 1993 (Cadman et al. 1993)

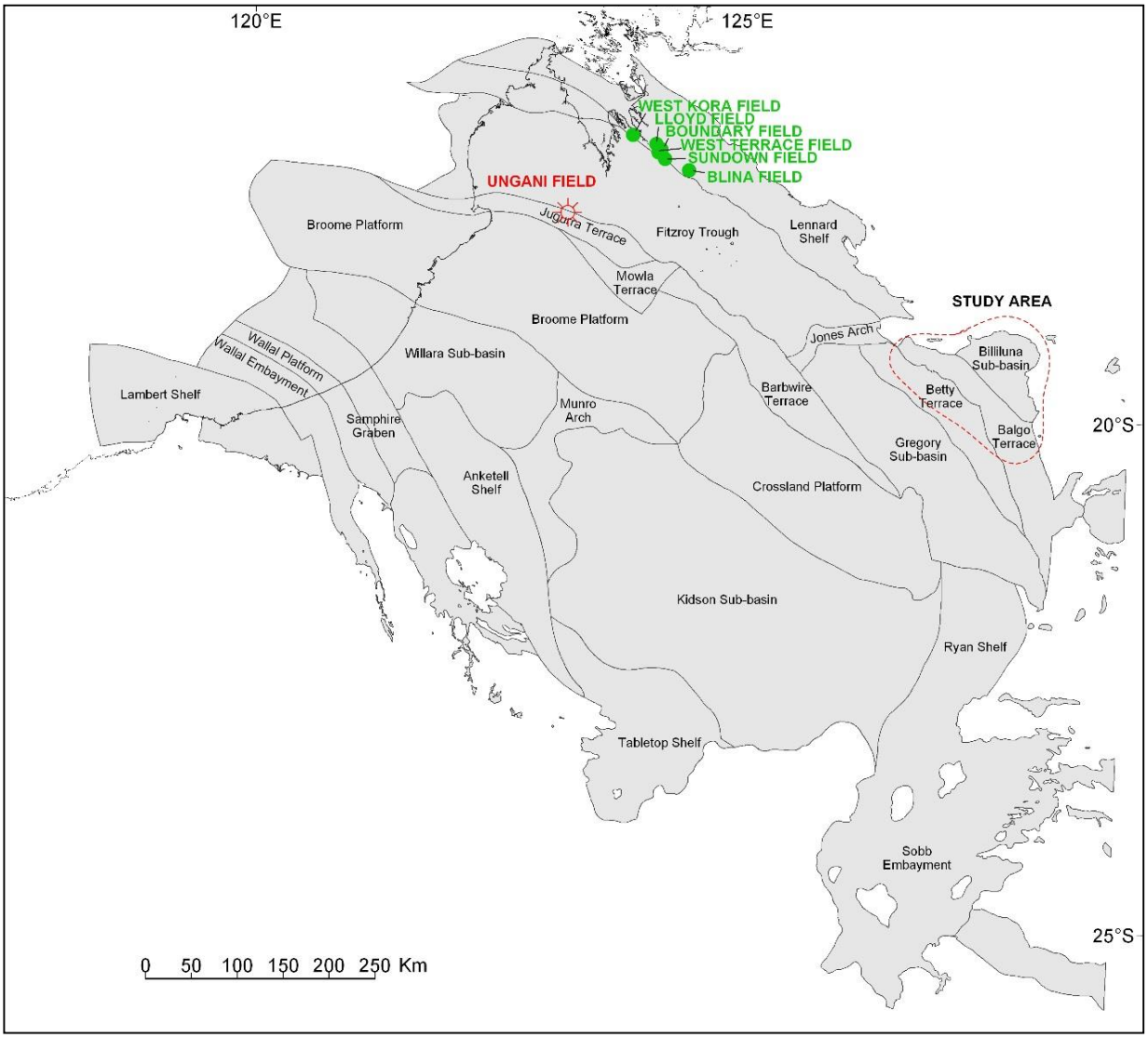

Figure 2.8. Regional production in the Canning Basin

3. Data Availability and Quality

Data for this project was obtained from the Geological Survey of Western Australia (GSWA). Data was accessed using the GSWA's online Petroleum and Geothermal Information library (WAPIMS). The data available for this project consisted generally of publicly accessible open-file information. With the exception of reprocessing that was applied to open-file 2D seismic, all other hard information used in the project is not proprietary to any organisation.

3.1 Well Data

Nine open-file petroleum exploration wells were used for this project. These wells are termed "study area wells" as they provide direct exploration tests within the study area. The study area wells are summarised in Table 3.1. Other regional petroleum wells that are also open-file were consulted for use of their geochemical data, and applied to the evaluation of source rock richness and maturity in later chapters. This was necessary as the study area wells did not penetrate stratigraphy deep enough to allow proper evaluation, nor did they contain enough geochemical information within the sections that they did intersect. Further, as this is a regional project, regional data sources are required to assess regional trends and the use of these wells will facilitate a regional investigation. Table 3.1 and Figure 3.2 illustrate the location of wells used for this project. The reader is referred to the Appendix A, C and D for a detailed disclosure of all well related data.

Well	Status	Total Depth	Completed	Data measurements			Summary and additional information
				TOC	RockEval Pyrolysis	VR	
Atrax 1	Plugged and Abandoned	786.0	15/7/1984	51	13	0	Full well completion report (WCR), Digital geophysical logs
Bindi 1	Plugged and Abandoned	2507.0	14/8/1984	19	14	7	Full well completion report (WCR), Digital geophysical logs
Kilang Kilang 1	Plugged and Abandoned	2300.0	03/12/1984	108	40	21	Full well completion report (WCR), Digital geophysical logs
Lake Betty 1	Plugged and Abandoned	3145.0	15/12/1971	141	39	15	Full well completion report (WCR), Digital geophysical logs
Lanagan 1	Plugged and Abandoned	1530.0	21/9/2008	0	0	0	Full well completion report (WCR), Digital geophysical logs
Lawford 1 (and Lawford 1 reentry)	Plugged and Abandoned	2698.0	27/10/2011	0	0	0	Full well completion report (WCR), Digital geophysical logs
Ngalti 1	Plugged and Abandoned	2758.0	17/10/1984	123	11	0	Full well completion report (WCR), Digital geophysical logs
Olios 1	Plugged and Abandoned	1963.0	02/11/1983	105	15	27	Full well completion report (WCR), Digital geophysical logs
Selenops 1	Plugged and Abandoned	1263.0	04/8/1984	85	3	0	Full well completion report (WCR), Digital geophysical logs

Table 3.1. Summary of the nine study area wells used in this project.

3.2 Well Data Quality

Before utilising the well data for this project, hard data measurements were screened for quality assurance. This was achieved numerous ways:

a) As a starting point, Well Completion Reports (WCR) that were obtained from the GSWA were checked for their completeness. This meant browsing through the reports to confirm that all of the reporting data types (i.e. WCR chapters, digital log data and paper log copies, appendices and attachments) were obtained from the GSWA when requested.
b) Well locations were converted from their native (original and reported) datum into the current Geodetic Datum of Australia (1994) projection. The converted locations were then loaded into Google Earth (satellite image viewing software) and referenced to nearby physiographic features reported for each well (for example road access, property fence lines, etc.) to ensure that the location of the well is correct with respect to current mapping projection systems. This was an important step because well locations need to be accurate when performing well-to-seismic ties in later stages of this project. Generally, most of the wells were noted to lie in the correct area, however some of the wells were given an updated location based on WCR surveyors' notes. The wells that were shifted from the datum-converted location are noted in Figure 3.2, along with comments.

WELL NAME	REPORTED LOCATION (CONVERTED TO GDA94, MGA z51S)					REVISED LOCATION (GDA94, MGA z51S)		COMMENTS
	Seismic profile	Latitude	Longitude	Easting	Northing	Rev Easting	Rev Northing	Google Earth location
Atrax 1	82GE31 VP1025	19° 24' 05.49188" S	126° 36' 18.23851" E	248486.775 m E	7852996.793 m S	249015.00 m E	7852827.00 m S	Well surveyed, though possible access track and pad visible 545m towards ESE, Need to QC with seismic to confirm
Bindi 1	82C1 SP344	19° 43' 14.81535" S	126° 48' 01.50719" E	269465.288 m E	7817922.76 m S	269465.288 m E	7817922.76 m S	Converted location is good
Kilang Kilang 1	RB81-6	20° 12' 41.93338" S	127° 07' 41.54882" E	304437.132 m E	7763993.515 m S	304422.27 m E	7763993.53 m S	GDA94 location is correct, visual pad disturbance
Lake Betty 1	"Godfrey K" SP42 (82GE34 for synthetic)	19° 34' 02.95169" S	126° 19' 49.53925" E	219914.846 m E	7834193.031 m S	220258.00 m E	7834192.00 m S	Visible well pad disturbance
Lanagan 1		19° 35' 00" S	126° 25' 36" E	230173.742 m E	7832750.408 m S	230043.00 m E	7832593.00 m S	Recent well - should be in correct position, but Google earth images pre-dates WCR date. Location lies on seismic line. Use WCR converted location
Ngalti 1	RB82-31 SP580	19° 52' 02.66036" S	127° 18' 50.51775" E	323472.083 m E	7802308.642 m S	323472.083 m E	7802308.642 m S	Well surveyed "144.0m>255 deg WSW of Dopper Stn"
Olios 1	83GN15A VP240	19° 30' 15.19105" S	126° 47' 34.75023" E	268375.83 m E	7841890.262 m S	268329.47 m E	7841877.80 m S	Converted location is good, small adjustment
Lawford 1	S87L-08 SP 534	19° 59' 38.8" S	126° 37' 51.3" E	252115 m E	7787570 m S	252115 m E	7787570 m S	Recent well. Location is good.
Selenops 1	82GE31 VP1369	19° 24' 50.14033" S	126° 43' 05.52977" E	260391.471 m E	7851784.825 m S	260446.00 m E	7851654.00 m S	Using QC'd navigation locations (+/- 40m) the well sits nearer WCR location. At this location can see dark grey possible well pad area. Adopt this location as it sits on correct VP

Table 3.2. Quality control applied to study area wells

c) Geophysical logs from each well were inspected to draw attention to any acquisition and recording matters that are pertinent to further interpretations. The principal inspection was carried out on the Caliper log for every well (Figure 3.1). It was noted that well bore rugosity was a common feature in most of the core study wells. It is important to note the presence of these imperfections because this can affect accurate recording of other geophysical tools. Refer to Chapter 5.5.2 for further comments. It was found, that although well bore rugosity was prevalent during drilling of the study area wells, rugosity did not seem to have a significant negative impact on the affected well Density (RHOB) and Porosity/Sonic (DT) tools, and successful well-to-seismic ties were achievable as a result (Chapter 5.2.2).

d) The GSWA provide open-file well bore measurements in a compilation (excel format). The compilation contains a large variety of data, including an archive of geochemistry (TOC measurements, Rock-Eval Pyrolysis measurements) and petrophysical properties (porosity and permeability), amongst many other data types. These databases were found to be very useful as a starting point for this project. The data summaries were screened for accuracy, by browsing through WCR records and other existing data acquisition reports for the original numerical forms. This was found to be a particularly important step in quality assurance because on occasion some numbers had been incorrectly entered into the database. This screening process was also useful for familiarisation with the availability of well bore data.

Once a diligent quality assurance process was completed, well data was extracted from GSWA archives and partitioned into more user friendly excel spreadsheets for future examination. For example, separate documents were created for data type availability, well summaries, geochemistry, petrophysical data, etc.

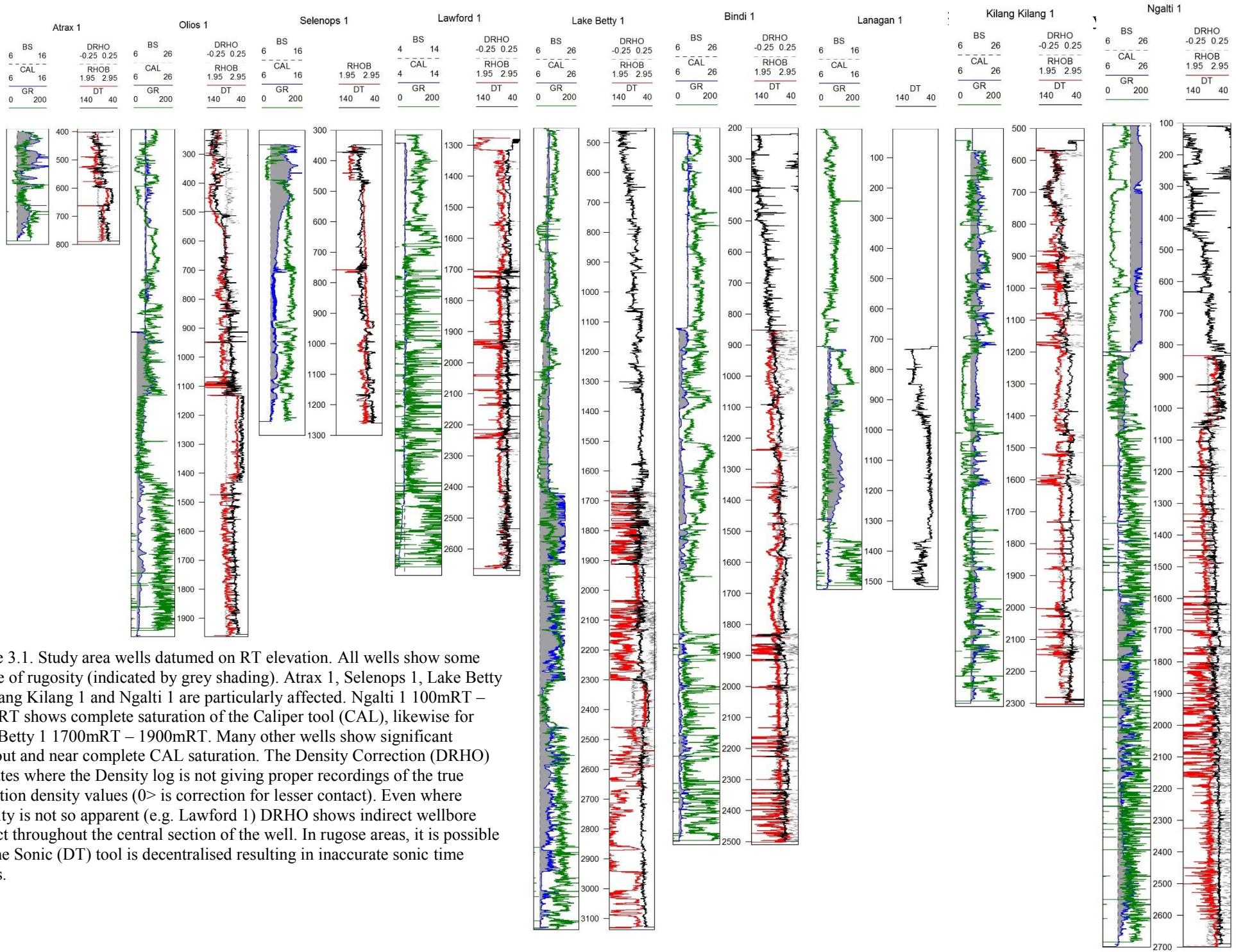

Figure 3.1. Study area wells datumed on RT elevation. All wells show some degree of rugosity (indicated by grey shading). Atrax 1, Selenops 1, Lake Betty 1, Kilang Kilang 1 and Ngalti 1 are particularly affected. Ngalti 1 100mRT – 800mRT shows complete saturation of the Caliper tool (CAL), likewise for Lake Betty 1 1700mRT – 1900mRT. Many other wells show significant washout and near complete CAL saturation. The Density Correction (DRHO) indicates where the Density log is not giving proper recordings of the true formation density values (0> is correction for lesser contact). Even where rugosity is not so apparent (e.g. Lawford 1) DRHO shows indirect wellbore contact throughout the central section of the well. In rugose areas, it is possible that the Sonic (DT) tool is decentralised resulting in inaccurate sonic time values.

3.3 Seismic Data

The study area is covered by a reasonable selection of 2D reflection seismology data. The data was obtained from the GSWA online archives (WAPIMS) in SEGY format and loaded into IHS Kingdom for interpretation. All of the publicly available 2D reflection seismic data was freely available for this project. An example of the data as it was initially obtained is shown in Figure 3.3. Table 3.3 summarises the surveys that were used in this project.

SURVEY	LINE ABBREVIATION	YEAR
Betty Terrace SS	81C	1981
Mt Bannerman 1982 SS	82GN, 82GE	1982
Billiluna SS	RB81	1981
Bloodwood 1982 SS	RB82	1982
White Hills SS	80WH	1981
Samphire Terrace SS	81B	1981
Roberts Range SS	81RR	1981
Doman SS	82C	1982
Lake Havern SS	82LH	1982
Lake Doman SS	82LD	1982
Ryan High Regional SS	86RH	1986
Pinbilly SS	A-79	1979
Barbwire Range Semi-Detail SS	BR65	1965
Orange Pool SS	BV93	1993
Barbwire Terrace SS	C72	1972
Meda 1982 SS	H82	1982
Nibil SS	NIB86	1986
Sturt SS	PS85	1985
Anna Plains SS	S84	1984
Lake McLernon SS	S85	1985
Willara SS	S87	1987
Lawford SS	S87L	1987
Great Sandy SS	S98C	1998

Table 3.3. Seismic surveys utilised in this project.

3.3.1 *Improvements to Seismic Data*

It was anticipated that interpreting the publicly available grid in its original form would be relatively difficult. Figure 3.3 demonstrates the quality of original seismic acquisition processing. It was determined by Pangaea that 120 seismic lines were to be reprocessed to aid in the evaluation of their exploration acreage STP-EPA-0030 and STP-EPA-0031. A total of 4,707 line km was reprocessed in this workflow. Pangaea selected which lines to reprocess based on the expected improvement the 2D line would have compared to its original image. All of the reprocessed lines were made available for use in this project. Figure 3.3 demonstrates an example of the improvement to a significant regional seismic line within the study area. The general improvement is dramatic. Figure 3.2 illustrates the distribution of the seismic grid that was interpreted as part of this project. Further examples of the quality of the seismic reprocessing is shown throughout chapters 5 and 6.

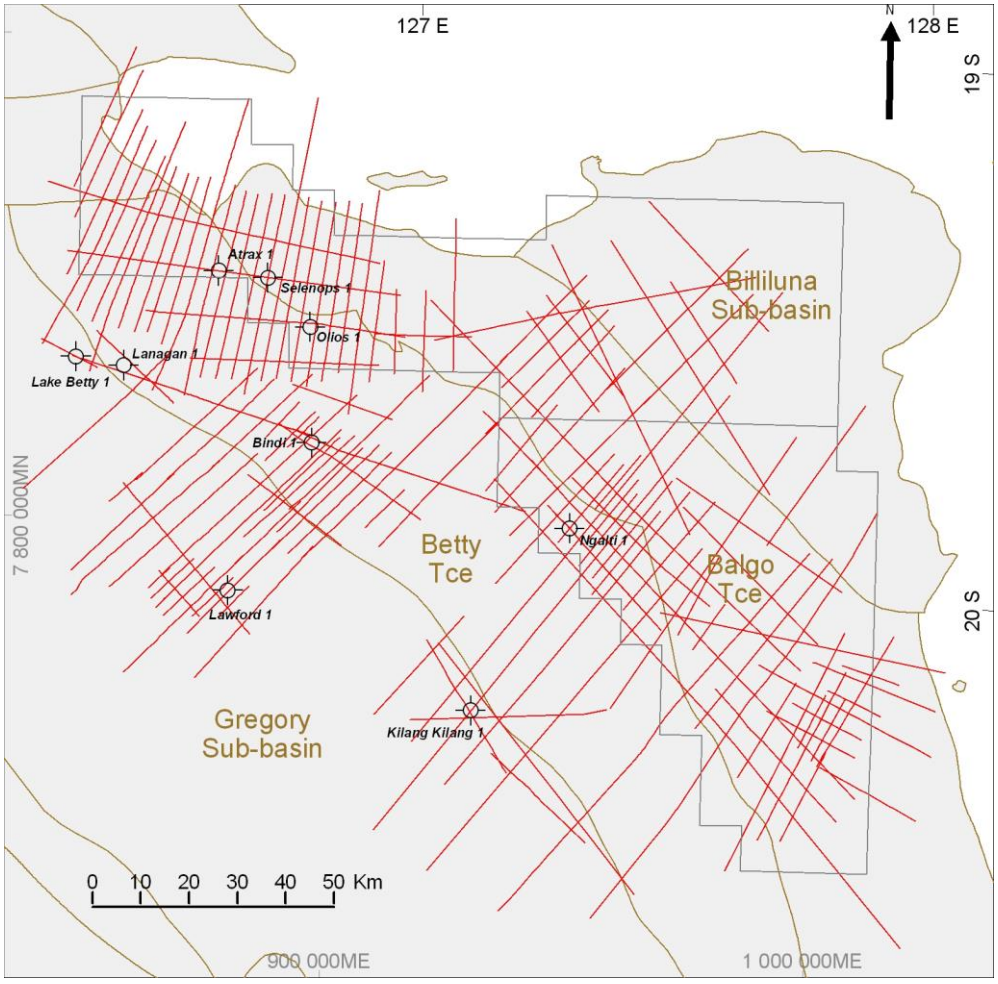

Figure 3.2. Seismic grid and well locations.

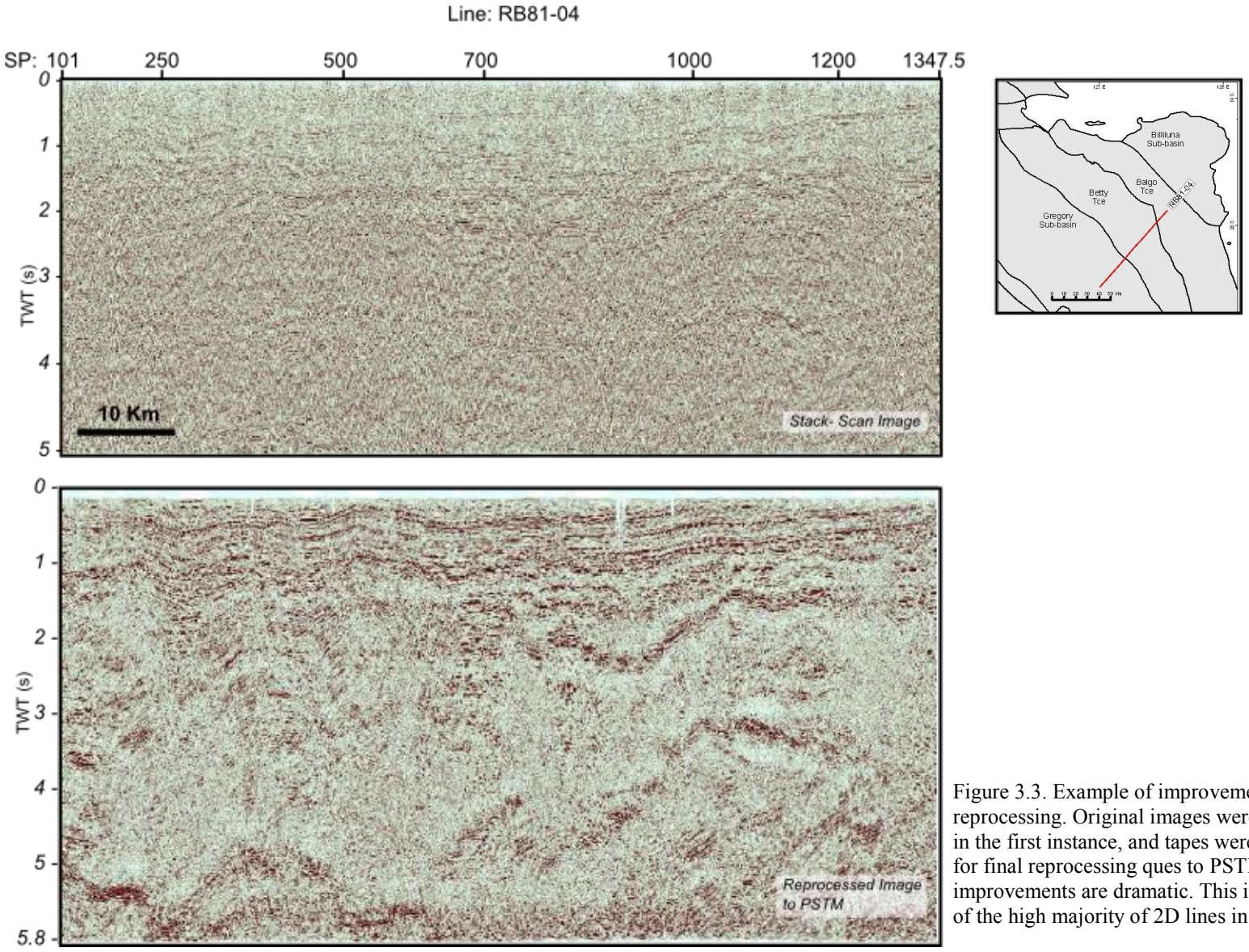

Figure 3.3. Example of improvements to seismic data post-reprocessing. Original images were scanned from data tape (top) in the first instance, and tapes were sent to reprocessing houses for final reprocessing ques to PSTM (bottom). Resulting improvements are dramatic. This improvement is representative of the high majority of 2D lines in this dataset.

It is noted that the seismic reprocessing, although exploited in the project, is not a material component of the research, and so the data is taken on board from an interpretation point of view. None of the reprocessing workflow formed part of this research project. The data, once received from the reprocessing house, was simply loaded into IHS Kingdom interpretation software and interpretations are based on the newly reprocessed seismic. Due to the poor quality of the original seismic processing, the majority of the original seismic grid was not utilised in this project. An exception to this is that in a small number of places the original processed version of a 2D line was the only version available (because the line was not reprocessed along with the other surveys), and to aid in loop ties. The only option was to refer to the original line.

3.3.2 *Seismic Data Quality*

The seismic grid utilised in project, shown in Figure 3.2 and summarised in Table 3.3, is generally 1980's vintage and has poor visual quality (in its' un-reprocessed and publicly available form). Most reflection events are subtle, and the data is generally noisy. As a result of the reprocessing, overall seismic imaging of the study area was improved. The key difference for the purposes of this project are the clearer reflection events of regional features (for example the Meda Transpression unconformity – Chapter 5.3.1). The selected mapping events, shown in Table 5.3, were strikingly more distinct when using the reprocessed grid. Events such as the Meda Transpression Unconformity, the Near Top Ordovician marker and Near Top Basement marker were generally easier to map with the reprocessed seismic. The Meda Transpression and Basement markers are far more difficult to map on un-reprocessed seismic, because the reflector terminations used to identify the correct position of the horizons are surrounded by low amplitude, noisy reflection events.

Spatially, the seismic grid over the study area adequately enables the interpreter to characterise the tectonic regions in question. The only minor problem with the grid layout, is that in certain regions there are less seismic lines to resolve loop ties. An example is shown in the centre of Figure 3.4 northwest of Ngalti 1 (19° 39'S, 127° 08'E), where there is a deficiency in seismic coverage (area between red and blue lines, where the blue lines were key lines for a central loop tie). This results in lower confidence in the interpretation because there are lesser available lines to loop tie within the parts of the Bloodwood 1982 and Betty Terrace 1981 surveys northwest of Ngalti 1. Further, correlation was more difficult between the Ngalti 1 and Bindi 1 wells on the east-west oriented 81C (Betty Terrace 1981 SS) line

(lower red line pairs on Figure 3.4). This grid deficiency is again notable in the Billiluna Sub-basin; the seismic model would have been more geologically resolved if line PS85-60 (Sturt 1985 SS) or RB81-7 (Billiluna 1981 SS) allowed intersection with Proterozoic outcrop to the North East of the basin. The red highlighted lines in Figure 3.4 were found to be key in regionally correlating between the northwest and southeast project areas.

Conclusively, reprocessed seismic imaging is generally good across the whole of the study area and seismic imaging of major faults is clear. This is assisted by strong reflection events at the Near Top Laurel Carbonate marker due to its high reflection coefficient contrast at the event and below the event into the Knobby Sandstone level. Another Intra-Devonian reflection event (which was not chosen for mapping in this project) aids the interpreter in relative positioning within the seismic section, and provides several “train track” events to juxtapose across faults. Seismic imaging of minor faults is adequate for the purposes of this research project.

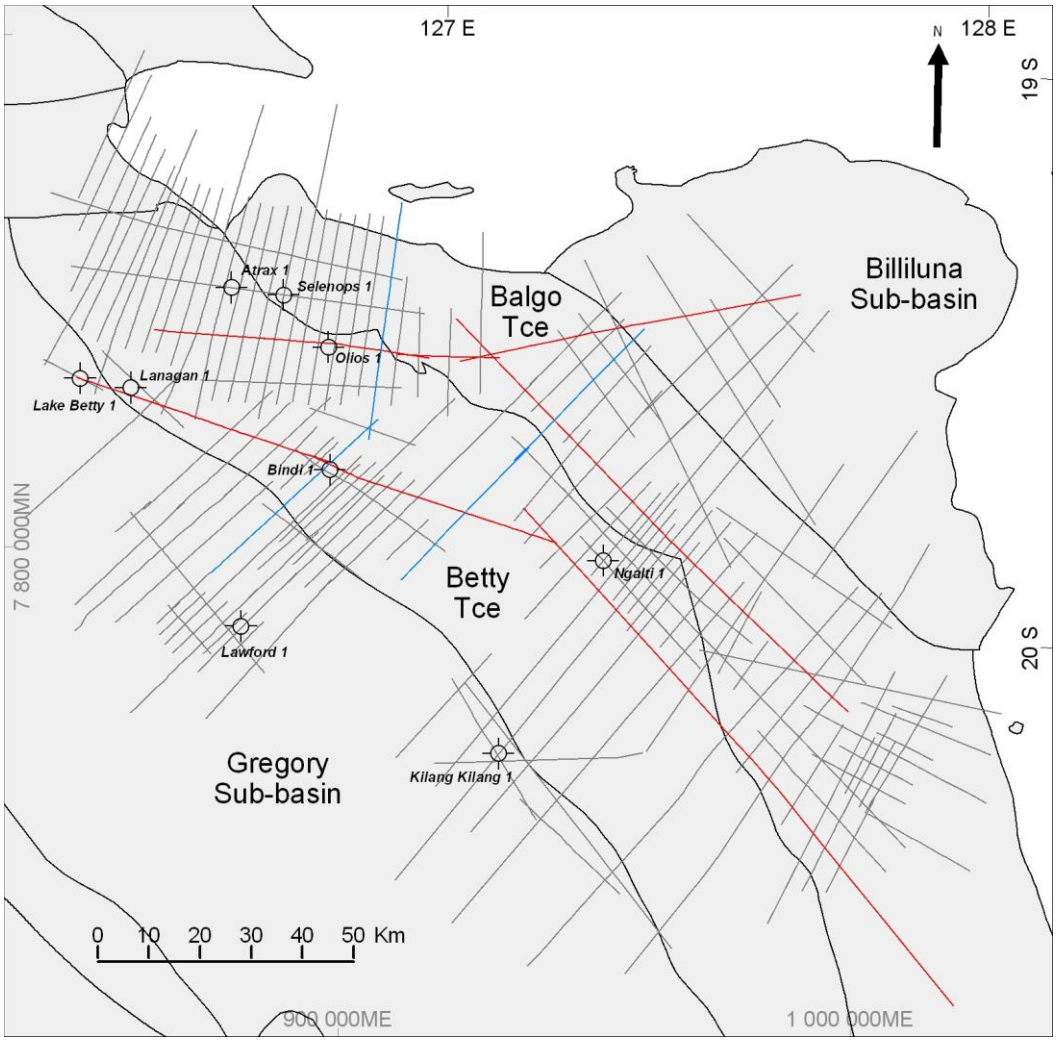

Figure 3.4. Seismic grid with key regional lines (red) and key lines for central area loop tie (blue). More seismic within the central 'pentagon' area would have enabled a more confident loop tie in seismic interpretation.

4. Stratigraphic Framework

The Canning Basin is presently filled with sedimentary rocks of Ordovician to Cretaceous age. The objective for this Chapter is to produce a meaningful stratigraphic framework of regionally extensive stratigraphy that is identifiable from Geophysical Log Characteristics. The framework will then be discussed in terms of a regional setting and inferences for hydrocarbon prospectivity for the study area.

This Chapter also discusses results of Isochron (TWT thickness) maps derived from seismic interpretation (Chapters 5 and 6), because isochrons inform of stratigraphic spatial variability that cannot be derived from well correlations alone. This Chapter (Chapter 4) is prior to seismic (Chapters 5 and 6) to comprehensively introduce the reader to the stratigraphy. Well correlation cross sections (Figure 4.44 to Figure 4.46) are available at the end of this Chapter. Isochron maps (Figure 6.19 to 6.25) are available at the end of Chapter 6.

Pre-Cambrian, Cambrian, Ordovician and Silurian aged rocks are not penetrated by wells within the project area so their existence is considered where the limits of the seismic and published literature will allow. It remains possible that older sequences exist at depths within the study area that are potentially prospective for hydrocarbons, however conclusions can only be drawn as a function of the seismic and well data at hand.

Inferences for older rocks are derived from two wells (Percival 1 and Lake Havern 1, Figure 4.1). Text concerning deeper stratigraphy will be general in nature. Stratigraphy with good well intersections (i.e. where better well coverage and well data exists) allow a more detailed, hierarchical discussion to convey a characterization of regional setting and relationships; and identify potential petroleum system reservoirs and sealing intervals.

Most of the information within this section was ultimately derived from WCR files (discussed in Chapter 2). GSWA provided a tabled summary of regional reservoir quality data. Geophysical logs were loaded into Rockware Logplot 7 for editing and presentation in this study. Core data is scarce within the project area and surrounds, particularly to enable a quantifiable characterization of sealing capacity, so deductions from cuttings lithology and geophysical log characteristics are all that is available to the interpreter.

4.1 Pre-Ordovician

4.1.1 *Precambrian*

Surface geological maps show Precambrian rocks outcropping along the northeastern basin margin, and belonging to the Halls Creek Province (Figure 2.2). They are of Archaean to Early Proterozoic age. The Pre Cambrian section dips to the west under the project area, the top of which is represented by a steeply dipping angular unconformity under Paleozoic strata (mapped as the Near Top Basement horizon on 2D Seismic, Figure 5.7). Klappa et al. (1985) noted similar Proterozoic sequences in the Amadeus Basin that are hydrocarbon bearing (for example the Neoproterozoic Heavitree Quartzite) and that the sequence in the Canning Basin should not be overlooked in regards to hydrocarbon prospectivity. However, the Precambrian rocks are mostly very deep, commonly exceeding 4 seconds in TWT on 2D seismic. For the purposes of this research project the petroleum systems of the Pre Cambrian are not considered.

4.1.2 *Cambrian*

Rocks of Cambrian age are not known to exist in the sedimentary sequence of the Canning Basin. Some horizontal reflections were noted to occur below the Near Top Basement horizon (Figure 6.7) – these could possibly represent Cambrian strata, but no wells are available to verify this, so for simplicity these ‘intra-basement’ reflections were mapped as Basement.

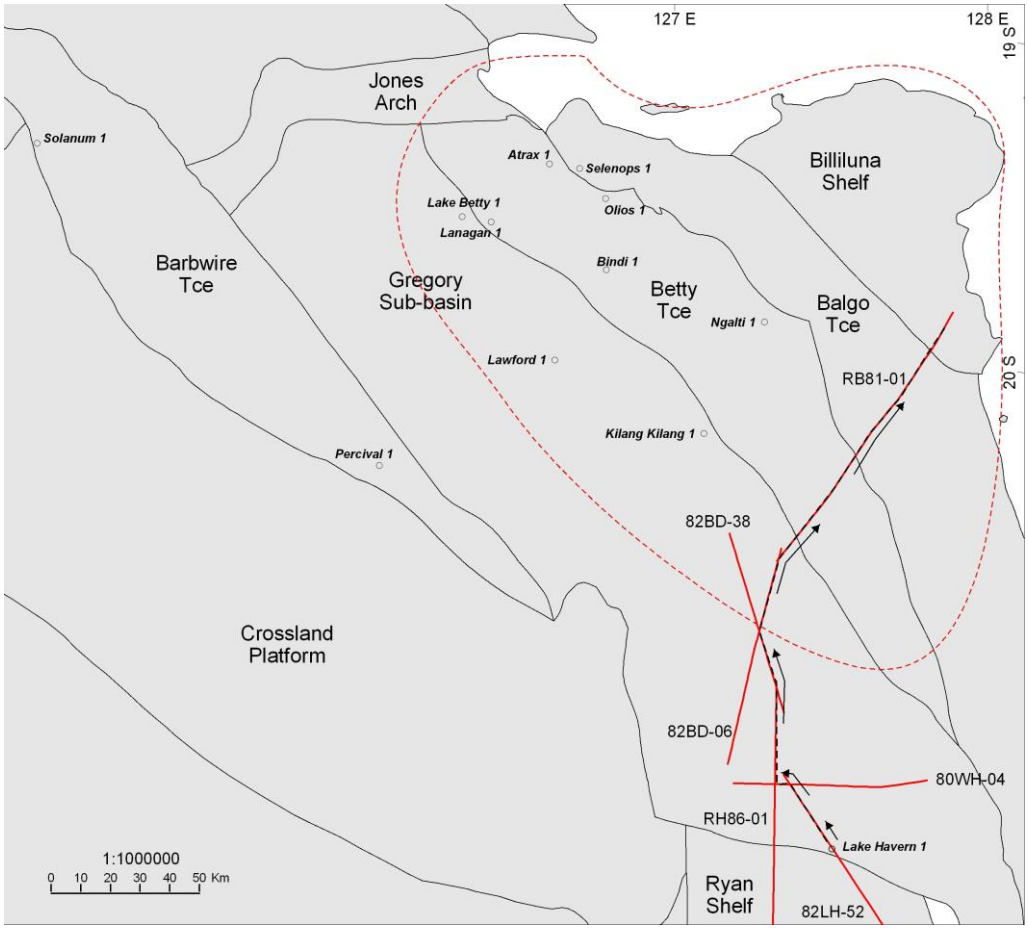

Figure 4.1. Study area in a regional context. Seismic tie to Lake Havern well. Seismic lines (red) show the arbitrary line (black dashed and arrows). Study area circled in red. Interpretation is shown in Figure 5.8.

4.2 Early to Middle Ordovician

Overview

Early to Middle Ordovician rocks in the Northeastern Canning Basin comprise a relatively comfortable succession containing the Early Ordovician Nambeet Formation, Early to Middle Ordovician Willara Formation, Middle Ordovician Goldwyer Formation and Nita Formation (France, 1984). The Ordovician sequence is divided into 5 super-sequences by Kennard et al (1994) and Romine et al (1994) (summarized in Figure 4.2). There are no wells within the study area that intersect Ordovician age sedimentary rocks. The following investigation of regional wells, together with seismic evidence in subsequent Chapters, provides some confidence that an Ordovician package is present within the Billiluna Sub-basin, Balgo and Betty Terraces, however the study area may sit in a paleogeographic setting that discourages the accommodation of shale lithologies.

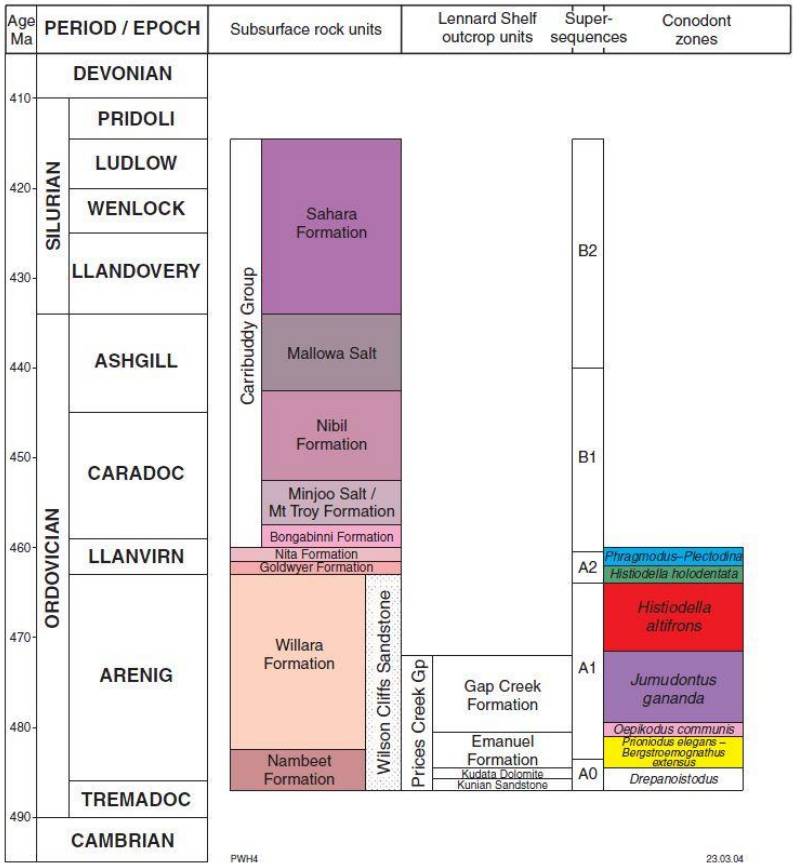

Figure 4.2. Stratigraphic column of Ordovician and Silurian stratigraphy (Modified after Haines, 2007)

Percival 1 (Figure 4.3) - drilled on the Barbwire Terrace (on the southwestern flank of the Gregory Sub-basin); and Lake Havern 1 (Figure 4.5) – drilled on the northern edge of the Ryan Shelf, are the two nearest wells to intersect a portion of preserved Ordovician stratigraphy. Percival 1 intersected a sequence that is most readily correlatable to regional Ordovician markers, whereas Lake Havern 1 intersected a sequence of Ordovician rocks that appear to be of different paleogeographic origin.

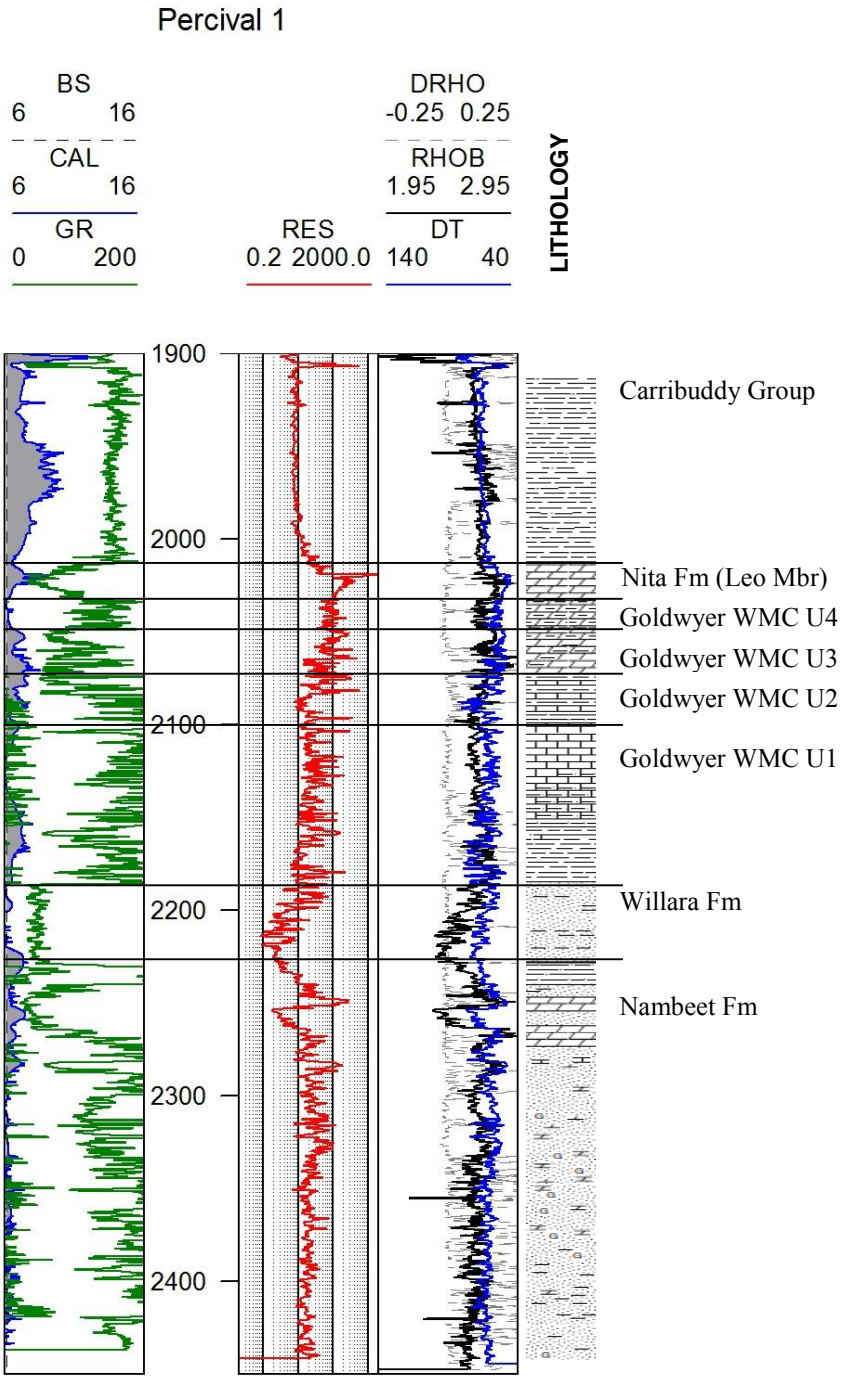

Figure 4.3. Percival 1 geophysical log. Lithology indicated on right (modified after France, 1984).

4.2.1 *Nambeet Formation*

Characteristics

The Early Ordovician (Tremadocian) fluvial to marginal marine Nambeet formation is described at Percival 1 primarily as an orthoquartzitic medium grained well-sorted sandstone with dolomite and shale banding, capped by interbedded dolomite, blackish fissile shale and argillaceous fissile siltstone (France, 1984).

Geophysical Log Characteristics

The top of the formation is marked by a spike in the gamma ray log underneath a blocky Willara Formation sandstone (Figure 4.3). The Orthoquartzitic section of the Nambeet Formation shows a generally homogenous resistivity log, sonic log and high gamma ray values (increasing gamma ray trend towards the base of the formation). The density log shows generally high values reflecting the dolomitic and indurated characteristics of the formation.

The Nambeet Formation does not directly correlate to wells within the study area, and a regional seismic tie (encapsulated within the Goldwyer Formation correlation and Figure 5.8) to Lake Havern 1 is the only indication that the interval exists within the project area.

4.2.2 *Willara Formation*

Characteristics and Geophysical Log Characteristics

The Early to Middle Ordovician (Arenig to Llanvirn) Willara Formation at Percival 1 is a relatively homogenous sandstone unit, described predominately as fine grained, moderately well-sorted and massive in character (France, 1984). As such, the gamma ray response of the interval is clean and blocky. Logs show low resistivity and density values and the unit is relatively slow on the sonic log compared to intervals above and below.

The Willara Formation does not directly correlate to wells within the study area, and a regional seismic tie (encapsulated within the Goldwyer Formation correlation and Figure 5.8) via Lake Havern 1 is the only indication that the interval may exist within the study area.

4.2.3 *Goldwyer Formation*

Overview

The Middle Ordovician (Llanvirn) Goldwyer Formation is separated into four stratigraphic subunits, Unit 1 to Unit 4 (oldest to youngest). Recent workers Kennard et al. (1994) utilized wireline log data, whole core and relations to regional tectonic events to subdivide the Formation. Kennard et al's recent work generally correlates to earlier subdivisions proposed by Western Mining Corporation (WMC, operators of the Percival 1 well), though Goldwyer Formation relationships were originally thought to be restricted to the Mowla Terrace and Broome Platform (close to the West Australian seaboard). Associations have recently (experimentally) been made to further regions in the northwest (Admiral Bay, Willara Sub-basin, etc.) utilizing the earlier subdivisions of WMC (Haines, 2004) because of their simple definition. The same WMC subdivisions are carried here.

Goldwyer Formation Type Section

Kennard et al. (1994) proposed a type section for the Goldwyer Formation at Solanum 1 on the Barbwire Terrace between 283 mRT to 563 mRT. The type section is shown in Figure 4.4, along with the preserved section at Percival 1.

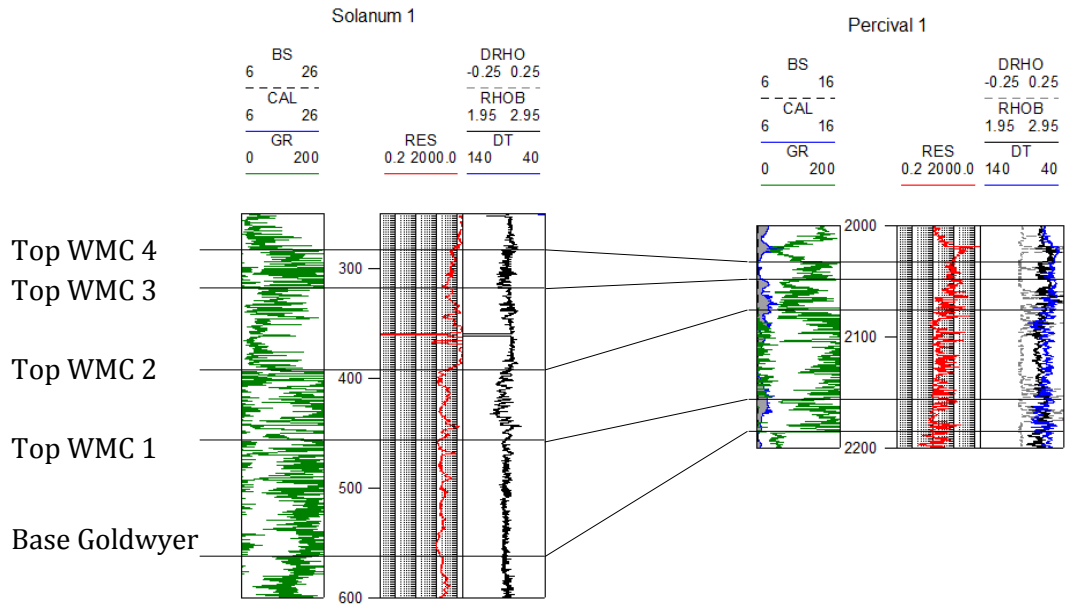

Figure 4.4. Solanum 1 (left) and Percival 1 (right) show Goldwyer Formation correlation (modified after France, 1984; France and Scibiorski, 1984).

Unit Division at Percival 1: Characteristics and Geophysical Log Characteristics

Unit 1

Percival 1 (Figure 4.3) intersected a mostly complete section of the Middle Ordovician Goldwyer Formation, with a gross thickness of 153 metres. The basal unit (Unit 1) comprises soft dark grey calcareous sub-fissile micromicaceous shale capped by interbedded dark grey argillaceous siltstone, dolomitic limestone and grey sucrosic dolomite (France, 1984). Geophysical logs over Unit 1 show a consistently hot gamma ray response, invariable mid-range resistivity and homogeneous sonic log. The density log increases over the lower part of the package representing the change from limestone to argillaceous siltstone. Unit 1 is 86 metres thick at Percival 1.

Unit 2

Unit 2 of the Goldwyer formation is observed as interbedded blackish firm fissile shales, with firm argillaceous pyritic siltstone and microcrystalline limestones (France, 1984). Unit 2 is characterized by an invariably fast sonic log, decreasing density log with increasing depth and marked increasingly hot trend in the gamma ray log response with depth, showing a blocky character. Goldwyer Formation Unit 1 is separated from Unit 2 by a hotter and blockier gamma ray log response (where Unit 2 shows a decreasing upwards GR trend). Unit 2 is 16 metres thick at Percival 1.

Unit 3

Unit 3 is observed as interbedded black infrequently carbonaceous shales, microcrystalline to sucrosic dolomite and massive microcrystalline limestone (increasing dolomite towards base) (France, 1984). Geophysical logs over the interval reflect these lithologies, showing marked increases in sonic transit times (increases at base) and generally lower gamma ray (with spikes over the carbonaceous shales). The gamma ray shows a subtle overall fining upwards trend. Unit 3 is separated from Unit 2 by a lower gamma ray log response and faster sonic transit times. Unit 3 is 35 metres thick at Percival 1.

Unit 4

The upper-most subdivision (Unit 4), is observed as grey to black finely crystalline argillaceous and carbonaceous dolomite (France, 1984). Unit 4 is observed as an unvarying high-range resistivity and sonic log, and a hot blocky gamma ray log response over the interval. The gamma ray character differentiates Unit 4 from the surrounding intervals. The top of the Goldwyer Formation (uppermost section of Unit 4) is commonly situated below a marked deflection (decrease) in gamma ray resembling a "U" or "V" shape. A similar (though inverted) form can be seen in the resistivity and sonic logs (an inflected response over the same interval), which separates the Nita Formation above. Unit 4 is 16 metres thick at Percival 1.

4.2.4 *Nita Formation*

The Ordovician Nita Formation at Percival 1 is described as finely crystalline and sucrosic Dolomite (France, 1984). Geophysical logs over the interval (Figure 4.3) show a 'characteristic' "U" or "V" shape in the gamma ray log, increases in resistivity, density and sonic logs that represent the tight and dense dolomite lithology. The Nita Formation is 16 metres thick at Percival 1.

Comparison between Percival 1 and Lake Havern 1: Does an Ordovician package exist within the study area?

Percival 1 geophysical logs were compared to Lake Havern 1 logs. The Lake Havern 1 well was then correlated seismically to the study area.

The Ordovician aged rocks at Lake Havern 1 are not characterized by the same features as at Percival 1. Top of the Ordovician section at Lake Havern 1 (Figure 4.5) is interpreted from logs to be at 1756 mRT. The section is purported to belong to the Goldwyer Formation, and is described as dominantly fine grained sandstone with thin dolomitic fissile shales, claystones and banded dolomite. The section is recorded as an increase in gamma and resistivity logs due to an increase in shale content from the overlying Carribuddy Group at

the well location. The gamma ray over the interval is observed as a "saw tooth" variable and noisy log character. The Nita Formation was not intersected above the Goldwyer Formation at Lake Havern 1.

Below the Goldwyer Formation, Lake Havern 1 intersected 646 metres (1950 mRT to 2296 mRT, described as Ordovician aged "Middle Formation") of fine grained sandstone and minimal thin shales with dolomite, distinguished only from the overlying Goldwyer Formation by a change to a more-so invariable gamma ray and sonic log response below 1950 mRT. This section may belong to the Willara Formation (correlating the cooler blockier gamma ray log response to 2188 mRT to 2230 mRT at Percival 1). Further inspection of the Lake Havern 1 geophysical logs over the "Middle Formation" indicates a basal section (2224 to 2296 mRT) that looks to represent a portion of Nambeet Formation, indicated by a coarsening gamma ray trend, increasing trend in resistivity and increasing shift in density curve responses (that signals an increase in dolomitic content). However, palynology (discussed below) from Lake Havern 1 does not assist with this allocation.

Age Control at Lake Havern 1

In the northeastern portion of the Canning Basin, well intersections of Ordovician aged rocks are limited, and because the described Goldwyer Formation is vastly different between Lake Havern 1 and Percival 1, some doubts are raised about the correct age association of Lake Havern 1's Ordovician aged section. Palynological evidence was sought by the Lake Havern 1 well operator to alleviate these doubts. The identified microspores found below 1756 mRT are reported to be of a 'younger Late Famennian period, though possibly older' (Purcel in Irwin, 1998). The "Middle Ordovician" section identified from logs at 1950 mRT was not age-datable from Palynology evidence, though a lower portion of this "Middle Ordovician" section (at 2291 mRT) was shown to be 'at least of Devonian age' (Purcel in Irwin, 1998), which could also imply the samples tested at these depths are cavings from shallower in the well.

The operator of the tenement commissioned further age dating of this zone by Ostracod and Conodont analysis. The analysis concluded that organic matter and phosphatic fragments found within 2 of the 3 samples at 2200 mRT to 2300 mRT supported an Ordovician age of the sediments (Jones and Niccol in Irwin, 1998), which gives some confidence that the

intersected package belongs somewhere within either the Goldwyer Formation, Willara Formation or Nambeet Formation. It is also possible that all three formations are present and correlation difficulties are due to facies changes.

The conclusion here is that an Ordovician aged package is present at Lake Havern 1.

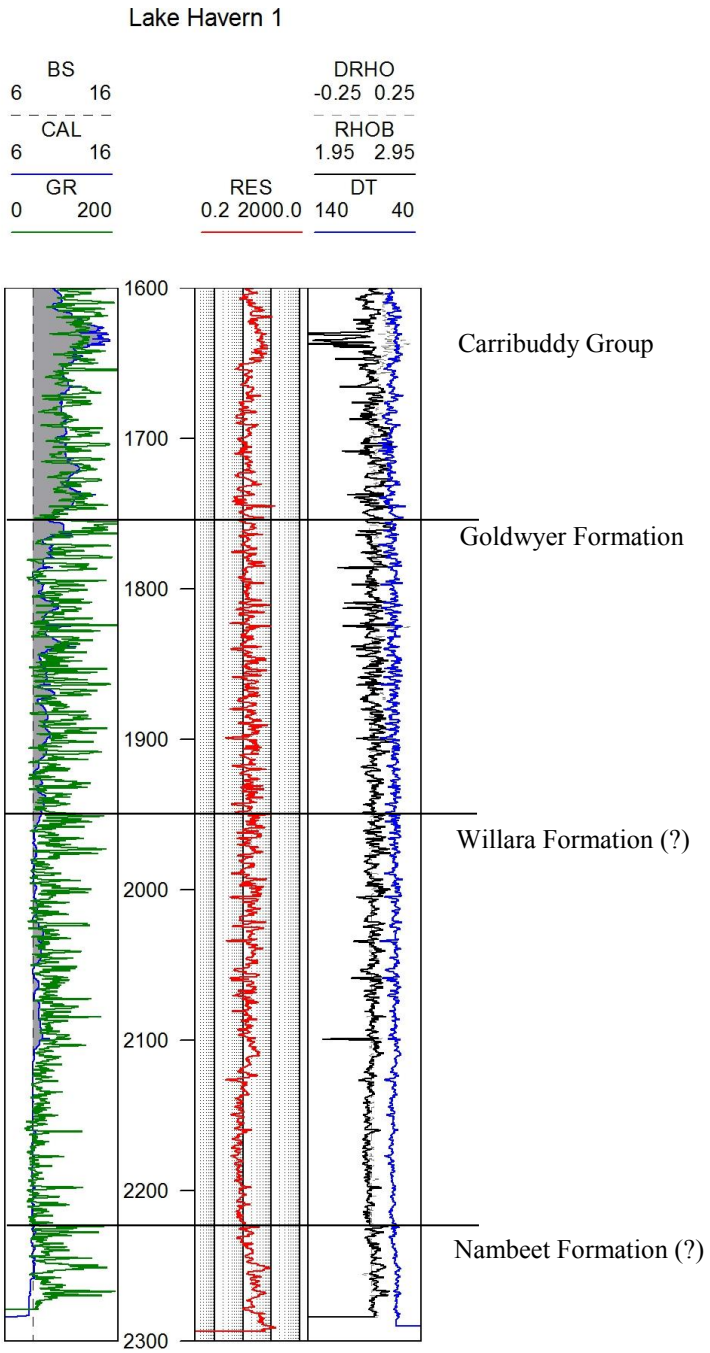

Figure 4.5. Lake Havern 1 geophysical log (modified after Irwin, 1998).

A lack of seismic data precludes the ability to correlate the preserved section from Percival 1 to the study area, however a regional seismic correlation (Figure 4.1 and Figure 5.8) from the project area to Lake Havern 1 shows Ordovician aged rocks to be present on the Balgo and Betty Terraces and within the Billiluna Sub-basin. Correlating the geologic units within the Ordovician package is more difficult due to poor seismic imaging over deeper stratigraphy across the Gregory Sub-basin.

A key question is thus answered; Ordovician aged stratigraphy exists within the project area. Another key question – whether the Goldwyer Formation organic shale is present within the project area; will be considered using paleogeographic reconstructions (discussed below).

Middle Ordovician Depositional Setting

The Lake Havern 1 Ordovician section appears sandier than the preserved section at Percival 1. This is likely because Lake Havern 1 is located nearer to the coastline of the Ordovician Larapintine Seaway (Cook and Totterdell, 1990, Figure 4.6), whereas Percival 1 is likely within the neritic zone. The source of the Ordovician sediments at Lake Havern 1 are perhaps more so derived from a supratidal near shore influence (noted fine grained siliciclastic rocks) rather than shallow marine/intertidal (carbonates) (Figure 4.7). Both Percival 1 and Lake Havern 1 indicate periods of intermittent carbonate deposition, which indicates either paleo-highs or lower base level (relative to marine seaways). The Epeiric Sea present during the Late Arenigien accommodated basinal shales along the developing Fitzroy Graben (Figure 4.7) noting that the extensional tectonic regime present at the time (Haines and Ghori, 2010) facilitated increased rates of accommodation generation due to subsidence. The observations at Percival 1 and particularly Lake Havern 1 portray intersections of low relative base level, where the Ordovician section may be sandier. It is anticipated that the Ordovician section (particularly the Goldwyer Formation) in a more basinal location (to the northwest in Figure 4.7) may contain thicker sections of mud-rich (and possibly more organic) stratigraphy.

Abundant macrofossil fauna identified throughout the Goldwyer Formation at Percival 1 suggest a marine influence on sedimentation (Haines, 2004), where individual subunits of the formation imply varying water depths. The gamma ray log at Percival 1 suggests an overall base level increase from the base to the top of the Formation, where the top of Unit 2 and Unit 4 represent flooding surfaces related to broad deepening and shallowing patterns.

Goldwyer Formations Unit 1 and Unit 2 are interpreted as shallow marine, and Unit 3 and Unit 4 are interpreted as shallow to restricted marine (possibly lacustrine) (France, 1986).

In answering the second key question; it appears that the study area may have experienced a greater (coarse-grained) siliciclastic dominated paleogeographic setting than Percival 1. This means that the Goldwyer Formation lithotypes, if present, are potentially sandy in nature and may lack the organic rich shale lithologies required for a generative source rock for the Larapintine L2 petroleum system.

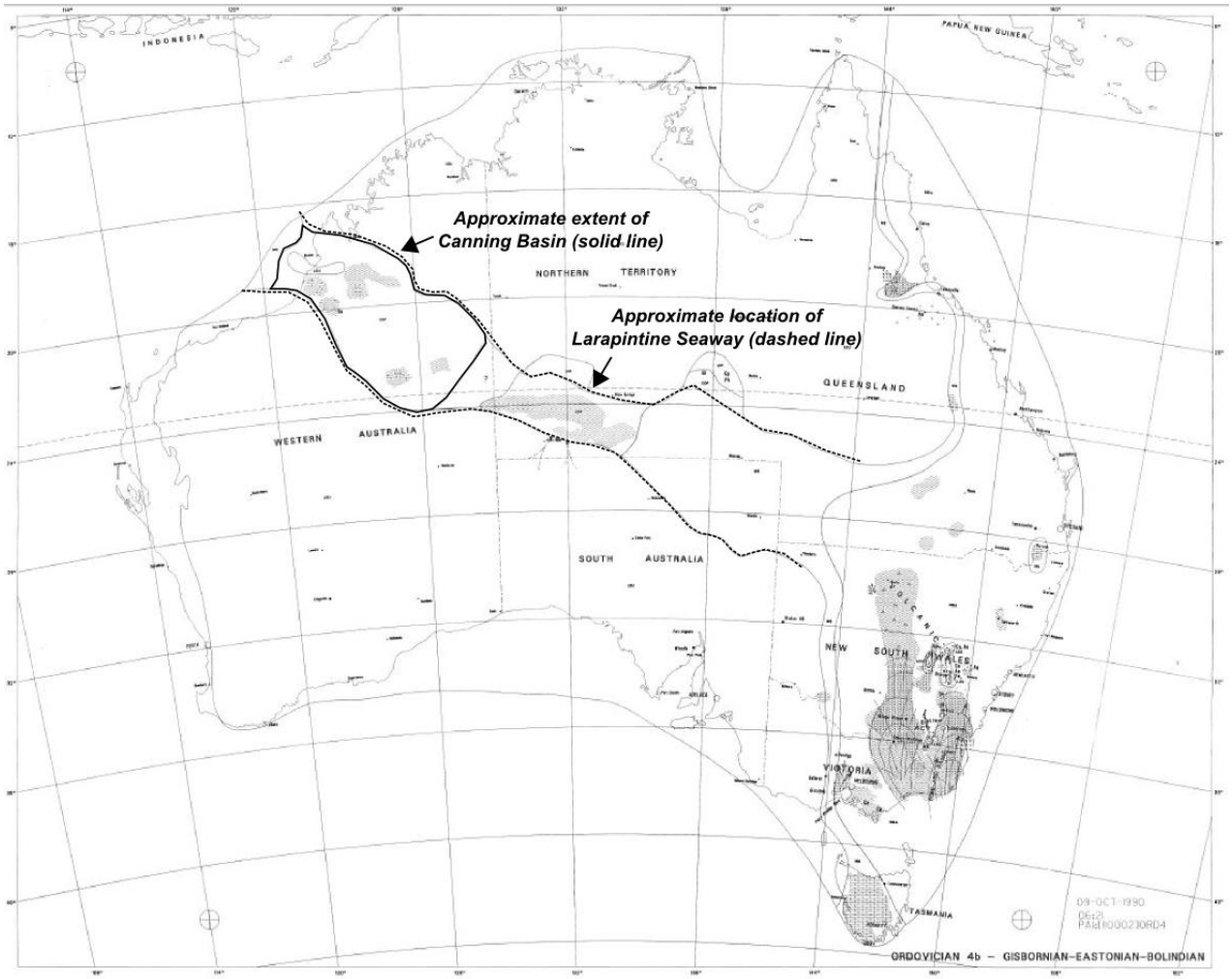

Figure 4.6. Paleogeographic map of the Ordovician (modified after Cook and Totterdell, 1990).

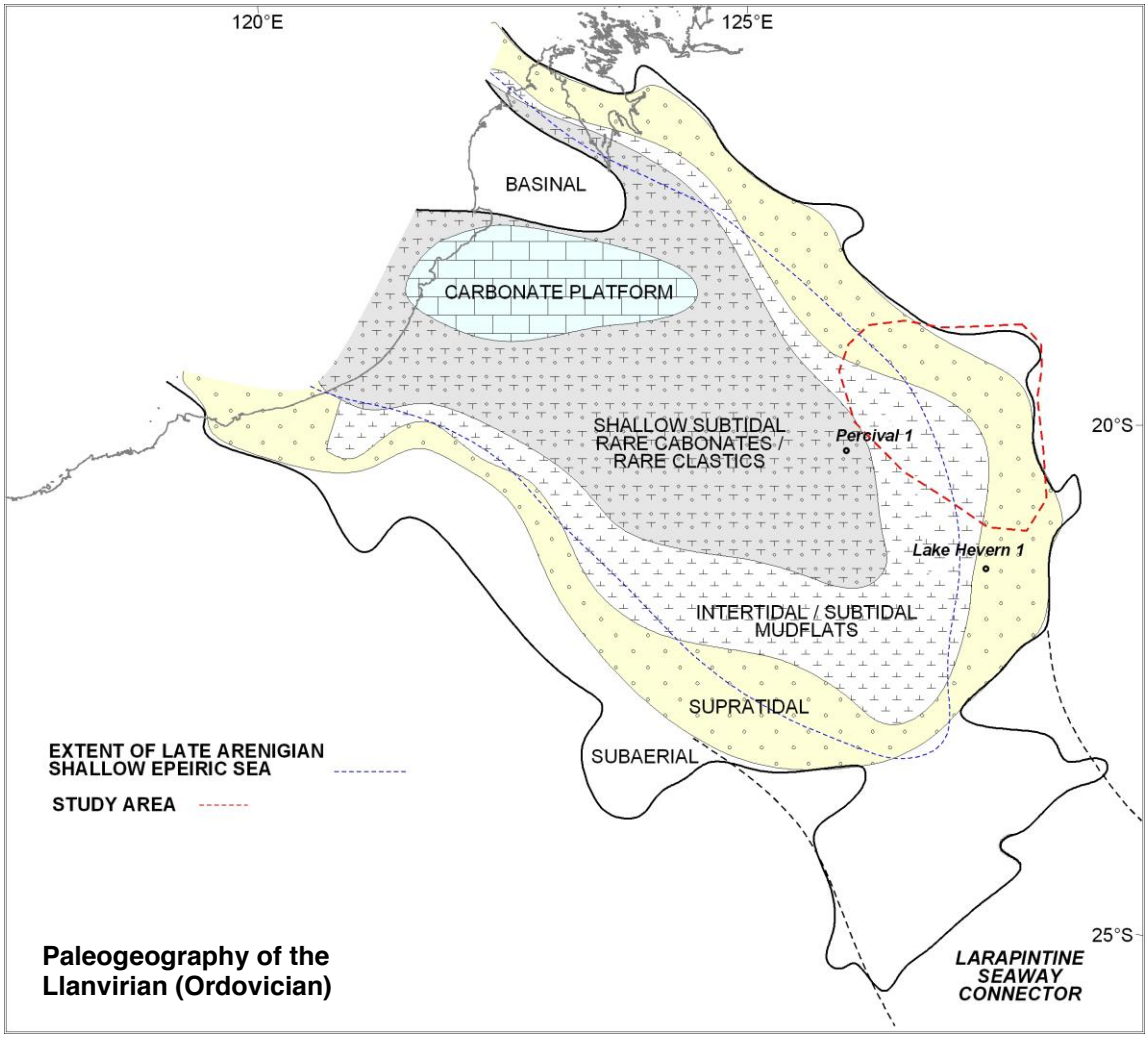

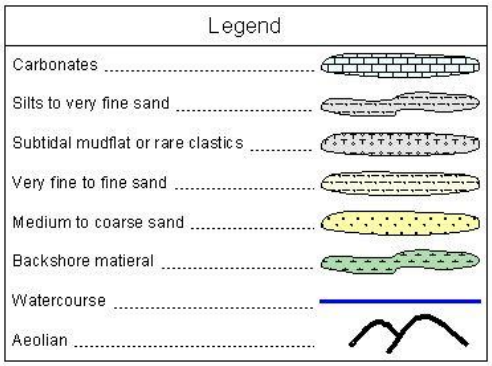

Figure 4.7. Paleogeography of the Llanvirnian. Legend on right applies to all paleogeography maps in this study (modified after Brown, in Purcel 1984)

Reservoir Properties

Reservoir quality data is elusive for Ordovician aged stratigraphy, however some core derived porosity and permeability data was obtained from Percival 1 by the well operator (Figure 4.8). At Percival 1, porosity in the Nita Formation ranges 0.8% to 0.9%, averaging 0.85%. Permeability is reported nil. In the Goldwyer Formation Unit 4 shows porosities of 1.2% to 2.4%, averaging 1.7%, and Unit 3 similarly shows porosities 0.8% to 2.3%,

averaging 1.5%. Permeability is a maximum of 0.01 mD in Unit 4 and a maximum of 0.3 mD in Unit 3. Reservoir property data is not available for the Nambeet Formation or Willara Formation.

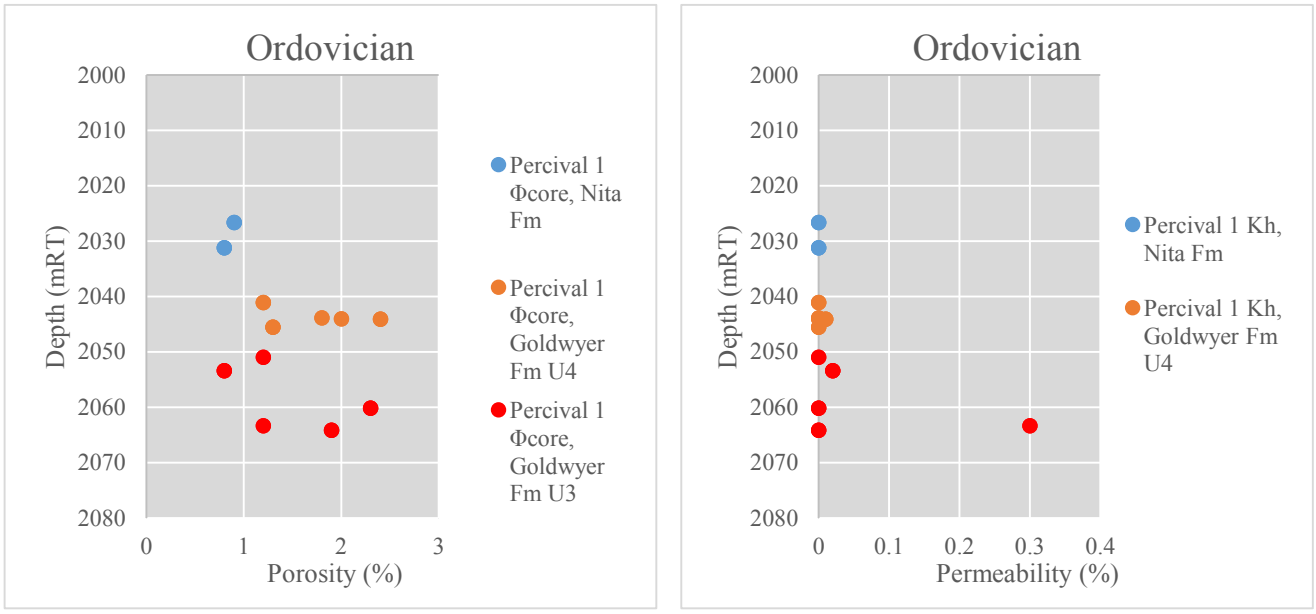

Figure 4.8. Ordovician porosity and permeability data (modified after France, 1984)

The dolomites of the Nita Formation could provide a suitable seal within the Larapintine L2 petroleum system, where Percival 1 shows the interval to be 16 metres thick. Tight porosity, nil permeability and fast sonic velocities (indicative of low porosity) is suggestive of good sealing potential in the Nita Formation.

4.3 Late Ordovician

Late Ordovician strata are also not intersected by wells within the study area; however their occurrence is documented across the Gregory Sub-basin. Stratigraphy of this age primarily includes the Carribuddy Group. Percival 1 is the nearest well to intersect Late Ordovician stratigraphy (Figure 4.9). Lake Havern 1 also intersects rocks of similar age, however Percival 1's section is regionally correlatable using Haines (2004). The Carribuddy Group was found to be an interbedded claystone and dolomite sequence containing the Nibil Member, the Minjoo Marker Bed and the Bongabinni Member.

A discrete Late Ordovician package was not mappable on seismic data, so inferences of stratigraphic presence, extent and thickening are summed within the Near Top Ordovician seismic horizon and seismic interpretation maps, described in subsequent sections.

4.3.1 *Carribuddy Group – Bongabinni Member*

Characteristics

The Bongabinni Member is described at Percival 1 as deep brownish-grey to blackish sub-fissile to fissile claystone that is silty and sandy in part (France, 1984). The formation is known in other regions of the Canning Basin (such as the Willara Sub-basin on the West Australian coast, Figure 2.1) to be a potential source rock within the present day oil window (Haines and Ghori, 2006), and excellent oil shows (oil bleeds from core) have been noted at Cudalgarra 1, along the Admiral Bay Fault Zone (northern margin of the Willara Sub-basin, Figure 2.1). If the Bongabinni Member is present at depths within the Gregory Sub-basin, or within the project area, the unit may provide to be a suitable source rock for the Larapintine L2 petroleum system, and if the unit is sufficiently thick, it's description leads to the possibility of it acting as a seal for deeper Ordovician reservoirs.

Geophysical Log Characteristics

Geophysical logs (Figure 4.9) over the interval show a uniform resistivity log response, invariable sonic and density response, and a hot blocky gamma ray with a slight deflection in the centre of the unit.

4.3.2 *Carribuddy Group – Minjoo Marker Bed*

Characteristics

The Minjoo Marker Bed at Percival 1 comprises a thin (3 metre thick) brownish yellow microcrystalline, argillaceous dolomite (France, 1984).

Geophysical Log Characteristics

Geophysical logs over the interval show a spike in resistivity, sonic and density logs, and a sharp deflection in the gamma ray log response over the interval, representing a sharp contact with the thin dolomite zone (Figure 4.9).

4.3.3 *Carribuddy Group – Nibil Member*

Characteristics

The Nibil member at Percival 1 is observed as brownish grey soft dolomitic claystone (France, 1984).

Geophysical Log Characteristics

The Top of the Nibil Member (also top of the Carribuddy Group) is marked by a baseline shift in gamma ray, resistivity, sonic and density values underneath the overlying basal Worral Formation carbonate unit. Geophysical logs over the Nibil Member show generally high gamma ray log values, slight deflections of the resistivity log, sonic and density log in the upper portion of the Member (1877 mRT to 1885 mRT) (Figure 4.9).

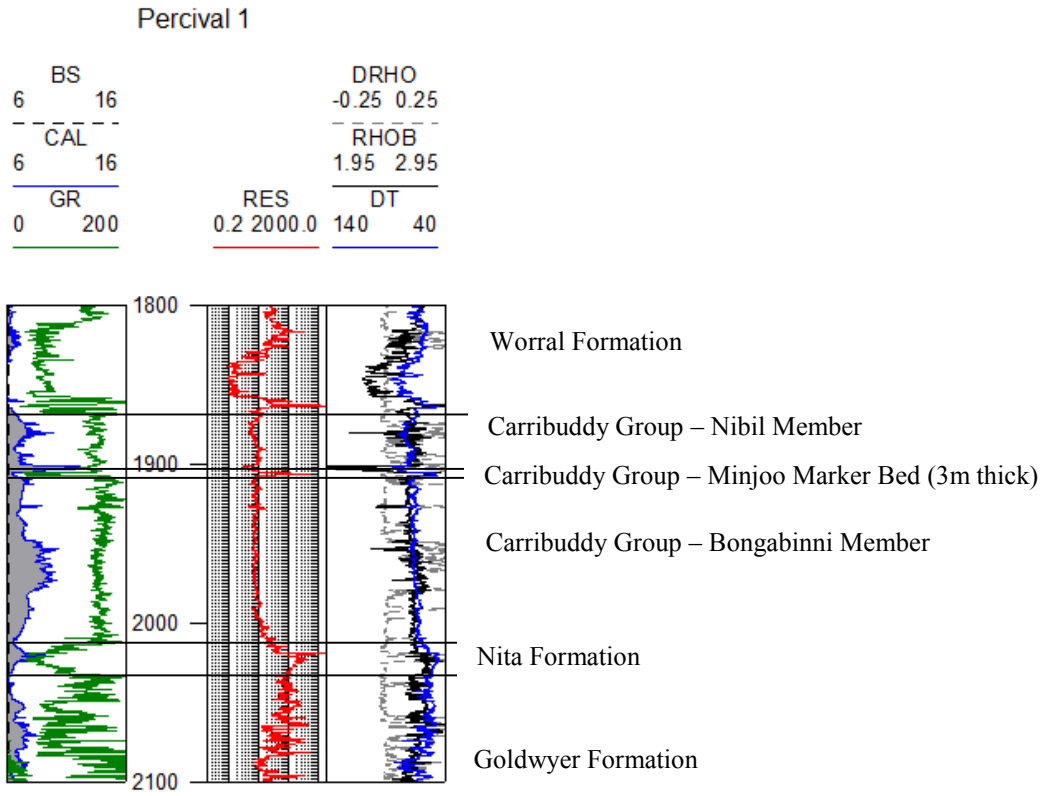

Figure 4.9. Percival 1 geophysical log over Siluro-Ordovician section (modified after France, 1984).

Depositional Setting

Overall, the Carribuddy Group represents a supratidal to intertidal/restricted marine depositional influence, with accommodation also influenced by an extensional tectonic regime.

The Bongabinni Member is representative of lower flow regime deposition (sub-fissile claystone and fine sandstone) that appears oxidized in part (Haines, 2009), and was likely deposited in an intertidal or restricted marine (lagoonal) environment. Haines (2009) notes that the Admiral Bay Fault Zone hanging wall (nearer the Willara Sub-basin, on the West Australian coast) includes thicker deposits of the Bongabinni Member due to syn-tectonic accommodation generation. Brown (in Purcell, 1984, Figure 2.4) notes that the Admiral Bay Fault Zone was active at a similar time to the Fitzroy Graben, therefore a similar package of thicker Bongabinni Member mud-rich rocks may exist within the Gregory Sub-basin.

The Minjoo Member, elsewhere in the basin, is represented by a dolomitic mudstone that grades to halite (Haines, 2009). The observations at Percival 1 indicate that extensive hypersaline conditions likely did not exist on the Barbwire Terrace, instead mud-rich and carbonate lithofacies prevailed, indicating lower flow regime deposition and marine influence. Hypersaline basins were likely present elsewhere at the time.

The Nibil Member is a dolomitic claystone, also indicative of lower plane bed energy. The Nibil Member was likely deposited in a restricted marine environment, not significantly different to environmental conditions experienced by that of the other Carribuddy Group members.

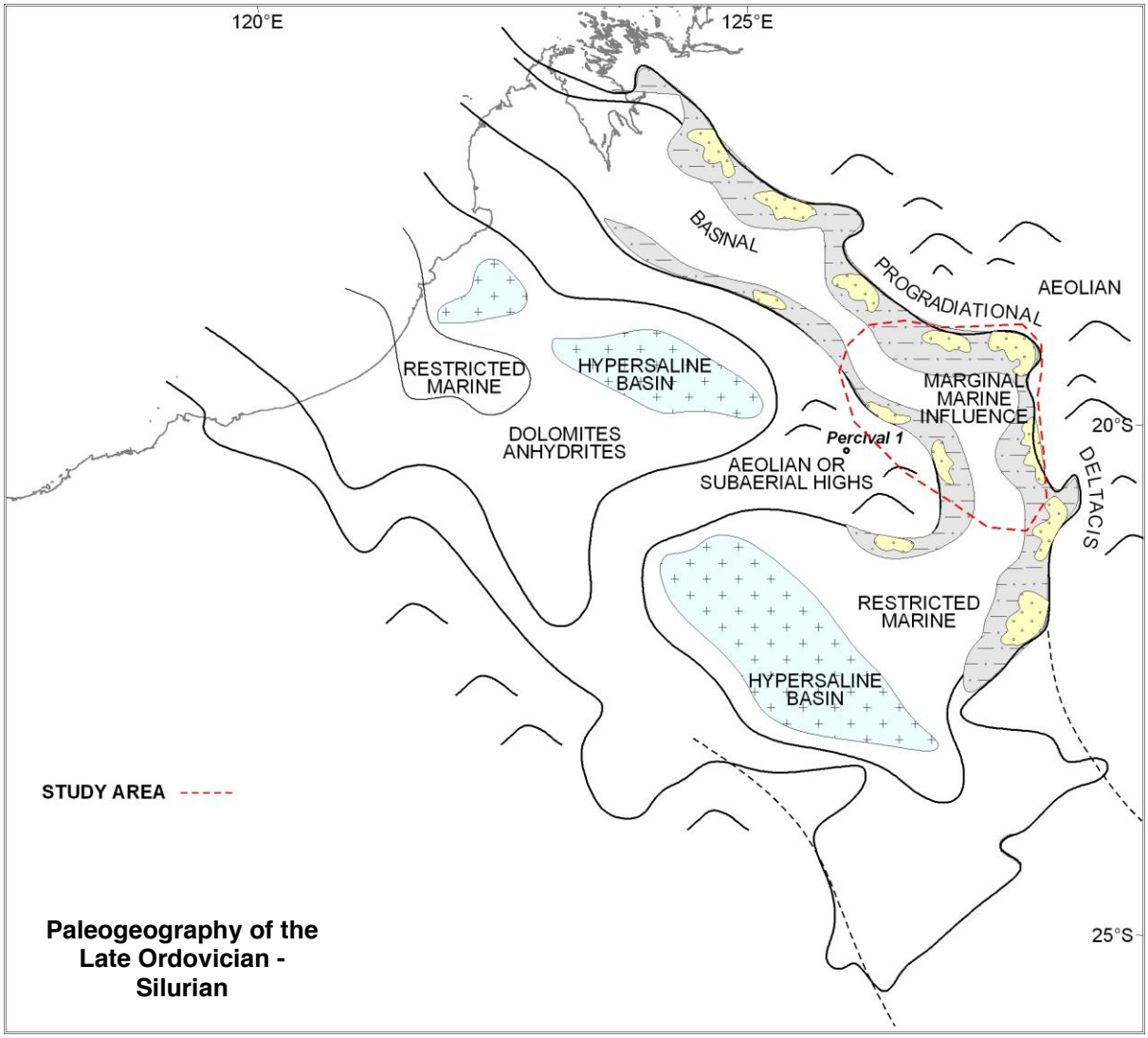

Figure 4.10. Paleogeography of the Late Ordovician to Silurian (modified after Brown, in Purcel 1984)

Reservoir Properties

Description of the Carribuddy Group Bongabinni and Nibil members (fine grained and therefore tight) indicates possible sealing potential in the Ordovician package. The Bongabinni log character alludes to source rock potential.

Discussion – Ordovician Aged Section

There are no discrete mappable packages of intra-Ordovician stratigraphic units on 2D seismic (Chapter 5.3.7), so TWT seismic interpretation and the products of seismic interpretation capture a general package under a single Near-Top Ordovician horizon. Two-way travel time thickness (Isochron) mapping of the Near Top Ordovician package shows the thickest section preserved is on the order of 1.6 seconds TWT thickness, down dip of the Stansmore Fault in the Gregory Sub-basin. The Ordovician thins to 0.3 seconds TWT westward towards the Jones Arch (a basement high northwest-ward of the study area). The package thins to approximately 0.4 to 0.6 seconds TWT on the Balgo and Betty Terraces. Within the Billiluna Sub-basin the Ordovician section is approximately 1 second thick at the Mueller Fault and thins to approximately 0.3 seconds TWT (and assumed to continue to thin onto Pre-Cambrian basement) at the near zero edge on the northern basin margin. Generally, the Ordovician appears thicker in the southern portion of the study area, averaging approximately 0.6 seconds TWT on the terraces and as thick as 1.6 seconds in the central project area depocentre. The Ordovician thickens in a southwest direction (basinward), and is thinner in the north and northwestern portions of the project area.

A clear uncertainty surrounds what Ordovician lithologies exist within the project area, however as the Pre-Carboniferous stratigraphy thickens into the Gregory Sub-basin (seismic line RB81-07, Figure 6.5) some confidence is provided that the Ordovician aged section will thicken from the Barbwire Terrace and Ryan Shelf areas (using the Lake Havern 1 correlation) towards the study area. Paleogeographic reconstructions indicate that the Goldwyer Formation is potentially sandy in nature and may lack the organic rich shale lithologies required for a generative source rock for the Larapintine L2 petroleum system.

The Ordovician section has been demonstrated by Haines (2004) to exist regionally across the Canning Basin. Haines performed a high-resolution correlation using geophysical logs. The reader is referred specifically to Plate 3 of Haines (2004), where the Ordovician section is carried from Contention Heights 1 (Kidson Sub-basin) to Percival 1 (Barbwire Terrace) and across the Fitzroy Trough to Blackstone 1 (Lennar Shelf). Plate 3 demonstrates that the Ordovician packages (Goldwyer Formation and Nita Formation) thicken substantially from the Kidson Sub-basin along strike in a northeast direction, and towards the Fitzroy Trough. The Ordovician correlation across the Fitzroy Trough is perhaps more difficult due to poor

seismic imaging across the Gregory Sub-basin thick sediment accumulation, and the Carribuddy Group is shown to be eroded at Blackstone 1.

4.4 Early to Middle Silurian

Regionally, the Silurian aged section comprises the upper-most portion of the Carribuddy Group known as the Sahara Formation and the marginal marine Worral Formation. Although these early to middle Silurian aged rocks are not intersected by wells within the study area, the Worral Formation was intersected at Percival 1 on the Barbwire Terrace. The top of the Silurian Worral Formation corresponds with the top of the Larapintine L2 Petroleum System.

4.4.1 *Worral Formation*

Characteristics

The Silurian marginal marine Worral Formation generally unconformably overlies the Late Ordovician Carribuddy Group. The Worral Formation encompasses a lower Dodonea Member, a middle Elsa Sandstone Member and an upper Waldecks Member (France, 1984). The Dodonea Member is a pale grey microcrystalline to cryptocrystalline dolomite that is 11 metres thick at Percival 1. The fluvial Elsa Sandstone Member is an orange fine grained sub-angular poorly sorted friable sandstone with minor dolomite at its base (France, 1984). It is 42 metres thick at Percival 1. The upper portion of the Worral Formation is the Waldecks Member, which is an interbedded succession of laminar sub-fissile micromicaceous claystone, brown calcitic arenaceous siltstone, and translucent medium grained sub-angular to well-rounded and moderately-sorted indurated sandstone (France, 1984). The Waldecks Member is 63 metres thick at Percival 1.

Geophysical Log Characteristics

The top of the Worral Formation (Waldecks Member) is marked on geophysical logs (Figure 4.11) as a baseline increase on gamma ray log, resistivity, density and sonic log responses from the overlying Tandalgoo Formation. The interval has an invariably fast sonic, high density and mid-range resistivity response; though the gamma ray displays heterogeneity

over the interbedded claystone lithologies with a coarsening upwards trend. On geophysical logs the Elsa Sandstone Member is distinguishable due to a blocky gamma ray log response, and decreasing baselines in the resistivity, sonic and density logs. The Dodonea Member is observed as an increasing shift in the resistivity, sonic and density logs, and an increase in gamma ray values over the interval.

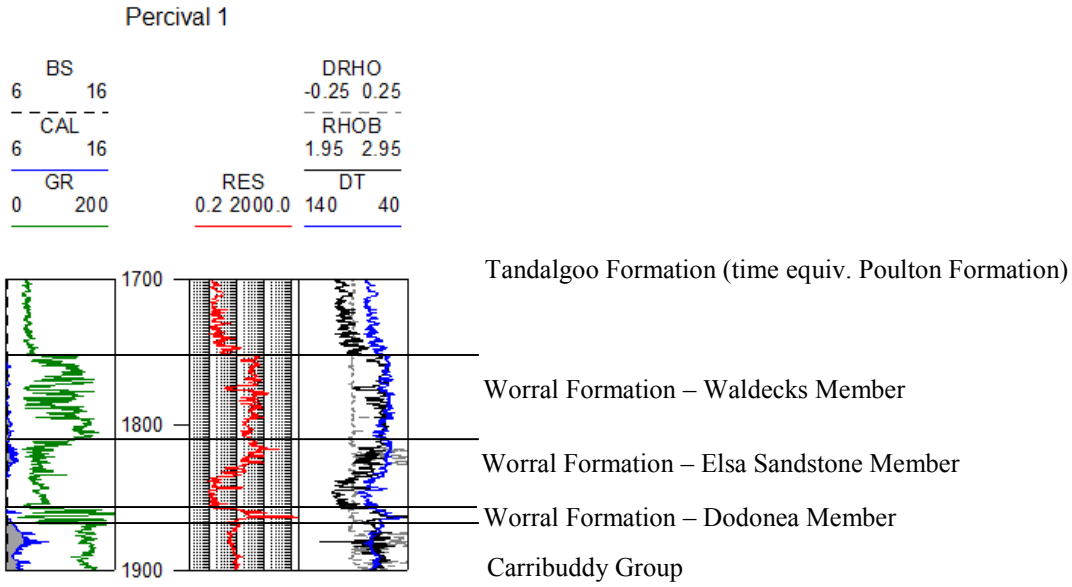

Figure 4.11. Percival 1 geophysical log over Worral Formation (modified after France, 1984).

Depositional Setting

Overall, the Worral Formation is representative of regressive base level. The Worral Formation's basal Dodonea Member suggests some marine influence during Middle Silurian time. The Elsa Member's blocky sand is either channel facies with regressed sea level or aeolian. The Waldecks Member's interbedded clays and siltstone with sandy intervals suggests alternating base level and movement of shallow distributaries in a general low energy environment. It is probable that the coarsening upwards trend on the gamma ray log suggests a progradational episode. The Top of the Elsa Member's blocky character could represent a small scale flooding surface. The Worral Formation's lower carbonate is probably a high-stand. The top of the Elsa Sandstone member is likely a sequence boundary, and the Waldecks Member is evidence of a low-stand systems tract.

Reservoir Properties

The description of the Worral Formation's Elsa Sandstone leads to the possibility of the interval as potential reservoir unit (42 metre thick fluvial sandstone), and the 63 metre thick sub-fissile claystone. The Waldecks Member may provide a suitable overlying seal. No reservoir property data was obtainable for the Worral Formation.

4.5 Late Silurian to Devonian

An unconformity (not regionally mappable on 2D seismic data) related to the Late Silurian Prices Creek Compressional Event separates the Silurian aged section from Devonian aged rocks. Devonian strata are the oldest that are penetrated by wells within the study area. The Devonian (Figure 2.3) comprises (oldest to youngest) the Poulton Formation (Tandalgoo Formation age equivalent), a Devonian aged Conglomerate, Bungle Gap Limestone, Gogo Formation, Virgin Hills Formation and Knobby Sandstone (with time equivalent Luluigui Formation and Nullara Limestone).

4.5.1 *Poulton Formation*

The Early to Middle Devonian Poulton Formation (time equivalent of the Tandalgoo Formation at Percival 1) was intersected within the project area at Lake Betty 1. Crank (1972) described the formation in Lake Betty 1 as a grey, fine grained, angular well-sorted micaceous sandstone, with minor interbeds of brownish grey siltstones and mudstones.

Geophysical Log Characteristics

The top of the interval on geophysical logs (Figure 4.12) is marked by a deflection on the gamma ray log. Logs over the zone show a slight increasing resistivity trend and coarsening upward gamma ray log character that represents a transition from interbedded argillaceous units to sands underneath. The base of the zone shows increases in the GR log and density log over mud rich intervals. Lake Betty 1 reached Total Depth (TD) within the Poulton Formation, intersecting 67 metres of the unit.

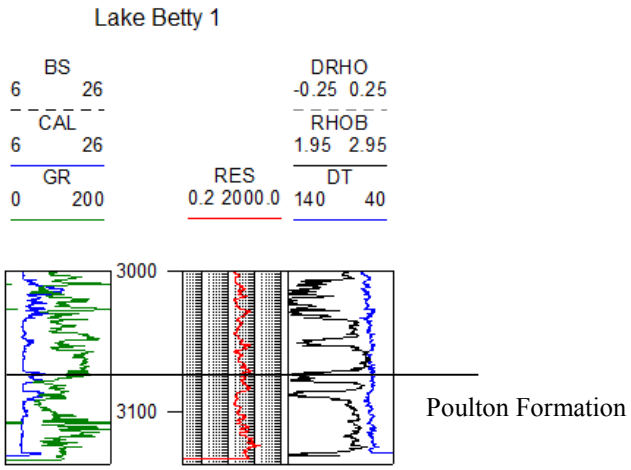

Figure 4.12. Lake Betty 1 geophysical log over Poulton Formation (modified after Crank, 1972).

Depositional setting

The fine grained sediments (fine sand, siltstone and mudstone) indicates lower flow regime, or sediment settling out of suspension. The gamma ray log over the interval shows an overall upward coarsening sequence, suggestive of a progradational package. A marginal marine environment is proposed for the Poulton Formation, potentially a deltaic sequence (delta mouth or prodelta sediments).

Reservoir Properties

The description of the Poulton Formation leads to the possibility of the interval as a potential reservoir unit, however the fine grained sandstone may be tight (low permeability). No reservoir property data was obtainable for the Poulton Formation.

4.5.2 *Devonian Conglomerate*

A Devonian aged conglomeratic sequence (125 metres thick at Atrax 1 and 336 metres at Selenops 1) is present along the northern border of the project area (partly shown on cross section A-A', Figure 4.13). The unit is observed as a range of boulder (200+ mm), cobble (64 – 128 mm) and pebble (2 – 64mm) sized polymict clasts containing orthoquartzite, granite, dolerite and quartz diorite material (Klappa et al., 1985). Argillaceous siltstones and feldspathic sandstones commonly make up the matrix. Multiple zones of conglomerate are

intersected (tops 662 mRT and 721 mRT at Atrax 1 and tops 927 mRT, 1027 mRT, 1034 mRT, and 1187 mRT at Selenops 1) with an interbedded argillaceous siltstone and sandstone sequence between the deposits.

Geophysical Log Characteristics

Geophysical logs over the interval at Selenops 1 show a marked increasing shift in the resistivity and sonic log from the Gogo Formation above and decreasing density and gamma ray log responses within sandier intervals. At Atrax 1 the conglomerate shows a decreasing shift underneath the Bungle Gap Limestone, within an increase in gamma ray and slowing in sonic log responses. The interval is observed as an overall coarsening upward gamma ray log response, shows high-range blocky resistivity, and mostly homogeneous sonic and density log responses with infrequent stepwise increases over thicker conglomerate horizons. The interval shares similar variability in all logs throughout the interval (Figure 4.13).

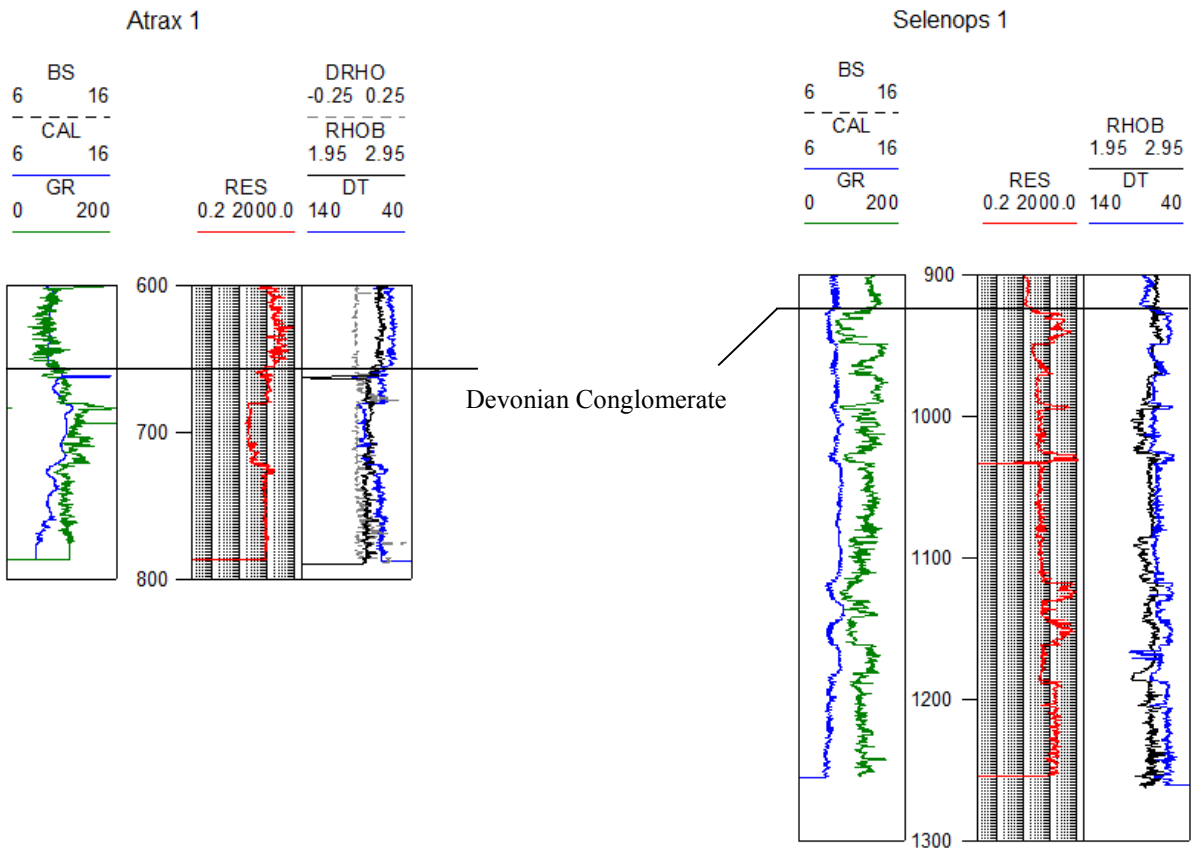

Figure 4.13. Atrax 1 (left) and Selenops 1 (right) geophysical logs over the Devonian Conglomerate (modified after Klappa et.al, 1985a; 1985b).

Depositional Setting

The conglomerates are probably proximal features of alluvial fan deposits (fan apex or upper fan) along the northern basin margin, where the interbedded finer clastics represent either changes to base level or altered positioning of fan distributary systems. The occurrence of alluvial fans along the northern basin margin follows the Prices Creek Compressional Movement, which likely provided the uplift to which sediments were then stripped and are now redeposited as Devonian aged coarse clastics and surrounding associated lithotypes.

Reservoir Properties

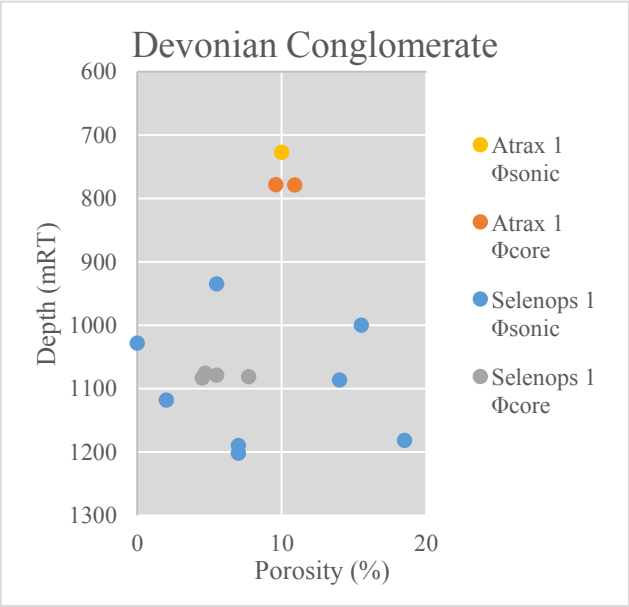

Figure 4.14. Devonian Conglomerate porosity measurements (modified after Klappa et al., 1985a; 1985b)

Reservoir property data for the Devonian Conglomerate was obtained via core measurements and sonic calculated porosities at Atrax 1 and Selenops 1 (Figure 4.14). The Devonian Conglomerate is shown to have 4.5% to 7.7% porosity at Selenops 1 and 9.6% to 10.9% porosity at Atrax 1, which makes the interval an attractive reservoir, however no permeability data is currently at hand. The sonic porosity measurements from Atrax 1 are in good agreement with core results. The Selenops 1 sonic porosities show variable results, and vary

by as much as a factor of 2.5 across a similar depth interval, and given the Selenops 1 core results, the sonic porosities at the same well are perhaps non-representative.

4.5.3 *Bungle Gap Limestone*

The Middle to Late Devonian Bungle Gap Limestone was intersected at Selenops 1 on the Balgo Terrace. No other wells intersected the formation. Selenops 1 intersected 59 metres of Bungle Gap Limestone.

Characteristics

The Bungle Gap Limestone is observed as a grey thick-bedded to massive arenaceous limestone grading to very calcareous sandstone in part, categorized as a grainstone or packstone (Klappa et al 1985). Very fine to fine grained quartzose sands are common throughout the limestone interval. The unit commonly shows biogenic inclusions; commonly gastropod, foram, bryozoan and ostracod constituents; along with ooids, peloids and intraclasts. Klappa et al (1985) noted that calcite occludes primary porosity, and fracturing is also similarly filled.

Geophysical Log Characteristics

Geophysical logs over the interval show a low gamma ray log response that is subtly coarsening upwards, and also a high-ranging resistivity and sonic log that display a broad bell shape curve. The resistivity and sonic logs show sharp increasing boundaries that makes the unit readily distinguishable from the surrounding lithologies (Figure 4.15).

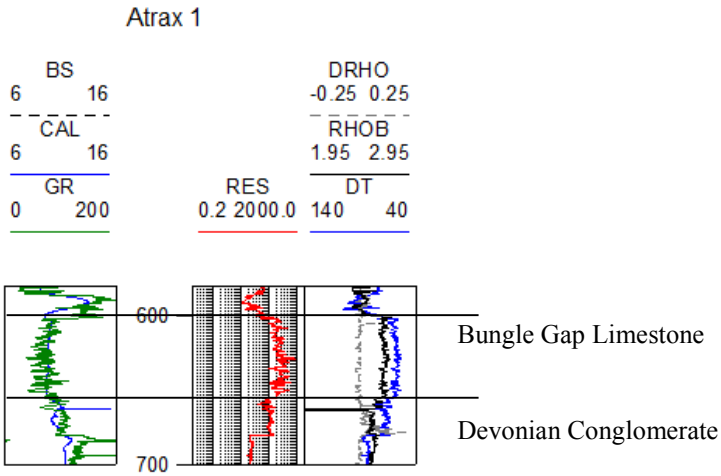

Figure 4.15. Atrax 1 geophysical log over Bungle Gap Limestone (modified after Klappa et al., 1985a).

Depositional Setting

Klappa et al. (1985) suggests that the clastic components are debris flow deposits of a marginal slope environment. It's probable that the Bungle Gap Limestone was deposited in a transgressive systems tract, where accommodation for carbonate accumulation was provided by a rising water level that introduced a shallow marine influence within the sequence. Marginal slope-type sandstones could then represent either higher energy flow (laminar) style remnants or a brief shallowing of the marginal marine environment with partial distributary influence.

Reservoir Properties

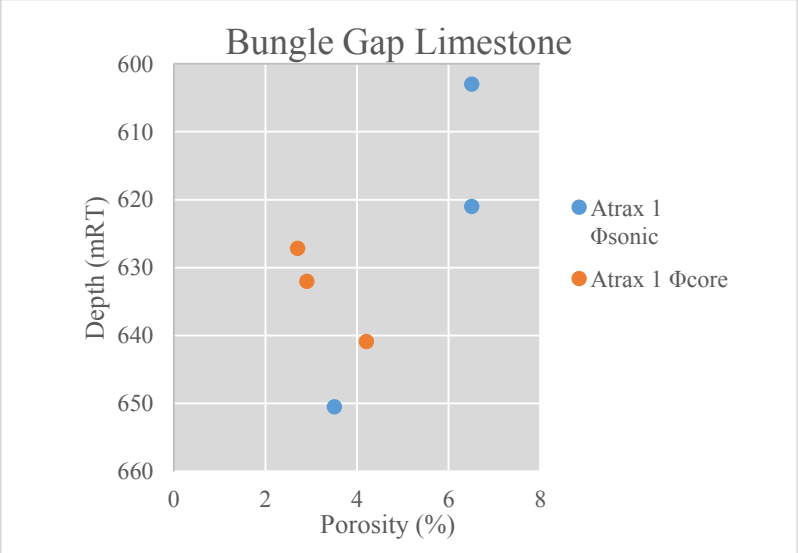

Figure 4.16. Bungle Gap Limestone porosity measurements (modified after Klappa et al., 1985a).

Reservoir property data for the Bungle Gap Limestone was obtained at Atrax 1 via core measurements and sonic porosity calculations (Figure 4.16). Core porosities range 2.4% to 4.2%, while sonic derived porosities vary up to 6.5%. Permeability data is unavailable for the interval. Lithological descriptions (secondary calcite and fracture fill) and porosity data suggest the limestone may not be a suitable reservoir within the study area.

4.5.4 *Lennard River Group*

The Middle to Late Devonian Lennard River Group was intersected at the Ngalti 1 well on the Betty Terrace. Ngalti 1 reached Total Depth within the Lennard River Group.

Characteristics

The Lennard River Group is comprised of interbedded limestone, sandstone, siltstone and minor amounts of claystone. Limestone content increases with depth. The limestone is observed off-white to buff, cryptocrystalline, silty and slightly fossiliferous, with minor argillaceous intervals (Smith, 1985b). The basal portion of the Lennard River Group's limestone is observed as fossiliferous, with common brachiopods, molluscs and bryozoans, and shows common peloidal carbonate mud intraclasts, giving evidence of reworking of limestone sediments (Martin, in Tybor 1985). The sandstone is white, very fine to fine grained, angular to sub-angular, moderately to poorly sorted, siliceous in part and dolomitic in part. The Siltstones are light grey, micromicaceous, rarely calcareous and rarely argillaceous. The claystone is dark blackish grey, firm, micromicaceous, sub-fissile and dolomitic in part (Smith, 1985b).

Geophysical Log Characteristics

The top of the Lennard River Group (transition) is marked on wireline logs (Figure 4.17) as an increasing baseline shift in the gamma ray response, increasing baseline shift in resistivity response, is slightly noisier and faster in the sonic log, and is slightly denser and less variable in the density response than the overlying Knobby Sandstone. The interval is shown to have

increasing sonic and resistivity log responses with increasing depth, and an intermittently high gamma ray log over claystone interbeds.

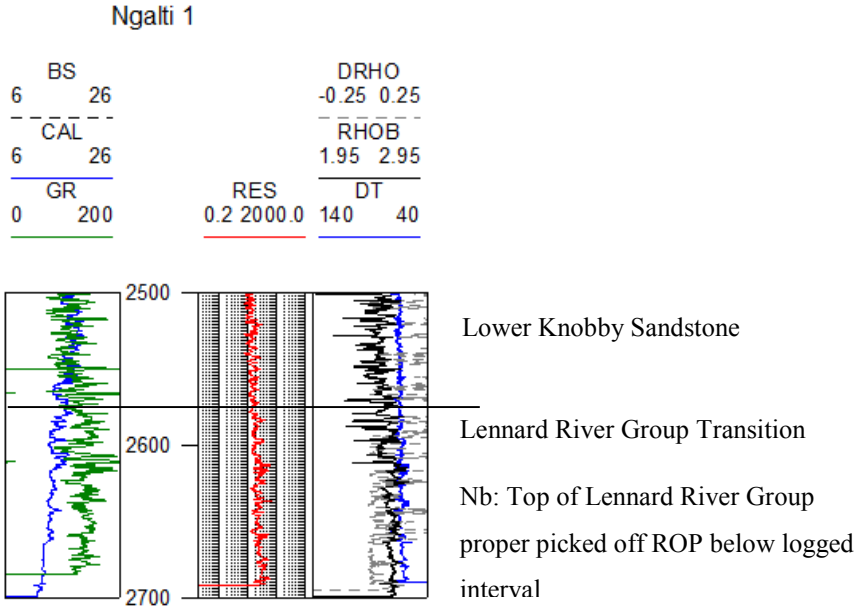

Figure 4.17. Ngalti 1 geophysical log over Lennard River Group (modified after Smith, 1985b).

Depositional Setting

The interbedded sandstone, siltstone, claystone and limestone character of the Lennard River Group alludes to alternating base level between high velocity laminar flow and lower velocity (turbidity?) currents. It was revealed in work by Martin (in Tybor, 1985) that limestones commonly show evidence of reworking, so the limestones are possibly redeposited rip-ups from a near shore marine (suggesting wave influence), into a delta-mouth type environment, in either the intertidal or swash zone.

Reservoir Properties

The description of the Lennard River Group's lithology leads to the assumption that the interval will be impermeable (cryptocrystalline limestone and fine grained siliceous dolomitic sandstones). If hydrocarbons are present in this zone, it would require a stimulated recovery. The interval may be a suitable seal. No reservoir property or seal potential data was obtainable for the Lennard River Group.

4.5.5 *Gogo Formation*

Characteristics

The Devonian Gogo Formation consists of laminated and thin bedded medium grey, soft to firm massive and blocky micromicaceous shales, light greenish grey soft calcareous argillaceous siltstones, and very fine grained white well-sorted argillaceous sandstone. Interbedded clastic lithotypes are observed commonly interlaminated with fossiliferous microcrystalline limestone stringers (Klappa et al, 1985).

Geophysical Log Characteristics

The Gogo Formation is dominated by an aggradational log character of thick, monotonous, high gamma-ray shales and infrequent lower gamma-ray spikes of thinly interbedded fine-grained sandstones (Figure 4.18). The gamma-ray log response is accompanied by a markedly uniform, mid-range resistivity and mid-range density log character. The sonic log shows only slight variability. The top of the Gogo Formation is marked on geophysical logs (Figure 4.18) as a gradual increasing baseline shift in the gamma ray log, and decreasing baseline shift in the resistivity and sonic logs. The top of the interval is also marked by a deflection in the density curve.

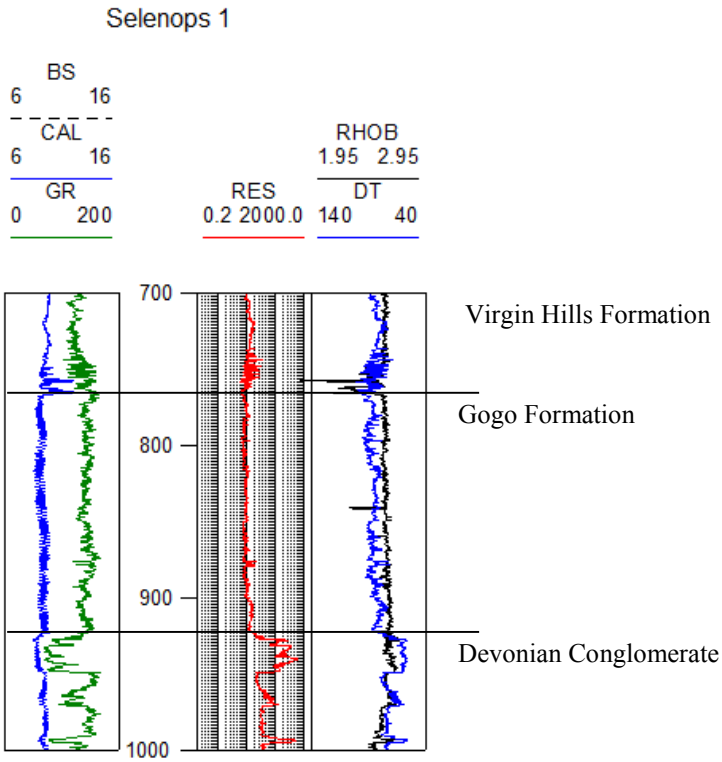

Figure 4.18. Selenops 1 geophysical log over Gogo Formation (modified after Klappa et al., 1985b).

Depositional Setting

The Gogo Formation is characterized by aggradational gamma-ray log patterns that are dominated by finer grained shales and siltstones deposited from suspension settling. Fine-grained sandstones that are thinly interbedded within the shale-rich sequence were deposited from traction current processes, suggesting deposition from infrequent turbidity currents. Regionally, fossiliferous microcrystalline limestone stringers are commonly observed interbedded with the clastic lithologies suggesting either brief platformal carbonate deposition or wave energy reworking (thin limestones). The Gogo Formation is interpreted as resulting from a deeper water basinal environment, with intermittent shallow marine influence or intertidal zone wave energy reworking.

Reservoir Properties

Description of the Gogo Formation (blocky, massive shales and argillaceous siltstones) implies the possibility of a potential sealing unit within the Devonian section, or a potential source rock. Source rock potential is examined in Chapter 7. No reservoir property data was obtainable for the Gogo Formation.

4.5.6 *Virgin Hills Formation*

The Devonian Virgin Hills Formation was intersected only at Selenops 1 in the northern project area, between 464 mRT to 767 mRT.

Characteristics

The Virgin Hills Formation consists of interbedded sandstone, siltstone, shales, and limestone. A limestone interval caps the formation. The sandstone is observed as grey, very fine to fine grained, sub-angular to sub-rounded, moderately well-sorted, argillaceous, bioturbated, ripple and cross laminated (Klappa et al, 1985). The siltstone is observed as medium to dark grey, firm, micaceous, pyritic, bioturbated and very argillaceous. The shales are medium to dark grey, soft and crumbly, micromicaceous and sub-blocky to sub-fissile. The interval is also interbedded (1 to 3 metre interbed thicknesses) and also capped by tan to cream, fine and coarsely crystalline, brittle and blocky to massive limestone. The limestone is described by Klappa et al (1985) as a grainstone or packstone, noting the occurrence of crinoids, bryozoans, molluscs, brachiopod and peloid fragments.

Geophysical Log Characteristics

The top of the Virgin Hills Formation is marked on wireline logs (Figure 4.19) as a sharp baseline increase on the gamma ray log, sonic log and density log due to an increase in argillaceous and calcareous (limestone) rock types over the interval. The Resistivity log shows a spike at the top of the unit coinciding with a thick (14 metres) limestone bed. The Virgin Hills Formation unconformably underlies the Grant Group at this location. The geophysical logs over the interval show a generally homogeneous resistivity and density log

response, though the sonic log shows slower values along with a lower gamma ray response between 635 mRT to 717 mRT due to a slight increase in sand content and less limestone over the zone. The base of the formation is observed as a chaotic response in wireline logs, however after looking at the logged drilling cuttings, the reason for this chaotic response is unclear. One possibility is an increase in argillaceous siltstone content.

Depositional Setting

The fine grained character of clastic lithologies suggest a low energy depositional influence. Bioturbation indicates oxygenation, so deep water is less likely than near shore. Cross bedding and ripple lamination from core evidence suggests pro-delta sedimentation for mud rich facies and mouth-bar for fine sands. The erratic interbedded carbonates (packstones and grainstones) suggest that the limestone zones are perhaps allocthonous detrital (rip ups) rather than insitu carbonate deposition – a carbonate reef was probably located some distance away from this location. This is suggestive of wave influence. A progradational system is plausible here, possibly within a low-stand system.

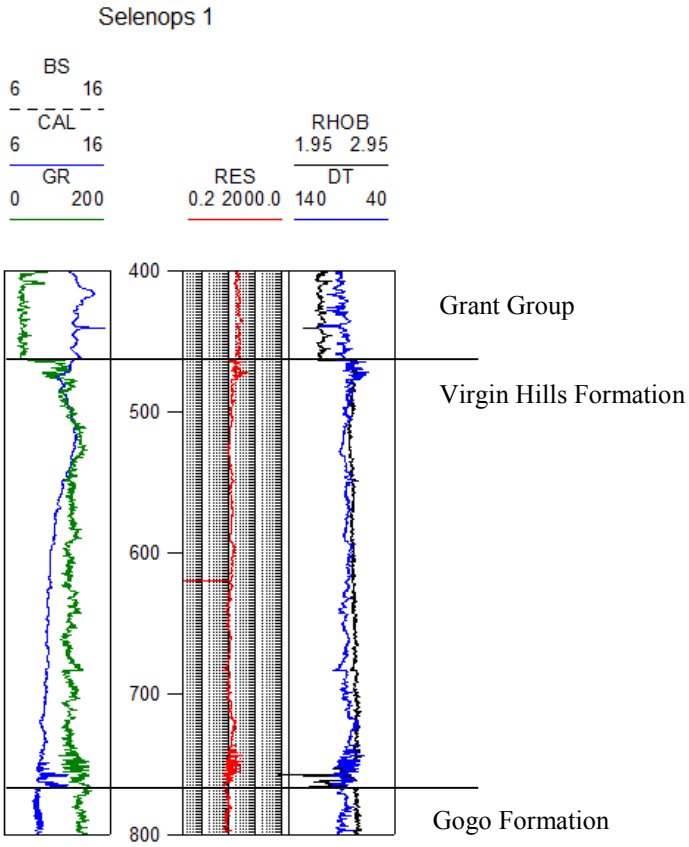

Figure 4.19. Selenops 1 geophysical log over Virgin Hills Formation (modified after Klappaet al., 1985b).

Reservoir Properties

Reservoir property data was obtained from core measurements and also calculated from sonic logs at Selenops 1 on the Betty Terrace (Figure 4.20). Sonic calculations indicated 9% porosity in the upper (purer) limestone interval. Core derived porosities are much more variable in the upper limestone (though more siliciclastic) zone, ranging 3.7% to 10.5%. Permeability ranges 0.25 to 1.2 mD at Selenops 1. Porosity data suggests that the Virgin Hills Formation may be a suitable reservoir target, however permeability data indicates that the clastic zone may be tight.

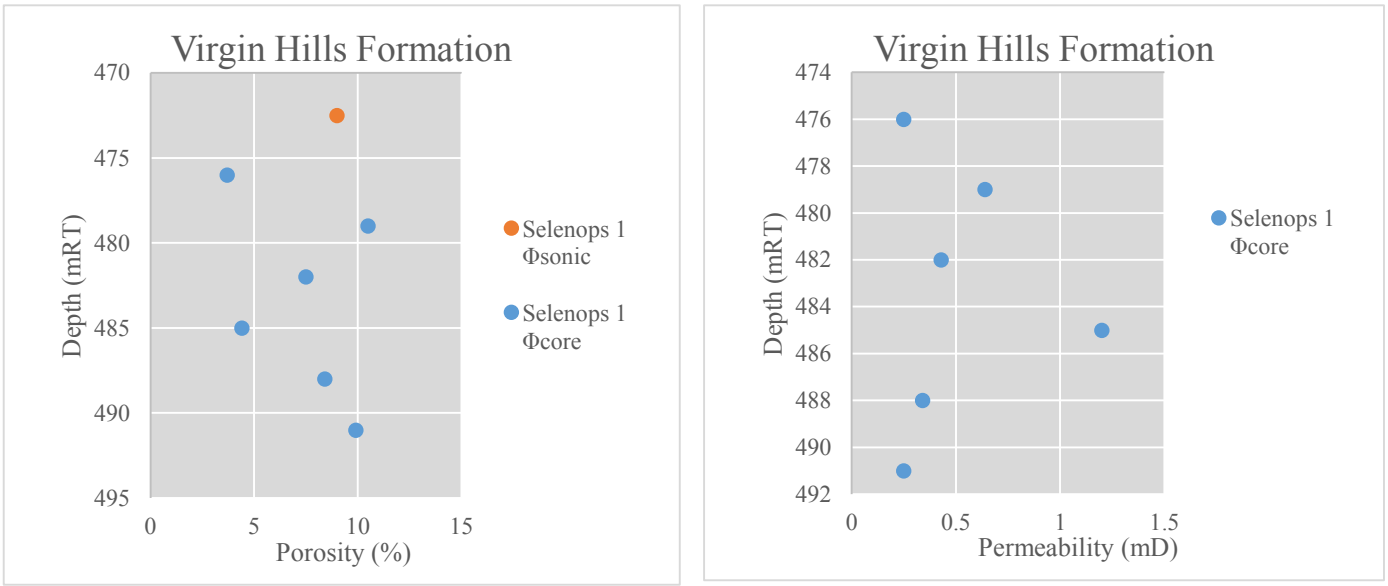

Figure 4.20. Virgin Hills Formation porosity and permeability measurements (modified after Klappa et al., 1985b).

4.5.7 *Knobby Sandstone*

The Late Devonian Knobby Sandstone is a prominent Formation within the study area. Historically, explorers have viewed it is a conventional reservoir target. It is intersected in wells Atrax 1 (586.5 mRT to 602 mRT), Lanagan 1 (1508 mRT to 1530 mRT), Ngalti 1 (1067 mRT to 2705 mRT) and Olios 1 (1560 mRT to 1962 mRT). It is mapped from seismic data to exist regionally across the study area's tectonic regions.

Characteristics

At Atrax 1 and Olios 1 (on the Balgo Terrace near the northern basin margin) the Knobby Sandstone is classified as mostly sandstone with minor shale at the base of the interval (for example 588.4 mRT to 599 mRT at Atrax 1). The sandstone is observed as medium to dark grey but lightening in colour towards the base, very fine to fine grained, sub-rounded to rounded, moderately well-sorted, silty in part and planar to cross bedded with rare burrowing (Klappa et al, 1985). The silty sections are greenish grey, firm, micromicaceous and sub-blocky to sub-fissile. The basal shale is observed as light to medium grey, sub-fissile, micromicaceous, pyritic and non-calcareous. Shale rip-ups and a minor zone (trace amounts to 5% returned cuttings) of black vitreous conchoidal coal also occur at the base of the interval at Olios 1.

Lanagan 1 (on the Betty Terrace, down dip of Atrax 1 and Olios 1) only intersected the upper 22 metres of the Knobby Sandstone (Lanagan 1 reached TD at 1530 mRT). The formation is classified as sandstone with minor claystone (NSO, 2008). The sandstone is described as light grey, very fine to fine grained, sub-angular to angular, well-sorted, calcareous in part and micromicaceous. The claystone is observed as medium grey, firm, sub-blocky to sub-fissile, calcareous, arenaceous in part, and grades to dark grey shale in part with trace limestone.

At Ngalti 1 (on the Betty Terrace in the central project area) a thick section of Knobby Sandstone was intersected. At 1512.3 metres, it is the largest intersection of the formation within the project area. The Knobby Sandstone is divisible into three sub-units at this location (Upper 1067 mRT to 1701.4 mRT, Middle 1701.4 mRT to 2179.7 mRT, Lower 21179.7 mRT to 2579.3 mRT).

Upper Unit (1067 mRT – 1701.4 mRT)

The upper unit of the Knobby Sandstone is classified as sandstone; clear and translucent, fine to medium grained. It is also coarse grained in part and grain size coarsens with depth within the upper unit, where it's sub-angular, moderatelysorted and argillaceous. Rare zones in core (e.g. 1072.8 mRT to 1073.8 mRT) include mud pellet rip-ups and show cross bedding and trough-cross bedding, though is mostly planar bedded. The upper-most portion of the upper unit also comprises interbedded shale that decreases in occurrence with depth; medium to dark grey, micaceous and firm (Smith, 1985b).

Middle Unit (1701.4 mRT – 2179.7 mRT)

The middle unit is observed as an interbedded sequence of sandstone and claystone rip-ups, and rare interbeds of siltstone. The sandstone is observed as clear, fine to medium grained but also rarely coarse grained, angular to sub-angular, poorly sorted, rarely argillaceous and commonly micaceous. The siltstone is observed as medium grey, slightly siliceous and argillaceous. The claystone rip-ups are pelletal, and occur below 1786.07 mRT. The middle unit shows common cross beds, trough-cross bedding, rare soft-sediment deformation structures and is also planar bedded (Smith, 1985b).

The unit shows a slump structure at 1780.3 mRT, consisting of fine grained angular micaceous sandstone with quartz flour matrix material.

Lower Unit (2179.7 mRT – 2579.3 mRT)

The lower unit is observed as a sandstone interbedded with minor siltstone and claystone. The sandstone is translucent, fine to medium grained, angular to sub-rounded, well-sorted and has minor amounts of siliceous cement. Carbonaceous flecks and trace mica is noted. The siltstone is grey and reddish brown, firm and blocky, micromicaceous, non-calcareous and pyritic in part. The claystone is white to off-white, moderately firm, carbonaceous in part, micaceous in part and grades to silty shale in part (Smith, 1985b).

Geophysical Log Characteristics

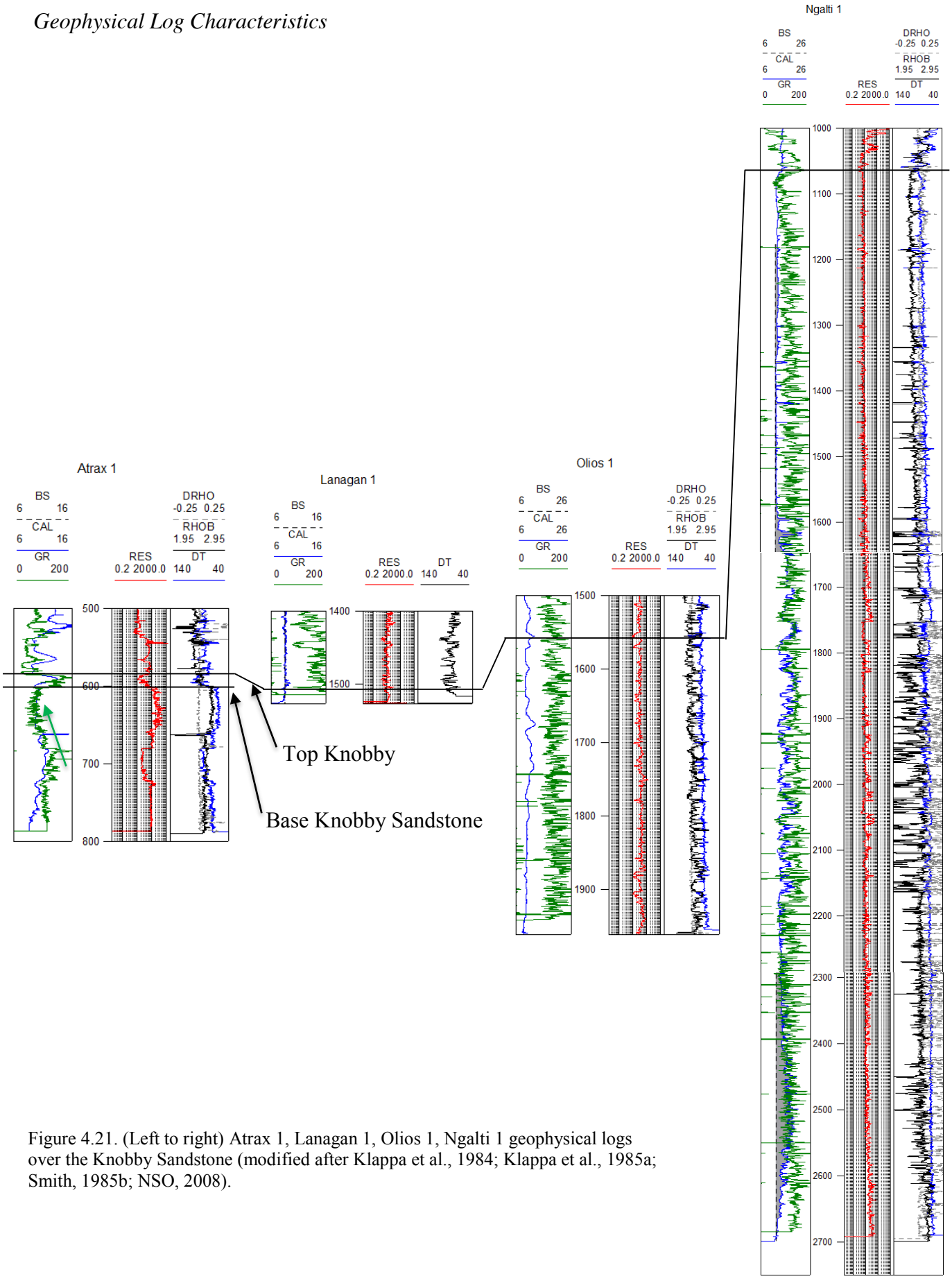

Figure 4.21. (Left to right) Atrax 1, Lanagan 1, Olios 1, Ngalti 1 geophysical logs over the Knobby Sandstone (modified after Klappa et al., 1984; Klappa et al., 1985a; Smith, 1985b; NSO, 2008).

The top of the Knobby Sandstone is marked at Atrax 1 and Lanagan 1 by an inflection on the gamma ray log, sonic log and density log responses (Figure 4.21). At Olios 1 the top of the formation is marked by a subtle baseline increase to the gamma ray log response. At Ngalti 1 the top is marked by an increasing baseline shift to the gamma ray log and a decreasing baseline shift to the resistivity, sonic and density tool responses.

The Knobby Sandstone is observed on wireline log data to show little variability in the resistivity log response over the interval, except for an increase in values across the blocky sandstone at Atrax 1. The log response across the interval in all wells shows generally fast sonic values. The gamma ray response at Atrax 1 shows a characteristic sandstone response. The gamma ray logs at Lanagan 1, Olios 1 and Ngalti 1 are different in character, with consistently high trends and is generally quite chaotic (resembling a "saw tooth" character). The reason for this is likely a combination of altering grain size (very fine grained sandstones and zones with clays) along with mineralogy – the formation is representative of a fluvial system that may have a high influx of uranium-rich sediments that results in a 'hot sand' gamma ray response. The Knobby Sandstone is observed to contain interbedded zones of clays however the clay content is probably not prominent enough to produce the observed geophysical response. A Spectral Gamma Ray log was not acquired in any well, however a petrography study at Olios 1 suggests that Monazite is the likely radioactive mineral causing high value responses influencing the gamma ray log (Klappa et al, 1984).

Lanagan 1 and Olios 1 reached TD within the Knobby Sandstone. There is no Wireline log data below 2693 mRT at Ngalti 1 (i.e. wireline log data does not reach the base of the Formation).

Depositional Setting

The overall fine-grained character of the sediments observed across all the well intersections suggests a general low energy and low flow velocity environment of deposition. The observations at Atrax 1, Lanagan 1 and Olios 1 suggest mid to lower plane bed energy systems whereas the coarser grains sizes (medium to coarse grained sandstones) observed at Ngalti 1 suggest mid plane bed grading to upper plane bed (higher velocity planar flow). The slump deposit in the Middle Unit (1701.4 mRT to 2179.7 mRT) at Ngalti 1 is a collapse structure during either subaerial exposure or higher-energy soft sediment deformation. One

key paleogeographic clue is the minor amount of coal observed at Olios 1, which indicates a near-by terrestrial environment, such as delta plain deposits (the observations of coal at Olios 1 are likely rip-ups). The cross beds, planar beds and burrowing observed at Atrax 1 alludes to fluvial flood deposits with tidal influence. It is likely that the Knobby Sandstone is representative of a fluvial dominated depositional setting (Figure 4.22); with Atrax 1, Olios 1 and Lanagan 1 situated distal of sediment supply such as mouth bar or pro delta flood plain. Observations at Ngalti 1are interpreted to suggest the Knobby Sandstone is likely a mid-meandering system deposit. The “saw tooth” gamma ray response is suggestive of aggradation (equal accommodation and sediment supply). The Knobby Sandstone, showing erosive (slumping) and coal/clay rip-ups (evidence of exposure), is likely representative of a low-stand or transgressive systems tract.

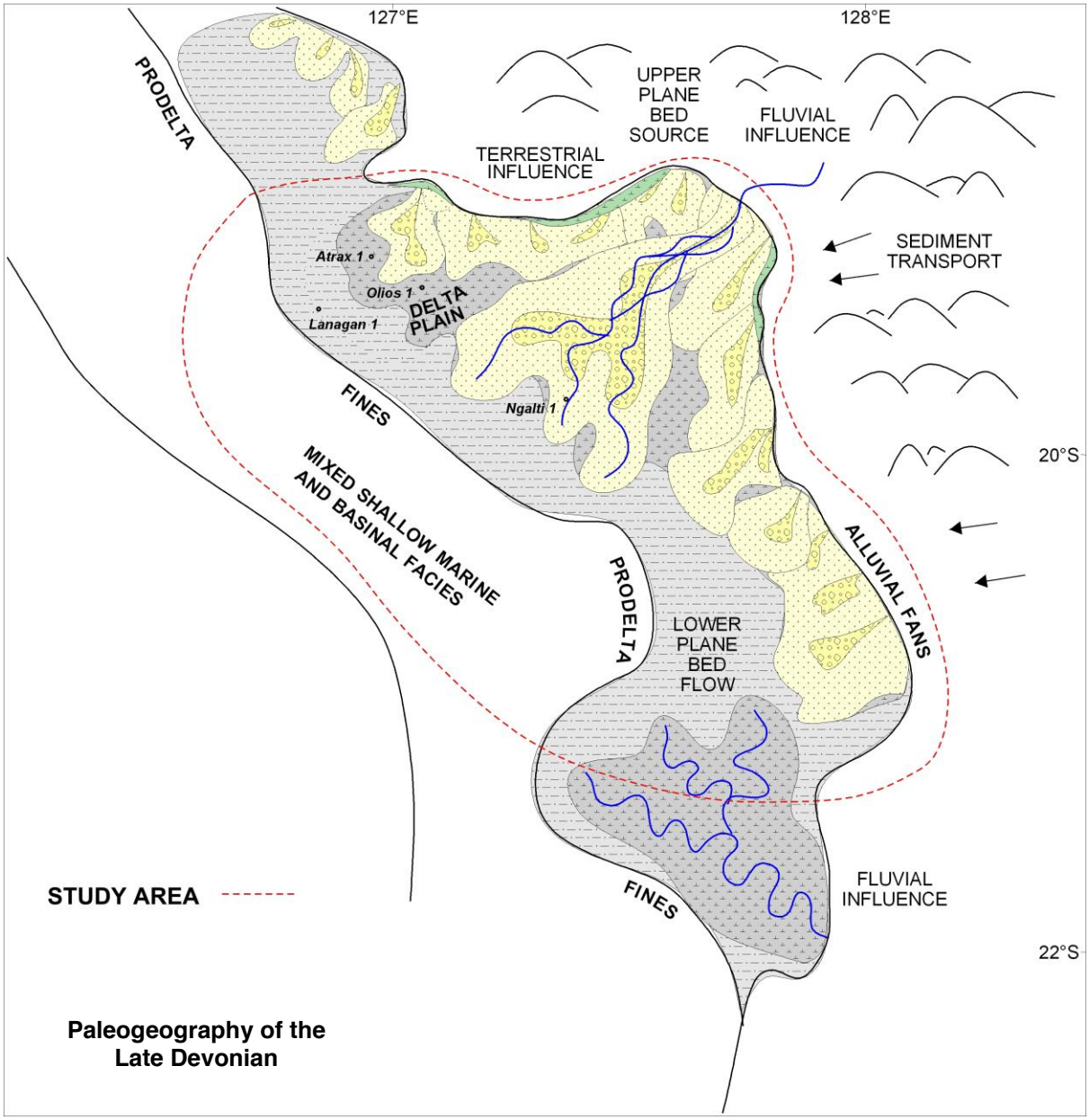

Figure 4.22. Paleogeography of the Late Devonian (modified after Wulff, 1987)

Reservoir Properties

The Knobby Sandstone shows excellent reservoir quality (Figure 4.23). The operators of Ngalti 1 also calculated sonic porosities from the Knobby Sandstone, which show good agreement with core derived measurements (Table 4.1). It is clear that the best reservoir section at Ngalti 1 is the Upper Unit of the Knobby Sandstone, above 1071 mRT, with an average of 20.6 % porosity and 567 mD of permeability. Only sonic derived porosities were derived from the Lower Unit at Ngalti 1 (Table 4.1).

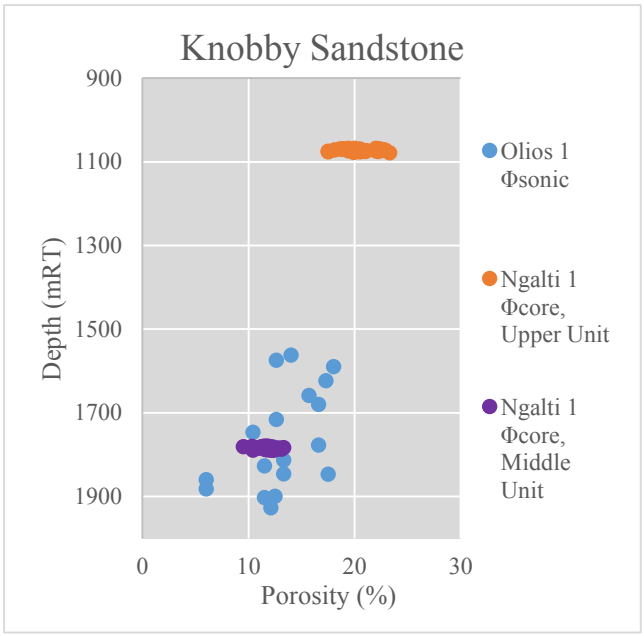

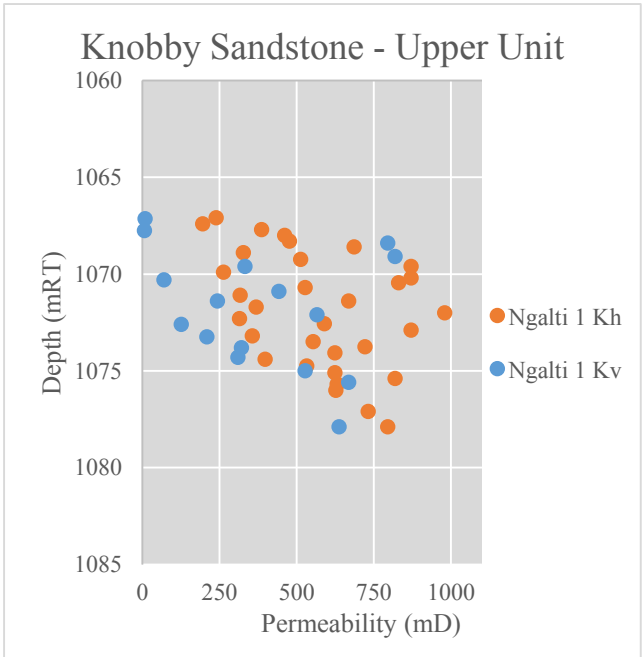

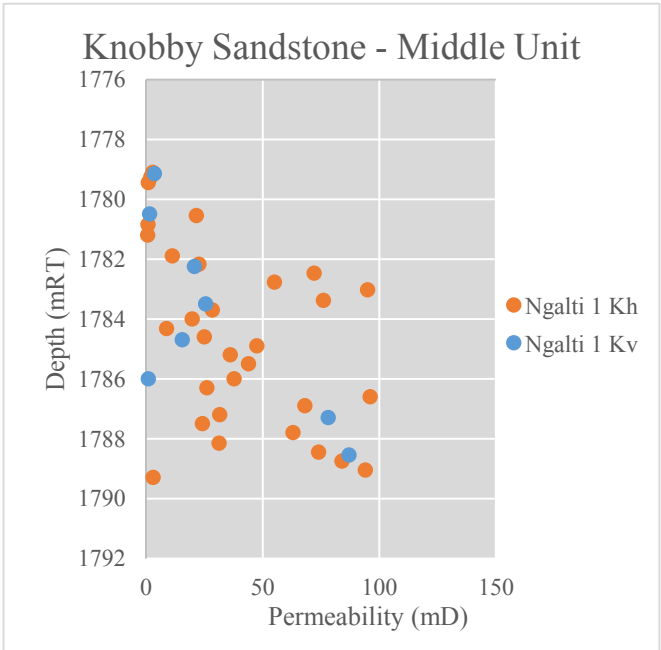

Figure 4.23. Knobby Sandstone porosity and permeability measurements (modified after Klappa at al., 1984; Smith, 1985b)

Well	Interval	Porosity (%, Sonic derived)
	Upper Unit	
	1067 – 1078 mRT	20%
	1078 – 1594 mRT	10 – 20%
	1600 – 1071 mRT	8 – 11%
	Middle Unit	
	1720 – 1753 mRT	6%
Ngalti 1	1781 – 1802 mRT	8%
	2012 – 2021 mRT	8%
	2045 – 2062 mRT	5%
	2097 – 2105 mRT	5%
	Lower Unit	
	2180 – 2476 mRT	5%
	2477 – 2566 mRT	5%

Table 4.1. Ngalti 1 porosity measurements (Smith, 1985b).

4.5.8 *Luluigui Formation*

The Late Devonian Luluigui Formation is restricted within the project area to the Gregory Sub-basin (Smith et al., 2013). It was intersected at Lake Betty 1 (2579.5 mRT to 3078.5 mRT).

Characteristics

The Late Devonian Luluigui Formation is observed as an interbedded sequence of sandstone and siltstone with minor shale (Crank, 1972). The sandstone is described as whitish to light and medium grey, fine grained, sub-angular, moderately sorted, micaceous, kaolinitc, rarely pyritic and variably calcareous. Cross beds and laminations, pebbly claystone and thin (centimeter-scale) limestones are observed as core features. The siltstone is described as medium to dark grey, argillaceous but also arenaceous in part, variably calcareous (containing one inch veins in core), occasionally fossiliferous (pelecypods and ostracods), and sub-fissile in part. Minor shale is described as dark grey, sub-fissile to blocky, slightly calcareous, micaceous, and silty in part. Rare slumping is observed (at 2944 mRT in Lake Betty 1) (Crank, 1972).

Geophysical Log Characteristics

The top of the Luluigui Formation is marked on geophysical logs by a subtle baseline decrease in the resistivity log and gamma ray log, and a decreasing trend in the density log response (Figure 4.24). Over the interval, the Formation is characterized by a subtly increasing though otherwise homogeneous resistivity and sonic response. The decreasing density log response and increasing resistivity corresponds with gradual increases in calcareous cuttings. At 2857 mRT there is a baseline increase in the resistivity log and gamma ray log response along with a sharp increase in the density log, as well as a spike in the gamma ray. This change corresponds with an increase in calcareous content (calcite crystals and calcite veining) and a zone of claystone observed in returned core and cuttings. The Luluigui Formation shows three broad coarsening upwards gamma ray trends (capped at 3000 mRT, 2772 mRT and 2579 mRT).

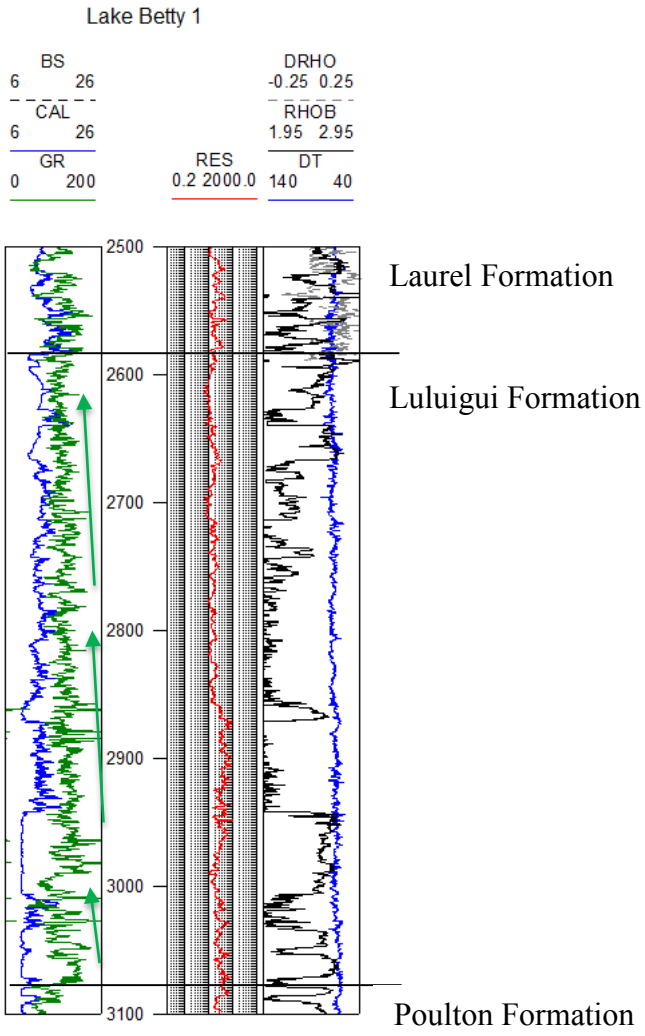

Figure 4.24. Lake Betty 1 geophysical log over Luluigui Formation (modified after Crank, 1972). Gamma ray trends in green arrows.

Depositional Setting

The observed overall fine grain sizes noted at Lake Betty 1 are representative of a lower plane bed energy system (low velocity flows). The cross bedded and planar laminated evidence alludes to flood plain type deposits (lower energy and altering depositional dips) which were likely subjective to tidal influence. The broad coarsening upward cycles are an indicator of channel bank or distributary channel facies. This could place the Lake Betty 1 location in a fluvial flood plain or pro delta/delta plain environment, distal from fluvial sediment supply, showing tidal influence. The Luluigui Formation is likely within a low-stand systems tract.

Reservoir Properties

The description of the Luluigui Formation (interbedded fine grained siliciclastics) suggests that the interval may be a potential reservoir, however it may be tight (low permeability, indicated by fine grained characteristics). No reservoir property data was obtainable for the Luluigui Formation.

Discussion and Framework – Devonian Aged Section

The Devonian Conglomerate (found at Atrax 1 and Selenops 1) and Bungle Gap Limestone (only at Atrax 1) are localized occurrences found in the northwest. Cross section A-A' (Figure 4.44) demonstrates the framework for this section of the stratigraphy. Note that with only two well intersections for the lower Devonian packages, the framework represents a likely overly simplified view of the sequence. Klappa et.al. (1985) suggest that the continuous high amplitude reflection event that is labeled on seismic line 82GE-33 as an 'Intra-Devonian Reflection Event' (Figure 6.4, SP 760 1.7 seconds TWT, below the reflection poor Knobby Sandstone – the top of which is interpreted as Near Top Devonian) may represent the Bungle Gap Limestone. Another possibility is that this reflection event represents the Devonian aged Pillara Limestone (not intersected by wells within the study area). The Bungle Gap Limestone is not intersected in wells in the southeastern project area; however the 'Intra Devonian Reflection Event' is a commonly noted regionally mappable horizon (though was not mapped for this project) within the seismic dataset.

The seismically 'quiet' zone under the Near Top Devonian horizon makes it difficult to map the extent of the Devonian Conglomerate, the Gogo Formation and the Virgin Hills Formation, however as the Poulton Formation is present down dip at Lake Betty 1, it is thought that the Conglomerate, Gogo and Virgin Hills Formations transition basinward to equivalents from the Northwestern project area (and the Devonian Conglomerate transitions into a finer grained lateral equivalent lithology), shown on section A-A' (Figure 4.44). The Lanagan 1 and Olios 1 wells are not of assistance as these wells reached TD in the younger Knobby Sandstone. The Devonian Conglomerate, Gogo Formation and Virgin Hills Formation are not intersected in wells in the southeastern project area.

The Knobby Sandstone and time equivalent Luluigui Formation are arguably the most prominent Devonian formations in the region (intersected by all wells except Bindi 1, Kilang

Kilang 1 and Selenops 1). The Knobby Sandstone is generally thick – in excess of 400 metres in most of the wells across the study area, shown on cross sections A-A', B-B' and C-C' (Figure 4.44 to Figure 4.46). Well correlation illustrates that the unit slightly thickens down dip into the Gregory Sub-basin in the northern project area (A-A'). In the south the unit is anticipated to thicken dramatically, demonstrated on B-B' and the Siluro-Devonian Isochron (Figure 6.24, southwest of Ngalti 1). Seismic line RB81-7 (Figure 6.5) also suggests thickening of the entire Siluro-Devonian section down dip across the Stansmore Fault. The Knobby Sandstone is known to exist on the Betty Terrace (at Ngalti 1) and interpreted to continue across the Balgo Terrace in the central and southern portion of the study area. The Knobby Sandstone is anticipated to be more limited in its occurrence in the northwestern study area – it thins at Atrax 1 to 15m thick, and truncates under the Meda Transpression Unconformity before reaching the Selenops 1 well to the west (Klappa et.al, 1985). The Knobby Sandstone is suggested to be the youngest formation in the Billiluna Sub-basin from surface geology information (aside from an alternative Fairfield Group interpretation; refer seismic interpretation in Chapter 6.2.3, which has no external data tie).

4.6 Carboniferous

4.6.1 *Fairfield Group – Laurel Formation*

The Early Carboniferous (Tournaisian) Laurel Formation is a regionally prominent stratigraphic package across the Canning Basin. The Formation contains a regionally mappable carbonate marker. The Laurel Formation is mapped using 2D seismic data to exist within the project area. The formation was intersected in six petroleum exploration wells within the project area. The tops of the formation are shown in Table 4.2 and Figure 4.25.

WELL	Lake Betty 1	Kilang Kilang 1	Bindi 1	Lanagan 1	Ngalti 1	Olios 1
Top Laurel Formation (mRT)	1658.28	1717.0	2474.0	983.3	796.0	883.0
Top Laurel Carbonate (mRT)	2305.0	Not Intercepted	Not Intercepted	983.3	796.0	1131.0
Base Laurel Carbonate (mRT)	2459.7	Not Intercepted	Not Intercepted	1292.3	1015.6	1431.0
Base Laurel Formation (mRT)	2579.5	Not Intercepted (Well TD within Formation)	Not Intercepted (Well TD within Formation)	1508.0	1037.5	1560.0

Table 4.2. Summary of Laurel Formation intersections within project area. Tops derived from geophysical logs.

Characteristics

The Laurel Formation is mainly a clastic sequence with zones of limestone (the Laurel Carbonate). Within the project area, the Laurel Formation is characterized by interbedded sandstone, siltstone, minor claystone, shale and limestone (Smith, 1985a; 1985b; and Klappa et al, 1985). The Sandstone across most of the project area is coloured clear translucent to medium grey, very fine to fine grained, silty in part and also argillaceous in part, sub-angular to sub-rounded, moderately sorted, slightly calcareous and also friable in part (at Olios 1) (Klappa et al, 1985). The sandstone is noted fine to medium grained at the Bindi 1 location (Lehmann and Haines, 1985) and generally medium grained and massively-bedded at the Kilang Kilang 1 location (Smith, 1985a). The siltstone is observed as greyish brown, calcareous, slightly to moderately carbonaceous, micaceous and sub-blocky to sub-fissile (at Kilang Kilang 1) (Smith 1985a). The claystone is observed as grey to dark grey, very soft, non-calcareous, arenaceous in part, micromicaceous and blocky to sub-fissile. The shale is

observed as medium to dark grey, blocky to fissile, shows a waxy texture in part, pyritic in part and arenaceous in part (Smith, 1985a).

The limestone is generally concentrated to thick intervals, known as the Laurel Carbonate marker (for example 2305.0 mRT to 2459.7 mRT at Lake Betty 1, Table 4.2) however relatively thin limestone interbeds are noted within the Laurel Formation. The interbedded limestone is noted as cream, buff and light brown to grey, finely to microcrystalline and fossiliferous (Crank, 1972).

The Laurel Carbonate marker is composed of a limestone, or interbedded unit of predominant limestone with fine-grained clastics. Within the project area, the Carbonate markers limestone is tan and greyish brown, finely to microcrystalline and cryptocrystalline, moderately fossiliferous (noting crinoids, pelecypods and brachiopods), and is classified as a wackestone to grainstone (Klappa et al, 1985). Interbedded zones contain brownish siltstone grading to very fine sandstone. The carbonate at Lanagan 1 is also interbedded with medium grey, soft, sub-blocky claystone. At Olios 1 the marker is interbedded with minor very fine grained sub-angular to sub-rounded silica cemented sandstone (Klappa et al, 1985).

Geophysical Log Characteristics

The Early Carboniferous Laurel Formation is truncated in part by the Meda Transpression Unconformity. The reader is referred to Chapter 5.3.1 and Chapter 6.2 of this study for insights into the degree of erosion. The seismic interpretation Figures, particularly line RB81-7 and RB81-10 (Figures 6.5 and 6.7), demonstrate the relationship between the top of the Laurel Formation (or top of the Laurel Carbonate where the upper Laurel Formation sequence is eroded by truncation) to the Meda Transpression Unconformity. Importantly, the truncation effect of the unconformity means that the top of the Laurel Formation is often different between wells, and consequently there are varying amounts of preserved Laurel Formation above the Laurel Carbonate.

The thickest succession of Laurel Formation above the Laurel Carbonate was encountered at Lake Betty 1 (646.72 metres) and a 248 metre thick section is preserved above the carbonate at Olios 1 (Figure 4.25). All other locations either did not intersect the Laurel Carbonate, or the upper portion of the Laurel Formation was eroded.

In every case where the upper Laurel Formation is encountered within the project area, the top of the interval is marked by a baseline increase in the gamma ray log response and a baseline decrease in the sonic log. The Laurel formation (both the section above the Laurel Carbonate and the section below the Laurel Carbonate) are characterized by a "saw tooth" gamma ray response (e.g. 1750 mRT to 1850 mRT at Kilang Kilang 1 and 1450 mRT to 1550 mRT at Olios 1) and coarsening upward gamma ray responses (1000 mRT to 1020 mRT at Olios 1 and 1800 mRT to 1900 at Lake Betty 1). Blocky gamma ray log responses are also noted (for example 1900 mRT to 1950 mRT at Kilang Kilang 1). Two funnel (or bell curve) trends in the gamma ray log are noted at Kilang Kilang 1, that show a coarsening upward and then fining cycle capped by an abrupt deflection in the log at 2210 mRT to 2300 mRT, followed by a (inverted) fining then coarsening upward cycle at 2120 mRT to 2210 mRT.

A major character change in wireline log response occurs at the intersection of the Laurel Carbonate (Figure 4.25). The top of the Laurel Carbonate is marked on geophysical logs by a pronounced baseline decrease in gamma ray log, together with a distinct increasing shift in baseline to the sonic, density and resistivity log responses. Over the carbonate interval the sonic and density log responses remain invariable, and are high (density) and fast (sonic). The resistivity log response over the interval is invariable at Lake Betty 1, though other wells that intersect the Laurel Carbonate show "saw tooth" variability in the resistivity log. The gamma ray log over the interval displays a very subtle funnel character toward lower values (lowest response in the centre of the carbonate and higher in the transition zones at the top and base of the carbonate interval).

The lower portion of the Laurel Formation (below the Laurel Carbonate) is similar in appearance to the upper portion in observed geophysical log characteristics. The base of the Laurel Carbonate is marked by an increase in baseline in the gamma ray response, and baseline decreases to the resistivity, density and sonic log responses. The gamma ray log over the lower portion of the Laurel Formation shows a "saw tooth" response, and perhaps shows a very subtle overall fining upwards trend in all wells that intersect this lower portion (for example 2480 mRT to 2550 mRT at Lake Betty 1, Figure 4.25).

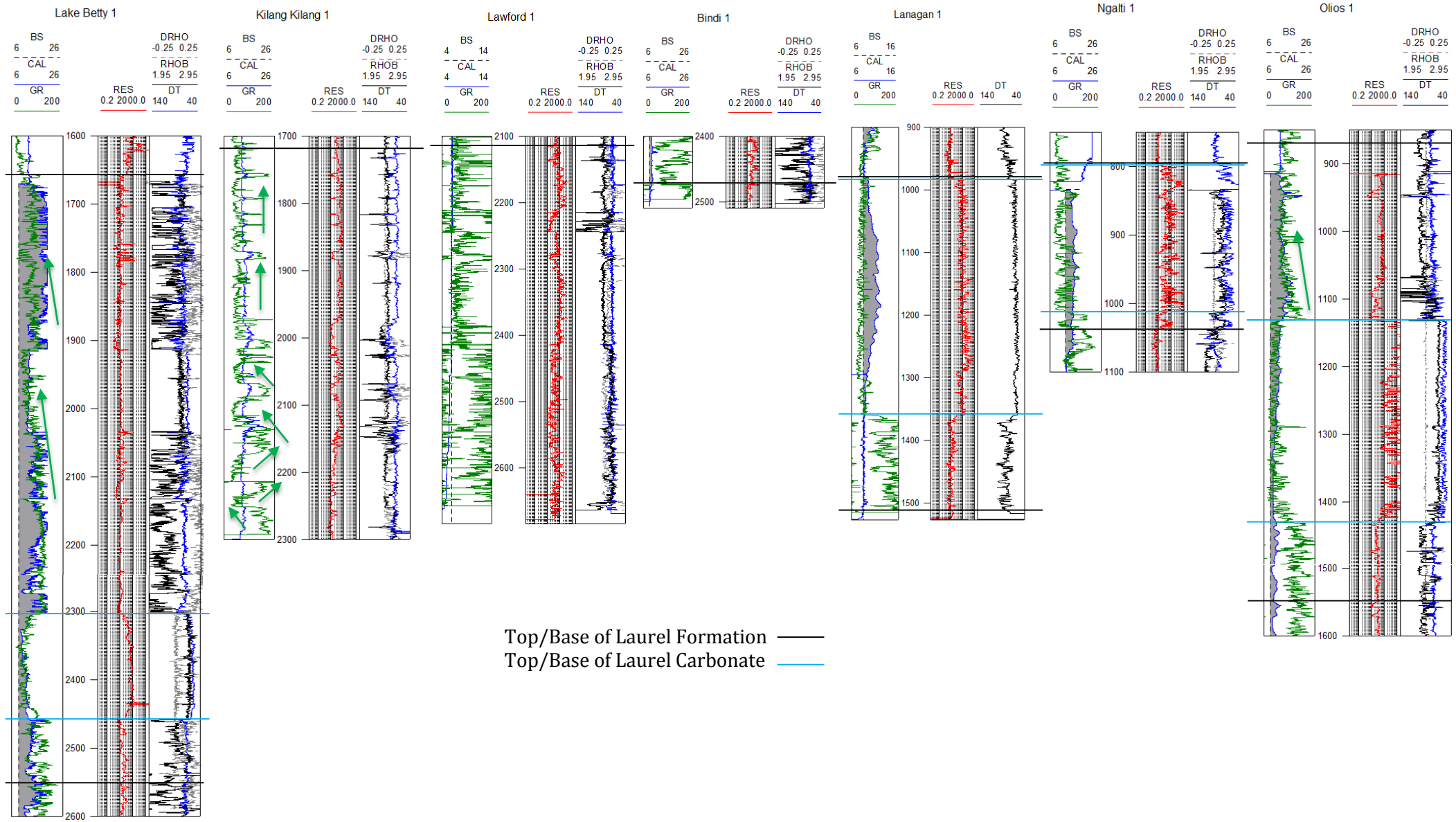

Figure 4.25. Geophysical logs over Laurel Formation across project area. Wells are labelled, (modified after Crank, 1972; Klappa et al., 1984; Lehmann and Haines, 1985; Smith, 1985a; 1985b; NSO, 2008; Cookson and Jones, 2013). Fining patters indicated by green arrows.

Depositional Setting

The overall fine to very fine sandstone, and finer grained clastic lithologies indicate a low energy depositional setting, suggestive of lower plane bed energy. Intermittent limestone deposition and a significant limestone package (The Laurel Carbonate) is key to determining some marine influence in Early Carboniferous time. The interbedded fine sandstone, siltstone and clays suggest periods of altering water levels. This is supported by the funnel shape gamma ray curves at Kilang Kilang 1; 2210 mRT to 2300 mRT illustrates a coarsening up trend followed by a fining parasequence cycle capped by an abrupt deflection in the log that likely represents a transgressive surface, followed by a second (inverted) funnel shape; fining then coarsening upward cycle at 2120 mRT to 2210 mRT (Figure 4.26).

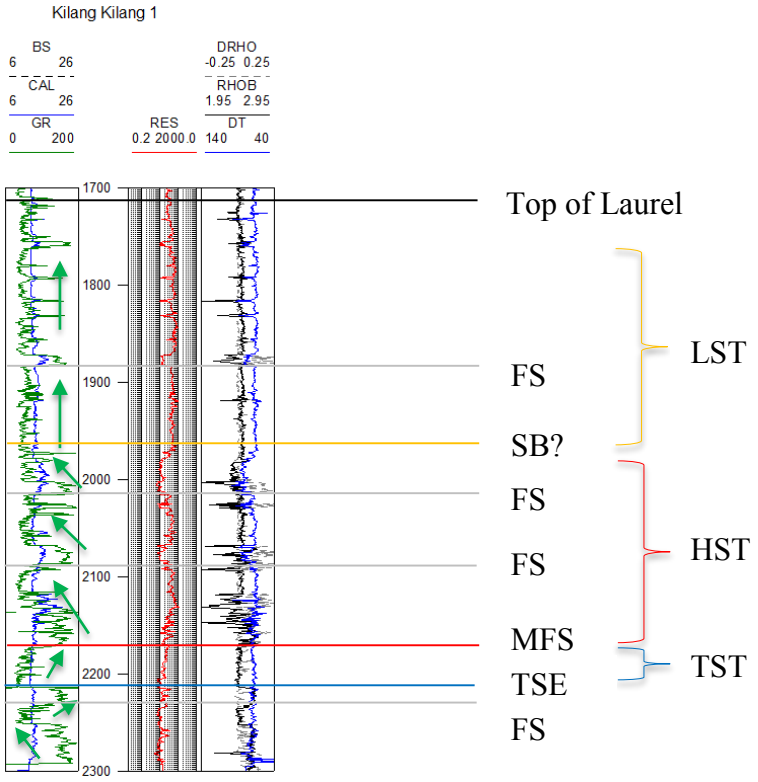

Figure 4.26. Kilang Kilang 1 geophysical log. Sequence stratigraphic analysis overlain (modified after Smith, 1985a). Green arrows indicate fining patterns.

Figure 4.26 illustrates alternating base level in sequence stratigraphic terms. A maximum flooding surface (MFS) is noted at 2170 mRT. The sharp deflection in the gamma ray log response at 2210 mRT is likely a transgressive surface of erosion (TSE). Together, the Laurel Formation at Kilang Kilang 1 represents a Transgressive sequence followed by a period of high relative base level accommodating sediment supply (high stand systems tract, HST). A low stand systems tract (LST) follows to the top of the Laurel Formation. The inference from this analysis, is that the time equivalent section to the Laurel Carbonate (not present in this well) is potentially in the zone between 2000 mRT to 2200 mRT; where a high stand at Kilang Kilang 1 allows higher base level in an up-dip location, thus facilitating a carbonate prone environment (refer paleogeographic map, Figure 4.27).

The Kilang Kilang 1 well is likely in a basinal position (down dip) relative to prime reefal carbonate deposition, which explains why the primary carbonate zone is not found in the well. The Bindi 1 well was not drilled deep enough to intersect the Laurel Carbonate. The Laurel formation was likely deposited in a marginal marine or lacustrine type setting.

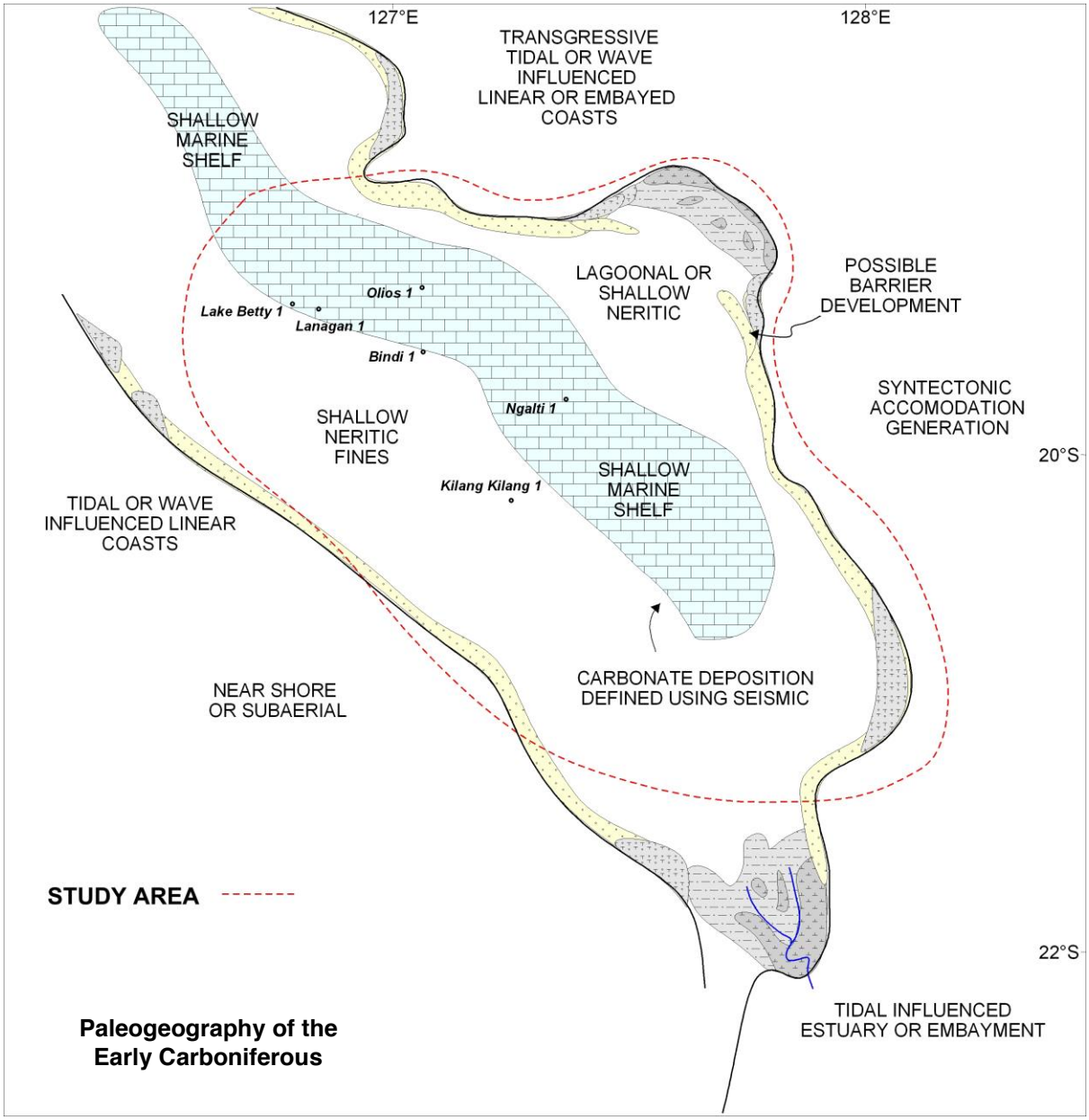

Figure 4.27. Paleogeography of the Early Carboniferous (modified after Wulff, 1987).

Reservoir Properties

Sonic derived porosities were calculated at Kilang Kilang 1 and Olios 1 for zones in the Laurel Formation (Table 4.3). Olios 1 sonic porosities show excellent reservoir potential in the upper clastic zone (ranging 12.1% to 22%) and also in the lower clastic zone (16.7% to 19.8%), below the carbonate (Figure 4.28). At Kilang Kilang 1, reservoir quality decreases (though is still attractive) likely due to deeper burial at Kilang Kilang 1, and likely higher proportions of finer grained clastics; with a more porous zone below 1981 mRT (up to 17%

sonic porosity). No data is available for the carbonate section, however the description (finely crystalline fossiliferous limestone) suggests that reservoir potential exists for the zone.

Well	Interval	Porosity (%, Sonic derived)
Kilang Kilang 1	1714 – 1755 mRT	9%
	1760 – 1872 mRT	8%
	1883 – 1978 mRT	8 – 9%
	1981 – 2003 mRT	17%
	2016 – 2068 mRT	8 – 10%
	2086 – 2124 mRT	8 – 10%
	2173 – 2214 mRT	10%
	2235 – 2251 mRT	12%

Table 4.3. Kilang Kilang 1 porosity data for the Laurel Formation (Smith, 1985a).

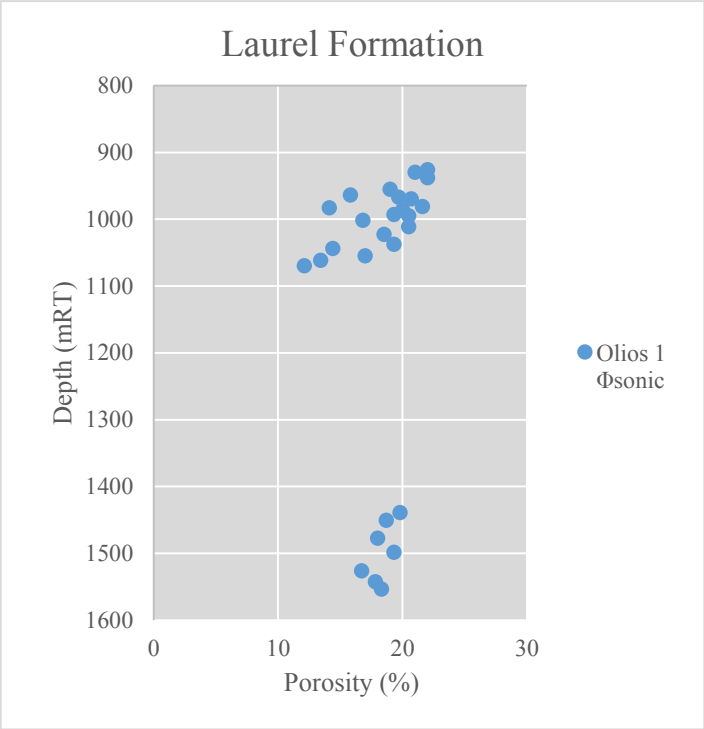

Figure 4.28. Laurel Formation porosity measurements (modified after Klappa, 1984).

4.6.2 *Anderson Formation*

The Early-Middle Carboniferous Anderson Formation is a conformable sequence of variable amounts of interbedded sandstone, siltstone and claystone, subdivided into seven units; 'A' to 'G', oldest to youngest. The Anderson Formation lies conformably above the Laurel Formation. The top of the Anderson Formation lies unconformably underneath the Grant Group. The Carboniferous Meda Transpression divides the Grant Group from the Anderson, often implicating significant truncation. The Anderson Formation is completely removed by erosion across large portions in the northern project area and southeastern project areas, and is preserved in complete package in the central project area (refer to Anderson Formation Isochron, Figure 6.22). Kilang Kilang 1 intersected a condensed section (1448 mRT to 1717 mRT, 269 metres thick), whereas the preserved section at Bindi 1 (1832 mRT to 2474.5 mRT, 642.5 metres thick) is the fullest in the project area. Figure 4.29 illustrates sub-unit division at Kilang Kilang 1 and Bindi 1.

Age

Biostratigraphic dating at Bindi 1 places the following ages on the observed stratigraphy, obtained from side-wall cores (Purcel, in Lehmann and Haines, 1985).

Depth (mRT)	**Sub-unit**	**Palynological unit**	**Suggested Age (stage)**
1918.7	Lower Unit G	*G. maculosa* Assemblage / *A. frustulentus* Microflora	Tournaisian – Westphalian
1999.4		Indeterminate	
2173 – 2481.4	Unit C, Unit B, Unit A	*G. frustulentus* Microflora	Tournaisian – Visean

Table 4.4. Age of the Anderson Formation (Purcel, in Lehmann and Haines, 1985).

Characteristics

Unit A

The deepest unit of the Anderson Formation comprises interbedded white, coarse-grained, loose angular well-sorted quartzose sandstone; mottled brown micaceous, massive, slickensided claystone; and dark brown micaceous arenaceous siltstone (Lehmann and Haines, 1985). Unit A at Kilang Kilang 1 is similarly observed as at Bindi 1, however the concentrations of siltstone and claystone are considerably less (Smith, 1985a).

Unit B

Unit B of the Anderson formation comprises a massively bedded quartzose sandstone; pale greenish grey, coarse grained but also medium in part, rarely granular in part, sub-angular to sub-rounded, and poorly sorted. Rare siltstone occurs in the unit, described as per Unit C below (Lehmann and Haines, 1985).

Unit C

Unit C is observed as a medium purplish brown rarely carbonaceous massively bedded siltstone that grades in part to non-fissile claystone; and grey and greenish brown fine to medium grained, sub-angular to sun-rounded quartzose and micaceous sandstone (Lehmann and Haines, 1985). The basal 13.5 metres of the sub-unit grades to very-coarse grained, and is also described as loose and well-sorted.

Unit D

Unit D is observed as massively bedded quartzose sandstone. The sandstone is described as transparent off-white to pale grey, mainly coarse with minor medium and also very coarse grains in part, angular to sub-angular, occasionally aggregated showing variably silicified quartzose grains, and a pyritic and argillaceous matrix. Variably developed quartz crystals and secondary overgrowths visible (Lehmann and Haines, 1985).

Unit E

Unit E is a mottled and variably coloured purplish to brownish micromicaceous massively bedded claystone that is arenaceous in part and grades to siltstone in part (Lehmann and Haines, 1985).

Unit F

Unit F is similar to Unit D. It is observed as a massively bedded quartzose sandstone. The sandstone is described as transparent off-white to pale gray, coarse grained with minor medium and also very coarse grains in part, angular to sub-angular, occasionally aggregated showing variably silicified quartzose grains, and a pyritic and argillaceous matrix. Variably developed quartz crystals and secondary overgrowths are noted (Lehmann and Haines, 1985).

Unit G

The shallowest subunit, Unit G, is comprised of claystone and sandstone. The claystone is observed as pale and light green to maroon, moderately firm to slightly friable, rarely carbonaceous, micaceous, occasionally slickensided and massively bedded. The Sandstone is off-white to pale grey, medium to coarse grained but also fine to medium grained aggregates noted, angular to well-rounded, loose, moderately to well-sorted, showing quartz crystal faces and overgrowths (Lehmann and Haines, 1985). The unit at Kilang Kilang 1 is also observed to contain an argillaceous dolomitic zone between 1462 mRT to 1480 mRT (Smith, 1985a). A Trace amount of greyish black to black brittle coal is observed at Lawford 1 (Cookson and Jones, 2013).

Geophysical Log Characteristics

The top of the Anderson Formation is marked on geophysical logs by a large inflection on the gamma ray log and subtle deflection (over the uppermost 3 metres) on the resistivity log response. The wireline log responses over the Anderson Formation's 7 subunits are variable, and provide the basis for the subunit division that is shown in Figure 4.29.

Unit A

The top of Unit A at is marked by an inflection on the gamma ray log that is well pronounced at the Bindi 1 location. The top of the subunit is also noted by a slight baseline decrease in the resistivity log, sonic and density log responses. The gamma ray log over the zone at Kilang Kilang 1 is relatively clean and subtly fining upwards, whereas the same zone at Bindi 1 shows a hotter and more variable gamma response, due to a higher concentration of fine grained clastics (siltstone and claystone interbeds) than at Kilang Kilang 1. The resistivity and sonic logs are generally mid-range and homogeneous. Correlating Unit A of the Anderson Formation is perhaps the most dubious..

Unit B

The Top of Unit B is marked on wireline logs by a distinct baseline decrease in the gamma ray log underneath Unit C. The top is also marked by a pronounced baseline increase to the resistivity and sonic logs. The zone is characterized by a relatively clean and blocky gamma ray log response (with the exception of increases to the log response at 2310 mRT at Bindi 1 and 1650 mRT), and largely invariable resistivity, density and sonic log responses.

Unit C

The top of Unit C is shown by a significant baseline increase to the gamma ray log response underneath Unit D, along with baseline decreases to the resistivity sonic and density tools. Unit B is characterized by a hot and blocky gamma ray log response, invariable resistivity and sonic responses, and a chaotic response in the density log across the unit.

Unit D

The Top of Unit D is marked by a baseline decrease to the gamma ray log underneath Unit E. The resistivity, sonic and density logs also show a baseline increase to their respective responses. The gamma ray log is generally blocky over the zone however is also subtly fining upwards in the upper portion of the subunit (from 2090 mRT at Bindi 1 and 1560 mRT at Kilang Kilang 1). The sonic and density log responses are homogeneous. The resistivity log response is also generally invariable although shows a subtle decreasing upwards trend from 2090 mRT at Bindi 1.

Unit E

Unit E is a thin zone at both well locations (thickest at Bindi 1; 26 metres), and is observed on geophysical logs as a pronounced baseline increase on the gamma ray log, and a baseline decrease to the resistivity, sonic and density log responses (though the resistivity log at Kilang Kiang 1 shows an inflection). The gamma ray, sonic, density and resistivity log responses are variable in character with infrequent zones of high values in each log corresponding to high percentages of claystone (observed as a similar log package as Unit C).

Unit F

The top of Unit F is observed as a prominent baseline decrease to the gamma ray log and sonic log responses. The resistivity log response at Bindi 1 shows a baseline increase though the opposite response is noted in the same interval at Kilang Kilang 1. Across the unit, all log responses are invariable and blocky. The inconsistency is also noted in the density log response.

Unit G

Unit G is observed as an (upper) fining-upward gamma ray log response and a (lower) hot and blocky gamma ray response at Bindi 1 (1860 mRT to 1900 mRT, not observed at Kilang Kilang 1). The resistivity log is invariable across the zone at Bindi 1, though the log shows a blocky character at Kilang Kilang 1 together with a step up (blocky character) in density and sonic responses at 1463 mRT, which represents the zone of argillaceous dolomite observed in drill cuttings. The density log and sonic logs at Bindi 1 show reduced and variable (chaotic) responses over the Unit G interval.

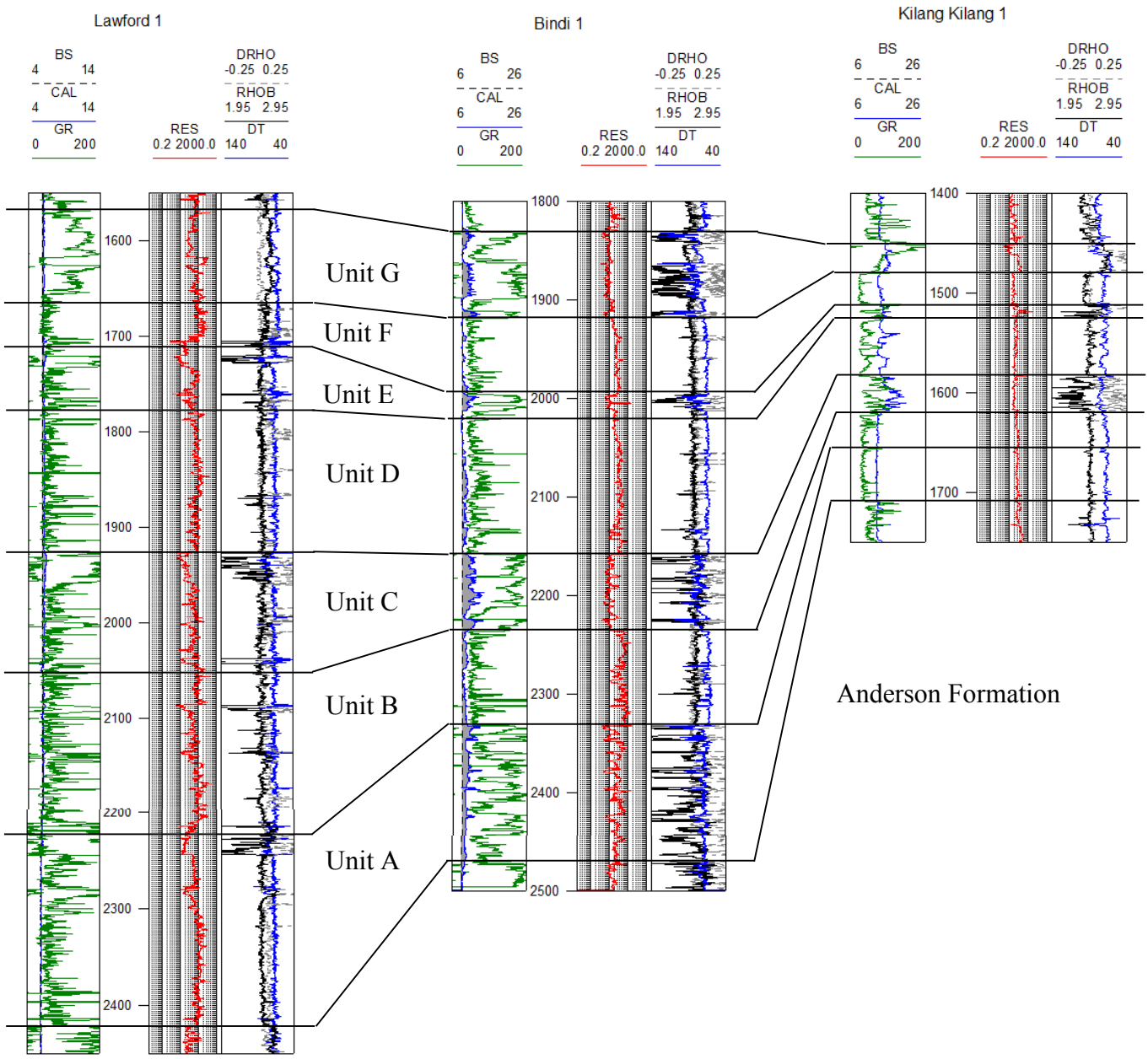

Figure 4.29. Geophysical logs over the Anderson Formation. Wells are labelled (modified after Lehmann and Haines, 1985; Smith, 1985a; Cookson and Jones, 2013).

Depositional Setting

Noticeable variability in observed lithologies and geophysical log characteristics across the Anderson Formation allude to alternating water depths and flow velocities, suggestive of variable depositional settings during Early – Middle Carboniferous time.

Units A, C, E and G represent periods of lower energy environments and likely lower plane bed velocities, whereas Units B, D and F represent periods of higher energy environment, likely upper plane bed energy.

Palynology evidence acquired at Bindi 1 between 1641.1 mRT to 2224.9 mRT (Units C to G) and 2348.1 mRT to 2481.4 mRT (Unit A) both concluded that preserved palynomorphs were severely oxidized, suggesting sub-aerial exposure of the sediments. A Trace amount of coal observed in Unit G at Lawford 1 alludes to either an exposed terrestrial environment or a high energy (rip ups) from a neighboring coal deposit.

Considering the deeper Laurel Formation represents a period of marginal marine influence, it is possible that the lower-most unit of the Anderson (Unit A) also shares a similar influence. This is supported in sequence stratigraphic terms by Figure 4.30, showing Unit A within a transgressive sequence (TST), leading into a high stand (HST) at the top of Unit C. the gamma ray log clearly represents a trend of coarsening overall grain size throughout Anderson Formation sedimentation (common finer clastics at the base, and abundance of coarser clastics up-section). A low stand is evidenced in Figure 4.30 from the sequence boundary (SB) at 2160 mRT toward the top of the Formation.

It is probable that the lower section (Unit A) represents a conclusion to a marginal marine (or estuarine) setting (that was prevalent during Laurel Formation deposition). Units B and C probably signal a transgressive coast, such as a strand-plain or wave dominated estuary (noting that sedimentary structures were not observed in the absence of whole core data, however coarse grained sands are prevalent in Units B, D and F). A change to a regressive coast is likely from the sequence boundary (SB) at 2160 mRT. At this point base level decreased to accommodate a progradational marine influence with fluvial influence such a deltaic environment, suggested by upper plane bed flow regimes and observed coal rip ups. The sand bodies within Units B, D and F are probable stacked delta lobes.

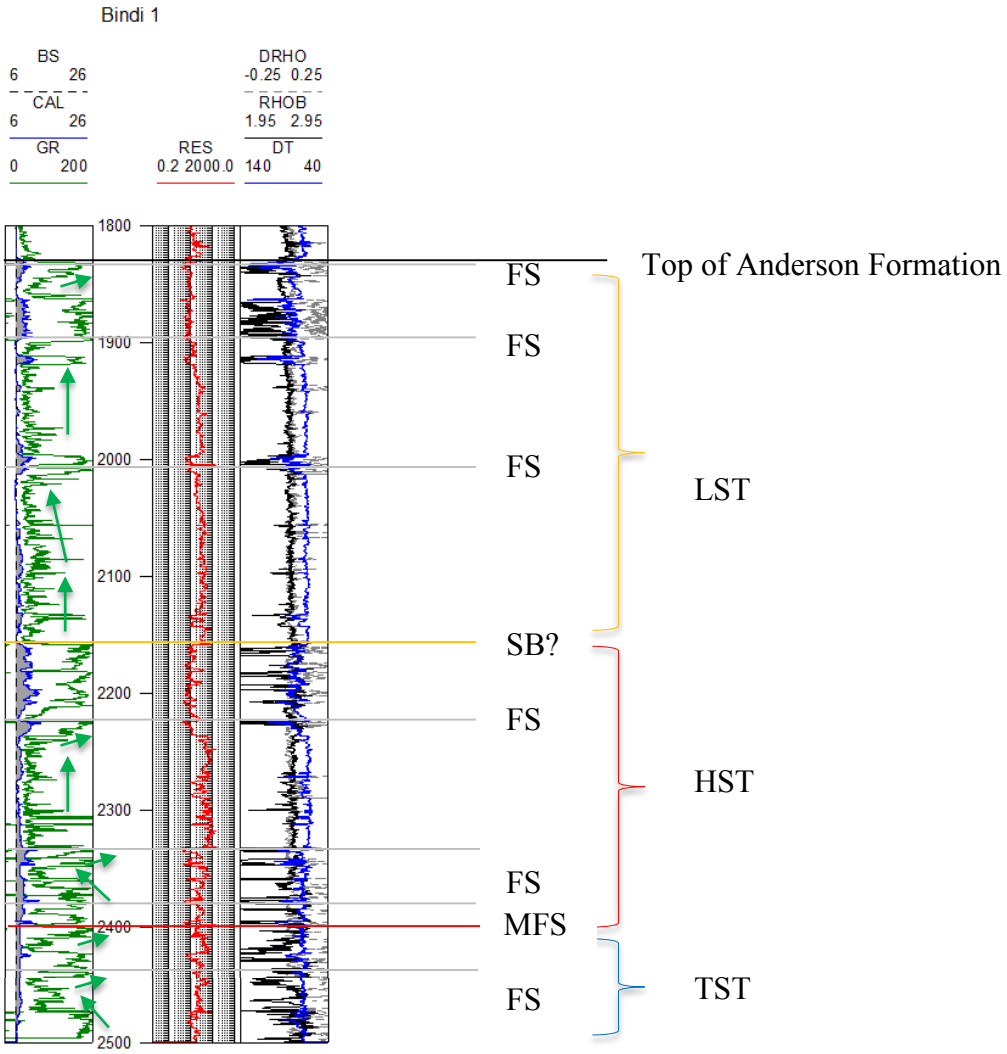

Figure 4.30. Bindi 1 geophysical log. Sequence stratigraphic analysis overlain (modified after Lehmann and Haines, 1985). Green arrows indicate fining patterns.

Reservoir Properties

Sonic derived porosities were calculated by the well operators at Kilang Kilang 1, Bindi 1 and Lawford 1, presenting average to good reservoir quality (Table 4.5). Sonic porosities at Bindi 1 suggest that Units A (6% - 11%), C (8.5%), and G (13%) retain the better reservoir quality data, however this is arguably deceptive given the gamma ray log; where it is perhaps expected to have more favourable reservoir properties in units D and F (a low stand system). Sonic porosities are lower in these zones at Bindi 1 (averages of 5% and 7% respectively), though the sonic log clarifies the reasons for the reported results (due to slower average transit values in zones A, C and G). No core derived data exists for the Anderson Formation.

From the gamma ray log at Bindi 1, it is anticipated that Anderson Units B, D and F represent candidate reservoir intervals, and Units A, C, E and G represent candidate sealing intervals.

Well	Unit	Interval	Porosity (%, Sonic derived)
Kilang Kilang 1	Anderson Fm G and F	1481 – 1511 mRT	13%
	Anderson Fm E to A	1515 – 1710 mRT	10 – 20%
Bindi 1	Anderson Fm G	1832 mRT	8 – 20%, Average 13%
	Anderson Fm F	1919 mRT	3 – 11%, Average 7%
	Anderson Fm D	2023 mRT	3 – 10%, Average 5%
	Anderson Fm C	2158.5 mRT	5 – 15%, Average 8.5%
	Anderson Fm B	2237 mRT	3 – 10%, Average 5%
	Anderson Fm A	2332.5 mRT	5 – 13%, Average 8%
	Anderson Fm A	2386 – 2389.5 mRT	11%
	Anderson Fm A	2398 – 2405 mRT	6%
	Anderson Fm A	2409.5 – 2421.5 mRT	9%
	Anderson Fm A	2436.5 – 2439.5 mRT	11%
	Anderson Fm A	2443.5 – 2452 mRT	9%
Lawford 1	Anderson Fm G to A	1661 – 2645 mRT	9.4%

Table 4.5. Anderson Formation porosity measurements (Lehmann and Haines, 1985; Smith, 1985a; Cookson and Jones, 2013).

Discussion and Framework – Carboniferous Section

The Carboniferous aged section is known from well data to exist within the study area, and has been mapped from 2D seismic to extend regionally. The Fairfield Group isochron (containing the Laurel Formation and Laurel Carbonate) is presented in Figure 6.23 and the Anderson Formation isochron is shown on Figure 6.22. The Fairfield Group is mapped to be the thickest down dip of the Stansmore Fault, thickening to 800 milliseconds TWT before thinning to 231 milliseconds thickness on the Kilang Kilang 1 high (20° 08'S, 127° 08'E). The Fairfield Group continues as a thick package to the south into the southern Gregory Sub-basin (20° 26S, 127° 31E), where it is anticipated to exceed 903 milliseconds TWT thickness. Across most of the Betty and Balgo Terraces the Fairfield Group package exists averaging 200 milliseconds TWT thickness. The Fairfield Group is truncated in the northern project area before reaching the Atrax 1 and Selenops 1 wells. A thicker portion of the Fairfield Group is noted atop the Billiluna Sub-basin graben (on the foot wall of the Mueller Fault, 19° 36S, 127° 34E) at a maximum of 519 milliseconds TWT thickness. The seismic interpretation (refer RB81-7, Figure 6.5) indicates a possible package of Fairfield Group in the Billiluna Sub-basin that reaches a near zero edge at the northeast basin margin (19° 30'S, 127° 35'E).

The Fairfield Group is intersected in wells Bindi 1, Kilang Kilang 1, Lake Betty1, Lanagan 1, Ngalti 1, Lawford 1 and Olios 1. Cross sections A-A' (Figure 4.44), B-B' (Figure 4.45) and C-C' (Figure 4.46) demonstrate the stratigraphic framework for the Fairfield Group (including the Laurel Carbonate). Well data confirms that the Fairfield Group thickens basinward (section A-A' and B-B') off the Betty and Balgo Terraces into the Gregory Sub-basin. It is apparent that primary carbonate buildup (the Laurel Carbonate) was concentrated on the Betty Terrace during Early Carboniferous time, between the Selenops 1/Atrax 1 area (19° 25'S, 127° 40'E) to the Lanagan 1/Lake Betty 1 area (19° 35S, 126° 25'E), and along depositional strike towards Ngalti 1 (19° 52'S, 127° 18'E). As Ngalti 1 intersected a similar thickness of carbonate to that at Lake Betty 1 (approximately 200 metres at each), and as the carbonate thickens substantially up dip at Olios 1, a suitable model would show carbonate development continuing up dip from Ngalti 1. The Carbonate transitions to fine grain lithotypes before reaching the Kilang Kilang 1 location (section B-B', Figure 4.45). A schematic showing a primary Laurel Carbonate depositional model is shown in Figure 4.27.

Seismic interpretation and isochron mapping demonstrates the extent of the preserved section of Anderson Formation within the project area. The Anderson Formation is either partially

removed (shown on line 82GE -33, Figure 6.4) or completely removed (shown on RB81-7, Figure 6.5) by truncation of the Meda Transpression Unconformity. The Anderson Formation isochron (Figure 6.22) clearly reveals the erosive outcome of the Meda Transpression Unconformity. The Anderson Formation is completely removed from large tracts of the project area. The Formation is only partly preserved to approximately 200 milliseconds TWT thickness across the southeastern Betty and Balgo Terraces. The thickest mapped preserved section is in the central project area, surrounding the Bindi 1 location (19° 43'S, 126° 49'E). It is anticipated that more preserved section of Anderson Formation could exist northeast of Bindi 1 (around 19° 34'S, 126° 58'E) where the isochron reaches a maximum of 1439 milliseconds TWT thickness. A relatively thick section (between 303 to 831 milliseconds TWT thickness) of preserved Anderson Formation is also mapped to exist in the hanging wall of the Stansmore Fault west of Kilang Kilang 1 (20° 11'S 127° 17'E). A preserved section is mapped to continue northwest along the Betty Terrace out of the project area, west of Atrax 1. The Anderson Formation does not extend north of the Mueller Fault onto the Billiluna Sub-basin.

4.7 Permo-Carboniferous

4.7.1 *Grant Group and Reeves Formation*

The Grant Group is a variably conformable succession of interbedded sandstones, siltstones and claystones. The Grant Group lies uncomfortably above the Anderson Formation (where the Anderson Formation is preserved) or over the Laurel Formation (where the Anderson Formation is removed by truncation). The base of the Grant Group is mapped on 2D seismic data as the regional Meda Transpression Unconformity, which separates Carboniferous and older strata from the Permo-Carboniferous and younger sediments. The Grant Group is mapped from seismic data to exist regionally within the project area, cropping out on the Balgo Terrace (refer to the Grant Group isochron, Figure 6.21) in the north and on the eastern basin margin. The Grant Group is intersected in all wells within the project area.

Age

Subdivisions of the Grant Group have proved difficult to correlate across the Canning Basin (Apak and Backhouse, 1999), and age control is sparse due to a lack of well intersections. Figure 4.31 demonstrates the variations in nomenclature of the Grant Group members. Apak and Backhouse (1998) redefined the Grant Group using available palynology data over the Barbwire Terrace, where they carry the upper section as the 'Grant Group' and a lower blocky sandstone renamed as the Reeves Formation (after Reeves Hill, a location west of the exploration well Fraser River 1, where the type-section for the Reeves Formation is derived). Apak and Backhouse (1999) place the members of their Grant Group within the *Pseudoreticulatispora confluens* Zone (Asselian to Sterlitamakian stage of the Early Permian). The Reeves Formation (formerly included within the Grant Group) is Visean to Stephanian (Figure 4.31).

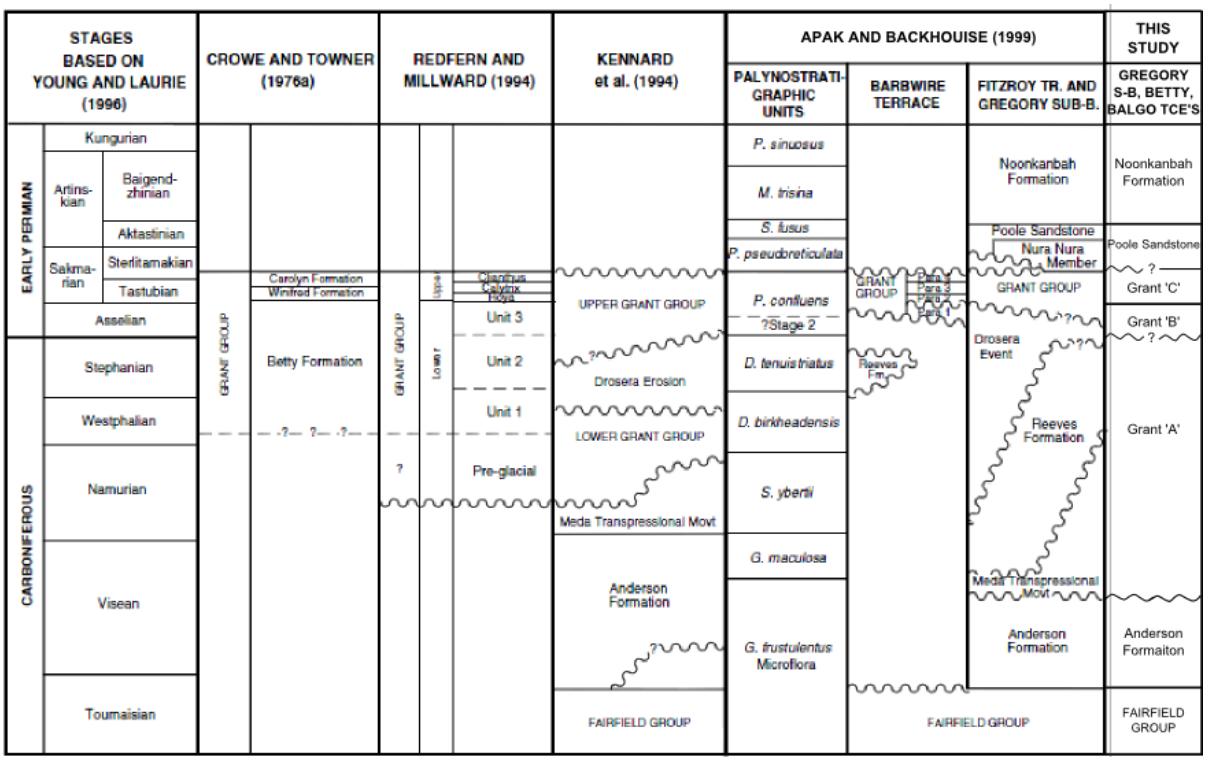

Figure 4.31 Age of the Grant Group (Modified after Apak and Backhouse, 1999).

Members of the Grant Group are challenging to correlate from the Barbwire Terrace (the focus area of Apak and Backhouse's work) across the Gregory Sub-basin to this study area. The Reeves Formation is generally the simplest to carry using geophysical logs, however the formation becomes challenging on the Balgo Terrace, where the blocky-sandstone log response becomes interbedded (refer Olios 1 and Atrax 1, Figure 4.32). The upper Grant Group members (Apak and Backhouse's parasequences 1-4, or older nomenclature – 'Carolyn', 'Winifred' and 'Betty' Formations) can be risky to nominate in a regional setting on well log data alone. To avoid nomenclature-related issues in this project, the members of the Grant Group and Reeves Formation are simply referred to using a genetic interval approach; Grant Group units 'A', 'B' and 'C' (oldest to youngest) (Figure 4.31) and correlated on that basis. No age related re-definition is proposed here. As a reminder, correlation sections A-A', B-B' and C-C' show the optimal frame for understanding the correlatives of the Grant Group, so the reader is referred to the correlations sections (Figure 4.44 to Figure 4.46) for visual assistance. The correlation framework is outlined in the Permo-Carboniferous discussion that follows.

Characteristics

Grant A

The lowermost member (also the Reeves Formation; Apak and Backhouse, 1998) is composed of an upper claystone and sandstone sequence, and a lower sandstone. The upper claystone is described as medium grey to greenish grey, finely micaceous, rarely carbonaceous, with variable amounts of very fine to coarse Diamictite ('dropstone' deposits). The upper sandstone is off-white to pale grey and translucent quartzose, medium to coarse grained, sub-angular to angular and rarely sub-rounded to rounded, pyritic in part, micaceous in part and feldspathic in part. Quartzite and biotite flakes are noted in variable amounts (Klappa et al, 1985a; 1985b).

The lower sandstone interval is described as pale grey, fine to coarse grained, angular to sub-angular and also sub-rounded to rounded in part, poorly sorted and loose, rarely pyritic, rarely feldspathic, variably coloured coarse grained (orange, rose, green grey and black) lithics and granitic fragments, rare quartzite chips and biotite are noted. The sandstone becomes better sorted to a predominant coarse grainsize with increasing depth. The lower interval also

features pale grey mottled micromicaceous claystone, grey carbonaceous siltstone and black hard fibrous coal fragments (Klappa et al, 1985a; 1985b).

Grant B

The Grant B member is comprised of sandstone, siltstone and claystone. The sandstone is pale grey to frosted, medium grained but rarely coarse, loose, sub-angular to rounded and rarely well-rounded, calcareous in part, trace pyritic, with trace lithic and carbonaceous fragments noted. The siltstone is light to medium grey and bluish grey, firm, massive, arenaceous in part and also argillaceous in part, rarely carbonaceous, with rare biotite noted. The claystone is light to pale grey, occasionally medium grey, very finely micaceous, arenaceous in part, carbonaceous, and contains sporadic very fine to fine quartzose grains in varying abundance (Klappa et al, 1985a; 1985b).

Grant C

The uppermost interval of the Grant Group consists of a sandstone interbedded with siltstone and claystone. The sandstone is pale to light grey, fine to medium grained but rarely coarse and also rarely silty in part, loose, angular to sub-angular, quartzose, coarsely micaceous, pyritic and feldspathic in part. The siltstone is light to medium grey, very finely micaceous, and carbonaceous. The claystone is dark grey, micromicaceous, blocky, and grades to carbonaceous shale in part, with black brittle coal fragments noted (Klappa et al, 1985a; 1985b).

Geophysical Log Characteristics

Grant C

Within the project area the top of the Grant Group is mostly represented on wireline logs as a sharp inflected gamma ray contact that represents a disconformity between the Permian Poole Sandstone and the Grant Group. Where the sharp contact is not present and the contact is gradual (Lanagan 1 and Bindi 1) a conformable contact is proposed. A mostly complete

section of Grant C is observed at Bindi 1, where the interval 990 mRT to 1060 mRT is removed in other wells in the project area.

The top of Grant C is marked by a shale that shows an inflection on the gamma ray response and deflection on the resistivity and sonic log responses. Underneath the capping shale, the Grant C interval shows either a coarsening upward gamma ray (as at Selenops 1, Olios 1), a low baseline gamma ray (as at Lake Betty 1, Lanagan 1, Ngalti 1), or an interbedded gamma ray log response (such as at Bindi 1 or Kilang Kilang 1). Where the gamma ray response shows a low sandstone baseline or sandstone interbeds (for example at Olios 1, Bindi 1 and Kilang Kilang 1) the resistivity log shows elevated values and the density log shows a decreased trend.

Grant B

Grant B is the most inconsistent in terms of geophysical log characteristics within the Grant Group. Lanagan 1, Lake Betty 1, Olios 1 and Ngalti 1 show the top of Grant B represented by a sharp contact inflection on the gamma ray log. The Sonic log shows a similarly shaped deflection at the same point. Kilang Kilang 1 shows a sharp contact deflection at the top of the interval with a similarly shaped inflection on the sonic log. The sharp contact may indicate a disconformable contact to the overlying Grant C interval. The top of Grant B at Bindi 1 is picked at the top of an invariable gamma ray response below a fining upwards sequence. The gamma ray log in all wells is variable over the interval, showing a variety of fining upwards and coarsening upwards patterns, as well as blocky interbedded signatures. At Lake Betty 1 and Lanagan 1, a stepwise increasing shift in the resistivity and sonic logs are observed approximately in the middle of the interval.

Grant A

Grant A is the simplest interval in the Permo-Carboniferous section to identify and correlate on geophysical logs. The top of Grant A is identified by a decrease baseline shift in the gamma ray response. Over the interval, the gamma ray log is both consistently low and blocky (Lake Betty 1, Lanagan 1, Bindi 1, Ngalti 1, Kilang Kilang 1), or shows a blocky variable interbedded sequence (Olios 1 and Lawford 1) but in every case the gamma ray

response shows a generally low baseline. The resistivity, density and sonic logs over the interval is generally invariable with the exception of Olios 1 that shows a variable character to match the interbedded gamma ray response.

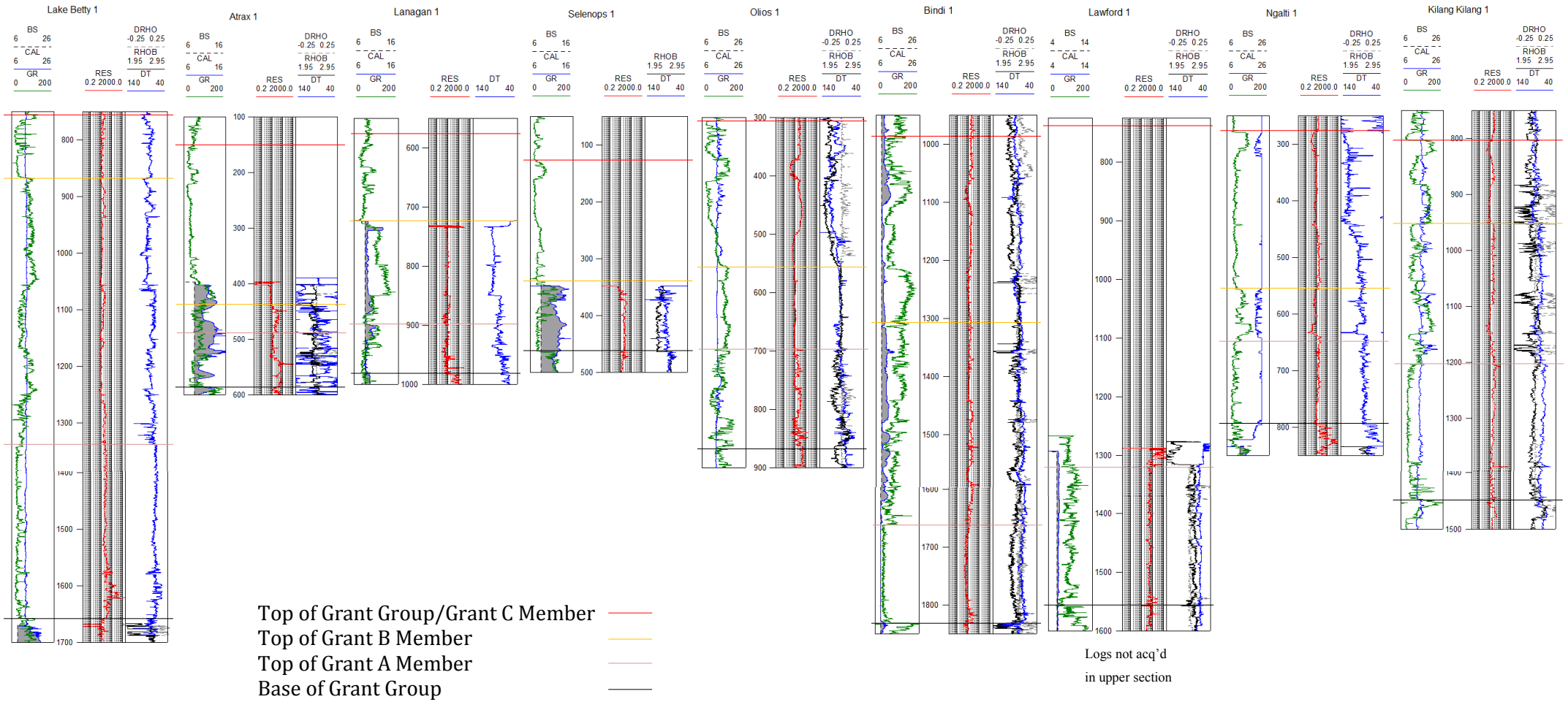

Figure 4.32. Geophysical log definition of the Grant Group across the project area. Well are labelled (modified after Crank, 1972; Klappa et al., 1984; Lehmann and Haines, 1985; Klappa et al., 1985a; 1985b; Smith, 1985a; 1985b; NSO, 2008; Cookson and Jones, 2013).

Depositional Setting

The overall mixed grainsize components (medium to coarse grained sandstones) with poorly sorted character represent variable flow regimes, with an overall larger grainsize, representative of higher energy depositional flows, likely upper flow regime. The rip up clasts of claystones, vari-coloured lithics and granitic fragments is evidence of reworking. Coal fragments in the lower section hint at a near-by terrestrial environment. The interval comprising both Grant A and the lower-most section of Grant B (1500 mRT to 1830 mRT) at Bindi 1 capped by a probable transgressive surface (TSE) points to a low stand system (higher rate of sediment supply relative to rate of accommodation generation). This is suggestive of a regressive environment, with high percentage coarse-grainsize sedimentation, possibly a delta mouth or strand plain (Figure 4.33 and Figure 4.34).

A transgressive systems tract overlies the low stand, between a potential TSE at 1500mRT, to a maximum flooding surface (MFS) at 1260 mRT at Bindi 1. Aggradational sequences are observed on the gamma ray log separated by minor flooding events at 1360 mRT and 1445 mRT. This transgressive system, comprised of finer grained sediments (medium sands, siltstone and claystone) reflected in a higher baseline gamma ray response, indicates slightly lower energy deposition (than the lowermost LST) due to higher base level; likely mid-plain to lower plane bed energy. This is indicative of a transgressive environment, such as an embayed coast or tidal influenced estuary. The Diamictite (‘drop stones’) noted throughout Grant A are validation of a glacial period in the Late Carboniferous, discussed by Apak and Backhouse (1999).

A maximum flood lies at 1247 mRT. This MFS indicates higher base level, and higher rates of accommodation relative to the rate of sediment supply. A transgressive surface lies at 1215 mRT. This transgressive surface likely represents a period of erosion due to higher local energy flows, where the erosional surface is potentially a remnant of subaerial exposure, removing some (or most) of the underlying high stand (HST) and subsequent low stand (LST), and is therefore also the location of a sequence boundary (SB). Surface incisions (incised valleys) are expected due to subaerial exposure and are identified by Apak and Backhouse (1999).

The upper section of the Grant Group in Bindi 1 represents a transgressive system (TST), above the SB at 1215 mRT. The finer grained sediments (fine grained sandstones, siltstones and claystones) represents lower plain bed energy, and a higher base level. The gamma ray

log response confirms intermittent aggradational periods as well as fining up sections. The observed coal fragments (rip ups) suggests a nearby terrestrial environment (Figure 4.35). The upper unit is suggestive of a transgressive setting, such as a tidal influenced estuary. A flooding surface caps the top of the Grant Group.

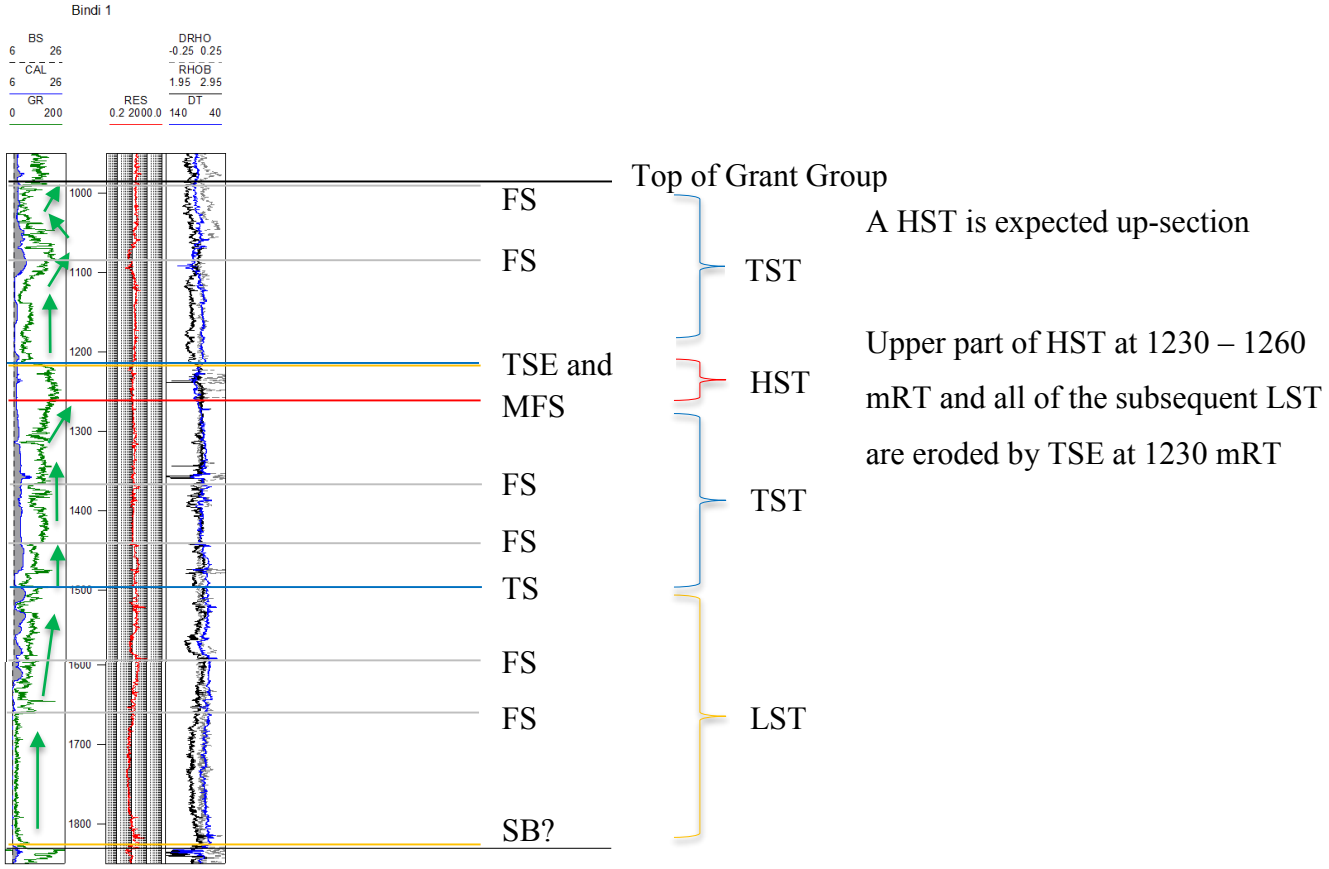

Figure 4.33. Bindi 1 geophysical log. Sequence stratigraphic analysis overlain (modified after Lehmann and Haines, 1985).

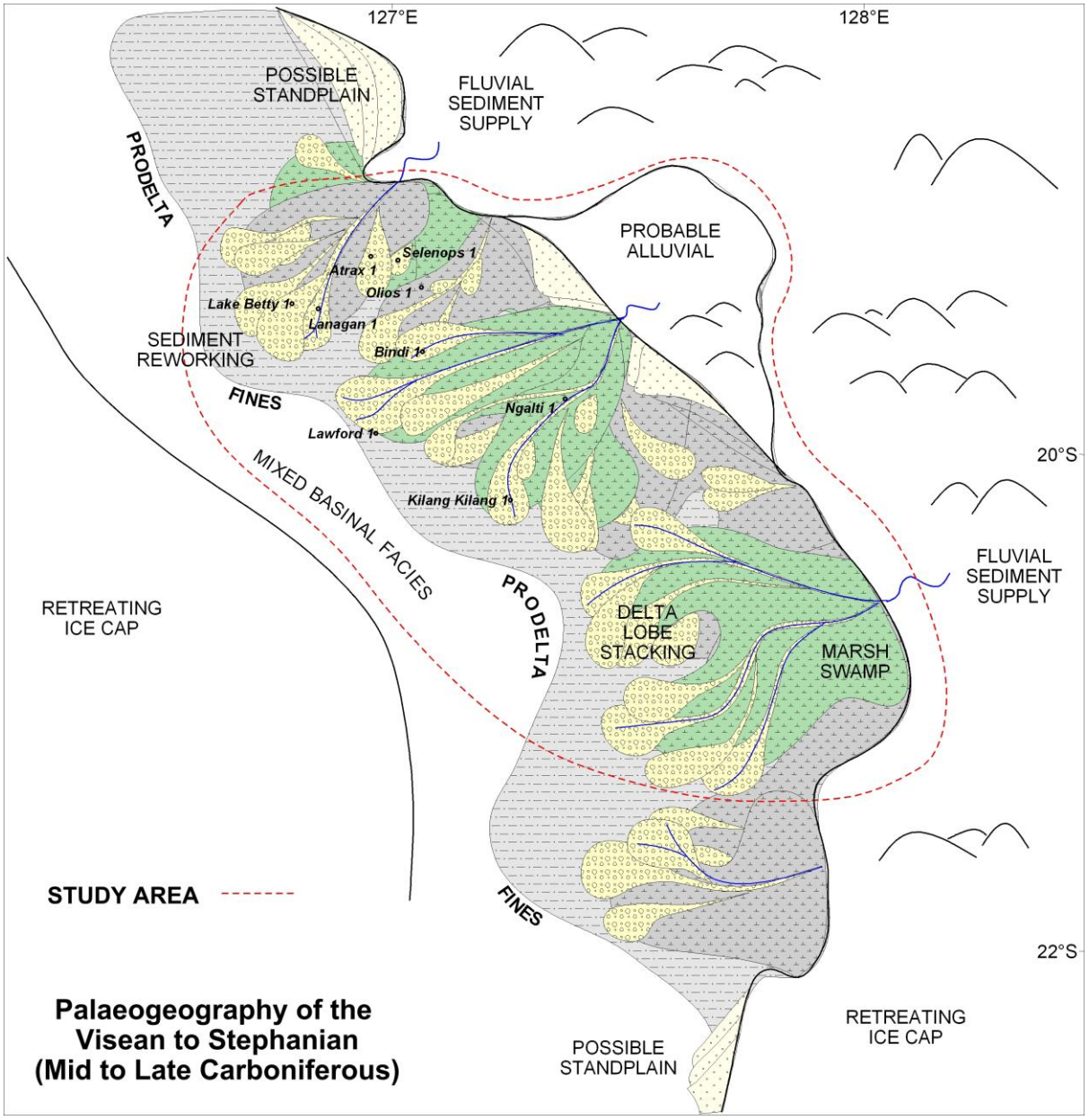

Figure 4.34. Palaeogeography of the Visean to Stephanian (modified after Wulff, 1987).

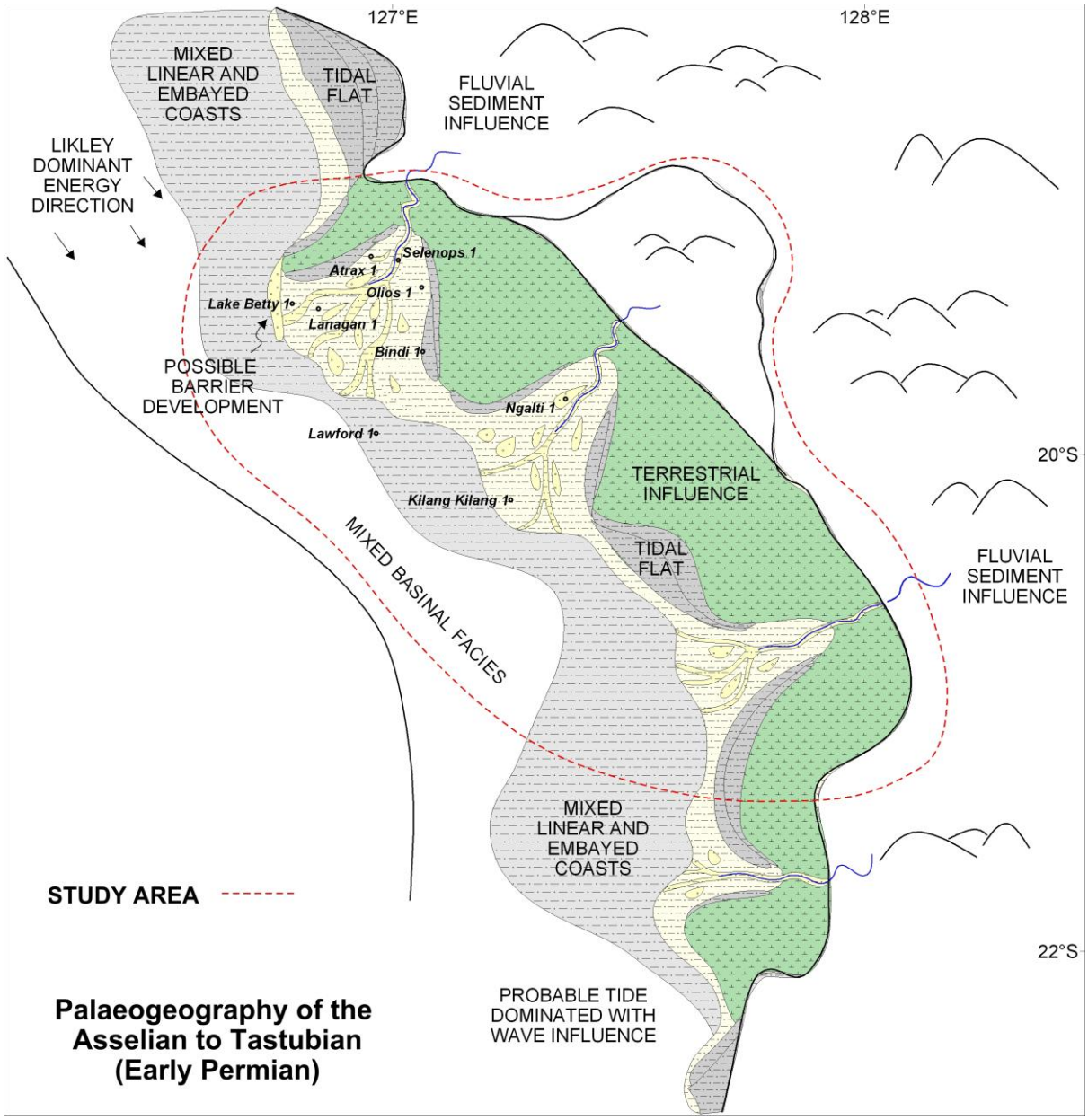

Figure 4.35. Palaeogeography of the Asselian to Tastubian (modified after Wulff, 1987).

Reservoir Properties

Sonic derived porosities were calculated at Bindi 1, Olios 1, Atrax 1, Ngalti 1 and Kilang Kilang 1 by the well operators, revealing excellent reservoir quality (Table 4.6 and Figure 4.36). Excellent reservoir properties are confirmed by core data measurements at Atrax 1, showing 18.5% porosity and 754 – 1015 mD permeability in Grant unit A (Figure 4.36).

Well	Unit	Interval	Porosity (%, Sonic derived)
Ngalti 1	Grant C to A	280 – 796 mRT	13 – 40%, Average 20%
Kilang Kilang 1	Grant C	831 – 882 mRT	18 – 25%
	Grant B	952 – 985 mRT	20%
	Grant B	1005 – 1097 mRT	10 – 18%
	Grant B	1149 – 1161 mRT	20%
	Grant A	1204 – 1447 mRT	8 – 18%, Average 12%
Bindi 1	Grant C	990 mRT	13 – 30%, Average 21%
	Grant C	1303.5 mRT	5 – 22%, Average 13%
	Grant B	1583 mRT	7 – 18%, Average 10%
	Grant A	1662 mRT	7 – 20%, Average 12.5%

Table 4.6. Grant Group porosity measurements (Lehmann and Haines, 1985; Smith, 1985a; 1985b).

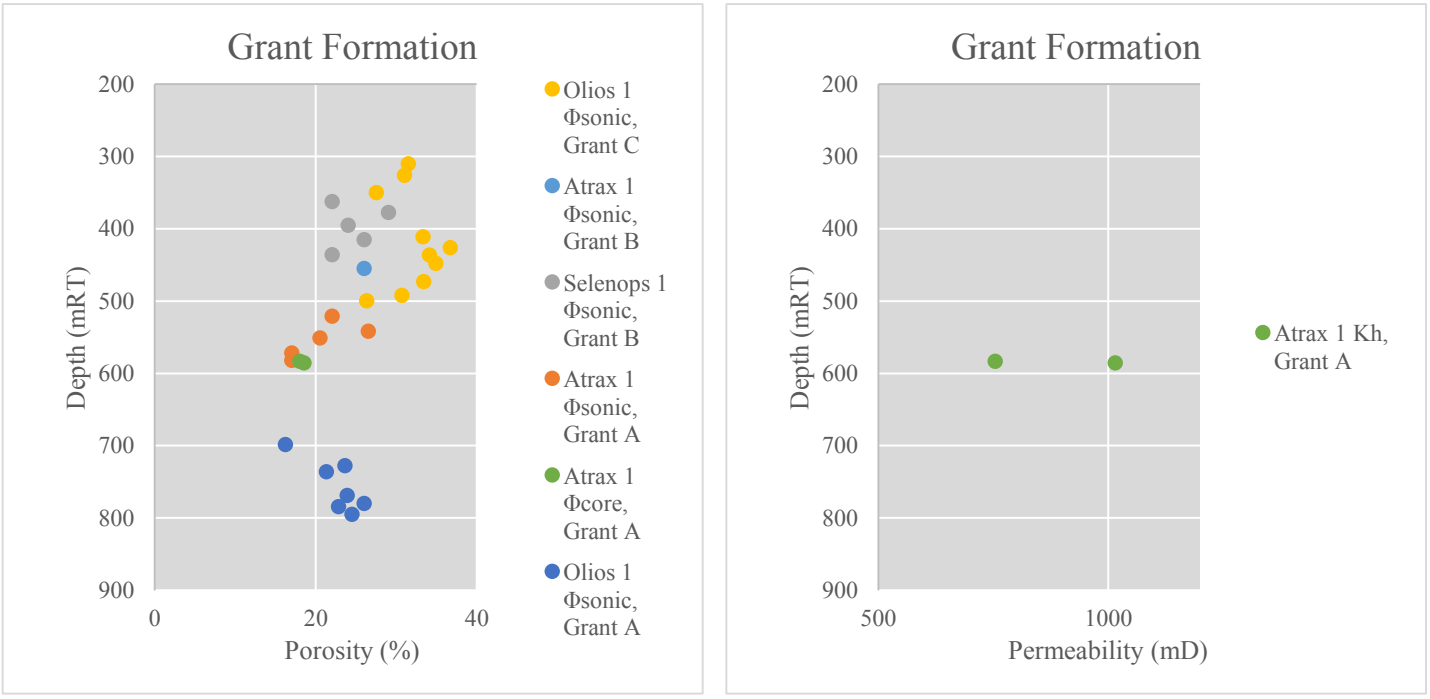

Figure 4.36. Grant Formation porosity and permeability measurements (Klappa, 1984; Klappa et al., 1985a; 1985b).

Discussion – Permo-Carboniferous Section

The Grant Group isochron (Figure 6.21) shows that the Grant Group exists regionally within the project area. The Grant Group thins to a near zero edge on the Balgo Terrace in the north (16° 21’ S, 126° 46’ E) and in the north east (19° 43’ S, 127° 33’ E) or intersects the Mueller Fault at the Billiluna Sub-basin boundary. The Grant Group A, B and C intervals gradationally thicken and deepen in a south-southwest direction off the Balgo Terrace in the northern project area (around the Selenops 1 well towards Lawford 1) to 500 milliseconds TWT thickness, as is also demonstrated on the section A-A’ (Figure 4.44). In the central project area (19° 37’ S, 127° 12’ E), the isochron shows that the Grant Group thickens in the central area depocentre to 1 second TWT thickness, before thinning over Ngalti 1 and the Kilang Kilang 1 area to 200 milliseconds TWT thickness (section B-B’, Figure 4.45). In the south eastern study area the Grant Group is mapped to thicken in broad patches to 900 milliseconds TWT thickness on the Betty Terrace (20° 06’ S, 127° 29’ E) and Balgo Terrace (20° 20’ S, 127° 59’ E) before intersecting the

eastern basin margin. Section C-C' (Figure 4.46) confirms that the Grant Group thickens between Kilang Kilang 1 and Lake Betty 1, through the central depocentre (at Bindi 1), which is confirmed by seismic mapping. The Grant Group is mapped to thicken southwestward into the Gregory Sub-basin in excess of 600 milliseconds TWT thickness.

4.8 Permian

4.8.1 *Poole Sandstone*

The Permian (Sakmarian) Poole Sandstone is a regionally extensive sandstone package that is intersected by all wells within the study area. The unit underlies the Noonkanbah Formation, where the contact is generally conformable though sharp (Kilang Kilang 1, Ngalti 1, Bindi 1, Lake Betty 1) in the basinward portion of the study area, but also gradual in places (Lanagan 1, Olios 1) in the northeastern project area. The Poole Sandstone overlies the Grant Group with a disconformable contact.

Age

Two sidewall cores at Bindi 1 (921 mRT and 930.1 mRT) reveal high palynomorphs yields, and indicate the Poole Sandstone to be of Asselian to Sakmarian (Early Permian) age (Lehmann and Haines, 1985).

Characteristics

The Early Poole Sandstone is predominantly a sandstone unit, with interbeds of siltstone and claystone. The sandstone is clear to frosted, medium to coarse grained but also fine grained in part, rounded to sub-angular, moderately to poorly sorted, commonly friable and unconsolidated, micaceous in part, in a argillaceous quartzose flour matrix. The siltstone is dark grey to black, micromicaceous and argillaceous. The claystone is black, soft, micromicaceous and slightly arenaceous. Minor amounts of black, blocky, vitrinitic to sub-vitrinitic coal is also observed in the interval (for example at Kilang Kilang 1), giving a 'salt and pepper' texture to cuttings (Smith, 1985a).

At Bindi 1 (central study area) the Poole Sandstone is more argillaceous; comprised mostly of interbedded claystones and sandstones (Lehmann and Haines, 1985) (described as above) with 10 metres of blocky sandstone at the top of the interval. A 3 metre thick claystone lies at the base.

At Lake Betty 1 (northeastern project area) the Poole Sandstone was observed mainly as a sandstone; finer grained than in the southern area (observed as a very fine to fine grained interval and silty in part; Crank, 1972), and often grades to siltstone and minor shale; grey, sub-fissile to blocky and pyritic in part. A lower (5 metre thick) claystone is present in the northern project area at Atrax 1, described as dark grey, soft to firm, massive to sub-fissile, micaceous, carbonaceous to coaly and resinous to earthy (Klappa et al, 1985a).

Geophysical Log Characteristics

The top of the Poole Sandstone on geophysical logs (Figure 4.37) is represented by a sharp deflection in the gamma ray log (at Lake Betty 1, Bindi 1, Ngalti 1 and Kilang Kilang 1) or a gradational reduction in gamma ray response (at Lanagan 1 and Olios 1). A subtle but sharp infection in the sonic log response is also noted (at Lake Betty 1 and Ngalti 1) though a sharp deflection in the sonic log at the top of the interval is noted at Kilang Kilang 1.

Over the interval, the gamma ray response is usually observed as a low base line and shows a blocky character. Exceptions to this are at Bindi 1, Olios 1 and Lanagan 1, where the Poole Sandstone is more argillaceous. The resistivity log response is uniform over the interval, as is the sonic and density log responses (an exception to this is noted at Ngalti 1 and Kilang Kilang 1; where the sonic log reduces in baseline character (below 250 mRT at Ngalti1) or increases in baseline character (below 730 mRT at Kilang Kilang 1, representing calcareous content in the lower Nura Nura member).

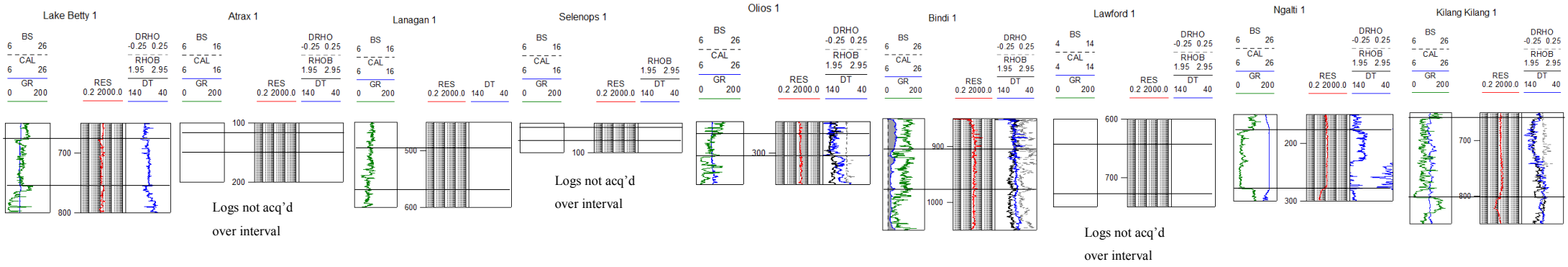

Figure 4.37. Geophysical logs over Poole Sandstone across project area. Wells labelled (modified after Crank, 1972; Klappa et al., 1984; Lehmann and Haines, 1985; Klappa et al., 1985a; 1985b; Smith, 1985a; 1985b; NSO, 2008; Cookson and Jones, 2013).

Depositional Setting

The lower claystone at Bindi 1 and Lake Betty 1 is labelled elsewhere in the basin as the Nura Nura member. The Nura Nura member represents the flooding surface separating the Poole Sandstone from the Grant Group.

Acritarchs observed in the Poole Sandstone at the Bindi 1 location indicate a marginal marine to shallow marine environment. Increasing concentrations of acritarchs at the base of the interval (also featuring a claystone zone at the base) suggests a lower marine portion and a higher energy environment up-section, terminating in blocky sandstone at the top. Coal observed at Kilang Kilang 1 indicates a nearby terrestrial environment. This indicates a regressive environment for the Poole Sandstone overall; possibly a tide dominated estuary at the base connected to a fluvial sediment source, prograding to a deltaic environment. The blocky sandstones are possible stacked delta lobes (Figure 4.38).

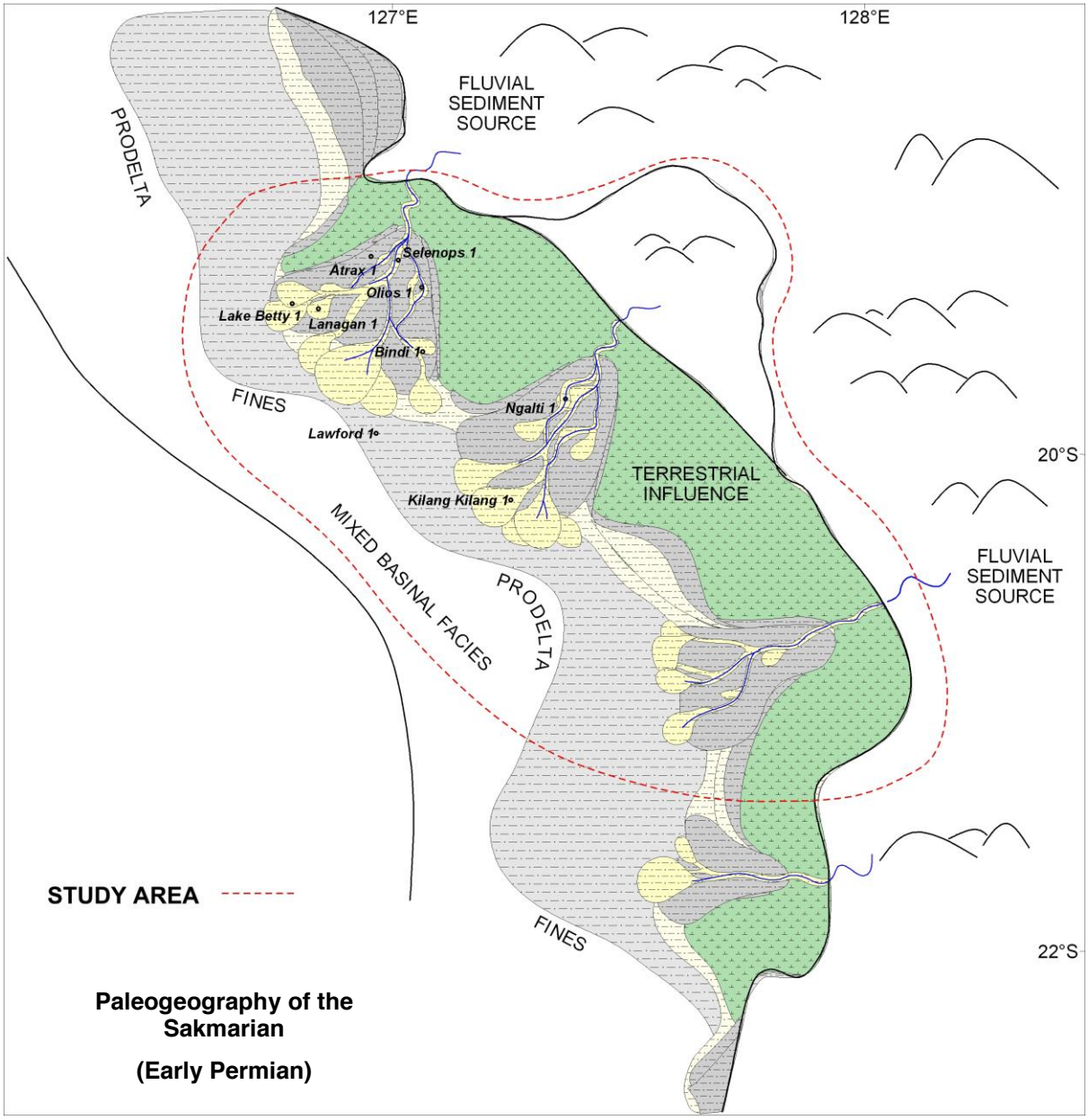

Figure 4.38. Paleogeography of the Sakmarian (modified after Wulff, 1984)

Reservoir Properties

Sonic derived porosities were calculated at Ngalti 1, Bindi 1, Olios 1 and Kilang Kilang 1 for the Poole Sandstone, revealing excellent reservoir quality (Table 4.7), in excess of 20% porosity across the study area. Note that as the porosity results are derived from the sonic log, the very high sonic porosities observed at Ngalti 1 are perhaps unrealistic, given the baseline decrease in the sonic log from 231 mRT.

Well	Interval	Porosity (%, Sonic derived)
Ngalti 1	178 – 280 mRT	29 – 40%
Kilang Kilang 1	661 – 803 mRT	23 – 35%
Bindi 1	910 mRT	20 – 27%, Average 25%
Olios 1	275 – 299 mRT	28 – 32.6%, Average 30%

Table 4.7 Poole Sandstone porosity measurements (Klappa et al., 1984; Lehmann and Haines, 1985; Smith 1985a; 1985b).

Discussion and Framework

The Poole Sandstone is mapped to exist regionally throughout the project area. Isochron mapping (Figure 6.20) demonstrates the package thickens to 210 milliseconds TWT in the southern project area within the Gregory Sub-basin (20° 34’ S, 127° 29’ E). The Poole Sandstone gradually thins northwards onto the Betty Terrace to 100 milliseconds TWT (20° 02’ S, 127° 27’ E), and continues to thin in a northward direction onto the Balgo Terrace, averaging 50 milliseconds TWT thickness in broad areas across the northern half of the project area. The Poole Sandstone thins to 21 milliseconds TWT thickness on the Balgo Terrace (20° 03’ S, 127° 58’ E) before reaches a near-zero edge on the eastern and northern basin margins. The Pool Sandstone is mapped to not exist on the Billiluna Sub-basin.

Isochon mapping of the Poole Sandstone (Figure 6.20) shows little variability in TWT thickness across the study area. This is confirmed in cross sections A-A’, B-B’ and C-C’

(Figure 4.44 through Figure 4.46). Sections A-A' (Figure 4.44) and B-B' (Figure 4.45) show a uniform thickness correlation for the package, which is agreeable with the isochron mapping. Section C-C' (Figure 4.46) shows a slight thinning between Kilang Kilang 1 and Bindi 1 (142.5 metres to 80 metres), also visible on the isochron (thinning from 100 milliseconds to 49 milliseconds TWT).

4.8.2 *Noonkanbah Formation*

The Early Permian (Aktastinian to Baigendzhinian) Noonkanbah Formation is a regionally mappable shale and interbedded siltstone interval that conformably overlies the Poole Sandstone. The Noonkanbah Formation represents the Maximum Permian Transgression in the Canning Basin.

Age

Palynological evidence at Lake Betty 1 (431 – 635 mRT) suggests an Early Permian – Artinskian (Vittanina Assemblage of Balme 1964) age for the Noonkanbah Formation.

Characteristics

The Noonkanbah Formation is observed as mostly shale interbedded with siltstone. The shale is described as light and dark grey to blackish grey, soft and sticky, blocky to sub-fissile, micaceous, arenaceous in part, calcareous in part, carbonaceous in part, and pyritic. The siltstones are observed as light and dark grey, argillaceous, micaceous, carbonaceous in part and rarely grade to very fine sandstone. The rare thin sandstone interbeds are described as light to medium grey, very fine grained, sub-angular, poorly sorted and unconsolidated in part (Klappa et al, 1985a; 1985b; Lehmann and Haines, 1985; Smith, 1985a; 1985b).

Geophysical Log Characteristics

The Noonkanbah Formation is characterized with an increase in gamma ray baseline from the overlying Triassic aged rocks and underlying Poole Sandstone (Figure 4.39). The baseline

difference is more pronounced in the southeastern project area at Ngalti 1 and at Kilang Kilang 1 (though the top of the interval is not acquired on logs at Kilang Kilang 1). The gamma ray response is subtly variable in small blocky packages over the zone. A subtle decrease in resistivity baseline is also noted over the interval. The Noonkanbah Formation is observed to have a generally invariable resistivity and sonic log response.

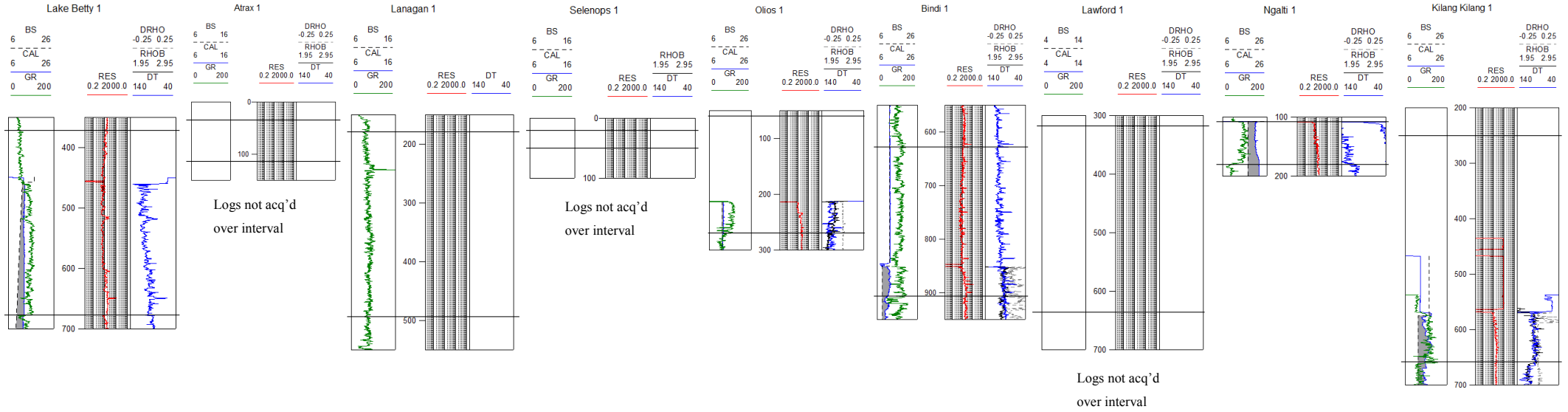

Figure 4.39. Geophysical logs over the Noonkanbah Formation across the project area (modified after Crank, 1972; Klappa et al., 1984; Lehmann and Haines, 1985; Klappa et al., 1985a; 1985b; Smith, 1985a; 1985b; NSO, 2008; Cookson and Jones, 2013).

Depositional Setting

The overly fine-grained nature of the formation (shale and siltstones) indicates low velocity flow (lower plane bed) energy. Rare intermittent sandstones indicate periods of higher energy environments or lower base level. The Noonkanbah Formation represents a maximum base level during Permian time. A shallow marine to marginal marine depositional environment is evident; potentially influenced by a restricted marine environment such as an estuary (Figure 4.40).

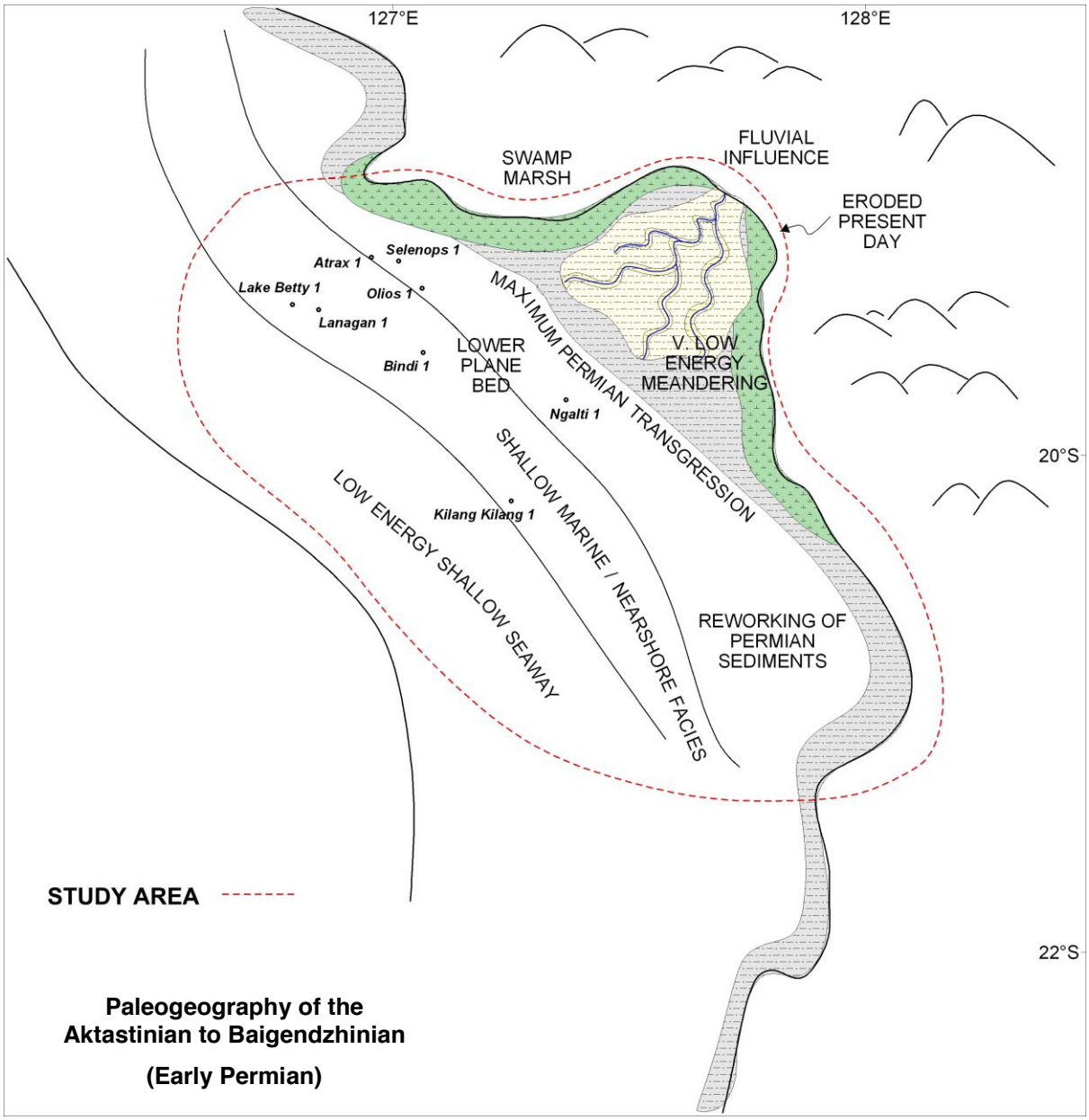

Figure 4.40. Paleography of the Aktastinian to Baigendzhinian (modified after Wulff, 1984).

Reservoir Properties

Sonic derived porosities were calculated at Bindi 1 and Olios 1 (Table 4.8). The sonic calculated results are potentially deceptive given the fine grained nature of the formation. Lithologic descriptions and well log character suggest the Noonkanbah Formation to be a regional seal across the study area, where it is expected to be tight. There is no core data on hand for the Noonkanbah Formation.

Well	Interval	Porosity (%, Sonic derived)
Bindi 1	629 mRT	10 - 30%, Average 17%
Olios 1	235.5 – 254 mRT	14.9 – 19.1%, Average 17%

Table 4.8. Noonkanbah Formation porosity measurements (Klappa, 1984; Lehmann and Haines, 1985).

Discussion and Framework

The Noonkanbah Formation is mapped to exist across the project area. Isochron mapping shows that the package thickens to 443 milliseconds TWT southwest of Kilang Kilang 1 (20° 15' S, 127° 02' E). The Noonkanbah Formation is essentially isopachus (invariable in time-thickness) across large portions of the project area, averaging 270 milliseconds TWT thickness (ranging 250 to 300 milliseconds TWT thickness) in the southern portion of the project area. The package gradually thins to 70 to 120 milliseconds TWT in the northwestern study area (around Lake Betty 1 and Lanagan 1). The Noonkanbah Formation continues to thin to a near-zero edge in the northeast, and does not exist on the Billiluna Sub-basin.

Cross sections A-A', B-B' and C-C' (Figure 4.44 to Figure 4.46) show good agreement between the isochron mapping and the well thicknesses. The Noonkanbah Formation thickens into the Gregory Sub-basin between Ngalti 1 and Kilang Kilang 1 (66 metres to 406.5 metres; section B-B', Figure 4.45) and thins between the southeast and northwestern areas via Bindi 1 (section C-C', Figure 4.46). In the northwestern project area (section A-A', Figure 4.44) the package is generally isopachus until it thins dramatically at Selenops 1 (where it is 26 metres thick).

4.8.3 *Liveringa Group*

Age

The Liveringa Group is a conformable succession of sandstone and siltstone intersected in all study area wells, except Atrax 1. The Liveringa Group (in complete preserved section) comprises the Condren Sandstone, Godfrey Beds, Hardman Formation, Lightjack Formation and Triwhite Sandstone. The preserved section within the study area, however, is limited to the Condren Sandstone and Lightjack Formation, implying a period of erosion or non-deposition between members. Palynological evidence at Lake Betty 1 suggests a Late Permian age (Dulhuntyspora Assemblage of Balme, 1964) for the Liveringa Group.

4.8.4 *Liveringa Group – Condren Sandstone*

Characteristics

The Condren Formation comprises sandstone and siltstone. The sandstone component is off-white, light to medium grey, coarse grained, rarely fine grained, sub-angular to sub-rounded and rounding improves with depth, clean and loose quartzose, rarely pyritic and carbonaceous. Minor coal is observed. The lower portion of the formation shows very fine to fine grained sandstone that is angular to sub-angular and grading to siltstone in part. The main siltstone component is medium grey, grading to very fine sandstone in part, micromicaceous, rarely pyritic, and shows fine carbonaceous flecks.

4.8.5 *Liveringa Group – Lightjack Formation*

Characteristics

The Lightjack Formation is characterized by sandstone interbedded with siltstone and claystone. The sandstone is off-white and pale grey grading to medium brownish grey, very fine grained and grading to siltstone in part, angular to sub-angular, quartzose, micaceous and pyritic. The claystone intervals are light to medium grey, sub-fissile to blocky, arenaceous in part and grading to very fine sandstone in part, occasionally carbonaceous, rarely pyritic and rarely calcareous (Crank, 1972; and Lehmann and Haines, 1985). The siltstone is light grey, grades to very fine sandstone in part, very micaceous, slightly to moderately calcareous in

part and carbonaceous in part. Brachiopods are observed at Bindi 1 between 520 mRT to 525 mRT and 560 mRT to 565 mRT along with shell fragments (Lehmann and Haines, 1985).

Liveringa Group – Geophysical Log Characteristics

Note: Geophysical logs were only recorded over the interval at Bindi 1, Lanagan 1 and Ngalti 1. Referring to Bindi 1; the top of the Liveringa Group (Condren Sandstone) is marked on wireline logs as a baseline decrease in the gamma ray, resistivity and sonic log responses (Figure 4.41). The gamma ray is generally low and blocky over the interval and shows a coarsening upwards trend, whereas the sonic and resistivity logs parallel each other with a gradual increase in baseline with increasing depth. The top of the Condren Sandstone member is represented on geophysical logs as a baseline increase in gamma ray response and increases in baseline to the resistivity and sonic log responses. Over the Condren Sandstone member, all geophysical logs display a homogeneous response. In cuttings (where no logs were acquired) the Condren Sandstone is represented by the intersection of finer grained lithologies

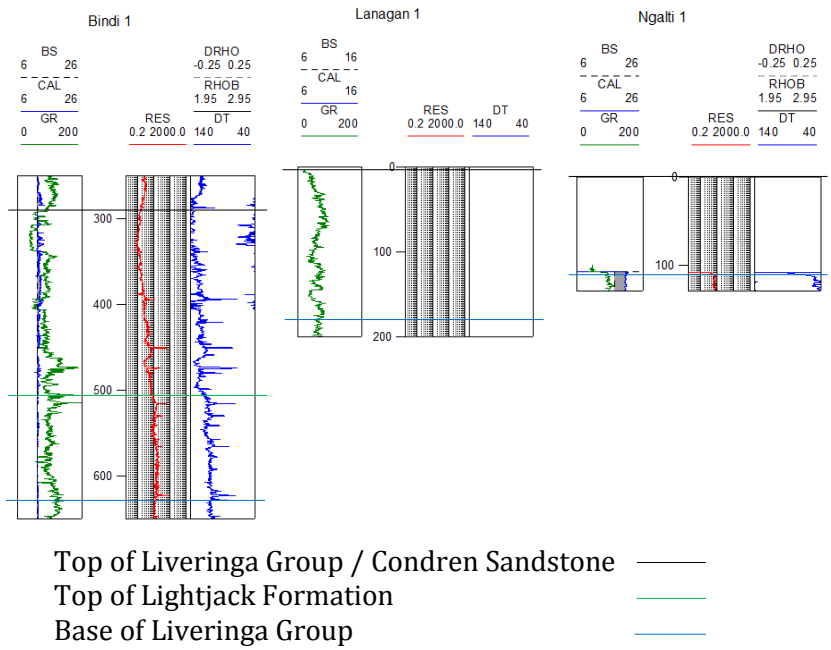

Figure 4.41. Geophysical logs over Liveringa Group (modified after Lehmann and Haines, 1985; Smith, 1985b; NSO, 2008).

Depositional Setting

The fine grained sandstone, siltstone and claystone indicates low energy flow (low plane bed deposition) within the Lightjack Formation. The brachiopods and shell fragments observed at Bindi 1 indicate a marine influence on deposition. The coarser grained sediments within the Condren Sandstone indicate a change to a higher energy environment. An overall coarsening trend is apparent up section. A maximum flooding surface (MFS) is located within the Noonkanbah Formation (Figure 4.42), which places the lower Liveringa Group within a high stand (HST). A sequence boundary is likely present at 463.5 mRT at Bindi 1, with the upper Liveringa Group (most of the Condren Sandstone) representing a low stand (LST). A shallow marine or marginal marine environment is assigned to the Lightjack Formation (evidenced by Palynology confirmation at Lake Betty 1, and brachiopods at Bindi 1), and a regressive fluvial dominated environment is assigned to the Condren Sandstone.

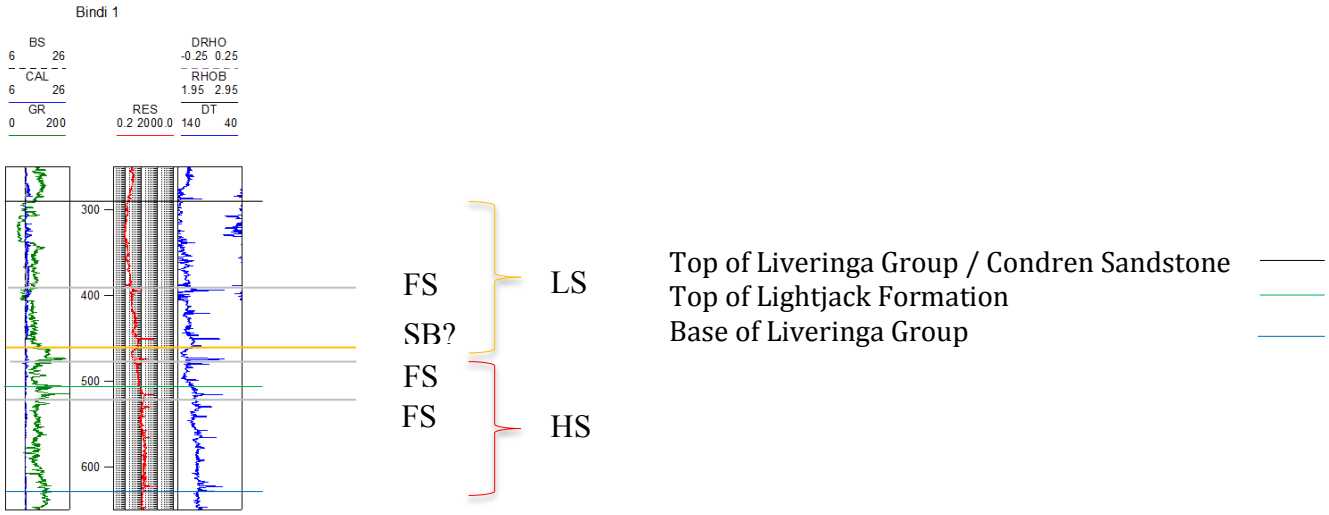

Figure 4.42. Bindi 1 geophysical log. Sequence stratigraphic analysis overlain (modified after Lehmann and Haines, 1985).

Reservoir Properties

Sonic derived porosities were calculated at Kilang Kilang 1 for the Liveringa Group, presenting excellent reservoir quality, ranging between 21% and 30% porosity (Table 4.9).

Well	Interval	Porosity (%, Sonic derived)
Kilang Kilang 1	48 – 167 mRT	25 – 29%
	200 - 320 mRT	21 - 30%

Table 4.9. Liveringa Group porosity measurements (Smith, 1985a).

Framework

No mappable package exists for the Liveringa Group on seismic data, and only 3 wells intersected the formation. A thin, generally isopachus unit is anticipated for the Liveringa Group within the project area, potentially thickening slightly towards the southwest, similar to the way of other Permian sediments.

4.8.6 *Millyit Sandstone*

The Late Permian – Early Triassic Millyit Sandstone is only present at Bindi 1.

Characteristics

The Millyit Sandstone is predominantly a sandstone unit. The sandstone is observed light grey to brownish grey, very fine grained grading to fine and medium grained with depth (though also rare well-rounded coarse grains are noted), sub-angular, quartzose, micaceous in part, rarely glauconitic, showing occasional carbonaceous flecks. Occasional small bivalve shell fragments are noted at Bindi 1 between 260 mRT to 286 mRT (Lehmann and Haines, 1985).

Geophysical Log Characteristics

The top of the Millyit Sandstone is characterized by a baseline increase on the gamma ray log response (Figure 4.43). The top is only marginally recorded on wireline logs (sonic and resistivity) but show an elevated subtle broad bell shape response over the zone. The gamma ray response is subtly bell shaped to blocky, with subtle variability.

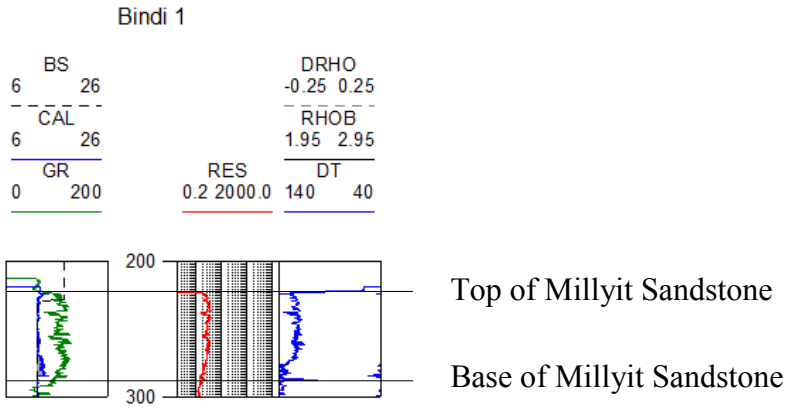

Figure 4.43. Bindi 1 geophysical log over Millyit Sandstone (modified after Lehmann and Haines, 1985).

Depositional Setting

The variable grain sizes present throughout the Millyit Sandstone indicates either changes to base level or a mixture of depositional influences during Late Permian – Early Triassic time. The concentration of sandstone along with the presence of carbonaceous lithotypes and shell fragments suggests multi-environment influences, potentially in a near-shore dominated territory. The low stand present in the underlying upper Liveringa Group indicates the Millyit is likely a continuation of a regressive environment, potentially near-shore shallow marine, such as strand plain or intertidal zone.

Framework

No mappable package exists for the Millyit Sandstone on seismic data. A thin, generally isopachus unit is anticipated for the Millyit Sandstone within the project area, potentially thickening slightly to the southwest, with other Permian sediments.

4.9 Triassic and Younger

Triassic and younger rocks were intersected at Bindi 1 and Lake Betty 1.

4.9.1 *Blina Shale*

The Blina Shale was intersected at Bindi 1 and Lake Betty 1.

Characteristics

The Blina Shale is predominantly a siltstone, based on the single well intersection at Bindi 1 (Lehmann and Haines, 1985). The siltstone is observed as pale to light grey, firm and slightly friable, mostly argillaceous in part but also arenaceous and grading to very fine sandstone in part. It is micaceous, showing occasional carbonaceous flecks and is rarely glauconitic. Minor silty light grey glauconitic claystone is also noted in the interval.

Geophysical Log Characteristics

No geophysical logs were acquired over the interval.

Depositional Setting

The overall fine grain sizes within the Blina Shale indicates a low energy flow regime, with subtle base level alterations suggested by the minor claystone and arenaceous components. The observations noted for the Blina Shale (without log data) are consistent with the tidal flat

environment presented by Yeates and Muhling (1977). The siltstone at Bindi 1 is potentially a shoreline component with sediment supply from longshore drift.

4.10 Summary of Results

Table 4.10 summarizes the stratigraphy within the project area, highlighting lithological characteristics and reservoir properties, as a quick guide for future reference.

AGE	FORMATION	UNIT / MEMBER	RESERVOIR	SEAL	AVE POROSITY (%)	AVE PERMEABILITY (mD)	LITHOLOGY	COMMENTS
TRIASSIC	Blina Shale			Seal?			Firm siltstone	No data
PERMIAN	Millyit Sandstone		Reservoir?				Predominantly sandstone	No data
	Liveringa Group	Condren	Reservoir		25 % (sonic)		Sandstone and siltstone	Excellent reservoir potential
		Lightjack	Reservoir		25 % (sonic)		Interbedded sandstone, siltstone and claystone	Excellent reservoir potential
	Noonkanbah Formation			Seal	17% (sonic)		Shale with siltstone interbeds	Sonic porosity overestimated?
	Poole Sandstone		Reservoir		≥ 20 % (sonic)		Predominantly sandstone with siltstone and claystone interbeds	Excellent reservoir quality
	Grant Group	C	Reservoir		21 % (sonic)		Interbedded sandstone, siltstone and claystone	

		B		Seal	10 % (sonic)		Interbedded sandstone, siltstone and claystone	
		A	Reservoir		18.5 %	754 – 1015 mD	Blocky sandstone	Excellent reservoir quality
CARBONIFEROUS	Anderson Formation	G		Seal	13 % (sonic)		Interbedded claystone and sandstone	
		F	Reservoir		7 % (sonic)		Massively bedded quartzose sandstone	
		E		Seal?			Massively bedded claystone	
		D	Reservoir		5 % (sonic)		Massively bedded quartzose sandstone	
		C		Seal	8.5 % (sonic)		Massively bedded siltstone and non-fissile claystone	
		B	Reservoir		5 % (sonic)		Massively bedded quartzose sandstone	
		A	Reservoir		9 % (sonic)		Loose coarse grained sandstone	

	Laurel Formation	Clastic	Reservoir	18.4 % (sonic)		Interbedded sandstone, siltstone and minor shale	Good reservoir quality
		Carbonate	Reservoir?			Finely crystalline and fossiliferous limestone, also blocky shales	No data
DEVONIAN	Luluigui Formation		Reservoir?			Interbedded sandstone, siltstone and minor shale	No data
	Knobby Sandstone		Reservoir	20.6 %	567 mD	Fine grained sandstone and minor siltstone	Excellent reservoir quality
	Virgin Hills Formation		Reservoir	7.4 %	0.52 mD	Interbedded sandstone, siltstone, shale and limestone	May be tight
	Gogo Formation		Seal?			Grey, blocky micromicaceous shales	No data
	Lennard River Group		Reservoir?			Interbedded limestone, sandstone, siltstone and claystone	No data
	Bungle Gap Limestone		Seal	3.3 %		Thick bedded massive arenaceous limestone, with secondary calcite	Calcite and fracture fill indicate impermeable

	Devonian Conglomerate		Reservoir	10.3 %		Polymict conglomerate	
	Poulton Formation		Reservoir?			Fine grained well-sorted sandstone	No data
SILURIAN	Worral Formation	Waldecks		Seal?		Sub-fissile micromicaceous claystone, siltstone and medium grained sandstone	No data
		Elsa	Reservoir?			Fine grained poorly sorted friable sandstone	No data
		Dodonea		Seal?		Microcrystalline to cryptocrystalline dolomite	No data
ORDOVICIAN	Carribuddy Group	Bongabinni	Reservoir?	Seal?		Grey blackish sub-fissile to fissile claystone, silty in part	Possible source rock?
		Minjoo		Seal?		Brownish yellow microcrystalline argillaceous dolomite	No data, potential seal?
		Nibil		Seal?		Brownish grey soft dolomitic claystone	No data, potential seal?
	Nita Formation			Seal	0.85 %	Nil	Finely crystalline sucrosic dolomite	

		WMC 4	Reservoir	Seal?	1.7 %	0.01 mD	Black finely crystalline argillaceous carbonaceous dolomite	Possible source rock?
	Goldwyer Formation	WMC 3	Reservoir	Seal?	1.5%	0.3 mD	Carbonaceous shale and sucrosic dolomite	
		WMC 2					Firm blackish fissile shale	No data
		WMC 1					Dark grey sub-fissile shale and siltstone	No data
	Willara Formation		Reservoir?				Massive, well-sorted fine sandstone	No data
	Nambeet Formation		Reservoir?				Medium grained well-sorted sandstone	No data

Table 4.10 Summary of lithology, characteristics and reservoir properties for stratigraphy in this study.

4.11 Well Correlation

Three well correlations were built across the project area (Figure 4.44 to Figure 4.46). The results were discussed in the text within this chapter.

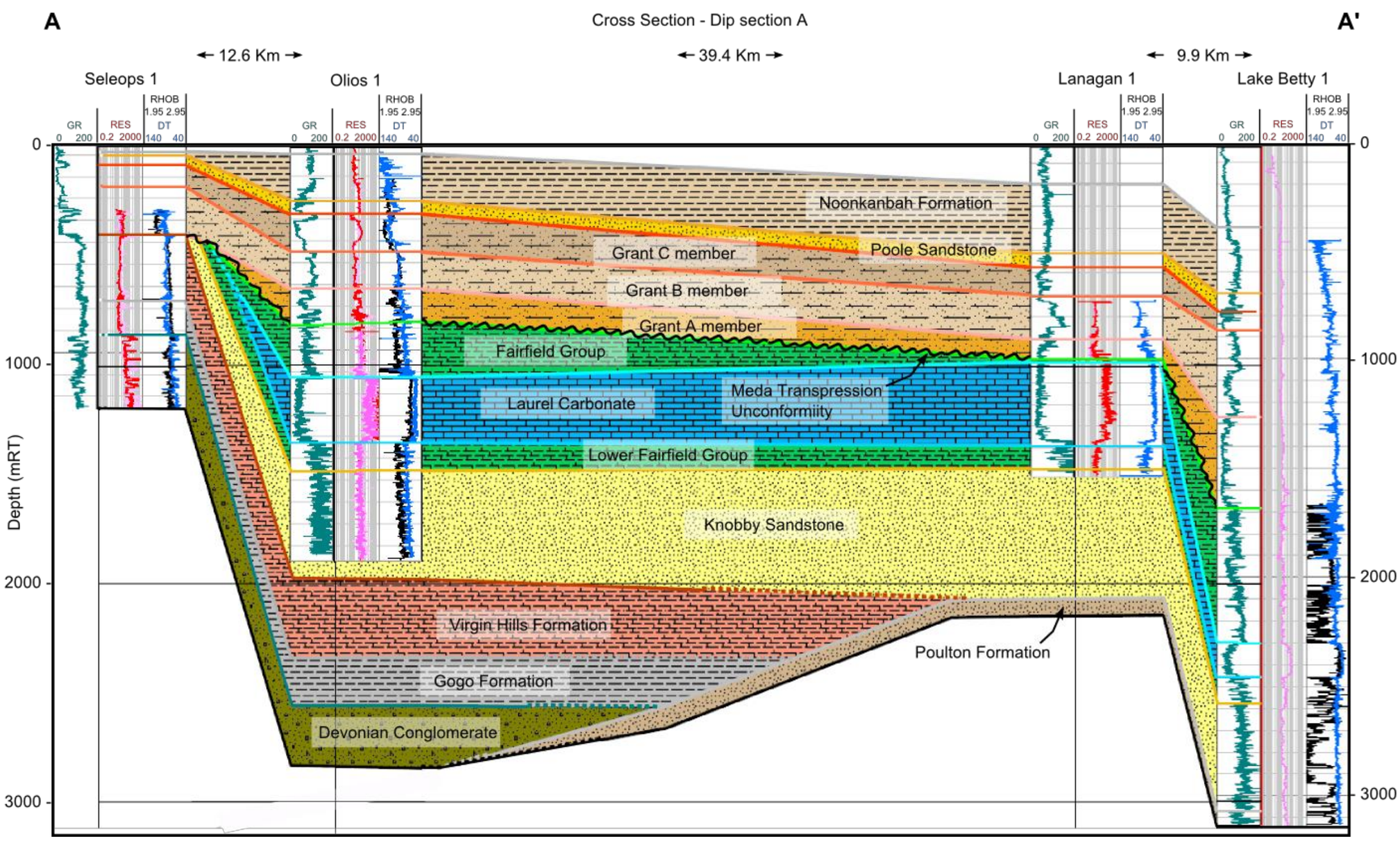

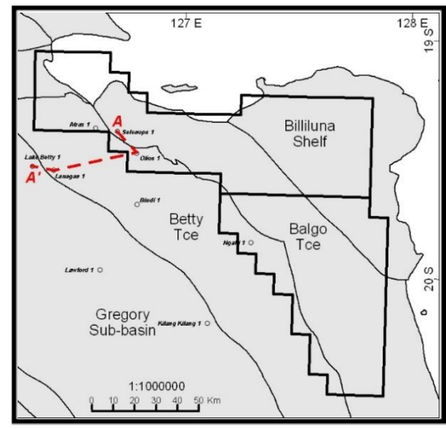

Figure 4.44. Dip section A - A' in the northwestern project area.

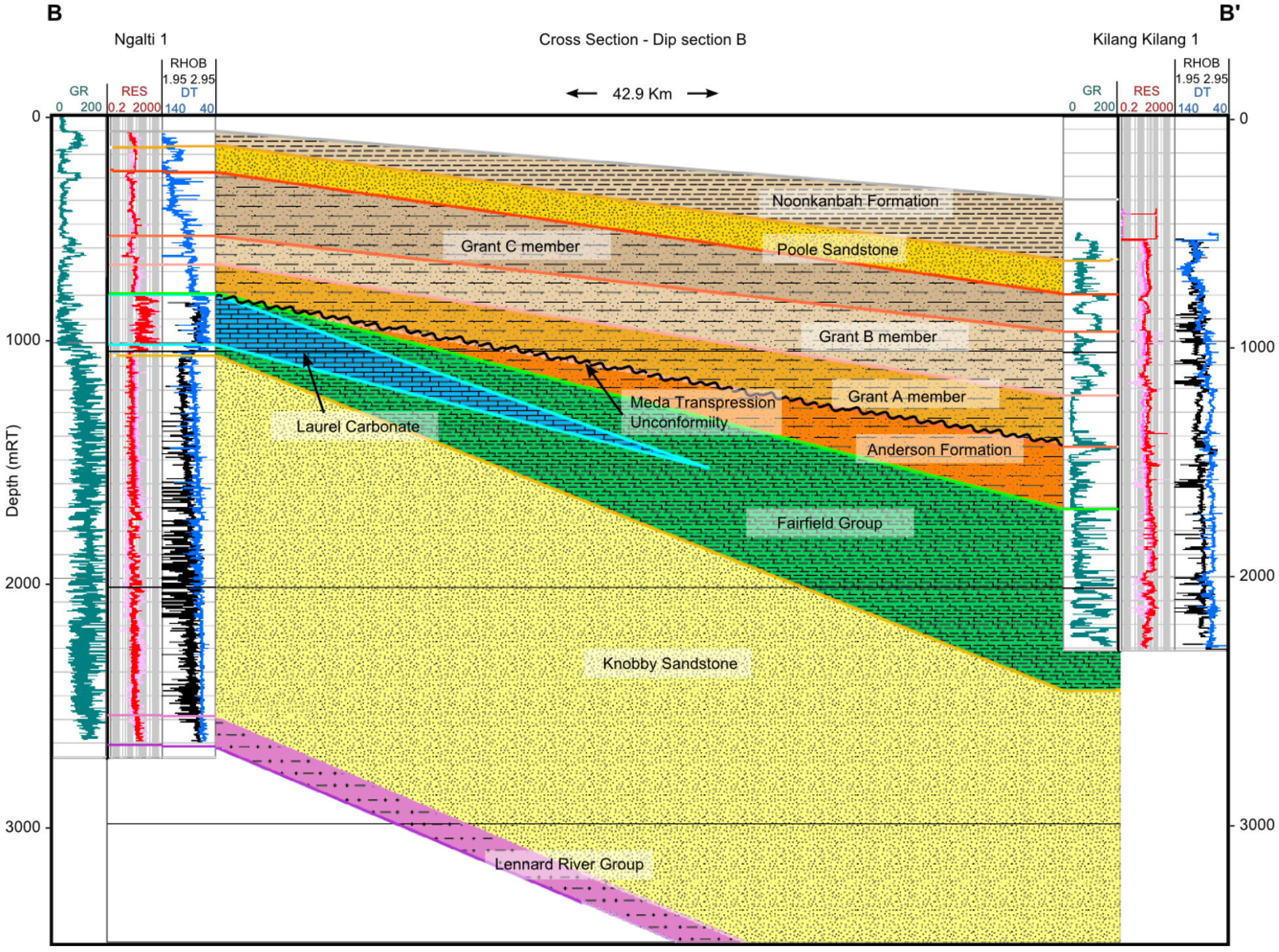

Figure 4.45. Dip section B - B' in the southeastern project area.

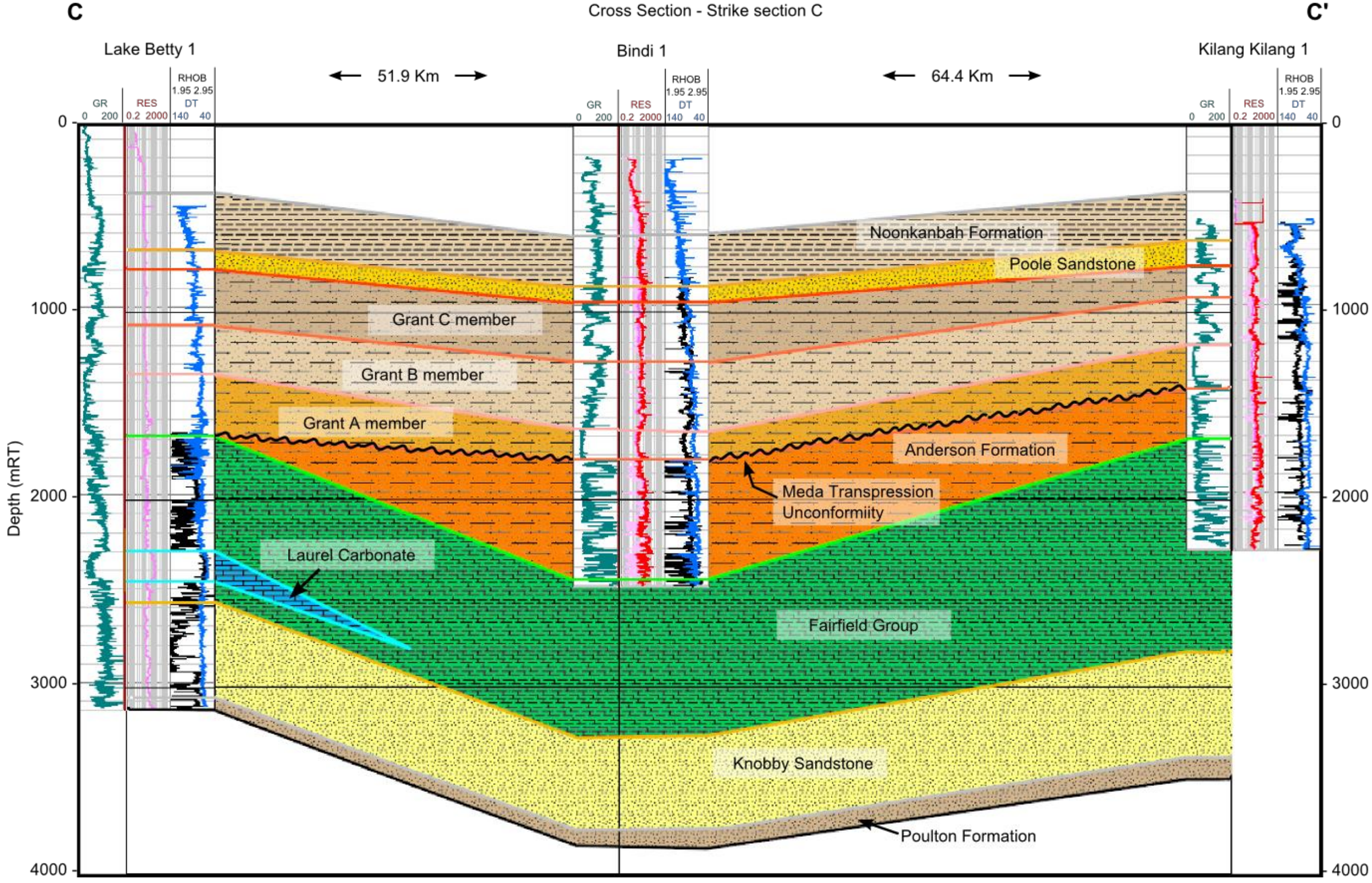

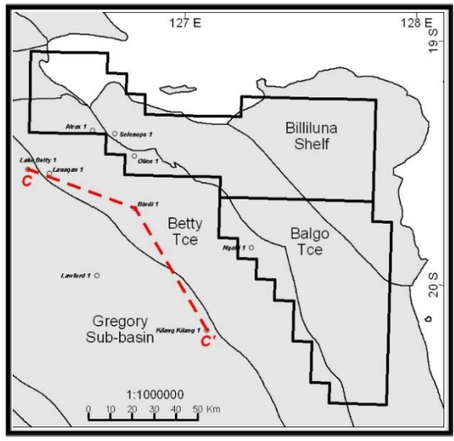

Figure 4.46. Strike section C - C' across the project area.

5. Seismic Interpretation

Seismic interpretation was a key component of this study. Mapping horizons across the project area enabled a thorough investigation of subsurface geometries.

Chapter 5 details the methodology used in the seismic interpretation workflow. The key objectives of the seismic interpretation workflow were to:

- Tie the 2D seismic dataset to external well data via synthetic seismograms, so that formation tops at the wells could be correctly identified on 2D data;
- Internally tie the seismic interpretation across the study area to ensure a robust horizon mapping package;
- Correlate seismic horizons between wells;
- Map the distribution of prominent regional seismic markers that represent key stratigraphic formations;
- Define the tectonic framework and identify the key faulting geometries;
- Produce maps of structure and time-thickness (isochron); and,
- Derive an estimate of depth of the mapped packages for use in petroleum systems modelling.

5.1 The Use of Seismic in this Project

Mature source rocks, reservoir rocks, lithologies with sealing potential and trapping geometries are all fundamental elements of an active petroleum system, therefore it is important in this study to determine the existence and extent of source rocks, reservoirs, seals and traps. To achieve this, stratigraphic horizons that are representative of petroleum system elements were mapped throughout the study area in order to determine their presence, spatial variability and geometric form.

To resolve the research questions it is clear that the interpretation needs to focus on mapping the elements of the three petroleum systems that exist within the study area. The seismic dataset was tied to the nine wells within the study area (Chapter 5.2). Eight seismic surfaces

were readily identified and regionally mappable on the 2D seismic data (Chapter 5.3). These surfaces define the major stratigraphic units of the northeastern Canning Basin and encompass the three petroleum systems of the region (Table 5.3). Each of these surfaces are characterized by particular seismic amplitudes and/or seismic geometries, and have genetic significance within the stratigraphy.

5.2 Well-To-Seismic Ties:

Synthetic seismograms were generated for all wells in the study area, and tied to seismic lines in Table 5.1 (illustrated in Figure 5.1). No synthetic seismograms were generated for wells outside of the study area.

Well	Seismic line
Atrax 1	82GE-31
Selenops 1	82GE-31
Olios 1	83GN-15A
Lanagan 1	S85LM-06
Lake Betty 1	82GE-34
Bindi 1	81C-1A
Lawford 1	S85LM-22
Ngalti 1	RB82-31
Kilang Kilang 1	RB8106

Table 5.1. Well ties in this study.

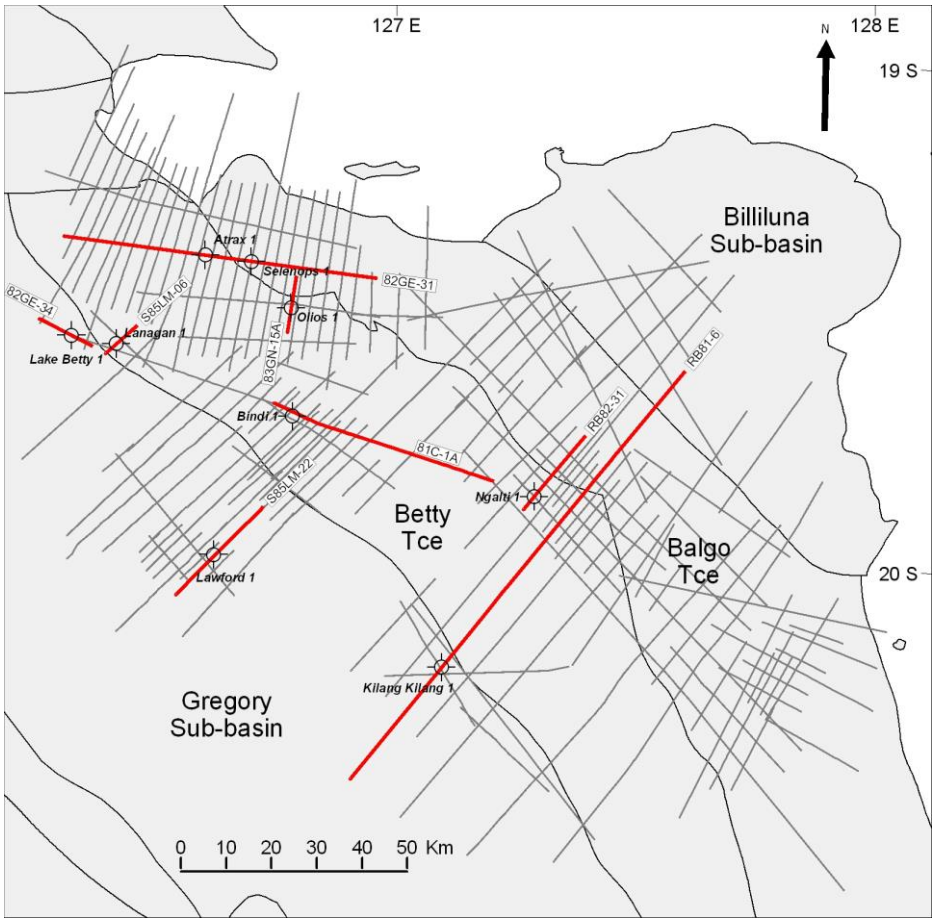

Figure 5.1. Distribution of wells ties in project area. Seismic lines used for synthetic ties are shown in red.

5.2.1 *Synthetic Generation:*

Table 5.2 summarizes the parameters to recreate each synthetic seismogram utilizing the synthetic generation wizard in IHS Kingdom.

Well	T-D Chart	Velocity	Density	Wavelet	Trace
Ngalti 1	Ngalti 1 original check shots recorded at the well – Datum 250m AMSL	DT log converted from feet to meters below RT	Constant density value of 1	Extracted from seismic by frequency matching: 500m radius along RB82-31, 39 traces, phase angle 0	Extracted 4 traces at the borehole, within a 50m radius, along RB82-31
Kilang Kilang 1	Kilang Kilang 1 original check shots recorded at the well – Datum 250m AMSL	DT log converted from feet to meters below RT	Constant density value of 1	Extracted from seismic by frequency matching: 500m radius along RB81-6, 28 traces, phase angle 0	Extracted 6 traces at the borehole, within a 100m radius, along RB81-6
Lanagan 1	Lanagan 1 original check shots recorded at the well – Datum 250m AMSL	DT log converted from feet to meters below RT	Constant density value of 1	Extracted from seismic by frequency matching: 200m radius along S85LM-06, 39 traces, phase angle 0	Extracted 7 traces at the borehole, within a 50m radius, along S85LM-06

Table 5.2. Examples of synthetic seismogram parameters used to perform synthetic ties in this project.

5.2.2 *Effect of Well Bore Rugosity on Synthetic Seismograms:*

Well bore rugosity was illustrated in Chapter 3.2 and Figure 3.1. Shallow well data that intersects stratigraphy above the Meda Transpression event have generally good quality wireline log data. Wireline log data quality depreciates quickly below the Meda Transpression Unconformity event due to borehole rugosity (Figure 3.1). It is common to see complete (or nearly complete) saturation of the caliper tool, and consequently, it is inferred that the Density tool experiences poor well bore contact resulting in spurious values. Further, the sonic sonde is likely to decentralize within the bore hole revealing inaccurate sonic times.

In all scenarios, the Density log (DT) was omitted from the synthetic generation to avoid contamination from any borehole rugosity. This was undertaken to produce good quality synthetic ties across all wells. The sonic log was utilised as a minimum to compute velocity in all synthetics. This procedure found that the overall effect of well bore rugosity was minimal on synthetic seismograms, and successful ties were resolved for all wells. Thus, confidence is provided that the horizon identification is correct when interpreting seismic in this project. Three well ties are produced here for illustration, the remainder are available in Appendix B.

5.2.3 *Synthetic Seismograms:*

Out of all the wells, Ngalti 1, Kilang Kilang 1 and Lanagan 1 arguably gave the best tie to the extracted trace for each respective well location. A small discussion is presented here to highlight some of the success and pitfalls of synthetic ties in this study.

At Ngalti 1, there is good agreement between the generated synthetic and the extracted trace (Figure 5.2). Although the synthetic trace does not always equal the extracted trace in amplitude or travel time throughout the entire well, there are sections where the correlation between the trace and the synthetic are very good. Importantly, all formation tops (Devonian and younger) referred to in Table 5.3 are resolved with very good matches between the synthetic and extracted trace. The good correlation at Ngalti 1 (and other wells generally) is attributed to proper wellbore readings of the Density (RHOB) and Sonic (DT) tools above 1250 mRT (approx. 0.8 seconds TWT). Note that the Caliper log (800 mRT to 1600 mRT at Ngalti 1) is less saturated than other wells in the project area (refer to Caliper tool comparison in Figure 3.2). A large washout is apparent below 1500 mRT at Ngalti 1. Note that the

synthetic has a high amplitude peak-trough-peak at approximately 1.0 seconds, related to the poor well bore contact of the logging tools at this depth. The seismic only shows a single large peak at the same location.

Largely, it can be said that the synthetic ties for each of the wells are good to very good, illustrated by ties for Ngalti 1, Kilang Kilang 1 and Lanagan 1 in Figure 5.2 through Figure 5.4. The results obtained from successfully tying the wells to seismic data gave confidence in placing horizon interpretation at correct levels on the seismic dataset.

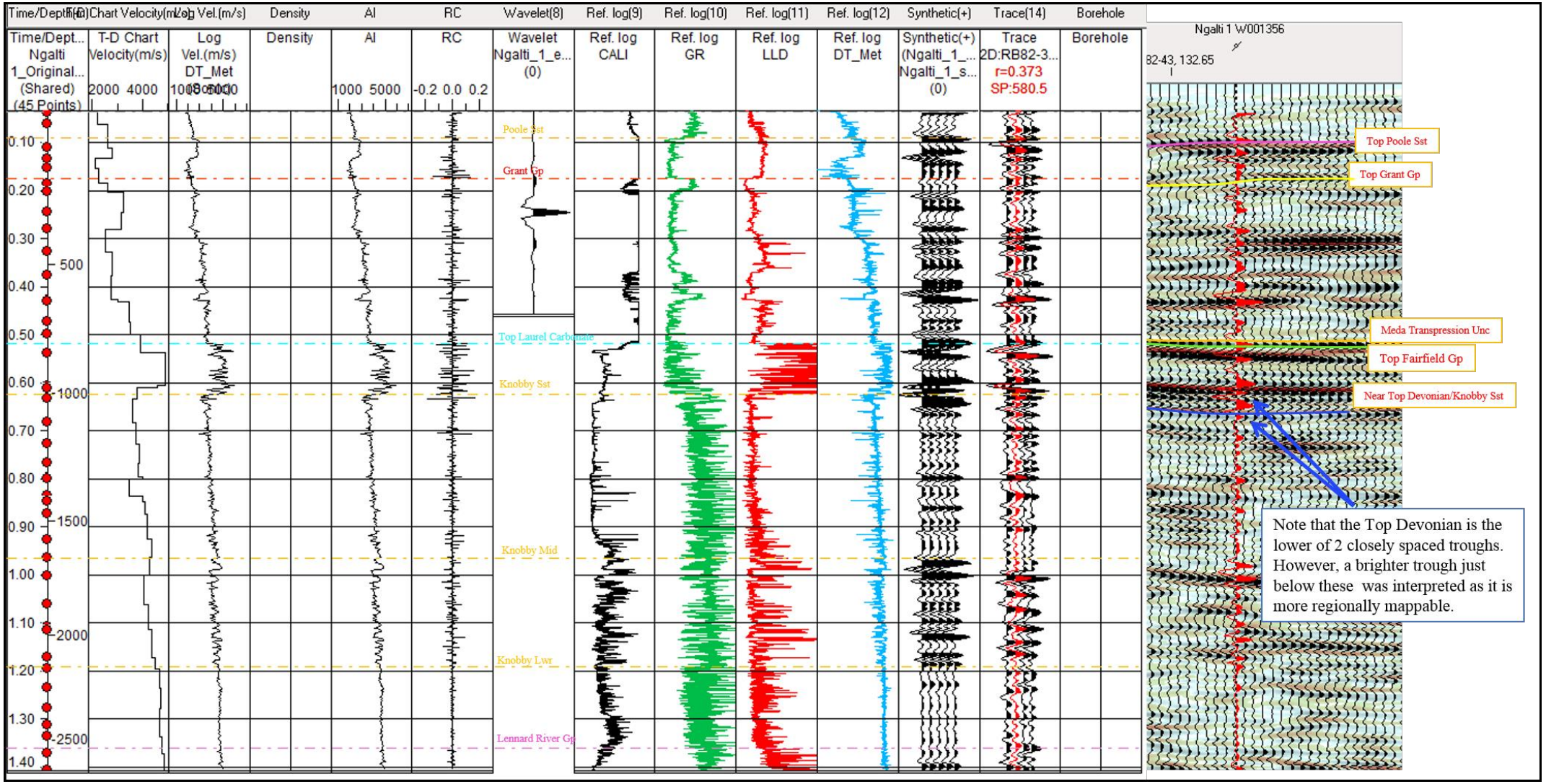

Figure 5.2. Ngalti 1 synthetic seismogram (left), synthetic overlay on seismic RB82-31 (right).

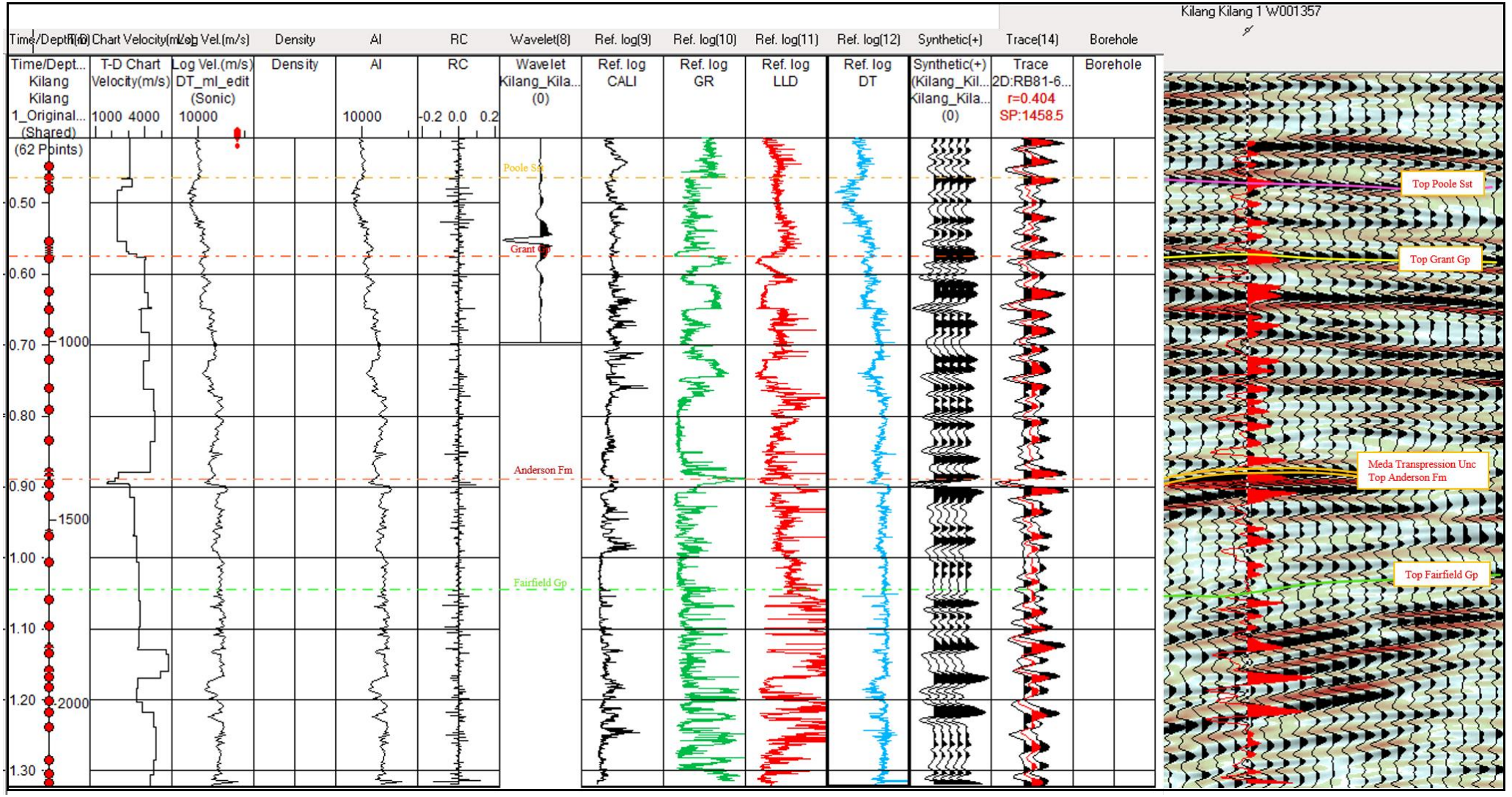

Figure 5.3. Kilang Kilang 1 synthetic seismogram (left), synthetic overlay on seismic RB81-6 (right).

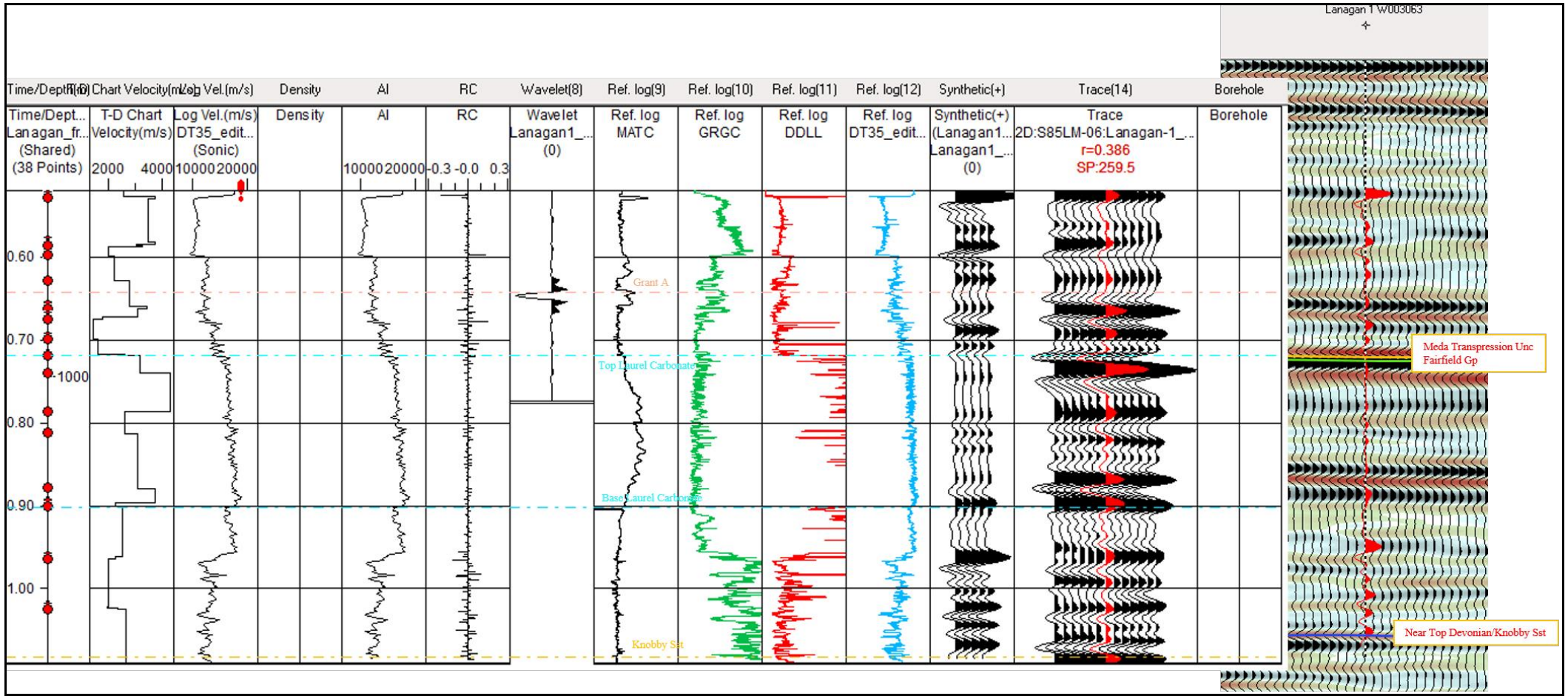

Figure 5.4. Lanagan 1 synthetic seismogram (left), synthetic overlay on seismic S85LM-06 (right). Note that the deeper reflection events (below the Meda Transpression/Fairfield group, between 0.8 – 0.9 seconds) do not tie to the extracted trace in amplitude or travel time, likely due to the bell-shaped washout in the caliper log below 1000mRT (MATC).

.

5.3 Interpretation of Horizons:

Table 5.3 summarises the seismic characteristics of each correlated seismic package in this study. The reader is referred to Chapter 6.1 to view the horizon interpretation.

Stratigraphic surface	Horizon colour	Seismic package characteristics
Near Top Noonkanbah Formation		• Identified by moderate to strong peak in seismic amplitude • Moderately bright, continuous, lateral intra-sequence reflectivity due to massively bedded shale character • Maximum Flooding Surface of the Permian transgression
Near Top Poole Sandstone		• Identified by moderate peak in seismic amplitude • Sequence of partially irregular to partially laterally continuous brightly amplified reflections • Transgressive Systems Tract
Near Top Grant Group		• Identified by strong peak in seismic amplitude • Interbedded Grant units (C, B and A) observed as non-continuous to irregular, brightly amplified events • Flooding Surface above Low Stand Systems Tract
Meda Transpression Unconformity		• Identified by truncation of seismic reflectors and marked change in seismic character across the unconformity • Unconformable surface between Grant Group and Anderson Formation (where preserved) or Fairfield Group

Near Top Laurel Carbonate		• Identified by strong peak in seismic amplitude • Package of bright amplitude, highly laterally continuous events • Often displayed as bright 'tram tracks' • Regional carbonate marker
Near Top Knobby Sandstone		• Identified by moderate to strong trough in seismic amplitude • Package of moderate to bright amplitude non-laterally continuous events • Underlies Fairfield Group Carbonate marker • Low Stand Systems Tract
Near Top Ordovician		• Identified by strong peak in seismic amplitude • Interpretation observes a package of upper moderately bright generally laterally continuous but partly irregular events atop a lower package of low amplitude and seismically dull irregular reflections. • Maximum Flooding Surface of the Ordovician
Near Top Basement		• Identified as irregular to chaotic, moderately bright to bright reflections that dip steeply towards the west (on seismic lines in a NW-SE or E-W orientation) • Identified as irregular to chaotic, moderately bright reflections (no apparent dip) (on seismic lines in a N-S orientation

Table 5.3. Major seismic stratigraphic surfaces and their sequence characteristics.

5.3.1 *Near Top Meda Transpression*

The Near Top Meda Transpression horizon was the first event to be mapped throughout the dataset. It is an important horizon because it represents a good regional marker, is easily identifiable on seismic and is a good surface upon which to datum for further interpretation. It is also significant because the surface indicates the top of the Larapintine L4 Petroleum System. All of the wells within the study area penetrate the horizon, providing good well control, however because the Near Top Meda Transpression horizon is a regional unconformity, lithological relationships across this horizon change. The Grant 'A' sand consistently overlies the unconformity but strata below the unconformity vary from carbonates of the Fairfield Group to shale-rich interbedded siliciclastics of the Anderson Formation where preserved.

Due to the nature of the unconformity, the seismic character of the horizon changes between a peak and trough, and so internal loop ties are based more on the change in seismic character above and below as opposed to a specific amplitude response. Generally, the location of the horizon is interpreted to be at the place of maximum discordance between the overlying Grant Group and underlying strata (Figure 5.5).

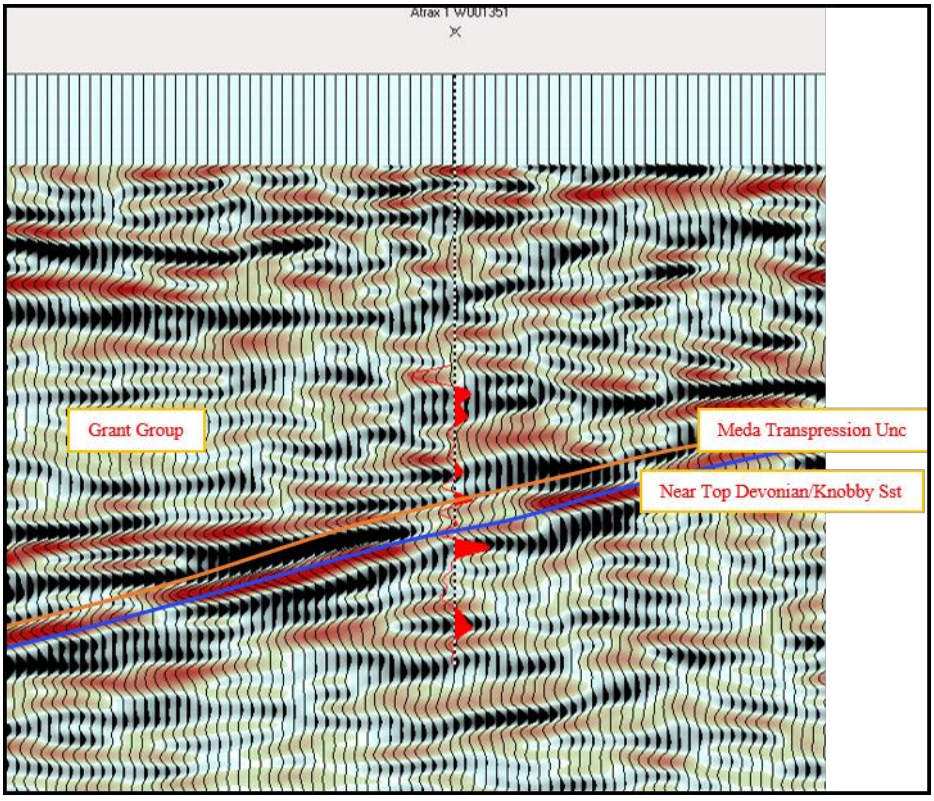

Figure 5.5. The Meda Transpression Unconformity is at the place of maximum discordance between the overlying Grant Group and underlying strata.

The interpretation on line RB81-10 (Figure 6.7) demonstrates the onlap of the Grant Group over the older, broadly folded pre-Permian strata below the Meda Transpression unconformity. The onlapping geometries and the angular discordances were key characteristics used to map this horizon within the study area. Note that there are some subtle disconformities within the lower Grant Group that can blur the exact position of the Meda Transpression pick, which places a minor uncertainty on the precise location of the horizon in some areas, particularly where deformation of Middle Carboniferous and older strata is minimal. Because this truncation is represented by reflector terminations (not a consistent peak or trough), there were a few places where there were slight misties with the regional interpretation – principally in the central portion of the study area over the horst block separating the Billiluna Sub-basin from the Balgo Terrace (Figure 3.4, and RB81-07, SP1200, Figure 6.5) – though they were resolved to an acceptable standard as they were observed. Seismic mapping shows that the unconformity is indeed regional, as the truncation event can be mapped across the whole study area.

Confidence in the interpretation of the Meda Transpression event is high over most of the project area, particularly on the up-thrown side of the Muller Fault (Balgo Terrace) and throughout the central project area, where the truncation of the Anderson Formation and Fairfield Group sediments is clear. Mapping of the horizon into the Gregory Sub-basin is less confident because the reflection terminations that are used to map the character of the horizon are not as clear (the events above and below the horizon are less angular in their non-conformance).

5.3.2 *Near Top Laurel Carbonate*

The Near Top Laurel Carbonate was the second horizon to be mapped throughout the study area. The horizon was critical to map because it signifies the near top of the Larapintine L3 petroleum system (and indicates the absence of the L4 petroleum system where the Anderson Formation is eroded). The Larapintine L3 and L4 systems have been targeted as primary objectives since exploration in the Canning Basin began. The L3 and L4 petroleum systems host stratigraphy that have revealed the majority of positive basin-wide drilling results to date (Table 2.1 and 2.2, and Figure 2.8). Therefore, mapping the Laurel Carbonate is an important horizon to map in this project.

The Near Top Laurel Carbonate is marked by a package of bright amplitude events equaling approximately 300 milliseconds two-way-travel time (TWT) thickness in the central portion of the study area, and the package generally thins basinward. The horizon is clearly visible on RB81-07 (approximately 0.8s TWT, SP 950, Figure 6.5). Thicker packages are also present on the hanging wall blocks of large normal faults (i.e. within the Stansmore Fault hanging wall, RB81-7 SP 550, Figure 6.5). The Laurel Carbonate splits into two thinner bright reflection packages in the northern study area (for example at Lanagan 1, Figure 5.4) with seismically dull reflection character in the middle, due to lesser intra-Laurel carbonate interbeds that causes lesser intra-Laurel reflectivity. The carbonate package is the lower section of the Laurel Formation within the Early Carboniferous Fairfield Group.

Within the study area, the upper partition of the Laurel Formation is largely truncated by the Meda Transpression unconformity. The marker is intersected by most petroleum wells in the study area, which produced confidence in the interpretation via good well-to-seismic ties. The

horizon allows confident internal loop ties due to a readily identifiable, high amplitude, laterally continuous seismic response.

The Upper clastic section of the Laurel Formation is truncated by the Meda Transpression Unconformity on up-thrown fault blocks on the Betty Terrace. Seismic mapping shows that the carbonate is present throughout the study area, though two-way travel-time structure and time thicknesses are variable. Seismic mapping shows that the carbonate marker occurs on the terraces up dip of the Gregory sub-basin and occurrence of the carbonate is less common basin-ward (into the Gregory Sub-basin) where the continuous bright amplitudes diminish and the carbonate transitions to shale lithotypes of the surrounding Laurel Formation.

5.3.3 *Near Top Grant Group*

The Near Top Grant Group was the third horizon to be carried through the study area. The top of the Grant Group is generally marked by a strong peak on seismic data (thought also a low amplitude peak at Ngalti 1), representing a shale rich member (Grant 'C') at the top of the formation appearing laterally continuous throughout the project area. The interbedded relationships of the Grant Group are visible on seismic as non-continuous to irregular, brightly amplified events. The Grant Group constitutes sandstones interbedded with shale packages and is divisible in this project into 3 units (Grant C, B and A, youngest to oldest). The seismic characteristics of these individual members are difficult to correlate within the Group due to the intricate interbedded marginal marine depositional history (deltaic sandstones interbedded with prodelta shale lenses). The Grant Group is intersected by all wells within the study area.

The Horizon for the Near Top Grant Group ties well to external well data and the Near Top Grant Group package fits the expected seismic character given the above lithological description. Loop ties for the Grant Formation are satisfactory within the data set. Both the external and internal seismic ties provide confidence in the interpretation. Seismic mapping of the Near Top Grant Group reveals that the package exists across the study area, and reaches near time zero near the northeastern margin of the Balgo Terrace. This is validated by outcrop on surface geology maps.

5.3.4 *Near Top Knobby Sandstone.*

The Near Top Knobby Sandstone is recognized to be a moderate to strong trough in the seismic dataset due to a negative Reflection Coefficient Impedance Contrast that is observed across the faster velocities of the Carbonate rich Laurel Formation (Fairfield Group) into the relatively slow velocity sediments of the predominantly clastic Knobby Sandstone. The seismic package is observed as moderate to bright amplitude non-laterally continuous events representing high sand content partially interbedded with finer clastic lithologies.

The Knobby Sandstone marker location is the last bright amplitude event at the base of the Laurel Formation package (base of the bright amplitude events at SP 600, 1.2s TWT on line 82GN-20, Figure 6.2). The benefit of mapping the Near Top Knobby Sandstone in this project, is that the Laurel Formation marker provides a well pronounced 'tram track' of parallel reflections to map (Figure 5.2), which places higher confidence in the mapping of the Knobby Sandstone horizon throughout the dataset. This procedure saved considerable time.

The Knobby Sandstone is interpreted to exist regionally throughout the study area and thickens basinward (refer to Chapter 4.5.7). The Knobby Sandstone is suggested to be the youngest level of stratigraphy (other than Cenozoic cover) within the Billiluna Sub-basin, however the interpretation here questions this by the inclusion of Fairfield Group packages in the Billiluna area. Cenozoic cover is abundant and sections of Carboniferous age may be inaccessible. An isopachus Devonian and Fairfield Group interpretation into the Billiluna Sub-basin supports the interpretation presented in this thesis. This is an uncertainty, and Chapter 6.2.3 attempts to provide some resolution.

5.3.5 *Near Top Poole Sandstone*

The Near Top Poole Sandstone was the fifth horizon carried through the study area. The horizon is recognized as a moderately strong peak on seismic data due to a positive Reflection Coefficient Impedance Contrast between the Noonkanbah Formation and the Poole Sandstone. The seismic sequence is mostly observed as a package of partially laterally continuous but also partly irregular events caused by interbedded rock packages of variable porosity (sands and shales). The Poole Sandstone was intersected by all wells within the study area which produced good well to seismic ties for the horizon (Kilang Kilang 1 synthetic, Figure 5.3). A strong RC impedance contrast present at the top of the unit provides

a good marker to correlate across the study area, which facilitates good internal loop ties, and gives confidence in the interpretation.

Seismic mapping reveals that the Poole Sandstone is present throughout the Balgo and Betty Terraces, and sub-crops on the down-thrown side of the Mueller Fault. The Poole Sandstone is interpreted to be absent within the Billiluna sub-basin, verified by surface geological maps.

5.3.6 *Near Top Noonkanbah Formation*

The Near Top Noonkanbah Formation was the sixth horizon to be carried through the seismic dataset. The horizon represents the position of the maximum Permian marine transgression. As such, the marker is observed as a moderate to strong peak, caused by slower velocity sediments within the Triassic section interfacing faster velocity sediments within the Permian Noonkanbah Formation. This contrast produces a positive Reflection Coefficient Impedance Contrast at the horizon. The seismic package is generally observed as moderately high intraformational reflectivity occurring as continuous lateral events representing a massively bedded shale, though irregular events are noted due to packages of intraformational sandstone deposits. The Noonkanbah Formation is penetrated by all wells within the study area and confidently ties to external wells (for example Olios 1, Appendix B). The horizon has an excellent internal loop tie. Seismic mapping shows that the Noonkanbah Formation is present throughout the dataset, though is not present within the Billiluna Sub-basin, verified by surface geological maps.

5.3.7 *Near Top Ordovician*

The Near Top Ordovician Horizon is a character interpretation based on its published geological model (Deep burial, argillaceous lithologies, thickens basinward off the terraces and into the Gregory Sub-basin). A reasonably strong Reflection Coefficient Impedance Contrast is expected to be present at the top of this unit contrasting the coarser grained Nita Formation and Carribuddy Group above, thus giving a strong peak on seismic. Based on seismic mapping, the interpreted Ordovician package is a sequence of two parts; a moderately bright generally laterally continuous (but partly irregular) events atop a lower package of low amplitude and seismically dull irregular reflections. As there are no intersections of Ordovician rocks within the study area, and the only correlation is via a

character tie to the Lake Havern 1 well (Figure 5.8), there is low confidence in the accurate selection of reflection events chosen to represent the Near Top Ordovician. However, the argument for the presence of an Ordovician package within the project area is still strong irrespective of the interpretation accuracy. The Ordovician section is mapped throughout the dataset within a reasonable amount of error or uncertainty.

The interpretation suggests that Ordovician rocks are present in the study area, giving evidence to confirm the presence of rocks of the Larapintine L2 petroleum system, which is a significant component of overall prospectivity of the study area. Figure 5.8 demonstrates the Ordovician tie.

The Near Top Ordovician horizon is based on a seismic character tie to the Lake Havern 1 well (south of the project area. The well reached total depth in Ordovician aged stratigraphy) (Figure 5.8). The Lake Havern 1 well does not have a time-depth chart. Other wells within the study area do not penetrate deeper than the Devonian section, which does not allow a local well-to-seismic tie.

There is some uncertainty in internally tying the Near Top Ordovician horizon between the northern and southern parts of the project area. There are only two north-east oriented lines that provide the main route of correlation between the southern and northern parts of the study area; Betty Terrace SS line 81C-1A and Billiluna SS line RB81-11 (Figure 5.6). The lines RB81-11 and the RB82-17 were reprocessed by different processing houses and a reasonable mistie is apparent at its intersection (attributed to slightly different processing sequences which results in time variances in the phase). A small section of line RB81-16 is also required to complete an arbitrary line to view the tie in a wider context. The southern correlation path via 81C-1A, which relies somewhat on line 81C-07 which was not reprocessed to Pre-Stack Time Migration (PSTM) and the reflection events are poorly imaged, especially for the deeper Near Top Ordovician marker. This results in a less confident internal tie for the Ordovician.

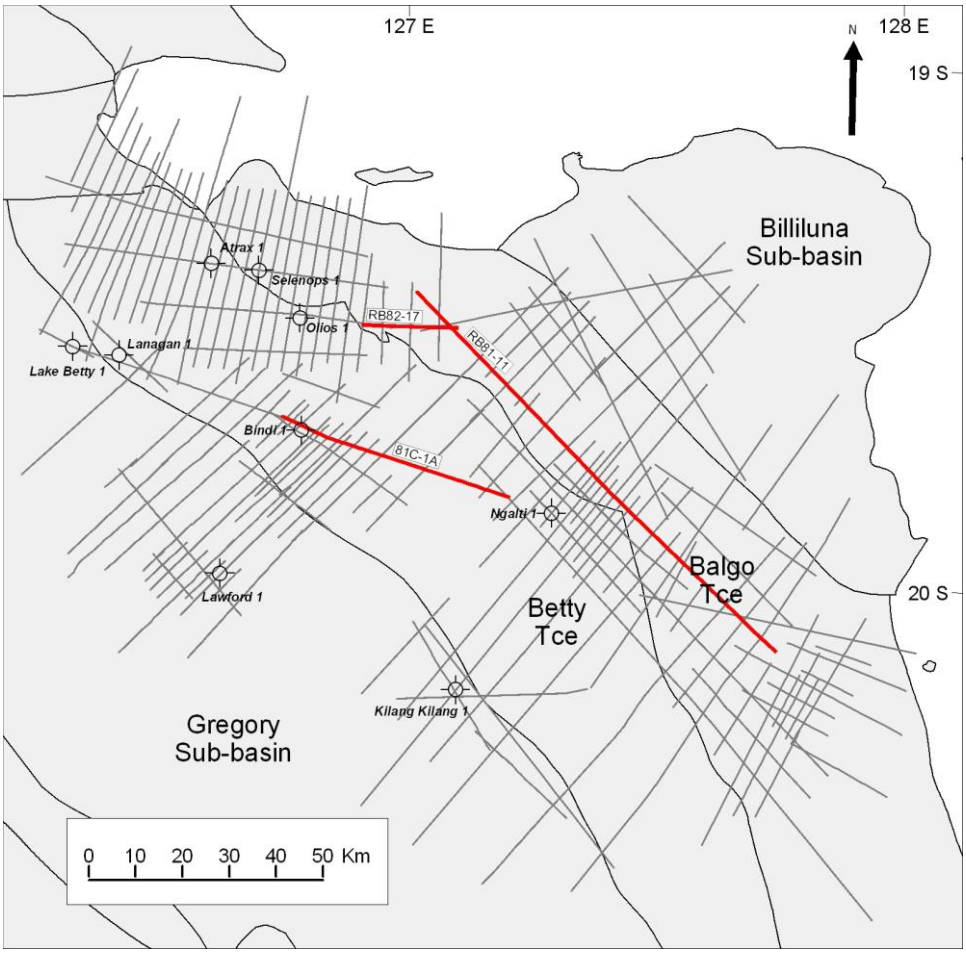

Figure 5.6. Seismic grid. Red lines indicate main path to tie horizons across the central project area.

5.3.8 *Near Top Basement*

Near Top Basement is not penetrated by any well in the study area or immediate surrounds, so the basement horizon is solely mapped on its reflection character. The Near Top Basement horizon is based on seismic imaging of a steeply westerly dipping Precambrian rock 'fabric' underneath interpreted Ordovician strata (Figure 5.7), presenting a steep angular unconformity (refer Chapter 2.3.1 and Irwin, 1998). The sequence is observed as irregular to chaotic, moderately bright to bright reflections that dip steeply towards the west. The basement fabric provides for a reasonable and consistent marker in the southern part of the study area, as the seismic surveys in the south are oriented in general alignment with the fabric dip (east-west). In the northern part of the study area the fabric is not as clear, because the surveys are oriented in a north-south direction, which does not allow the seismic to best image the Precambrian fabric. Although the steeply dipping fabric is not as clear in the

northern part of the study area, the basement is represented by a chaotic reflection character that maintains a reasonable reflection interpretation.

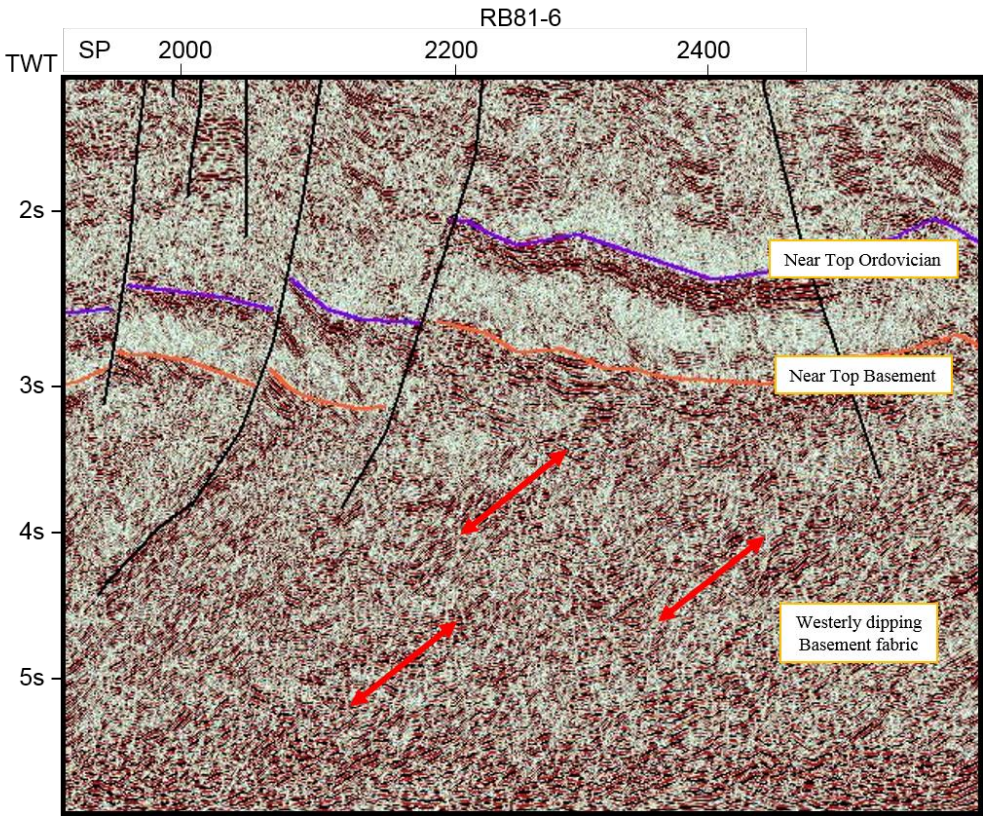

Figure 5.7. Example of seismic on RB81-6. Westerly dipping reflection events used to identify Basement are clear (red arrows).

In some localities (for example the most northeastern section of Line RB81-6) there are pockets of horizontal strata immediately below the Basement horizon. These strata might be features of Ordovician rocks in this immediate locality rather than Precambrian. These features are not regularly present on adjacent dip lines. They have been mapped as basement features for consistency in the interpretation, and probably do not have significant meaning within the scope of this project.

The only method to tie the Basement horizon to any external data is via surface geology maps. Precambrian rocks outcrop to the northeast of the Billiluna Sub-basin and to the north of the Balgo Terrace. Mt Bannerman 1982 seismic line 82GN-02 is acquired over basement outcrop to the north of the study area and images the chaotic reflections representative of basement. It would have been beneficial to be able to tie the westerly dipping fabric to

outcrop on the eastern edge of the study area, however seismic coverage precludes this. A reasonably confident interpretation of the Near Top Basement horizon is presented here within the scope of this study.

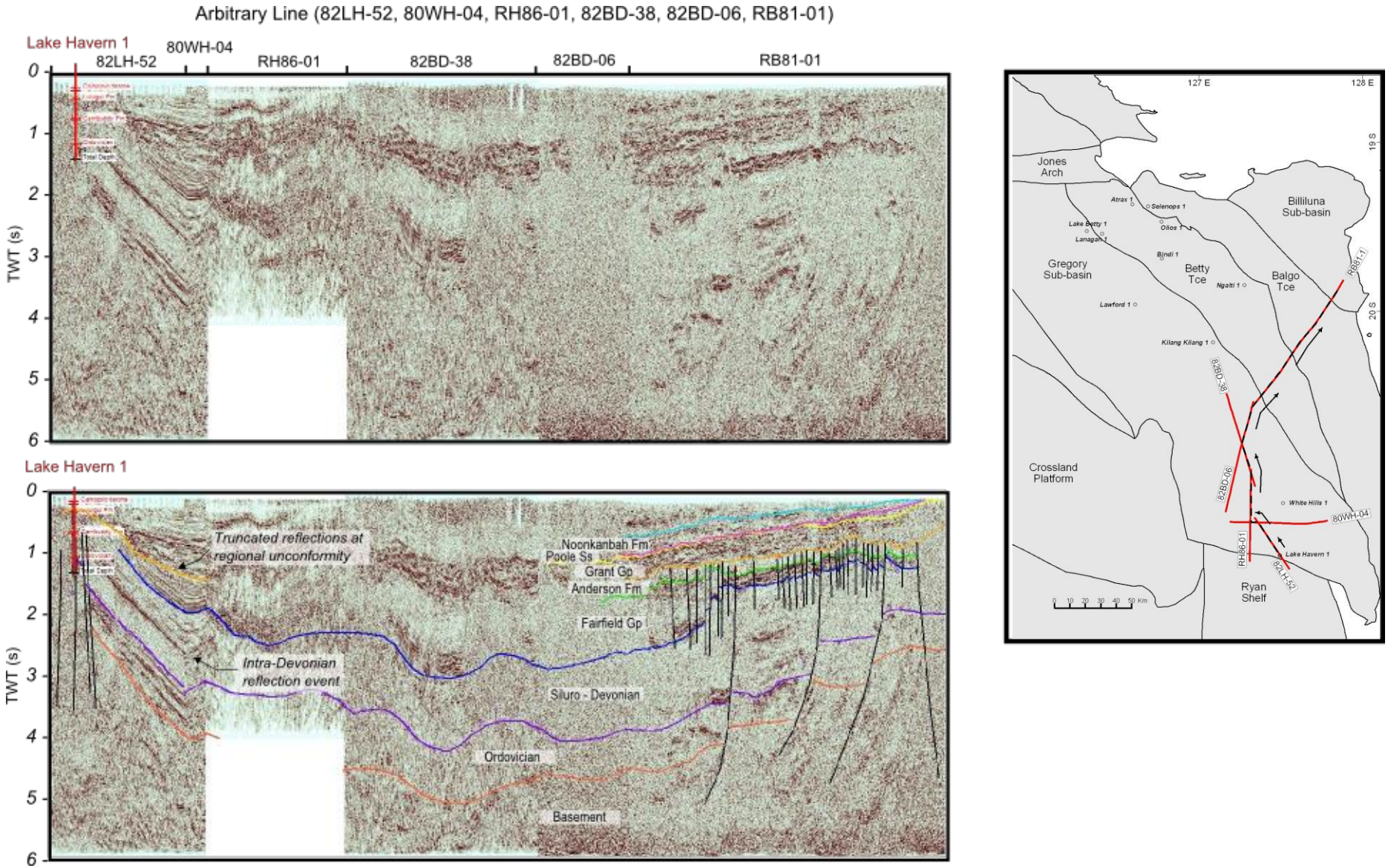

Figure 5.8. Arbitrary line used to tie Ordovician package from Lake Haven 1 to the study area. Map (right) shows the arbitrary line (dashed with arrows).

5.4 Interpretation of Faults

The study area is located on the northeastern corner of the Canning Basin, and comprises several terraces with stratigraphy thickening into a regional depocentre. Pursuant to reviewing work by previous authors (Brown, et al., 1984; Smith, 1984; and Yeates, et al., 1984), the expectation is to see large, down-to-the-basin normal faults between these terraced areas. This expectation is validated by seismic mapping. Large normal faults are observed, some exemplifying large throws. Figures 6.2 through 6.7 illustrate faulting geometries and highlight the structural overprint within the study area.

It is evident from seismic interpretation that the structural overprint is significant. Some faults are relatively small with minor throws (only affecting stratigraphy within limited shallow sections) and are too small and erratic within the study area to warrant correlating within the scope of the project.

The process of fault interpretation in this study essentially comprised defining the tectonic elements (depocentres and terraced areas) to form a significant basin scale framework, as well as mapping faults that are likely to provide large structural traps for prospect generation. The larger faults were correlated by block or 'package' across the study area. Given that there is a finite time available for the interpretation of this dataset (a number of weeks allocated to correlating faults), spending more than the allotted time presented a case of diminishing returns with regards to the fault correlation interpretation at the seismic interpretation stage of this project.

Fault interpretation was largely undertaken prior to horizon interpretation. This was for the purpose of familiarization and creating an understanding in the interpreter’s mind of faulting styles. It was also more practical to have the common faults in place prior to horizon mapping so that mapping horizons in close proximity to faults was faster.

5.4.1 *Confidence in Fault Interpretation*

Confidence is generally high in mapping horizons across faults within most of the study area. Assurance is provided by correlation polygons used within IHS Kingdom to compare packages of seismic reflection events across fault planes. Further to this, seismic reflection character is optimized by the seismic reprocessing that was applied to the dataset prior to

interpretation. Bright ‘tram track’ amplitudes associated with the Fairfield Group (discussed in section 5.3.2) also assures of confident correlation.

There are, however, two aspects where horizon correlation across faults is less confident. The first uncertainty is correlating the Near Top Meda Transpression Unconformity horizon across the Stansmore Fault into the Gregory Sub-basin. Shot point 250 on RB81-7 (Figure 6.5) illustrates a broad anticline in post-Devonian stratigraphy, resultant of compression associated with the Triassic Fitzroy Movement. Because the unconformity surface parallels the other post-Devonian surfaces the unconformity loses its distinct character and reflection terminations.

The second less confident aspect is in regards to the Horst system that separates the Balgo Terrace from the Billiluna Sub-basin. The lack of confidence in this scenario revolves around not having any wells within the Billiluna Sub-basin in which to tie the seismic interpretation. The only method to correlate regional line RB81-7 (Figure 6.5) into the Billiluna Sub-basin is via surface geology maps showing Devonian outcrop. Near Top Ordovician and Near Top Basement horizons in the Billiluna Sub-basin rely on an isopachus interpretation.

The Near Top Devonian horizon ties surface geology in the Billiluna Sub-basin (RB81-7, Figure 6.5), though it’s questionable whether there is any Fairfield Group within the Billiluna Sub-basin, and if so, how much section is preserved. There are no wells to tie seismic data in the Billiluna Sub-basin. The interpretation shown on RB81-7 (Figure 6.5) between shot point 1300 and 1400 assumes that the Laurel Carbonate isopach remains consistent across the top of the Billiluna Horst block and into the Billiluna Sub-basin. Unfortunately Cenozoic cover prevents validation of the interpretation. The reflection character of the Laurel Carbonate deteriorates at the top of the Horst (shot point 1200, RB81-7; Figure 6.5). The sediments may be time equivalent siliciclastic sediments rather than carbonates.

5.5 Velocity Analysis and Depth Conversion:

Velocity Analysis and Depth Conversion are frequently performed in most seismic interpretation projects. Given the objectives of this petroleum systems study, a subsequent important workflow in this project was simulating petroleum systems and their potential hydrocarbon accumulations in petroleum systems models (discussed in Chapter 8). Schlumberger PetroMod basin modeling software was used for this workflow. To create and simulate the structural and stratigraphic geometries of the seismic interpretation in petroleum systems models, the seismic interpretation (which is constructed in the time domain) needs to be converted to the depth domain so that the depth domain interpretation can be digitized and then simulated in Petromod.

Whilst considering the seismic and modelling workflows for this project, and given the time constraints, it was decided that extensive time spent on Velocity Analysis and Depth Conversion was not required. Depth maps were deemed to be unnecessary within the scope of this project, and instead, a simple depth approximation utilizing IHS Kingdom's 'Dynamic Depth Conversion' tool would be sufficient, and also produce the suitable 2D depth sections for Petromod.

5.5.1 *Dynamic Depth Converter (DDC)*

The dynamic depth conversion (DDC) is performed by specifying time and depth data pairs; such as horizons, formation tops, grids or control points, and selecting a velocity model type (average or interval velocity). These parameters are specified within HIS Kingdom's DDC module.

A time-depth (TD) chart was compiled to gain an understanding of any obvious lateral variations to velocity across the project area. Figure 5.9 shows that there is good agreement with time-depth relationships between wells within the project area. The depth conversion was performed using the 2D seismic interpretation horizons and well formation tops to develop an average velocity model.

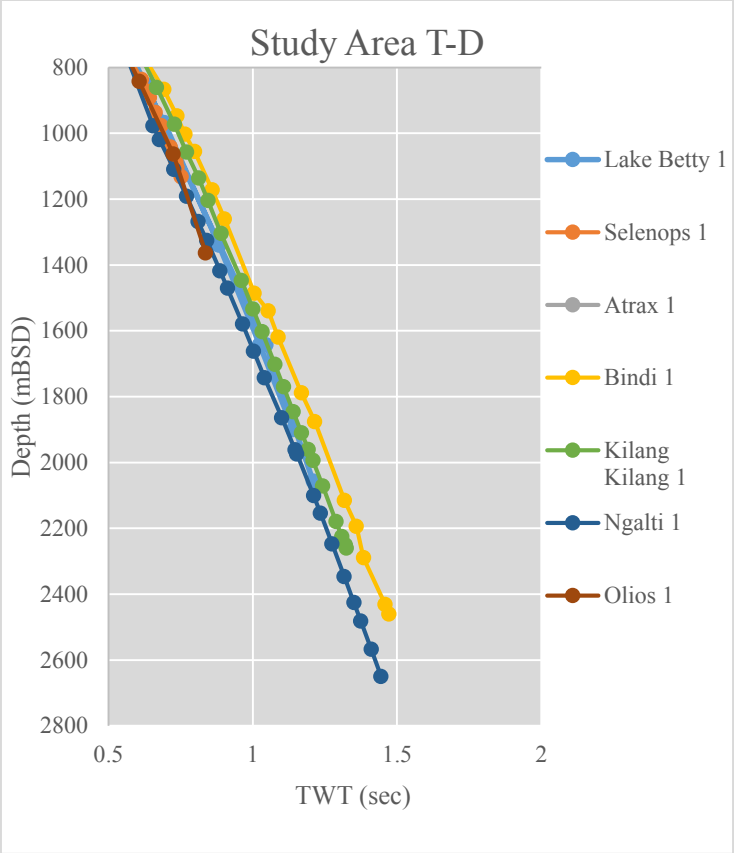

Figure 5.9. Time-Depth relationship between wells within the project area.

For dynamic depth conversion IHS Kingdom takes the horizon and formation top data through a process to generate a number of time, depth, velocity, isochron and isochore grids for each layer of stratigraphy in the model (Kingdom, 2013), according to the following;

1. Create first time grid
2. Compute first time/depth pairs
3. Create average velocity grid
4. Create depth grid
5. Create second layer time, average velocity and depth grids
6. Create isochron grid
7. Create isochore grid
8. Repeat for each additional layer

The DDC's resulting conversion is activated within Kingdom by selecting 'Virtual Depth' within a 2D section, thus dynamically converting the seismic from the time domain into the depth domain.

Depth structure maps were not produced because a rigorous depth conversion was not performed. Therefore, the only insight to spatial structural variability was allowed via TWT structure maps. There is a large uncertainty present because a complete understanding of the depth structure is not at hand, and any structure that is presented in any discussion is therefore an 'apparent time structure'. Structure maps (in TWT) will not take account of velocity variability. For example, there may be areas of thick higher velocity material that may be observed evenly deposited atop an apparent structural trap, thus causing "pull-up". The example in Figure 5.10 demonstrates that time interpretation without a proper depth conversion can falsely pronounce structures. Simply, the structures presented here in time may not actually occur in depth. This uncertainty is relevant here because there are several levels of stratigraphy assumed to contain high velocity material, namely the Laurel Carbonate within the Fairfield Group, the Devonian Bungle Gap Limestone and carbonates in the Ordovician section (likely within the Nita Formation and Goldwyer Formation).

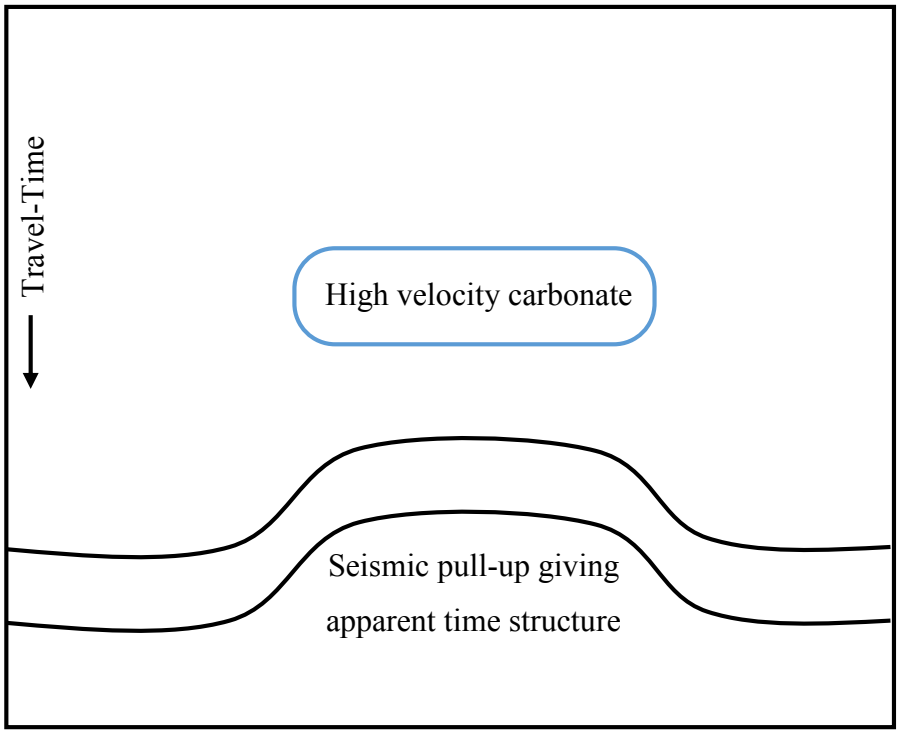

Figure 5.10. Schematic illustrating apparent time structures.

5.6 Two-Way-Travel Time Structure and Time-thickness (Isochron) Mapping

The horizon PSTM interpretation was exported from IHS Kingdom to a Petrosys mapping Seismic Data File (SDF). IHS Kingdom fault interpretation was similarly taken from Kingdom into Petrosys for use in contouring. TWT maps were prepared using this data for each interpreted horizon.

Each horizon was contoured within Petrosys. The contouring was successful with use of standard gridding functions. Hand contouring was useful in all of the maps to a small extent to remove anomalous features (bull's-eyes etc.) that were not verifiably present in the actual interpretation. Gridding anomalies were most common in areas of greater seismic line spacing or where there is a lack of data to constrain the grid. Hand contouring was also useful at the 'near zero edge' of shallower units to tie the interpretation to surface geology maps. Hand contouring was necessary to contour the deeper areas of the Gregory sub-basin where only few seismic lines allow proper definition of the subsurface, and to clip the gridding function to a clipping polygon (so that the grid does not extrapolate further than the seismic grid).

TWT thickness (isochron) maps were produced in Petrosys by subtracting a deeper TWT structure map from the TWT surface immediately above. Hand contouring was required for the isochron maps for the shallow Near Top Poole Sandstone as well as the deeper Near Top Ordovician. The Ordovician only required minimal assistance with guide contours that could then be applied to the gridding function and allowed to infill, similarly for most other horizons in places of less seismic data.

The Near Top Poole Sandstone isochron required extensive hand contouring. This was principally because this layer of the stratigraphy is generally quite thin and fairly isopachus across the study area, with only a few exceptions in fault hanging walls, thus hindering the ease at which the gridding algorithm can ascertain values or trends to contour. Hand contouring for the Near Top Poole Sandstone isochron is made fairly obvious by the lack of detail in contouring compared to other isochron maps, though I expect that the true variability of the Poole Sandstone stratigraphic unit to be much more inhomogeneous in reality (the same could be said about the other isochron maps presented here also, even though their isochrons show more erraticism represented by each contour). Figures 6.11 to 6.25 demonstrate the TWT structure and isochron maps within the study area.

6. Basin Architecture: Structural Framework

Basin architecture determines the distribution (extent and thickness) of likely source rock and reservoir rock intervals, and defines structural styles and trapping geometries. Therefore, the characterisation of basin architecture is a critical component of petroleum systems analysis. Together, with source rock richness (Chapter 7) and petroleum systems modelling (Chapter 8), the mapping of basin architecture formed a significant portion of this research project.

Chapter 6 discusses the structural and stratigraphic framework of the Balgo Terrace, Betty Terrace and Billiluna Sub-basin, which is the result of workflows outlined in Chapter 4 and Chapter 5.

The key research questions that Chapter 6 aims to answer are:

- What is the nature of regional faulting within the study area?
- What is the distribution of prominent source rocks and reservoir rocks?
- Do regionally prominent source rocks and reservoir rocks exist within the study area?
- Are favourable trapping geometries and packages likely to contain sealing rocks present in the study area?
- What is the likely time-thickness and time-configuration of the key stratigraphic units?

6.1 Seismic Interpretation Results

The following section presents the results of the seismic interpretation to give insight into structural features. Figure 6.3 through Figure 6.7 demonstrates a representative example of the seismic grid in different regions of the project area. Key lines were chosen to demonstrate structural and stratigraphic variability. The lines that are presented are summarised in Table 6.1, and the distribution of the lines are highlighted in Figure 6.1.

Survey name	Line
Mt Bannerman 1982 SS	82GE-33
Mt Bannerman 1982 SS	32GN-01
Mt Bannerman 1982 SS	82GN-20
Billiluna SS	RB81-1
Billiluna SS	RB81-7
Billiluna SS	RB81-10

Table 6.1. 2D seismic lines presented to demonstrate seismic interpretation and geologic features with the project area.

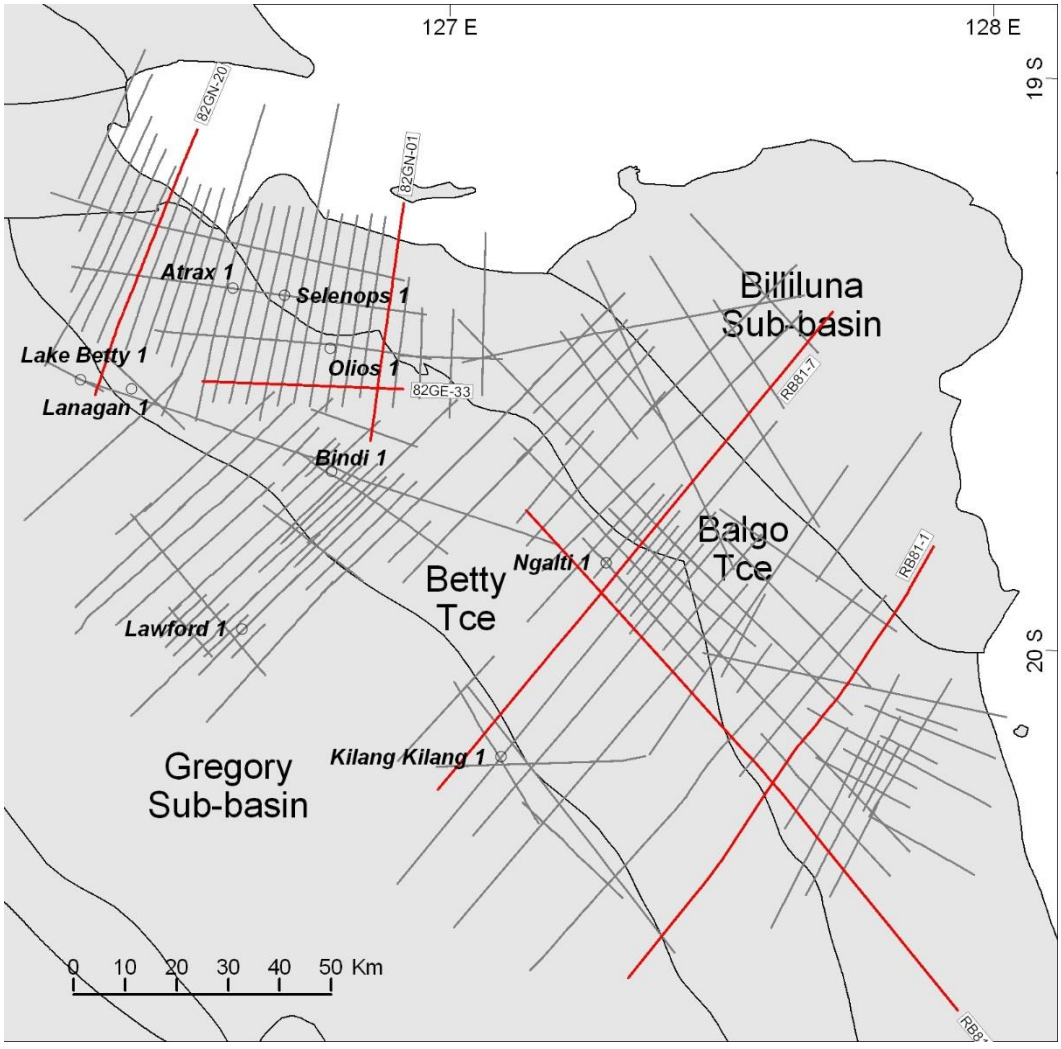

Figure 6.1. Distribution of seismic lines presented in Table 6.1.

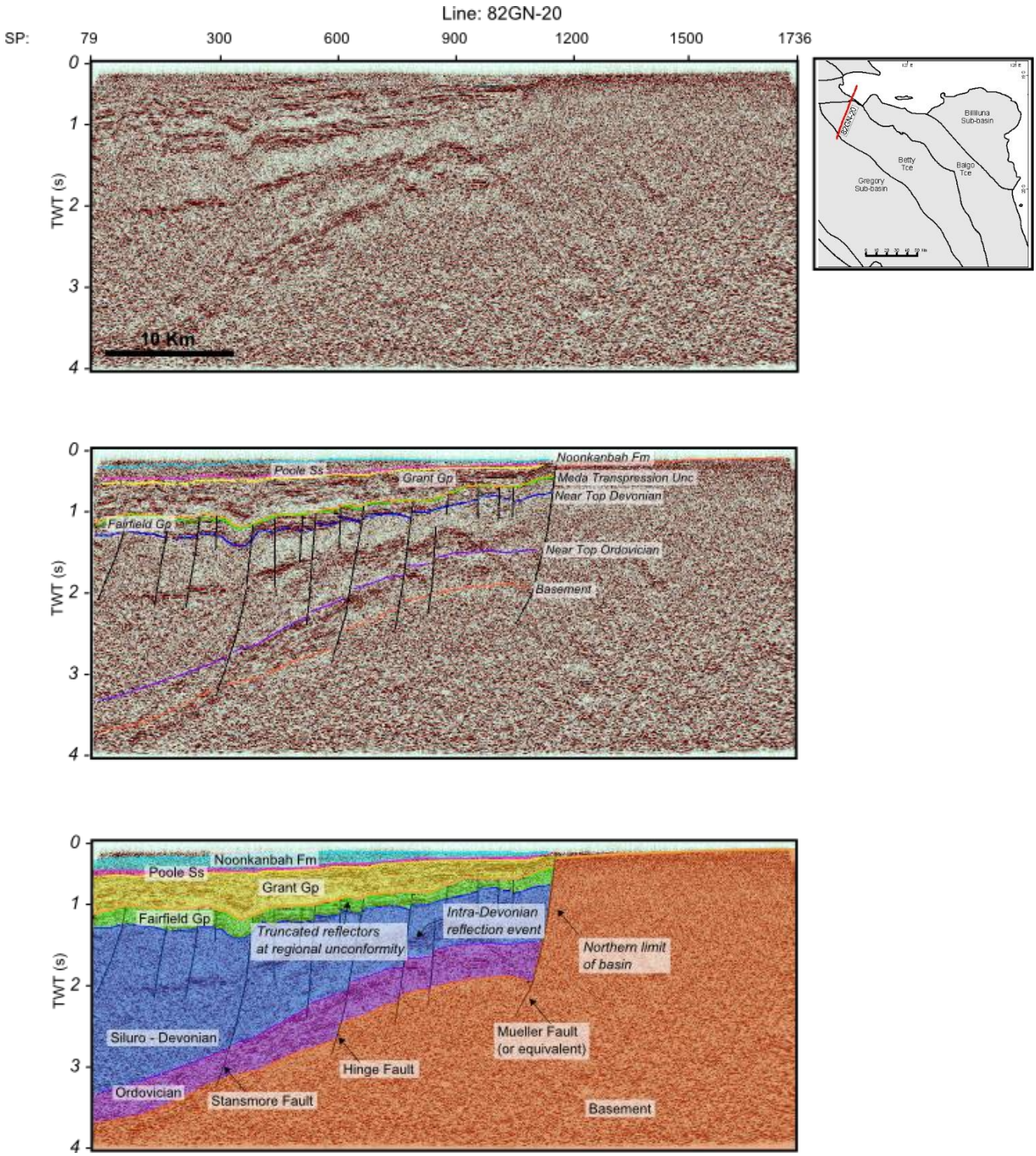

Figure 6.2. Line 82GN-20 demonstrates structural configuration (dip section) in the north western portion of the study area. Bare seismic (reprocessed) (top), interpretation of reflection events (middle) and geologic model from 2D (bottom).

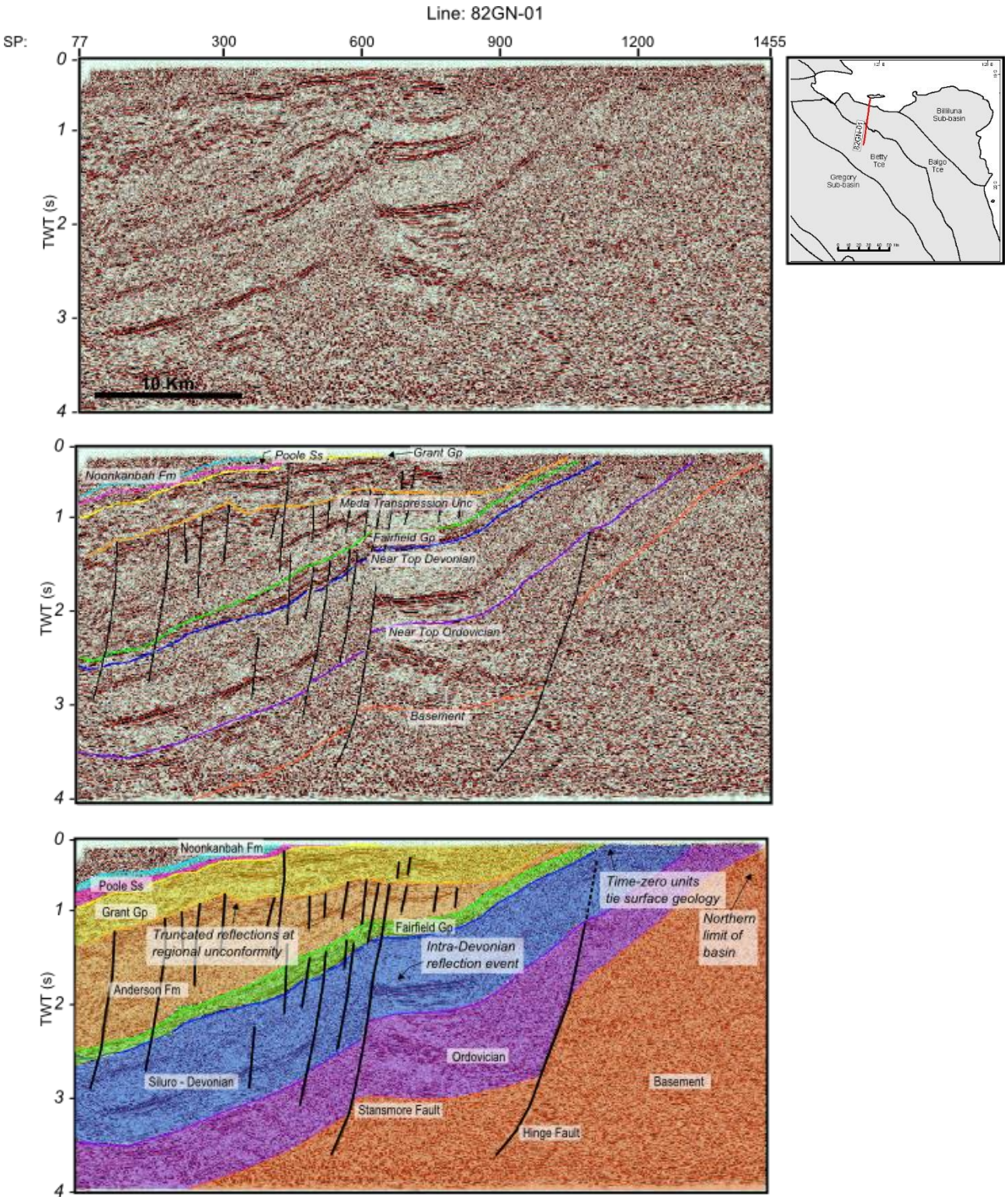

Figure 6.3. Line 82GN-01 demonstrates structural configuration (dip section) in the mid-north portion of the study area. Bare seismic (reprocessed) (top), interpretation of reflection events (middle) and geologic model from 2D (bottom).

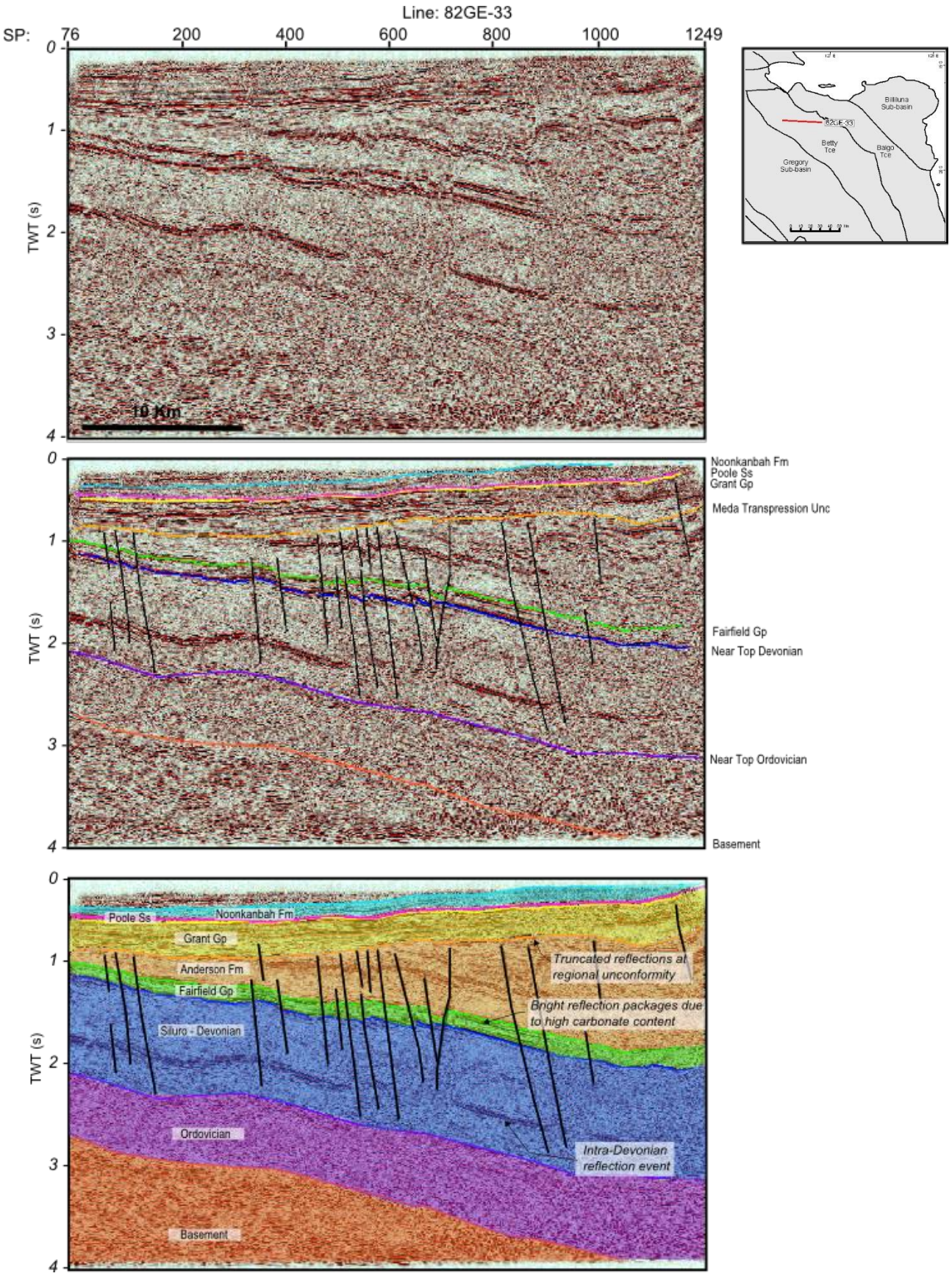

Figure 6.4. Line 82GE-33 demonstrates structural configuration (strike section) in the northern portion of the study area. Bare seismic (reprocessed) (top), interpretation of reflection events (middle) and geologic model from 2D (bottom).

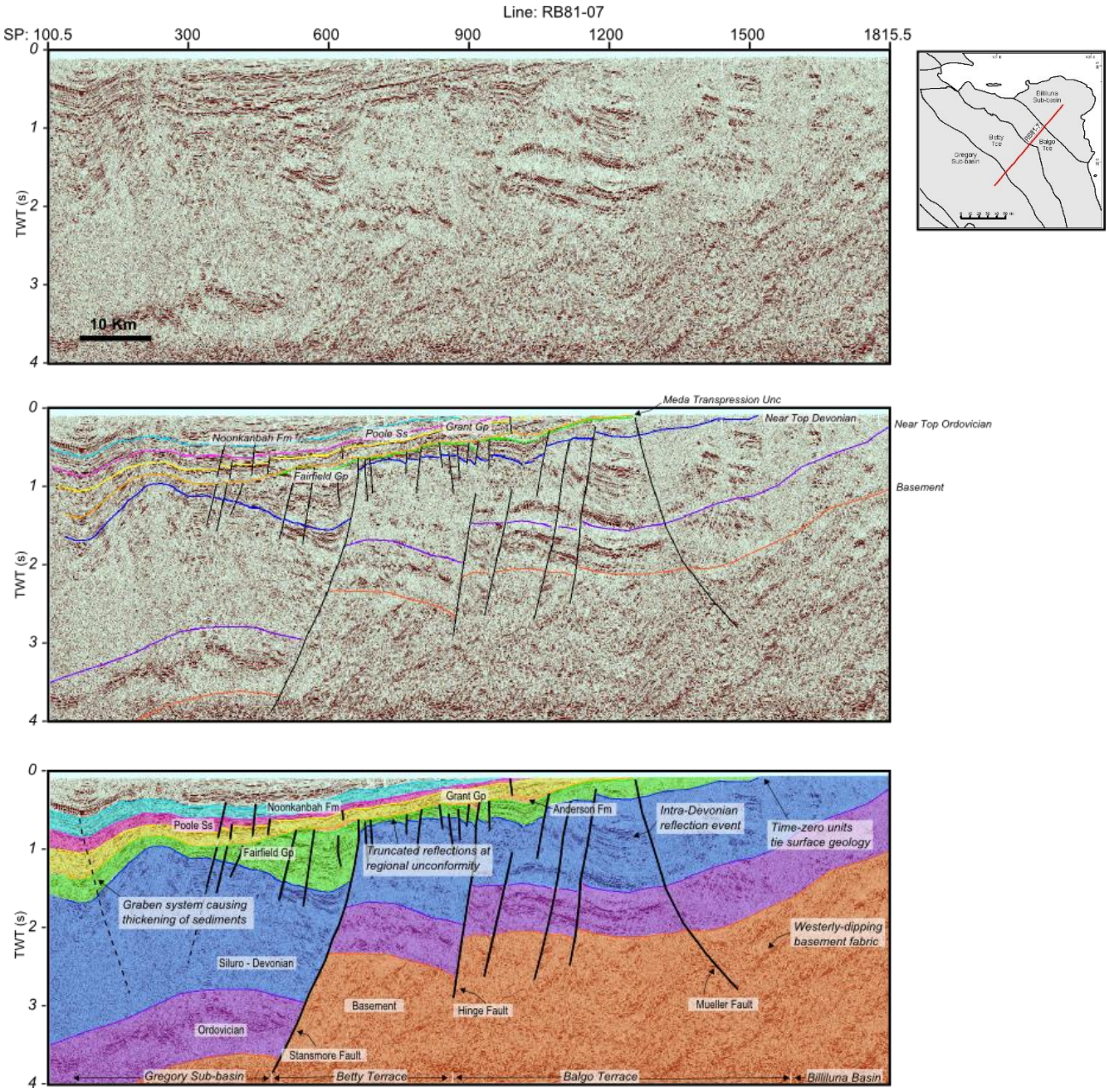

Figure 6.5. Line RB81-07 demonstrates structural configuration (dip section) in the north eastern portion of the study area. This line gives the longest cross section image of the geologic configuration across all tectonic provinces within the study area. Westerly-dipping pre-Cambrian fabric that is used to identify Basement is clear in the image. Bare seismic (reprocessed) (top), interpretation of reflection events (middle) and geologic model from 2D (bottom).

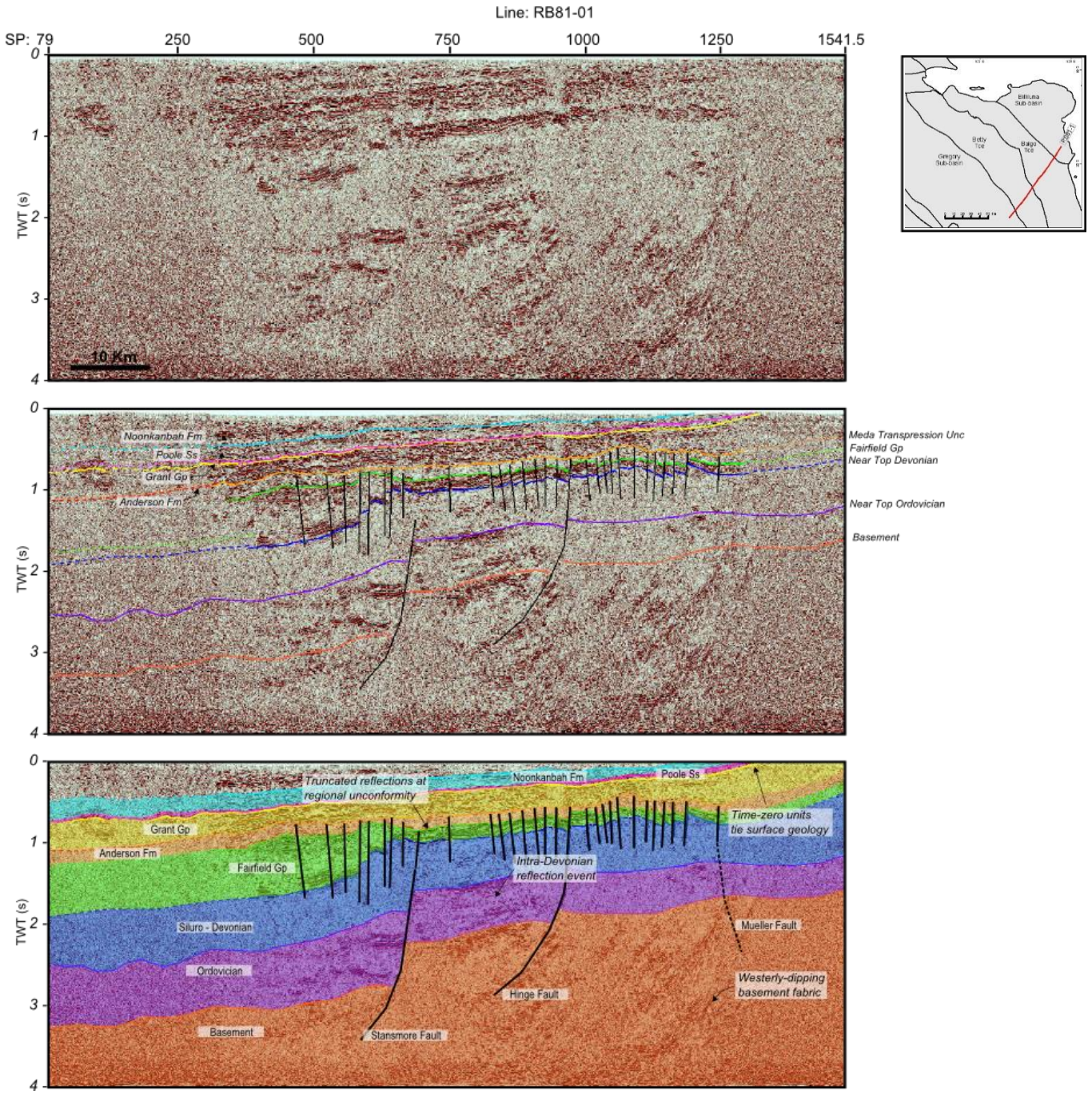

Figure 6.6. Line RB81-01 demonstrates structural configuration (dip section) in the south eastern portion of the study area. Bare seismic (reprocessed) (top), interpretation of reflection events (middle) and geologic model from 2D (bottom).

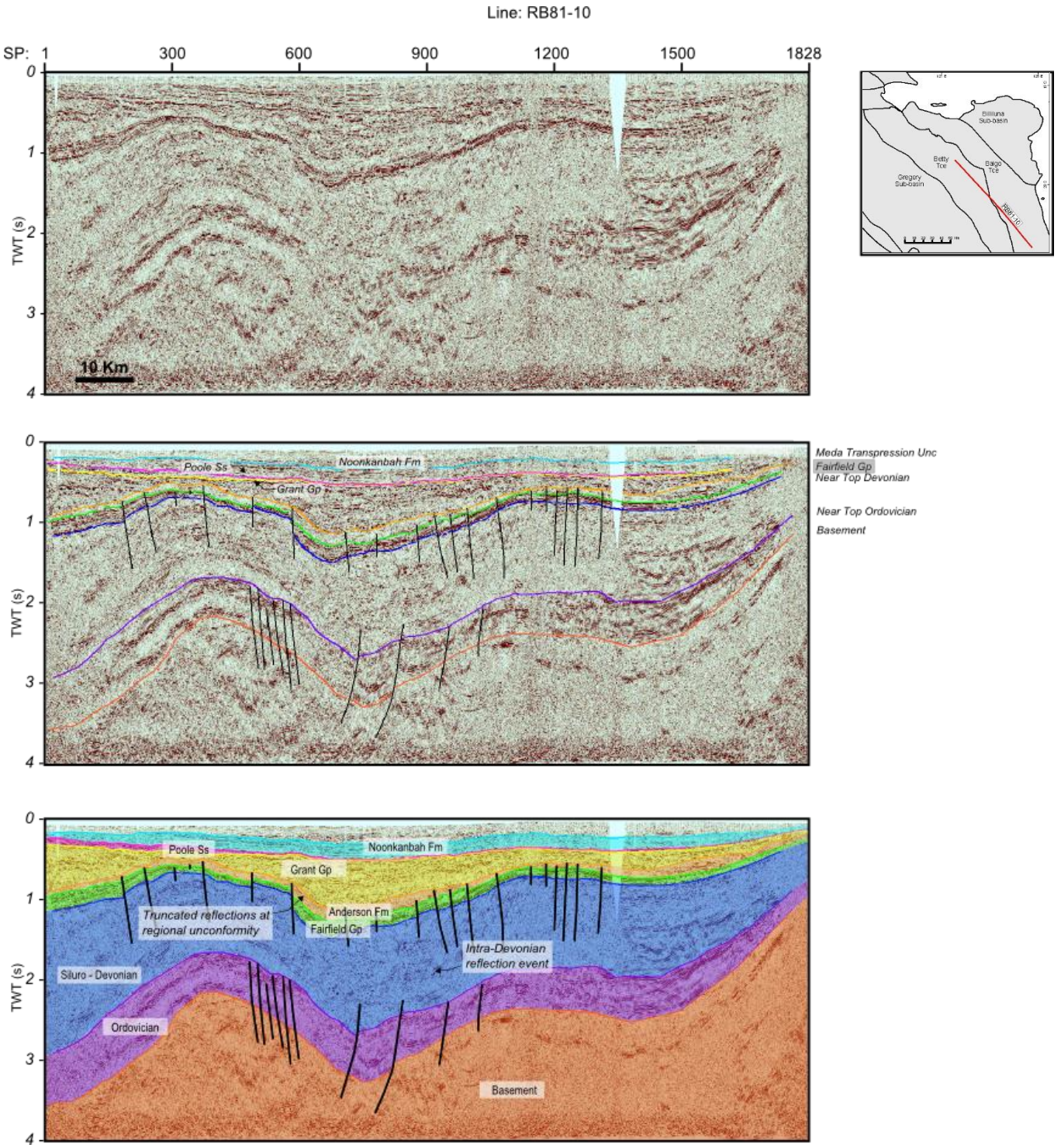

Figure 6.7. Line RB81-10 demonstrates structural configuration (strike section) in the central-south eastern portion of the study area. Bare seismic (reprocessed) (top), interpretation of reflection events (middle) and geologic model from 2D (bottom).

6.2 TWT Structure and Isochron Maps

Two-Way-Time (TWT) structure maps were produced for the interpreted horizons in Table 6.2. The results are shown in Figure 6.11 through Figure 6.18 at the end of this Chapter.

Isochron maps were produced for the interpreted horizons in Table 6.2. The results are shown in Figure 6.19 through Figure 6.25 at the end of this Chapter.

6.2.1 *The Case for a Revised Tectonic Elements Map*

The tectonic elements that are provided by the Western Australia Geological Survey (GSWA) are shown in Figure 6.8. A revision to the tectonic elements map (Figure 6.8) is supported here by correlating larger faults within the project area. Dashed-lines in Figure 6.8 represent uncertainty in the correlation in the central portion of the study area due to lesser data, and also on the northern basin margin where there is either no seismic, or data quality diminishes. The revision is not extreme, although it implies that the geological characteristics of the Gregory Sub-Basin are closer to the centre of the project area. As the Gregory Sub-basin is considered to host significant organically rich source rocks, it suggests that source rocks within the Gregory Sub-basin are nearer to potential reservoirs and trapping geometries that may exist within the study region, and that hydrocarbons require less lateral migration to fill traps. The interpretation here is similar to a map presented in Smith (1984), though the tectonic elements described here show the inferred faulting (dashed lines) to follow the boundary of the central depocentre, rather than cutting across it.

The revised tectonic element outlines are utilized in all TWT structure and isochron maps in this Chapter.

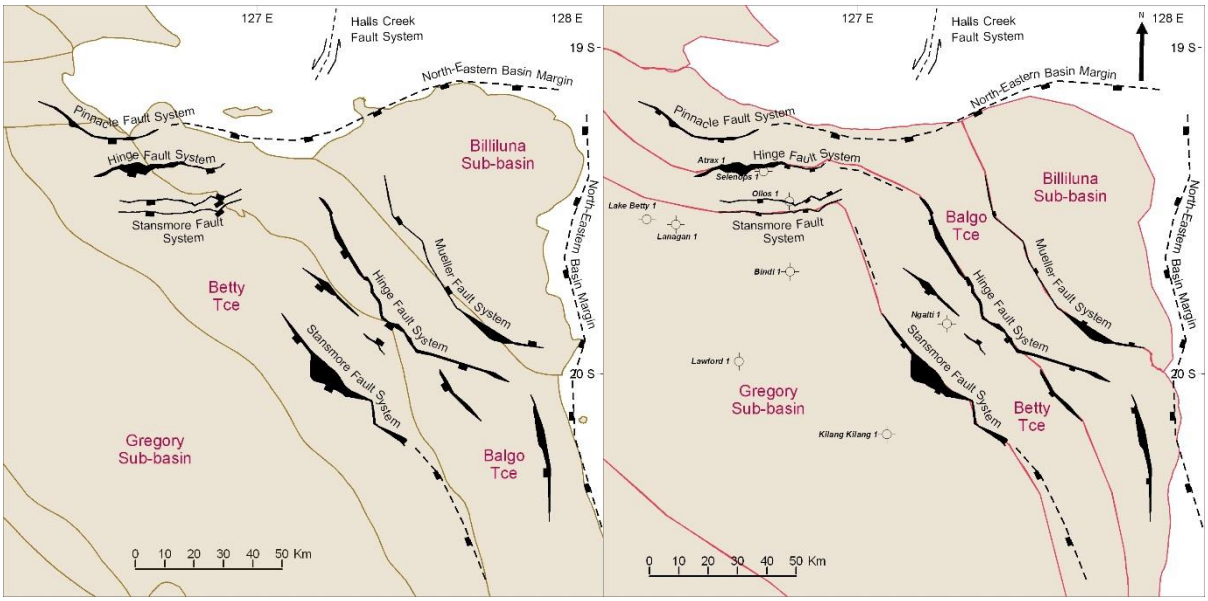

Figure 6.8. Tectonic divisions provided by GSWA (left) and proposed revision to the tectonic divisions pursuant to seismic interpretation (right). The spatial positioning is similar, but implies that the Gregory Sub-basin extends further to the northeast.

The Discussion below divides the study area into two main portions; the northwest, and southeast. The central study area is intermittently referred to in the ensuing sections (Figure 6.9). The division is not based on any geologic feature but rather makes the interpretation more manageable.

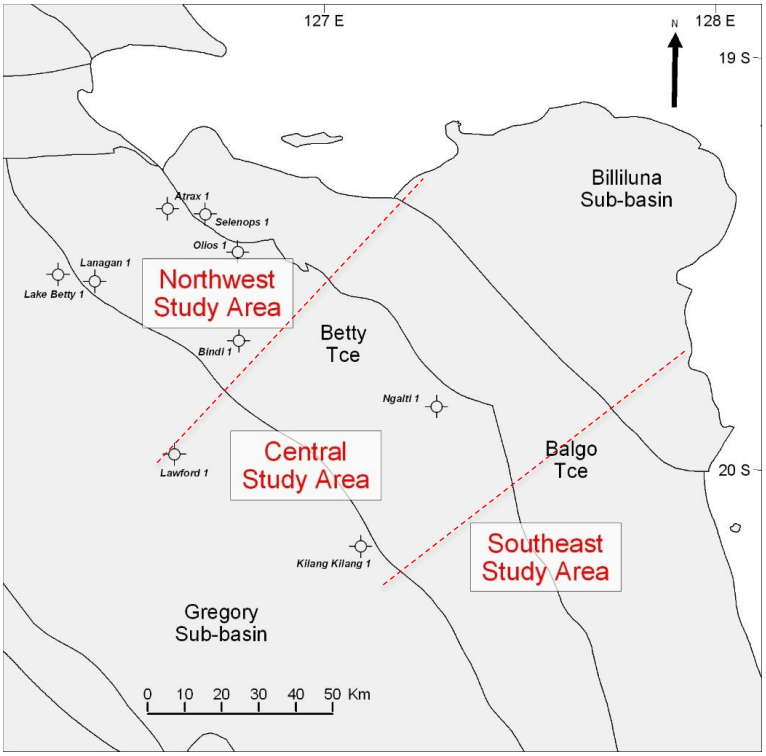

Figure 6.9. The northwestern, central and southeastern portions of the study area. Separation is arbitrary, but provided to aid in managing the interpretation.

6.2.2 *Northwestern Study Area*

Seismic interpretation reveals that there are two collections of stratigraphic (apparent seismic) dips in the northwestern portion of the study area. The regionally extensive Carboniferous Meda Transpression unconformity (Near Top Meda Transpression Horizon) separates the geology and represents an angular unconformable surface in most of the project area, most clearly observed on strike line 82GE-33 (Figure 6.4) where Carboniferous and older strata are truncated. Stratigraphy below the Meda Transpression unconformity (i.e. the Anderson Formation (where preserved), Fairfield Group, the Siluro-Devonian and Ordovician aged rocks) shows gentle apparent dips (approximately 15-20 degrees in time section on Figure 6.4) into the basin dipping towards the south and southeast, whereas stratigraphy above the Meda Transpression (ie the Grant Group, Noonkanbah Formation and Poole Sandstone) is generally flatter lying, and dip towards a similar south-southeast direction. The interpretation shows deeper packages of Ordovician to Early Carboniferous age are conformable and parallel in their extent, as is the stratigraphy post-Meda Transpression erosion. In the northwestern portion of the study area stratigraphic dips are generally similar across the Balgo and Betty Terraces, where the only variation is due to the proximity of the central depocentre (ie dips on line 82GN-01 appear steeper than on 82GN-20, which is also consistent with TWT structure of Carboniferous and older strata).

It is clear from contour mapping that the dips observed from lines 82GN-20, 82GN-01 and 82GE-33 are on the northern edge of a depocentre located in the central portion of the study area (considered here an extension of the Gregory Sub-basin rather than a separate feature – per revision of tectonic elements, Chapter 6.2.1). The depocentre is more pronounced in pre-Carboniferous time (see TWT maps of the Fairfield Gp, Figure 6.15; Siluro-Devonian, Figure 6.16; and Ordovician sections, Figure 6.17), and there is a slight thickening of pre-Meda Transpression sediments in this part of the region towards and within the Gregory Sub-basin. Stratigraphy above the Meda Transpression remain fairly isopachus and the trend into this central depocentre is less pronounced.

Basement in the northwestern portion of the study area is mapped as a chaotic reflection character underneath a package of Ordovician age reflections. The westerly dipping ‘fabric’ (Chapter 5.3.8) is not clearly observed in this northern area. Basement is seen to deepen in accordance with the central depocentre (southwards) and is in excess of 4 seconds TWT on 82GE-33. Lines 82GE-33 and 82GN-20 (Figure 6.4 and Figure 6.2 respectively) demonstrate

a shallowing basement trend (to 2 seconds TWT) towards the west as the strata moves towards the Jones Arch (west of the study area). All pre-Carboniferous stratigraphy appears to thin towards the Jones Arch and towards the northern basin limit. The Anderson Formation is generally preserved in the central depocentre and thins to the north with other strata, though The Meda Transpression truncates the units of the Anderson Formation completely to the west (towards the Jones Arch) (there is no preserved Anderson Formation on line 82GN-20), and the Anderson Formation subcrops before reaching Selenops 1 or Olios 1 in the north (Meda Transpression TWT structure, Figure 6.14).

Dip lines 82GN-20 (Figure 6.2) and 82GN-01 (Figure 6.3) demonstrate the main fault elements within the northwestern part of the study area. Most of the faulting was active throughout the Ordovician extension, and again in the Mid Carboniferous. Fault throws are difficult to quantify in Early Ordovician time as reflection events within acoustic basement are not clearly identifiable. It is assumed that fault throws observed within the main stratigraphic section are generally representative of throws that are not clearly visible due to poor reflections.

82GN-20 (Figure 6.2) shows sediments intersecting the northern limit of the basin at the eastern end of the Pinnacle Fault; a normal fault that is a more prominent feature on the Lennard Shelf (a similar strike-related shelfal position to the northwestern portion of the study area). The Pinnacle Fault is shown to be active throughout the Ordovician and appears to control sedimentation through to the Permian (Poole Sandstone). Near surface data quality issues make the shallow parts of the Pinnacle Fault difficult to identify, though it is likely that the Pinnacle Fault controlled sedimentation along the northern basin margin into the Triassic. 82GN-20 (Figure 6.2) and 82GN-01 (Figure 6.3) demonstrate the Hinge Fault in this portion of the study area. The Hinge Fault is a large normal fault the separates that Balgo Terrace from the Betty Terrace. The Hinge Fault was active throughout the Ordovician and in periods through to the mid-Carboniferous, evidenced by slight thickening in Devonian and Carboniferous reflection packages. 82GN-20 also shows the normal Stansmore Fault system. The Stansmore Fault system is one of the most significant faults in the study area, and separates the Betty Terrace from the Gregory Sub-Basin. The Stansmore Fault was active throughout Ordovician times and in periods through to the Mid-Carboniferous, shown by slight thickening of the Siluro-Devonian section below the Intra-Devonian reflection event (labeled on 82GN-20, Figure 6.2). The fault does not appear to control sedimentation post-Meda Transpression time.

Strike line 82GE-33 (Figure 6.4) demonstrates faulting geometries within the Betty Terrace. Here, normal faults are consistent with main faulting regimes (the nearby Stansmore and Hinge Faults). The faulting patterns are illustrated to offset Siluro-Devonian to Carboniferous stratigraphy (related to mid-Carboniferous Meda Transpression deformation). The seismic suggests that these faults do not extend to the Ordovician strata, though data quality also deteriorates and some of the large faults in 82GN-33 may in fact penetrate Ordovician aged section (Figure 6.4).

82GN-01 (Figure 6.3) and 83GE-33 (Figure 6.4) show some instances of shallower faulting through the Anderson Formation and into the Grant Group. The shallow faulting observed here is possibly remnants of the Triassic aged Fitzroy movement, or more recent Jurassic events. Duddy et al. (2003) concluded that Triassic to Jurassic tectonic events removed up to 2500 metres of Triassic sediment within the Canning Basin, and faulting seen in shallow parts of the preserved section may be related to this exhumation.

6.2.3 *Southeastern Study Area*

Seismic lines RB81-07 (Figure 6.5), RB81-01 (Figure 6.6) and RB81-10 (Figure 6.7) of the Billiluna 1981 Seismic Survey are some of the longest 2D lines in the project and present a good reflection image of the subsurface across the southeastern project area. Line RB81-07 specifically, provides an excellent cross section of the otherwise data-poor Billiluna Sub-basin, as well as the Balgo Terrace, Betty Terrace and proximal section of the Gregory Sub-basin.

Seismic interpretation of lines RB81-07 (Figure 6.5) and RB81-01 (Figure 6.7) show that stratigraphic (apparent seismic) dips of post-Carboniferous stratigraphy (Grant Group, Noonkanbah Formation and Poole Sandstone) are at approximately 10 degrees to the southwest (basinward), conformable, and thickening basinwards. There is, however, a greater variability in pre-Carboniferous stratigraphic dips in the southeastern portion of the study area due to a broad anticline that developed in the Triassic (RB81-7, SP 300, Figure 6.5), though dips overall appear to trend towards the Gregory-sub basin. Reflections in the Billiluna Sub-basin (RB81-07) dip towards the Mueller Fault between approximately 10 and 15 degrees.

Reflections in the Betty Terrace and Gregory Sub-basin tend to show a broad anticline appearance (RB81-07, Figure 6.5) in the central project area, where the Stansmore Fault cuts the anticline between the Gregory Sub-basin and Betty Terrace. It is difficult to confirm whether the stratigraphic thickening of the post-Carboniferous units at the southwestern-most edge of line RB81-07 (left flank; basinward side of the broad anticline, Figure 6.5) is related to the large graben system of the Gregory Sub-basin, possibly reactive in periods up to the mid-Jurassic. The RB81-7 line is not quite long enough for this, though the opposing listric fault to the Stansmore, on the southwestern edge of the Gregory Sub-basin (illustrated by the dashed line), is likely related to a mirror image of what is visible on the southwestern flank of RB81-7.

Stratigraphic reflections within the Balgo Terrace and Betty Terrace appear generally horizontal; also appearing as a subtle broad syncline on the Balgo Terrace (RB81-07, Figure 6.5), though the same synclinal form cannot be seen in the southern end of the project area (RB81-01, Figure 6.6). TWT structure over the Balgo Terrace in this region (refer to intersection of RB81-07 and RB81-10 and TWT maps for Fairfield Group, Figure 6.15, and Devonian sections, Figure 6.16) reveals a trough in the Balgo Terrace, and a structural nose developing through Ordovician to Early Carboniferous time. The Ngalti 1 well was drilled on the ridge at the apex of this structural nose.

Basement in the southeastern portion of the study area is characteristically different than observed in the northwestern area. Lines RB81-07 (Figure 6.5) and RB81-01 (Figure 6.6) show a westerly dipping ‘fabric’ (steeply dipping pre-Cambrian beds, or tilted fault blocks). Reflection events are also slightly more chaotic here than in the younger Canning Basin stratigraphy. The Ordovician rocks appear to unconformably overly the basement in this regard. As noted in text earlier in this Chapter, only the northwest-southeast oriented lines (such as RB81-07, Figure 6.5) reveal this fabric because seismic imaging on lines oblique to the fabric do not capture these ‘intra-basement’ reflections and instead represent basement as a chaotic package.

Basement in the southeastern study area is in excess of 4 seconds TWT trending into the Gregory Sub-basin (and continues below the section view on RB81-07). In the central part of the project area, basement averages 2 seconds TWT on the Balgo Terrace and shallows to 1 second TWT in the Billiluna Sub-Basin, eventually outcropping at the northeastern basin margin (TWT structure on Near Top Basement, Figure 6.18; not visible on seismic data). The

southern-most part of the project area shows similar basement (apparent) depths, and is viewed on RB81-10 (Figure 6.7) shallowing to 1 second TWT towards the southeastern basin margin. Basement continues to shallow out of the section view to approximately tie surface geology.

Seismic line RB81-07 (Figure 6.5) demonstrates the major faults that define the tectonic regions within the study area. The reader is also referred to the TWT structure map on the Near Top Basement (Figure 6.18) as this will aid in visualizing the geometries of the major faulting elements. The Stansmore Fault separates the Betty Terrace from the Gregory Sub-basin. All of the pre-Carboniferous stratigraphy appears to thicken in the Stansmore Fault hanging wall (into the Gregory Sub-basin, Figure 6.15 and Figure 6.16). The Fairfield Group is shown to be truncated by the Meda Transpression unconformity in the footwall in this vicinity, though small sections of preserved Anderson Formation may indicate an upper limit of Fairfield Group deposition on the Betty and Balgo Terraces, suggesting that Fairfield Group deposition is controlled by the Stansmore Fault in the Gregory Sub-basin. This demonstrates a synrift sequence, also observed with lesser throw on RB81-1 (Figure 6.6). A similar thickening can be seen in the Siluro-Devonian section across the Stansmore Fault, and also a slight thickening in the Ordovician strata (Figure 6.5; also isochron maps for the Fairfield Group, Figure 6.23; Siluro-Devonian, Figure 6.24; and Ordovician, Figure 6.25). This indicates that the Stansmore Fault (and the Gregory Sub-basin system in a larger context) was active in periods from the Ordovician through to the mid-Carboniferous, alluding to syndepositional faulting associated with the Gregory Sub-basin. The same thickening cannot be seen in Late Carboniferous and younger rocks.

The Hinge Fault in the southeast area (RB81-07, Figure 6.5) shows slight synrift thickening in the Ordovician and thickening of the Siluro-Devonian stratigraphy, terminating at the Meda Transpression Unconformity. Whilst deformation is clear in the Carboniferous at this location (for example in the Fairfield Group), the same influence on deposition is not as clearly observed in the preserved section of the Fairfield Group as it is across the Stansmore Fault, where only a minor amount of thickening is observed.

The Mueller Fault (imaged on RB81-07, Figure 6.5) is a large listric fault separating the Billiluna Sub-basin from the Balgo Terrace. A decline in seismic data quality makes identifying fault throws slightly more difficult in the Billiluna Sub-basin. The interpretation shows the Mueller Fault throwing down to the northeast into the Billiluna Sub-basin and

away from the Gregory Sub-basin. RB81-07 shows very slight TWT thickening of the Ordovician and Siluro-Devonian packages across the Mueller Fault into the Billiluna Sub-basin at the fault intersection (Figure 6.5).

The interpretation also indicates a package of Carboniferous Fairfield Group in the Billiluna Sub-basin (RB81-7, Figure 6.5). As mentioned previously, there are no wells in the Billiluna Sub-basin, and Cenozoic cover (per surface geology) makes tying the interpretation to external data nearly impossible, however younger units (Permian) and older units (Devonian) show outcrop on surface geology maps that tie the respective parts of the interpretation. To keep the mapping as isopachus as possible across the Mueller Fault, the Fairfield Group is interpreted to exist in the Billiluna Sub-basin. Note however, that if no Fairfield Group were to exist in the Sub-basin, the Devonian would be thicker than what is shown here (RB81-7, Figure 6.5), which could imply that the Mueller Fault might actually dip in the opposite direction towards the Gregory Sub-basin (assuming a normal/extensional stress regime, which is evident throughout Canning Basin geological history). Another alternative that would allow the Siluro-Devonian to exist at surface along the whole Billiluna Sub-basin in place of the Fairfield Group; is to suppose that the Fairfield Group (or equivalent) was deposited in the Billiluna Sub-basin, and due to reactivation on the Mueller Fault (potentially during the Triassic aged Fitzroy event) the fault was inverted, and the Fairfield Group eroded in Triassic time; thereby bringing the Siluro-Devonian to surface. An expectation though would be to see inverted reflection events with a possible null-point (though this may have also been eroded along with the Fairfield Group). Again, seismic data quality makes these determinations difficult, and it is thought that the interpretation represents the (simpler?) optimistic view for the purposes of this study.

Two-way-travel time (TWT) structure on the top of the Late Carboniferous to Permian units (Noonkanbah Formation, Poole sandstone and Grant Group; Figure 6.19 to Figure 6.21) show that these surfaces gently dip at approximately 10 degrees to the southeast into the Gregory Sub-basin. Dips of the Late Carboniferous to Permian strata steepen slightly in the northwest (mentioned above). There is a high at this level in the stratigraphic sequence in the Gregory Sub-basin at 20° 14’S, 127° 10’E (Kilang Kilang 1 the flank of this structure, approximately on line RB81-07, Figure 6.5; and cross section B-B’, Figure 4.45). The Noonkanbah Formation and Poole Sandstone outcrop on the northwestern and southwestern basin margin, and along a northwestern trend across the Balgo and Betty Terraces. The Grant Group is noted to outcrop further into the study area on the Balgo Terrace (Figure 6.13). Faulting is

likely to intersect these Late Carboniferous to Permian units, potentially a product of the Triassic Fitzroy Movement, however faults were not correlated across these surface as they were not significant to the tectonic province definition or prospect generation, or achievable within time constraints allocated for this stage of the project (refer to Chapter 5.4).

The Meda Transpression Unconformity is a regional marker across the study area and represents a regional exposure surface. The unconformity truncates Early Carboniferous stratigraphy across the Canning Basin (Figure 6.14). The Meda Transpression surface is also a proxy here for TWT structure of the Anderson Formation (Figure 6.22), because in many places the Anderson Formation is truncated to great extent by the regional unconformity. The Meda Transpression surface generally mirrors younger surfaces in apparent seismic dip with the exception of a low in the surface in the central project area on the Betty Terrace 19° 36'S, 127° 13'E (TWT structure on the Near Top Meda Transpression; Figure 6.14) that appears to develop a connection or 'trough' in the Gregory Sub-basin. The high that is present in the younger surfaces (at 20° 14'S, 127° 10'E, Figure 6.13) is also present in the Meda Transpression surface, suggesting that the feature was generated after the unconformity associated with this Carboniferous event. The high occurs generally consistently on reflections at this location (RB81-07) and is probably associated with compressional events in the Triassic Fitzroy Movement. Another subtle high in this surface is noted in the southeastern project area on the Betty Terrace at 20° 15'S, 127° 46'E.

TWT structure on the top of Late Carboniferous and older units (Fairfield Group, Siluro-Devonian, Ordovician and Basement packages, Figure 6.15 through Figure 6.18) show a very different structural form than younger units, explained by the structural overprints introduced by the Carboniferous Meda Transpression event and also the Triassic Fitzroy Movement.

Two broad (approximately 50 kilometers wide each) northeast-southwest oriented lows are noted as major structural features separated by a ridge in the central project area (20°S, 127° 10'E, RB81-10; Figure 6.7), deepening to approximately 2.4 seconds TWT in each low at the Fairfield Group level (Figure 6.15). The northern-most low continues over the Betty and Balgo Terrace and appears to continue to the northern basin margin. The southern low appears more disconnected from the basin margin and is generally more confined to the Gregory Sub-basin. A projected position (a useful but non-optimal cross section) of the lows and central ridge can be seen on RB81-10 (edge of the northern low at SP 1, central ridge at SP 400 and southern low at SP 750; Figure 6.7) The ridge appears on RB81-10 as an

anticline, and the lows are synflormal off the anticline flanks to the northeast and southwest. The features are probably the product of mid Carboniferous compression events, after uplift and erosion of the Pre-Carboniferous stratigraphy. The northern low may be influenced by north-south oriented strike slip faults of the Halls Creek region (Figure 6.8), as the low trend intersects the northern basin margin where the Halls Creek zone had greater influence on the basin.

Up dip across the Stansmore Fault (northeast-ward), the central area ridge (or anticline) broadens to a more complex faulted structural nose (19° 50'S, 127° 21'E, Figure 6.15). The nose trends similar to the central ridge – northeast-southwest, and is intersected and flanked along strike by grabens associated with the Hinge Fault system. Ngalti 1 tested the apex of this structural feature. The structure extends from the Stansmore Fault, across the Betty and Balgo Terraces and intersects the Mueller Fault. It is questionable from current seismic data as to whether the same structural feature continues across the Mueller Fault into the Billiluna Sub-basin.

In the southeastern project area, an elongate northeast trending high exists in the pre-Carboniferous levels at 20° 17'S, 127° 46'E (approximately 26 km x 13 km, Figure 6.16). The high spans across the Betty and Balgo Terraces. Viewing the projected position of the high on RB81-10 (Figure 6.7) shows that it probably formed as a product of Mid-Carboniferous tectonic events. The high is intersected by a graben at the crestal position (refer TWT structure on Near Top Fairfield Group, Figure 6.15), RB81-10 shows that there is a minor amount of apparent throw offsetting the Fairfield Group and Siluro-Devonian section.

6.2.4 *Structural Lead Identification*

Seismic interpretation has produced numerous apparent time structures within the project area, across several levels of stratigraphy. Structural development is most clearly noted on the TWT structure map on the Near Top Fairfield Group (Figure 6.10). Structural development also translates through other levels, illustrated in Figure 6.16 and Figure 6.17. Although many more traps are identifiable, it is prudent to identify a selection that appear common throughout the stratigraphy (Table 6.2). Closure areas are based on closing contours in Table

6.2. The purpose of identifying structural traps at this stage gives another goal to 2D basin modelling. It is not a goal here to construct a detailed prospect portfolio.

Trap	Closing contour (TWT msBSD)	Closure Area (Km^2)	Seismic reference	Nature of Trap
A	800	363	RB82-28	Structural; fault bound to northeast
B	900	139	Arbitrary line (S85LM-08, S85LM-08A, 82GN-03	Structural; fault bound to north
C	750	20	RB81-7	Structural; atop the Billiluna Horst, fault bound to north and south
D	700	308	RB81-7	Structural, fault bound to northeast and southwest
E	500	63	RB82-23	Structural; found bound to northeast

Table 6.2. Summary of key structural leads identified from seismic interpretation.

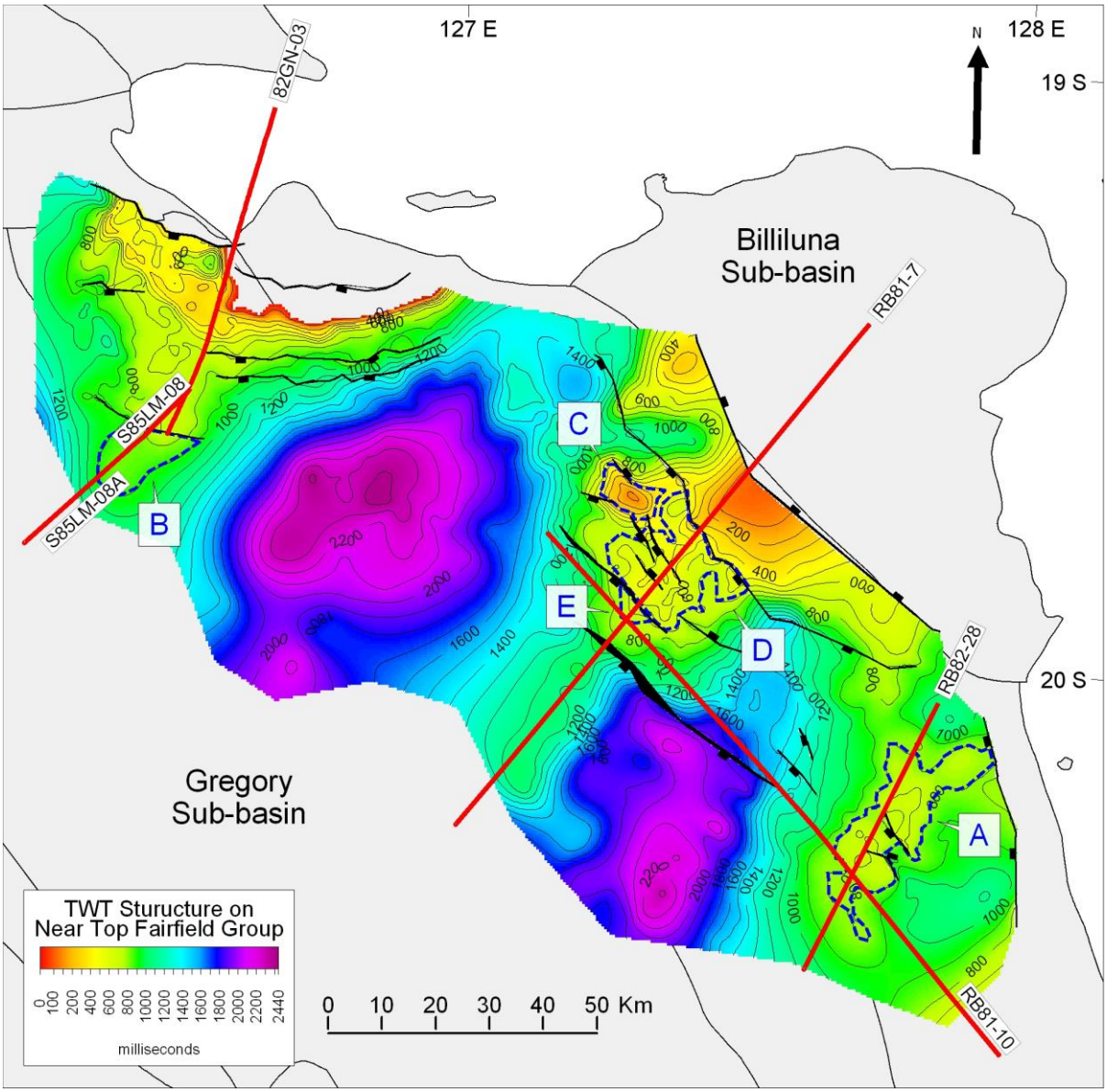

Figure 6.10. Key structural leads identified from seismic interpretation. Leads are apparent time structures that exist on multiple levels. Demonstrated on the Near Top Fairfield TWT map in this instance.

The red seismic lines on Figure 6.10 indicate where 2D modelling would be most valuable. 2D petroleum systems models will test apparent time structures, and importantly have regional distribution to enable a thorough understanding of thermal maturity and petroleum system evolution across the project area.

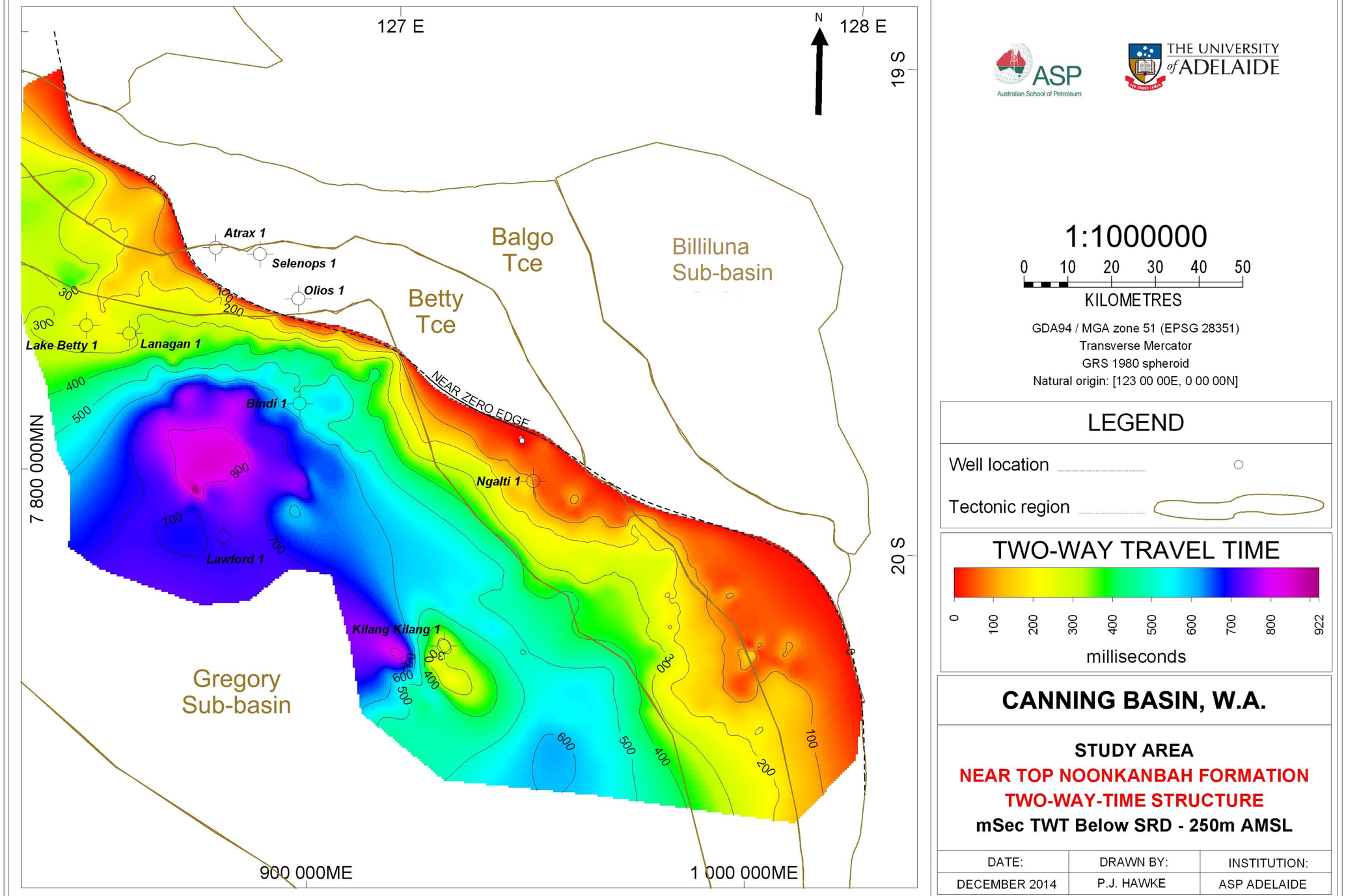

Figure 6.11. TWT structure on Near Top Noonkanbah Formation.

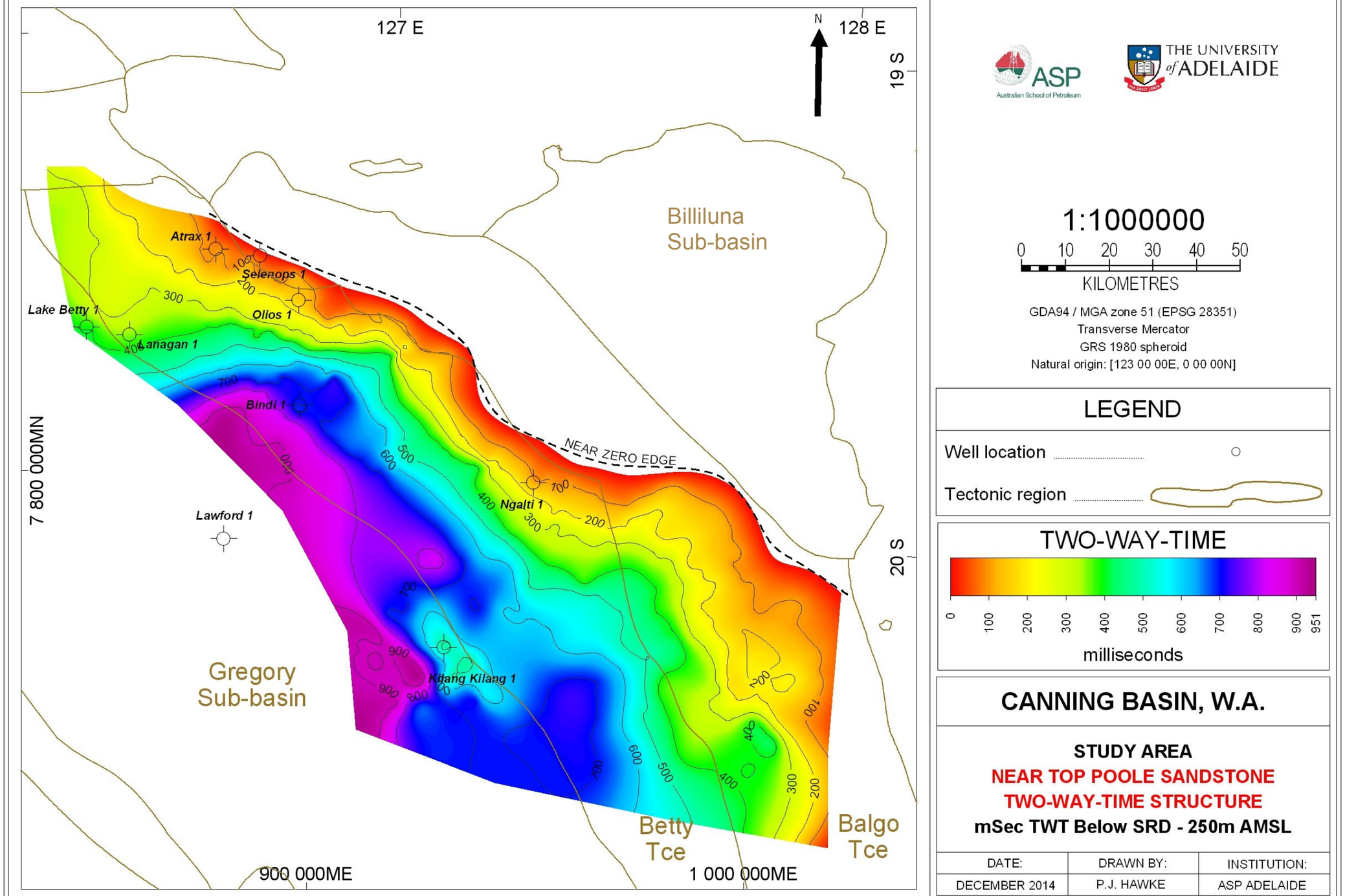

ASP
Australian School of Petroleum

THE UNIVERSITY of ADELAIDE

1:1000000

0 10 20 30 40 50

KILOMETRES

GDA94 / MGA zone 51 (EPSG 28351)
Transverse Mercator
GRS 1980 spheroid
Natural origin: [123 00 00E, 0 00 00N]

LEGEND

Well location

Tectonic region

TWO-WAY-TIME

0 100 200 300 400 500 600 700 800 900 951

milliseconds

CANNING BASIN, W.A.

STUDY AREA
NEAR TOP POOLE SANDSTONE
TWO-WAY-TIME STRUCTURE
mSec TWT Below SRD - 250m AMSL

DATE:	DRAWN BY:	INSTITUTION:
DECEMBER 2014	P.J. HAWKE	ASP ADELAIDE

Figure 6.12. TWT structure on Near Top Poole Sandstone.

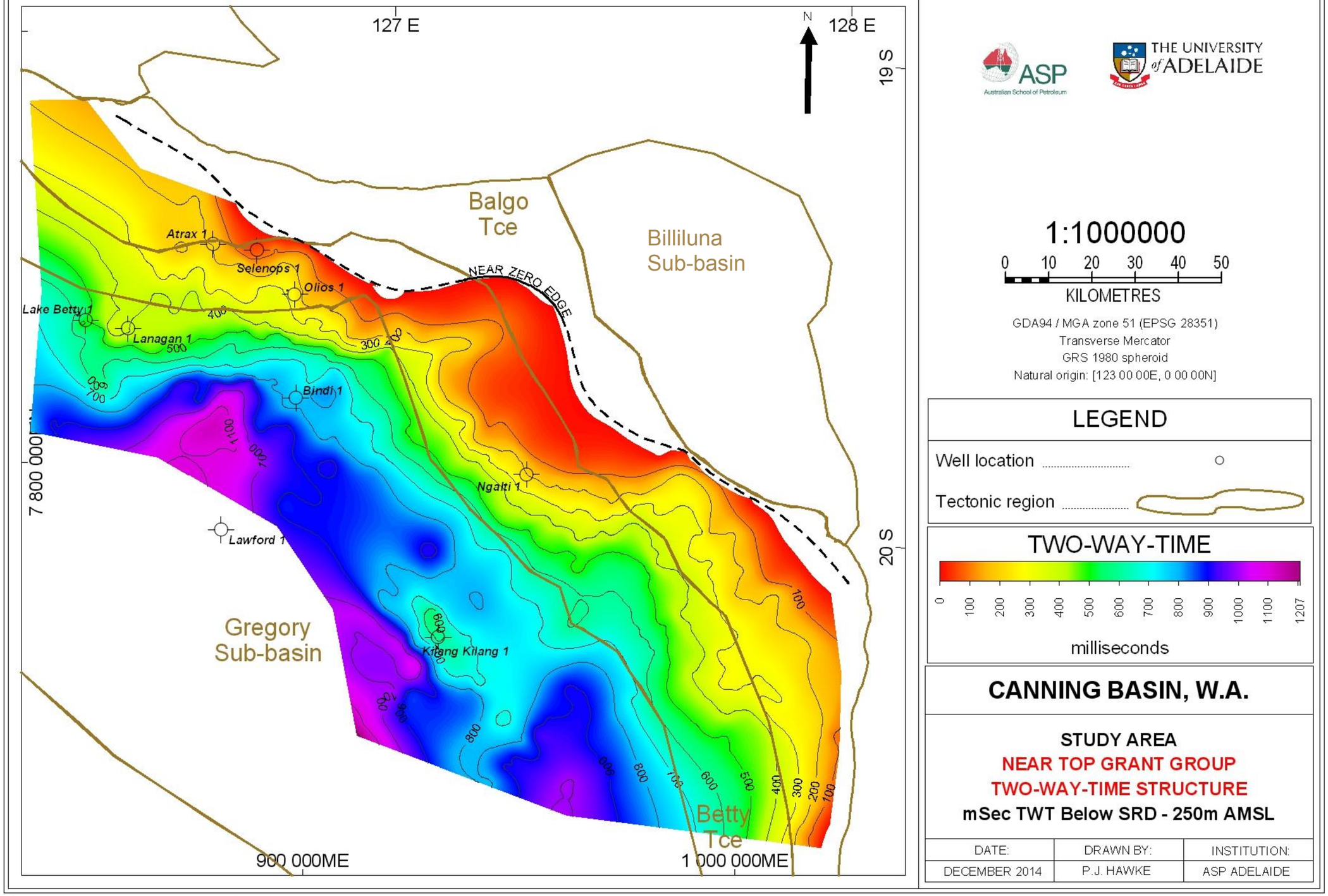

Figure 6.13. TWT structure on Near Top Grant Group.

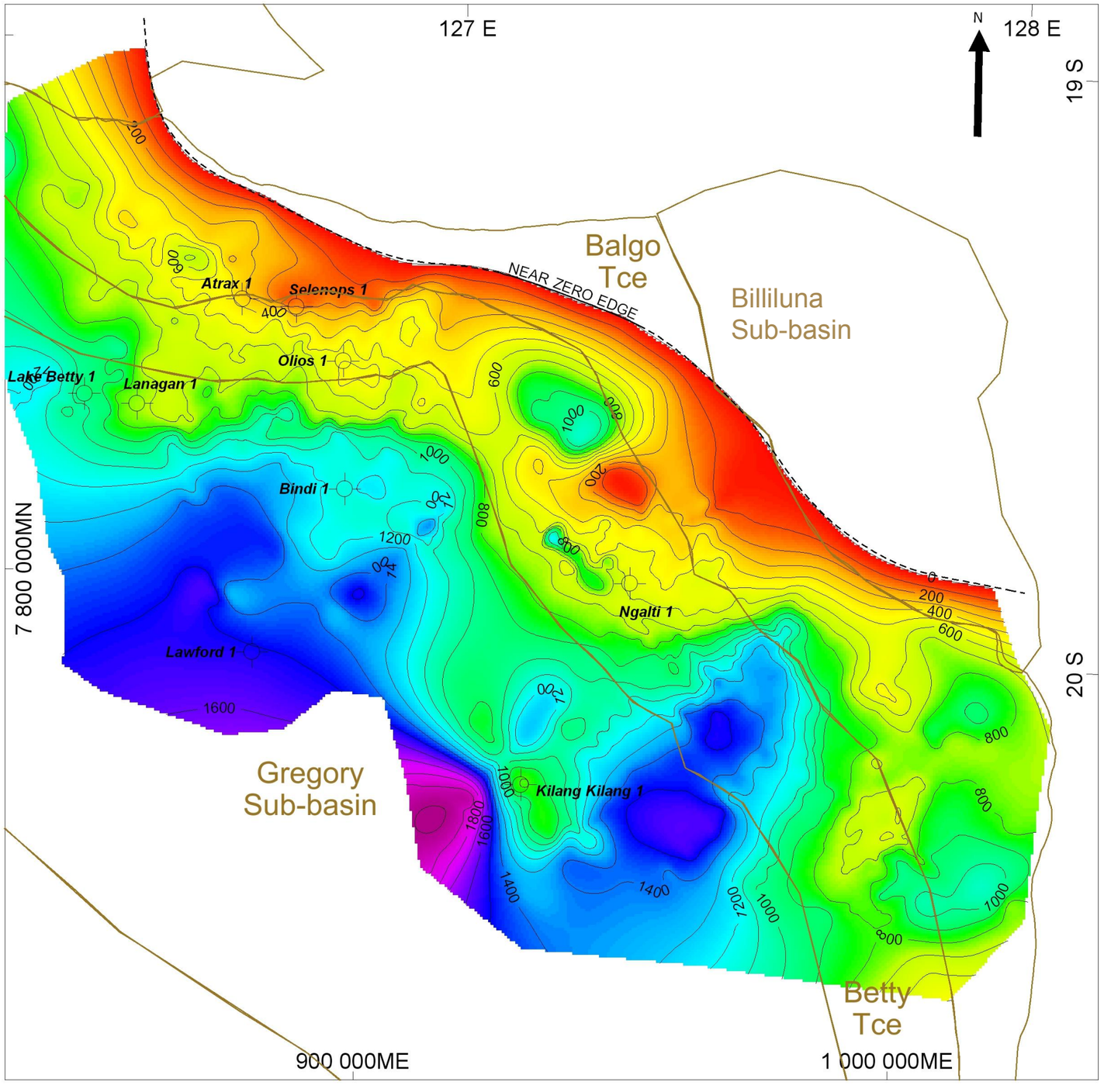

ASP Australian School of Petroleum

THE UNIVERSITY of ADELAIDE

1:1000000

0 10 20 30 40 50

KILOMETRES

GDA94 / MGA zone 51 (EPSG 28351)
Transverse Mercator
GRS 1980 spheroid
Natural origin: [123 00 00E, 0 00 00N]

LEGEND

Well location

Tectonic region

TWO-WAY-TIME

0 100 200 300 400 500 600 700 800 900 1000 1100 1200 1300 1400 1500 1600 1700 1800 1900 2016

milliseconds

CANNING BASIN, W.A.

STUDY AREA

TOP MEDA-TRANSPRESSION UNCONFORMITY

TWO-WAY-TIME STRUCTURE

mSec TWT Below SRD - 250m AMSL

DATE:	DRAWN BY:	INSTITUTION:
DECEMBER 2014	P.J. HAWKE	ASP ADELAIDE

Figure 6.14. TWT structure on Near Top Meda Transpression Unconformity.

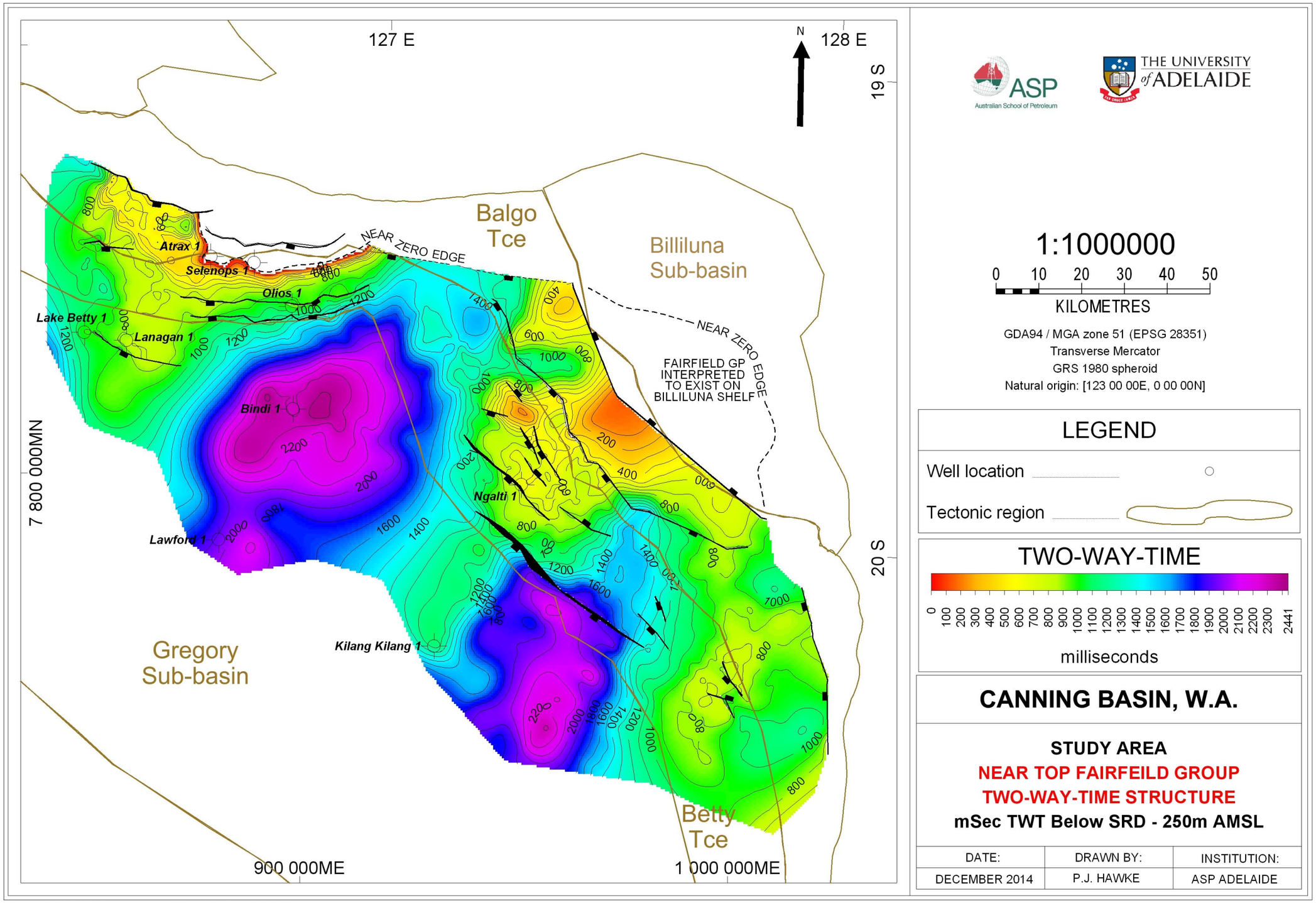

Figure 6.15. TWT structure on Near Top Fairfield Group.

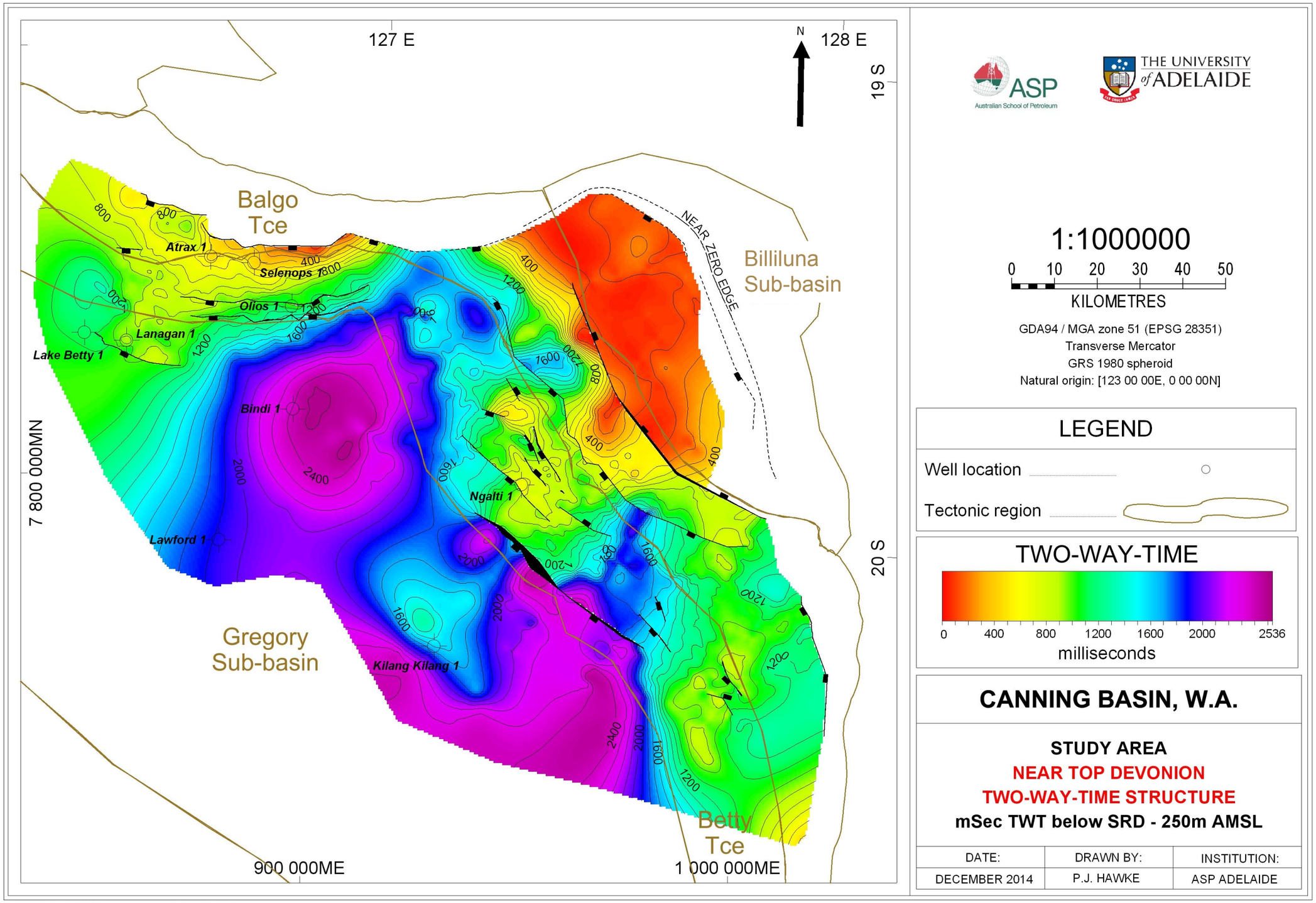

ASP Australian School of Petroleum

THE UNIVERSITY of ADELAIDE

1:1000000

0 10 20 30 40 50

KILOMETRES

GDA94 / MGA zone 51 (EPSG 28351)
Transverse Mercator
GRS 1980 spheroid
Natural origin: [123 00 00E, 0 00 00N]

LEGEND

Well location

Tectonic region

TWO-WAY-TIME

0 400 800 1200 1600 2000 2536

milliseconds

CANNING BASIN, W.A.

STUDY AREA
NEAR TOP DEVONION
TWO-WAY-TIME STRUCTURE
mSec TWT below SRD - 250m AMSL

DATE:	DRAWN BY:	INSTITUTION:
DECEMBER 2014	P.J. HAWKE	ASP ADELAIDE

Figure 6.16. TWT structure on Near Top Devonian.

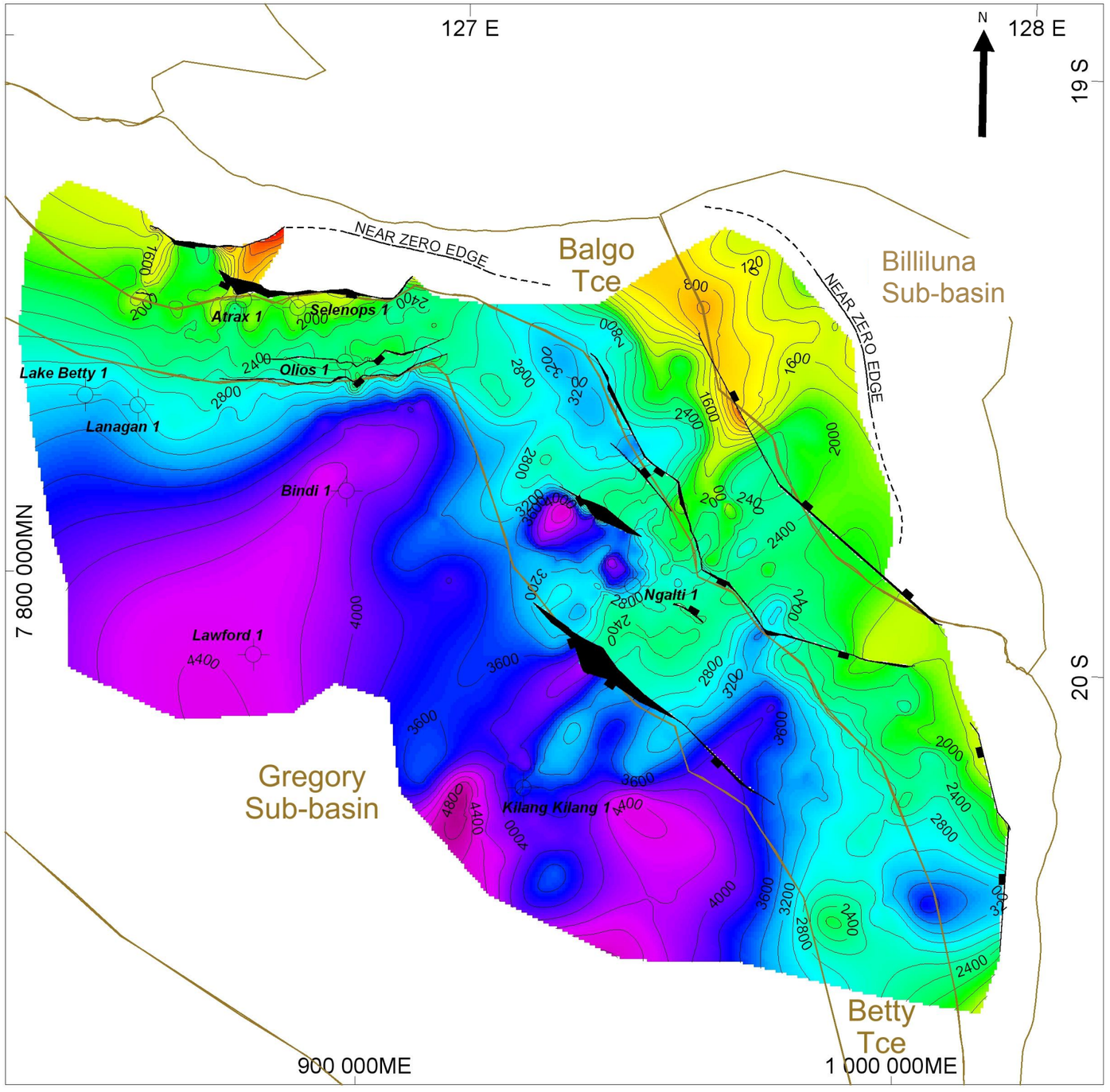

ASP
Australian School of Petroleum

THE UNIVERSITY of ADELAIDE

1:1000000

0 10 20 30 40 50

KILOMETRES

GDA94 / MGA zone 51 (EPSG 28351)
Transverse Mercator
GRS 1980 spheroid
Natural origin: [123 00 00E, 0 00 00N]

LEGEND

Well location

Tectonic region

TWO-WAY-TIME

0 200 400 600 800 1000 1200 1400 1600 1800 2000 2200 2400 2600 2800 3000 3200 3400 3600 3800 4000 4200 4400 4600 4800 4952

milliseconds

CANNING BASIN, W.A.

STUDY AREA
NEAR TOP ORDOVICIAN
TWT STRUCTURE
mSec TWT below SRD - 250m AMSL

DATE:	DRAWN BY:	INSTITUTION:
DECEMBER 2014	P.J. HAWKE	ASP ADELAIDE

Figure 6.17. TWT structure on Near Top Ordovician.

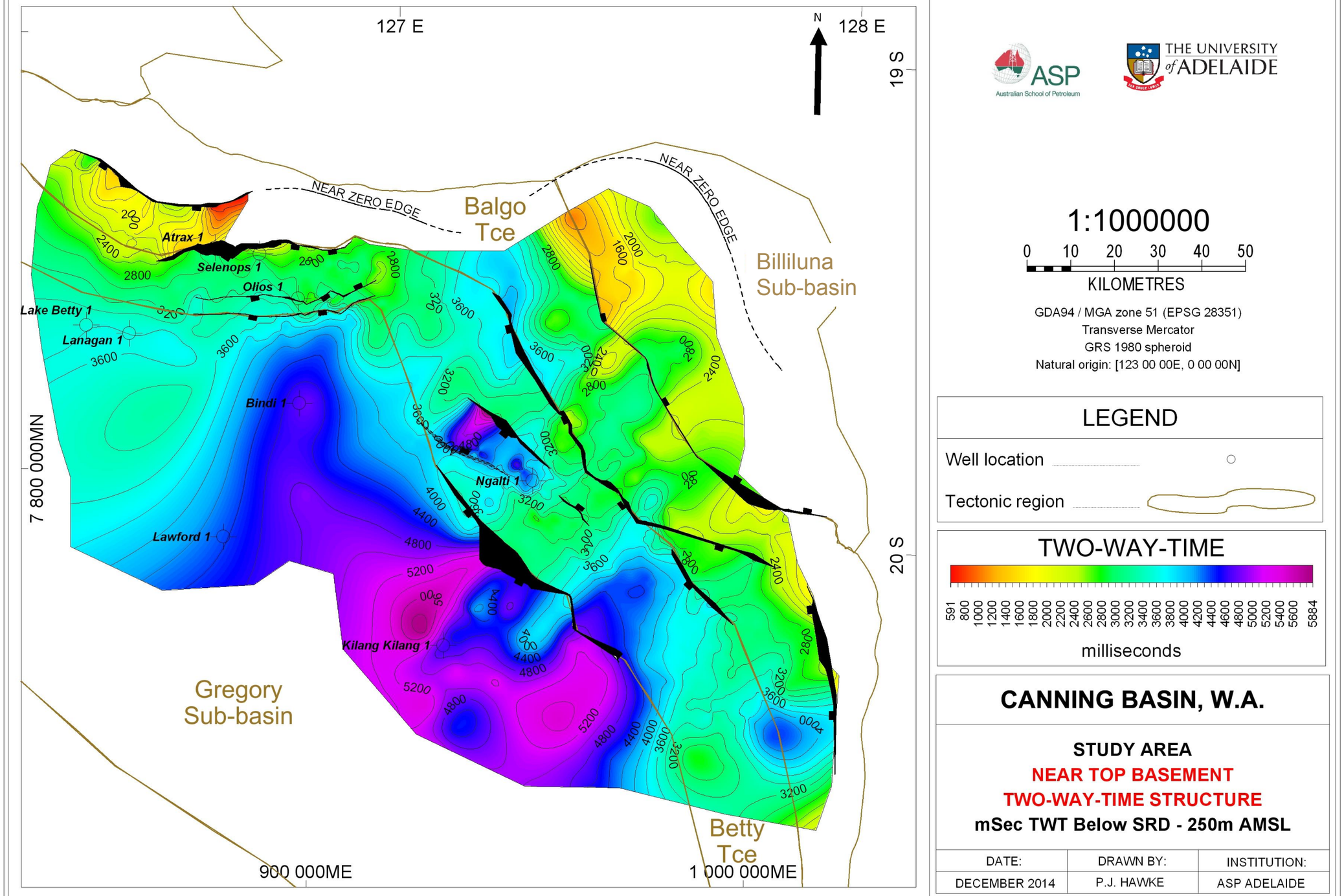

ASP
Australian School of Petroleum

THE UNIVERSITY of ADELAIDE

1:1000000

0 10 20 30 40 50

KILOMETRES

GDA94 / MGA zone 51 (EPSG 28351)
Transverse Mercator
GRS 1980 spheroid
Natural origin: [123 00 00E, 0 00 00N]

LEGEND

Well location

Tectonic region

TWO-WAY-TIME

591 800 1000 1200 1400 1600 1800 2000 2200 2400 2600 2800 3000 3200 3400 3600 3800 4000 4200 4400 4600 4800 5000 5200 5400 5600 5884

milliseconds

CANNING BASIN, W.A.

STUDY AREA
NEAR TOP BASEMENT
TWO-WAY-TIME STRUCTURE
mSec TWT Below SRD - 250m AMSL

DATE:	DRAWN BY:	INSTITUTION:
DECEMBER 2014	P.J. HAWKE	ASP ADELAIDE

Figure 6.18. TWT structure on Near Top Basement.

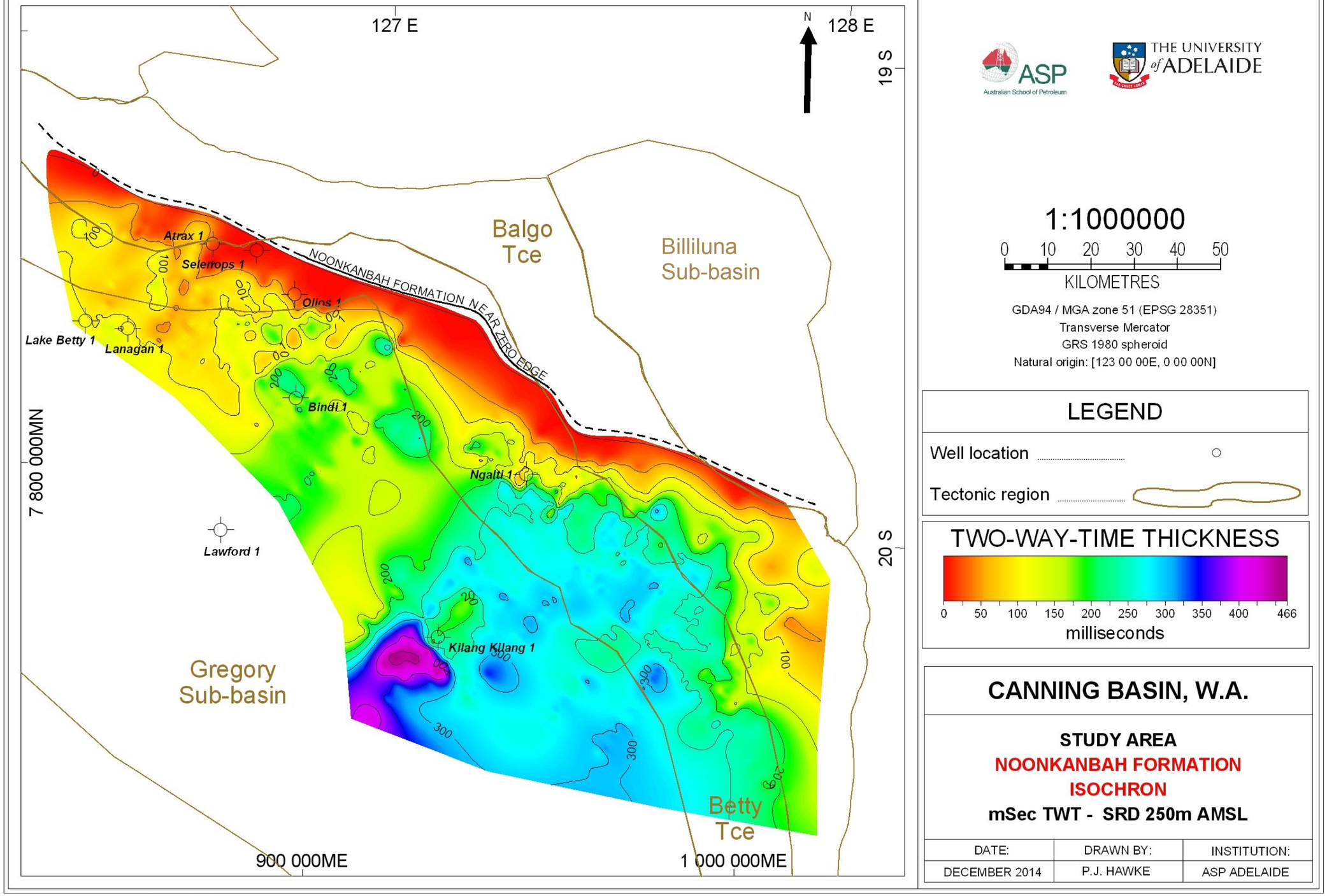

Figure 6.19. Noonkanbah Formation isochron.

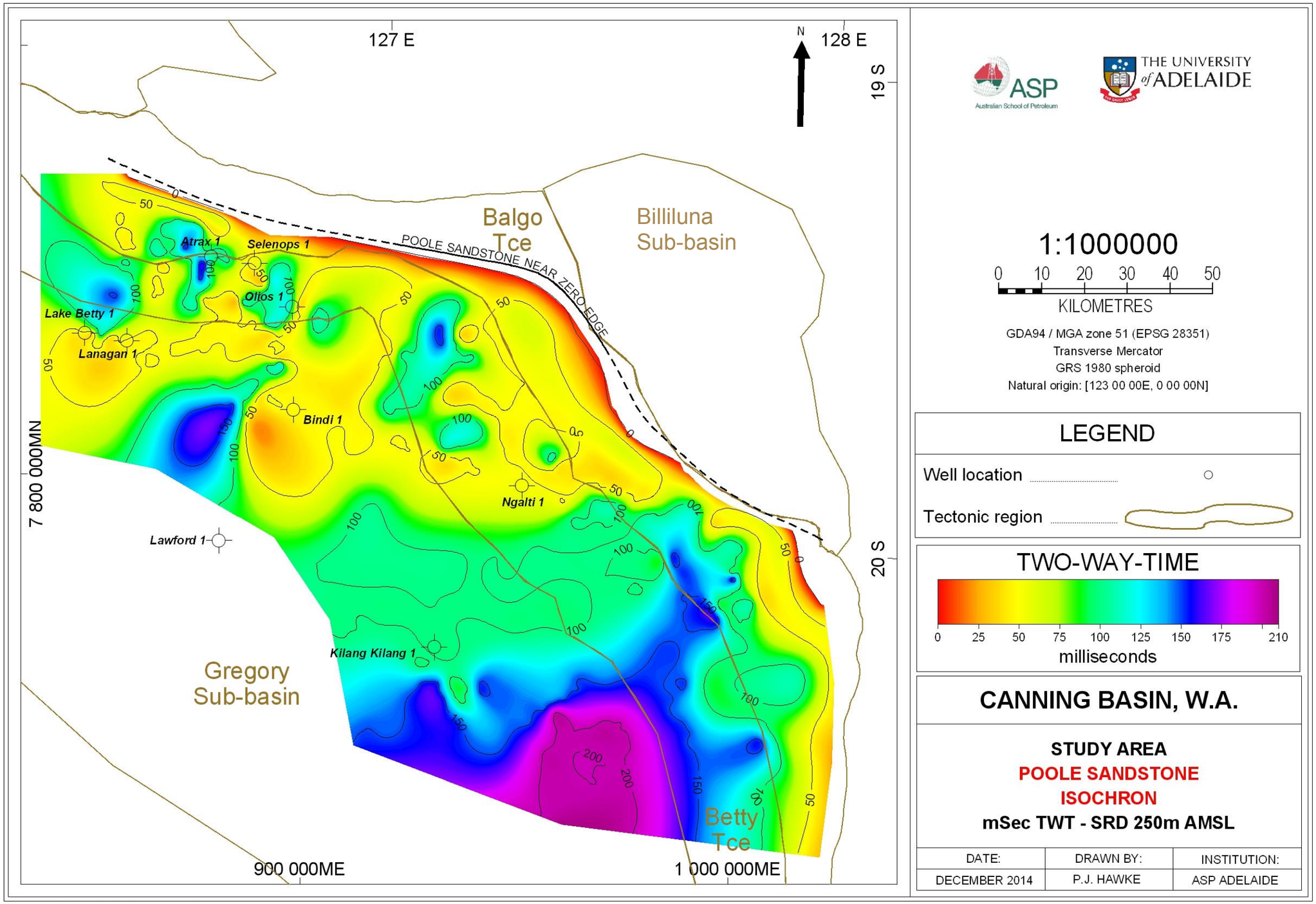

Figure 6.20. Poole Sandstone isochron.

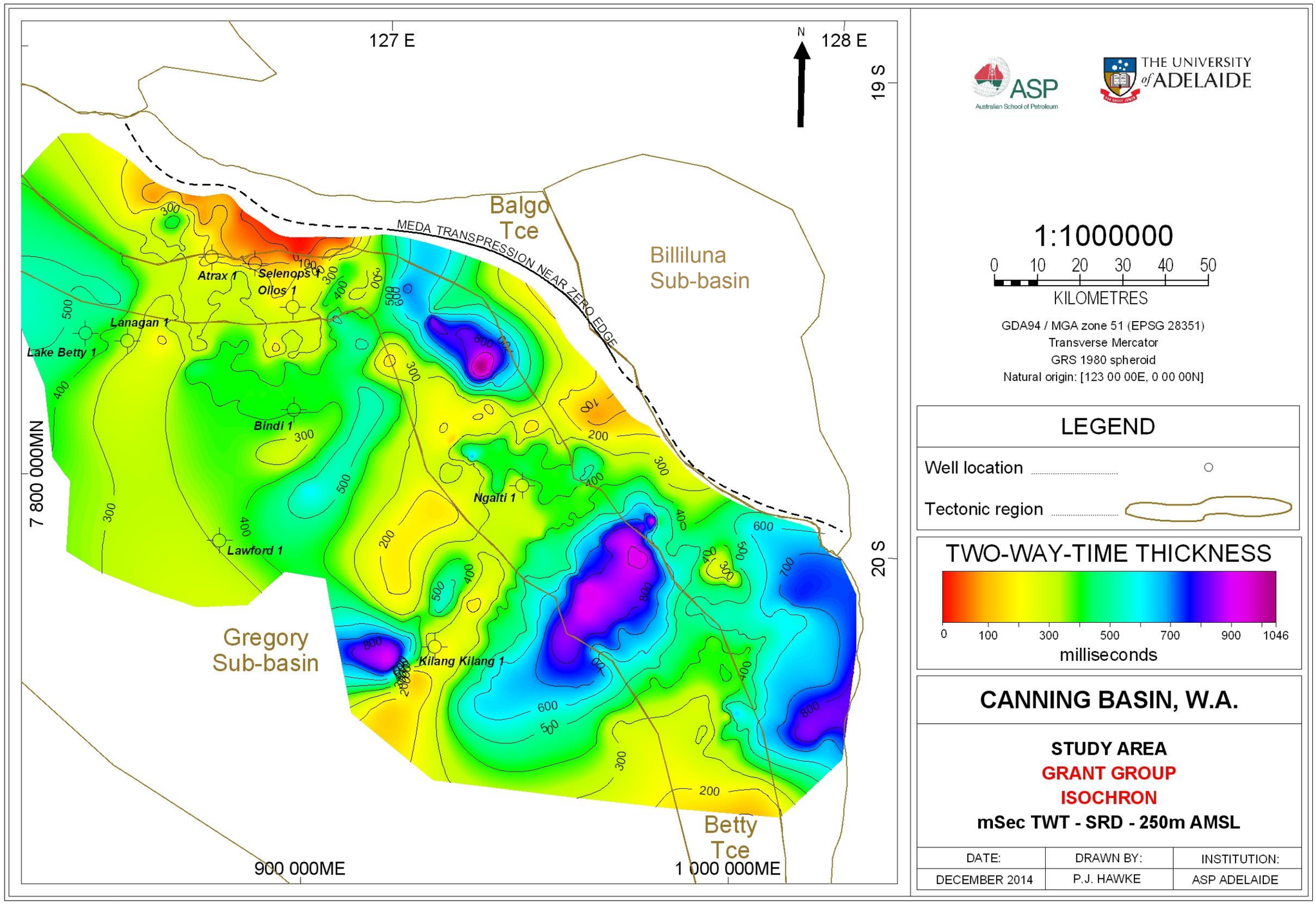

Figure 6.21. Grant Group isochron.

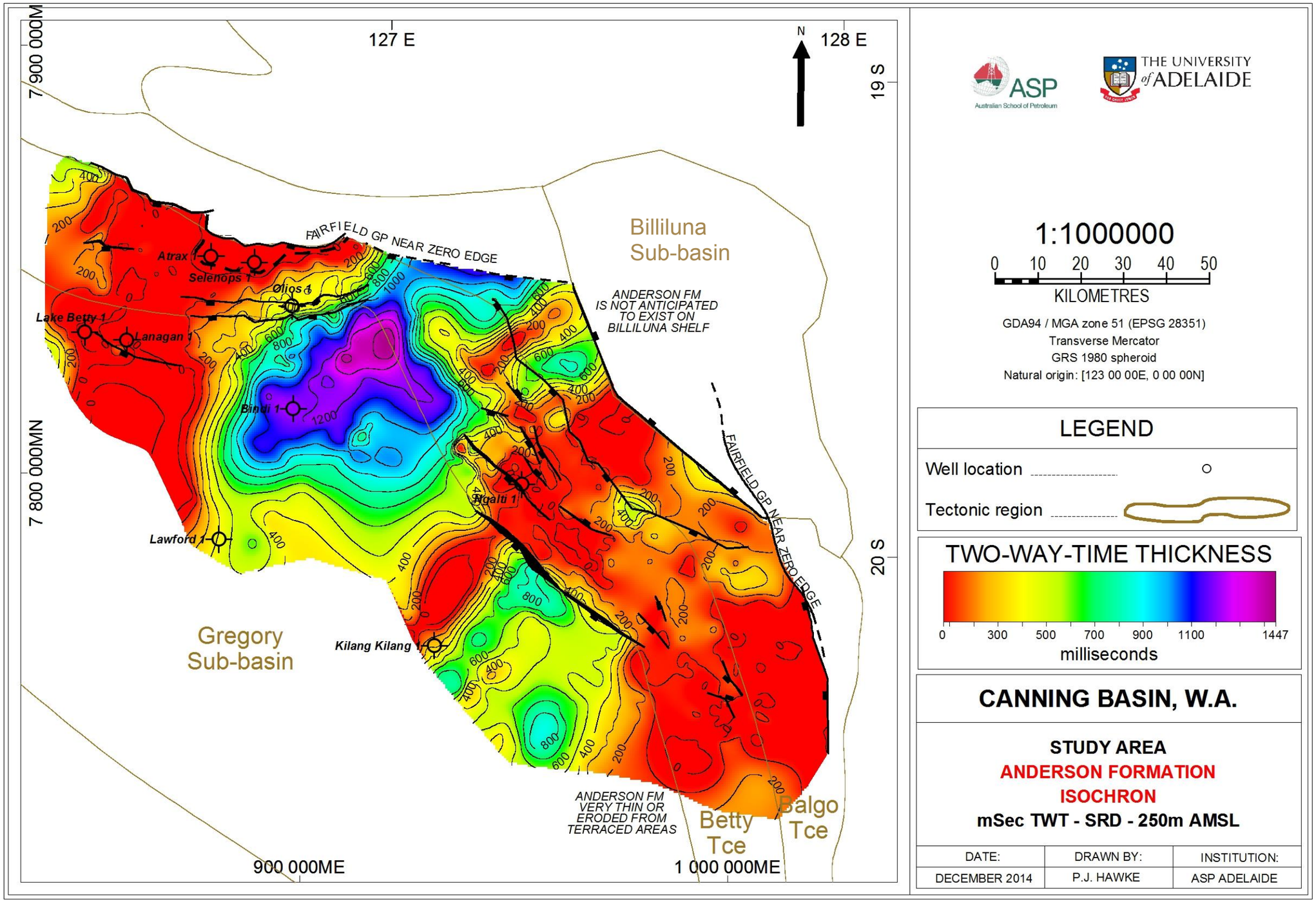

ASP
Australian School of Petroleum

THE UNIVERSITY of ADELAIDE

1:1000000

0 10 20 30 40 50

KILOMETRES

GDA94 / MGA zone 51 (EPSG 28351)
Transverse Mercator
GRS 1980 spheroid
Natural origin: [123 00 00E, 0 00 00N]

LEGEND

Well location

Tectonic region

TWO-WAY-TIME THICKNESS

0 300 500 700 900 1100 1447

milliseconds

CANNING BASIN, W.A.

STUDY AREA
ANDERSON FORMATION
ISOCHRON
mSec TWT - SRD - 250m AMSL

DATE:	DRAWN BY:	INSTITUTION:
DECEMBER 2014	P.J. HAWKE	ASP ADELAIDE

Figure 6.22 Anderson Formation isochron.

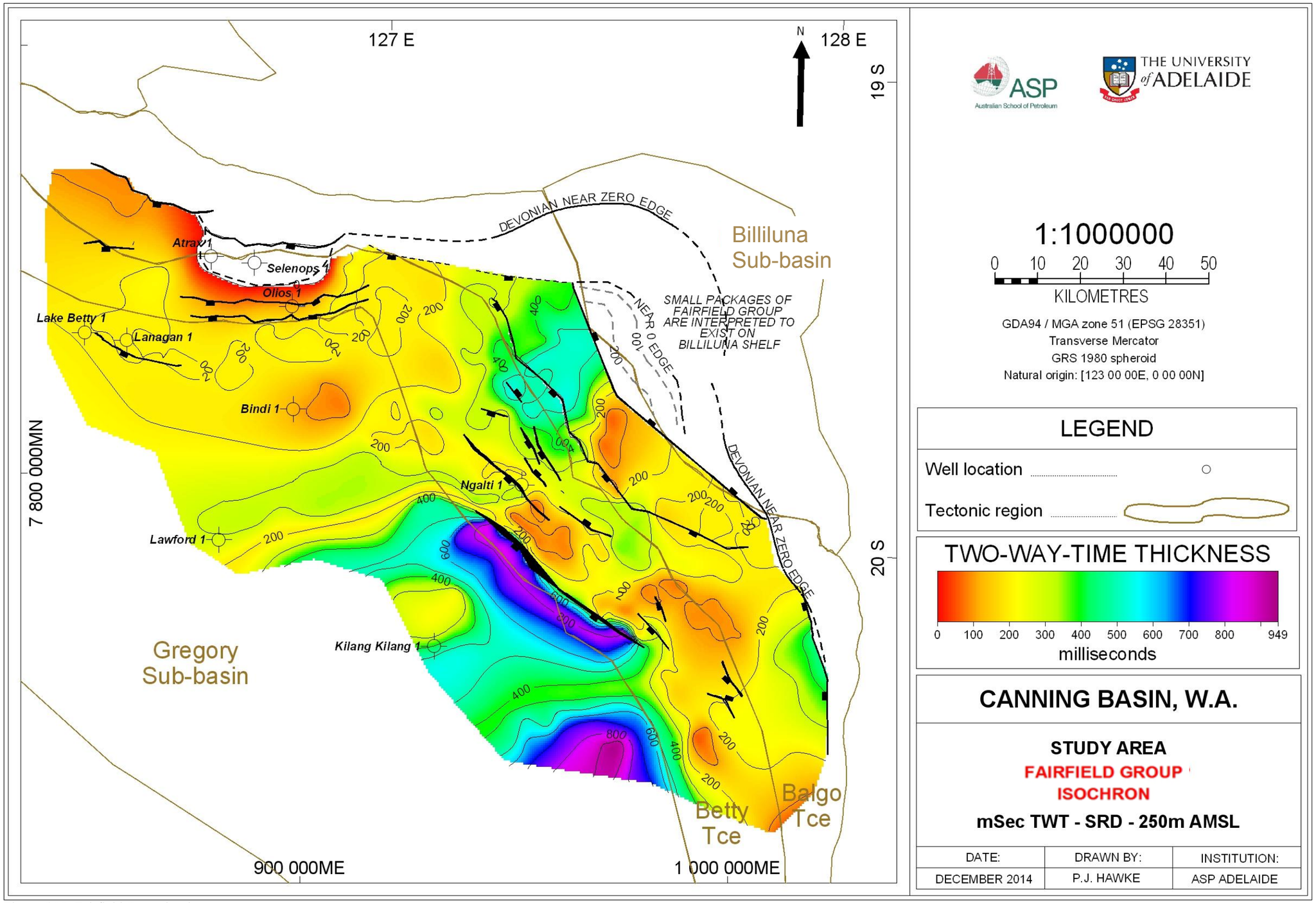

Figure 6.23. Fairfield Group isochron.

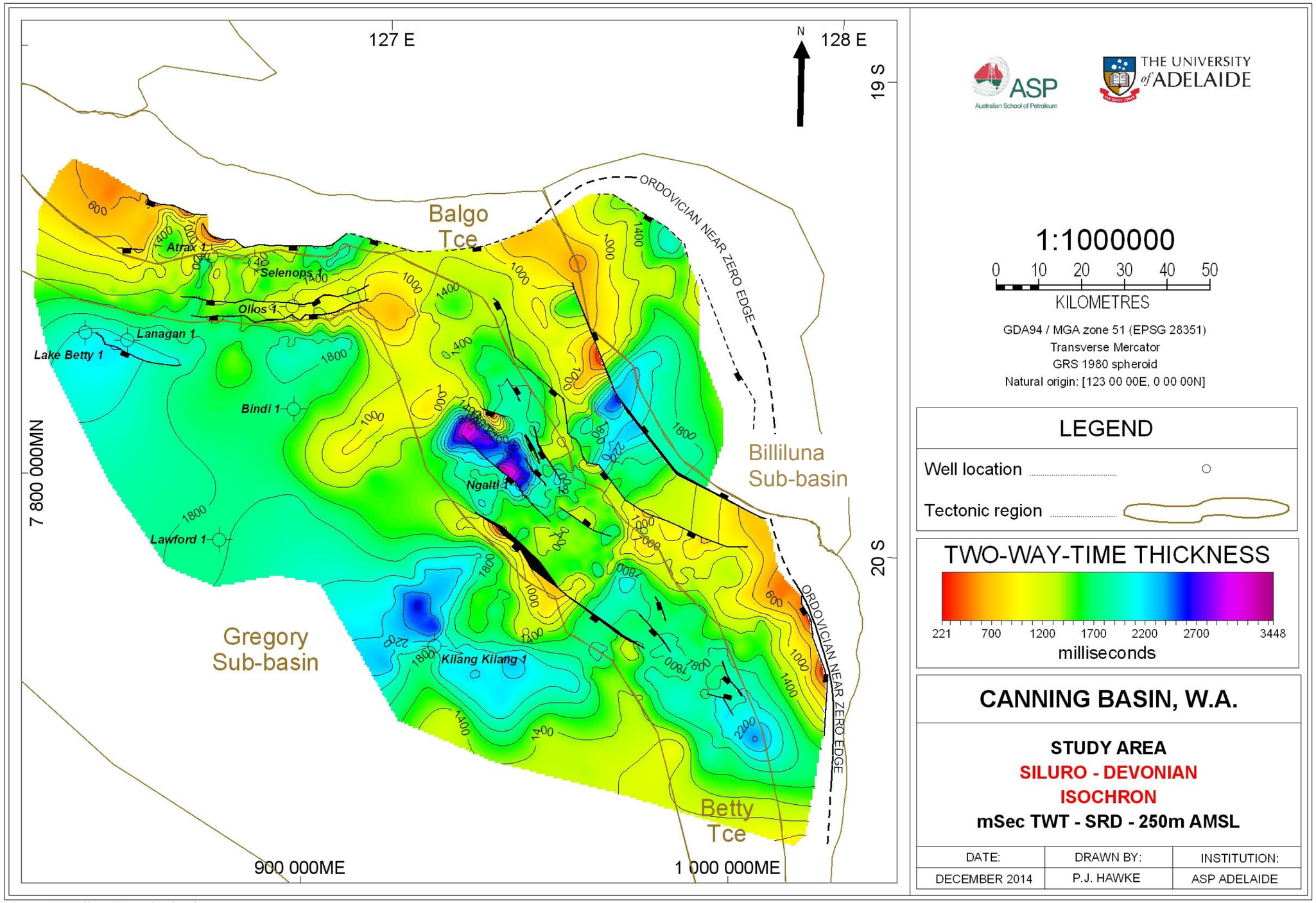

Figure 6.24. Siluro-Devonian isochron.

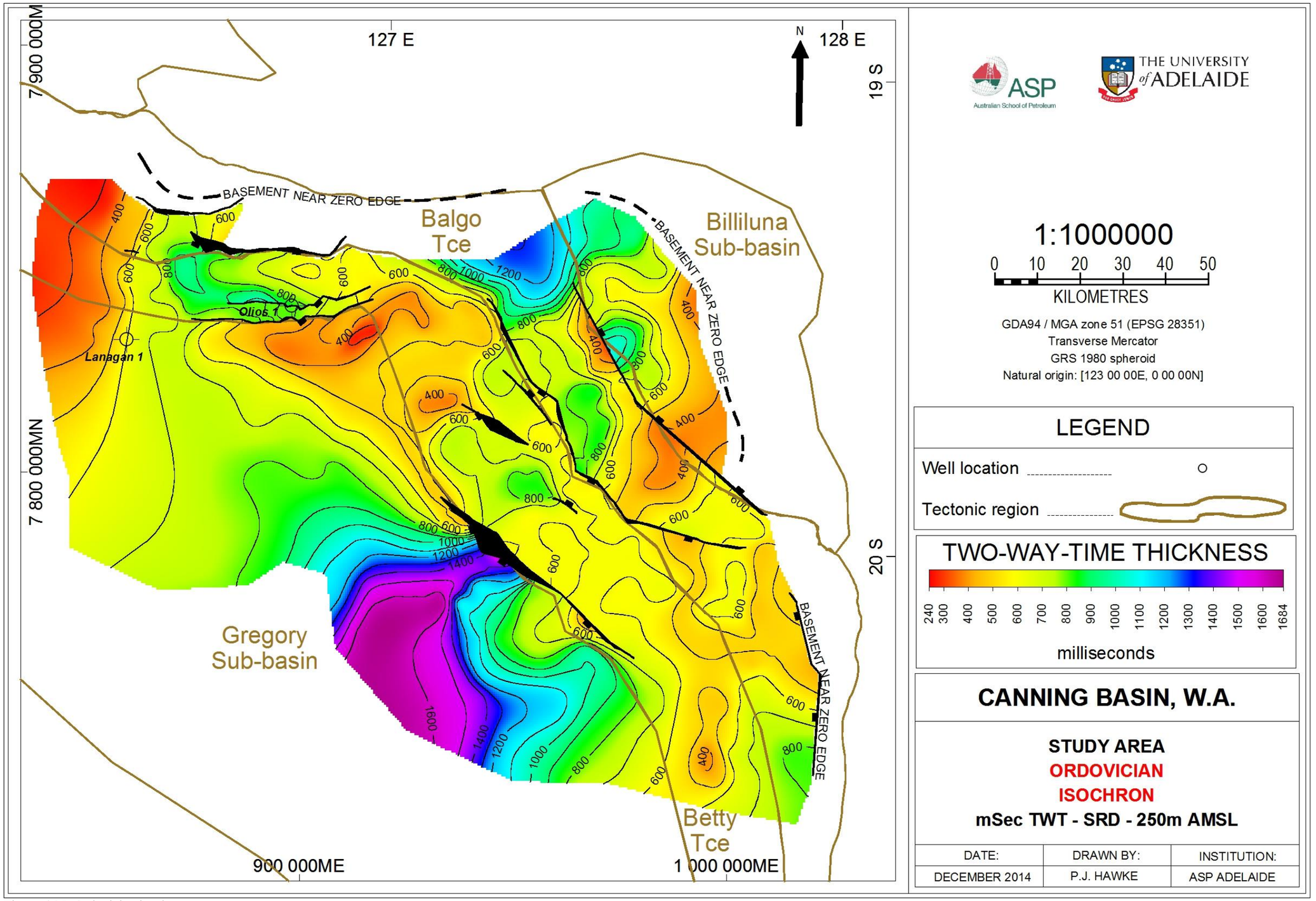

Figure 6.25. Ordovician isochron.

7. Source Rock Assessment

7.1 Introduction

A petroleum system, defined in Chapter 2, is a geologic system that encompasses the hydrocarbon source rocks and all related oil and gas, and which includes all of the geologic elements and processes that are essential if a hydrocarbon accumulation is to exist (Magoon and Dow, 1994). To investigate whether active petroleum systems exist within the project area, source rocks of sufficient organic richness and thermal maturity able to generate hydrocarbons must be identified, and the optimal timing of the occurrence of petroleum system elements and processes must be resolved to determine whether hydrocarbons may be preserved over geologic time to present day.

The goal for this Chapter is to investigate the stratigraphy within the study area to identify source rock potential in relation to organic richness. To accompany this assessment, the stratigraphy will also be examined for thermal maturity in Chapter 8. Between this Chapter and the next, the requirement is to understand source rock quantity (organic richness), quality (organic matter type) and thermal maturity.

7.2 Method and Data

To investigate source rock richness, Total Organic Carbon (TOC) and Rock Eval Pyrolysis data was obtained from published reports (refer to Reference List), Well Completion Reports (WCR) and also from the GSWA online database (GSWA, 2013), which is a collation of regional well data for the entire Canning Basin. The data was quality controlled for reporting accuracy and loaded into Microsoft Excel. It is important to note that the analysis within this Chapter contains data from outside of the project area, because the project area alone has a relatively lean number of wells compared to other shelfal positions in the Canning Basin. Where appropriate, wells located outside of the study area that provide information are identified in the text. All data used in this Chapter are available in Appendix C.

7.3 Analytical Techniques and Definitions

This analysis makes use of three parameters to consider candidate source rock quantity, quality and thermal maturity:

1. Total Organic Carbon (TOC)
2. Rock Eval Pyrolysis
3. Vitrinite Reflectance (%Ro)

7.3.1 *Definition of a Source Rock*

A source rock is a rock that is capable of generating or that has generated movable quantities of hydrocarbons (Beaumont and Foster, 1999). Source rocks within this Chapter are discussed regarding their 'potential' to generate hydrocarbons. Terms '*petroleum potential*', '*genetic potential*' and '*generative potential*' are arbitrary terms that are used interchangeably to deliberate how a prospective source rock may perform. In any case, the *potential* of a given source rock represents the amount of petroleum (oil or gas) that the kerogen within the rock is able to generate, if it were subjected to an adequate temperature over a sufficient time period (Tissot and Welte 1984).

The *potential* of a source rock also is variable (thus a qualitative term), and depends on the mineral and maceral (organic component) composition of a given rock. In a conventional sense, source rocks are usually represented as shales (siliciclastic mudstones that break along cleavages, known as fissile shales). Carbonate rocks are also able to be generative source rocks. Tissot and Welte (1984) state that carbonates can produce a higher amount of petroleum per amount of organic matter. This is because carbonates tend to contain lesser amounts of reworked terrestrial matter and high percentages of marine organics.

7.3.2 *Total Organic Carbon*

Total Organic Carbon (TOC, weight %) characterises the amount of organically derived carbon in a sample of rock and comprises kerogen and bitumen. TOC does not wholly define petroleum source rock capability, though is essential if a source rock is to generate any hydrocarbons at all (Peters and Cassa, 1994). TOC is most commonly measured using the Direct Combustion technique; whereby a small ground sample is first treated with

hydrochloric acid to remove carbonate based carbon, and is then washed and dried to 100°C for 30 minutes. The residue is combusted in a high-frequency induction furnace to 1200°C and measured as Carbon Dioxide (Peters and Cassa, 1994). Other methods of TOC determination are highlighted in Peters and Cassa (1994).

Results in the ensuing text utilise present-day TOC; that is, TOC measurements which reflect organic carbon at maximum thermal maturity settings. For mature source rocks, present-day TOC measurements echo quantities of organic carbon that have matured through hydrocarbon product windows over geologic time and have undergone some degree of conversion to petroleum. For mature source rocks, present-day TOC will be less than initial TOC (TOCi; organic carbon at initial burial). For immature source rocks, present-day TOC can be similar or equal to TOCi. It is important to recognise this difference because present-day TOC often underestimates the total source rock generative potential. TOCi estimates are utilised within petroleum systems modelling (Chapter 8). Peters et al. (2005) provides a method for estimating TOCi.

Peters and Cassa (1994) characterise source rock potential using the TOC parameter in Table 7.1.

Petroleum Potential	Organic Matter: TOC (wt. %)	Rock-Eval Pyrolysis: S_1[a]	Rock-Eval Pyrolysis: S_2[b]	Bitumen[c] (wt. %)	Bitumen[c] (ppm)	Hydrocarbons (ppm)
Poor	0–0.5	0–0.5	0–2.5	0–0.05	0–500	0–300
Fair	0.5–1	0.5–1	2.5–5	0.05–0.10	500–1000	300–600
Good	1–2	1–2	5–10	0.10–0.20	1000–2000	600–1200
Very Good	2–4	2–4	10–20	0.20–0.40	2000–4000	1200–2400
Excellent	>4	>4	>20	>0.40	>4000	>2400

[a]mg HC/g dry rock distilled by pyrolysis.

[b]mg HC/g dry rock cracked from kerogen by pyrolysis.

[c]Evaporation of the solvent used to extract bitumen from a source rock or oil from a reservoir rock causes loss of the volatile hydrocarbons below about *n*-C_{15}. Thus, most extracts are described as "C_{15+} hydrocarbons." Lighter hydrocarbons can be at least partially retained by avoiding complete evaporation of the solvent (e.g., C_{10+}).

Table 7.1. Petroleum potential classification based on organic matter TOC and Rock Eval Pyrolysis (Peters and Cassa, 1994).

7.3.3 *Rock Eval Pyrolysis*

Rock Eval Pyrolysis was first developed by Espitalié (1977) at the French Petroleum Institute as a rapid screening tool to characterise source rock capacity. The method, also highlighted by Tissot and Welte (1984), is a useful solution to characterise source rocks in place of other chemical methods that are time intensive and expensive to isolate kerogens. Rock Eval Pyrolysis is a suitable substitute to expensive and time consuming chemical analyses as it is relatively inexpensive, and takes about 20 minutes per analysis (Peters, 1986).

The method subjects a small (100 mg) sample to progressive heating up to 550°C in an inert atmosphere at a programmed temperature profile, stepping 25°C per minute. During the test, hydrocarbons that are existing within the sample (bitumen) are released at moderate (~300°C) temperatures (at the S1 peak). Programmed temperatures continue to rise at 25°C per minute in the test chamber where kerogen is 'pyrolised' to generate hydrocarbons and hydrogen-like compounds (at an S2 peak) utilising the remaining organic carbon. Oxygen rich volatiles (carbon dioxide) are later released (at an S3 peak). The compounds are passed through a flame-ionisation detector (FID) and a thermal conductivity meter to measure S2 and S3. The temperature at which maximum hydrocarbons are generated in the test chamber is recorded as the Tmax parameter (Tissot and Welte 1984). Figure 7.1 illustrates the temperature profile of a pyrolysis record. Tmax values always increase with higher thermal maturity (Hantschel and Kauerauf, 2009) and hence are a good tool for quick estimates. The correlation between Tmax and hydrocarbon product windows varies with organic matter type, where sensitivity is greatest in determining maturity in type II kerogens. Correlations can be made with vitrinite reflectance (Burrus, 1985).

Peters (1986) illustrates some pitfalls of the Rock Eval Pyrolysis method. A key take-away from the work of Peters (1986), is that interpretation of Pyrolysis and TOC data should be made encompassing lithological information, mineral matrix information, well conditions, locally generated or migrated hydrocarbon information and laboratory pyrograms. It is important to note that abundant mineral matrix information, data on locally derived hydrocarbons and laboratory pyrograms are unavailable at the time of this study.

Peters (1986) notes that due to the adsorption of pyrolytic organic compounds onto the mineral matrix of the Rock Eval sample, Pyrolysis results in the S2 and Tmax parameter that correspond with Total Organic Carbon content less than 0.5% should be discarded from interpretation (Peters, 1986). S2 and Tmax results corresponding to TOC less than 0.5% can

produce unreliable HI or OI values, or other by-products of ratios involving the S2 and Tmax parameter. This advice was taken on board when constructing interpretation charts in this study.

The reader is referred to Peters (1986), where he deliberates the various potential pit-falls of the Rock Eval Pyrolysis method. Laboratory equipment is assumed to be functioning, maintained and calibrated correctly. Pyrograms were not accessible during this study to confirm that the tabled data are recorded correctly.

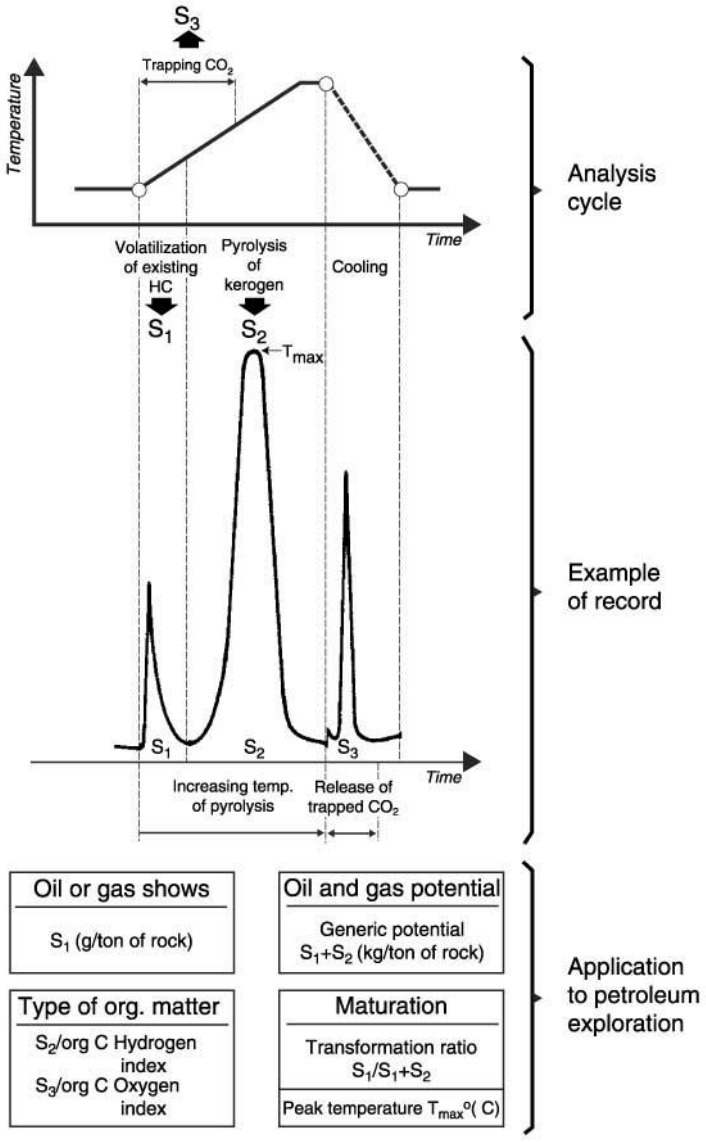

Figure 7.1. Summary of the outcomes and useful calculations related to source rock analysis by Rock Eval Pyrolysis (Tissot and Welte, 1984).

	Term	Description
Derived from Pyrolysis	S1	Amount of free hydrocarbons that can be volatilized out of the rock without thermal cracking of kerogen. S1 increases and S2 decreases in thermally mature rocks. Expressed as kg HC/ton or mg HC/g rock
	S2	Generated hydrocarbons from kerogen cracking (breakdown) suggestive of the reaming generative potential. Expressed kg HC/ton or mg HC/g rock
	S3	A measure of the oxygen content of the rock. Expressed in mg/kg or kg/ton rock.
	Tmax	A measure of the thermal maturity of the sample. Corresponds to the pyrolysis oven temperature observed at maximum hydrocarbon generation by kerogen breakdown.
Calculated from Pyrolysis	Potential Yield (PY) S1 + S2	Ultimate genetic capacity of rock
	Pyrolysable Carbon (PC) S1 + S2 x 0.803	Proportion of TOC that is capable of breaking down to hydrocarbons
	Production Index (PI) S1/S2 + S2	Ratio of hydrocarbons already generated and amount already generated. A measure of maturity of the sample
	Hydrogen Index (HI) S2/TOC x 100	Indication of the remaining generative capacity of a kerogen. Higher HI indicates higher generative potential. Expressed as mg HC/g TOC
	Oxygen Index (OI) S3/TOC x 100	Amount of CO_2 produced from Pyrolysis. Indication of the amount of Oxygen in a sample. Expressed as mg CO_2/g TOC

Table 7.2. A guide on making interpretations from TOC and Rock Eval Pyrolysis measurements (Peters, 1986; Peters and Cassa, 1994)

Kerogen Type	HI (mg HC/g TOC)	S_2/S_3	Atomic H/C	Main Expelled Product at Peak Maturity
I	>600	>15	>1.5	Oil
II	300–600	10–15	1.2–1.5	Oil
II/III[b]	200–300	5–10	1.0–1.2	Mixed oil and gas
III	50–200	1–5	0.7–1.0	Gas
IV	<50	<1	<0.7	None

[a]Based on a thermally immature source rock. Ranges are approximate.

[b]Type II/III designates kerogens with compositions between type II and III pathways (e.g., Figure 5.1) that show intermediate HI (see Figures 5.4–5.11).

	Maturation		Generation		
Stage of Thermal Maturity for Oil	T_{max} (°C)	TAI[a]	Bitumen/ TOC[b]	Bitumen (mg/g rock)	PI[c] $[S_1/(S_1 + S_2)]$
Immature	<435	1.5–2.6	<0.05	<50	<0.10
Mature					
Early	435–445	2.6–2.7	0.05–0.10	50–100	0.10–0.15
Peak	445–450	2.7–2.9	0.15–0.25	150–250	0.25–0.40
Late	450–470	2.9–3.3	—	—	>0.40
Postmature	>470	>3.3	—	—	—

Table 7.3. Kerogen type (top) and thermal maturity hydrocarbon products (bottom) from Rock Eval Pyrolysis measurements (Peters and Cassa, 1994).

Peters (1986) and Peters and Cassa (1994) provide a guide on making interpretations from TOC and Rock Eval Pyrolysis measurements (Table 7.2). Table 7.4 suggests relative quantities of hydrocarbons that can be generated based on Hydrogen Index (HI) (modified after Peters and Cassa, 1994; and Waples, 1985 in Wulff, 1987). Table 7.5 summarizes source rock generative potential based on the S2 parameter (Wulff, 1984).

HI (mg HC/g TOC)	**Relative Quantity of Hydrocarbons Generated**
> 600	Very large
300 - 600	Large
200 - 300	Moderate
50 - 200	Small
< 50	Small

Table 7.4. Relative quantity of generated hydrocarbons from HI (Modified after Peters and Cassa, 1994; Waples, 1985; in Wulff 1987)

S2 (mg HC/g or kg HC/ton)	Generative Potential Classification
0 - 1	Poor
1 - 2	Marginal
2 - 6	Moderate
6 - 10	Good
10 - 20	Very Good
20 +	Excellent

Table 7.5. Generative potential classification based on S2 (Waples, 1985; in Wulff, 1987)

7.3.4 *Organic Matter Type*

The amount of kerogen and the maceral type is useful for characterising petroleum potential in a source rock. Peters and Cassa (1994) categorise kerogens into four types for classification purposes; type I, II, III and IV. Wulff (1987) explains Peters and Cassa's (1994) kerogen types, summarised in Table 7.6.

Kerogen Type	Explanation
Type I	Derived from lacustrine algae. Occurrences are type I kerogens are limited anoxic lakes and a few restricted marine environments. Type I kerogens have high generative capacities for liquid hydrocarbons.
Type II	Derived from marine algae, pollen, spores, fossil resin, and bacterial cells lipids. Despite variable origins, type II kerogens have good capabilities to generate liquid hydrocarbons. Most type II are found in marine sediments deposited under reducing conditions.
Type III	Composed of terrestrial organic material lacking in waxy components. Cellulose and lignin are contributors. Type III kerogens have lower generative potential than type II. Considered to generate mainly gas
Type IV	Contain mainly reworked organic debris and highly oxidized material of various origins. Generally considered to have no source potential.

Table 7.6. Kerogen type classification (Wulff, 1987; Peters and Cassa, 1994)

Kerogen types are determined by cross-plotting laboratory derived measurements of the hydrogen-to-carbon ratio against the oxygen-to-carbon ratio (Atomic H/C vs Atomic O/C) on a *Van Krevalen* diagram, and was originally developed to characterised coals (Peters and Cassa, 1994). Tissot et al (1974) modified the method to include sedimentary source rock kerogens. The modified version of the *Van Krevalen* diagram utilises Rock Eval Pyrolysis calculated Hydrogen Indices and Oxygen Indices in place of the laboratory derived Atomic ratios, which makes the experiment far more rapid and cheaper (Peters and Cassa, 1994). Figure 7.2 demonstrates the Atomic display (A) and the Pyrolysis display (B). Kerogen type can also be identified by cross plotting the samples calculated HI against Tmax (Peters and Cassa, 1994).

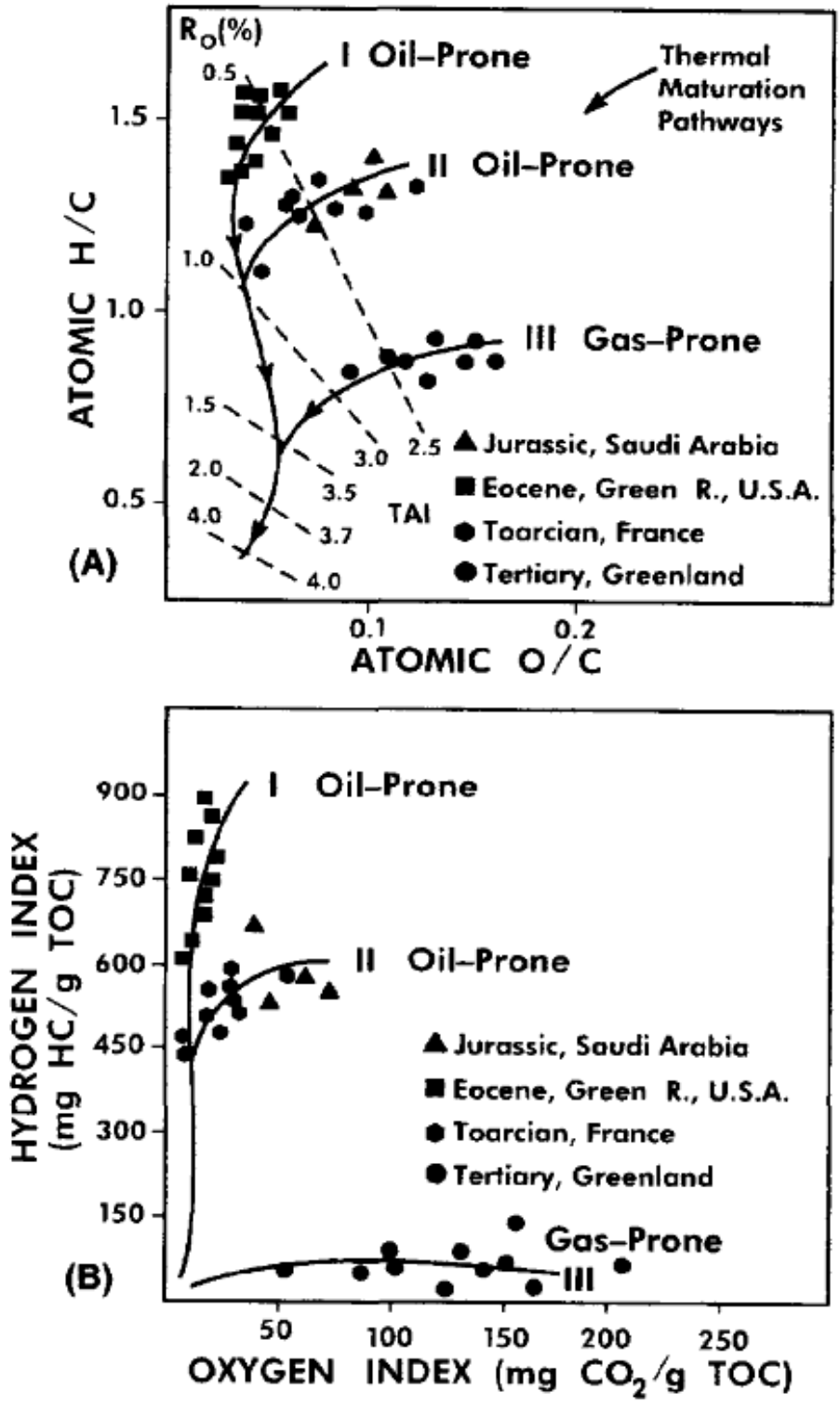

Figure 7.2. Kerogen type classification from H/C v O/C ratios and HI v Tmax (Peters and Cassa, 1994).

7.3.5 *Vitrinite Reflectance*

There are three primary groups of macerals (organic components, the equivalent of 'minerals' in igneous rocks) in sedimentary rocks. They are liptinite (previously known as exinite) vitrinite and inertinite (Tissot and Welte, 1984). Vitrinite macerals are derived from terrestrial plants and mature along the Type III kerogen pathway (Peters and Cassa 1994). Vitrinite Reflectance is a measure of the amount (presented as a percentage, %Ro) of incident light reflected from the surface of vitrinite maceral components in a sedimentary rock. The mean percentage is usually derived from a histogram of observed responses and presented as the mean vitrinite reflectance.

The vitrinite reflectance boundaries used in this project are derived from PetroMod to remain consistent with modelled thermal maturity overlays (Chapter 8). The boundaries are similar to widely published maturity windows of Dow (1977) and (Peters and Cassa, 1994), shown in Table 7.7.

Hydrocarbon product window	**Vitrinite reflectance (% Ro)**		
	PetroMod	**Dow (1977)**	**Peters and Cassa (1994)**
Immature	0 - 0.55	0 - 0.6	0.2 - 0.6
Early oil window	0.55 - 0.7	0.6 - 1.0	0.6 - 0.65
Main oil window	0.7 - 1.0		0.65 - 0.9
Late oil window	1.0 -1.3		0.9 - 1.35
Wet gas window	1.3 - 2.0	1.0 - 1.35	1.35 +
Dry gas window	2.0 - 4.0	1.35 - 3.0	
Over mature	4.0 +	3.0 +	

Table 7.7. Definition of hydrocarbon product windows from vitrinite reflectance. Petromod window are utilised in this project for consistency with modelling results. Comparison of definitions in published literature (modified after Dow, 1977; Peters and Cassa, 1994).

7.4 Source Rock Geochemistry

7.4.1 *Candidate Source Rock Intervals*

The investigation of the project area stratigraphy in Chapter 4 revealed that several packages contain candidate source rock intervals, based on their geological and petrophysical (wireline log response) character, summarised in Table 7.8.Table 7. Each formation in Table 7.8 will be examined for its capacity to generate hydrocarbons.

FORMATION / UNIT	LITHOLOGY	PETROPHYSICAL CHARACTER
Noonkanbah Formation	Shale with siltstone interbeds	Mid-range blocky gamma ray response
Anderson Formation Unit G	Rarely carbonaceous claystone and medium grained sandstone	Generally hot gamma ray response
Anderson Formation Unit E	Massively bedded claystone	Generally mid-range to hot gamma ray response
Anderson Formation Unit C	Massively bedded siltstone and non-fissile claystone	Generally mid-range to hot gamma ray response
Laurel Formation	Finely crystalline fossiliferous limestone and blocky shales	Interbedded gamma ray response, some hot zones
Gogo Formation	Grey, blocky micromicaceous shales	Gamma ray shows mid-high range blocky character
Bongabinni Formation	Grey blackish sub-fissile to fissile claystone, silty in part	Hot, blocky gamma ray
Goldwyer Formation / WMC 4	Black finely crystalline argillaceous carbonaceous dolomite	Hot gamma ray log response
Goldwyer Formation / WMC 2	Black fissile shale and siltstone	Hot gamma ray log response

Table 7.8. Candidate source rock intervals derived from Chapter 4.

7.4.2 *Noonkanbah Formation*

The Early Permian (Aktastinian to Baigendzhinian) Noonkanbah Formation is a sequence of shale interbedded with siltstone, deposited in a shallow marine to marginal marine depositional environment with fluvial influence (refer to Chapter 4.8.2 of this study).

The Noonkanbah Formation, regionally, shows good to very good organic content, averaging 2.17% TOC across the Canning Basin. TOC ranges from 0.07% in a very shallow (75 mRT) sample at Olios 1 to 9.37% at Cycas 1 (Figure 7.3). Within the project area, organic content in the Noonkanbah Formation is less than the basin average but is still classified as good, averaging 1.69% TOC, the highest is 4% at Ngalti 1 (Figure 7.3).

Despite high organic content, the Noonkanbah Formation regionally shows poor organic yields in Pyrolysis results. Free hydrocarbons in samples indicated by the S1 parameter are poor, averaging 0.11 kg HC/ton across the Canning Basin. Values range 0.1 to a maximum of 0.85 kg HC/ton. Generative potential shown by the S2 parameter is also poor to fair, averaging 1.09 kg HC/ton, ranging 0.04 to 5.04 kg HC/ton, throughout the Canning Basin (Figure 7.4). Ultimate potential yield is also therefore poor, averaging 0.98 kg HC/ton across the basin, ranging 0.1 to 5.50 kg HC/ton (Figure 7.3).

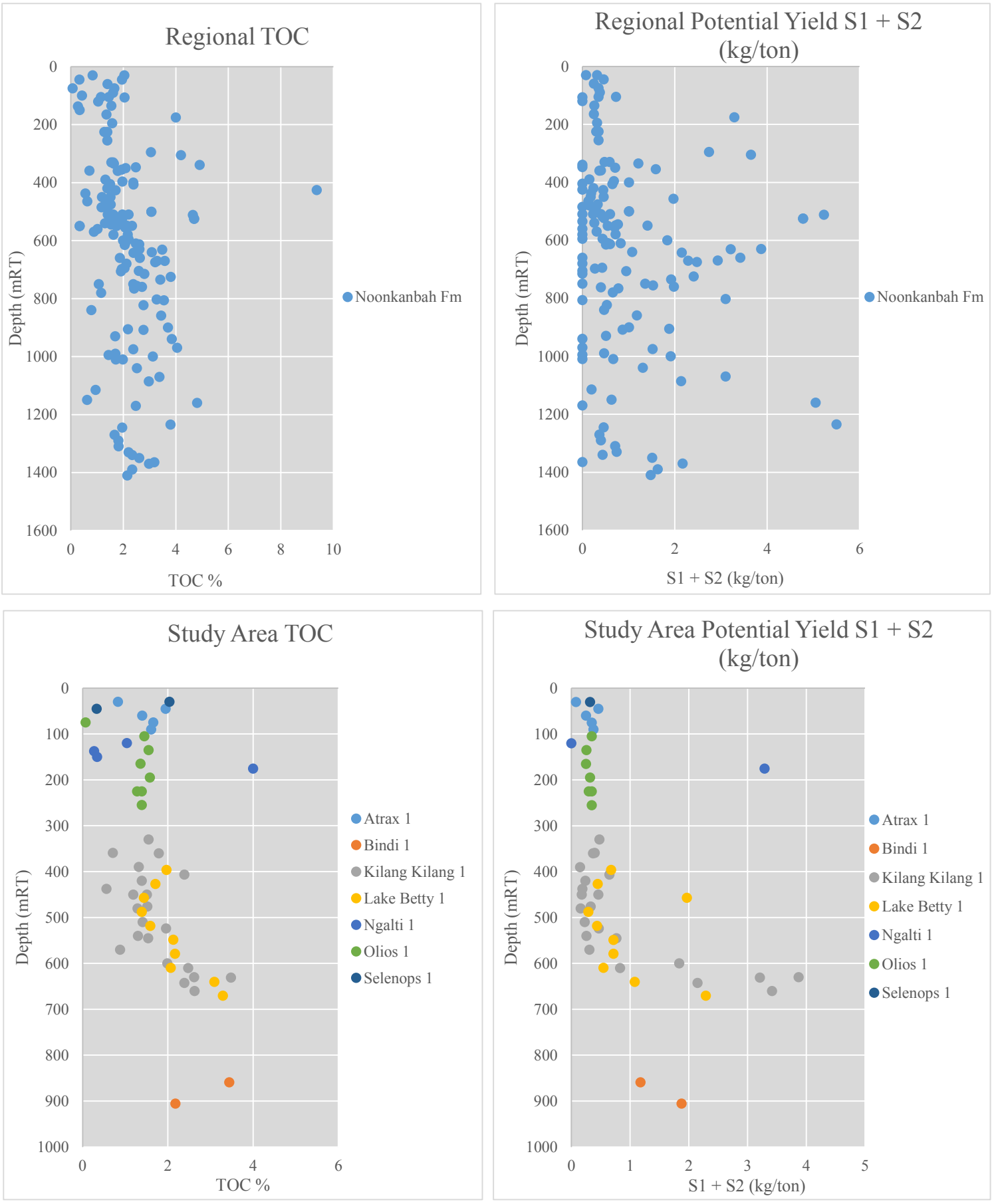

Figure 7.3. Noonkanbah Formation. Clockwise from top left: Regional TOC; regional potential yield; potential yield within study area; study area TOC (modified after GSWA, 2013).

Within the project area, free hydrocarbons as indicated by the S1 parameter are also poor, averaging 0.08 kg HC/ton, ranging 0.01 to 0.27 kg HC/ton. Generative potential is also characterised as poor to fair, averaging 0.76 kg HC/ton S2, ranging from 0.06 to 3.77 kg HC/ton. Figure 7.3 indicates that project area wells (such as Bindi 1, Kilang Kilang 1 and Lake Betty 1, Figure 3.2) show good to very good petroleum potential. These wells are located distal to the anticipated terrestrial influence indicated by paleogeographic reconstructions (Figure 4.40).

Wulff (1987) observed that there is a clear definition within the Noonkanbah Formation between an upper marine section and lower terrestrial section in Kilang Kilang 1, Ngalti 1, Lake Betty 1, Olios 1 and Bindi 1. Kilang Kilang 1 clearly demonstrates this trend (Figure 7.4), showing an average S2 of 2.41 kg HC/ton below 575 mRT (yield averages 2.55 kg HC/ton), whereas the zone above 575 mRT averages S2 at 0.27 kg HC/ton. S1 and TOC is consistent between the upper and lower portions of the well. Wulff (1987) points out that the TOC in these wells correlates to abundances of non-marine sporinite and cutinite within the lower terrestrial section. The cause, as suggested by Wulff (1987) and agreed here, is likely increased marine organism bioturbation and organic material consumption in the marine portion.

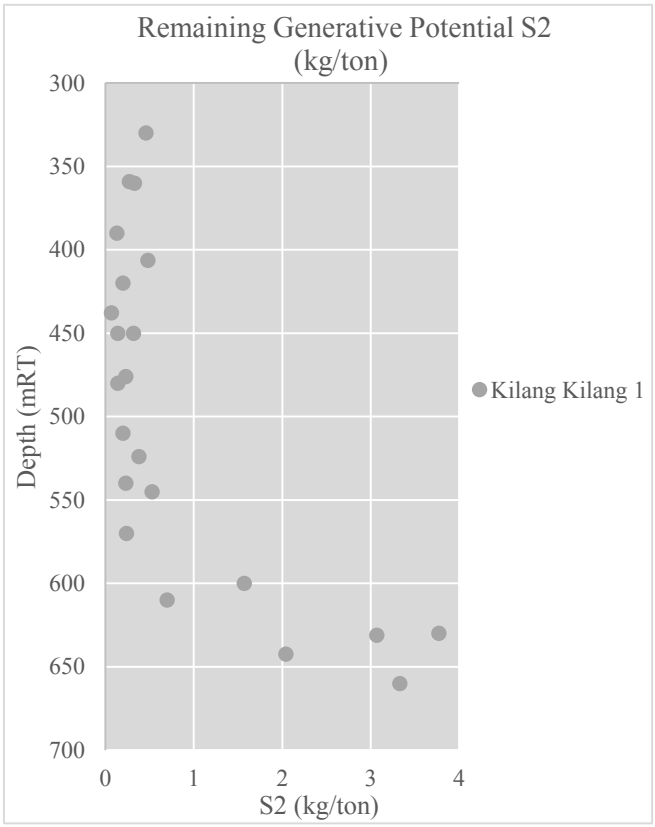

Figure 7.4. Noonkanbah Formation remaining generative potential (S2) (modified after GSWA, 2013).

Kerogen classification of the regional Noonkanbah Formation data suggests a type III to type IV kerogen, and it is likely inert. This is indicated by the HI and OI Van Krevalen diagram and also confirmed by cross-plotting HI and Tmax parameters (Figure 7.5). The HI classification provided by Peters and Cassa (1994) (Table 7.3) indicates a type III or type IV kerogen, with average Noonkanbah Formation HI across the basin at 33 mg HC/g TOC. The HI ranges 6.45 to 143.89 mg HC/g TOC. Typing the kerogen is indicative of a terrestrial or oxidised sedimentary source, which implies reworking of sediments from the nearby terrestrial influence, consistent with the paleogeographic reconstruction (Figure 4.40). Vitrinite and inertinite macerals were identified from side-wall cores (SWC) at Kilang Kilang 1 and Olios 1, confirming the terrestrial influence.

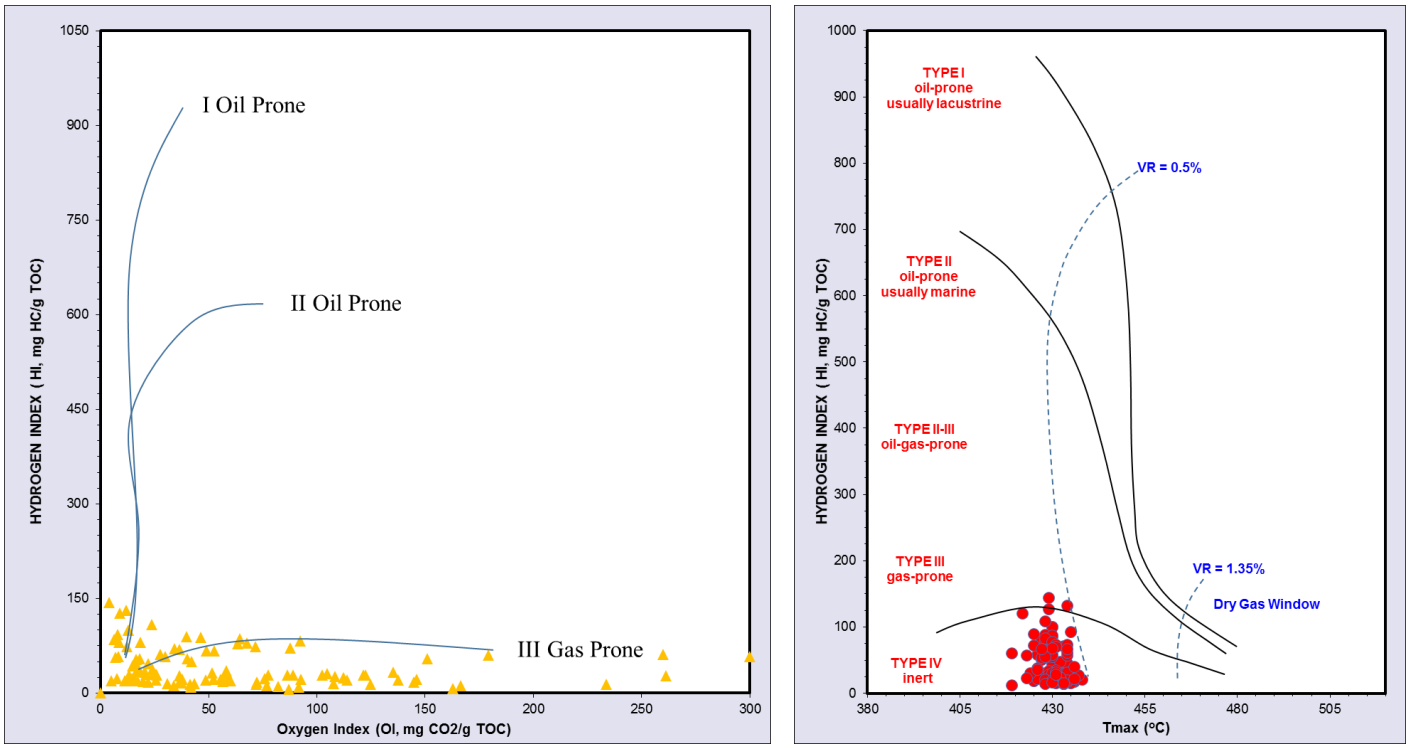

Figure 7.5. Noonkanbah Formation kerogen type; HI v OI (left), HI v Tmax (right) (modified after GSWA, 2013).

The low HI (6.45 to 143.89 mg HC/g TOC, averaging 33 mg HC/g TOC) is suggestive of a gas hydrocarbon product under optimal maturity conditions (Peters and Cassa, 1994).

The Noonkanbah Formation shows Tmax values ranging from 419°C to 438°C across the Canning Basin, averaging 430°C (Figure 7.6). This suggests that regionally, the Noonkanbah Formation is immature for hydrocarbon generation according to Tmax values. Tmax

measurements within the project area shows that the Noonkanbah Formation is immature on average (but marginally more mature than wells in the regional dataset; Figure 7.6), averaging 431°C (ranging 422°C to 437°C). Production Indices (PI) are also suggestive that the interval is regionally immature to early mature for hydrocarbon generation, with PI averaging 0.12 across the basin. PI within the study area averages slightly higher at 0.13 (ranges 0.02 to 0.63). Anomalously high PI ratios are observed at Kilang Kilang 1 (0.63); the cause for this is likely due to oxidation, or adsorption of pyrolytic oxygen compounds onto the mineral matrix of the sample and a low S2 (S3 of 2.56 kg/ton, S2 of 0.07 kg HC/ton and TOC of 0.56%) (Peters, 1986). PI can also be unreliable with small S1 and S2 products, because dividing a small number by a slightly larger number derives this index (Peters, 1986). Vitrinite reflectance at the same depth at Kilang Kilang 1 confirms the zone is immature to early mature for oil (Ro 0.63%).

Vitrinite reflectance data indicates that the Noonkanbah Formation within the study area ranges between 0.39 and 0.82 Ro%, averaging 0.60 Ro%. Refer to well maturation profiles in Chapter 8.6.8

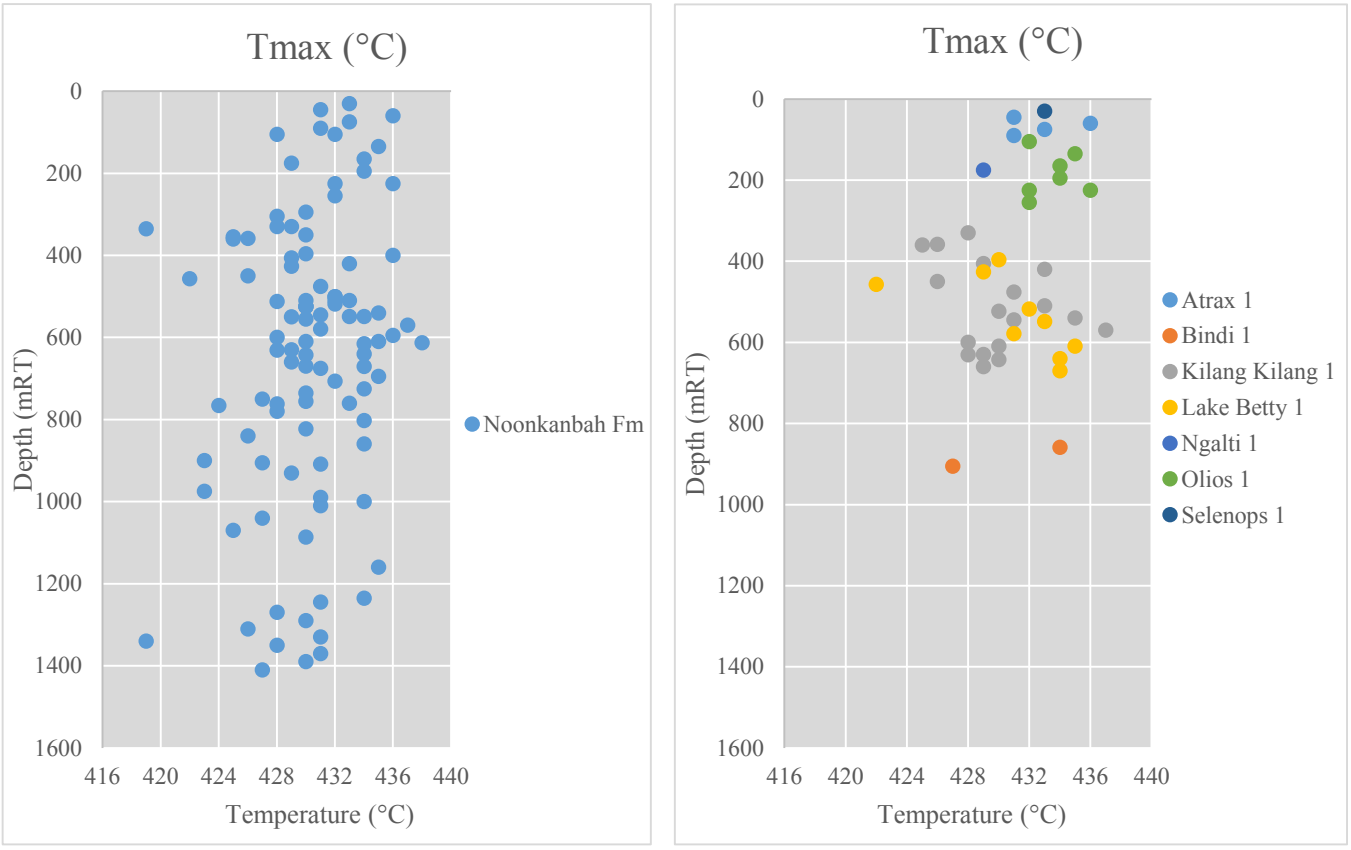

Figure 7.6. Noonkanbah Formation regional Tmax (left) and study area Tmax (right) (modified after GSWA, 2013).

Summary of Petroleum Potential

It is clear from TOC and Rock Eval measurements (Figure 7.3), that the Noonkanbah Formation contains enough organic carbon (TOC) to generate considerable quantities of hydrocarbons, showing very good petroleum potential. The Noonkanbah Formation, however, is thermally immature (and early mature for oil at best) for hydrocarbon generation at the sampled locations. Where buried deeper, maturity is expected to increase, and the Noonkanbah Formation may exist in a generative window for oil.

It is important to note, that in a basin with low well-density, conventional petroleum wells tend be located on highs generally targeting structural traps. Therefore, the samples may be acquired from locations that are perhaps biased toward shallower locations. This implies that the Noonkanbah Formation is likely to be found at a higher level of thermal maturity in a structurally deeper setting.

The interval has been evaluated using samples that are regionally immature, according to the data at hand. Because the samples are immature, production indices are low, indicating the samples have probably retained organic content from conversion to hydrocarbons. This means that ideal conditions are available here for characterising an accurate organic richness of the Noonkanbah Formation (Wulff, 1987).

7.4.3 *Anderson Formation*

The Early to Middle Carboniferous Anderson Formation is an interbedded sequence of sandstone siltstone and shale, divisible within the project area into seven subunits, based on lithology and geophysical log response (refer to Chapter 4.6.2). Anderson Formation Unit C, Unit E and Unit G are dominated by claystone lithologies with high gamma-ray log responses suggestive of high organic content, and were accordingly investigated for source rock potential. Unit C is a massively bedded siltstone and non-fissile claystone, represented on wireline logs as a generally mid-range to hot gamma ray response. Unit E is a massively bedded claystone with generally mid-range to hot gamma ray response. Unit G is a rarely carbonaceous claystone with a generally hot gamma ray log response.

Despite the encouraging gamma-ray log responses, the Anderson Formation regionally shows low total organic content, with poor to marginally fair hydrocarbon generating potential (Figure 7.7). The Anderson Formation shows 0.64% TOC on average, ranging from 0.02 to 12.7% TOC. The range of TOC is evidently skewed by the Wamac 1 well (located approximately 120 km northwest of Broome, in the offshore portion of the Canning Basin) which intersected 370 metres of organically rich Anderson Formation showing excellent TOC and petroleum potential (ranging 2.57 to 12.7% TOC).

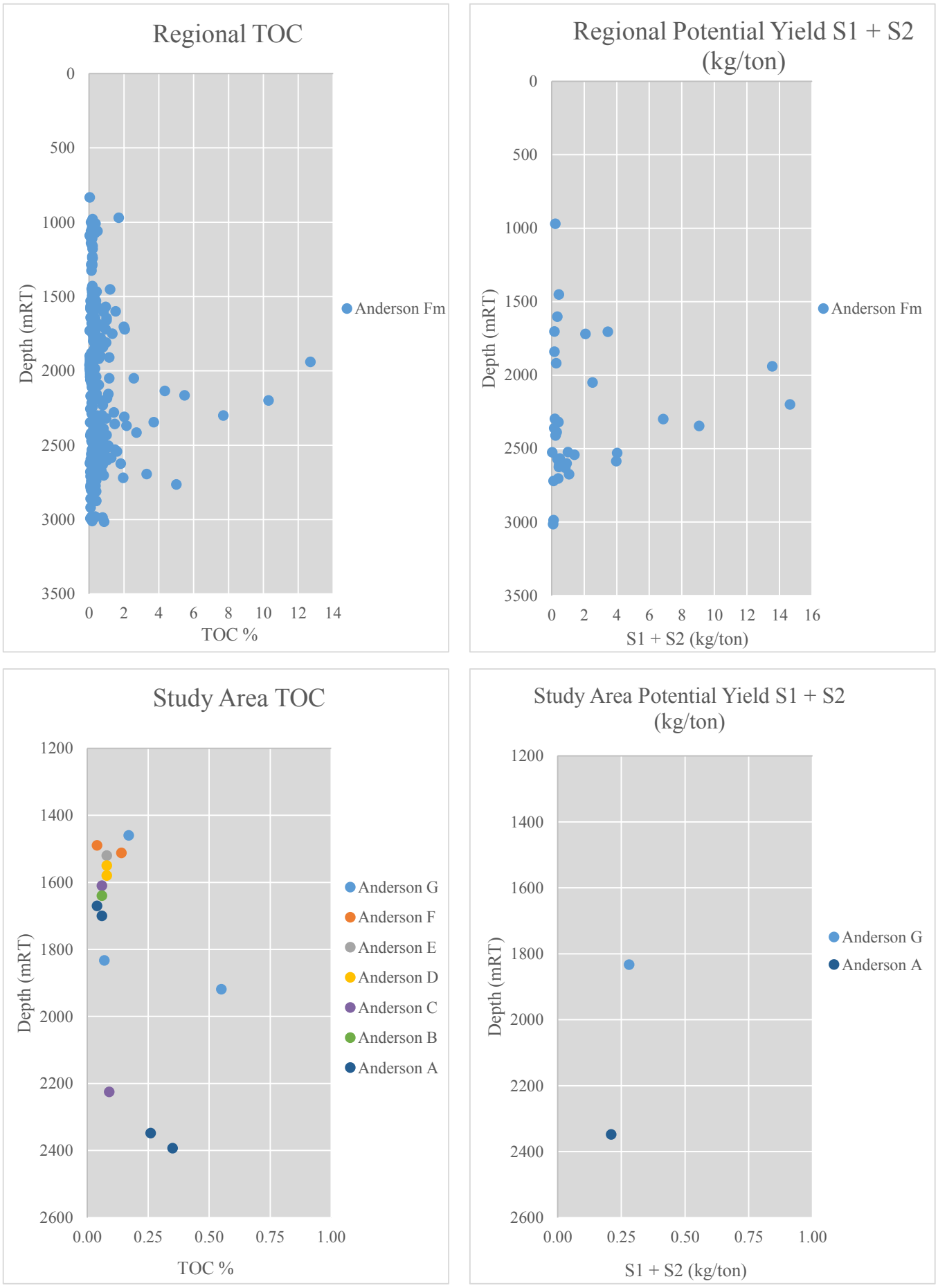

Figure 7.7 Anderson Formation. Clockwise from top left: Regional TOC; regional potential yield; potential yield within study area; study area TOC (modified after GSWA, 2013).

Within the project area, geochemical data characterising the Anderson Formation is available at Bindi 1 and Kilang Kilang 1 (the only two wells to intersect this formation). The Anderson Formation shows very low organic content and poor petroleum potential across all subunits, averaging 0.14% TOC. Table 7.8 indicates that Unit G represents the most organically rich zone averaging 0.26% TOC, where a single interval in Unit G at Bindi 1 reaches 0.55% TOC – the most organically rich portion within the project area. Unit E has a single data point – 0.08% TOC at Kilang Kilang 1, and Unit C shows very low TOC; 0.09% at Bindi 1 and 0.06% at Kilang Kilang 1. Anderson Formation Unit A (a quartzose sandstone interbedded with claystone) shows 0.26% and 0.35% TOC at Bindi 1; which is still very low organic contents, but therefore the second most organically rich Anderson Formation subunit within the project area (Table 7.8). Average ultimate genetic yield shows 0.25 kg HC/ton in the study area, and 1.68 kg HC/ton (1.06 kg HC/ton with Wamac 1 results removed) (Figure 7.7).

WELL	SUB-UNIT	DEPTH	TMAX	S1	S2	S3	S1+S2	TOC
Bindi 1	Unit G	1833.1						0.07
	Unit G	1918.7	425	0.17	0.11	0.19	0.28	0.55
	Unit C	2224.9						0.09
	Unit A	2348.1						0.26
	Unit A	2393	426*	0.08*	0.13*	0.24*	0.21*	0.35
Kilang Kilang 1	Unit G	1460						0.17
	Unit F	1490						0.04
	Unit F	1512.2						0.14
	Unit E	1520						0.08
	Unit D	1550						0.08
	Unit D	1580						0.08
	Unit C	1610						0.06
	Unit B	1640						0.06
	Unit A	1670						0.04
	Unit A	1700						0.06

Table 7.8. Anderson Formation pyrolysis and TOC measurements within study area. Note: * Denotes Rock Eval with TOC <0.5% (modified after GSWA, 2013).

The regional Anderson Formation has low free hydrocarbon content released in the S1 parameter at 0.32 kg HC/ton, ranging between 0.01 to 2.35 kg HC/ton. The S1 average quoted here is not regionally representative and is an over-estimation of free hydrocarbons released by pyrolysis for the Anderson Formation. To clarify, the Wamac 1 well shows good

petroleum potential with an average of 1.05 kg HC/ton S1, ranging 0.14 to 2.35 kg HC/ton, and is the reason the S1 basin average is above 0.2 kg HC/ton (Table 7.9).

The regional Anderson Formation also has low generative potential, with 1.74 kg HC/ton S2, ranging 0.02 to 13.58 kg HC/ton S2. Discounting the Wamac 1 pyrolysis results the basin S2 average drops to 0.86 kg HC/ton S2, which is a fairer representation of regional data.

WELL	DEPTH (mRT)	TMAX	S1	S2	S3	S1+S2	TOC
Wamac 1	1940	422	0.65	12.89	6.5	13.54	12.7
	2050	427	0.14	2.37	1.25	2.51	2.57
	2200	424	1.06	13.58	2.9	14.64	10.3
	2300	424	2.35	4.5	1.2	6.85	7.7

Table 7.9. Anderson Formation pyrolysis and TOC measurements at Wamac 1 well (modified after GSWA, 2013).

Kerogen classification of the regional Anderson Formation data suggests a type III kerogen, indicated by the HI and OI Van Krevalen diagram (type III gas prone), and also the HI and Tmax cross plot (Figure 7.8) showing type III to type IV. The HI classification provided by Peters and Cassa (1994) (Figure 7.8) concurs with a type III kerogen, with average Anderson Formation HI across the basin at 88 mg HC/g TOC. The HI ranges between 0.16 to 259 mg HC/g TOC. Typing the kerogen as type III supports a terrestrial or oxidised sedimentary source. Depositional setting conclusions drawn from lithological descriptions and sequence stratigraphic interpretation of wireline log data (Figure 4.30) indicates that a strong terrestrial influence was present during Anderson Formation deposition, which is reinforced here by kerogen typing. Coal observed in Unit G at Lawford 1 and palynological evidence in Units A and C through G confirm the terrestrial influence.

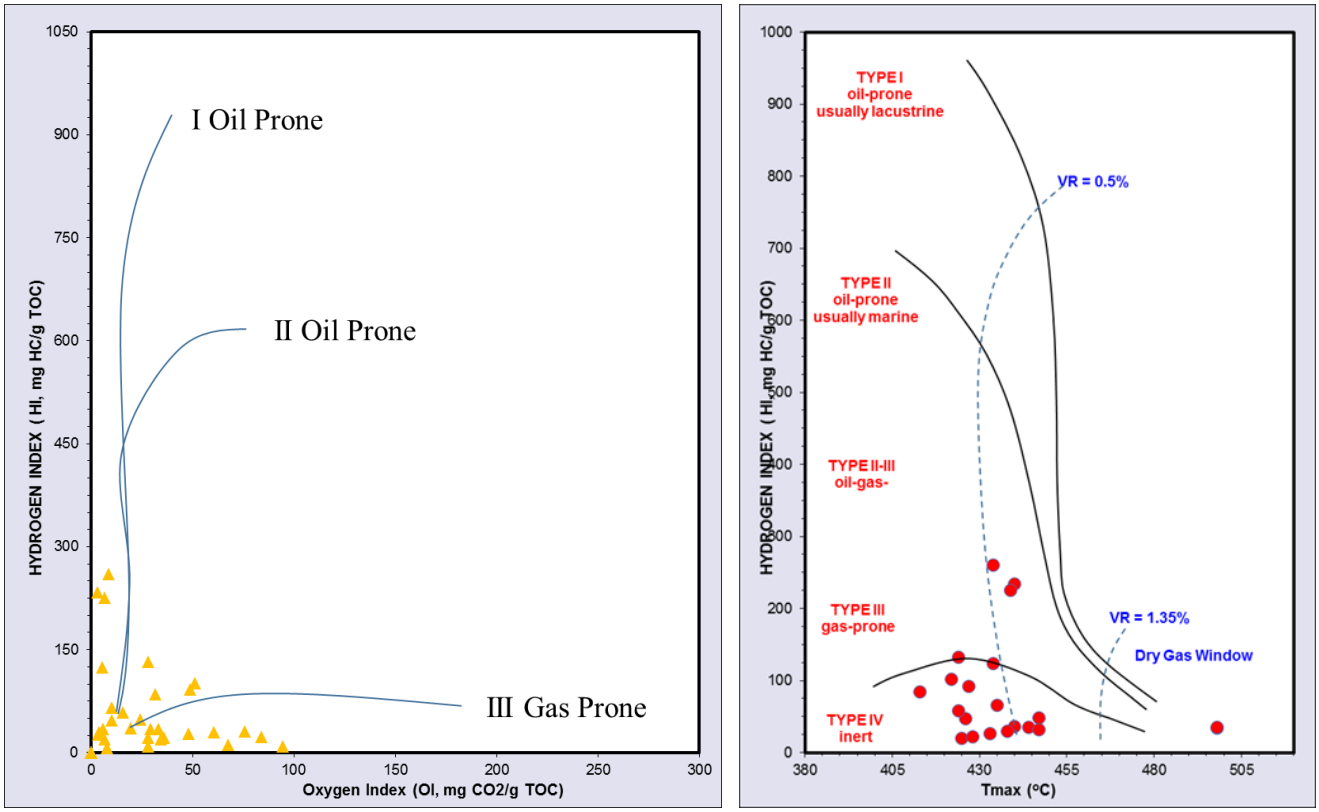

Figure 7.8 The Anderson Formation shows a type III kerogen indicated by the HI v OI cross plot (left) and the HI v Tmax (right) (modified after GSWA, 2013).

Within the project area, a single data point at Bindi 1 shows a HI of 20, indicating a type IV kerogen (Peters and Cassa, 1994). The low HI numbers indicate that a gas hydrocarbon product is likely under optimal maturity conditions (Peters and Cassa, 1994).

The Anderson Formation shows Tmax values ranging from 328°C to 498°C across the Canning Basin, averaging 429°C (Figure 7.9). This suggests that regionally, the Anderson Formation is immature for hydrocarbon generation according to Tmax values (note that the Tmax value of 498°C is anomalously high, caused by low S2 – 0.3 kg HC/ton). Data within the project area shows that the Anderson Formation is immature, with data at Bindi 1 indicating Tmax values at 425 °C. The Production Indices (PI) ratio is probably unreliable for the Anderson Formation; suggestive that the interval is regionally at peak maturity for oil generation, with PI averaging 0.34 across the basin. The S1 and S2 products directly impact PI, and because the pyrolysis results are very low, the PI is susceptibly high as a result

(dividing one small number by another slightly larger number). The same effect is observed at Bindi 1 within the study area, where the PI shows the interval is post-mature (0.61).

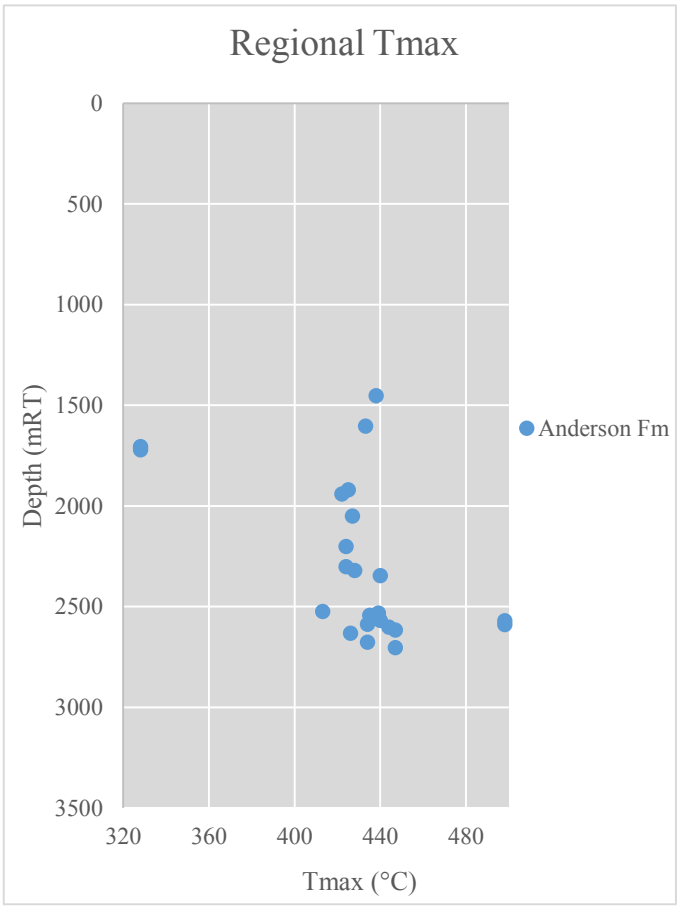

Figure 7.9. Anderson Formation Tmax indicates the formation is regionally immature (modified after GSWA, 2013).

Vitrinite Reflectance data (a single measurement at Kilang Kilang 1) suggests that the Anderson Formation has reached peak maturity for oil generation within the study area, at 0.76 Ro%. Note that a single data point is not a sufficient amount of data to characterise the maturity of the interval. Peters (1986) recommends that more reliable geochemical interpretations are based on datasets with measurements every 9 to 18 metres.

7.4.4 *Laurel Formation*

The Early Carboniferous (Tournaisian) Laurel Formation is predominantly a clastic sequence comprising interbedded sandstone, siltstone, claystone and shale. It shows and interbedded gamma-ray response with hot intervals. The sequence also comprises a regionally mappable carbonate package. The reader is referred to Chapter 4.6.1 for a comprehensive description of the Laurel Formation.

Regional assessment

Regionally, the Laurel Formation has fair petroleum potential with variable organic contents, ranging from 0.03% to 5.81% TOC and averaging 0.56% TOC across the Canning Basin (Figure 7.10). Average S1 and S2 data indicate poor petroleum potential across the basin – though S1 and S2 parameters are also variable, and zones (Figure 7.11) of Laurel Formation sediments in neighbouring tectonic provinces show fair to good organic contents. Regionally, pyrolysis yields are lean on average; S1 ranges 0.1 to 2.52 kg HC/ton, averaging 0.33 kg HC/ton. S2 ranges 0.1 to 14.6 kg HC/ton, averaging 0.56 kg HC/ton.

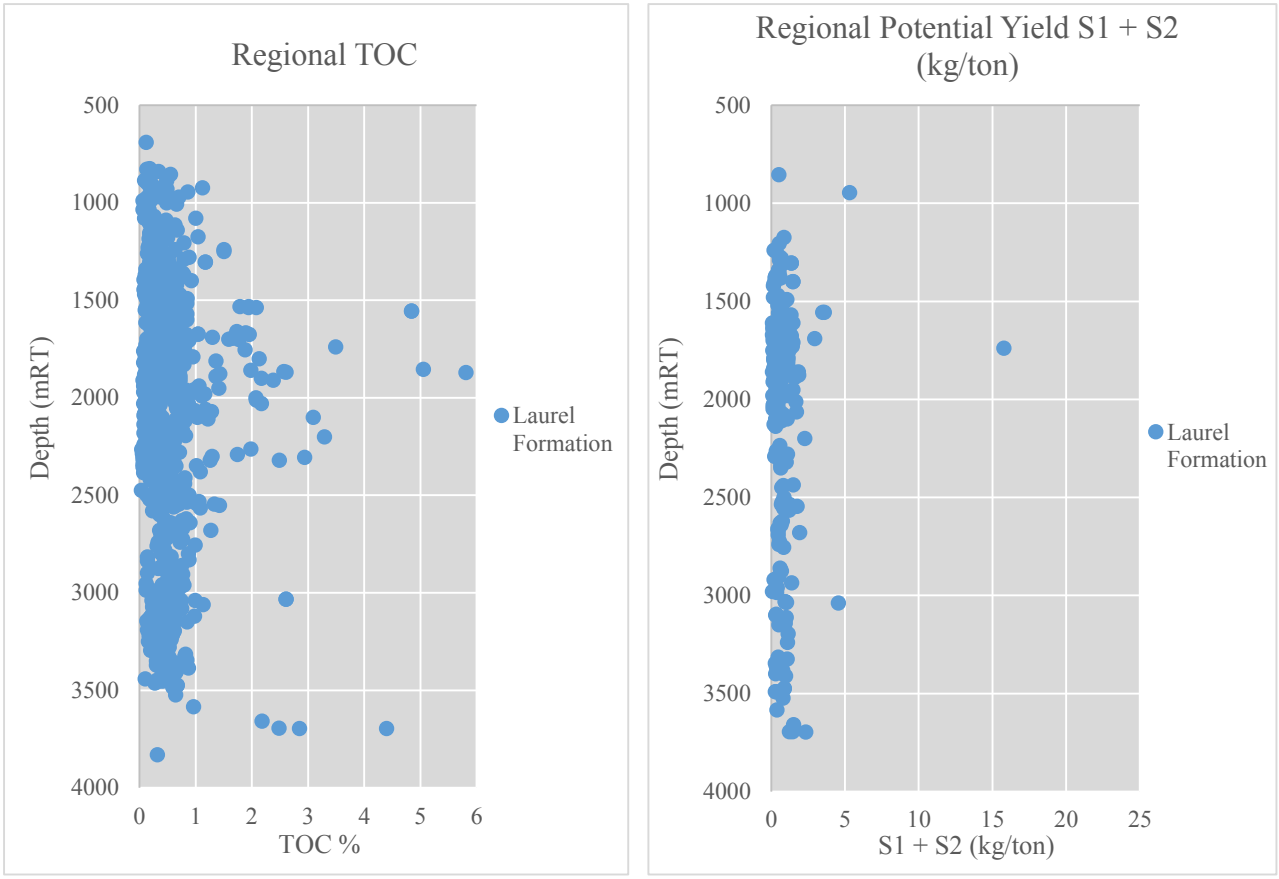

Figure 7.10. Laurel Formation regional TOC (left) and regional pyrolysis measurements (modified after GSWA, 2013).

Figure 7.11 demonstrates TOC and ultimate genetic potential across the basin, coloured by tectonic region. Lower images in Figure 7.11 show the same, but the data are filtered to only the neighbouring Gregory Sub-basin, as well as other similar shelfal-basinal 'pairs'; the Lennard Shelf and Fitzroy Graben (and also Pender Terrace). Figure 7.11 indicates that the basinal positions have the most encouraging organic content for the Laurel Formation in the Canning Basin – The Fitzroy Graben and Gregory Sub-basin show fair petroleum potential, averaging 0.61% TOC (ranging 0.03% to 5.81%), and 0.69 kg/ton ultimate genetic yield (S1+S2).

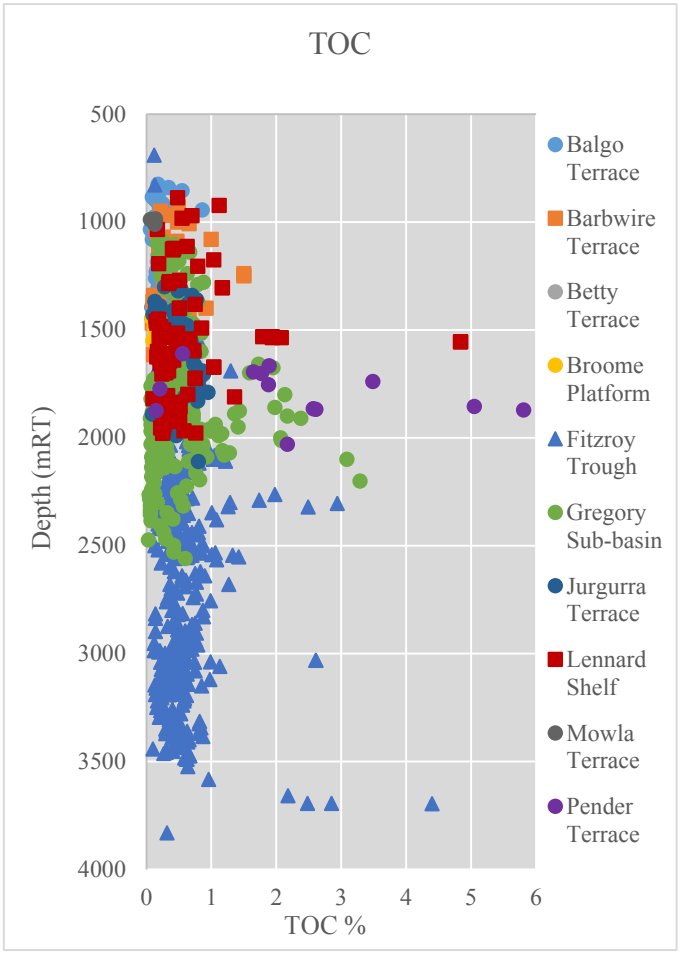

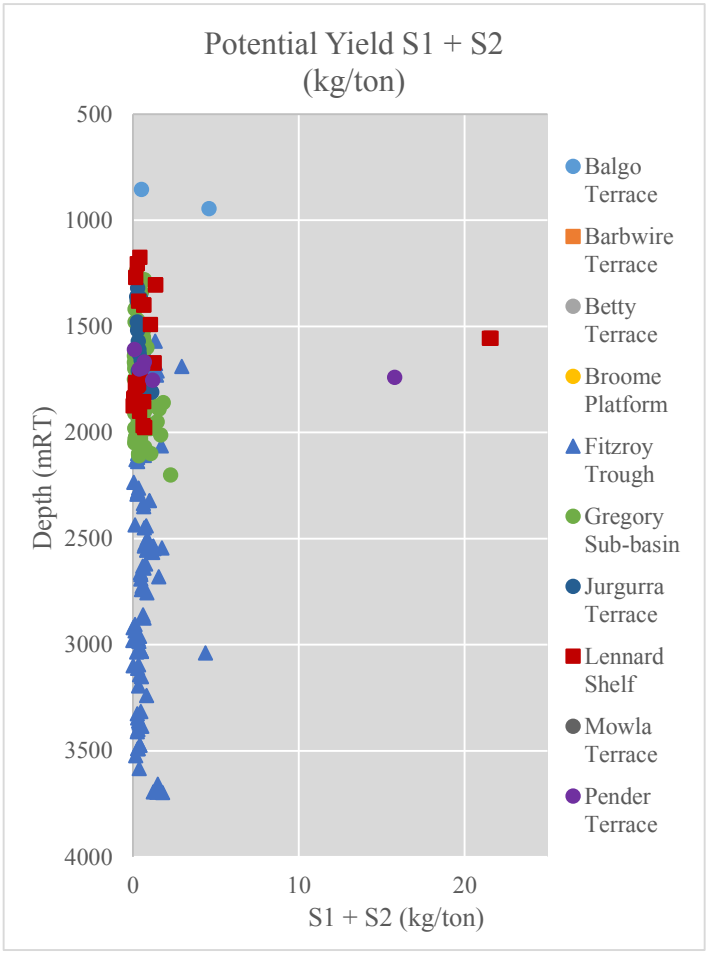

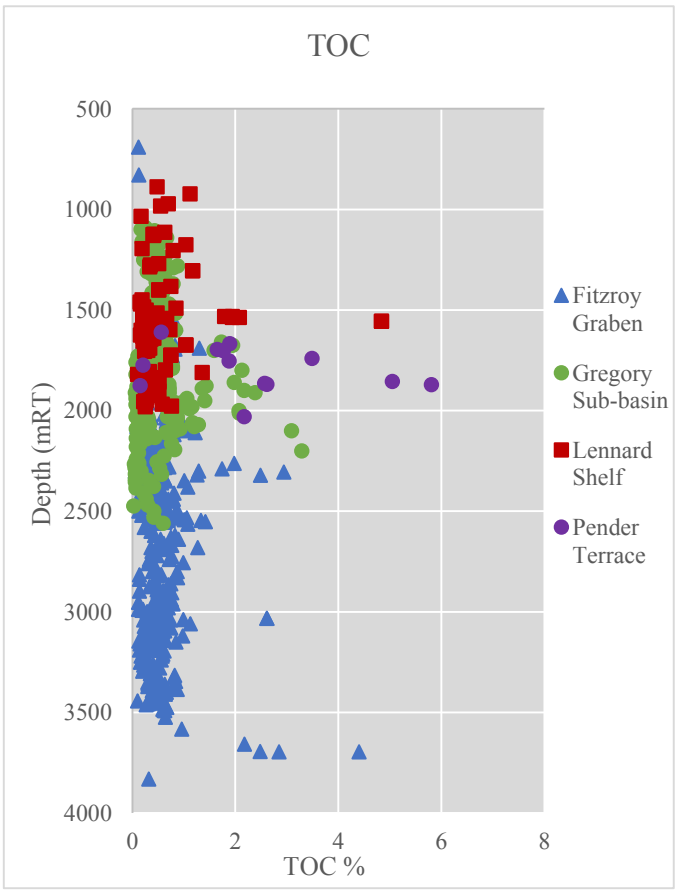

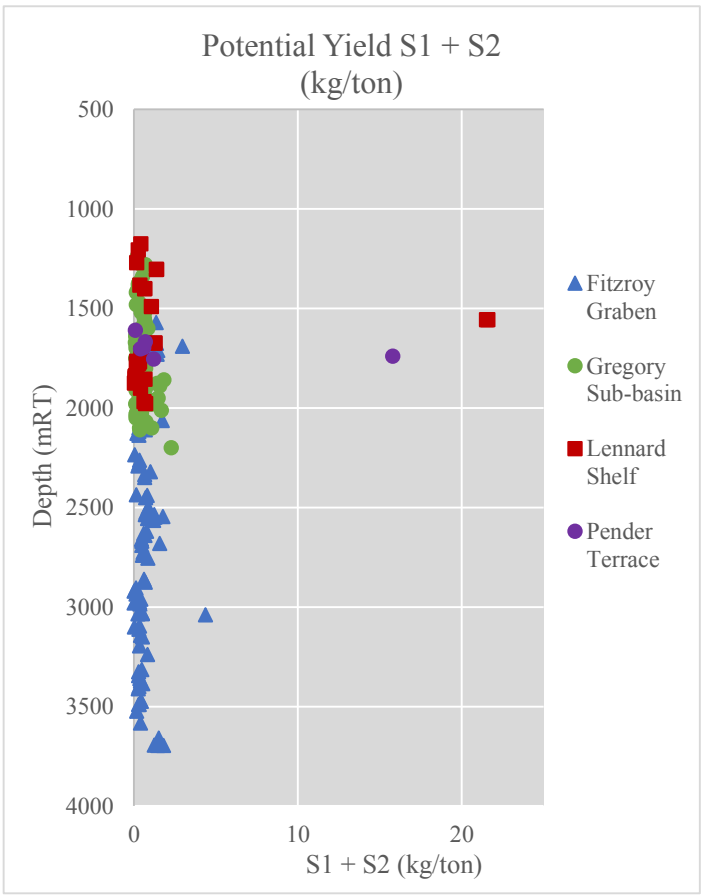

Figure 7.11. Laurel Formation regional TOC and Rock Eval Pyrolysis identified by tectonic province. Clockwise from left: Regional TOC; Regional potential yield; Potential yield nearer study area; TOC nearer study area (modified after GSWA, 2013).

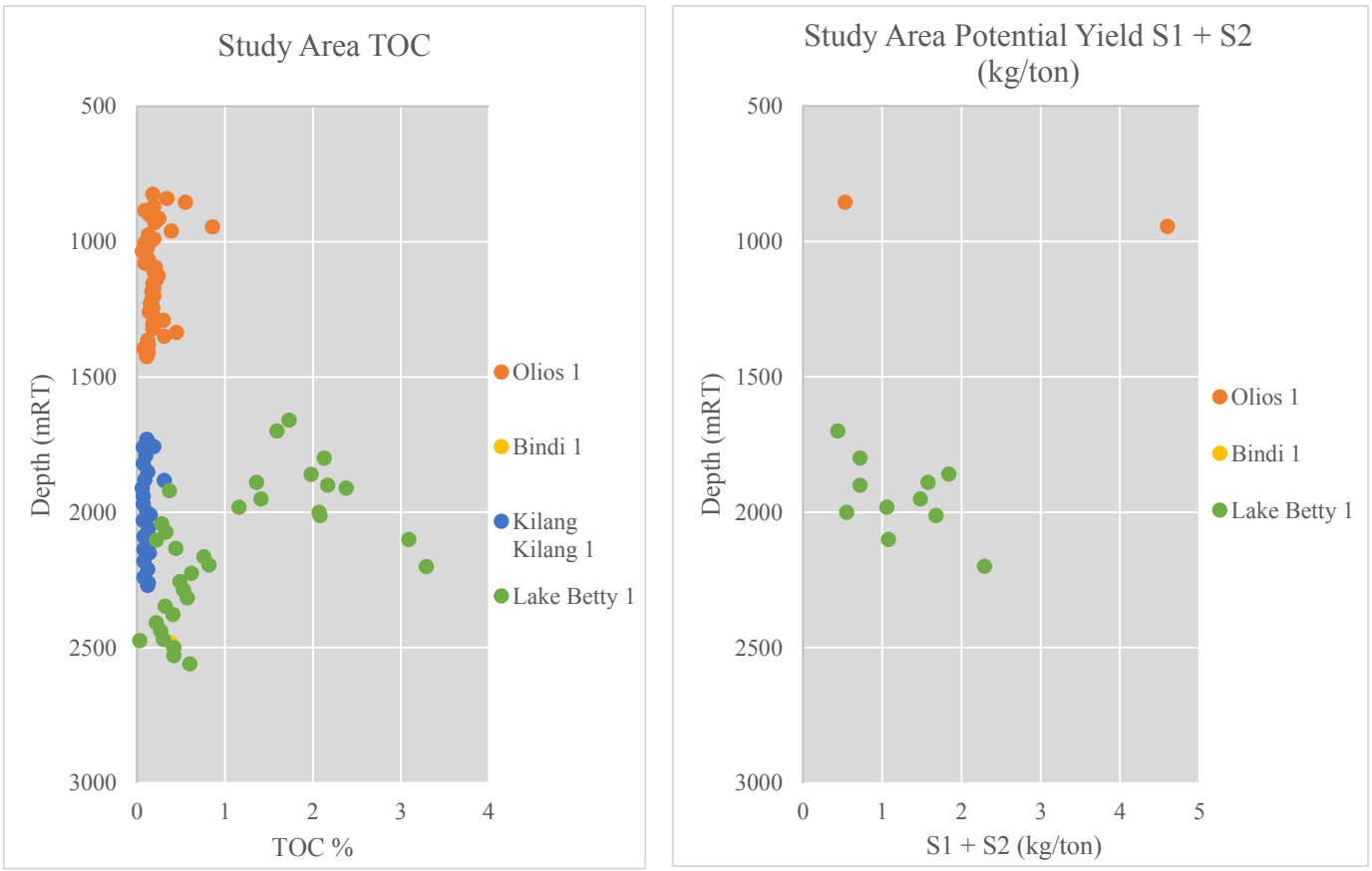

Figure 7.12. Laurel Formation Study area TOC (left) and study area potential yield (modified after GSWA, 2013).

Whilst the pyrolysis yields are subdued (keep in mind the sampling bias introduced by structurally higher drilling positions), the results support the concept of higher organic contents in a basinal setting with potential for hydrocarbon migration up-dip to shelfal reservoirs. Encouraging organic contents in a basinal paleogeographic setting (Figure 4.27) combined with an extensional tectonic environment (rapid accommodation generation and possible anoxic environment) present in the Gregory Sub-basin or Fitzroy Trough, supports stratigraphic thickening and the preservation of organic matter. This concept (also partially addressed by Wulff, 1987) supported by the elevated TOC in Figure 7.11 implies that thicker organically rich zones may be present in hanging wall sections of the Stansmore Fault (refer isochron maps, Figure 6.23; and RB81-07, Figure 6.5).

Local organic richness and pyrolysis yields

TOC data is available within the study area from Olios 1, Bindi 1, Kilang Kilang 1 and Lake Betty 1, pyrolysis data is restricted to Olios 1 and Lake Betty 1. Most of the well data indicates poor petroleum potential for the area; averaging 0.46% TOC (ranging 0.03% to 3.29%) (Figure 7.12). Organic content is also observed to be variable, and perhaps also supports the 'organically rich basin' concept – where Lake Betty 1 (located in the Gregory Sub-basin) shows richer organic content averaging higher than the regional at 1.07%, and as high as 3.29% TOC (ranging 0.03% to 3.29%). This is encouraging, and demonstrates that the basinal portion of the study area shows fair to good petroleum potential.

Tissot and Welte (1984) state that whilst 0.5% TOC is regarded as the low threshold for clastic source rock potential, carbonates can produce a higher quantity of petroleum per amount of organic matter, and 0.3% is considered the minimum (Tissot and Welte, 1984). This is because carbonates tend to contain lesser amounts of reworked terrestrial matter and high percentages of marine organics (e.g. algae) which could suggest an affinity with a type I kerogen (Wulff, 1987). Lake Betty 1 shows average organic content over the lower Laurel Carbonate averaging 0.36% TOC (ranges 0.22% to 0.57% TOC). Olios 1 shows an average of 0.18% TOC (ranges 0.08% to 0.45% TOC). Kilang Kilang 1 and Bindi 1 did not intersect the lower Laurel Carbonate interval. The data indicates that the carbonate within the project area is lean for organic contents and poor petroleum generating potential, even when considering Tissot and Welte's (1984) more accommodating thresholds.

Pyrolysis yields from all project area wells suggest poor petroleum potential. Free hydrocarbons (S1) average 0.31 kg HC/ton from Olios 1 and Lake Betty 1, raging 0.1 to 2.52 kg HC/ton. Remaining generative potential (S2) averages 1.12 kg HC/ton, ranging 0.34 to 2.19 kg HC/ton. Ultimate genetic potential indicates that the interval is lean (Figure 7.12) averaging 1.43 kg/ton.

Kerogen classification

Kerogen classification of the regional Laurel Formation data suggests a type III to type IV kerogen. This is indicated by the HI and OI Van Krevalen diagram (type III gas prone, but also encroaching on marginal type II), and also the HI and Tmax cross plot (Figure 7.13), indicating type III. The HI classification provided by Peters and Cassa (1994) (Table 7.3)

concurs with a type III kerogen, with average Laurel Formation HI across the basin at 58 mg HC/g TOC. The HI ranges from 3.4 to 419 mg HC/g TOC. Classifying the kerogen as type III supports a terrestrial organic matter influence. Depositional setting and paleogeographic reconstructions (Figure 4.27) indicate that a terrestrial influence was present in neighbouring provinces whilst a marginal marine influence was prevalent in the study area. The terrestrial organic material influence is reinforced here by kerogen typing. A HI of 241 is observed at Olios 1 (possibly contaminated by migrating hydrocarbons, suggested by an immature Tmax 422°C (Wulff, 1987), which suggests a type II kerogen (Peters and Cassa, 1994), signposting that a marine influence cannot be ruled out. Of course, more data would assist in typing the study area kerogens (pyrolysis data is only available at Olios 1 and Lake Betty 1). In any case, the carbonate platform that developed during the Tournaisian is expected to be reflected by a type II kerogen pathway, so an overall type II/type III kerogen could be anticipated with greater data coverage.

The HI data (as above), both regionally and within the project area, indicates that a gas hydrocarbon product is likely under optimal maturity conditions (Peters and Cassa, 1994).

Tmax maturity

The Laurel Formation shows Tmax values ranging from 317°C to 530°C across the Canning Basin, averaging 443°C. This suggests that on average, the Laurel Formation is regionally within the early mature hydrocarbon generative window according to Tmax temperatures. A better understanding of maturity characteristics is achieved by filtering Tmax temperatures by tectonic province (Figure 7.14). Tmax on the Lennard Shelf indicates that the Laurel Formation is largely immature to marginally early mature. In the basinal positions of the basin (Fitzroy Graben and the Gregory Sub-basin) the majority of well data suggest that the Laurel Formation is mature (most is at early to peak maturity) for hydrocarbon generation (between 435°C and 470°C).

Tmax within the project area shows that the Laurel Formation is immature to marginally early mature. Lake Betty 1 suggests samples reach peak maturation, with Tmax at 450 °C (Figure 7.14, lower right). Vitrinite reflectance confirms that the Laurel Formation is within the early mature oil generation window within the project area (averaging 0.6 %Ro). Refer to petroleum systems modelling for maturity trends (Chapter 8.6.6).

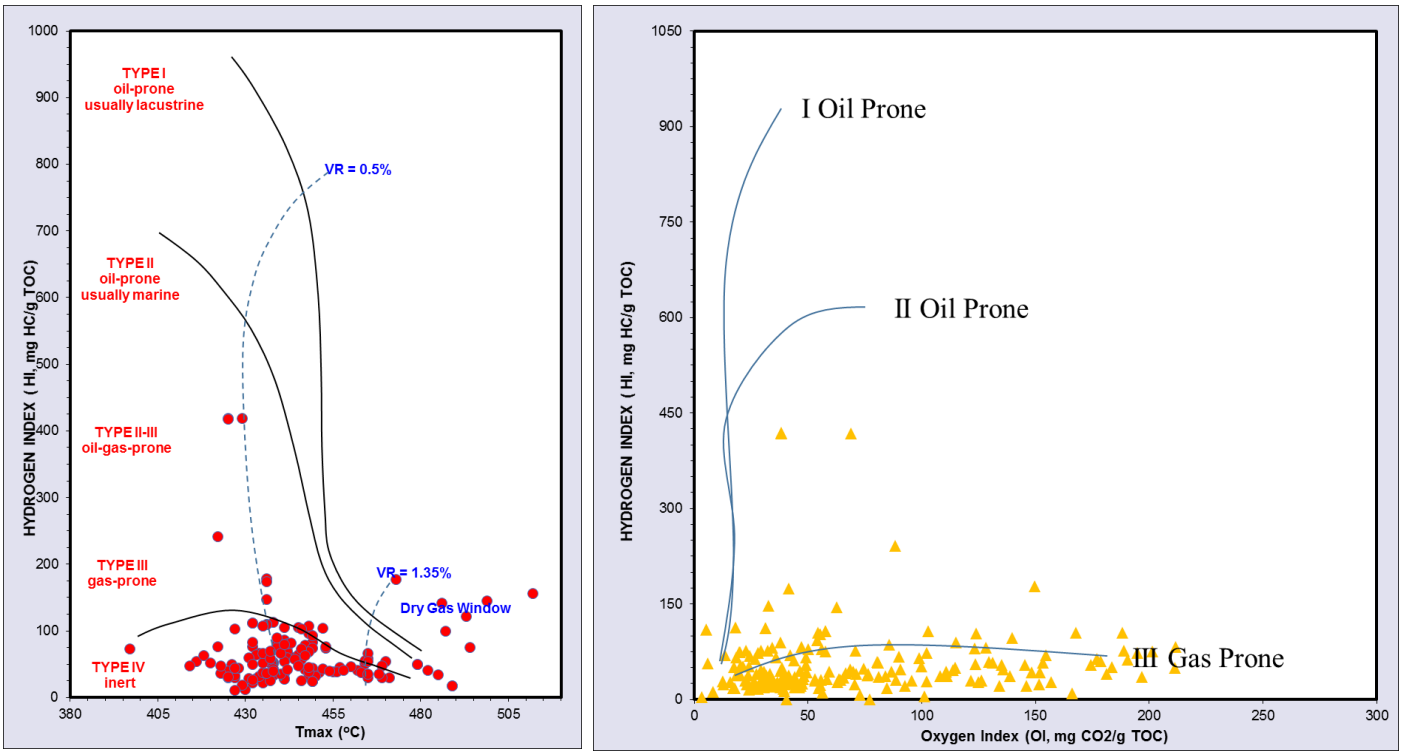

Figure 7.13. Laurel Formation kerogen classification on HI vs OI crossplot (left) indicates types IV and HI vs Tmax (right) shows type III (modified after GSWA, 2013).

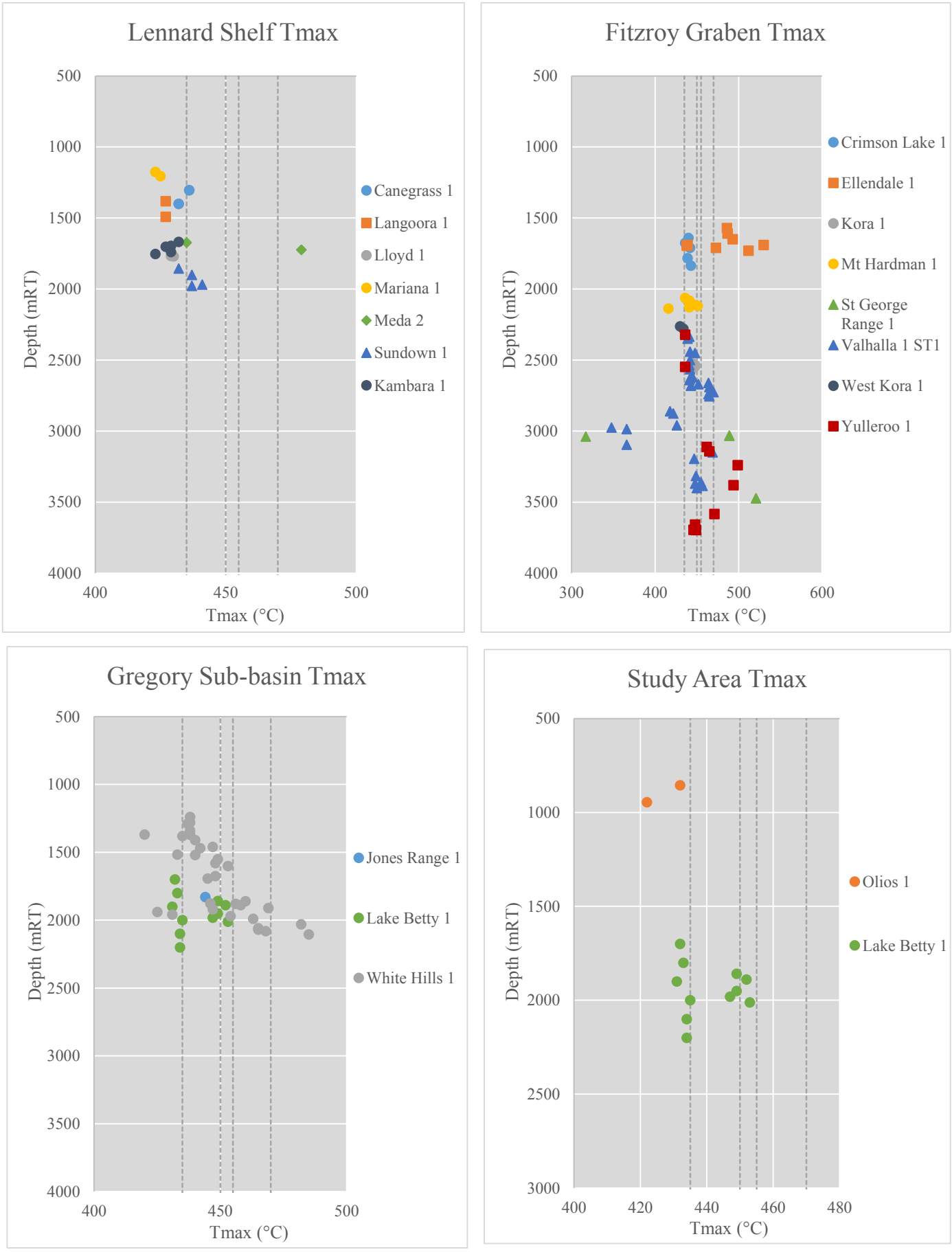

Figure 7.14. Laurel Formation Tmax measurements by tectonic province. Clockwise from top left: Tmax on Lennard Shelf; Tmax within Fitzroy Graben; Tmax within study area; Tmax within Gregory Sub-basin (modified after GSWA, 2013).

Summary of Petroleum Potential

It can be concluded, that the Laurel Formation is within the early to peak hydrocarbon generating maturity window to generate hydrocarbons within the project area, however the interval within the study area and neighbouring shelfal positions (Lennard Shelf) are lean in organic richness. Basinal positions contain encouraging indicators of elevated organic matter (from the well intersections at hand) and are also of a sufficient thermal maturity to generate hydrocarbons. The implication, is that the formation should be targeted for source rock potential in basinal positions, and in the case of the project area, migration would need to be relied upon to move hydrocarbons into shelfal reservoirs.

7.4.5 *Gogo Formation*

The Devonian Gogo Formation is a sequence of laminated to massively bedded shale and siltstone. The interval is represented as a generally mid to high-range, blocky, gamma-ray geophysical log response.

Very little data are available to appraise the formation for source rock potential. The Gogo Formation was only sampled for organic contents and pyrolysis yields at Gap Creek 1, Kambara 1, Matches Springs 1 and Selenops 1.

The Gogo Formation is believed to source the Blina Oil Field (Cadman, 1993; and Wulff, 1987). Notwithstanding this, data at hand suggests that the formation (regionally) has poor petroleum potential with low organic contents; ranging from 0.1% to 0.53% TOC and averaging 0.23% TOC across the Canning Basin (Figure 7.15). Only 1 data point (2819.62 mRT at Kambara 1) shows TOC over 0.5%, therefore most of the hydrocarbon yields stated here are unreliable.

Data obtained by Wulff (Table XIV in Wulff 1987) indicates that the Gogo Formation has better hydrocarbon source potential than what is shown here (but cannot be added here because no depth data is supplied by Wulff). TOC for the Gogo Formation in Wulff (1987) averages 1.25% (ranges 0.44% to 3.1% TOC). Pyrolysis yields are higher at 0.18 kg HC/ton S1 (ranges 0.02 to 1.08 kg HC/ton) and average 2.4 kg HC/ton S2 (ranges 0.33 to 7.02 kg HC/ton). This demonstrates fair to good petroleum potential for the Gogo Formation.

Within the project area, Selenops 1 shows very low organic content averaging 0.14% TOC (ranges 0.11% to 0.18% TOC) (Figure 7.15).

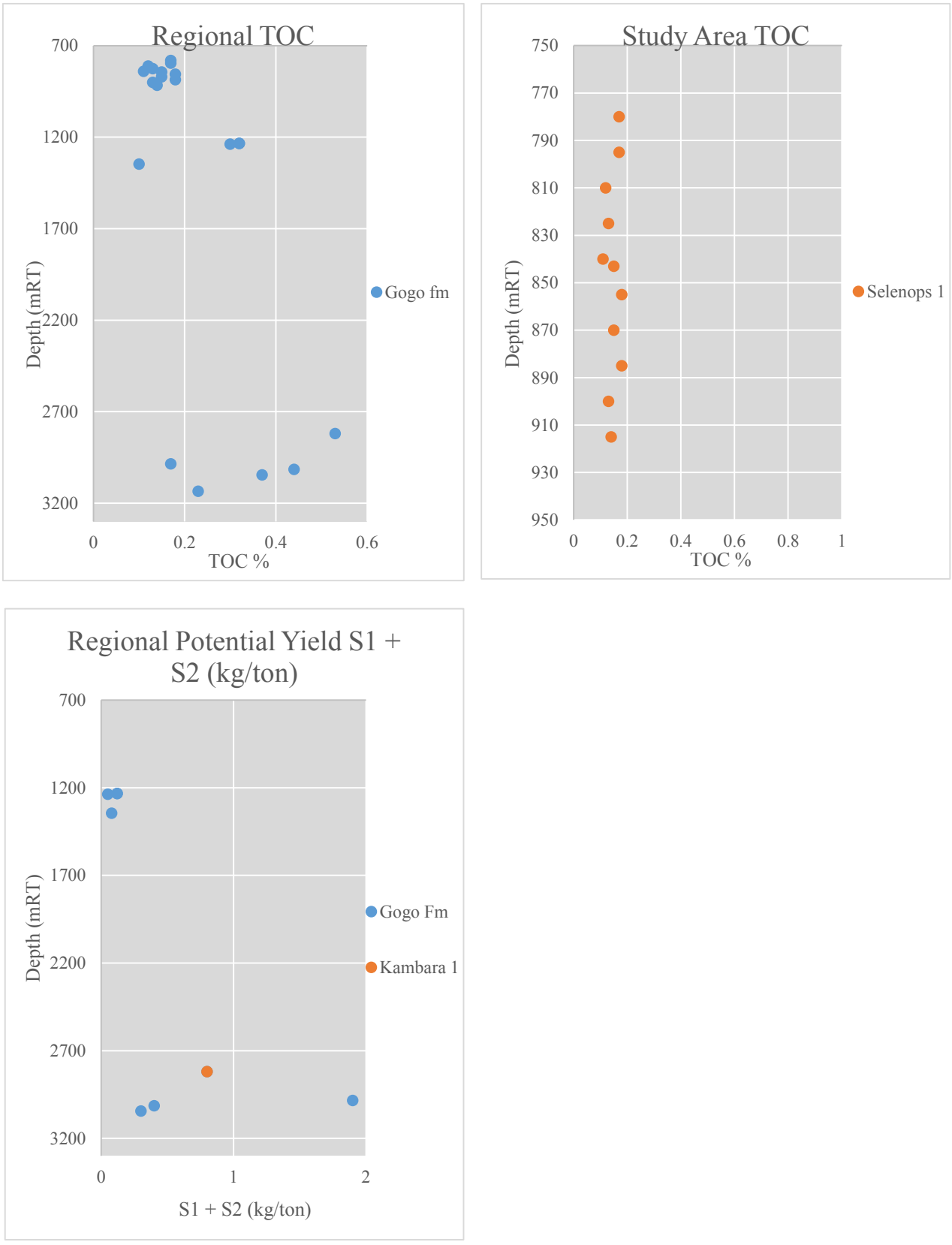

Figure 7.15. Gogo Formation TOC and pyrolysis measurements. Clockwise from top left: regional TOC; study area TOC; regional potential yeild (modified after GSWA, 2013).

The valid data point from Kambara 1 shows very low pyrolysis yields – 0.3 kg HC/ton S1 and 0.5 kg HC/ton S2, which indicates poor petroleum potential. Lean averages for S1 and S2 data also indicate poor petroleum potential across the basin – free hydrocarbon pyrolysis yield (S1) ranges 0.02 to 1.2 kg HC/ton, averaging 0.22 kg HC/ton. Hydrocarbons generated by kerogen cracking (S2) range 0.02 to 0.7 kg HC/ton, averaging 0.26 kg HC/ton. Ultimate genetic yield averages 0.48 kg/ton (Figure 7.15).

Classifying kerogen type using a single data point is unreliable as interpretation of Rock Eval data is best achieved using lots of data (Peters 1986), however the Van Krevalan cross-plots are provided here for completeness. Kerogen classification of the regional Gogo Formation data suggests a type III to type IV kerogen. This is indicated by the HI and OI Van Krevalen diagram (type III gas prone) and also the HI and Tmax cross plot (Figure 7.16). The HI classification provided by Peters and Cassa (1994) (Table 7.3Table 7.6) concurs with a type III kerogen (the Kambara 1 valid data point shows HI of 94 mg HC/g TOC), with average Gogo Formation HI across the basin at 92 mg HC/g TOC. The HI ranges from 6.6 to 411 mg HC/g TOC. Classifying the kerogen as type III to type IV supports a terrestrial organic matter influence, though again, this is probably unreliable given pyrolysis results are reflective of <0.5% TOC. Data within Wulff (1987) indicates average HI of 190 mg HC/g TOC, indicating type III kerogen. Although, as numerous data points within Wulff (1987) are above 200 HI, a type II kerogen is also plausible.

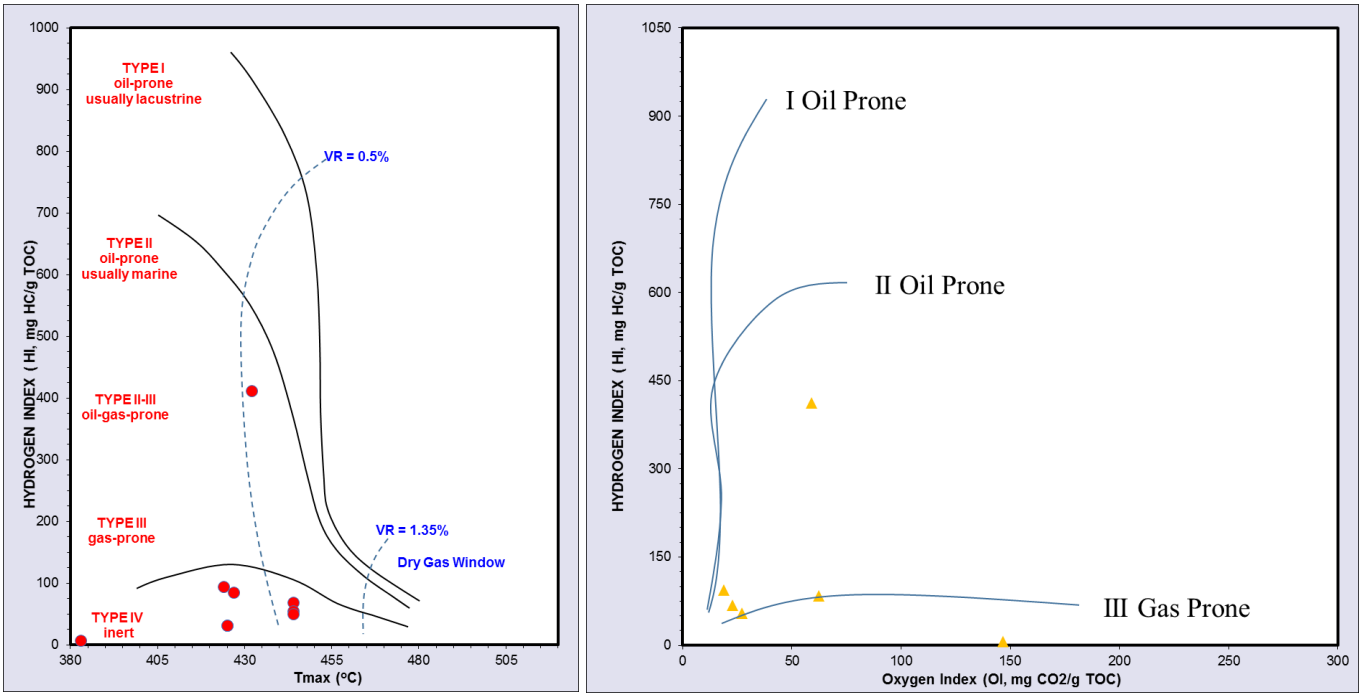

Figure 7.16. Gogo Formation regional pyrolysis indicates a type III to IV kerogen. HI v OI (left) and HI vs Tmax (right) (modified after GSWA, 2013).

The valid data point at Kambara 1 shows that the sample is immature for hydrocarbon generation at 424°C Tmax. The regional average (although invalid) also indicates immature samples averaging 427°C Tmax (ranging 383°C to 444°C) (Figure 7.17).

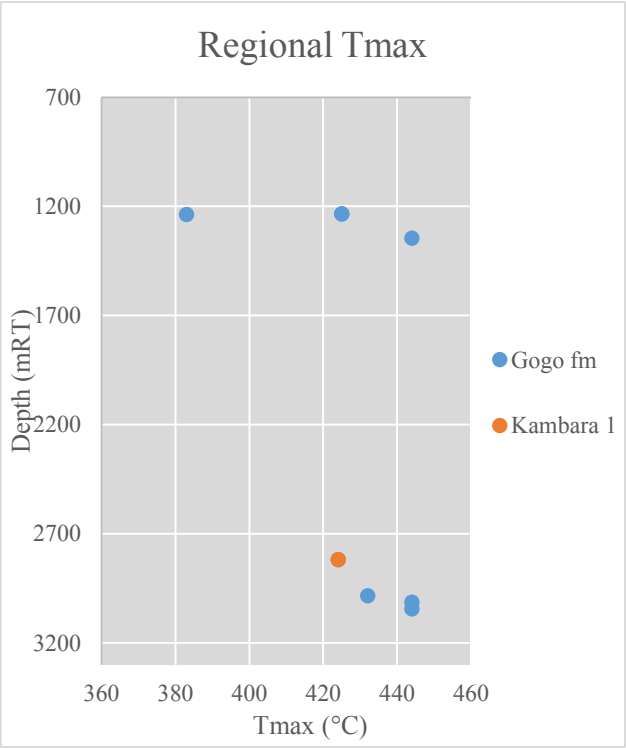

Figure 7.17. Gogo Formation regional Tmax (modified after GSWA, 2013).

Summary of Petroleum Potential

No data exists for the Gogo Formation on the Billiluna Sub-basin, however TWT structure (Figure 6.16) and isochron mapping (Figure 6.24) of the Siluro-Devonian aged section indicates thickening within hanging wall sections of listric faults within the project area, which is likely to encourage rapid accommodation generation for the preservation of organic matter. Combined with a deeper water depositional setting (Chapter 4.5.5), the Gogo Formation should be regarded as a potential source rock within, or down-dip of the project area.

TOC and Rock Eval measurements (Wulff, 1987) indicate encouraging source rock potential for the Gogo Formation, and demonstrate that the interval possesses good petroleum potential under optimal maturity conditions. Classification by Peters and Cassa (1994) suggests that the interval may generate moderate relative quantities of hydrocarbons (HI average of 190 mg HC/g TOC).

It is important to note here that it is very likely that the Gogo Formation samples are biased toward shallower depths as a function of structurally high drilling locations. The analysis here, therefore, is perhaps unfair and not an optimistic representation of interval potential as a source rock. If the Gogo Formation was to charge the Blina Field, it is likely that hydrocarbons migrated to reservoirs on the Lennard Shelf from deeper basinal positions that contain sufficient amounts of organic matter. It is possible that a similar play type may be available within the project area.

7.4.6 *Carribuddy Group – Bongabinni Member*

The Bongabinni Member of the Carribuddy Group is a greyish black, sub-fissile to fissile claystone with a hot and blocky gamma ray wireline log response. The Bongabinni Member is appraised as an organically rich, oil-prone source rock in the Admiral Bay Fault Zone (along the northern boundary of the Willara Sub-basin, Figure 2.1) (Ghori and Haines, 2007).

Very little data are available to appraise the Bongabinni Member for source rock potential. The Bongabinni Member was only sampled for organic contents at Frankenstein 1, Leo 1 and Sally May 1. Pyrolysis data is not available for the interval.

The Bongabinni Member contains low TOC, averaging 0.13% (ranging 0.03 – 0.32 %) across the regional dataset (Figure 7.18). This indicates that the Bongabinni Member has poor petroleum potential by TOC. These results are contradictory to work by Ghori and Haines (2007), where they attest that Ordovician source rocks are the most organically rich within the basin. It would therefore be unwise to discount the ability of the Bongabinni Member on TOC data alone. Thermal history modelling (Chapter 8.6.4) provides positive feedback to accompany future Rock Eval Pyrolysis lab work.

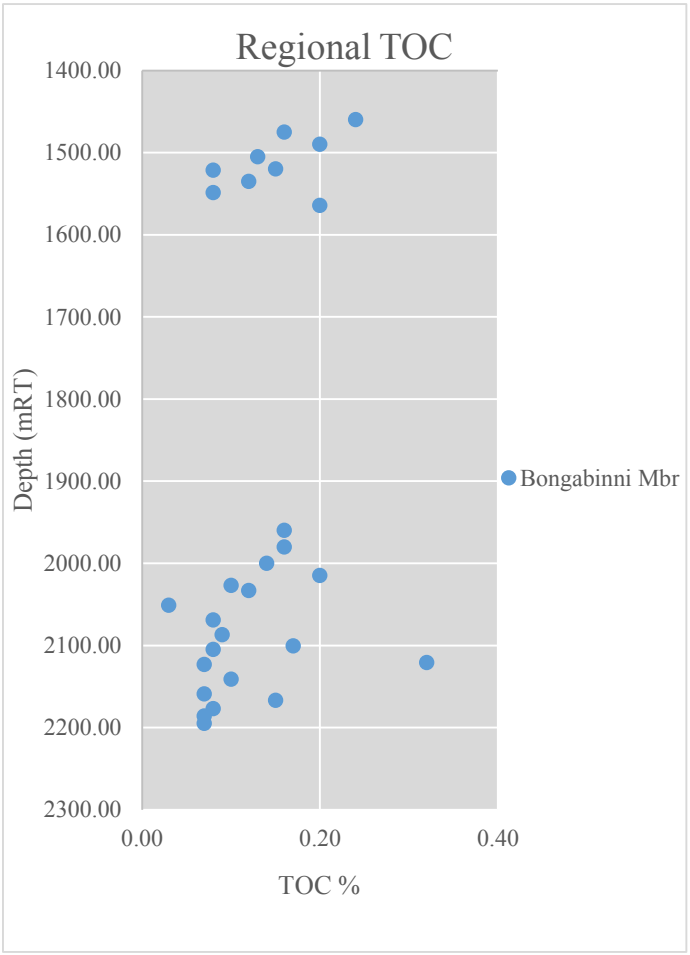

Figure 7.18. Bongabinni Member regional TOC (modified after GSWA, 2013).

7.4.7 *Goldwyer Formation*

The middle Ordovician (Llanvirn) Goldwyer Formation is considered to be an oil-prone marine source rock within the Larapintine L2 petroleum system (Haines, 2004). Several exploration programs by operators within the Canning Basin have searched regionally for organically rich, thick, and thermally mature packages of the Goldwyer Formation. Of note are recent efforts (in 2012) by New Standard Energy, ConocoPhillips and PetroChina within the Kidson Sub-basin. Further, Wulff (1987) claimed that the Goldwyer Formation is likely the best unit within the southern or central Canning Basin to generate hydrocarbons, thus the formation is anticipated to be organically rich and thermally mature within the Larapintine L2 Petroleum System.

The Goldwyer Formation is an interbedded sequence sub-divided into 4 units (WMC Units 1 to 4, oldest to youngest). The formation comprises a calcareous sub-fissile shale with occasional limestone (WMC Unit 1), a blackish fissile shale with siltstone and limestone (WMC Unit 2), a black occasionally carbonaceous shale (WMC Unit 3) and a grey to black argillaceous and carbonaceous dolomite (WMC Unit 4). WMC Units 2 and 4 show a high ranging gamma-ray log response.

The Goldwyer Formation has not been intersected by petroleum wells within the study area. The nearest well intersection that contains TOC and Pyrolysis data is Percival 1 on the Barbwire Terrace. Thirty-seven regional well intersections (refer to Appendix C) provide a sufficient dataset to appraise the formation for regional source rock potential.

The Goldwyer Formation has good regional petroleum potential with organic contents ranging from 0.5% to 4.8% TOC and averaging 1.5% TOC across the Canning Basin (Figure 7.19). Pyrolysis yields indicate that the Goldwyer Formation has very good to excellent regional hydrocarbon potential. Free hydrocarbons (S1) average 4.06 kg HC/ton (ranges 0.07 to 21.19 kg HC/ton). Hydrocarbons generated by kerogen cracking (S2) are also fair to good, averaging 4.11 kg HC/ton (ranges 0.2 to 41.45 kg HC/ton). Ultimate genetic yield averages 7.8 kg/ton, also indicating good hydrocarbon yields (Figure 7.19).

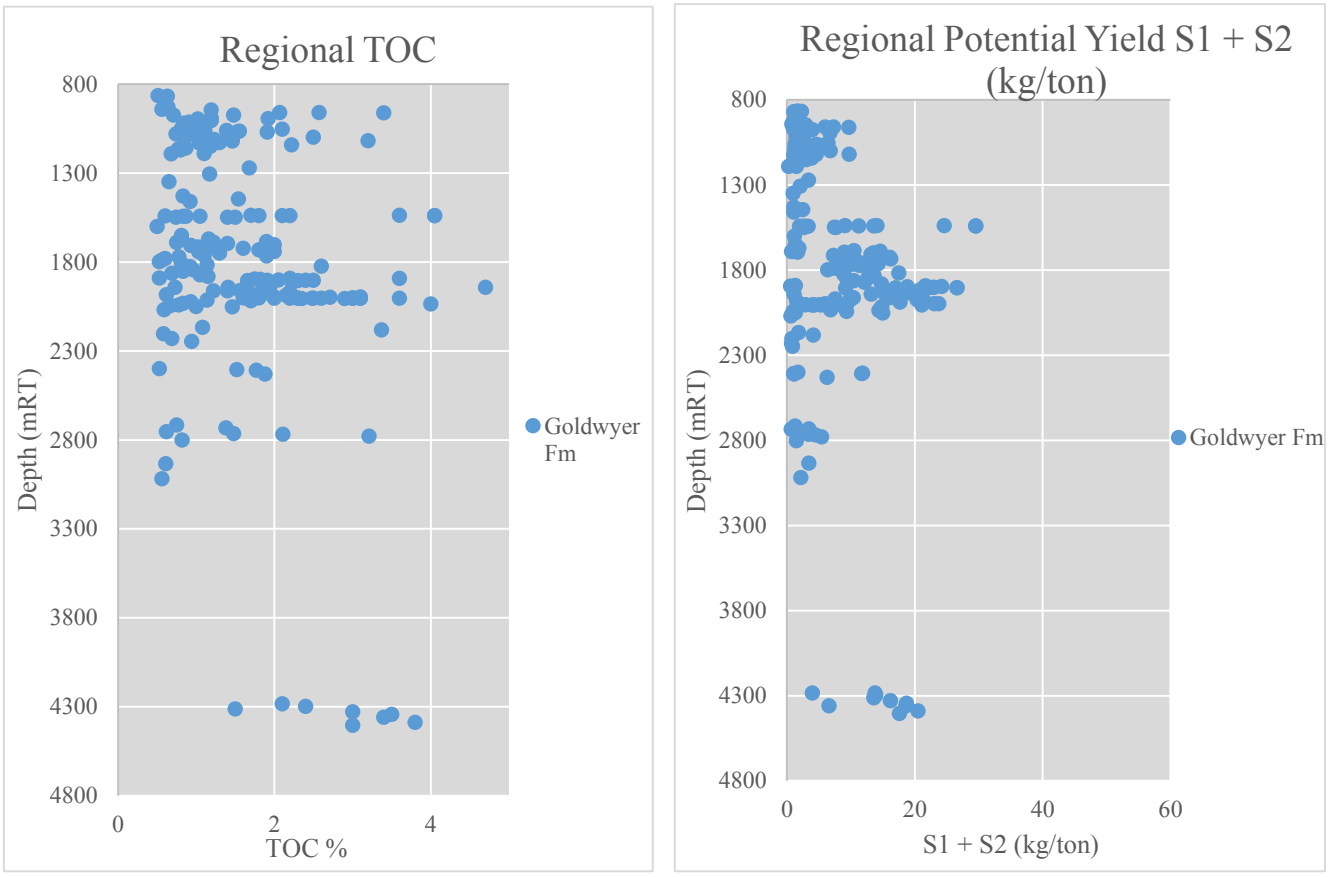

Figure 7.19. Goldwyer Formation regional TOC (left) and regional potential yield (right) (modified after GSWA, 2013).

Filtering the TOC and Pyrolysis dataset by tectonic region (Table 7.10) demonstrates that the Broome Platform, Kidson Sub-basin and Barbwire Terrace contain the most organically rich and highest yielding zones within the Goldwyer Formation. Figure 7.20 demonstrates that the Barbwire Terrace averages 8.21 kg/ton in ultimate genetic yield, the Kidson Sub-basin averages 9.26 kg/ton and the Broome Platform averages 9.22 kg/ton in ultimate genetic yield. Hydrocarbon yields are summarised by S1 and S2 components in Table 7.10.

Region	TOC (wt.%)			S1 (kg HC/ton)			S2 (kg HC/ton)		
	Ave	Min	Max	Ave	Min	Max	Ave	Min	Max
Barbwire Terrace	0.78	0.12	4.05	0.44	0.07	3.5	5.96	0.44	28.32
Broome Platform	0.89	0.06	4.8	6.11	0.07	21.9	3.23	0.1	41.45
Kidson Sub-basin	0.78	0.03	3.8	4.2	0.42	10.5	5.06	0.02	10

Table 7.10. Goldwyer Formation regional TOC and Rock Eval Pyrolysis seperated by tectonic region (modified after GSWA, 2013).

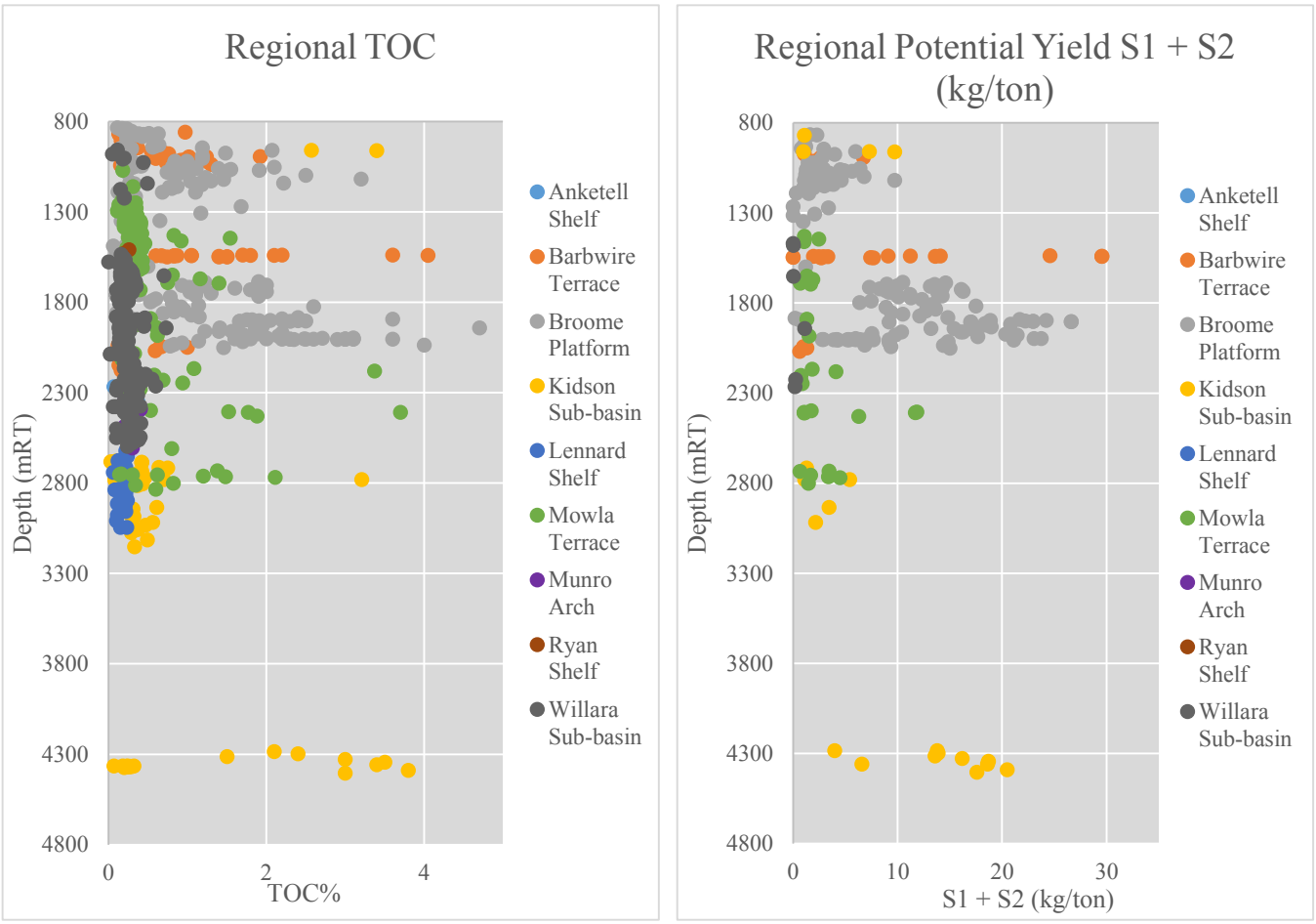

Figure 7.20. Goldwyer Formation regional TOC (left) and regional potential yield, separated by tectonic province (modified after GSWA, 2013).

Filtering TOC and Pyrolysis datasets by WMC subdivisions (Table 7.11) on a regional basis indicates that Unit 1 and 2 (the oldest two units) have the highest average TOC (1.18% and 0.86% TOC, respectively). Unit 2 has the highest average yield of free hydrocarbons (S1) at 7.9 kg HC/ton. WMC Unit 4 has the highest yield of cracked hydrocarbons from kerogen (S2) at 7.56 kg/ton. The low TOC of WMC Unit 4 does not preclude its ability to generate hydrocarbons – shown by excellent S1 and S2 numbers.

WMC Unit	TOC%			S1 kg HC/ton			S2 kg HC/ton		
	Ave	Min	Max	Ave	Min	Max	Ave	Min	Max
4	0.46	0.05	4.8	2.99	0.02	13.47	7.56	0.55	41.45
3	0.62	0.1	3.7	3.6	0.01	13.93	3.89	0.04	12.5
2	0.86	0.12	4.7	7.9	0.1	21.19	3.2	0.1	6.16
1	1.18	0.13	4	2.72	0.11	19.14	2.14	0.37	7.02

Table 7.11. Goldwyer Formation regional TOC and pyrolysis measurements separated by WMC subdivision (modified after GSWA, 2013).

Table 7.11 demonstrates a small inconsistency where average S2 shows to be the greatest for WMC 4, however regionally the same zone comprises the lowest average TOC (0.46%) and relatively lower averages of S1. This is likely due to sampling bias, rather than the characteristics of the rock. WMC 4 is the shallowest subunit, therefore it is likely more commonly intersected. Average measurements therefore comprise a larger sample population (note that the range of TOC is widest for WMC 4). Goldwyer Formation intersections are likely to be biased to structurally higher (less mature) settings due to a historical conventional exploration focus (refer Chapter 2.6). Note that pyrolysis yields appear good relative to low TOC. This is because Rock Eval pyrolysis is generally only run on samples with TOC greater than 0.5%, and all TOC measurements are still included in the analysis within Table 7.12.

Regional (averaged) Pyrolysis data demonstrates that free hydrocarbon (S1) yields are similar in quantity to hydrocarbons cracked from kerogen (S2) during the Rock Eval experiment. This indicates that regionally, the Goldwyer Formation has undergone a period of generation and thus consumed organic content, also summarised in a high average Production Indices (PI) of 0.47. PI demonstrates that the TOC data is potentially not sufficiently indicating initial TOC (TOCi) numbers, due to consumption. The TOC numbers here are likely under-represented and initial TOC is likely higher than what is shown. Due to maturation, TOCi numbers should be assumed slightly higher. Further, an apparent trend in Table 7.11 is that the older WMC units (which are those structurally deeper) have been regionally exposed to higher (deeper) maturation settings than the shallower units. The Goldwyer Formation in more immature locations should reveal more truthful TOCi.

Kerogen classification of the Goldwyer Formation suggests a regional type II kerogen, indicated by the HI and OI Van Krevalen diagram (type II oil prone) and also the HI and Tmax cross plot (Figure 7.21). Tmax trends suggest a type II to type III kerogen. The HI classification provided by Peters and Cassa (1994) (Table 7.3) concurs with a type II to type

III kerogen with average Goldwyer Formation HI across the basin at 269 mg HC/g TOC. The HI ranges from 5.5 to 1073 mg HC/g TOC. Classifying the kerogen as type II to type III supports a marine organic matter influence. Classification by Peters and Cassa (1994) also suggests that the Goldwyer Formation may generate moderate to large relative quantities of hydrocarbons under optimal maturity conditions (HI average of 269 mg HC/g TOC, ranges 2 to 2695 kg HC/g TOC).

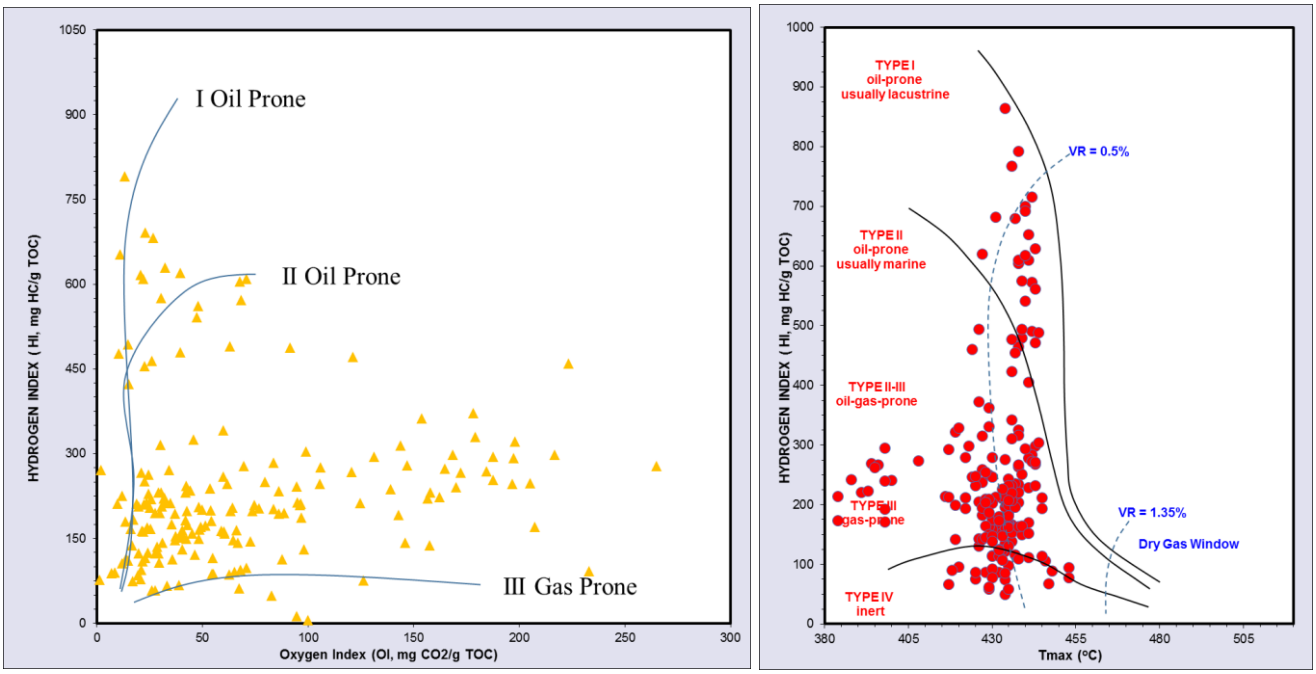

Figure 7.21. Goldwyer formation kerogen typing by OI vs HI crossplot (left) indicates type II. HI vs Tmax crossplot (right) indicates kerogen type II to III (modified after GSWA, 2013).

The Goldwyer Formation shows Tmax values ranging from 384°C to 453°C across the Canning Basin, averaging 431°C (Figure 7.22). This suggests that on average, the Goldwyer Formation is regionally marginally mature to early mature for generating hydrocarbons according to Tmax temperatures. A better understanding of Tmax maturity is achieved by filtering Tmax temperatures by tectonic province (Figure 7.22). Tmax on the Kidson Sub-basin and Broome Platform – two of the three regions that demonstrate the best petroleum potential (Figure 7.20) – indicates that the Goldwyer Formation is immature to early oil

mature respectively. Tmax shows that the formation on the Barbwire Terrace (another region of very good petroleum potential) is within the early to peak oil generation windows, summarized in Figure 7.22. The Barbwire Terrace shows average Tmax at 437°C (ranging 426°C to 453°C).

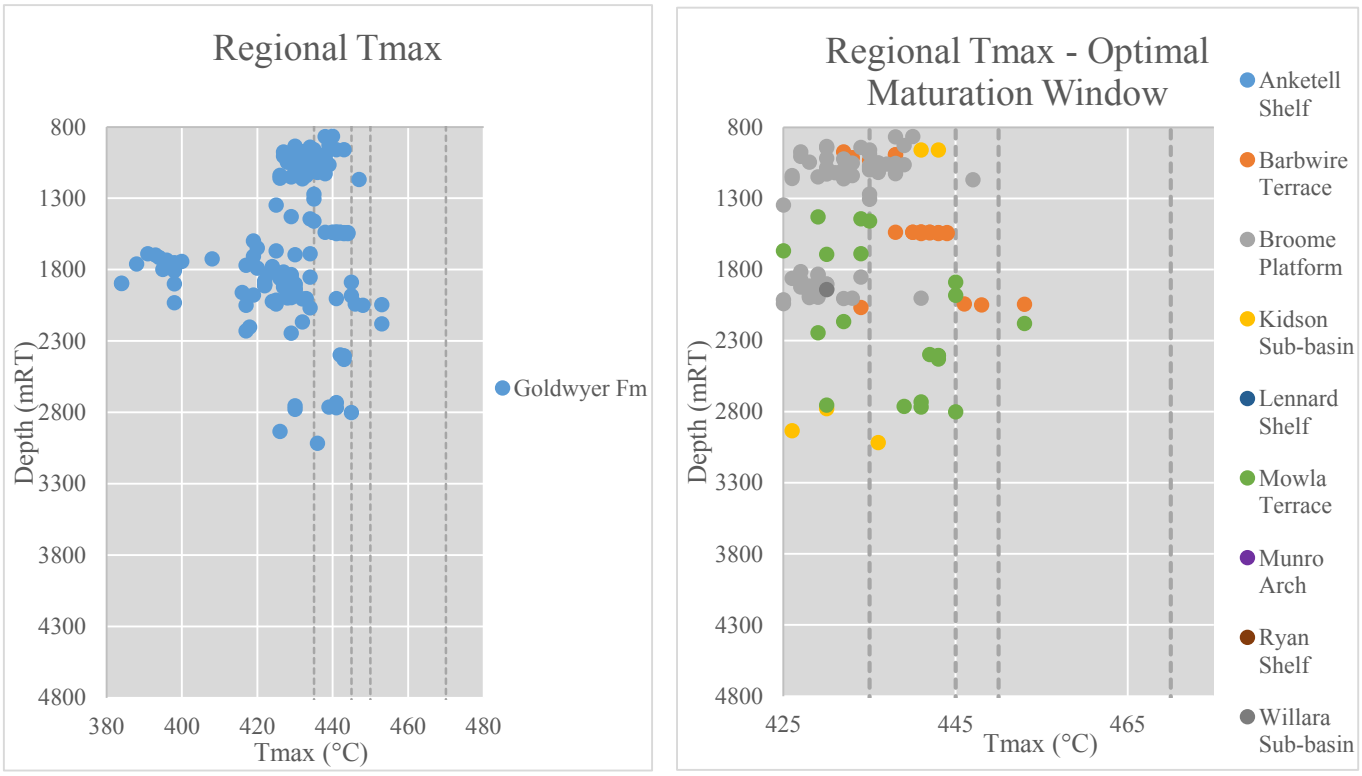

Figure 7.22. Goldwyer Formation regional Tmax (left) and regional Tmax separated by tectonic province (right) (modified after GSWA, 2013).

Tmax data (Figure 7.22) indicates that the Goldwyer Formation is within the early to peak mature hydrocarbon generative window on the neighbouring Barbwire Terrace (the nearest region to the project area to intersect the formation), averaging 437°C Tmax. Seismic evidence (Figure 5.8) demonstrates that the Ordovician aged section deepens and thickens dramatically from the project area off the Stansmore Fault into the Gregory Sub-basin. A similar structural style is assumed (though is documented in literature; i.e. Brown in Wulff, 1987) from the Barbwire Terrace into the Gregory Sub-basin. This implies that the Goldwyer Formation thickens and deepens into structurally deeper (likely higher maturity) settings

within the Gregory Sub-basin, in turn optimising a hydrocarbon generative window. Simply, to discount the availability of mature Goldwyer Formation zones near to the project area would be unwise because the formation is known to exist in deeper settings.

Vitrinite Reflectance data is unavailable for Ordovician aged stratigraphy, because Vitrinite macerals (terrestrial plants) did not develop until Devonian time (Peters et al, 2005).

Gloeocapsomorpha prisca

A marine algae – *Gloeocapsomorpha prisca* – is known to be prevalent during the early to middle Ordovician, with abundances of the organism reported to occur within WMC Unit 4. Occurrences of the algae are noted in other zones, related to the position of the Canning Basin during the Llanvirn (Figure 7.23; and Haines, 2004). Haines also states that the organic rich zone associated with *G. prisca* is restricted to the Mowla and Barbwire Terraces, however the organic horizon may continue into the Gregory Sub-basin (proposed here by seismic derived assumptions and geochemical log observations – discussed in this section). It is reported that there is a correlation between WMC Unit 4 and organic rich horizons with *G prisca* occurrence (Wulff, 1987). This may imply that *G. prisca* generally occurs where WMC Unit 4 is organically rich. To investigate the regional relationship between *G. prisca* and organic rich zones across the Canning Basin, geochemical logs were created for 28 regional wells, and are available in Appendix C. The light orange highlighting indicates zonation of *G prisca* on the geochemical logs.

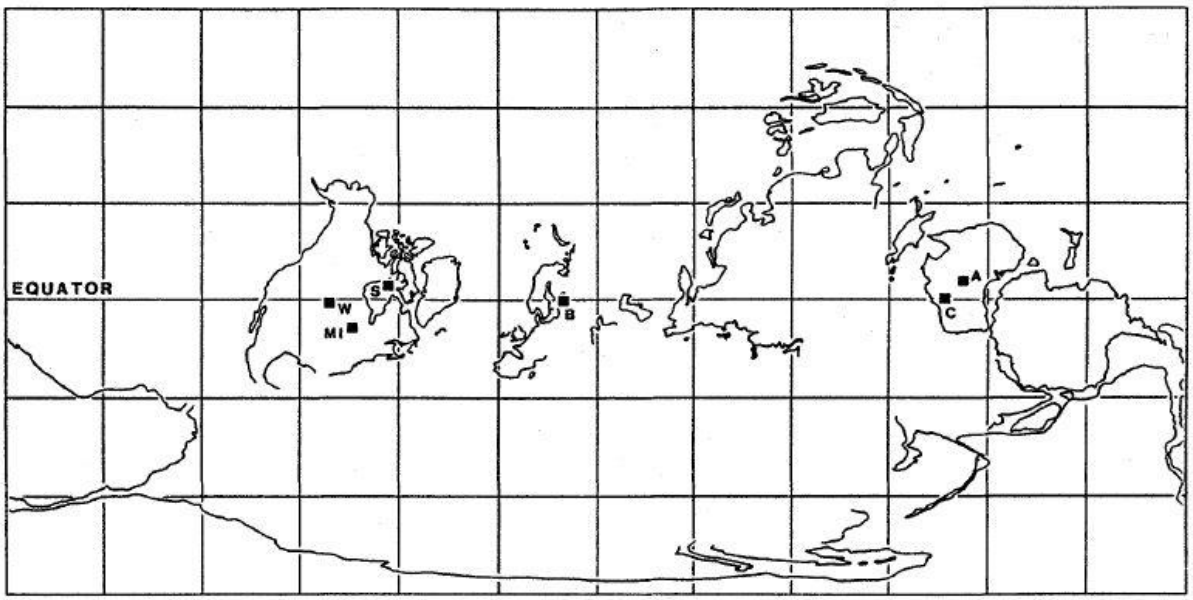

Figure 7.23. Paleogeographic position of continents in the Ordovician. 'C' represents the Canning Basin (Wulff, 1987).

Some conclusions can be drawn from inspecting the Goldwyer Formation geochemical logs. The principal conclusions are, that the *G prisca* zone was found more regionally than reported, and its occurrence is not always a precursor to higher organic content. To elaborate:

- Whilst *G. prisca* is advertised to be associated with WMC Unit 4 (Haines, 2004), the algae is found from regional palynology (within WCRs and illustrated in the geochemical logs) to occur in fairly even occurrences across the WMC subunits. Further, on many occasions within WMC Unit 4, the algae was reported to not occur. This indicates that the correlative is not required to find organic rich facies.
- The occurrence of *G. prisca* does not always indicate an organically rich zone (for example at Great Sandy 1, the presence of the algae corresponds with low TOC (<0.5%) and low yields.
- There are often other zones in wells that display lower organic contents occurring with the presence of *G. prisca*; for example the algae was found in WMC Unit 2 at Canopus 1, corresponding to low TOC, though WMC Unit 1 in the same well shows much higher organic content (up to 1.4% TOC) without the algae.
- *G. prisca* was found in WMC Unit 4 on the Willara Sub-basin (Willara 1, Darriwell 1, Great Sandy 1 and Calamia 1 wells) and Broome Platform (Edgar Range 1, Hedonia

1, Hilltop 1, Whistler 1 and Carina 1 wells), which is more regional than proposed in Haines (2004).

- The Percival 1 geochemical log gives an encouraging overview of the Goldwyer Formation nearest the study area, showing WMC Unit 4 to comprise up to 1% TOC and be within the early to peak hydrocarbon generation window.
- Solanum 1, also on the Barbwire Terrace, shows encouraging TOC and pyrolysis yields. The well displays up to 2.44% TOC, averaging 5.8 kg HC/ton ultimate genetic yield (S1+ S2), shows very good S1 (up to 3.5 kg HC/ton) and excellent S2 (up to 19.3 kg HC/ton) yields.

These conclusions are important because according to the source rock geochemical logs it is now apparent that prospectivity extends beyond WMC Unit 4, and other zones within the Goldwyer Formation clearly demonstrate the potential for hydrocarbon generation.

Summary of Petroleum Potential

TOC data (Figure 7.19) demonstrates that the Goldwyer Formation is regionally organically rich across the Canning Basin (averaging 1.5%). The Barbwire Terrace demonstrates fair to good petroleum potential by TOC (Table 7.11) and pyrolysis yields (Figure 7.20 and Table 7.10). WMC Units 1 and 2 show the best petroleum potential by TOC (averaging 0.86% and 1.18% TOC respectively) and Unit 2 has good pyrolysis yields (averaging 7.9 kg HC/ton S1 and 3.2 kg HC/ton S2). WMC Unit 4 shows excellent hydrocarbon yields and excellent remaining potential (averaging 2.99 kg HC/ton S1 and 7.56 kg HC/ton S2). Geochemical logs drawn for the Goldwyer Formation show encouraging petroleum potential in Percival 1 and Solanum 1 (wells on the nearby Barbwire Terrace – the nearest region to the study area known to intersect the Goldwyer Formation).

The Goldwyer Formation is shown to be an organically rich and thermally early-mature interval (grading to peak maturity) within the Larapintine L2 Petroleum System. Wulff (1987) demonstrated that the Goldwyer Formation is organically rich and thermally mature, utilizing a relatively small dataset. Work presented here is in agreement with those conclusions, though also demonstrates that a larger dataset incorporates a wider variety of inferences for the potential of the formation to be a good source rock.

7.4.8 *Summary of Source Rock Characteristics*

Table 7.12 provides a summary and quick reference guide of source rock characteristics within the project area. The results determined in this Chapter accompany petroleum systems modelling (Chapter 8) to fully evaluate source rock potential within the northeast Canning Basin.

Formation	Average TOC and Rock Eval Pyrolysis characteristics						
	TOC (%)	**S1 (kg HC/ton)**	**S2 (kg HC/ton)**	**PY (S1+S2)**	**Tmax (°C)**	**HI**	**Kerogen Type**
Noonkanbah Formation	2.17 (regional) 1.69 (study area)	0.11 (regional) 0.08 (study area)	1.09 (regional) 0.76 (study area)	0.98	430	33	III to IV
Anderson Formation	0.14	0.32	0.86	1.06	429	88	III
Laurel Formation	0.56 (regional) (0.46 study area)	0.33 (regional) 0.31 (study area)	0.56 (regional) 1.12 (study area)	0.69 (regional) 1.43 (study area)	443	58	III to IV
Gogo Formation	0.14	0.22	0.26	0.48	427	92	III to IV
Gogo Formation*	1.25	0.18	2.4				
Bongabinni Member	0.13						
Goldwyer Formation	1.5	4.06	4.11	7.8	437	269	II Oil prone

Table 7.12. Summary of source rock characteristics (modified after GSWA, 2013). Note: * indicates values from literature. Note that average PY here is not the sum of the average S1 and average S2 values. Refer to text for greater detail.

8. Petroleum Systems Modelling

8.1 Introduction

A petroleum system, defined in Chapter 2, is a geologic system encompassing the source rocks and includes all of the geologic elements and processes that are essential if a hydrocarbon accumulation is to exist (Magoon and Dow, 1994). Chapter 7 analysed geochemical data to determine source rock quantity (organic richness) and quality (organic matter type). This Chapter accompanies Chapter 7 to complete the source rock characterization of the northeast Canning Basin.

The goal for this Chapter is to investigate whether source rocks within the project area are buried deep enough to reach a sufficient level of thermal maturity to enable the source rocks to generate hydrocarbons. Chapter 8 also examines the timing of when petroleum source rocks reach thermal maturation windows to produce hydrocarbon products.

8.2 Definition of a Petroleum Systems Model

A petroleum systems model is a digital data model of a petroleum system where the interrelated elements and processes can be computer-simulated (Hantschel and Kauerauf, 2009). Petroleum systems modelling (similarly; 'Thermal history modelling', 'Source rock maturation modelling'; and collectively 'Basin modelling') is dynamic forward modelling of geologic processes in sedimentary basins tested over geologic time. Sediments within a basin are back-stripped to initial deposition and forward-modelled to present day to simulate the processes enacting within the petroleum system (Hantschel and Kauerauf, 2009).

Generally, the main goal of petroleum systems modelling is to simulate the geological history of a stratigraphic section in order to investigate whether the interval in question reaches optimal thermal maturity windows to generate hydrocarbons. A second goal is to understand the timing of hydrocarbon generation relative to the availability of reservoirs and the development of trapping geometries, where hydrocarbons may be preserved over geologic time to present day. The latter goal is a key focus of 2D modelling.

8.2.1 *General Structure and Method of a Petroleum Systems Model*

The general structure and method of a petroleum systems model involves specifying geological (stratigraphic, paleogeographic, lithological and structural), geothermal (heat flow, surface and sub-surface temperatures) and geochemical (source rock organic characteristics) parameters of a study area, computing compaction and thermal maturity profiles, and calibrating the results to laboratory measurements (Hantschel and Kauerauf, 2009; Prayitno et. al., 1992). A comprehensive review of the methodology is provided by Hantschel and Kauerauf (2009). A summary of the computer simulation workflow is illustrated in Figure 8.1 and Figure 8.2.

There are six elements of a thorough petroleum systems model (Hantschel and Kauerauf, 2009), which are are summarized below. Note that these elements are generally applicable to 3D models. The specific parameters defined for 1D and 2D models in this research project are explained in the ensuing sections. To avoid repetition, parameters for 2D modelling are often combined with the similar 1D controls as indicated below and in the sections to follow.

1. Present day model (1D and 2D modelling)
    - Horizons
    - Facies maps
    - Fault surfaces
2. Age assignment (1D and 2D modelling)
3. Paleo geometry of geological configuration (1D and 2D modelling)
    - Water depths
    - Erosion
    - Salt thickness (not required in this study)
    - Paleo thickness of sediments
4. Boundary conditions (1D and 2D modelling)
    - Surface-Water Interface temperatures
    - Basal heat flow
5. Facies (1D and 2D modelling)
    - Facies definition
    - TOC and HI (Geochemistry)
    - Rock composition
6. Seismic (2D modelling)

- Attributes (maps)
- Reference horizons (for depth conversion)

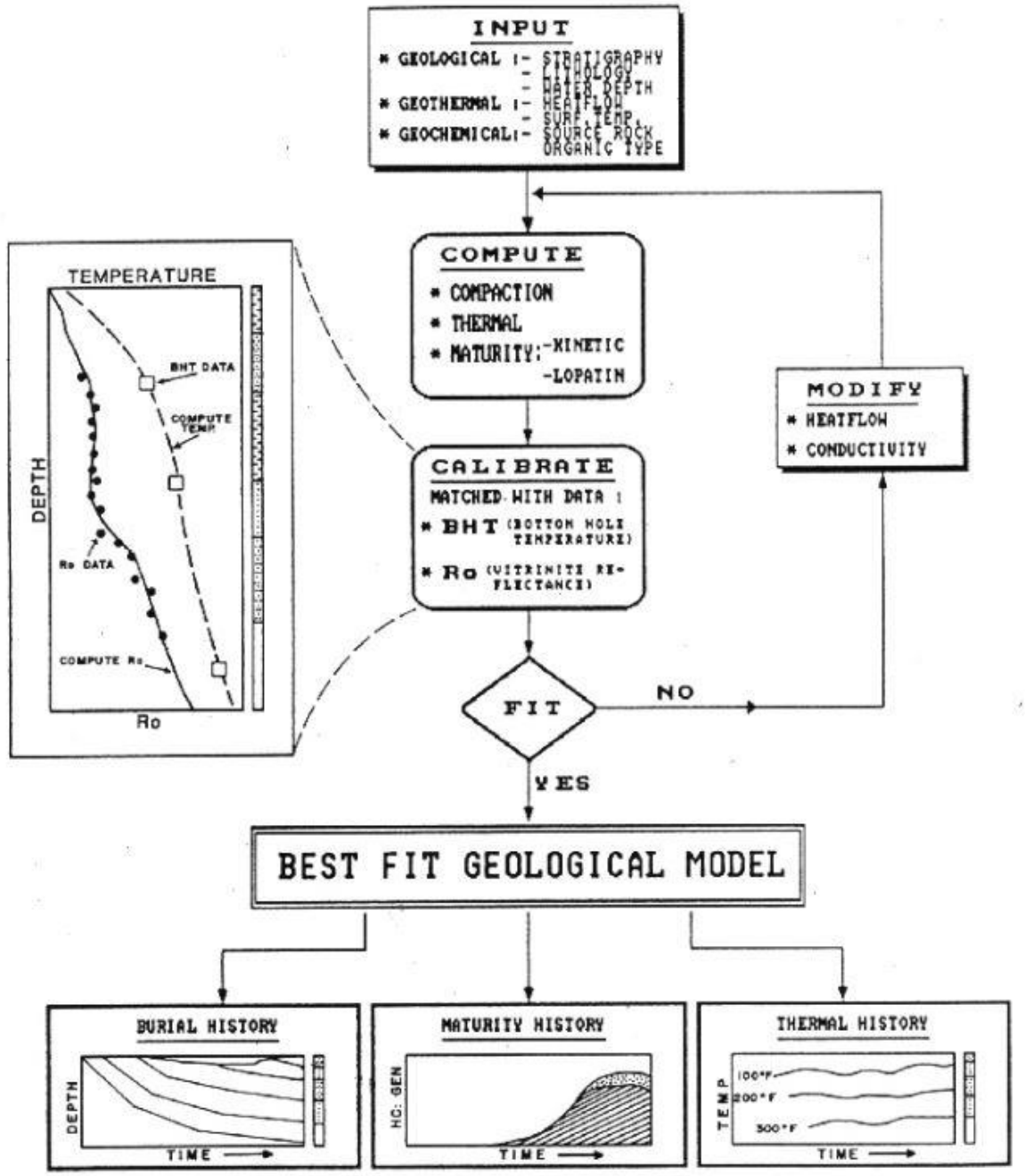

Figure 8.1. Illustration of a digital petroleum systems model workflow (Prayitno et. al., 1992).

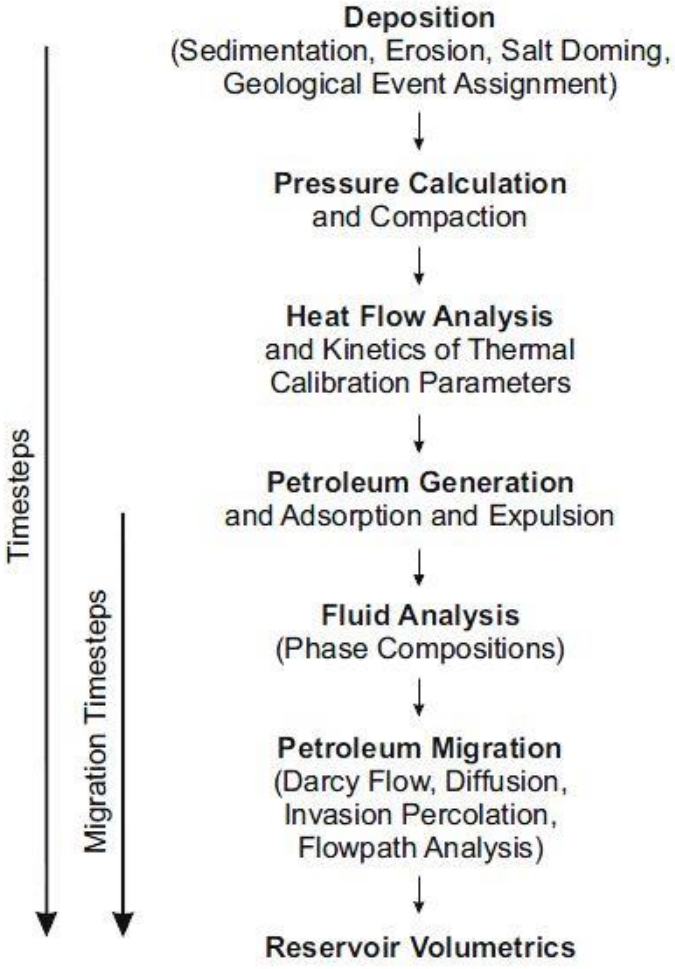

Figure 8.2. Summary illustration of petroleum systems model workflow, specific to PetroMod basin modelling software (Hantschel and Kauerauf, 2009)

8.2.2 *Structure and Method of Models in the Project Area*

To model source rock maturity, a variety of parameters, described in more detail in section 8.4 and 8.6, are inputted into PetroMod petroleum systems modelling software.

8.3 Model Locations

8.3.1 *1D Models*

1D models were constructed for wells in Table 8.1, illustrated in Figure 8.3. Well locations were chosen for geographic spread across tectonic regions, well depth (deeper wells intersect deeper stratigraphic units) and availability of maturity (Vitrinite Reflectance) data.

Well	Total Depth (mRT)	Well Completed
Bindi 1	2507	14/08/1984
Olios 1	1963	02/11/1983
Kilang Kilang 1	2300	03/12/1984
Ngalti 1	2758	17/10/1984
Lake Betty 1	3145	15/12/1971

Table 8.1. Well name and total depth summary of 1D models in this project.

8.3.2 *2D Models*

A regional 2D model; RB81-7, was built to simulate the evolution of petroleum systems across the Gregory Sub-basin, Betty Terrace, Balgo Terrace and Billiluna Sub-basin. Further 2D models were built to test the evolution of petroleum systems in association with structural traps where possible accumulations may exist (Chapter 6.2.4). These secondary (but no less important) 2D models were constructed using 2D seismic lines identified in Table 8.2, and illustrated in Figure 8.3. The line locations are based on areas that;

1. Are on key structural traps identified in Chapter 6.2.4;
2. Where the stratigraphy (outlined in Chapter 4) appears to host suitable reservoir and sealing elements; and

3. Where source rocks are organically rich and thermally mature for the generation of hydrocarbons (discussed in Chapter 7 and also this Chapter).

In summary, 2D model locations were selected to simulate the evolution of petroleum systems and to test petroleum system interactions across structural traps identified within the project area.

Seismic line	Line orientation
RB81-7	Dip line – NE-SW
RB81-10	Strike line – NW-SE
RB82-28	Dip line – NE-SW
Arbitrary Line 82GN-03, S85LM-08 and S85LM-08A	Dip line – NNE-SW

Table 8.2. Summary of seismic lines upon which 2D models were constructed in this project.

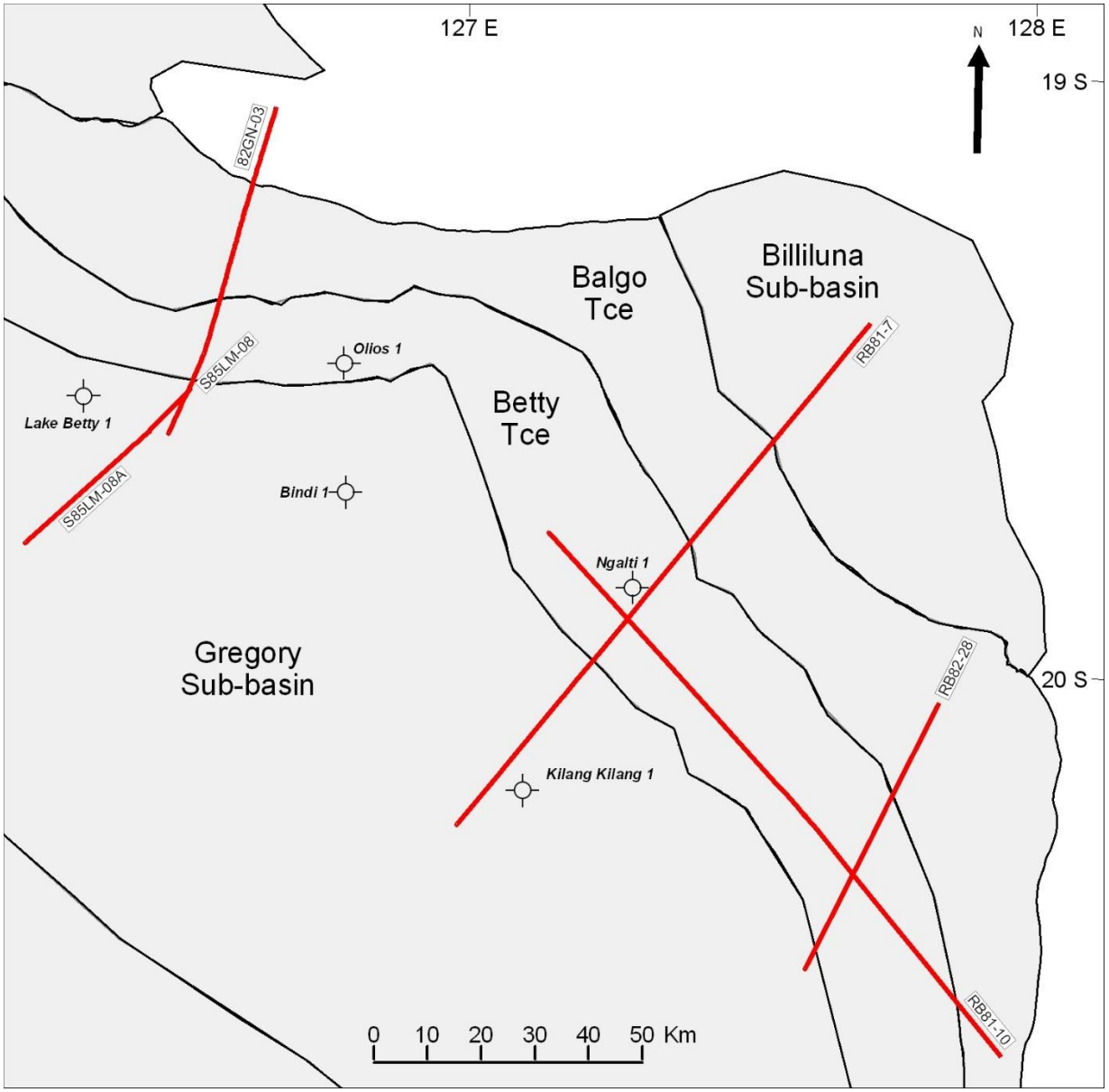

Figure 8.3. Location of wells and seismic lines used for 1D and 2D modeling.

8.4 Data Inputs and Parameters – 1D Models

8.4.1 *Present-day Model*

Age assignment

Age assignment relates the present day well bore intersections (or surfaces in 2D modelling) with their geological age of deposition and exhumation (Hantschel and Kauerauf, 2009). The age assignment input Table instructs PetroMod on geological formation attributes (such as geological age, quantities of preserved and removed section, and source rock TOC) to incorporate in the simulation. The age assignment for each 1D model is provided in Appendix E.

8.4.2 *Paleo Geometry*

Water depths

Water in geologic basins provide accommodation for sediment accumulation, thus influencing a control for sediment thicknesses and hence compaction. Paleo-water depths are therefore an important parameter in basin modelling because they impact the burial and uplift of a sedimentary basin. Paleo-water depths in PetroMod are also boundary conditions for fluid flow and heat flow equations. Water depths are generally derived from assumptions made about eustatic sea-level change and interpretations of paleogeographic settings (Hantschel and Kauerauf, (2009). Large uncertainties are associated with paleo-water depth estimates (Corcoran and Doré, 2005), and they are especially difficult to define in older rocks where less sedimentology-derived observations are on hand. In respect of this uncertainty, a wider range of error is anticipated to be present for Silurian and older sequences.

Paleo-water depth (PWD) estimates for this project were largely made from paleogeographic reconstructions (both from Chapter 4 and also various publications; Brakel et. al., 1990; Cook and Totterdell, 1990; Gorter, 1987; and Smith et. al., 2013), and estimates published in WCRs.

Average paleo-water depths are illustrated in Figure 8.4. Key PWDs concerning 1D and 2D modelling are explained in Table 8.2. A 40 metre water depth is selected for the

Mississippian epoch reflecting shallow or marginal marine conditions. A marine setting in the Permian was set at approximately 200 metre water depth. Another marine setting was set at 200 metres in the Triassic, related to the deposition of the Blina Shale. Smith et. al (2013) suggests a marginal marine water depth of approximately 20 metres accommodating the Late Jurassic Alexander Formation and Wallal Sandstone.

System / Epoch	Age	Paleo-water depth	Comments
Late Jurassic	160 Ma	20 m	Marginal marine paleogeographic setting (Smith et. al (2013)
Triassic	260 Ma	200 m	Marine paleogeographic setting (Chapter 4.9 and Gorter, 1987)
Permian	235 Ma	200 m	Marine paleogeographic setting, maximum Permian transgression (Chapter 4.8.2 and Brakel et. al., 1990)
Mississippian	344 Ma	40 m	Shallow marine/marginal marine paleogeographic setting (Chapter 4.6.1)
Devonian	380 Ma	35m	Marginal marine paleogeographic setting (Chapter 4.5.7)
Silurian	430 Ma	50 m	Marginal marine paleogeographic setting (Chapter 4.3.3)
Ordovician	475 Ma	150 m	Marine paleogeographic setting – Larapintine Seaway Development (Chapter 4.3.3. and Cook and Totterdell, 1990)

Table 8.3. Summary and explanation of paleo-water depths used in petroleum systems models.

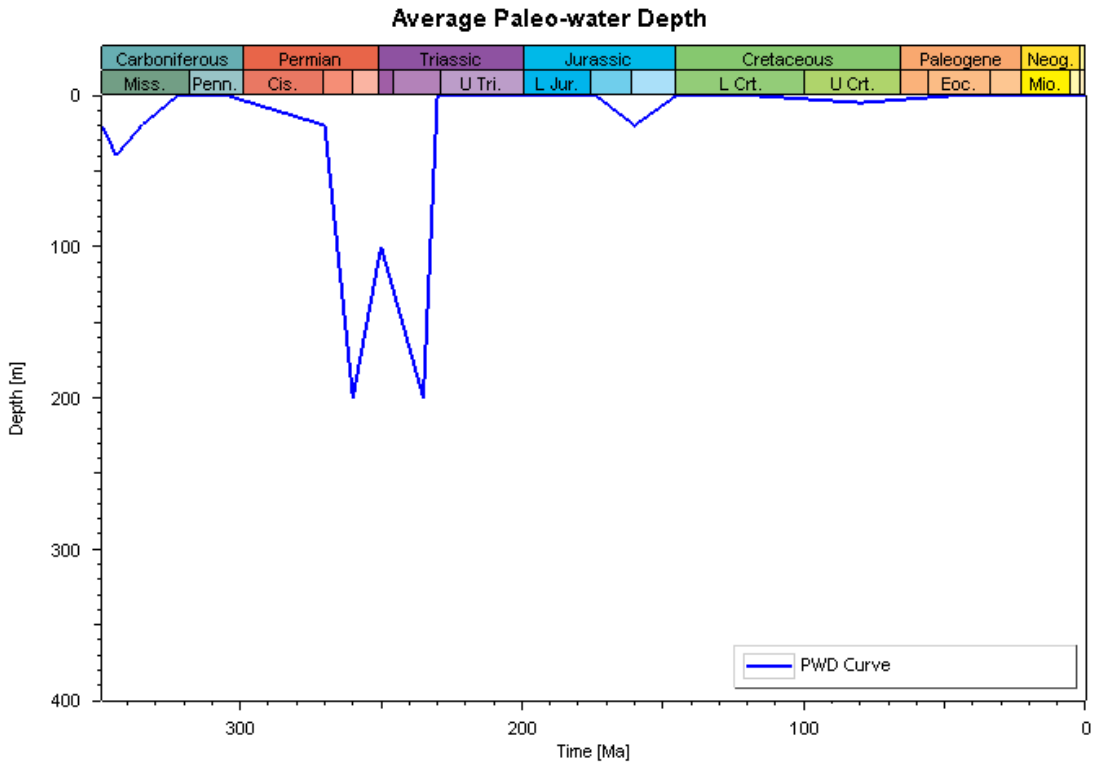

Figure 8.4. Average paleo-water depth used in 1D models.

Erosion – 1D and 2D modelling

Several tectonic episodes are reported to occur during the geological history of the Canning Basin (Yeates, et al., (1984) and Edwards, et al., (1997); refer to Chapter 2). The episodes that have likely led to exhumation of sediments are the Early Devonian Prices Creek Movement, the Middle Carboniferous Meda Transpression and the Triassic Fitzroy Movement. Recently, Duddy et. al., (2003) used Apatite Fission Track Analysis (AFTA) to determine an accurate burial history of eastern Canning Basin sediments, using the White-Hills 1 well, located south of the project area (Figure 8.5).

The eroded quantities described here, along with the procedures to estimate them, apply to 1D modelling and 2D modelling.

The 2D models simulate Carboniferous and older stratigraphy so consideration needs to be given to exhumation associated with the Early Devonian Prices Creek Movement. The 1D models do not intersect sediments as old as this structural episode. No Devonian inversion is visible on 2D seismic, and regional workers do not quantify Devonian exhumation in published literature (Edwards et al., 1997). Although uplift may have occurred during the

Devonian, no readily available present day evidence (for example, seismically visible unconformities) was observed, so it is assumed that the local effects of this tectonic episode are either minimal, or that the event described by regional Canning Basin workers were not as significant on the Betty or Balgo Terraces. Therefore, no exhumation was specified for the Early Devonian Prices Creek Movement.

Erosion during Carboniferous and Triassic periods need quantification for both timing and depth. For both exhumation events, final quantities were based on estimates derived during 2D modelling, and the 1D models were revised after the 2D models were complete.

Carboniferous Meda Transpression

Timing for Meda Transpression related exhumation is based on seismic observations (RB81-7, Chapter 6.2.3 and Figure 6.5). It is assumed that there was no deposition or hiatus between the boundary of Anderson Formation and Grant Group (i.e. Near Top Anderson Formation horizon). Erosion due to the Meda Transpression is estimated to start at 322 Ma until 305 Ma.

Quantifying the thickness of additional section removed during this event was achieved by using regional seismic line RB81-7. The eroded sequence was ‘restored’ during construction of the RB81-7 2D basin model (creation of erosion maps). RB81-7 (Figure 6.2.3) shows that the Anderson Formation and a large component of the Fairfield Group is eroded at SP 300. The top of the Anderson Formation was flattened in PetroMod and the eroded section digitized into the model. The eroded section is estimated to be equal to the thickness of the thickest preserved section, which is presently on the downthrown side of the Stansmore Fault, RB81-7 SP 900. On RB81-7 this is equal to approximately 250 metres. This eroded thickness was applied to all 1D models.

Two assumptions are made using this estimate:

1. That the eroded thickness is equal to the thickest preserved portion of the Anderson Formation and Fairfield Group. This may not be true, and a significantly larger amount of rock may have been eroded than what is preserved at RB81-7 SP 600. Alternatively, the exhumation enacted by the Meda Transpression may be spatially variable and less than 250 metres, however the input for PetroMod does not permit an error range for these allowances.

2. That the eroded thickness is isopachus across the project area, estimated from RB81-7. Again, it is likely that the eroded thickness varies considerably across the project area, though an estimate must be made for the PetroMod erosion parameter.

Mesozoic and Cenozoic exhumation

Very little indication of erosion is given by seismic data for exhumation during the Mesozoic and Cenozoic, other than a shallow angular unconformity at the present day surface. Timing and exhumed thicknesses were estimated after work by Duddy et.al. (2003). The workers used Apatite Fission Track Analysis (AFTA) to conclude that, based on the White Hills 1 well, three periods of uplift occurred. The reader is referred to Duddy et. al. (2003) for the methodology. The following are broad estimates of exhumation provided by AFTA:

1. 2900 m of total uplift and erosion between 230 Ma to 180 Ma;
2. 1450 m between 135 Ma and 120 Ma; and
3. 550 m between 45 Ma and 10 Ma. Re-burial occurs between each of these events (Figure 8.5).

It is acknowledged that techniques to estimate exhumation thicknesses in uplifted basins can have associated uncertainties on the order of several hundreds of meters, and that reconciling estimates of uplift is an important component of attempting to accurately estimate exhumation magnitude (Corcoran and Doré, 2005). It should be noted that ±500 metres or more of section may be in addition to the exhumed thicknesses stated here.

The above exhumed quantities were added to 1D models and also ‘restored’ during 2D modelling before simulation. A 1D pseudo well was extracted from 2D models to compare burial history and maturation curves at the location of Kilang Kilang 1; the result was compared to the Vitrinite Reflectance data, where it was found that the eroded thicknesses were causing the maturity profile to over-mature considerably. It was determined that the exhumation applied to each model needed to be reduced in order to honor the present day maximum paleo-temperatures represented by VR measurements.

Duddy et.al. (2003) confess that other thicknesses are within the allowances of AFTA (Figure 8.5, bottom left), so reduced thickness were attempted with much better fits for the VR data within the project area (refer VR vs. depth calibration, Figure 8.5):

1. 2200 m of total uplift and erosion between 230 Ma to 180 Ma;
2. 1050 m between 135 Ma and 120 Ma; and
3. 270 m between 45 Ma and 10 Ma. (Figure 8.5).

Again, these are broad estimates with proportional re-burial assumed between these episodes.

There is generally good agreement between exhumed quantities across the project area, where slight differences to exhumation between wells are attributed to unevenness in burial and spatial variability in the location of each respective well within the Gregory Sub-basin (Figure 8.5):

- Kilang Kilang 1 and Lake Betty 1 share similar present day depths (1620mRT and 1600mRT, respectively) and similar maximum maturity on the top of the Fairfield Group (0.8 – 1.1 %Ro).
- White Hills 1 is located towards the southeastern end of the Gregory Sub-basin, where the trough shallows onto the Ryan High (Figure 8.5). The Fairfield Group at this location reaches a similar maximum paleo-temperature on the top of the Fairfield Group (<0.95 – 1.1 %Ro) at a shallower present day depth (1100mRT).
- Bindi 1 is located in the central project area depocentre, presently 2350mRT to the top of the Fairfield Group, and shows a similar maximum paleo-temperature (>1.05 %Ro+), indicating a similar maximal burial in the Triassic, though less subsequent uplift relative to neighboring wells. This may be because the central project area (and central Gregory Sub-basin) was less adversely affected by exhumation in Triassic or later periods.

The net exhumation (gross erosion above minus the reburial component) estimate for each exhumation episode was used as input for PetroMod, and only varied slightly to ensure calibration parameters at each well were honored. The final Mesozoic and Cenozoic exhumation parameters used are as follows.

1. 1050 m of total uplift and erosion between 230 Ma to 180 Ma;
2. 550 m between 135 Ma and 120 Ma; and
3. 300 m between 45 Ma and 10 Ma.

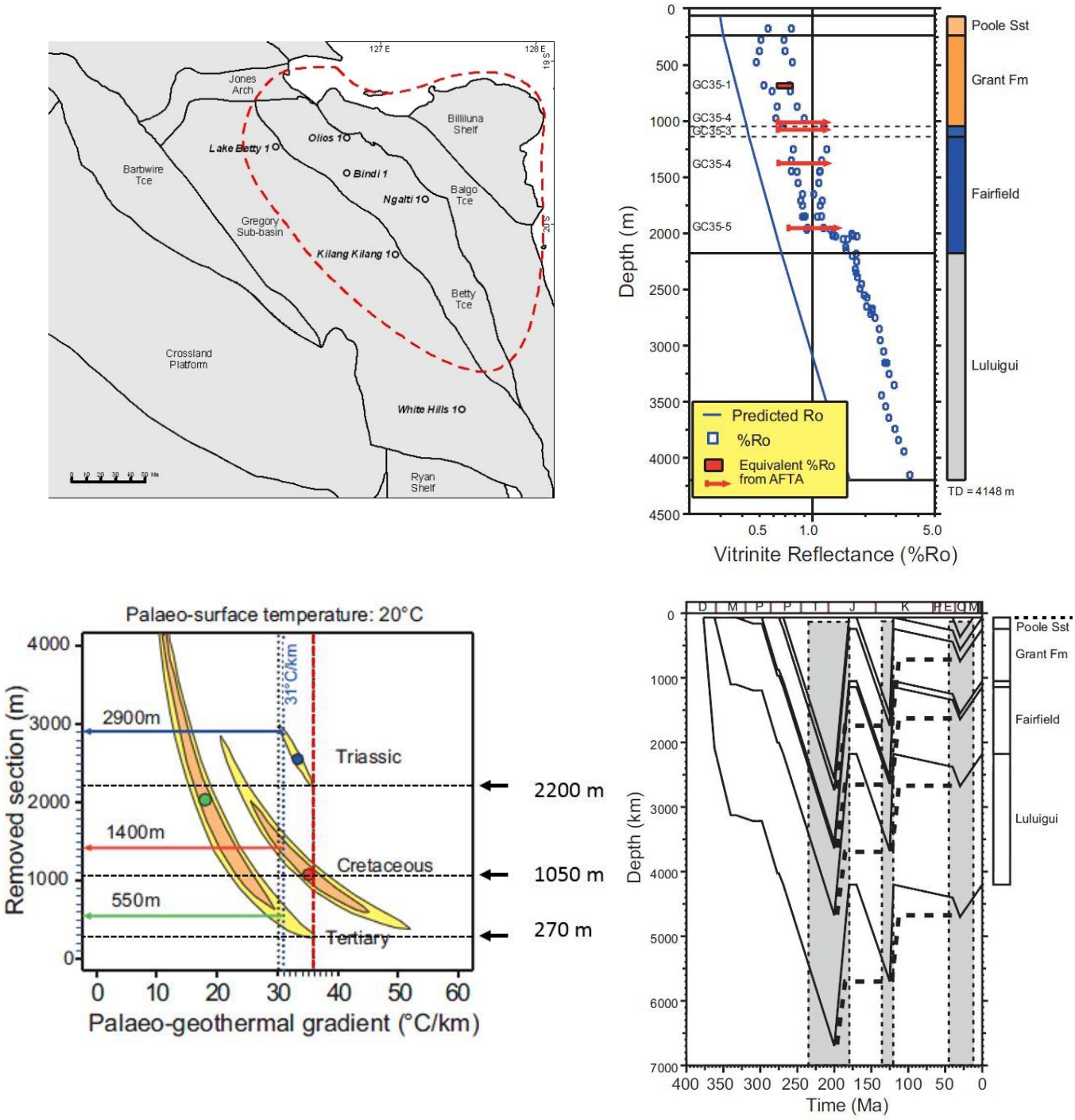

Figure 8.5. (Top left) Location of 1D models in bold, study area in red; White Hills 1 located south of the project area near the Ryan Shelf. (Top right) measured and predicted VR for White Hills 1; measured and predicted data trends are similar therefore qualifying heat flow at max. paleo-temp. is similar to present day. (Bottom left) Total section removed from top of Poole Sandstone at White Hills 1 at 95% confidence, numbers to right show modified depths for this project. (Bottom right) Burial history model for White Hills 1 after AFTA. (All figures except top right in Duddy et. al., 2013).

Paleo thickness

Paleo-thickness refers to the thickness of each formation within a 1D model, and was simply determined by formation tops at each well location. Well tops were loaded into PetroMod, along with starting and ending ages for deposition, taken from palynology where possible (Chapter 4). Generally, good age control is available for all formation boundaries. PetroMod automatically populates base and thickness values from well tops and the elevation datum that is assigned to a well location. Formation tops are tabulated in Appendix E.

8.4.3 *Boundary Conditions*

Sediment-water interface temperatures

Sediment-water interface temperature (SWIT) is the upper boundary in heat flow calculations (Hantschel and Kauerauf, 2009). SWIT is calculated using estimates of average paleo-surface temperatures with water depth corrections. Average surface temperatures are dependent on latitude (Wygrala, 1989; and Beardsmore and Cull, 2001).

PetroMod provides a simple utility to automatically estimate SWIT. By entering the present day latitude of the Canning Basin (18°S) and selecting 'southern Australia' as the basin continental association, PetroMod derives an estimate of SWIT over geologic time (Figure 8.6).

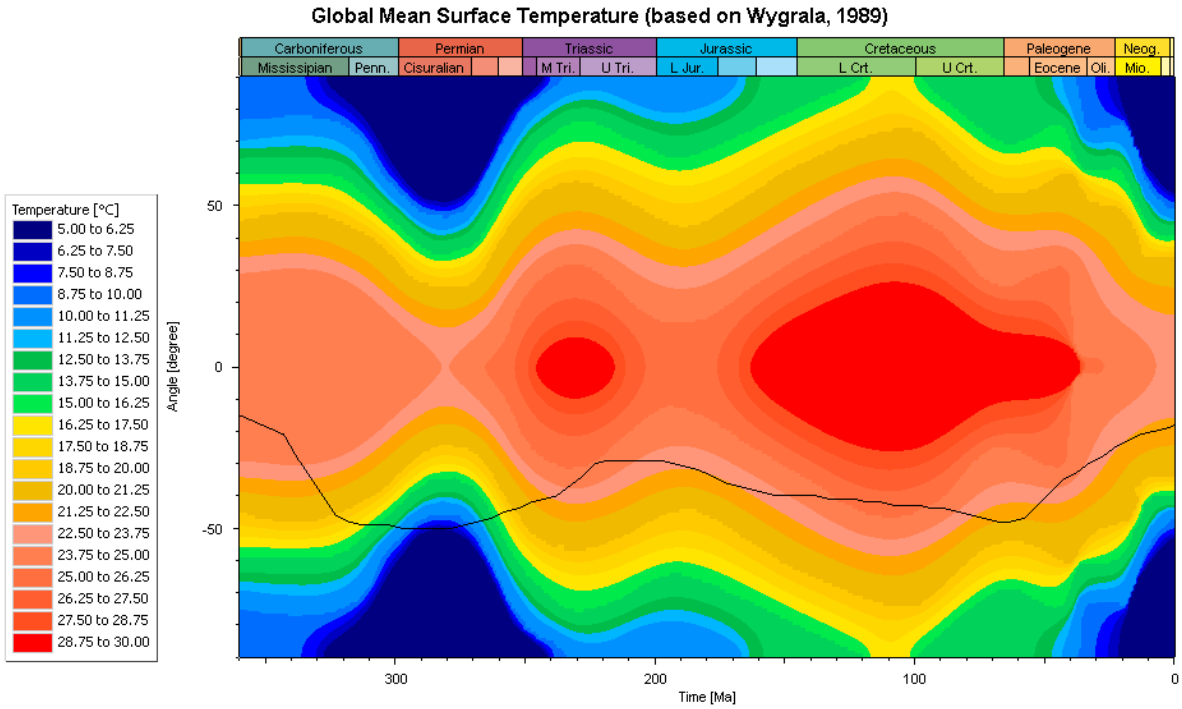

Figure 8.6. Mean surface temperatures used to configure PetroMod Surface-water-interface-temperatures. Black line indicates average temperature at 18° latitude (modified after PetroMod, 2014)

8.4.4 *Facies – 1D and 2D models*

Hantschel and Kauerauf, (2009) explain that in basin modelling terms, 'facies' are sedimentary groups with common properties, separated into the 'lithology group' and the 'organic facies group'.

Lithologies are characterised by thermal conductivities, heat flow capacity, radiogenic heat flow production, permeability, compressibility and capillary entry pressures (Hantschel and Kauerauf, 2009).

Organic facies are characterised by all kinetic parameters involved in the generation and cracking of petroleum; including Arrhenius-type activation energy and frequency data from primary and secondary petroleum cracking, total organic carbon (TOC) and hydrogen index (HI) numbers, adsorption parameters, densities, viscosities, and critical fluid parameters (temperatures, pressures and specific volumes) (Hantschel and Kauerauf, 2009).

PetroMod provides a relatively simple but comprehensive method for defining facies parameters for use in this study – the Lithology Editor. The Lithology editor is preloaded with a range of pre-defined lithologies and accompanying lithology group parameters.

Facies definition and Rock composition

In this study, facies were determined using cuttings descriptions and formational summaries from WCRs. The lithologies were compiled into a representative selection for each formation within the project area. The representative facies were then created in the Lithology Editor by 'mixing' (for example; sandstone, siltstone, claystone, shale, carbonate/limestone) from the predefined library within PetroMod. Table 8.4 shows the facies definition per formation.

Formation	Component %					
	Sandstone	Siltstone	Shale	Carbonate / Limestone	Conglomerate	Coal
Blina Shale		5	95			
Millyit Sandstone	90	5	5			
Liveringa Group	40	30	25			5
Noonkanbah Formation	10	30	60			
Poole Sandstone	85	5	10			
Grant Group	60	10	30			
Anderson Formation	70	15	15			
Laurel Formation	15	20	30	35		
Luluigui Formation	30	30	35	5		
Knobby Sandstone	80	10	10			
Virgin Hills Formation	15	20	50	15		
Gogo Formation	15	20	50	15		
Poulton Formation	100					
Bungle Gap Limestone	33	33	34			
Devonian Conglomerate	25		10		65	
Ordovician	80	10		10		

Table 8.4. Summary of lithology components for stratigraphic formations in the project area.

Predefined PetroMod constraints for the 'lithology group' used in this study shown in Table 8.5.

Lithology	Surface porosity (Φ; %)	Grain density (kg/m^3)	Thermal conductivity at 20°C	Radiogenic heat production at 40% porosity ($\mu W/m^3$)	Porosity-depth coefficient (Athy's factor k; km^{-1})
Sandstone	41	2700	3.95	0.42	0.31
Siltstone	55	2710	2.01	0.57	0.51
Shale	70	2610	1.45	1.38	0.85
Carbonate/Limestone	51	2680	2	0.84	0.52
Conglomerate	30	2700	2.3	0.51	0.3
Coal	74	1600	1	0.28	0.42

Table 8.5. Petrophysical properties for common lithologies in the PetroMod lithology editor.

TOC and HI (Geochemistry) – 1D and 2D models

PetroMod requires an average of measured TOC and HI for source rock intervals in order to simulate hydrocarbon generation and expulsion quantities. TOC and HI were derived from the same geochemical database compiled within Chapter 7 of this study, which was ultimately collated from WCRs. Refer to Chapter 7 and Appendix C for further detail on source rock parameters.

8.4.5 *Basal Heat Flow – 1D and 2D Models*

Basal heat flow refers to the amount of heat that enters a sedimentary basin sequence, and is a product of the mechanical and radiogenic state of the underlying lithosphere, asthenosphere and also the intra-basinal sequence (Hantschel and Kauerauf, 2009; and Waples 2001). Hantschel and Kauerauf, (2009) note that the McKenzie heat flow model (McKenzie, 1978) is frequently used in basin analysis, however recent work by Waples (2001) shows that the lithospheric stretching model proposed by McKenzie is not sufficient, as radiogenic sources can account for more than half of the heat flow at the top of basement. A common assumption; suggesting that all heat passing through the lithosphere originates from below the lithosphere, is incorrect (Waples, 2001).

Due to the difficulty of constraining paleo heat flow, this study adopted the admittedly simplistic assumption that heat flow has remained constant over geological time, and is equivalent to the present-day heat flow. The use of present day heat flow is supported by

Duddy et. al., (2003), where they demonstrated that the heat flow trend at the time of maximum paleo-temperatures is similar to trends of present day heat flow (Figure 8.5).

This method introduces an assumption that heat flow does not vary from the Ordovician to present day, which is undoubtedly incorrect. However by using the approach of Waples (2001), heat flow measurements due to radiogenic sources will total a higher quantity than that of a McKenzie model; which facilitates higher levels of maturity. Even though using constant heat flow removes variability to heat flow over geological time, a higher overall heat flow should more accurately model maturity at a time when paleo-temperatures were at a maximum.

Goutorbe et al., (2008) determined present day heat flow from wells within and around the study area, shown in Table 8.6. 1D and 2D models were assigned heat flow from the nearest present day measurement.

Well	Present Day Heat flow (mW/m^2)
Bindi 1	58
Kilang Kilang 1	56
Ngalti 1	60
Olios 1	62
White Hills 1	60

Table 8.6. Present-day heat flow for wells in the study area (Goutorbe et al., 2008).

8.4.6 *Calibration – Geothermal Gradients*

To ensure that temperature gradients in 1D and 2D models are realistic, they require calibration with measured data points. Models can be calibrated using various temperature or maturity controls including VR, AFTA and temperatures measured during the drilling of a well (Hantschel and Kauerauf, 2009).

Well	Total Depth (mRT)	BHT (°C)
Mean Surface Temp.	-	32.0
Atrax 1	786	53.8
Selenops 1	1262	59.3
Ngalti 1	2695	101.1
Olios 1	1965	88.3
Lake Betty 1	3146	155.0

Table 8.7. Mean surface temperature of project area (BOM, 2015) and bottom-hole static temperatures (corrected for drilling circulation times) for wells in the project area.

Simulated temperature gradient overlays were extracted in PetroMod from present day temperature inputs (calculated using the boundary condition inputs detailed above) and compared to Horner-plot-corrected bottom-hole (static) temperatures (BHT). Olios 1, Ngalti 1 Atrax 1, Selenops 1 and Lake Betty 1 have BHT data. Figure 8.7 provides the modelling results. Olios 1 and Ngalti 1 have good agreement between the modelled temperature profile and BHTs (85°C compared to 88°C measured at Olios 1, and almost precisely 101°C at Ngalti 1). Lake Betty 1 shows a temperature gradient too low for the measured BHT, although the Lake Betty 1 WCR notes that the 'circulation times' and 'observed time since circulation finished' is not confidently known, which may degrade the quality of the Horner correction for the well). Deviations in the calculated temperature curve are at formation boundaries are caused by slight variations to facies thermal properties (including thermal conductivity).

Vitrinite Reflectance (VR) maturity profiles were constructed in PetroMod using the Sweeny and Burnham (1990) Easy%Ro method. The maturation curves were plotted against measured VR obtained from well locations. All wells except Lake Betty 1 contained VR and Ngalti 1 has limited populations of VR, so these wells were compared to Vitrinite Reflectance Equivalent (VRe) calculated from Tmax, to aid in calibration in the absence of VR measurements. The results are shown in Figure 8.8.

Vitrinite data for post-Carboniferous stratigraphy within the project area is plentiful, where most formations in the northeast Canning Basin have some form of terrestrial influence. There is good agreement between the maturation curve and VR data at the well locations. Kilang Kilang 1 and Olios 1 demonstrate the best fits between simulated and measured maturity from VR. The maturity profile deviates from the VR population at Bindi 1, though

the VR data is insufficiently deep to build an optimal well maturation profile, relative to other wells. The VR population below 900 mRT at Bindi 1 is lower in reflectance than then modelled maturity. Cook, in Lehman and Haines (1985) report pyrite and iron oxides were present in the Bindi 1 VR samples along with commonly identified Inertinite, which indicates an oxidizing environment. This may be introducing a low level of suppression in the VR population at Bindi 1 (Carr, 2000). At Lake Betty 1, where no VR is available, the modelled maturity is in good agreement with VRe from Tmax.

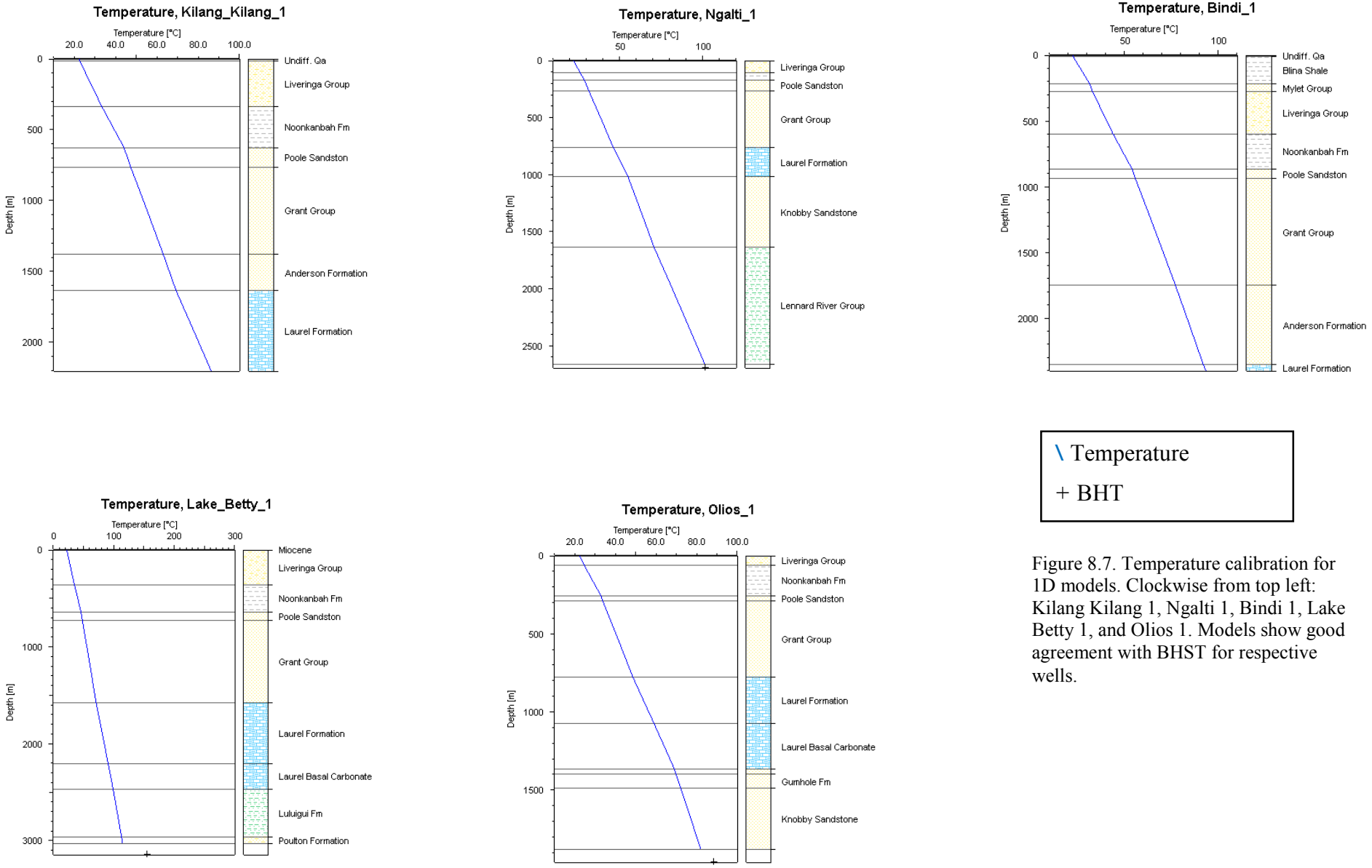

Figure 8.7. Temperature calibration for 1D models. Clockwise from top left: Kilang Kilang 1, Ngalti 1, Bindi 1, Lake Betty 1, and Olios 1. Models show good agreement with BHST for respective wells.

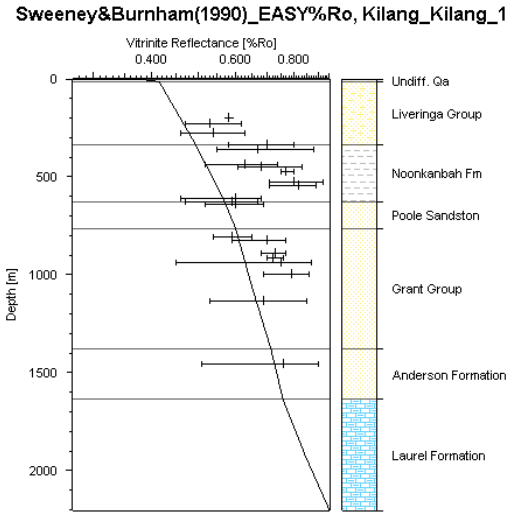

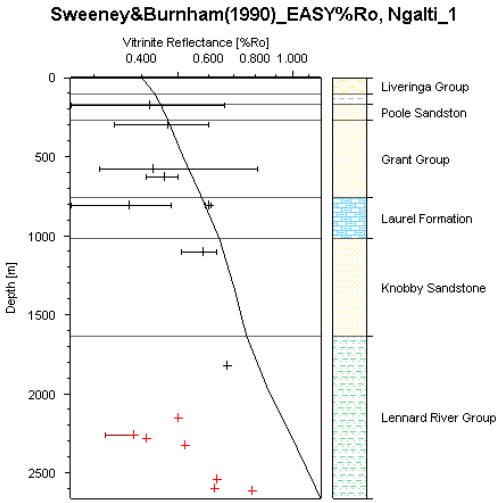

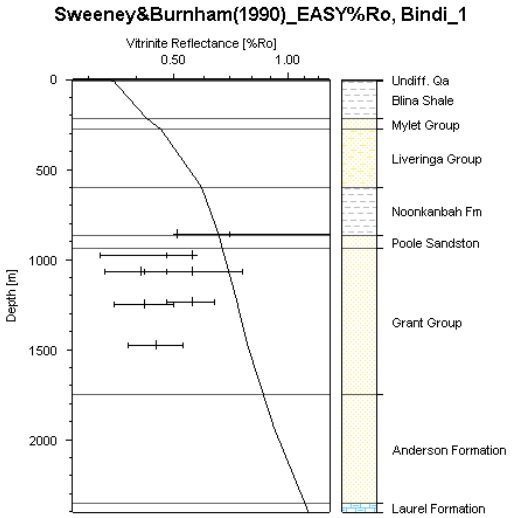

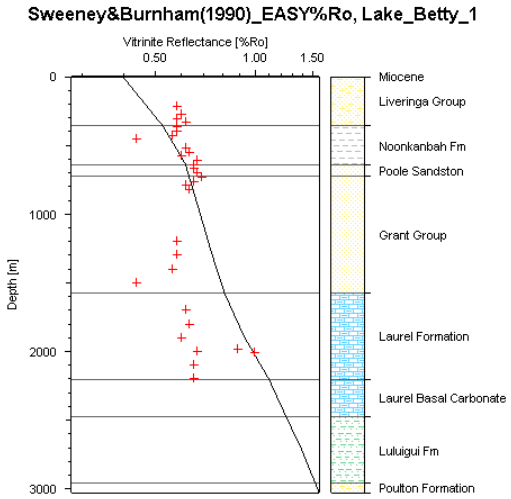

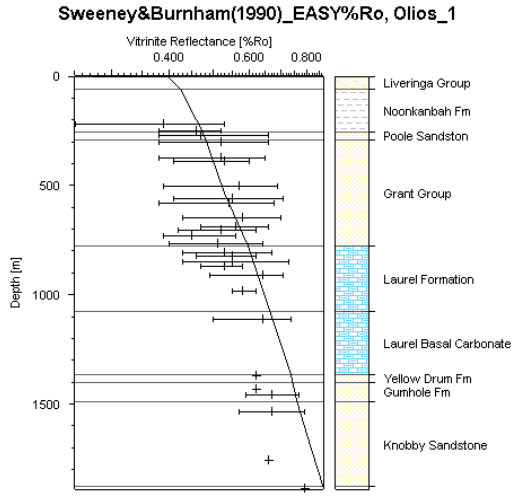

\ Predicted Vitrinite

\+ VR

\+ VRe from Tmax

Figure 8.8. Vitrinite reflectance calibration for 1D models. Clockwise from top left: Kilang Kilang 1, Ngalti 1, Bindi 1, Lake Betty 1, and Olios 1. Models show generally good agreement with VR and VRe measurements

8.5 Data Inputs and Parameters – 2D Models

2D basin models were constructed in this study to understand the evolution of petroleum systems in the northeast Canning Basin. The exercise was undertaken to;

1. Determine whether source rocks within the project area reach optimal thermal maturity to generate and expel hydrocarbon products, and to visualise this development via a 2D cross section through the Billiluna Sub-basin, Balgo and Betty Terraces into the Gregory Sub-basin;
2. Determine whether hydrocarbons migrate from kitchen areas into reservoirs and trapping geometries in shelfal positions;
3. Determine whether accumulations may exist, preserved through geologic time to present day; and
4. Facilitate the culmination of all of the work in the previous chapters of this study.

2D petroleum systems modelling has never before been undertaken within the project area, so the 2D models demonstrate an original contribution to the geoscientific discipline with respect to petroleum systems analysis in the northeast Canning Basin.

8.5.1 *Present-day Model*

PetroMod functions by taking a present day geological geometry along with all geological parameters, and strips the model to initial deposition. PetroMod then forward-simulates the geometries and parameters in a finite-element model (FEM), so that the model honors the present day configuration of the basin.

The present day model was derived from depth converted seismic interpretation, geochemistry and porosity data, heat flow parameters, and age assignments for deposition, exhumation and structural episodes.

Depth conversion

Seismic was converted to the depth domain using the IHS Kingdom Dynamic Depth Converter utility (Chapter 5.5.1).

Screen captures were obtained for the depth converted 2D seismic lines selected for 2D modelling (in Table 8.2 and Figure 8.3), and imported into PetroMod. The seismic images were then digitized in PetroMod to carry over the present day 2D geological model.

Horizons and Fault Surfaces

Horizons and faults were digitized from the depth converted seismic section for each 2D model. The horizons and faults were then gridded to mesh the pre-grid nodes (a node is created for each digitized mouse-click along a horizon or fault surface) to the Finite Elements in the model. The FEM was given a maximum cell sublayer thickness of 100 metres to give the present day geometry a realistic appearance. Increasing sublayer thicknesses did lengthen the simulation time, however it was deemed reasonable because a meaningful model in appearance is more intuitive than one that appears cubic and excessively simple.

Age assignment

As per 1D modelling, age assignment for 2D modelling involves instructing PetroMod on the attributes of a formation to include within a model. Age assignment relates the present day surfaces digitized from 2D seismic, with their geological age of deposition and erosion (Hantschel and Kauerauf, 2009). Age assignment for 2D modelling is slightly more complex than 1D, and requires parameters explained in Table 8.8 (model RB81-7 is used as an example in Figure 8.9).

Timing of Faulting

The timing of faulting in 2D models is important to define because it allows PetroMod the ability to correctly forward-model the geological history from initial deposition to final hiatus. Fault timing characterises the structural history in sedimentary basins. Correctly timed faults in 2D models can impact migration conduits and also can determine how trapping geometries are filled in accumulation analysis. The timing of faulting is estimated based on;

- Published literature concerning the tectonic history of the Canning Basin (Brown et al., 1984)

- Observations of fault timing drawn from seismic interpretation.

For example, The Stansmore Fault (a large listric fault that divides the Gregory Sub-basin from the Betty Terrace) was a major control on sedimentation at multiple stages during the basin's tectonic history, and is observed on seismic to be active to displace Pre-Cambrian (Basement) Ordovician, Siluro-Devonian, and probably at least Carboniferous stratigraphy, therefore is assigned ages 570 Ma until 330 Ma.

Header	Age (Ma)	Horizon	Pre-grid horizon	Gridded horizon	Erosion map	Layer	Event type	Facies map	Number of sublayers	Max time-step (Ma)
Explanation	*Age of horizon*	*Horizon name*	*Pre-gridded horizon digitized from 2D seismic (assigned upon gridding)*	*Gridded horizon. Represents the model geometry for a layer (assigned upon gridding)*	*Contains the thickness of the eroded part of a model layer (assigned upon defining erosion)*	*Layer name*	*User selected - deposition, erosion or hiatus. Instructs PetroMod on layer type and processes*	*2D map of facies definition properties (assigned during gridding)*	*Division of layer into sub layers, each can have different properties*	*If deposition exceeds Max time-step, Simulation will perform extra steps in modelling*

	Age [Ma]	Horizon	-	Pre-grid Horizon	Gridded Horizon	Erosion Map	Layer	-	Event Type	Facies Map	No. of Sublayers	Max. Time Step [Ma]
1	0.00	Hiatus_124_Top					Hiatus_124		Hiatus			10.00
2	180.00	Erosion_206_Top					Erosion_206		Erosion			10.00
3	200.00	Top_Triassic		Top_Triassic	Top_Triassic_Map	ErosionMapID22_200	Top_Triassic		Deposition	Map_Layer_121_Facies	10	10.00
4	253.00	Top_Noonkanbah		Top_Noonkanbah	Top_Noonkanbah_Map		Top_Noonkanbah		Deposition	Map_Layer_84_Facies	8	10.00
5	266.00	Top_Poole		Top_Poole	Top_Poole_Map		Top_Poole		Deposition	Map_Layer_85_Facies	3	10.00
6	271.00	Top_Grant		Top_Grant	Top_Grant_Map		Top_Grant		Deposition	Map_Layer_86_Facies	14	10.00
7	320.00	Erosion_98_Top				ErosionMapID11_320	Erosion_98_Top		Erosion			10.00
8	330.00	Top_Meda_Trans_Unc		Top_Meda_Trans_Unc	Top_Meda_Trans_Unc_Map	ErosionMapID10_330	Top_Meda_Trans_Unc		Deposition	Map_Layer_87_Facies	6	10.00
9	337.00	Top_Fairfield		Top_Fairfield	Top_Fairfield_Map	ErosionMapID9_337	Top_Fairfield		Deposition	Map_Layer_88_Facies	30	10.00
10	344.00	Top_Devonian		Top_Devonian	Top_Devonian_Map	ErosionMapID8_344	Top_Devonian		Deposition	Map_Layer_89_Facies	85	10.00
11	436.00	Top_Ordovician		Top_Ordovician	Top_Ordovician_Map		Top_Ordovician		Deposition	Map_Layer_90_Facies	54	10.00
12	570.00	Top_Basement		Top_Basement	Top_Basement_Map							

Table 8.8. (Top) Explanation of header terms used in PetroMod age assignment.

Figure 8.9. (Bottom) PetroMod age assignment input parameters used in 2D model RB81-7.

8.5.2 *Paleo Geometry*

Paleo-geometries for 2D models are largely similar to that of the 1D models, however a number of extra parameters are defined to characterise the older geology (1D models intersected Devonian aged rocks at the oldest).

Water depths

Paleo-water depth (PWD) estimates for 2D models were set identically to 1D models for Carboniferous and younger stratigraphy (Chapter 8.4.2). Estimates were derived from paleogeographic reconstructions (both from Chapter 4 and also various publications; Gorter, 1987; Brakel et al., 1990; Cook and Totterdell, 1990; and Smith et al., 2013), estimates published in WCRs, and initial rifting within the Gregory Sub-basin.

Extra parameters for 2D modelling are a 150 metre water depth to represent the marine Ordovician Larapintine Seaway (Cook and Totterdell, 1990). Paleo water depths are then estimated to shallow through the Silurian (40 metres) to the Devonian (25 metres), to accommodate carbonate development. Paleo-water depths are illustrated in Figure 8.10, and key PWDs are summarised in Table 8.3.

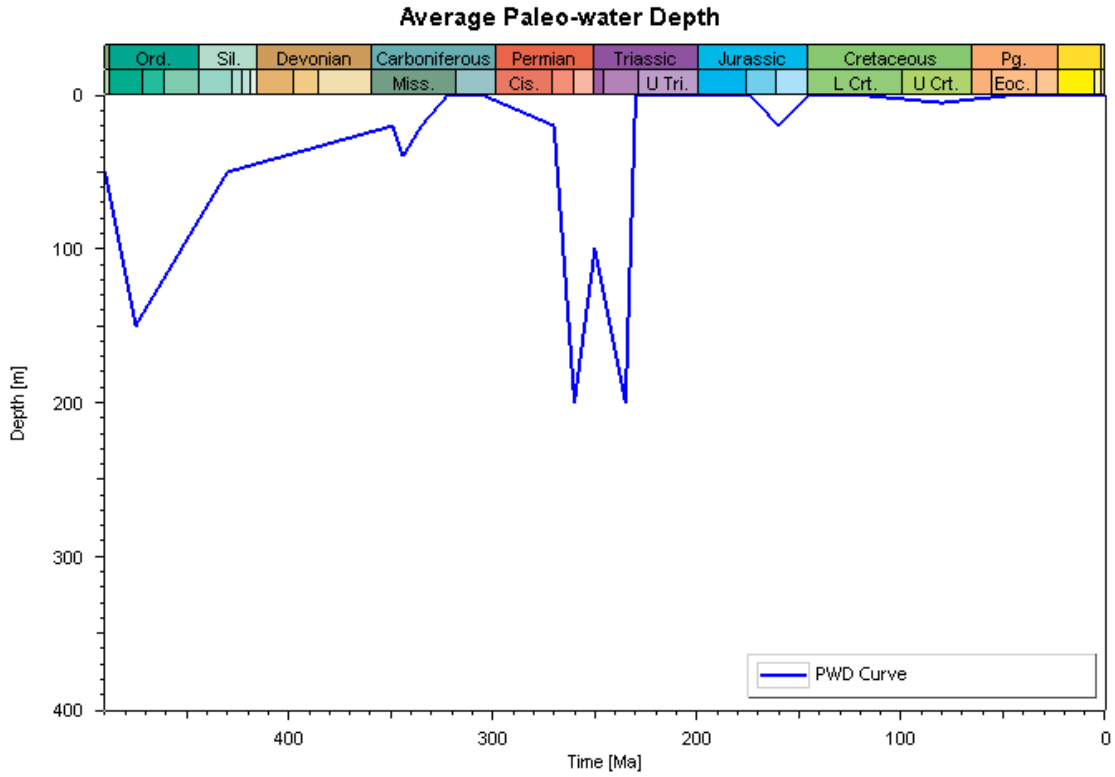

Figure 8.10. Average paleo-water depth for 2D models.

8.5.3 *Boundary Conditions*

Boundary conditions were defined essentially as per 1D modelling, with an extension to the parameters to allow for Carboniferous and older stratigraphy.

Surface-water interface temperatures

Sediment-water-interface temperature (SWIT) parameters were set identically as per 1D modelling, however the estimate of Beardsmore and Cull (2001) is only available in PetroMod until the Carboniferous. Wygrala (1989) estimates decreasing 1.5°C per 100 metres of water (up to deep water – 400 metres, where cold water artic conditions are proposed). Wygrala's calculation is applied to the PWD trend for Devonian and older stratigraphy (Figure 8.11).

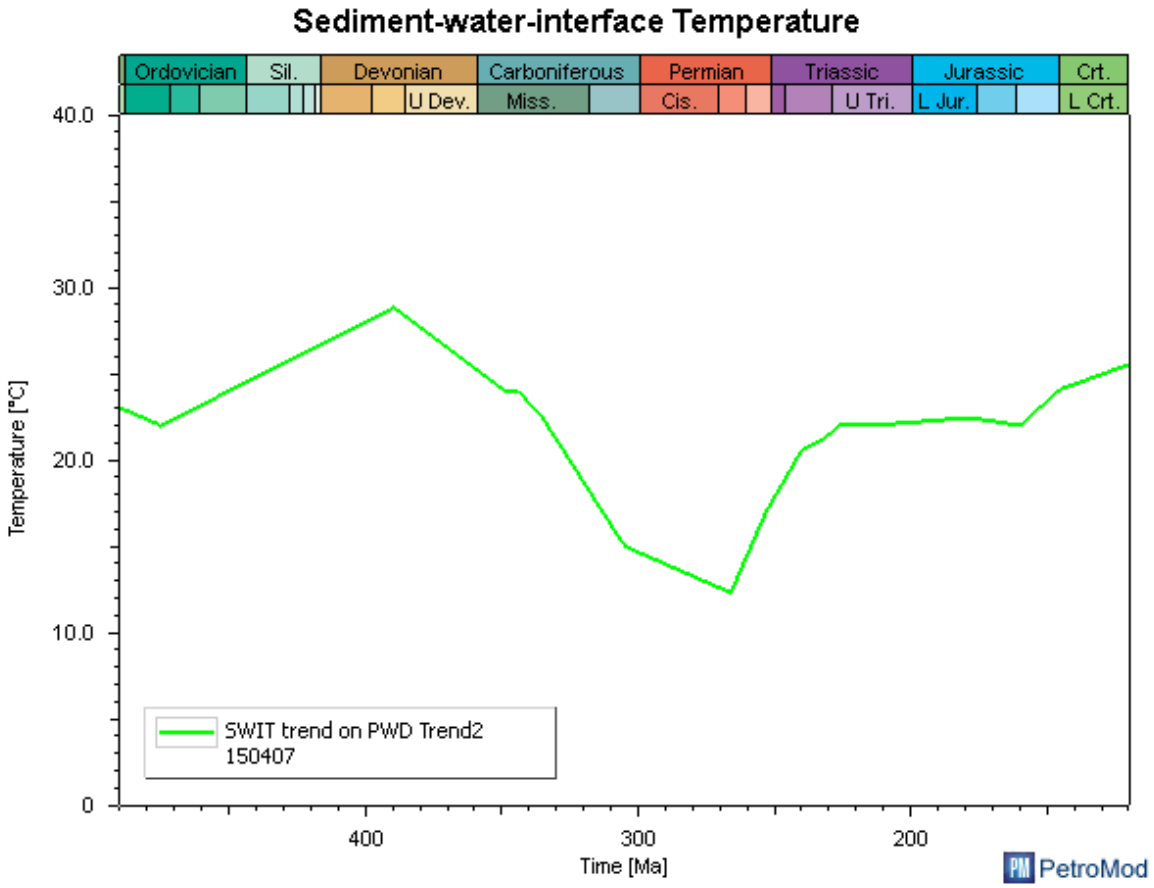

Figure 8.11. Sediment-water-interface-temperature curve for 2D models.

8.5.4 *Facies*

Facies definition, TOC and HI (Geochemistry) and Rock Composition parameters are set identical to 1D models (refer to Chapter 8.4.4).

It would be prudent to consider facies changes across 2D models, especially since the models are generally quite large (RB81-7 is 121 km long), and cover multiple tectonic provinces. Paleogeographic reconstructions (Chapter 4), demonstrate that facies change is likely within the study area. None of the models, however, intersect more than one well location to accurately estimate facies variability between well locations. In this study, variations in facies variability were 'mixed' within a customized Rock Composition library (a part of the PetroMod Lithology editor); a catalog created for this study (Table 8.4 and 8.5). Averages are representative of the formations across the study area. This implies that formation lithological composition is averaged across every model.

8.5.5 *Calibration*

The 1D models were extracted from 2D models at existing well locations (Kilang Kilang 1, Ngalti 1 and Lake Betty 1) to test the viability of the heat flow parameters to actual thermal maturity measurements (Figure 8.12). The 1D effective porosity profiles with core porosity data was also compared with 2D models for reassurance of overburden quantities that impact compaction (Figure 8.13.

Thermal maturity

The thermal maturity calibration results were variable at 1D pseudo well locations. In all cases the maturation profiles (%Ro per depth unit) are similar to existing 1D models. For example; 2D model RB82-28 closely matched the Vitrinite Reflectance measurements at Ngalti 1, indicating the RB82-28 model correctly simulates maturation at the Ngalti 1 well location.

RB81-7 shows a higher maturation curve at both calibration locations (Ngalti 1 and Kilang Kilang 1). RB81-7 at the top of the Laurel Formation in Kilang Kilang 1 shows 1.16% Ro; 0.4% Ro higher VR than the 1D well maturity profile. The RB81-7 model at the top of the Laurel Formation in Ngalti 1 shows 0.71% Ro; 0.14% Ro higher VR than the 1D well maturity profile. Despite the 1D extractions not exactly replicating the 1D maturation curve at Kilang Kilang 1 and Ngalti 1, RB81-7 extractions can still be correlated with VR measurements giving some validity to the simulation.

Arbitrary line 82GN-03 shows lower maturation than the Lake Betty 1 maturity profile. Note that Lake Betty 1 contains no VR measurements so VRe is calculated from Tmax. 82GN-03 at the top of the Poole Sandstone in Lake Betty 1 shows 0.43% Ro; 0.19% Ro lower VR than the 1D well maturity profile. Again, the 82GN-03 arbitrary line still lies within the broad VRe well profile. The RB81-10 2D model has a good match with Ngalti 1 VR measurements (Figure 8.12).

Effective porosity

2D modelling was also compared to core porosity measurements to gauge the effectiveness of the overburden digitized into the model to replace eroded material. There are no core porosity measurements available for Kilang Kilang 1.

RB81-7 and RB81-10 closely match effective porosity curves and intersect the Lennard River Group core data cluster in the Ngalti 1 well. This indicates that the overburden quantity digitized to replace Triassic and younger rocks reasonably compacts deeper stratigraphy to simulate present day effective porosity.

RB82-28 slightly over-compacts the effective porosity curve at Ngalti 1, though the modelled curve broadly fits the core porosity measurements in the Knobby Sandstone and Lennard River Group. This indicates that there is perhaps slightly too much overburden digitized into Triassic and younger rocks in RB82-28.

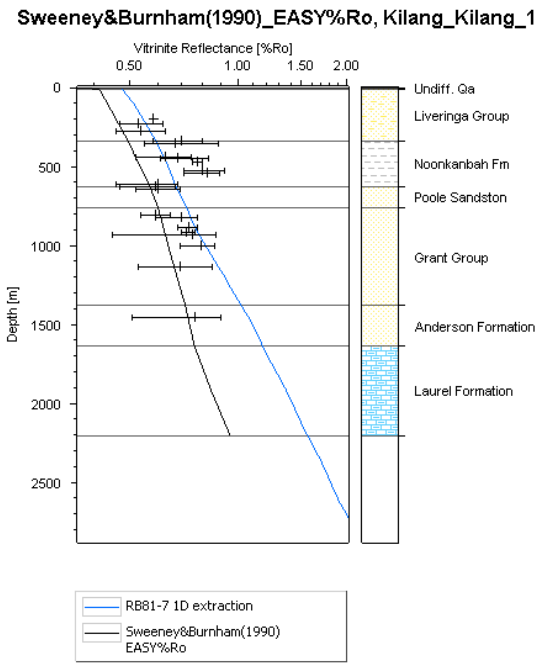

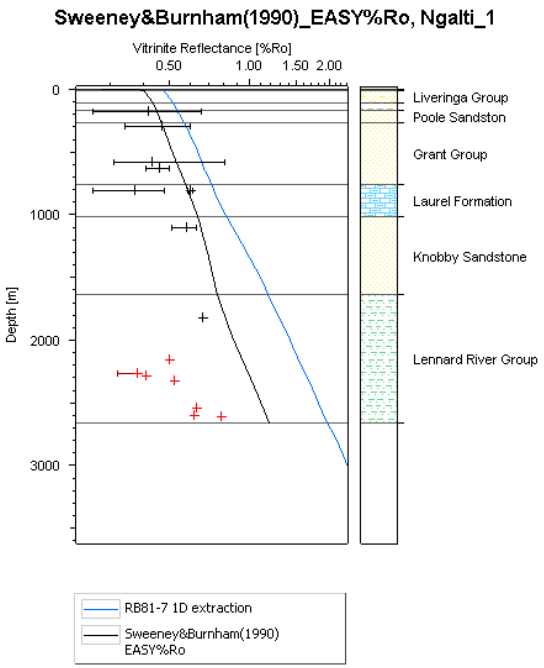

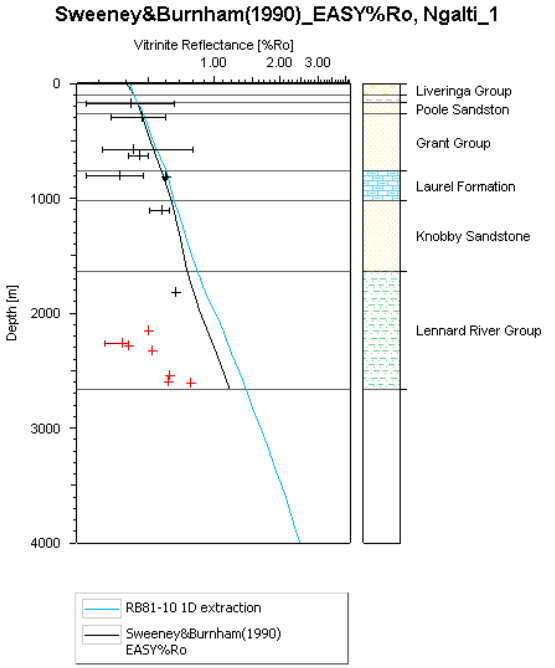

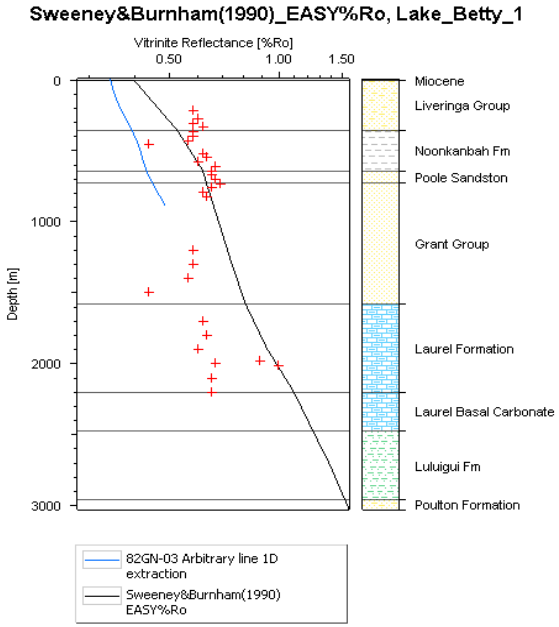

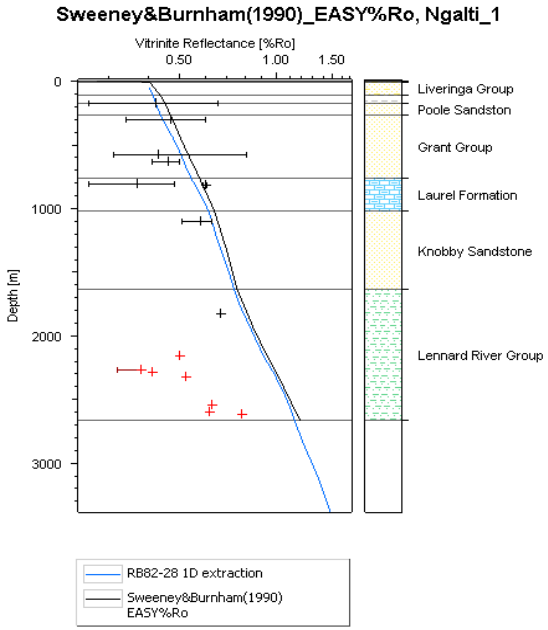

\ Predicted Vitrinite (well location)

\ Predicted Vitrinite (2D model)

\+ VR

\+ VRe from Tmax

Figure 8.12. VR calibration for 2D models. Original 1D model for respective well location in black, pseudo well extracted at projected location near 1D well in blue. 2D models show some variability in maturity profile though generally allowable within VR and VRe measurements.

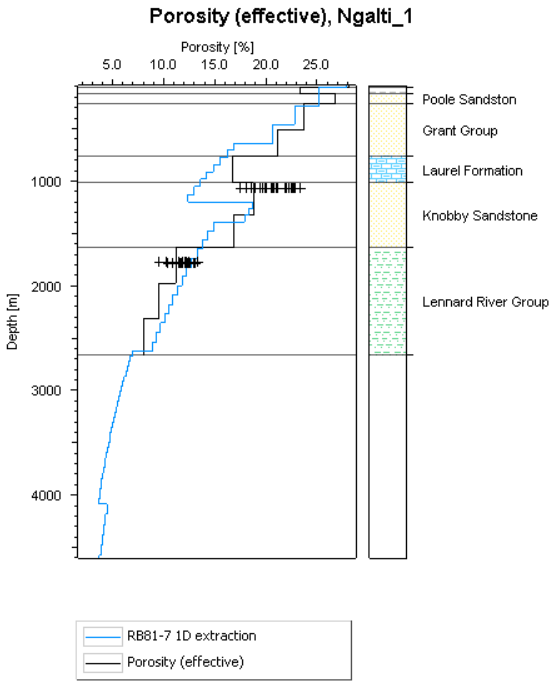

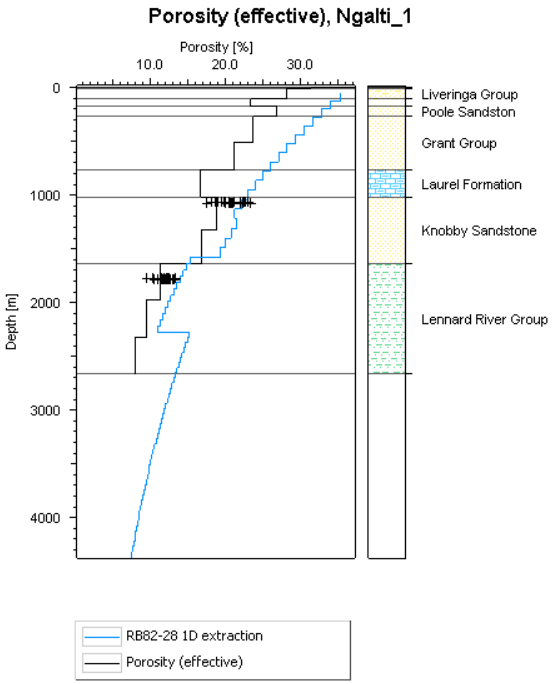

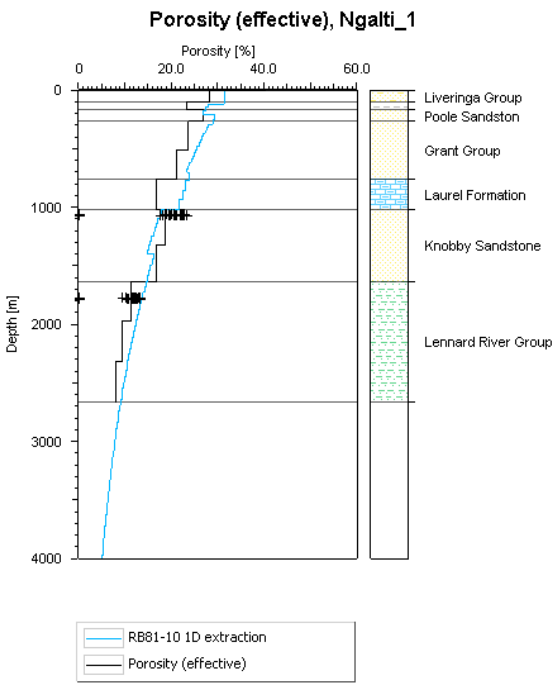

\ Predicted Effective Porosity (well location)

\ Predicted Effective Porosity (2D model)

\+ Core Porosity Measurement

Figure 8.13. Porosity calibration for 2D models against Ngalti 1 well (calibration restricted by porosity data availability). Predicted effective porosity for Ngalti 1 and respective 2D pseudo wells have good agreement with data measurements.

8.6 Results

Chapter 8.6 presents the results from 1D and 2D petroleum systems modelling within the northeast Canning Basin. Pseudo wells were extracted (Figure 8.14) to enable 1D investigations of 2D models across tectonic provinces within the study area. The results are presented in petroleum systems hierarchy; and discuss each formation in depositional sequence.

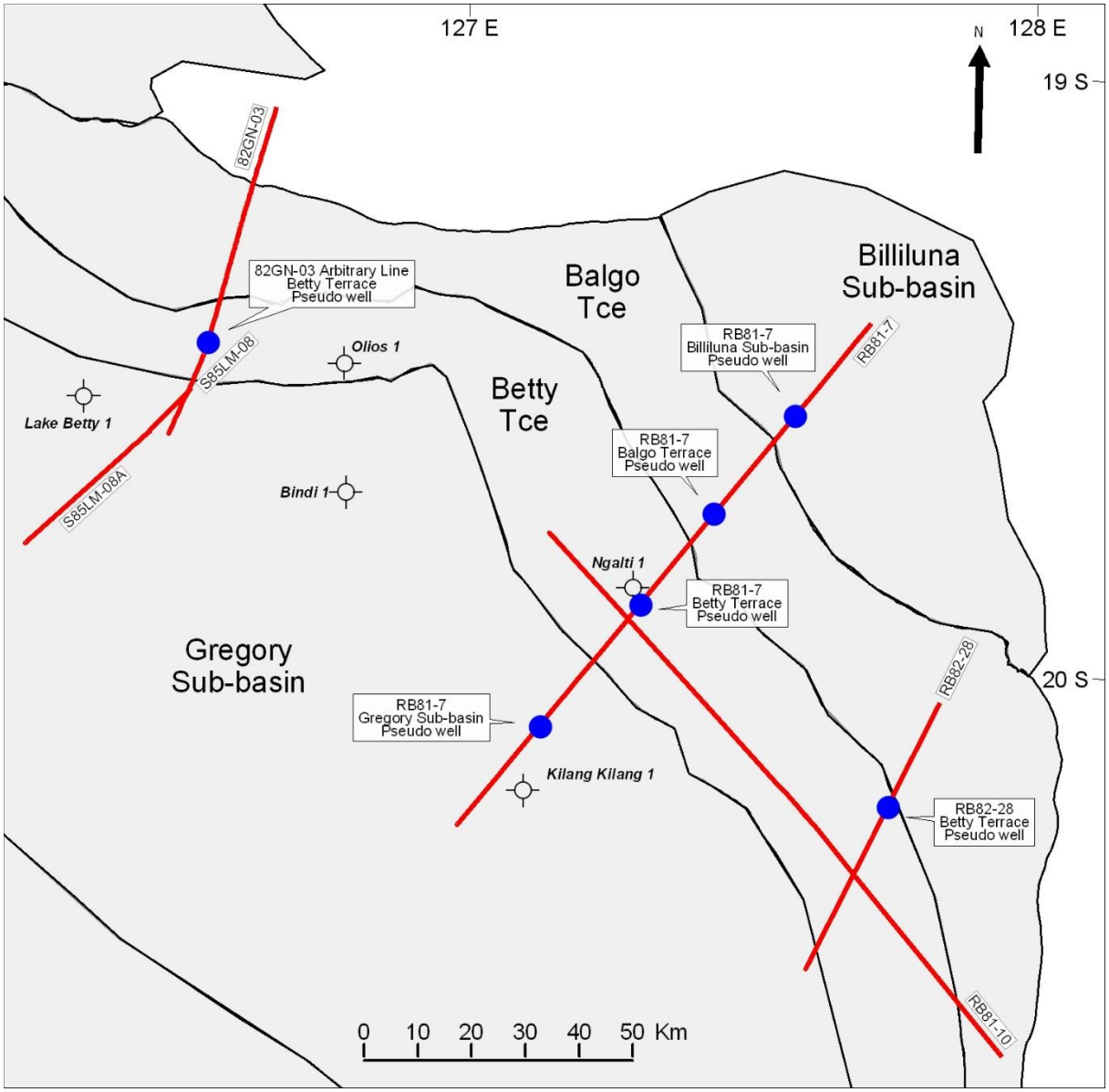

Figure 8.14. Location of 1D models, 2D models constructed on seismic lines (red), and 2D model pseudo well extractions (blue). Pseudo wells give good spatial spread throughout project area.

8.6.1 *Temperature*

Figures 8.15 and 8.16 demonstrate 1D well burial history results with temperature overlays for the modelled wells. It is clear that maximum paleo-temperatures occur in the Triassic as a result of deeper burial prior to uplift concluding in the Jurassic.

1D models (figures 8.15 and 8.16) demonstrate four periods of subsidence related heating:

1. Carboniferous: 338 – 309 Ma
2. Triassic: 225 – 191 Ma
3. Jurassic – Cretaceous: 160 – 126 Ma
4. Eocene – Miocene: 30 – 9 Ma

2D model RB81-7 demonstrates maximum paleo-temperatures in cross section through the study area (Figure 8.17). The base of the Gregory Sub-basin reached a maximum of 637°C during the Triassic. Results from RB81-7 indicate that the Balgo Terrace reached similar maximum temperatures to that of the Betty Terrace (280°C and 274°C respectively in Ordovician sediments) during the Triassic, and the Billiluna Sub-basin reaches only a slightly higher maximum paleo-temperature of 285°C.

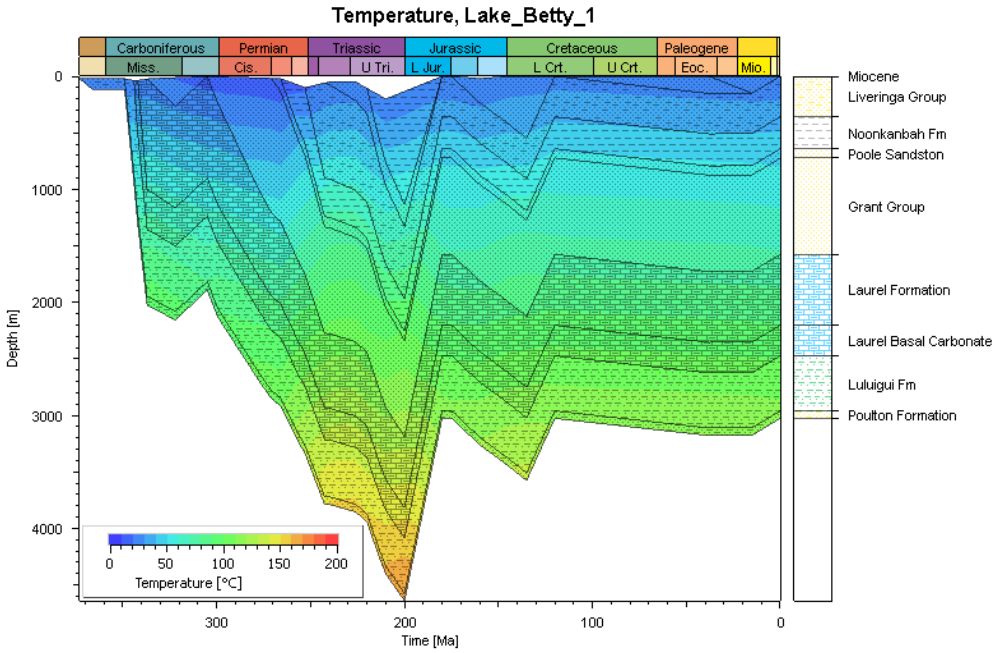

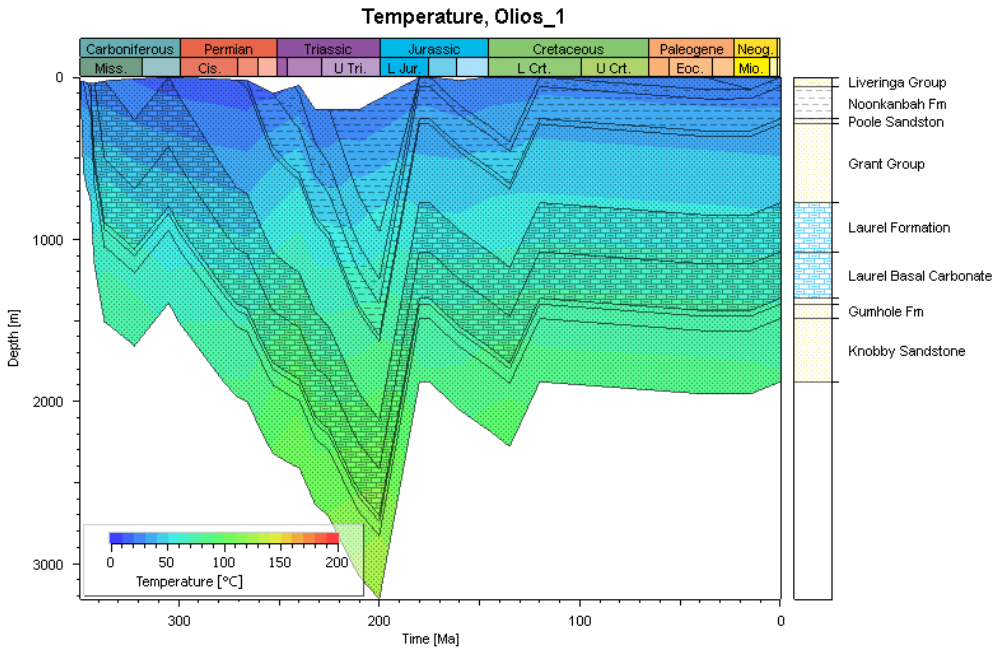

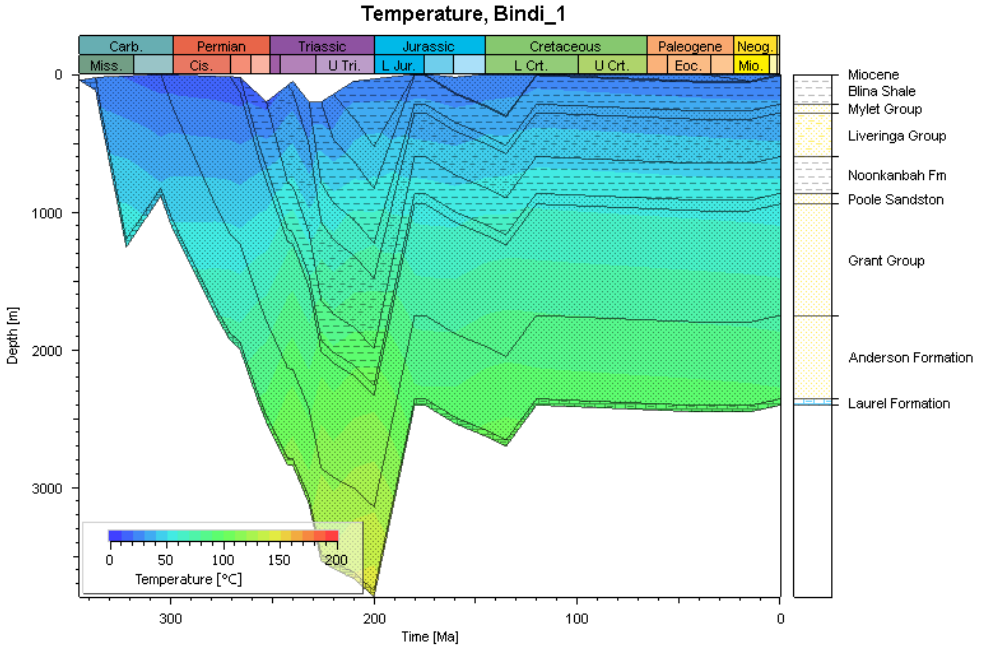

Figure 8.15. Well burial history results for Lake Betty 1 (top left), Olios 1 (top right) and Bindi 1 (bottom left) with temperature overlay for the respective well. Maximum paleo-temperatures occur in the Triassic as a result of deeper burial prior to uplift concluding in the Jurassic.

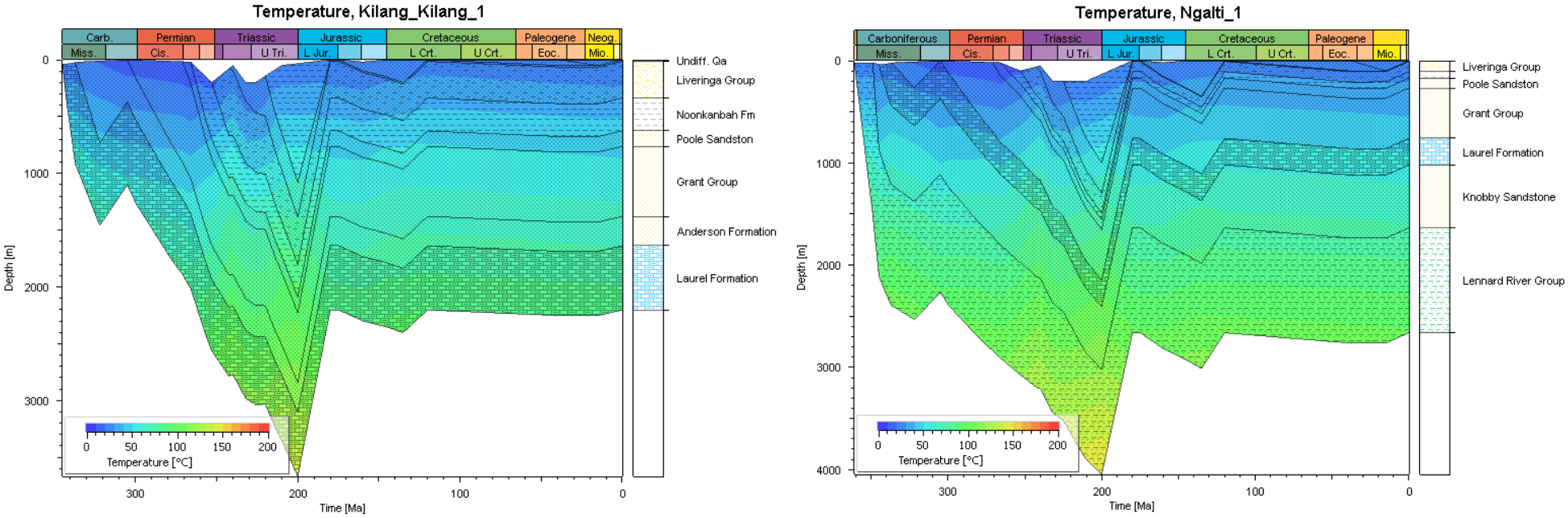

Figure 8.16. Well burial history results for Kilang Kilang 1 (left) and Ngalti 1 (right) with temperature overlays for the respective well. Maximum paleo-temperatures occur in the Triassic as a result of deeper burial prior to uplift concluding in the Jurassic.

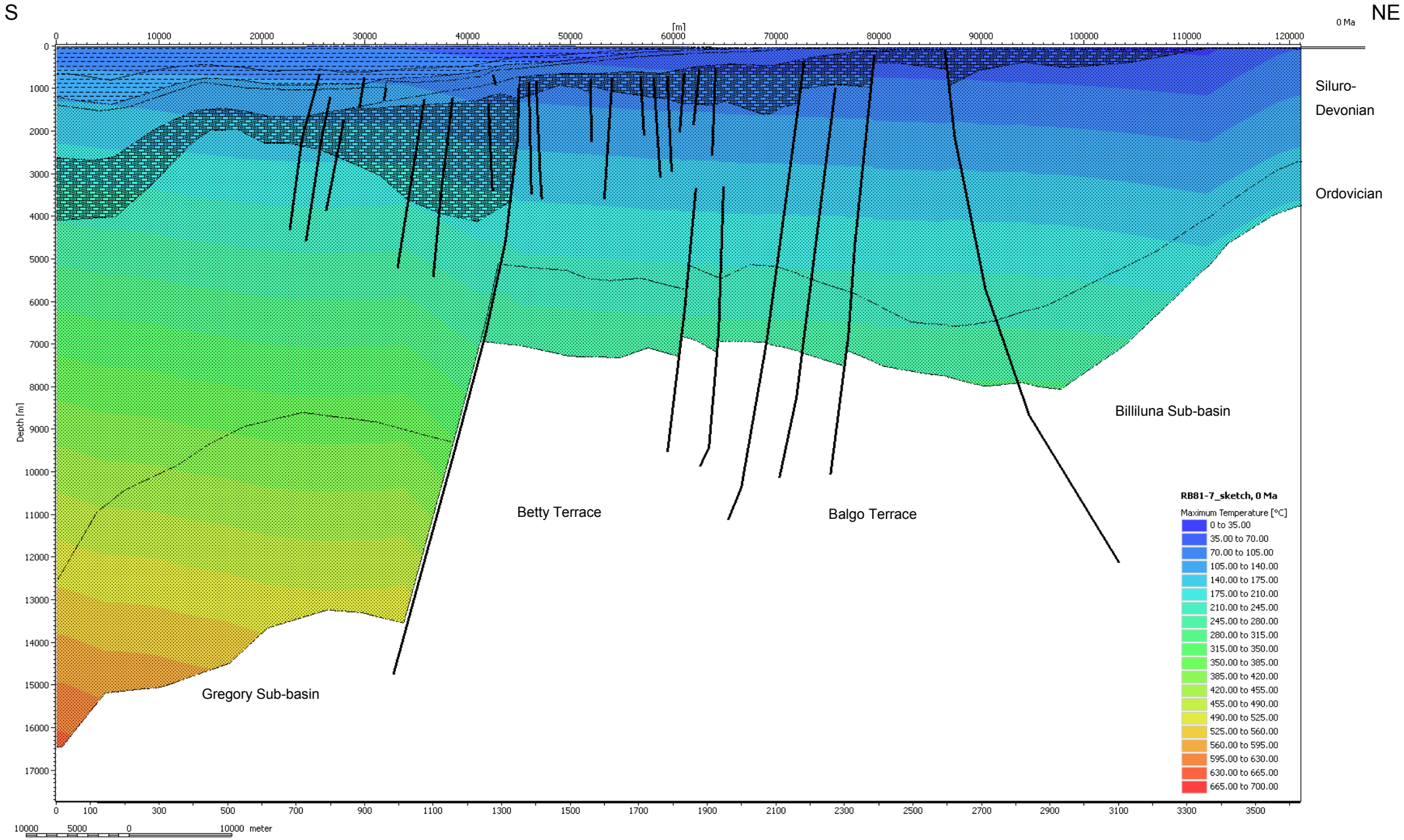

Figure 8.17. Present day RB81-7 model with pre-grid faults. RB81-7 demonstrates maximum temperature variations across the study area. Temperatures reach 637°C at the base of the Gregory Sub-basin.

8.6.2 *Thermal Maturity*

Figures 8.18 and Table 8.9 compare thermal maturity profiles for 1D wells within the Gregory Sub-basin and Betty Terrace. There is good agreement between individual well maturity profiles (%Ro per depth unit) within each province, suggesting that there are no variations to peak maturation within each respective tectonic region. Note that sediments within the Gregory Sub-basin reach higher levels of maturity than sediments within the Betty Terrace (Table 8.9). Figure 8.19 demonstrates maximum maturity in cross section attained in the Triassic across the study area. The Fairfield Group within the Gregory Sub-basin (as indicated in Figure 8.18 and Table 8.9) reaches the late oil window. The Fairfield Group reaches the early oil window on the Betty Terrace, but is immature on the Balgo Terrace and in the Billiluna Sub-basin.

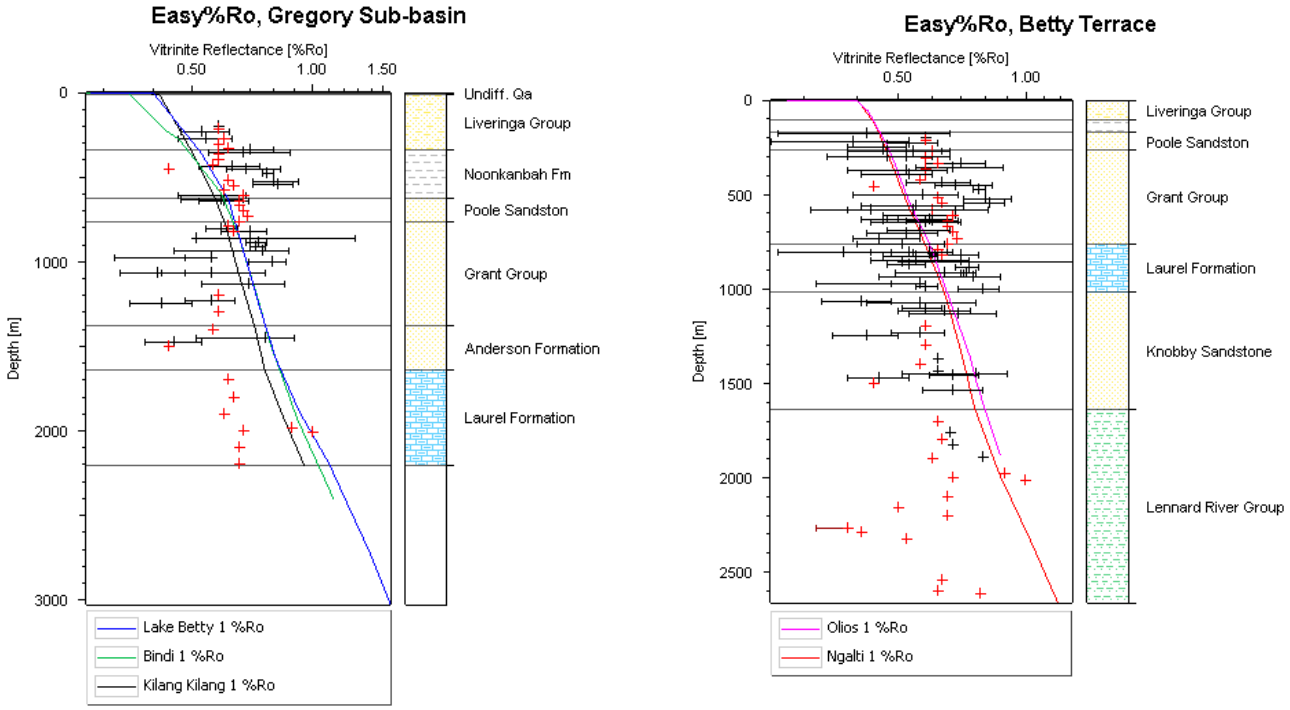

Figure 8.18. Maturity profiles for 1D models in the Gregory Sub-basin (left) and on the Betty Terrace (right). Models indicate that sediments within the Gregory Sub-basin are more mature that sediments on the Betty Terrace, due to deeper burial.

\ Predicted Vitrinite (vari-coloured)

\+ VR

\+ VRe from Tmax

Formation	Maximum maturity (%Ro)			
	Gregory Sub-basin		Betty Terrace	
	Top Fm	Base Fm	Top Fm	Base Fm
Noonkanbah Formation	0.51	0.6	0.43	0.45
Grant Group	0.63	0.75	0.47	0.58
Laurel Formation	0.82	1.05	0.58	0.65

Table 8.9. Summary of maturity on the top and base of key stratigraphic markers in the project area, from 1D models.

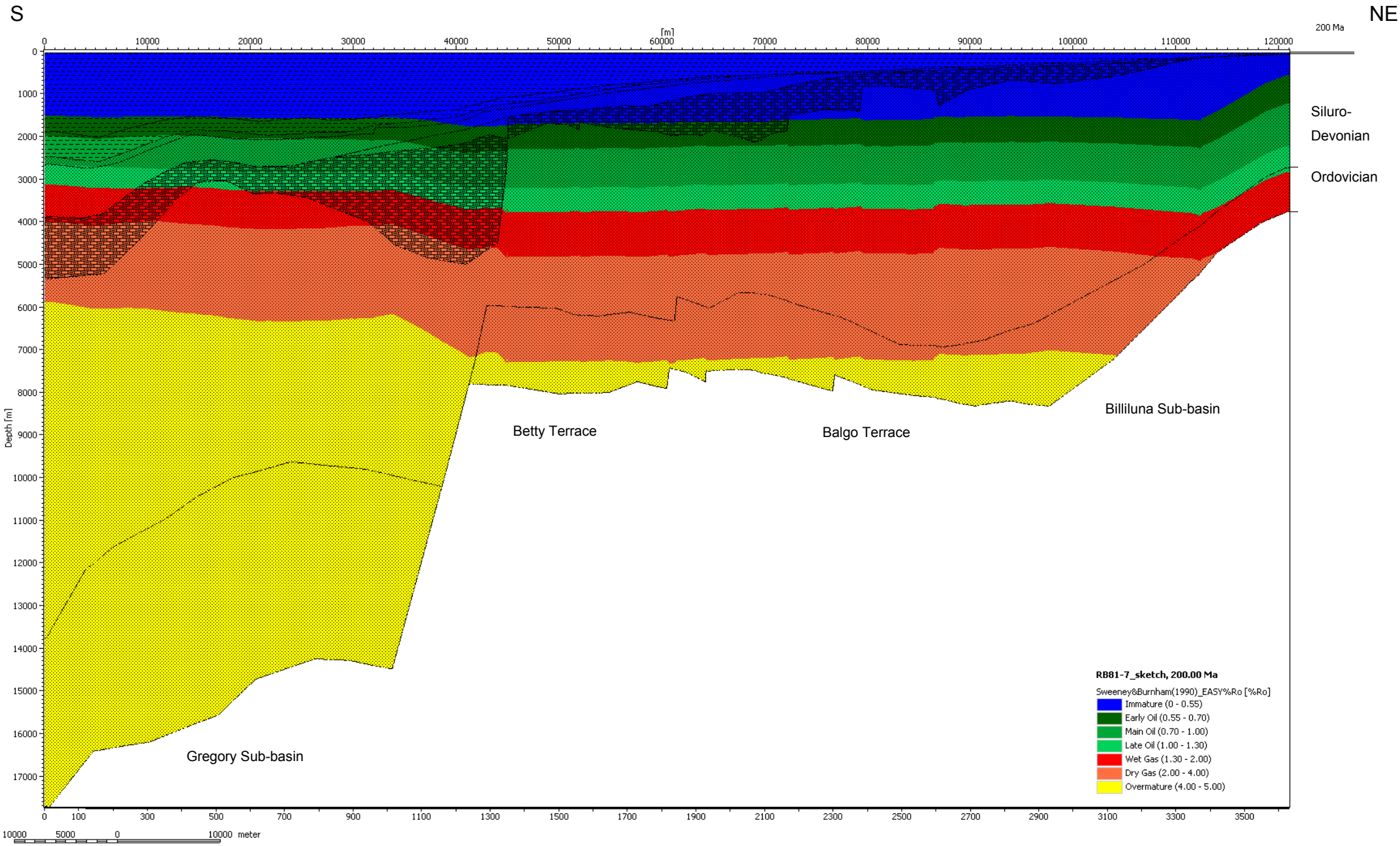

Figure 8.19. 2D model RB81-7 shows the regional maturity of sediments across the study area, restored to the time of peak maturation in the Triassic (time step 200Ma).

8.6.3 *Modelling Results – Goldwyer Formation*

Source rock maturity

Vitrinite vs. Time diagrams enable the determination of when the source rocks identified in Chapter 7 evolve through respective hydrocarbon maturation windows.

Sediments in the Gregory Sub-basin experience slightly higher maturation rates than sediments on the Betty Terrace, Balgo Terrace and in the Billiluna Sub-basin.

Figure 8.20 illustrates that the Goldwyer Formation undergoes initial subsidence after Early Ordovician rifting (475 Ma) until a dramatic increase in maturation rates in the Llandovery (Late Silurian, 435 Ma). Sediments continued to mature until the Mississippian (350 – 340 Ma) when the Goldwyer Formation within the Gregory Sub-basin reaches maximum maturity. Figure 8.5 shows that Gregory Sub-basin sediments are reburied in the Triassic where they attain maximum temperatures, confirmed by AFTA (Duddy et al, 2003), however Figure 8.20 indicates that maximum maturity for the Goldwyer Formation reaches 4.66% Ro; the same maturity as in the Carboniferous. This is the upper limit of the Sweeny and Burnham (1990) Easy%Ro kinetic, and in any case the sediments are over mature by the Carboniferous.

The Goldwyer Formation in the Gregory Sub-basin and Betty Terrace enters the early oil window (0.55 – 0.7 %Ro) in the Late Ordovician (450 Ma). Gregory Sub-basin sediments enter the main oil window (0.7 – 1.0 %Ro) in the Llandovery (Late Silurian, 435 Ma). Sediments in the Gregory Sub-basin rapidly mature from Llandovery time; entering the late oil window (1.0 – 1.3 %Ro) in the Wenlock (Middle Silurian 428 Ma), enter the wet gas window (1.3 – 2.0 %Ro) in the Ludlow (Early Silurian, 422 Ma), enter the dry gas window (2.0 – 4.0 %Ro) in the Early Devonian (410 Ma) and become over mature (4.0 – 5.0 %Ro) in the Late Devonian (365 Ma).

The Goldwyer Formation on the Betty Terrace, Balgo Terrace and in the Billiluna Sub-basin mature through respective hydrocarbon product windows slightly later and at slower rates than sediments in the Gregory Sub-basin (Figure 8.20). Balgo Terrace and Billiluna Sub-basin sediments enter the early oil window in the Wenlock (Middle Silurian, 427 Ma), and the three provinces enter the main oil window in the Pridoli to Lochkovian (~ 419 Ma).

Billiluna Sub-basin sediments enter the late oil window by the Early Devonian (407 Ma) and sediments on the terraces enter the same window 10 Ma later (~ 397 Ma).

The Goldwyer Formation on the Billiluna Sub-basin enters the wet gas window in the Middle Devonian (397 Ma) and enters the dry gas window by the Late Devonian (370 Ma). Betty Terrace and Balgo Terrace sediments enter the wet gas window in the Late Devonian (380 Ma) and reach the dry gas window in the Mississippian (345 – 332 Ma). Sediments on the Betty Terrace, Balgo Terrace and within the Billiluna Sub-basin undergo a further stage of maturation, remaining in the dry gas window during the Triassic Fitzroy Movement, concluding at 200 Ma.

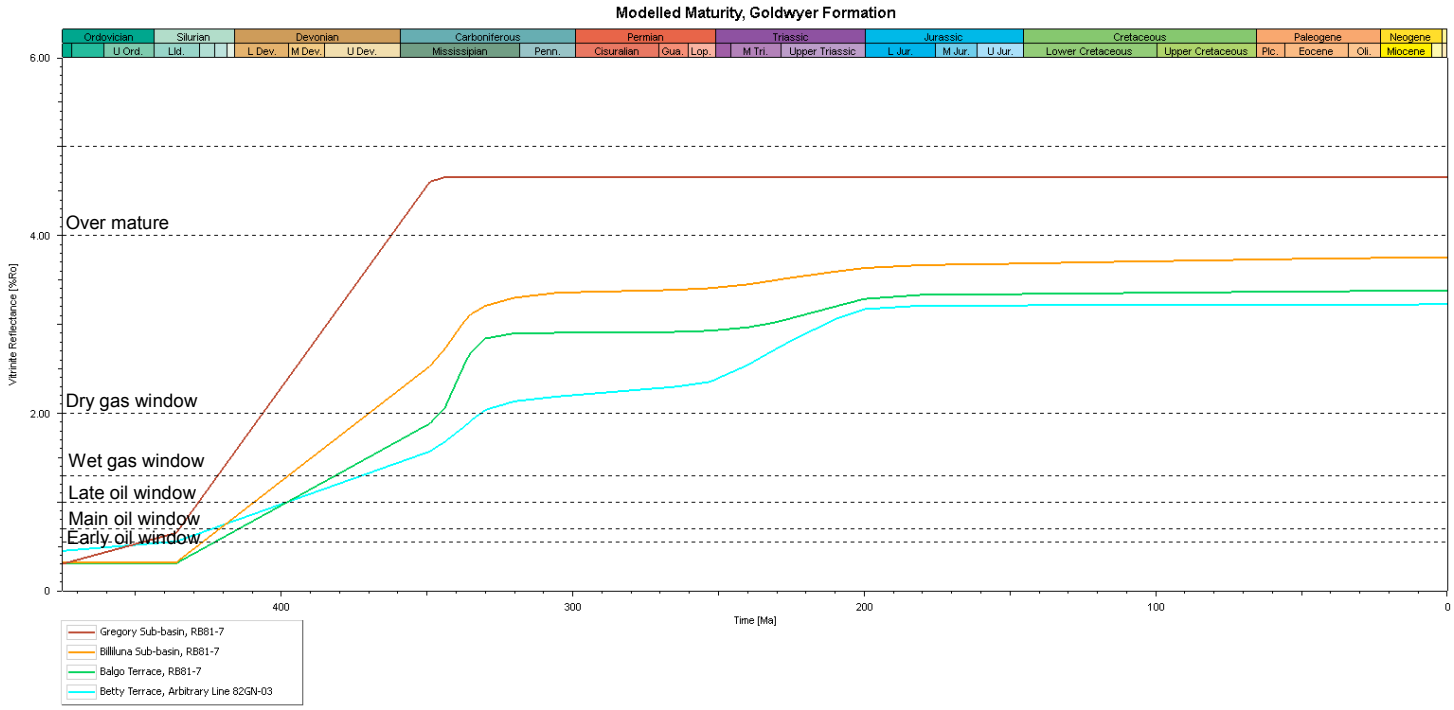

Figure 8.20. Goldwyer Formation maturity vs time diagram.

Transformation ratios

Transformation Ratios (TR) are an indication of how much kerogen has cracked to petroleum (%), and equals the Production Index (PI; = S_1 / (S_1+S_2)) if no petroleum has been expelled (Hantschel, T. and A. I. Kauerauf, 2009).

Goldwyer Formation kerogens undergo complete conversion to petroleum (Figure 8.21). Kerogens in the Gregory Sub-basin initiate cracking in the Early Ordovician (475 Ma), shortly after deposition. Rapid accommodation generation facilitates rapid burial and hence, maturation of Gregory Sub-basin sediments. Gregory Sub-basin kerogens convert at higher rates to kerogens on the Betty Terrace, Balgo Terrace and in the Billiluna Sub-basin. Conversion rates increase in the Llandovery (Early Silurian, 436 Ma) across all wells. Complete conversion occurs (100% TR) by the Mississippian (Early Carboniferous, 350 Ma). Maximum maturity obtained on terraced areas in the Triassic have no impact on kerogen conversion as the source rock is already exhausted.

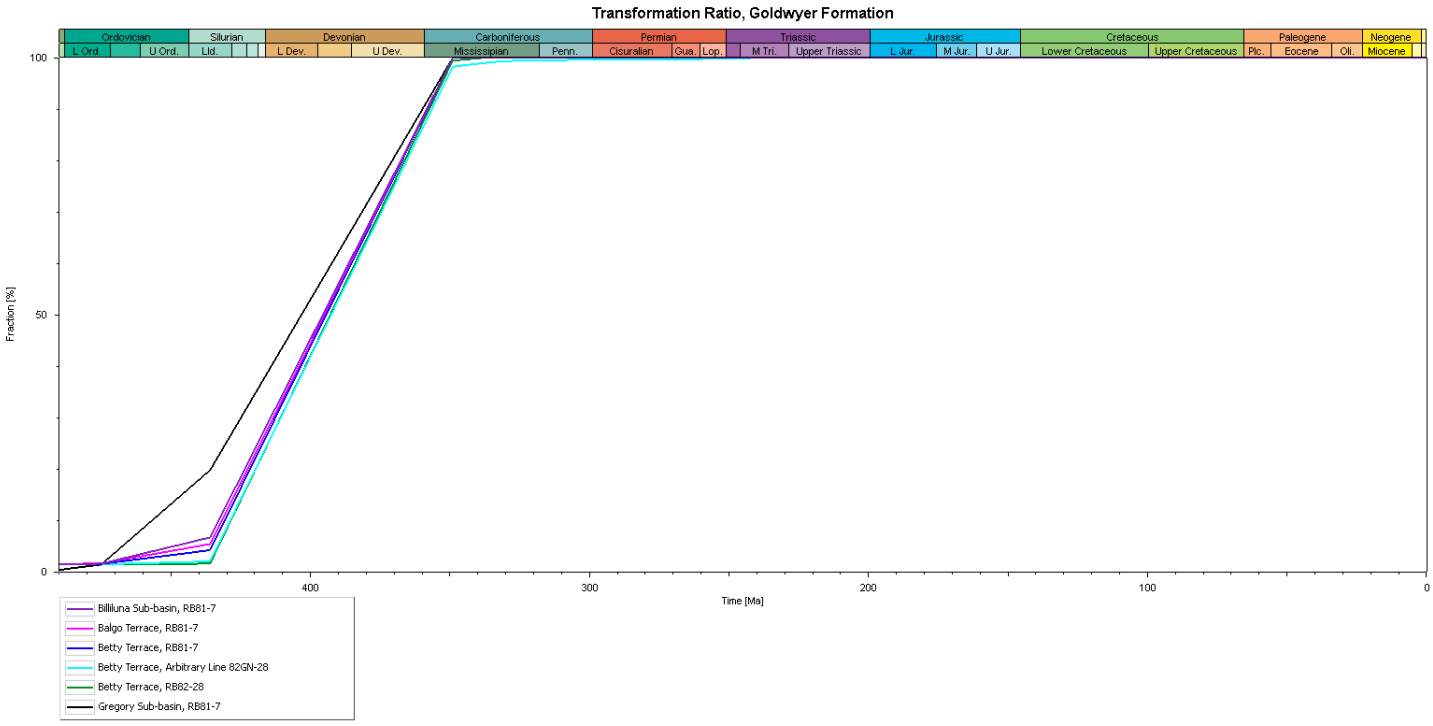

Figure 8.21. Goldwyer Formation transformation ratio vs time diagram

Hydrocarbon generation

Source rock generation occurs as a decomposition reaction when kerogen cracks to petroleum. The critical point of source rock generation is defined as when transformation ratios (TR) reach approximately 50% (Hantschel, T. and A. I. Kauerauf, 2009).

Generation masses in PetroMod are likely to be incorrect within the models presented here because average generative capacities are assigned from a regional source rock analysis (Chapter 7). In reality, source rock geochemical characteristics are likely to vary more than what is assumed here. The models are configured this way because timing is arguably more important for this project to determine than generated quantities.

Figure 8.22 shows that generation in the Goldwyer Formation commences in the Llandovery (437 Ma), slightly earlier than the Bongabinni Member, attributed to its deeper burial and hence marginally higher maturity. Generation in the Gregory Sub-basin peaks at a maximum (though still low) rate of 0.005 mg HC/g TOC/Ma in the Early Devonian (407 Ma), and ceases by the Mississippian (346 Ma) when Goldwyer Formation kerogens are exhausted. There is a second, limited period of generation on the Betty Terrace and Balgo Terrace in the Triassic caused by renewed subsidence; when the Goldwyer Formation on the Betty Terrace, Balgo Terrace and Billiluna Sub-basin obtain maximum paleo-temperatures (240 Ma); however this is likely meaningless given that kerogens are essentially exhausted by the Mississippian. There is no further generation in the Gregory Sub-basin post-Mississippian as the Goldwyer Formation source rock is already spent. Figure 8.22 illustrates that hydrocarbon generation is more rapid in the Gregory Sub-basin relative to the terraces due to sediments in the sub-basin attaining higher maturity at the faster rate.

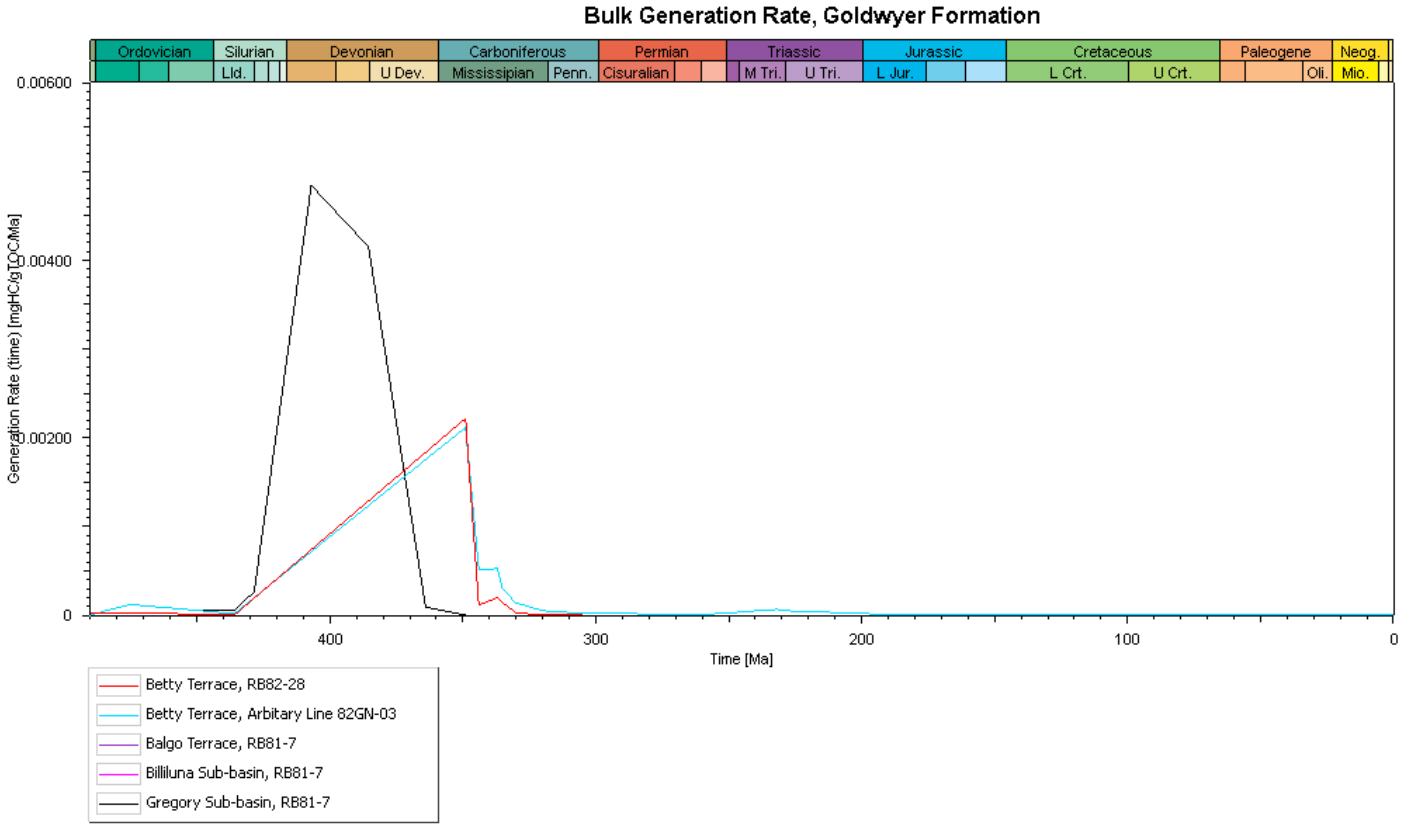

Figure 8.22. Goldwyer Formation generation rate vs time diagram.

Hydrocarbon expulsion

'Expulsion' specifies the amount of petroleum passing from the source rock to the carrier bed within a petroleum system (Hantschel, T. and A. I. Kauerauf, 2009), and refers to the phase of 'primary migration'; where hydrocarbons populate source rock pore space reaching a saturation threshold. At the saturation threshold, hydrocarbons are expelled from the source rock into a carrier system.

In PetroMod, the onset of expulsion is configured by saturation thresholds within the 'Lithology Editor'. Saturation thresholds are affected by generated volumes. The expulsion threshold is set to very low pore space saturations (0.5% oil saturation and 0% gas saturation), meaning that expulsion onset essentially occurs as soon as any hydrocarbons are generated. In turn, there are no (or very low) amounts of residual hydrocarbons in the models. Application of this method results in earlier expulsion times (Neumann et al., 2008). For the

purpose of this study, PetroMod is configured to presume that onset of expulsion occurs immediately after the onset of generation.

Figure 8.23 demonstrates that expulsion from the Goldwyer Formation in the Gregory Sub-basin commences in the Llandovery (Early Silurian, 436 Ma) and ceases in the Frasnian (Late Devonian, 385 Ma), when generation decreases due to waning generation rates. Expulsion on the terraces and within the Billiluna Sub-basin occur at similar times at very low rates (maximum 0.49 Mtons at 349 Ma).

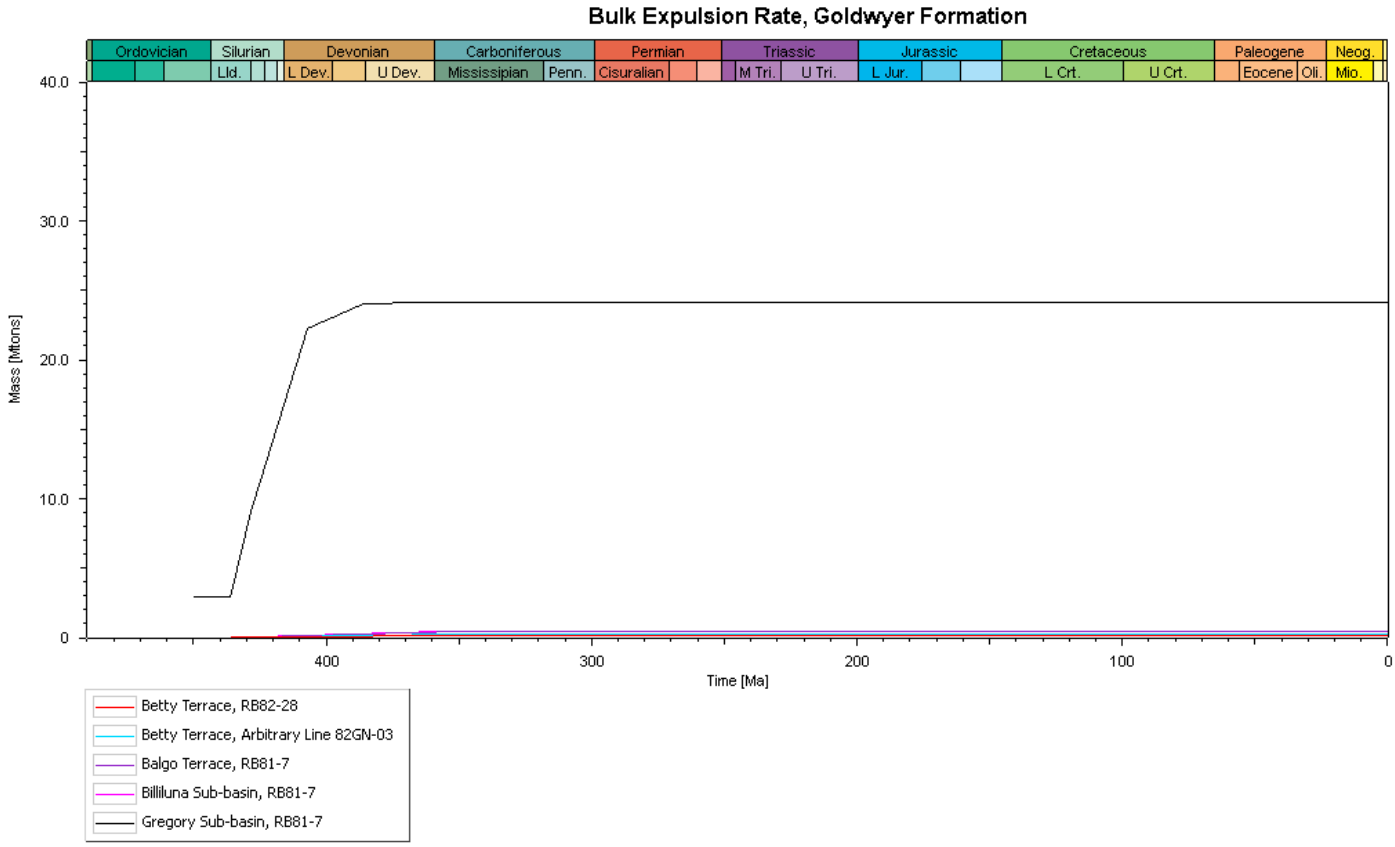

Figure 8.23. Goldwyer Formation expulsion rate vs time diagram.

8.6.4 *Modelling Results – Bongabinni Member*

Source rock maturity

The Bongabinni Member demonstrates a similar maturation history to the Goldwyer Formation (expected given similar ages). The Bongabinni Member is considerably more mature in the Gregory Sub-basin than on the terraces (Figure 8.24). Sediments throughout the study area undergo continual burial commencing in the Llandovery (Late Silurian, 435 Ma). Sediments in the Gregory Sub-basin continually subside until the Mississippian (345 Ma), however sediments on the Betty Terrace, Balgo Terrace and Billiluna Sub-basin undergo periods of increased maturation from the Mississippian and reach maximum maturity in the Triassic (200 Ma).

Initial subsidence is at a higher rate in the Gregory Sub-basin, where sediments mature through the early oil window (0.55 – 0.7 %Ro) in the Llandovery (435 Ma), enter the main oil window (0.7 – 1.0 %Ro) in the Late Llandovery (430 Ma), continue to the late oil window (1.0 – 1.3 %Ro) in the Wenlock (Middle Silurian, 425 Ma), enter the wet gas window (1.3 – 2.0 %Ro) in the Ludlow (Late Silurian, 418 Ma), enter the dry gas window (2.0 – 4.0 %Ro) in the Early Devonian (402 Ma) and become over mature when sediments reach maximum maturity levels in the Mississippian (345 Ma).

Sediments on the Betty Terrace, Balgo Terrace and in the Billiluna Sub-basin enter the respective maturation windows at a slightly later time. Sediments enter the early oil window in the Ludlow (Late Silurian, 420 Ma), enter the main oil window in the Lochkovian (Late Devonian 415 – 410 Ma), and enter the late oil window in the Early to Middle Devonian (402 – 390 Ma). Sediments in the Billiluna Sub-basin enter the wet gas window in the Middle Devonian (389 Ma) whereas sediments on the terraces enter the wet gas window slightly later, in the Late Devonian (375 – 360 Ma). Billiluna Sub-basin sediments enter the dry gas window in the Early Mississippian (356 Ma) whereas sediments on the Balgo Terrace enter the dry gas window by the Mississippian (340 Ma). Betty Terrace sediments don't enter the dry gas window until the Early Permian (295 Ma). The Bongabinni Member on the Betty Terrace, Balgo Terrace and in the Billiluna Sub-basin remain in the dry gas window until present day.

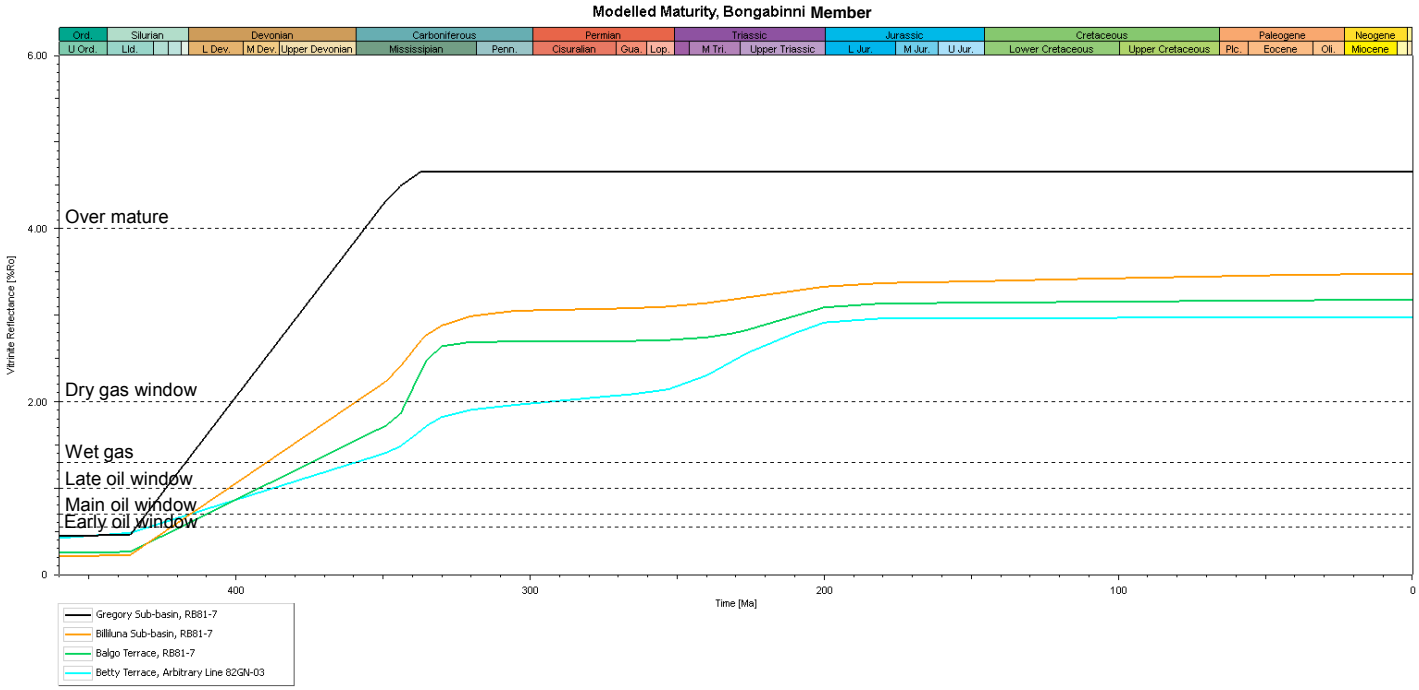

Figure 8.24. Bongabinni Member maturity vs time diagram.

Transformation ratios

Figure 8.25 illustrates the Bongabinni Member kerogens undergo complete conversion to petroleum, commencing in the Llandovery (Early Silurian, 436 Ma). Kerogens reach 100% conversion by the Mississippian (Early Carboniferous, 450 Ma), when Gregory Sub-basin sediments reach maximum maturity (over mature, 4.0 – 5.0 %Ro) and sediments on the Betty Terrace, Balgo Terrace and in the Billiluna Sub-basin enter the dry gas window (2.0 – 4.0 %Ro). A slight increase in maturity in the Triassic results in no further kerogen conversion as the source rock is already spent.

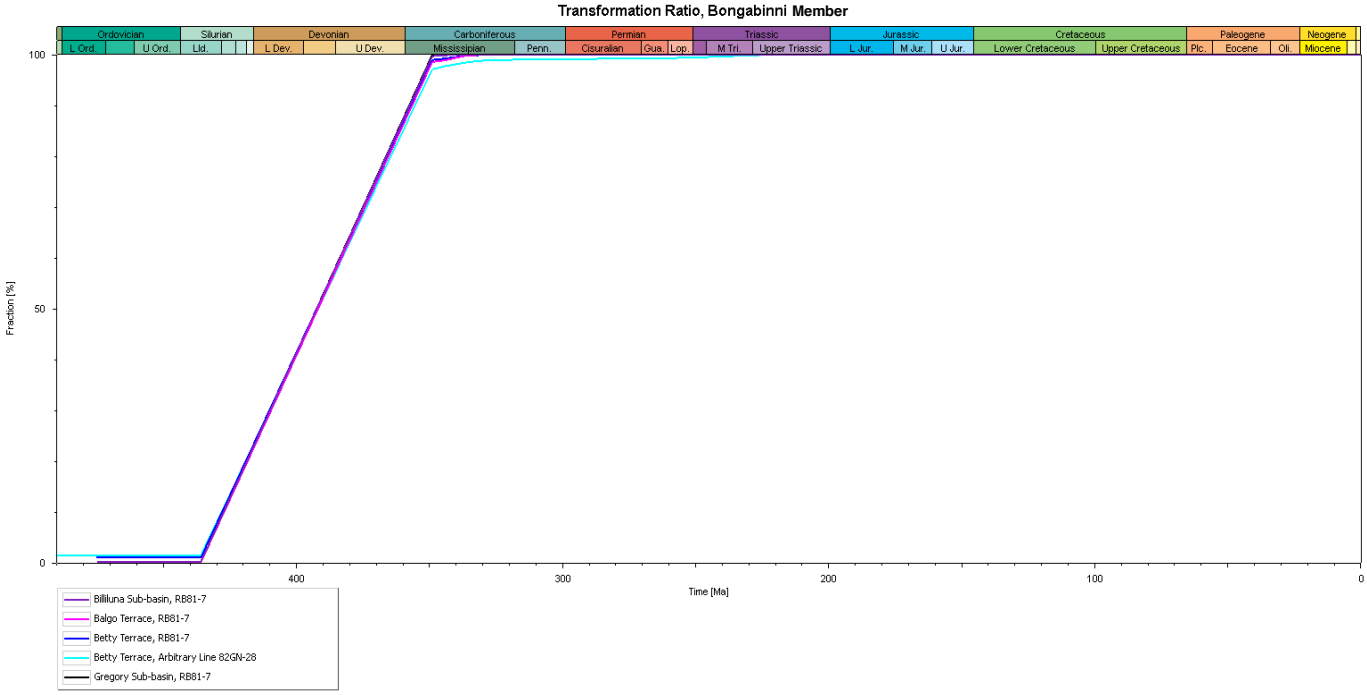

Figure 8.25. Bongabinni Member transformation ratio vs time diagram.

Hydrocarbon generation

Generation rates are low within the Bongabinni Member. Figure 8.26 illustrates that generation within the Gregory Sub-basin commences in the Early Devonian (407 Ma) and concludes by the Mississippian (Late Carboniferous, 350 Ma). Figure 8.26 indicates that the Bongabinni Member on the Betty Terrace (Pseudo well RB82-28) shows a generative period from the Silurian (435 Ma) until the Mississippian (~345 Ma) representing peak generation at 0.0022 mg HC/g TOC/Ma; however this is likely anomalous in the model as transformation ratios range close to 0% (unconverted kerogen). Meaningful generation is interpreted to occur close to the Late Devonian (or fractionally later) for terraced areas reaching a peak around 345 Ma. A second short generative period occurs in the Triassic (200 Ma) when maximum paleo-temperatures are obtained.

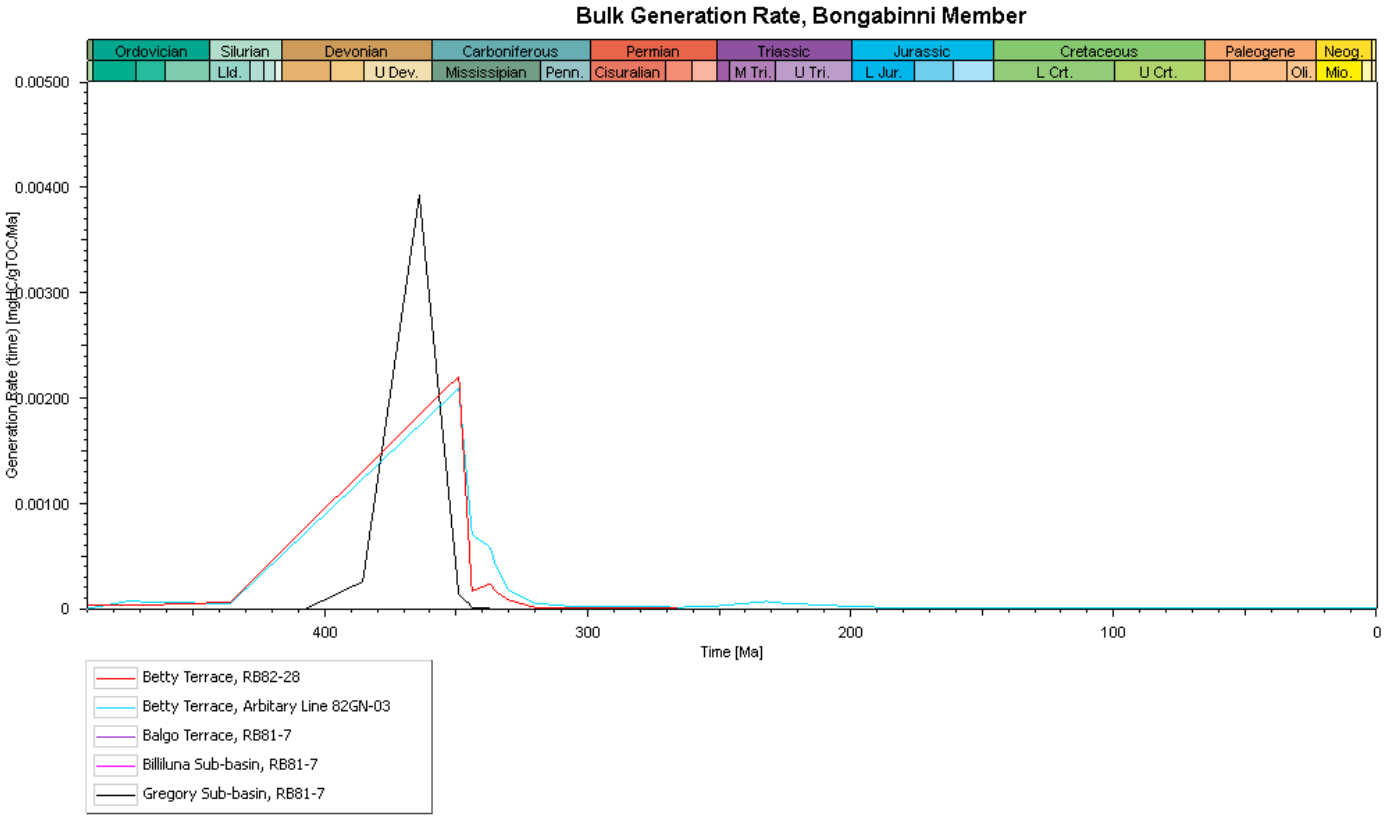

Figure 8.26. Bongabinni Member generation rate vs time diagram.

Hydrocarbon expulsion

Figure 8.27 illustrates that the Bongabinni Member expels hydrocarbons over one main period. Expulsion from sediments within the Gregory Sub-basin show onset in the Early Devonian (407 Ma) when generation commences. Expulsion continues until the Mid Devonian (385 Ma), with waning generation. Expulsion is also interpreted to occur on the terraced areas (indicated by a slight increase in expulsion rate on the Betty Terrace 82GN-03 pseudo well curve) within the Mississippian (350 Ma – 340 Ma) due to peak generation on the Betty and Balgo Terraces. No (or negligible) expulsion is interpreted to occur in the Billiluna Sub-basin or from the Betty Terrace RB82-28 and Balgo Terrace models.

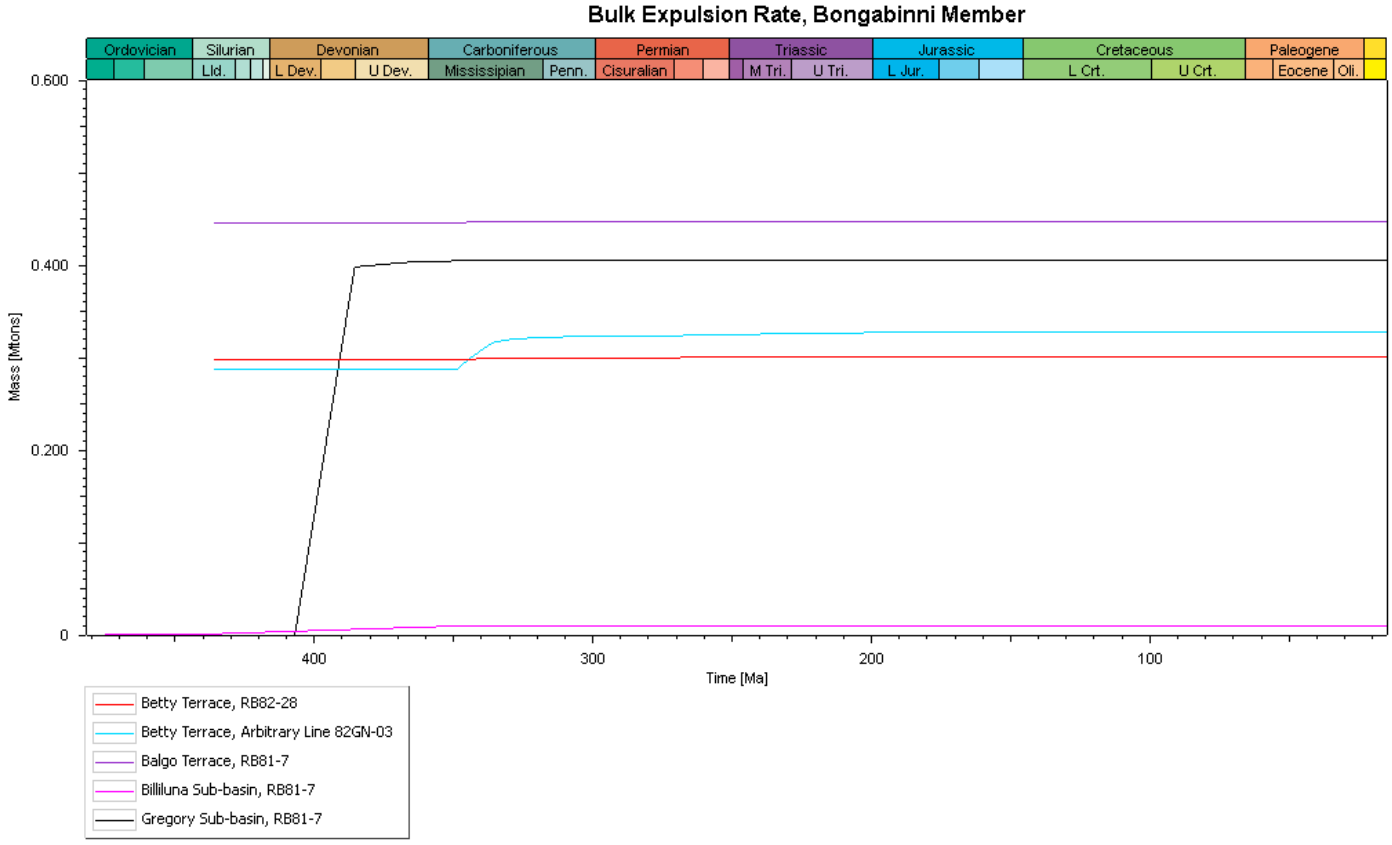

Figure 8.27. Bongabinni Member expulsion rate vs time diagram.

8.6.5 *Modelling Results – Gogo Formation*

Source rock maturity

The Gogo Formation shows to be considerably more mature in the Gregory Sub-basin than on neighboring terraces (Figure 8.28). All wells undergo significant burial in the Mississippian (345 Ma) following uplift of the Carboniferous Meda Transpression. The Gogo Formation in the Gregory Sub-basin rapidly matures through the main oil and late oil windows over a 10 My period, entering the wet gas window (1.3 – 2.0 %Ro) in the Mississippian (336 Ma) whilst sediments on the Betty Terrace and Billiluna Sub-basin effectively reach the main oil window (0.7 – 1.0 %Ro) at a similar time. Balgo Terrace sediments reach the main oil window (0.7 – 1.0 %Ro) and the late oil window (1.0 – 1.3 %Ro) within a 10 My period in the Mississippian (336 Ma).

Sediments continue to subside during the Triassic Fitzroy Movement. The Gregory Sub-basin matures the fastest, likely due to increased rates of rifting focused on the Stansmore Fault, where the Gogo Formation matures into the dry gas window (2.0 – 4.0 %Ro) in the Middle Triassic (240 Ma) and reaches peak maturity at 200 Ma. Sediments on the Betty Terrace gradually subside and enter the late oil window (1.0 – 1.3 %Ro) at the point of maximum maturity in the Late Triassic (200 Ma), whilst the Gogo Formation in the Billiluna Sub-basin remains in the main oil window (0.7 – 1.0%Ro) at peak maturity.

Figure 8.28 clearly demonstrates that the Gregory Sub-basin is repeatedly the focal point of rifting within study area, both during the Carboniferous Meda Transpression and Triassic Fitzroy Movement. This trend is consistent with most source rocks in the project area, however is clearly pronounced in relation to the Gogo Formation.

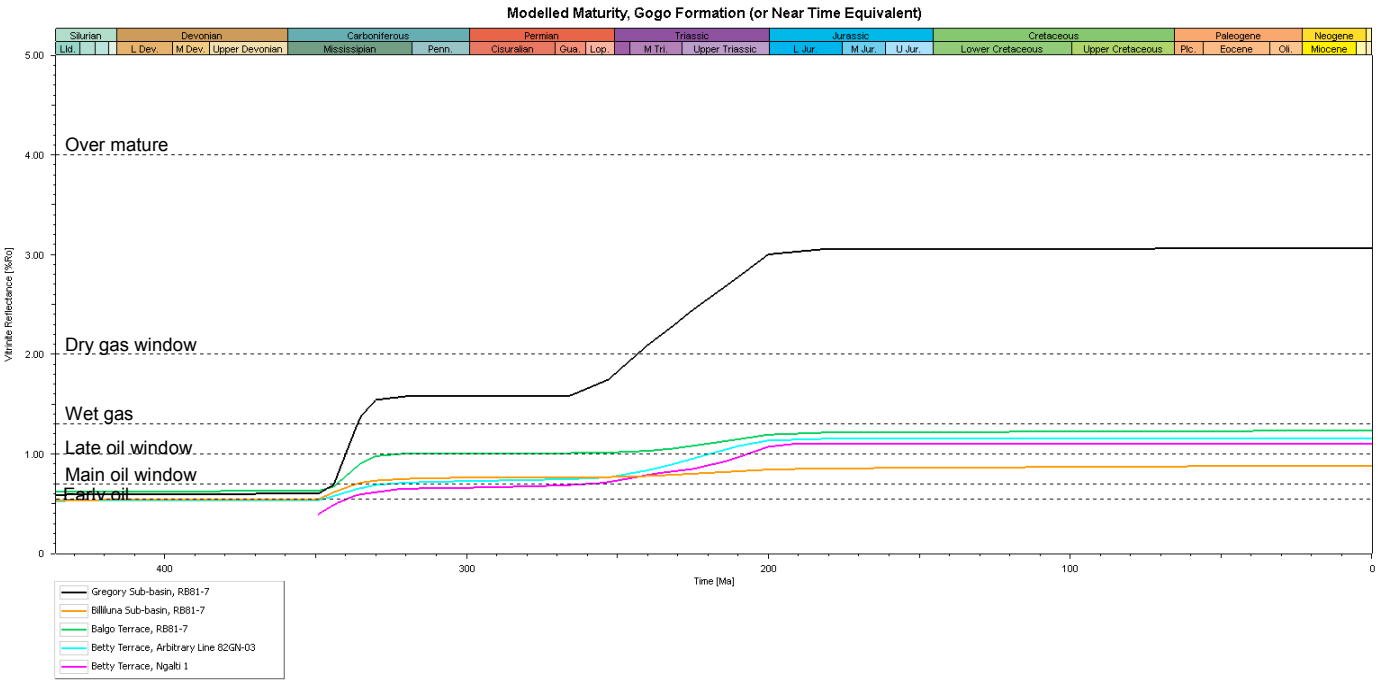

Figure 8.28. Gogo Formation maturity vs time diagram.

Transformation ratios

Kerogens in the Gogo Formation crack to petroleum in two periods; The Mississippian and Triassic (Figure 8.29).

Kerogens in the Billiluna Sub-basin and on the Balgo Terrace partly convert to petroleum in the Mississippian (Early Carboniferous, 342 Ma) reaching 20.5% on the Balgo Terrace and 40% in the Billiluna Sub-basin. Kerogens experience a second stage of cracking in the Late Triassic (between 235 Ma to 200 Ma) as sediments obtain maximum maturity, where they reach 60% – 70% TR.

Figure 8.29 illustrates that kerogens in the Gregory Sub-basin convert to petroleum at 79% TR in the Mississippian (345 – 330 Ma), and undergo complete conversion (100% TR) to petroleum at the end of the Triassic (200 Ma). The Gogo Formation in the Gregory Sub-basin is spent by the end of the Triassic.

Conversion in the Mississippian occurs when Gogo Formation sediments reach the early to main oil window (0.55 – 1.0 %Ro) on the Betty Terrace, Balgo Terrace and Billiluna Sub-

basin, and Gregory Sub-basin sediments mature through the oil window and reach the dry gas window (2.0 – 4.0 %Ro).

Kerogen conversion in the Triassic reflects sediments obtaining maximum maturity throughout the project area, where increases in maturity are high enough to encourage complete kerogen conversion in Gregory Sub-basin sediments.

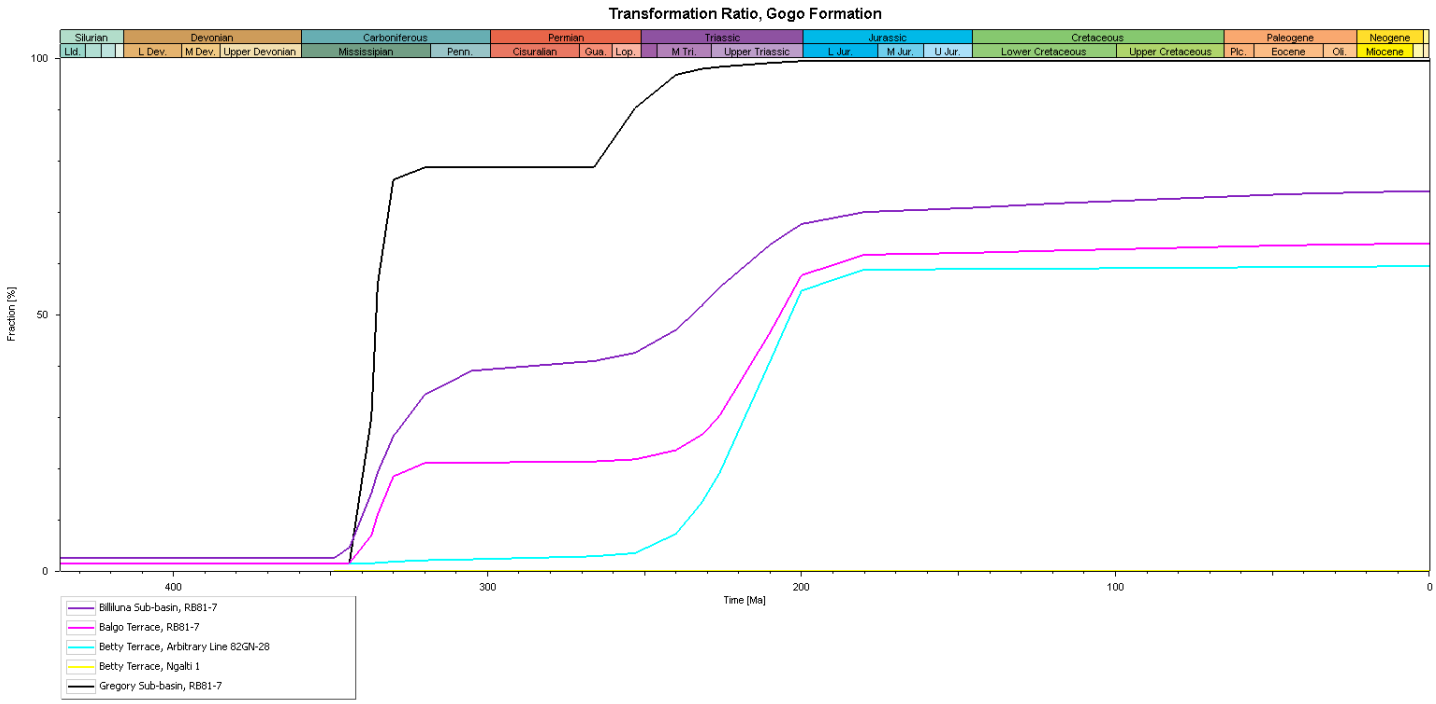

Figure 8.29. Gogo Formation transformation ratio vs time diagram.

Hydrocarbon generation

Figure 8.30 demonstrates that generation within the Gogo Formation commences in the Mississippian (349 Ma) when sediments enter the early oil window (0.55- 0.7 %Ro) and continue to the main oil window (0.7 – 1.0 %Ro). The Gogo Formation undergoes two periods of generation, the first in the Mississippian (349 – 335 Ma), and the second (main) generative period in the Middle Permian to Early Jurassic (280 – 175 Ma). Generation rates are low, reaching a peak at 0.0050 mg HC/g TOC/Ma in the Middle Triassic (240 Ma).

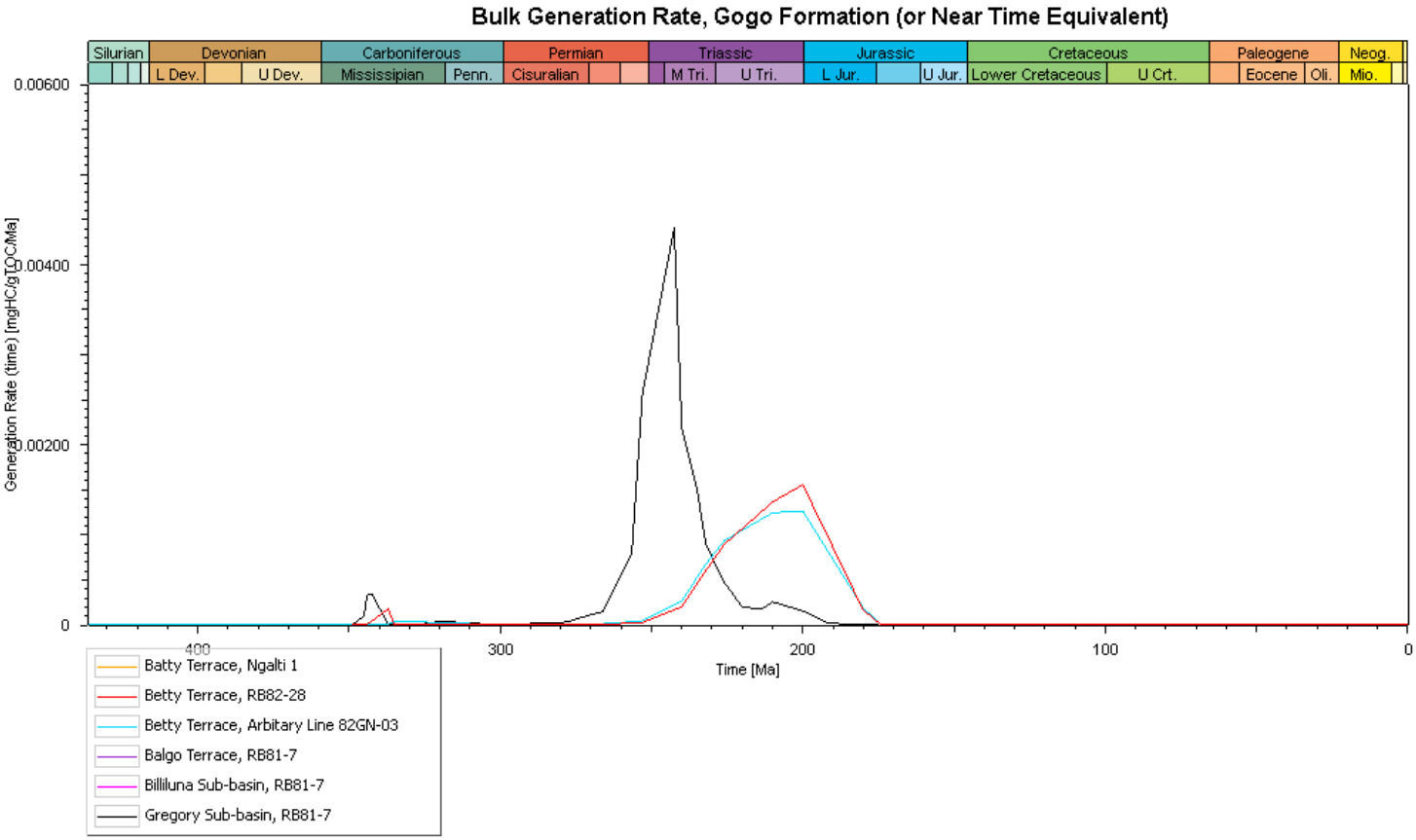

Figure 8.30. Gogo Formation generation rate vs time diagram.

Hydrocarbon expulsion

Figure 8.31 illustrates two expulsion periods for Gogo Formation sediments. The first (main) period of expulsion occurs in the Mississippian (Late Carboniferous, 344 Ma), 5 My after sediments commence generation. The first period of expulsion ceased in the Late Mississippian (330 Ma).

A second period of expulsion occurs from the Lopingian (Late Permian, 255 Ma) and ceases in the Late Triassic (200 Ma) due to waning generation rates.

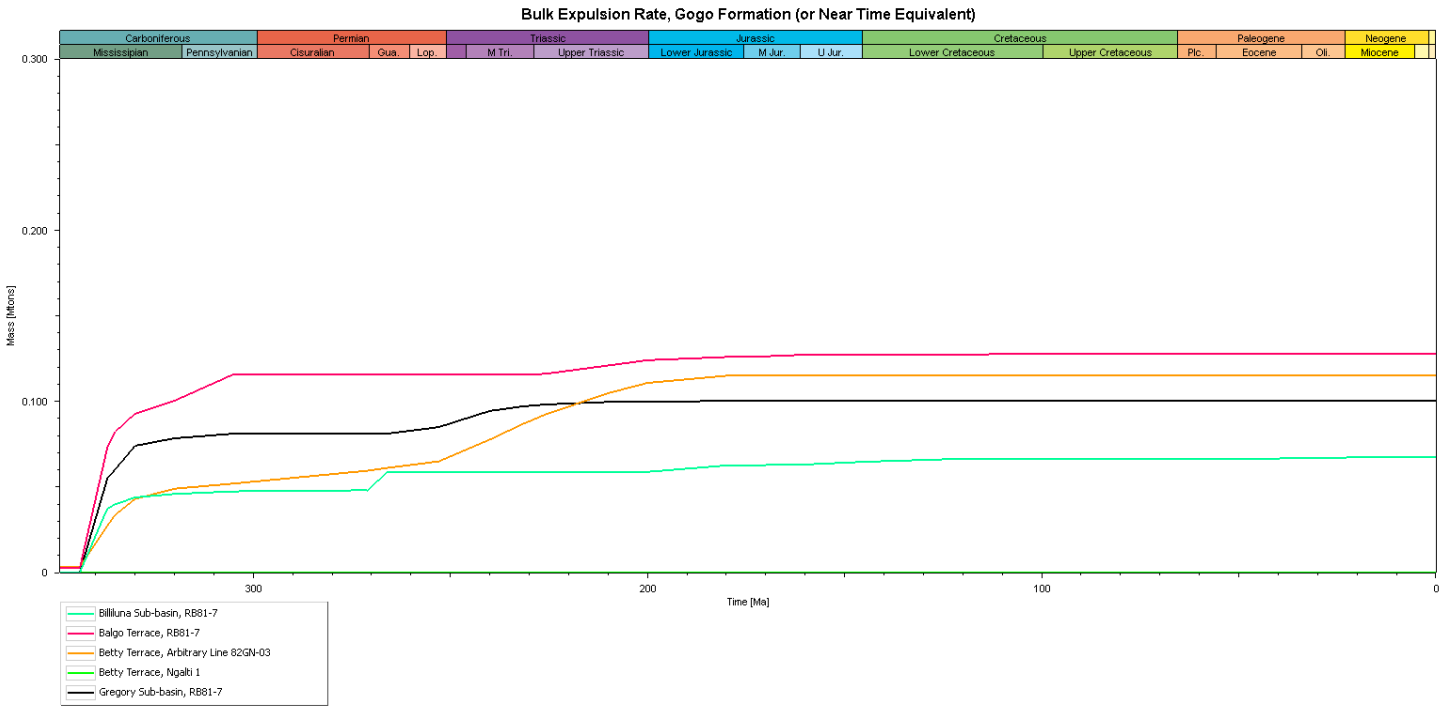

Figure 8.31. Gogo Formation expulsion rate vs time diagram.

8.6.6 *Modelling Results – Laurel Formation*

Source rock maturity

The maturity of the Laurel Formation is highest in the Gregory Sub-basin (Figure 8.32), showing the highest maturation rates; undergoing subsidence in the Mississippian and in the Guadalupian (Middle Permian) until the Middle Triassic (265 – 240 Ma). Subsidence wanes in the Middle Triassic and resumes in the Late Triassic until maximum maturity at 200 Ma. Laurel Formation sediments undergo slower maturation rates on the Betty Terrace and sediments very slowly subside on the Balgo Terrace and in the Billiluna Sub-basin. Sediments on the Betty Terrace, Balgo Terrace and Billiluna Sub-basin all reach maximum maturity in the Late Triassic (200Ma).

Gregory Sub-basin sediments enter the early oil window (0.55 – 0.70 %Ro) in the Late Permian (Lopingian, 252 Ma) and reach the main oil window (0.70 – 1.0 %Ro) in the Middle Triassic (240 Ma). Laurel Formation sediments in the Gregory Sub-basin continue towards (and essentially enter) the late oil window (1.0 – 1.3 %Ro) at the point of maximum maturity (200 Ma). Betty Terrace and Balgo Terrace sediments enter the early oil window (0.55 – 0.7 %Ro) at maximum maturity (200 Ma), whilst the Laurel Formation in the Billiluna Sub-basin remains immature at present day.

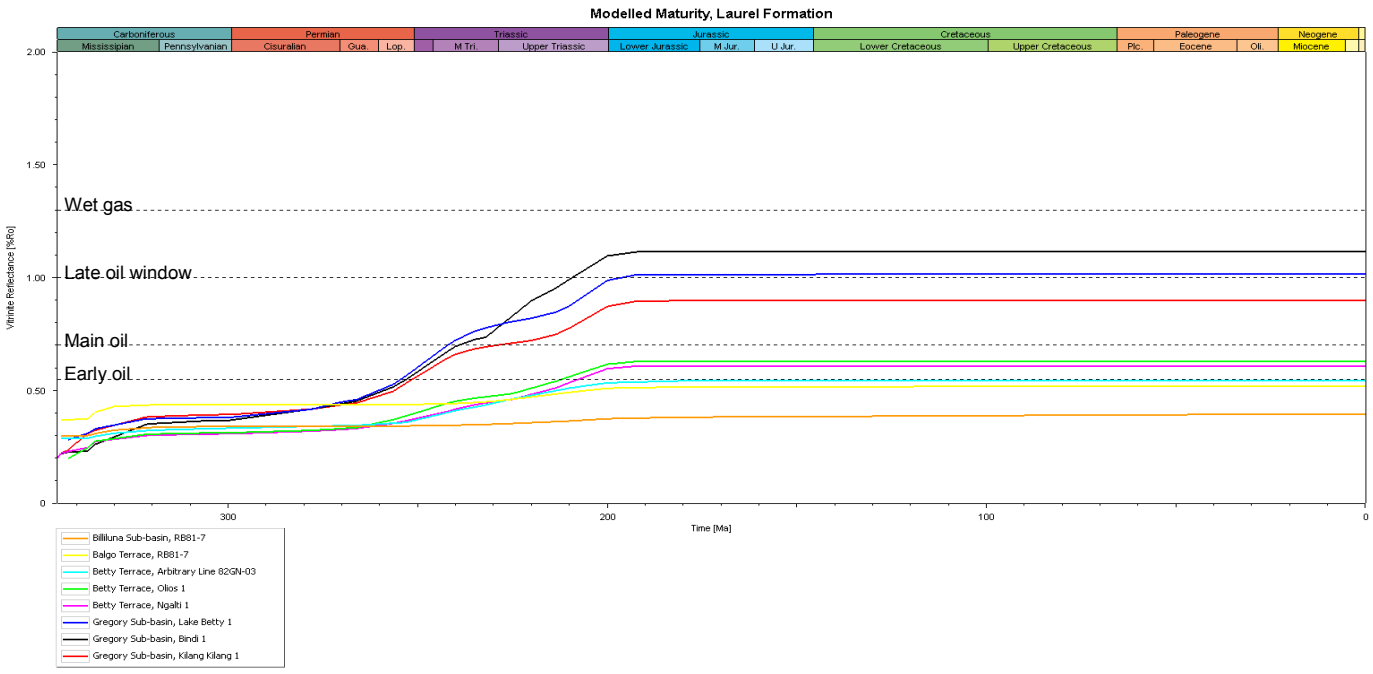

Figure 8.32. Laurel Formation maturity vs time diagram.

Transformation ratios

Laurel Formation kerogens on the Betty Terrace and Balgo Terrace undergo low fractions of transformation to petroleum (Figure 8.33). The Betty Terrace shows 10% conversion in the southern portion of the study area (RB82-28) when sediments reach maximum maturity in the Late Triassic (200 Ma). Kerogens at Olios 1 reach 4% conversion to petroleum at maximum maturity.

Kerogens in the Gregory Sub-basin undergo considerably higher ratios of cracking to petroleum. Transformation ratios of Laurel Formation kerogen in the Gregory Sub-basin ranges 69 % to 97%, suggesting kerogens within the Gregory Sub-basin effectively completely convert to petroleum in areas of optimal maturation (main to late oil window – 0.70 – 1.3% Ro). Kerogen conversion commences in the Early Triassic and ceases in the Late Triassic (252 – 200 Ma), in relation to the timing of maturation within the Gregory Sub-basin.

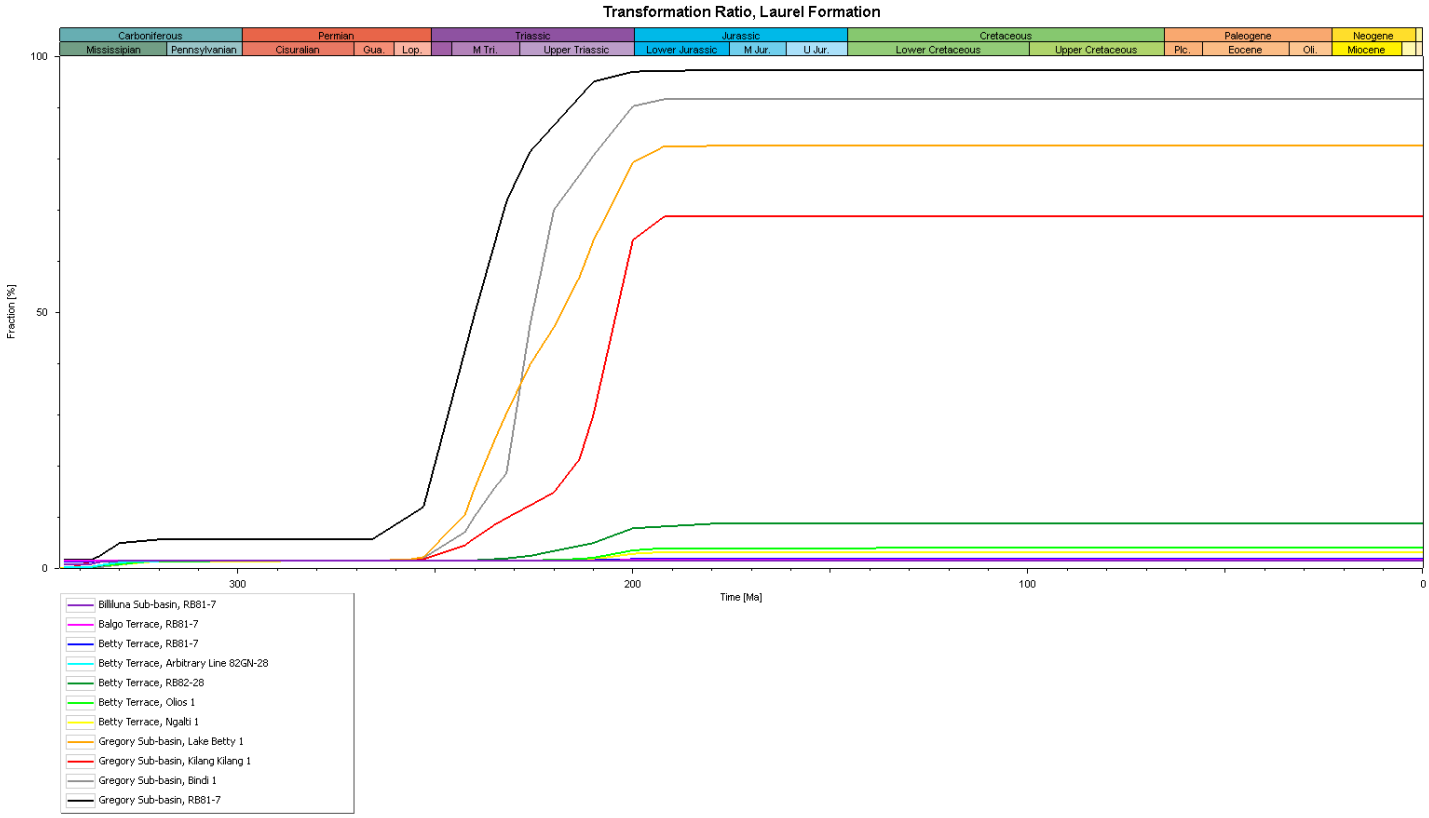

Figure 8.33. Laurel Formation transformation ratio vs time diagram.

Hydrocarbon generation

The Laurel Formation (Figure 8.34) within the Gregory Sub-basin commences generation in the Early Triassic (255 Ma) when sediments enter the early oil window (0.55 – 0.7 %Ro). Sediments in the Gregory Sub-basin briefly decrease in generation rates due to waning subsidence between 240 Ma – 231 Ma (Middle Triassic). The main generative phase for the central Gregory Sub-basin within the study area (Bindi 1) commences at 231 Ma and reaches peak generation in the Middle Triassic (226 Ma). Kilang Kilang 1 and Lake Betty 1 demonstrate that other portions of the Gregory Sub-basin vary in generative periods – Kilang Kilang 1 (southeastern Gregory Sub-basin) reaches peak generation in the Late Triassic (200 Ma). The northern portion of the Gregory Sub-basin appears to reach peak generation earlier, in the Middle Triassic (242 Ma). This illustrates a Laurel Formation generative trend; where the northern portion generates ahead of the central Sub-basin, followed by generation in the south. Laurel Formation generation within the Gregory Sub-basin ceases in the Early Jurassic (180 Ma). Generative rates are low, reaching 0.00245 mg HC/g TOC/Ma.

Modelling suggests that the Laurel Formation sediments generate at extremely low rates on the Betty Terrace and Balgo Terrace, with a brief generative period in the Late Triassic (200 Ma), at 0.0009 mg Hg/g TOC/Ma. This generative period commences as sediments on the Betty Terrace and Balgo Terrace enter the early oil window (0.55 – 0.7 %Ro). Sediments in the Billiluna Sub-basin do not generate, as these sediments remain immature (<0.55 %Ro).

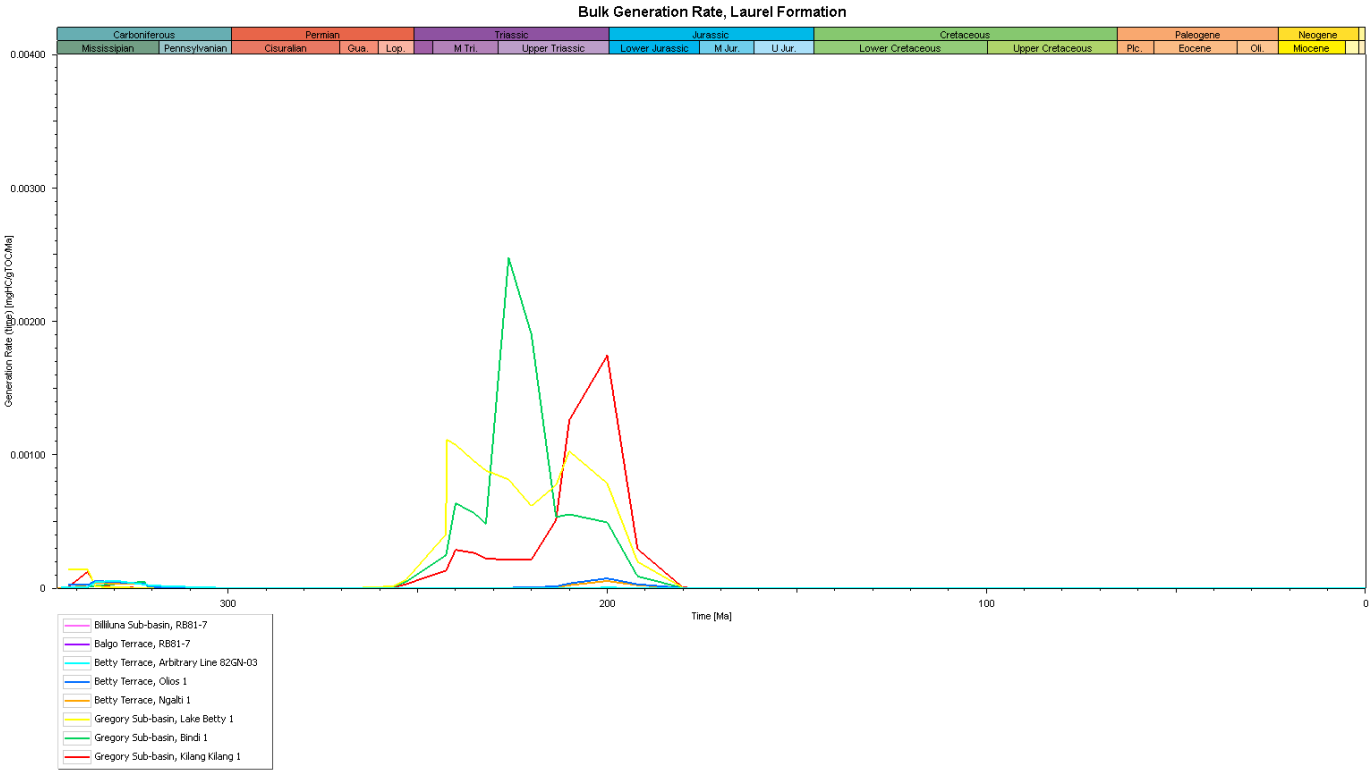

Figure 8.34. Laurel Formation generation rate vs time diagram.

Hydrocarbon expulsion

Expulsion from the Laurel Formation within the Gregory Sub-basin (Figure 8.35) commenced in the Late Triassic (220 Ma), 35 My after the Laurel Formation commenced generating. Expulsion continues as the Laurel Formation reaches maximum generation rates in the Late Triassic, and ceases in the Late Jurassic (192 Ma) when expulsion rates fall below the saturation threshold.

Modelling results (Figure 8.35) illustrate that the Laurel Formation on the Betty Terrace, Balgo Terrace and Billiluna Sub-basin undergo expulsion commencing in the Mississippian, however this is anomalous, because sediments do not enter the early oil window (0.55 – 0.70 %Ro) until the Late Triassic (214 Ma). Expulsion does not occur on the Betty Terrace, Balgo Terrace and Billiluna Sub-basin.

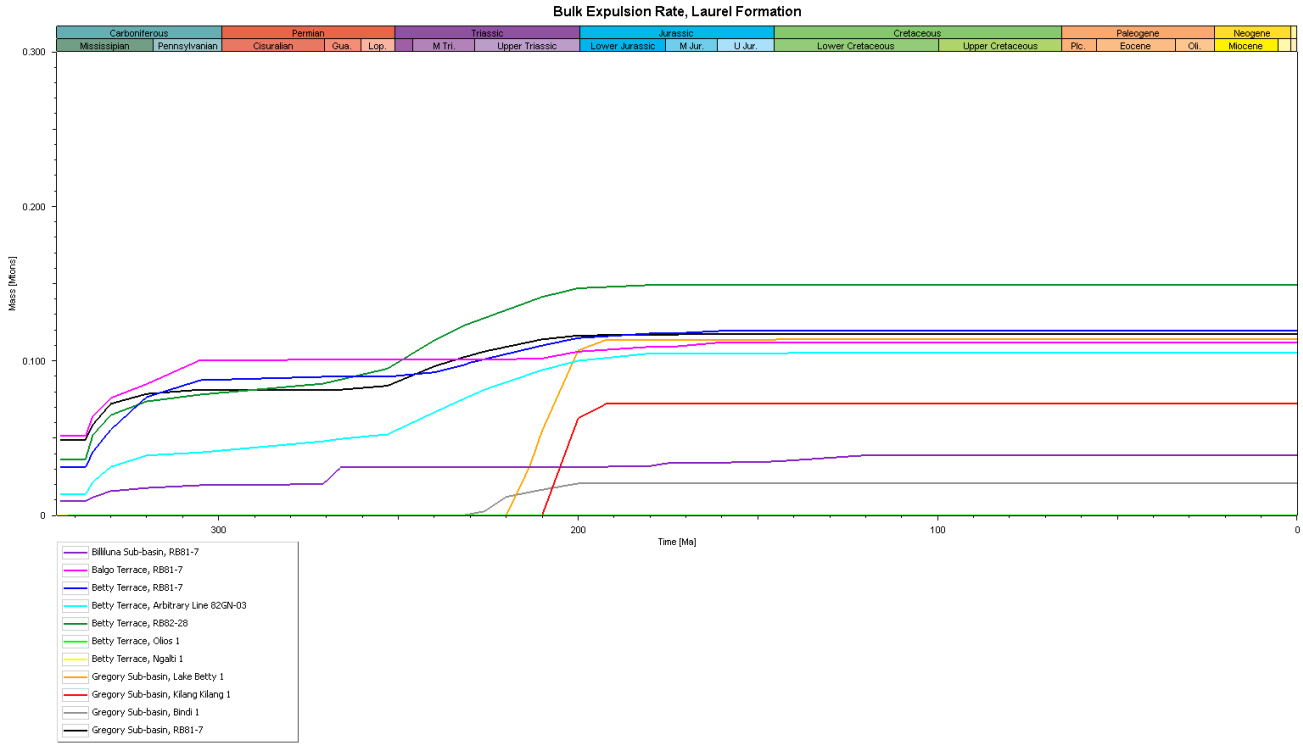

Figure 8.35. Laurel Formation expulsion rate vs time diagram.

8.6.7 *Modelling Results – Anderson Formation*

Source rock maturity

The Anderson Formation shows slightly different maturation rates between the Gregory Sub-basin and the Betty Terrace (Figure 8.36). Sediments undergo burial from the Mississippian after older stratigraphy was uplifted during the Carboniferous Meda Transpression Event. The Anderson Formation in the Gregory Sub-basin shows the highest rates of maturation during the Lopingian (Late Permian) to Late Triassic (255 – 240 Ma). The Anderson Formation on the Betty Terrace undergoes lesser subsidence. There appears to be a slight waning in subsidence rates in the Middle Triassic (230 Ma) prior to continued burial, where sediments reach maximum maturity in the Late Triassic (200 Ma).

The Anderson Formation in the Gregory Sub-basin enters the early oil window (0.55 – 0.70 %Ro) in the Middle Triassic (245 Ma) and enters the main oil window (0.70 – 1.0 %Ro) in the Late Triassic (225 – 205 Ma. Note that Bindi 1 matures faster – entering the main oil window at 225 Ma, reflecting a deeper structural setting relative to the Kilang Kilang 1 well).

Sediments within the Betty Terrace generally remain immature, however the RB82-28 pseudo well indicates Anderson Formation sediments reach the early oil window (0.55 – 0.7 %Ro) as a result of Triassic rifting (200Ma). This alludes to the Anderson Formation obtaining marginally higher maturity in the southwest portion of the Betty Terrace. Note that the Anderson Formation is only preserved in isolated packages throughout the study area (refer Chapter 6.23) because the Anderson Formation was largely eroded as a result of the Carboniferous Meda Transpression, well before sediments started to mature.

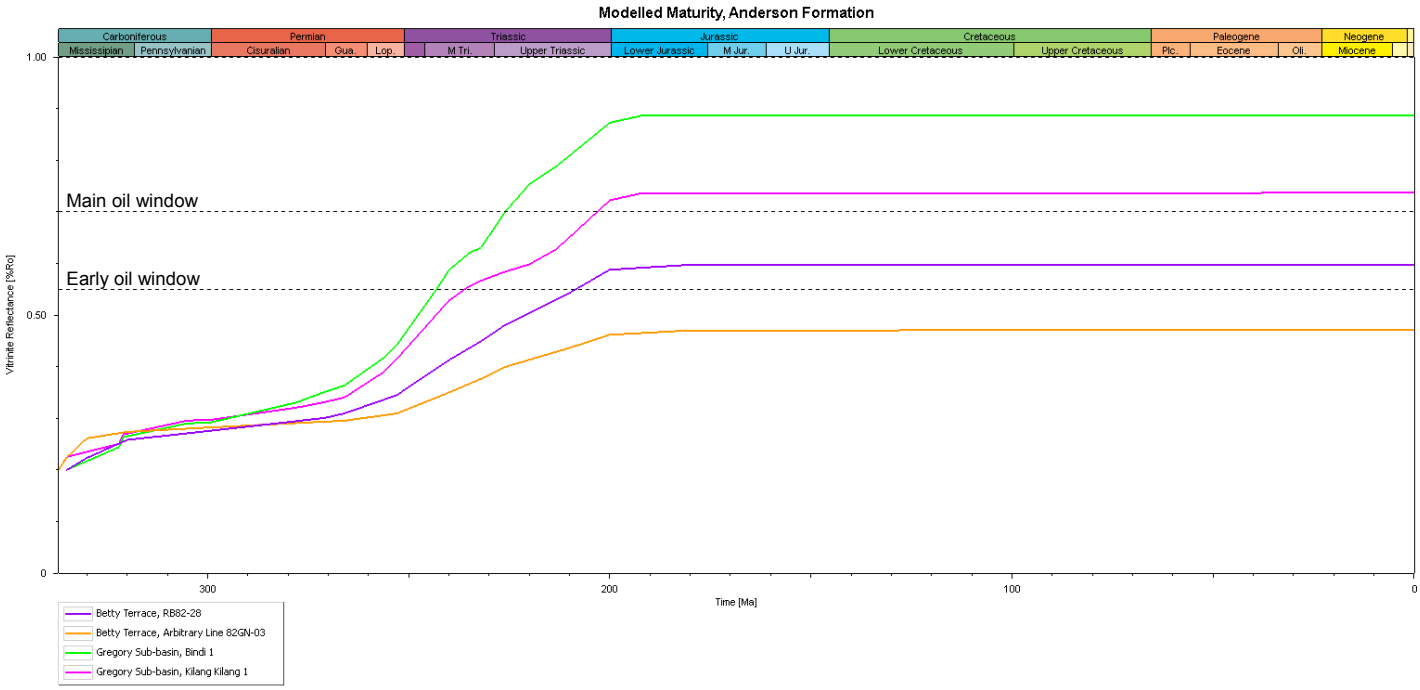

Figure 8.36. Anderson Formation maturity vs time diagram.

Transformation ratios

Anderson Formation kerogens on the Betty Terrace undergo relatively low conversion to petroleum, showing TR less than 10% (Figure 8.37). Maximum conversion is at 6% in the Early Jurassic (192 Ma).

Kerogens in the Gregory Sub-basin undergo high fractions of kerogen cracking. Kilang Kilang 1 kerogens show ratios of 18%, whilst Bindi 1 indicates ratios of 82%, also in the Early Jurassic. Maximum kerogen conversion occurs as a result of sediments within the project area reaching maximum maturation at the end of the Triassic (200 Ma), and are higher in the Gregory Sub-basin due to higher maturation obtained in the main oil window (0.7 – 1.0 %Ro, Figure 8.36).

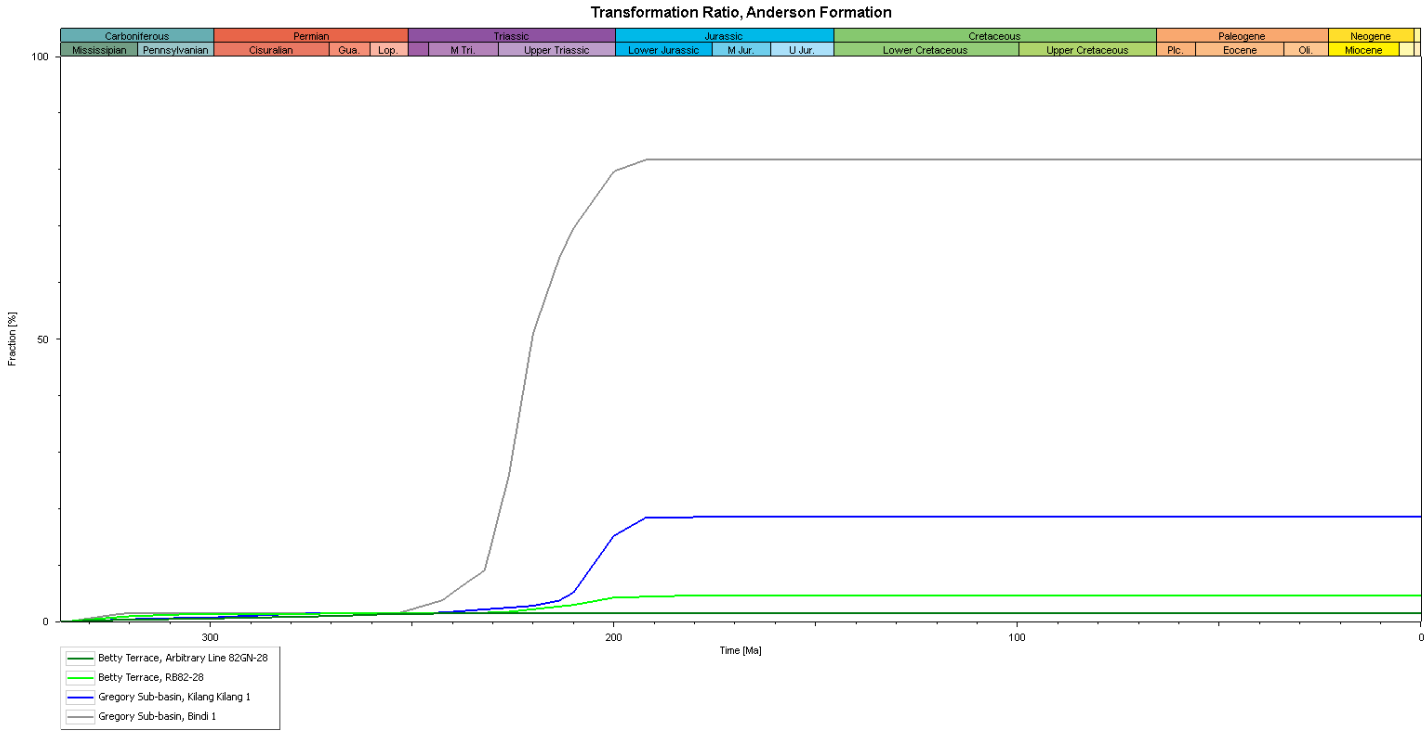

Figure 8.37. Anderson Formation transformation ratio vs time diagram

Hydrocarbon generation

Anderson Formation sediments in the Gregory Sub-basin commence generation in the Early Triassic (Figure 8.38) when the section enters the early oil window (0.55 – 0.7 %Ro). Generation rates for the Anderson are low (0.002 mg HC/g TOC/Ma). Peak generation occurs in the Late Triassic (220 Ma) once sediments enter the main oil window (0.7 – 1.0 %Ro). Betty Terrace sediments generate hydrocarbons at relatively low rates, where generation reaches a maximum at the end of the Triassic (200 Ma).

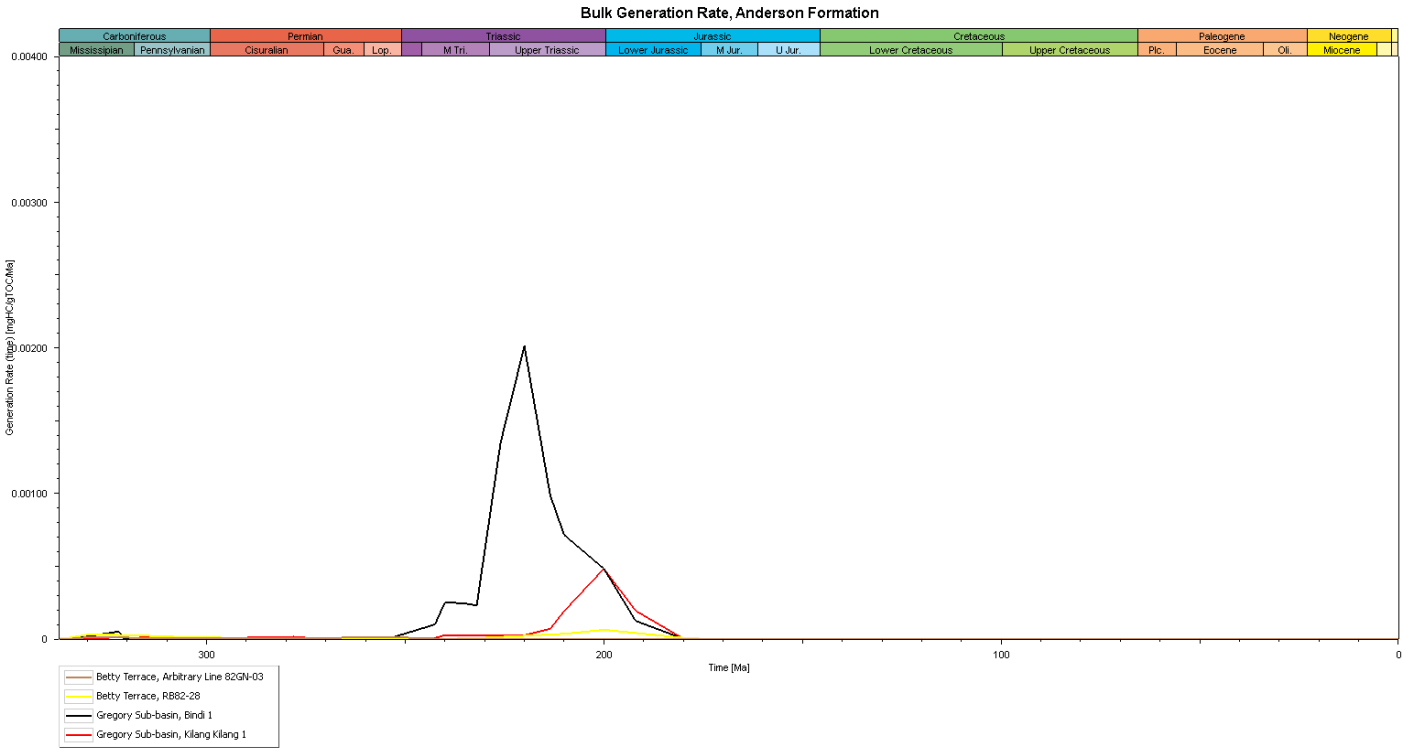

Figure 8.38. Anderson Formation generation rate vs time diagram.

Hydrocarbon expulsion

Anderson Formation sediments within the Gregory sub-basin expel hydrocarbons commencing in the Late Triassic (216 Ma), 36 My after sediments commenced generation (Figure 8.39). Results indicate that expulsion ceases in the Early Jurassic (192 Ma), once saturation levels fall below the expulsion threshold.

Figure 8.39 illustrates that Anderson Formation sediments on the Betty Terrace commence expulsion in the Pennsylvanian (Late Carboniferous, 320 Ma), however this is likely an anomaly in the model, because Betty Terrace generation is below the expulsion threshold at 200 Ma. No meaningful expulsion is interpreted here.

Further, Gregory Sub-basin sediments are the only region to achieve TR over 50%, thus initiating generation. The Anderson Formation on the Betty Terrace and Balgo Terrace only reaches the early oil window (0.55 – 0.7 %Ro) at peak maturity in the Late Triassic (200 Ma).

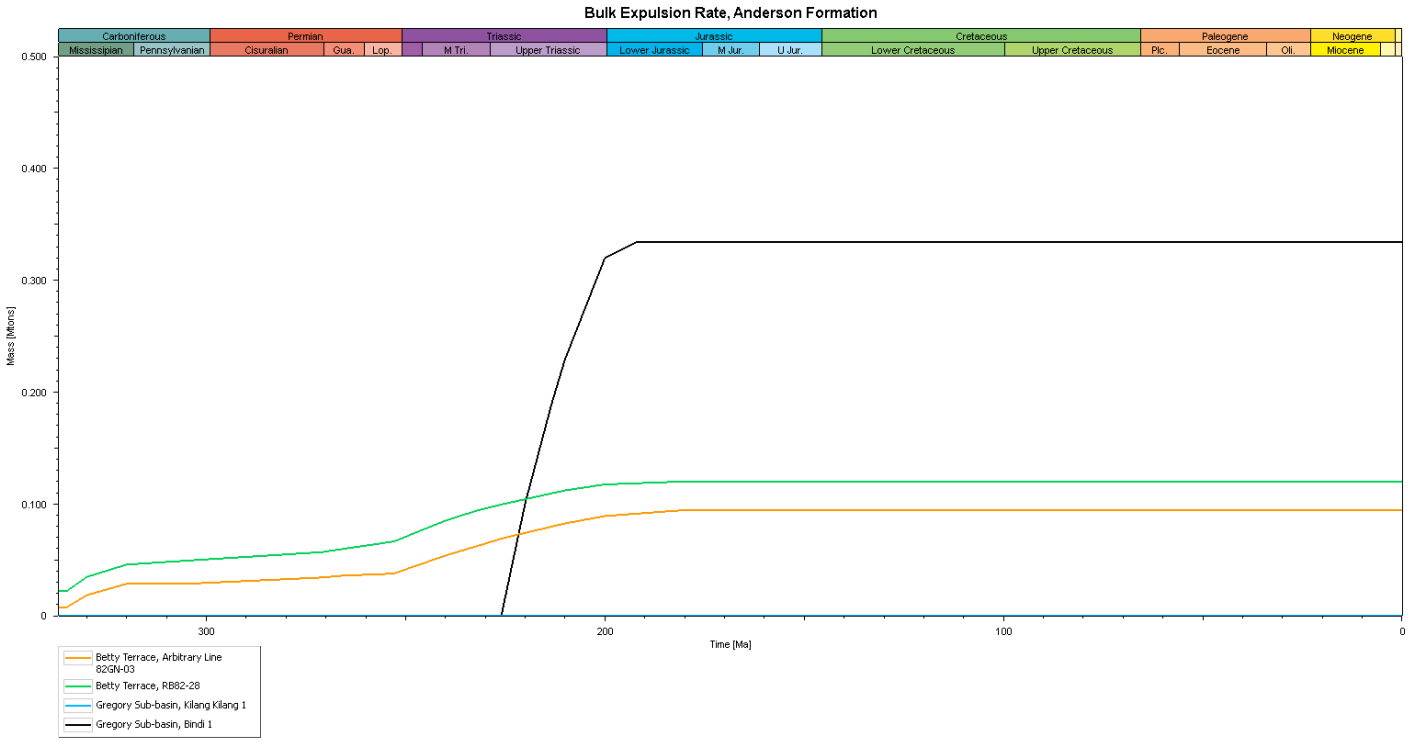

Figure 8.39. Anderson Formation expulsion rate vs time diagram.

8.6.8 *Modelling Results – Noonkanbah Formation*

Source rock maturity

There is slight variability in maturation of the Noonkanbah Formation between the Gregory Sub-basin and Betty Terrace (Figure 8.40). Wells in the Gregory Sub-basin undergo the highest subsidence rates, likely due to rapid accommodation generation developing along the Stansmore Fault. Wells on the Betty Terrace undergo shallower maturation gradients relative to other provinces. All wells undergo slow subsidence in the Lopingian (Late Permian). Subsidence increases at 250 Ma, due to the onset of rifting in the Triassic Fitzroy Movement, where sediments mature through the Early and Middle Triassic (250 – 230 Ma). The Noonkanbah Formation undergoes a second period of burial in the Late Triassic (210 – 200 Ma), however Bindi 1 undergoes earlier burial commencing from 232 Ma. TWT structure mapping on the Near Top Noonkanbah Formation (Figure 6.11) shows that Bindi 1 is situated in an area of focused subsidence, timing of which is indicated in Figure 8.15 and Figure 8.40. The Noonkanbah Formation in the Gregory Sub-basin reaches the early oil window (0.55 – 0.7 %Ro) in the Late Triassic (200Ma, and Bindi 1 from 215 Ma). Wells on the Betty Terrace remain immature (0.0 – 0.55 %Ro).

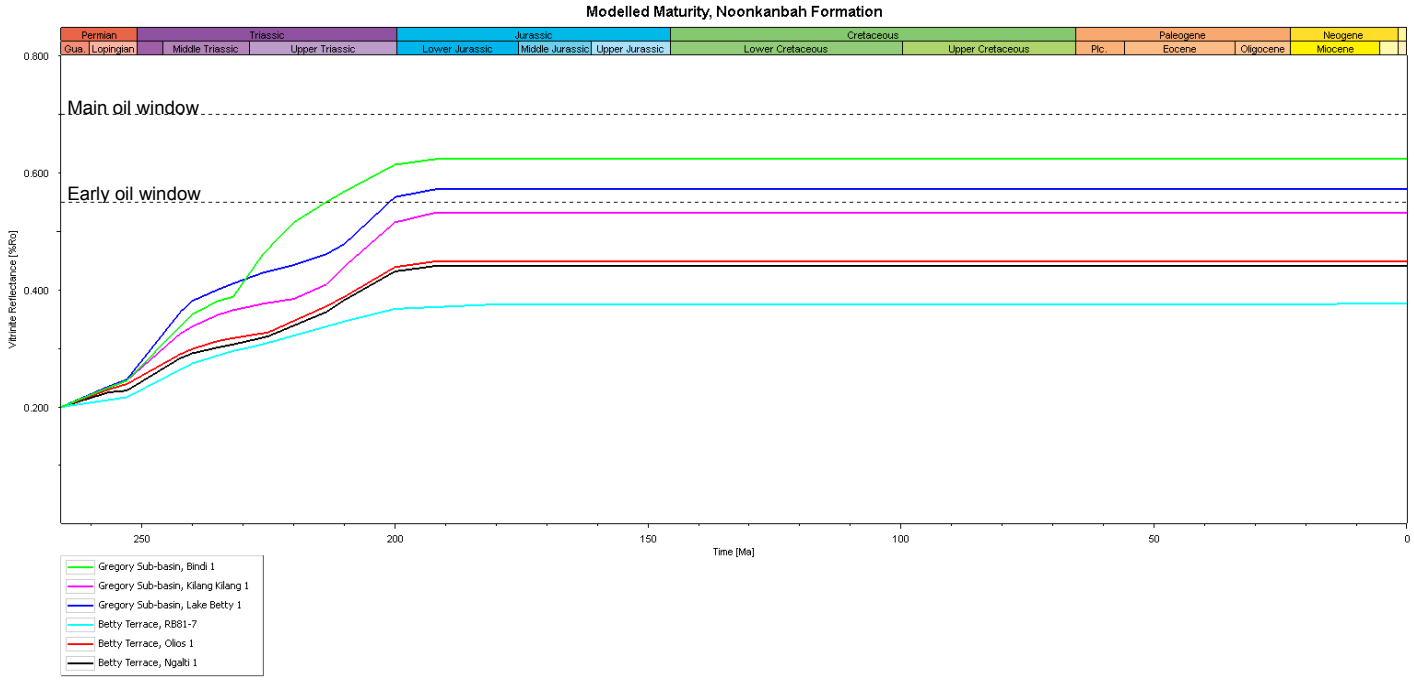

Figure 8.40. Noonkanbah Formation maturity vs time diagram.

Transformation ratios

Modelling results (Figure 8.41) indicate that Noonkanbah Formation kerogens have not undergone significant cracking to petroleum, with TR less than 10%. Low levels (2%) of conversion occur in the Early Triassic (245 Ma), and up to 4% is converted within Gregory Sub-basin sediments at peak maturity in the Late Triassic (200 Ma). Low TR is attributed to the largely immature character of the Noonkanbah Formation, and explains absence of meaningful generation (figures 8.41 and 8.42). The 4% TR in the Late Triassic reflects early oil window maturation in the Gregory sub-basin at the time.

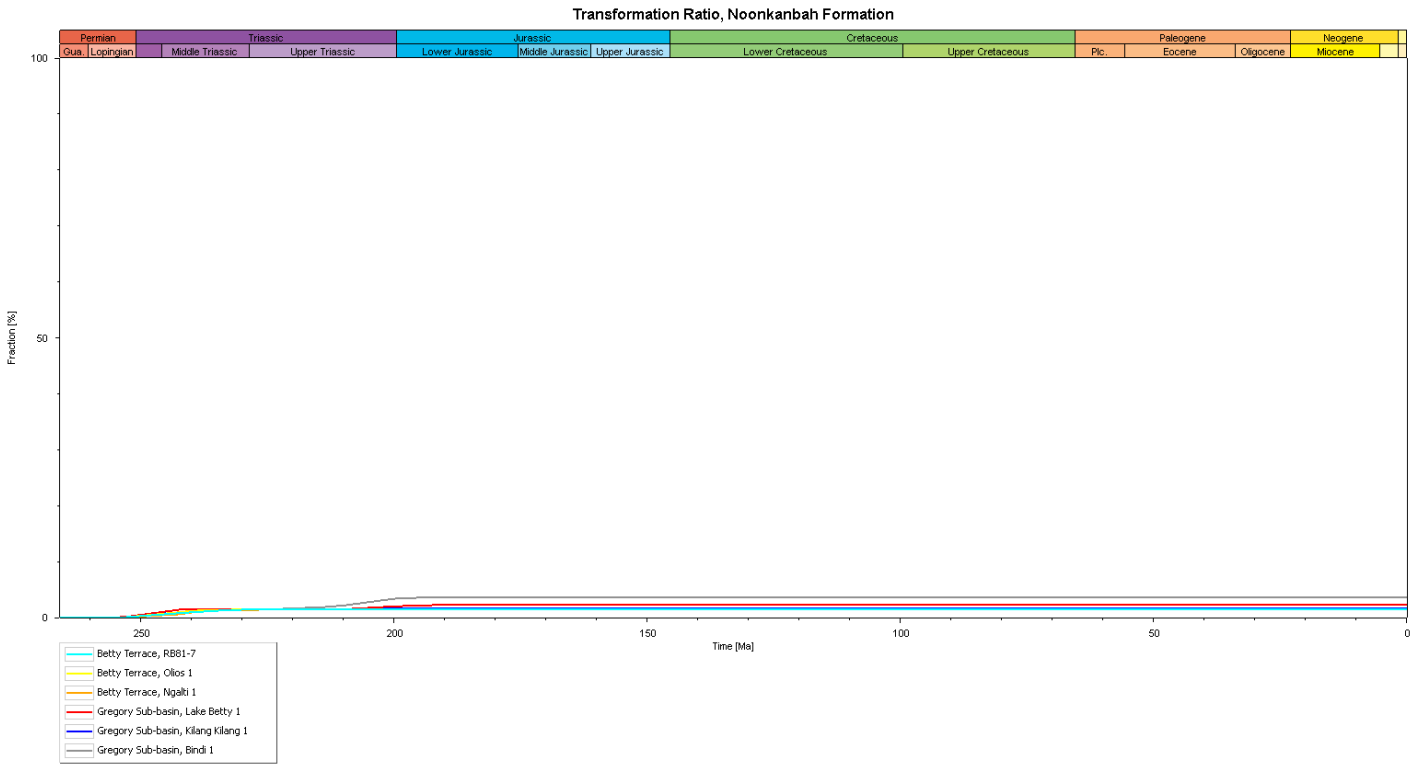

Figure 8.41. Noonkanbah Formation transformation ratio vs time diagram.

Hydrocarbon generation

Modelling results confirm that hydrocarbon generation from the Noonkanbah Formation does not meaningfully commence in the project area. Figure 8.42, shown here for completeness, indicates extremely small generation rates (maximum 0.000046 mg HC/g TOC/Ma) in accordance with timing of subsidence (Figure 8.40). The model is meaningless as the Noonkanbah Formation within the project area only reaches the early oil window (0.55 – 0.7 %Ro) at peak maturity in the Triassic, and is therefore deemed to be non-generative.

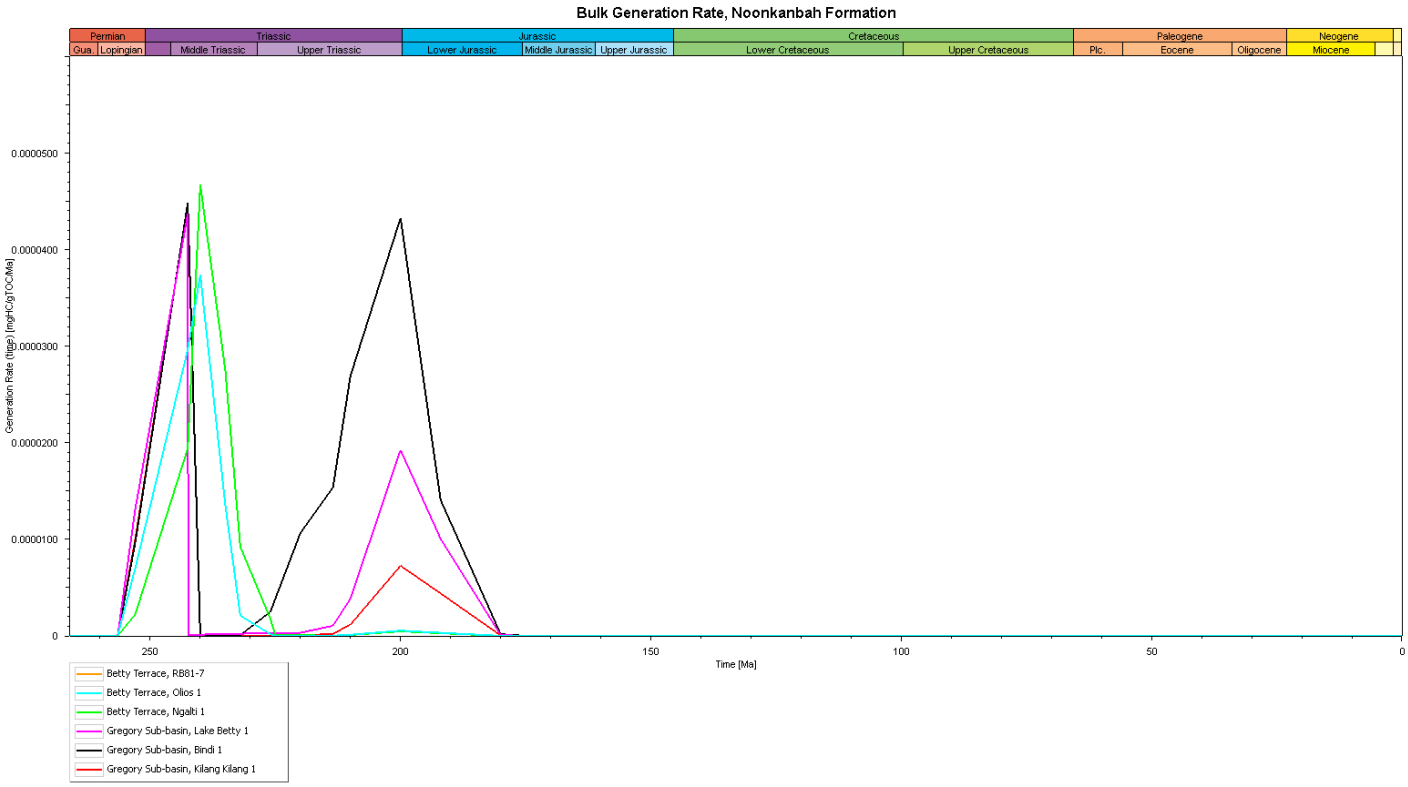

Figure 8.42. Noonkanbah Formation generation rate vs time diagram.

Hydrocarbon expulsion

Modelling results, shown here for completeness (Figure 8.43), demonstrate that the Noonkanbah Formation does not expel hydrocarbons within the project area. The Noonkanbah Formation does not generate hydrocarbons (Figure 8.42) to induce expulsion.

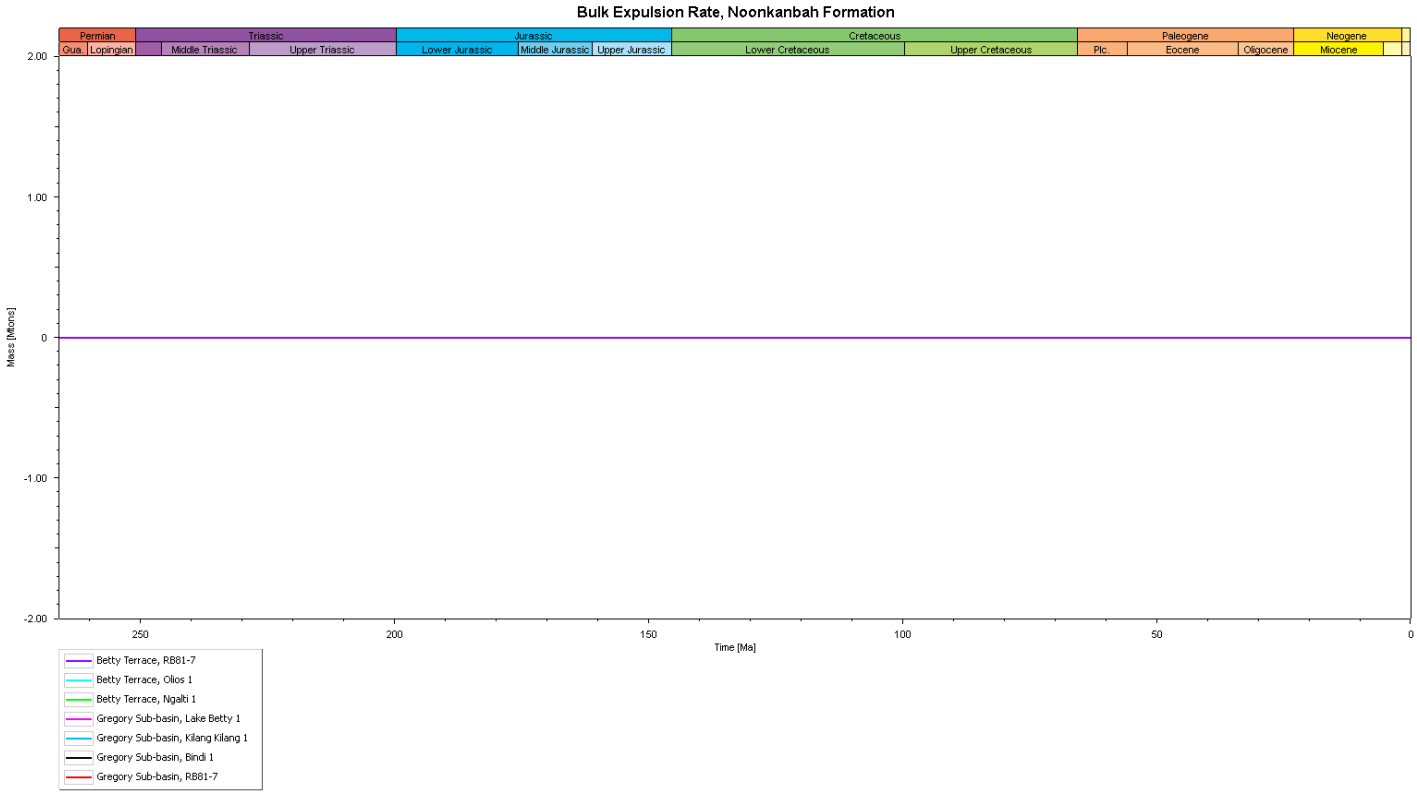

Figure 8.43. Noonkanbah Formation expulsion rate vs time diagram.

8.7 Hydrocarbon Accumulation Analysis

PetroMod migration and accumulation analysis is a valuable aspect of 2D basin modelling that can provide insights into hydrocarbon migration pathways and areas of hypothetical hydrocarbon buildups. 2D models were simulated (Figure 8.14) to test possible hydrocarbon accumulations within structural traps identified in Chapter 6.2.4.

Volumes: A word of caution

It is important to note here, that whilst occurrences of accumulations provides insights and validity to favourable petroleum system evolution, the following should be understood:

- Structures that host simulated accumulations were defined using simple depth conversion techniques (Chapter 5.5.1) that may not correctly accommodate effects of velocity of overlying stratigraphy on to underlying rocks. The Laurel Formation is an example of this possibility. A more detailed depth conversion is advised.
- Source rock TOC and Rock Eval Pyrolysis data is averaged in the models, which can artificially increase the generation and expulsion abilities of source rock intervals, hence volume.
- The Devonian aged section contains several layers of stratigraphy that are not sub-divided in models constructed in this study. For example, the thick Devonian section on RB82-28 is configured to represent the Gogo Formation (averaging 0.5% TOC according to available data). This induces the assumption that the whole Devonian aged section is at 0.5% TOC, rather than a relatively thin 0.5% TOC layer and other layers with possibly 0% TOC.
- Ages that are applied in Fault Definition are relative estimates from seismic interpretation and published literature, and could benefit from a more detailed consideration.
- Volumes assume a constant reservoir geometry 500 metres out of the 2D model plane.
- 2D models are unable to detect 3D mappable closure, and assume that trapping geometries are valid to support an accumulation if they are detected within the 2D plane.

8.7.1 *Modelling Results*

RB81-7

Regional seismic line RB81-7 was principally built to model the evolution of petroleum systems across all tectonic regions, and secondly to test the possibility of accumulations occurring at trap D and E (Figure 6.10).

Results illustrate that no present day accumulations were simulated within trap D or E. A small gas accumulation was simulated to be present (Figure 8.44) within the Poole Sandstone on a structural high in the Gregory Sub-basin (27°S 10’ 06”E, 127° 05’ 44”E). Kilang Kilang 1 tested the flank of the structure (4.7 km down dip to the southwest - out of the plane of the model), however no hydrocarbon shows were noted at the Poole Sandstone level.

The RB81-7 simulation indicates, that although the Kilang Kilang 1 well was dry, the simulation is still valid because it predicts a small accumulation at the crestal position of the structure, which is not detectable at the Kilang Kilang 1 location. TWT structure mapping on the Near Top Poole Sandstone (Figure 6.12) reveals that there is a subtle mappable closure at in this location.

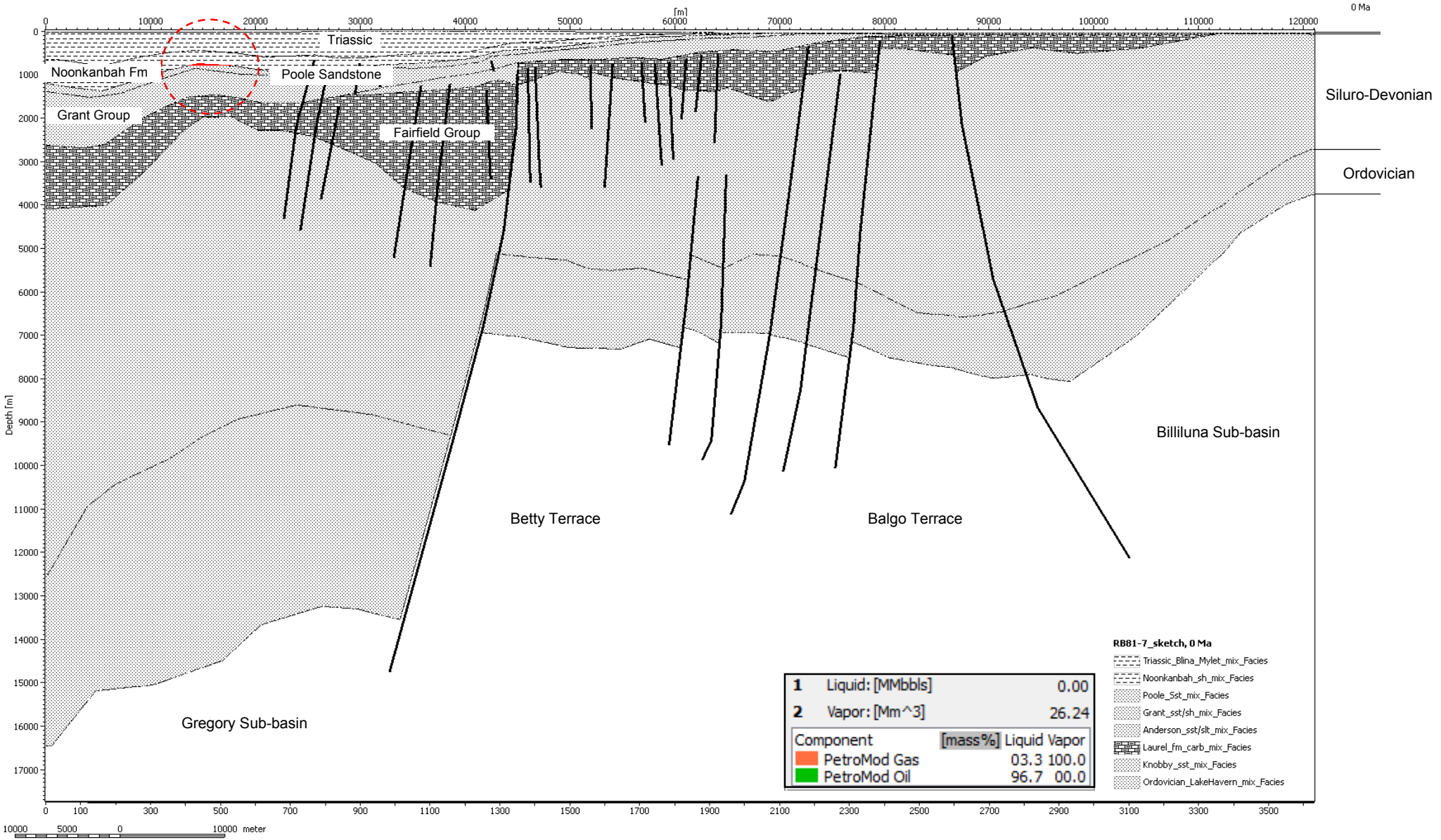

Figure 8.44. RB81-7 2D model at present day. Results show a small gas accumulation in the Poole Sandstone.

Arbitrary Line 82GN-03, S85LM-08, S85LM-08A

Arbitrary Line 82GN-03 was built to simulate the evolution of petroleum systems in the northern study area, and to also test for any accumulations within Trap B (Figure 6.10). Modelling results indicate the preservation of two small gas accumulations within the Devonian section and Poole Sandstone over Trap B (Figure 8.45). Results also indicate six large oil accumulations within the Devonian and Poole Sandstone in an area up-dip, across the Hinge Fault on the Betty Terrace and Balgo Terrace (19°S 32’ 29”E, 126° 31’ 23”E, Figure 6.10, and Figure 6.16). Trap B and the up-dip accumulations are untested by exploration drilling though there are a number of surrounding wells.

TWT structure on the Near Top Poole Sandstone reveals no mappable closure is present at this location, as closure only develops in Carboniferous and older stratigraphy. Therefore, the two Poole Sandstone accumulations are invalid as the model incorrectly assumes that trapping geometries have developed out of the 2D plane.

TWT structure mapping shows apparent fault bound closure at Trap B in pre-Carboniferous stratigraphy, so the model correctly assumes apparent closure for the Devonian gas accumulation in Trap B. Closure is more difficult to justify for accumulations on the Betty and Balgo Terrace, because the TWT interpretation (Figure 6.16) shows a likely leakage path to the north. There is a small apparent-time structural closure in the footwall of the Stansmore Fault that may support the validity of the southern-most Devonian accumulation. The modelling of other Devonian accumulations are therefore questionable in terms of out-of-plane trap assumptions.

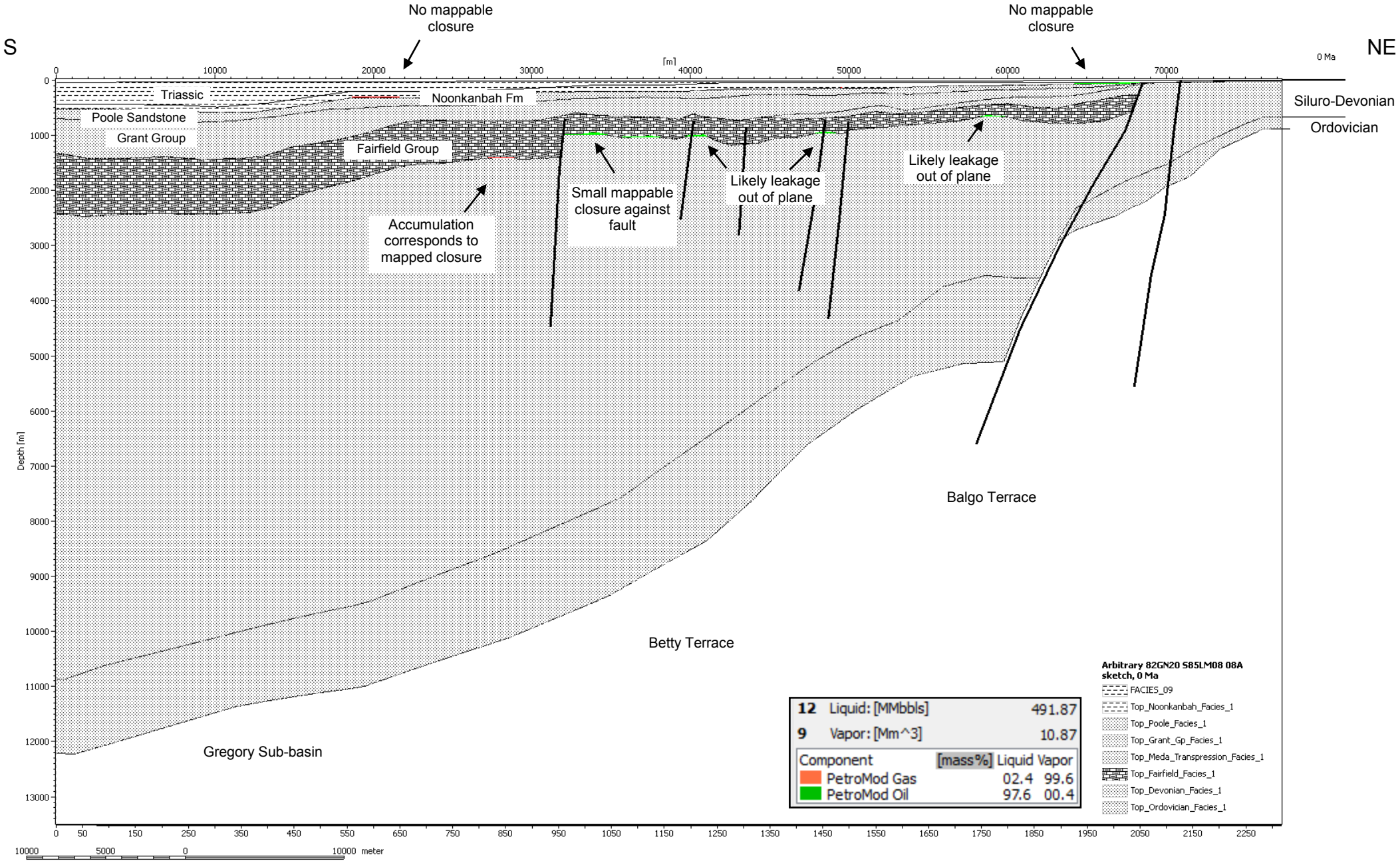

Figure 8.45. Arbitrary line 82GN-20 2D model. Results indicate sizable oil accumulations however a number of them are invalid as they are located within invalid structural traps.

RB82-28

Model RB82-28 was primarily built to test a large apparent time structural closure at Trap A in the southwestern project area. This large apparent structure has not been tested by exploration drilling. Results indicate eight large oil accumulations in Devonian stratigraphy and one oil accumulation with a gas cap in the Poole Sandstone.

No mappable closure exists for Poole Sandstone stratigraphy, so trap geometries in the Poole Sandstone are invalid assumptions in the model. Most of the closure in the Devonian sequence that is assumed by the model is validated by TWT structure maps. Closure is provided by a series of tilted fault blocks across a broad anticline. Note that faulting in the model is more detailed than on TWT maps (small scale faulting was not correlated across the study area) but all faulting is observed to occur within regional closure across the broad anticline. Apparent trap validity is highlighted in Figure 8.46.

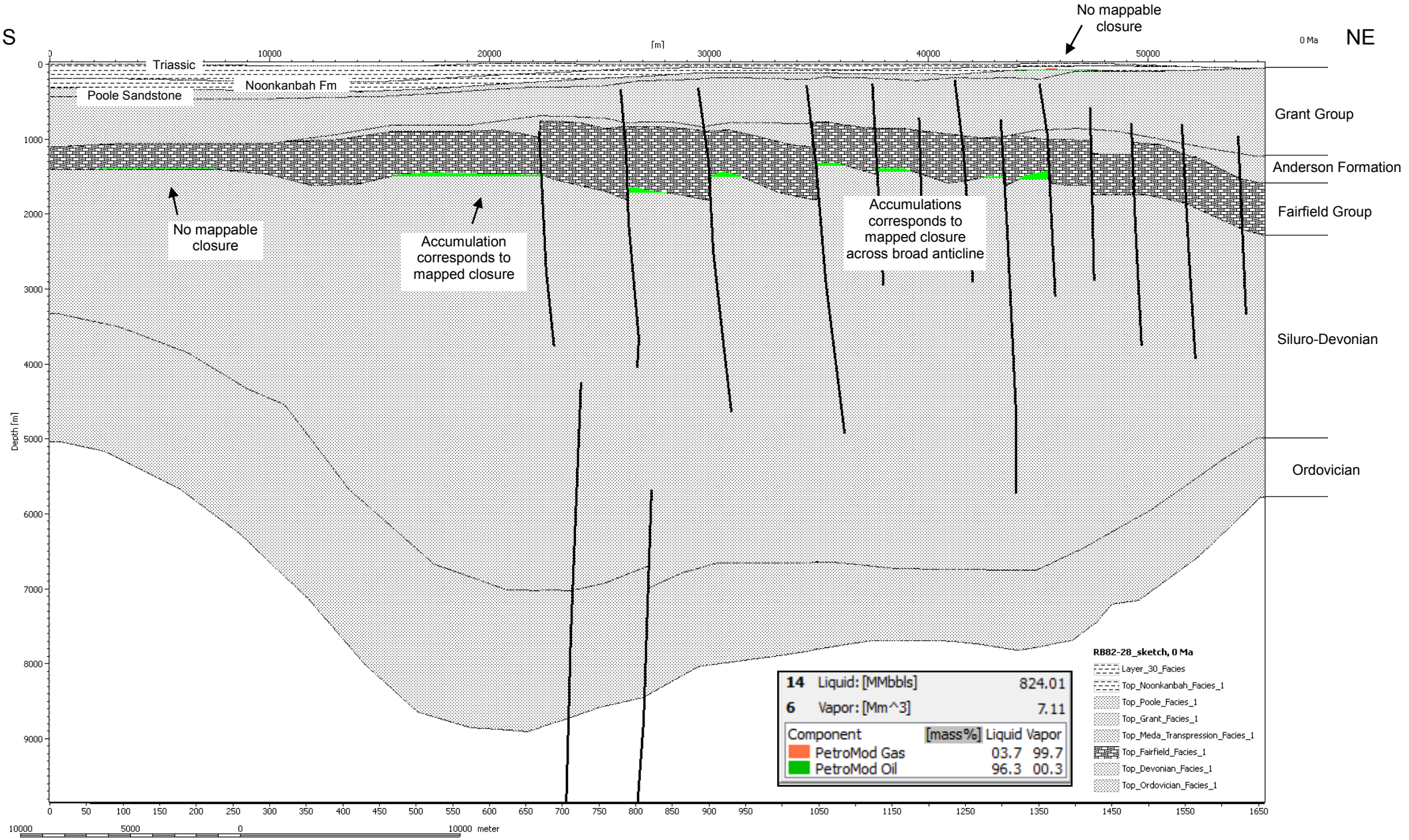

Figure 8.46. RB82-28 present day 2D model. Results indicate a large oil accumulation across a broadly folded anticline that corresponds to a mapped closure on seismic.

RB81-10

2D model RB81-10 was principally built to simulate the evolution of petroleum systems across the Betty Terrace. The model also intersects the southwestern portion of Trap A (Figure 6.10). Results indicate a moderate gas accumulation in the Poole Sandstone within the Trap A area, however no mappable closure exists at this location within the Poole Sandstone, so the model incorrectly assumes trapping geometry (Figure 8.47).

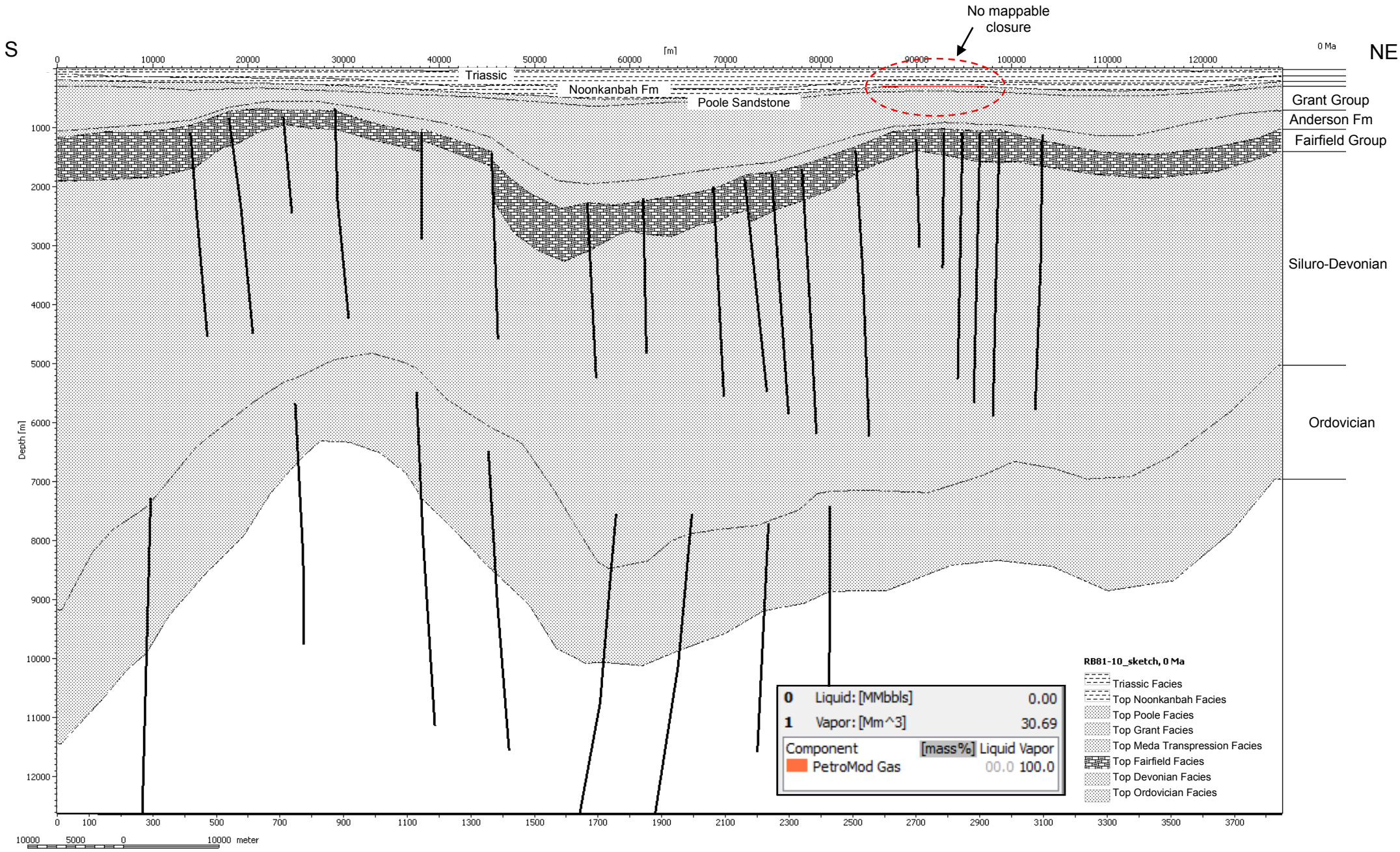

Figure 8.47. RB81-10 present day 2D model. Results indicate a small gas accumulation however it is not located within a mapped closure.

8.8 Summary of Results

This Chapter accompanies Chapter 7 to complete the source rock characterization of the project area. In this Chapter, five 1D models were constructed at existing well locations (Lake Betty 1, Olios 1, Bindi 1, Ngalti 1 and Kilang Kilang 1; Figure 8.3) and calibrated to existing thermal maturity measurements. Four 2D models were also constructed across 2D seismic lines in the project area (RB81-7, RB81-10, RB82-28 and Arbitrary line 82GN-03/S85LM-08/S85LM-08A; Figure 8.3). The main purpose of modelling was to characterise the thermal maturity of sediments within the Larapintine L2, L3, L4 and Gondwannan G1 petroleum systems, and to determine the timing of source rock hydrocarbon generation.

Apatite Fission Track Analysis (AFTA) was valuable in providing insight into the geological history and timing of thermal events. The incorporation of recent work by Duddy et. al., (2003) facilitated a thorough investigation into when petroleum system source rocks (The Goldwyer Formation, Bongabinni Member, Gogo Formation, Laurel Formation, Anderson Formation and Noonkanbah Formation) entered respective hydrocarbon production windows. Tables 8.10 and 8.11 summarise the results of this chapter, and also provide a useful quick-reference guide to accompany Table 7.13. Model RB82-28 (primarily built to test a large apparent time structural closure at Trap A), which is untested by exploration drilling to date, indicates eight large simulated oil accumulations in Devonian stratigraphy.

Petroleum System	Source rock	Geological province	Thermal maturity		Hydrocarbon product window	%Ro	TR%	Generation		Expels hydrocarbons	
			Attained by	Age (Ma)				From (Ma)	To (Ma)	From (Ma)	To (Ma)
Gondwannan G1	Noonkanbah Formation	Billiluna Sub-basin			Immature	< 0.5	No conversion	No meaningful generation		No expulsion	
		Balgo Terrace			Immature	< 0.5					
		Betty Terrace			Immature	< 0.5					
		Gregory Sub-basin	Late Triassic	200 - 215	Early oil window	0.55 - 0.7	2% conversion at 2445 Ma 4% conversion at 200 Ma				
Larapintine L4	Anderson Formation	Billiluna Sub-basin			Immature	< 0.5	No conversion	No generation		No expulsion	
		Balgo Terrace			Immature	< 0.5					
		Betty Terrace	Triassic	200	Generally immature. RB82-28 pseudo well indicates early oil window maturity where preserved	0.55 - 0.7	6% conversion at 192 Ma	Low generative period between 210 Ma - 190 Ma			
		Gregory Sub-basin	Middle Triassic Late Triassic	245 225 - 205	Early oil window Main oil window	0.55 - 0.7 0.7 - 1.0	Up to 82% conversion at 200 Ma	252 Ma, peak at 200 Ma	200 Ma	216 Ma	192 Ma
Larapintine L3	Laurel Formation	Billiluna Sub-basin			Immature	< 0.5	Effectively no conversion	No generation		No expulsion	
		Balgo Terrace	Late Triassic	200	Early oil window	0.55 - 0.7	Up to 10% conversion by 200 Ma	Low, brief period at 200 Ma		No expulsion	
		Betty Terrace	Late Triassic	200	Early oil window	0.55 - 0.7					
		Gregory Sub-basin	Late Permian Middle Triassic Late Triassic	252 240 200	Early oil window Main oil window Late oil window	0.55 - 0.7 0.7 - 1.0 1.0 - 1.3	69-97% conversion between 252 Ma to 200 Ma)	First phase commences 225 Ma Main phase commences 231 Ma	First phase ends 240 Ma Main phase ends 226 Ma to 180 Ma	200 Ma	192 Ma
	Gogo Formation	Billiluna Sub-basin	Mississippian	336	Main oil window	0.7 - 1.0	40% at 342 Ma 60-70% by 200 Ma	First phase commences 349 Ma Main phase commences 280 Ma	First phase ends 335 Ma Main phase ends 175 Ma	First phase commences 344 Ma Second phase commences 255 Ma	First phase ends 330 Ma Second phase ends 200 Ma
		Balgo Terrace	Mississippian Mississippian	336 330	Main oil window Late oil window	0.7 - 1.0 1.0 - 1.3	20.5% at 342 Ma 60-70% by 200 Ma				
		Betty Terrace	Mississippian Late Triassic	336 200	Main oil window Late oil window	0.7 - 1.0 1.0 - 1.3	<5% by 330 Ma 60-70% by 200 Ma				
		Gregory Sub-basin	Mississippian Middle Triassic	~ 336 240	Oil thru Wet gas window Dry gas window	1.3 - 2.0 2.0 - 4.0	79% by 330 Ma 100% by200 Ma				

Table 8.10. Summary of modelling results for the Gondwannan G1 and Larapintine L3 and L4 petroleum systems.

Petroleum System	Source rock	Geological province	Thermal maturity		Hydrocarbon product window	%Ro	TR%	Generation		Expels hydrocarbons	
			Attained by	Age (Ma)				From (Ma)	To (Ma)	From (Ma)	To (Ma)
Larapintine L2	Bongabinni Member	Billiluna Sub-basin	Ludlow	420	Early oil window	0.55 - 0.7	Conversion commences in Llandovery (436 Ma) 100% converted by Mississippian (350 Ma)	407	350	407	385
			Lochkovian	415 - 410	Main oil window	0.7 - 1.0					
			Early to Middle Devonian	402 - 390	Late oil window	1.0 - 1.3					
			Middle Devonian	389	Wet gas window	1.3 - 2.0					
			Mississippian	356	Dry gas window	2.0 - 4.0					
		Balgo Terrace	Ludlow	420	Early oil window	0.55 - 0.7					
			Lochkovian	415 - 410	Main oil window	0.7 - 1.0					
			Early to Middle Devonian	402 - 390	Late oil window	1.0 - 1.3					
			Late Devonian	375 - 360	Wet gas window	1.3 - 2.0					
			Mississippian	340	Dry gas window	2.0 - 4.0					
		Betty Terrace	Ludlow	420	Early oil window	0.55 - 0.7					
			Lochkovian	415 - 410	Main oil window	0.7 - 1.0					
			Early to Middle Devonian	402 - 390	Late oil window	1.0 - 1.3					
			Late Devonian	375 - 360	Wet gas window	1.3 - 2.0					
			Early Permian	295	Dry gas window	2.0 - 4.0					
		Gregory Sub-basin	Llandovery	435	Early oil window	0.55 - 0.7					
			Late Llandovery	430	Main oil window	0.7 - 1.0					
			Wenlock	425	Late oil window	1.0 - 1.3					
			Ludlow	418	Wet gas window	1.3 - 2.0					
			Early Devonian	402	Dry gas window	2.0 - 4.0					
			Mississippian	345	Overmature	4.0 >					
	Goldwyer Formation	Billiluna Sub-basin	Wenlock	427	Early oil window	0.55 - 0.7	Conversion commences in Llandovery (436 Ma) 100% by Mississippian (350 Ma)	437	346	436	385
			Pridoli - Lochkovian	~ 419	Main oil window	0.7 - 1.0					
			Early Devonian	407	Late oil window	1.0 - 1.3					
			Middle Devonian	397	Wet gas window	1.3 - 2.0					
			Late Devonian	370	Dry gas window	2.0 - 4.0					
		Balgo Terrace	Wenlock	427	Early oil window	0.55 - 0.7					
			Pridoli - Lochkovian	~ 419	Main oil window	0.7 - 1.0					
			Early Devonian	397	Late oil window	1.0 - 1.3					
			Late Devonian	380	Wet gas window	1.3 - 2.0					
			Mississippian	345 - 332	Dry gas window	2.0 - 4.0					
		Betty Terrace	Late Ordovician	450	Early oil window	0.55 - 0.7					
			Pridoli - Lochkovian	~ 419	Main oil window	0.7 - 1.0					
			Early Devonian	397	Late oil window	1.0 - 1.3					
			Late Devonian	380	Wet gas window	1.3 - 2.0					
			Mississippian	345 - 332	Dry gas window	2.0 - 4.0					
		Gregory Sub-basin	Late Ordovician	450	Early oil window	0.55 - 0.7					
			Llandovery	435	Main oil window	0.7 - 1.0					
			Wennlock	428	Late oil window	1.0 - 1.3					
			Ludlow	422	Wet gas window	1.3 - 2.0					
			Early Devonian	410	Dry gas window	2.0 - 4.0					
			Late Devonian	365	Overmature	4.0 >					

Table 8.11. Summary of results for the Larapintine L2 petroleum system.

9. Discussion – An Evaluation of Petroleum Systems in the Northeast Canning Basin

The Canning Basin contains sediments belonging to three major Palaeozoic petroleum systems: the Larapintine L2 (Ordovician – Silurian), Larapintine L3 and L4 (Devonian – early Carboniferous), and Gondwannan G1 and G2 (late Carboniferous – Permian) (Bradshaw et al, 1994). Determining the extent to which these petroleum systems are present and active within the study area was the primary goal of this study.

This Chapter aims to address unanswered questions concerning the petroleum prospectivity within the study area, such as:

- Why did key exploration wells fail to detect hydrocarbon accumulations?
- What can paleogeography predict about suitability of source rocks, reservoirs and seals?
- How does the timing of petroleum system evolution relate to prospectivity (petroleum system elements diagrams)?
- What play-types should be targeted within each petroleum system?
- What are the key recommendations that can help in reducing risk of exploring in the northeast Canning Basin?

9.1 Prospectivity – Are Active Petroleum Systems Present within the Northeast Canning Basin?

A synthesis of the analysis of reservoir quality and seal integrity (Chapter 4), hydrocarbon trapping configurations (Chapter 6), source rock richness (Chapter 7), and thermal maturity and timing of hydrocarbon generation and migration (Chapter 8) indicates that the exploration prospectivity within the study area is high risk. Stratigraphic and seismic frameworks (chapters 4 and 6) indicate that rocks belonging

to all three petroleum systems are present within the study area, but confidence that all the elements critical to dynamic petroleum systems are active across all three petroleum systems is lacking. Source rock richness and timing/migration appear to be the criteria of greatest exploration risk and contributed to the failure of 6 of the 7 dry holes drilled in the project area (Table 9.1). Structural integrity of the trap is the next greatest exploration risk and played a role in the failure of the 7th dry hole, and was also a contributing factor in 4 others. A lack of thermal maturity was only an issue in the shallowest petroleum system, the Permian Gondwannan G1. Reservoir and seal are criteria with the least exploration risk.

Although the Larapintine L2 petroleum system contains the world class source rock, the Ordovician (Llanvirn) Goldwyer Formation, paleogeographic facies reconstruction suggests that the Goldwyer is in a proximal depositional setting within the study area and characterised by organically lean sand-rich siliciclastic facies. In the Larapintine L3 and L4 petroleum system, the source rocks such as the Anderson, Laurel, and Gogo Formations are thermally mature, but are organically lean. Conversely, the main source rock in the Gondwannan G1 petroleum system, the Noonkanbah Formation, is organically rich, but thermally immature. The Triassic aged Fitzroy Movement created a structural overprint that imposes a significant threat to trap integrity of Carboniferous aged structures. Triassic aged structures may have developed marginally too late to trap hydrocarbons that generated at the time of peak thermal maturity in the Triassic.

Given the current geochemical dataset, hydrocarbon migration is required from basinal settings (for example the Gregory Sub-basin) to charge shelfal positions within the study area to consider all petroleum systems prospective (the only regional exception is the Larapintine L2 petroleum system, where a self-sourcing unconventional play could be targeted in a distal marine environment).

Synopsis of the Larapintine L2 Petroleum System

There are no wells drilled deep enough within the study area to directly test the exploration prospectivity of the Larapintine L2 petroleum system. However, analysis of regional 2D seismic data indicates that rocks of Ordovician-Silurian age are present in the subsurface across the project area. Petrophysical analysis of Lake Havern 1, which lies to the southwest of the study area, indicates good quality sandstone reservoirs and rocks with sealing potential are present within the Ordovician-Silurian stratigraphy. Projection of these results into the study area, along with the regional 2D seismic that defines large traps in the hanging wall of the Stansmore Fault, is encouraging for the prospectivity of the Larapintine L2 petroleum system. However, the petroleum system is likely inactive, for two reasons. Firstly, paleogeographic reconstructions for the Goldwyer Formation source rock (Figure 9.8) indicates that the Goldwyer Formation was deposited in a supra-tidal setting and the lithotypes that accumulated would have been sand-rich. The paleogeographic reconstruction suggests that the organically rich marine facies were deposited further basinward in the Gregory Sub-basin. Secondly, vitrinite-time diagrams and criterial moment charts created for the source rock (Figure 9.11) indicates that the Ordovician sediments rapidly mature through all hydrocarbon generative windows (expulsion concludes at 385 Ma), and thus predating the Late Devonian or Mississippian trap development. Hydrocarbons, if generated, are likely to have migrated out of the system.

Synopsis of the Larapintine L3 and L4 Petroleum System

Exploration prospectivity of the Larapintine L3 and L4 petroleum system is ranked higher than the Larapintine L2, however is also considered to be high risk. All wells within the project area intersect Larapintine L3 and L4 stratigraphy, providing tests of the petroleum system. Rocks of the L3 and L4 petroleum systems are present within the study area, indicated by seismic interpretation and well correlations (chapters 4, 5 and 6). Although several wells (for example Bindi 1 and Kilang Kilang 1; refer to Table 9.1) indicate that good quality reservoir rocks, optimal trapping configurations, and lithologies with probable sealing capacity are present, the petroleum systems are interpreted to be largely inactive, restricted by source rock organic richness. Source rock geochemical analysis indicates that the regional source rocks are lean; the Gogo

Formation averages 0.14% TOC (and averaging 1.25% TOC by Wulff, 1987), the Laurel Formation averages 0.56% TOC regionally and 0.46% TOC within the study area, and the Anderson Formation averages 0.14% TOC. Geochemical data from individual wells (Chapter 4.6.1) and paleogeographic reconstructions (Figure 4.27) indicate that source rock organic richness for the Laurel Formation is likely to increase basinward within the Gregory Sub-basin. Modelling (summarised in Table 8.10) advises that L3 and L4 source rocks are mature for hydrocarbon generation across the project area (though the Anderson Formation is immature on the Betty and Balgo Terraces, and within the oil window in the Gregory Sub-basin), therefore lateral hydrocarbon migration is required for any prospectivity to eventuate in the Larapintine L3 and L4 petroleum system.

Synopsis of the Gondwannan G1 and G2 Petroleum System

Exploration prospectivity of the Gondwannan G1 petroleum system is marginal. Analysis of regional data, and information provided by the Bindi 1 and Kilang Kilang 1 wells, have indicated that even though good quality reservoir rocks, sealing rocks and optimal traps are accounted for, the Gondwannan G1 petroleum system is largely inactive within the project area because it lacks a mature source rock. Geochemical analysis (Chapter 4.8.2) indicates that the Noonkanbah Formation is organically rich in the study area (averaging 2.17% TOC regionally and 1.69% TOC locally), however petroleum systems modelling demonstrates that the Noonkanbah Formation is immature across the Billiluna Sub-basin, Betty and Balgo Terraces, and only reaches the early oil window (0.55 – 0.7 %Ro) deeper within the Gregory Sub-basin (Figure 8.10). This requires that hydrocarbons must laterally migrate up dip from the Gregory Sub-basin to fill the shelfal reservoirs targeted within the study area. A scenario involving vertical hydrocarbon charge from the underlying Laurel Formation is also considered marginal because geochemical analysis indicates that the Laurel Formation is organically lean.

9.2 Analysis of Exploratory Tests within the Study Area

Nine exploration wells have been drilled within the project area. Selenops 1 and Atrax 1 were purely stratigraphic tests and did not target any hydrocarbon accumulations. The remaining seven wells were dry (summarised in Table 9.1). A dry hole analysis of these wells indicates that source rock richness and timing/migration are the most common reason for well failure (Table 9.1). Structural integrity of the trap is the second most common reason for failure followed by seal reliability. Thermal maturity was a contributor to well failure only in the Gondwannan G1 and G2 petroleum system. Reservoir development was found to never impact well failure and is thus considered the criterion of lowest exploration risk. A detailed summary of the dry hole analysis for each of the wells drilled within the project area is presented herein.

Well	Larapintine L2					Larapintine L3 / L4						Gondwannan G1 / G2					
	Source	Res.	Seal.	Trap	Tim/Mig.	Source	Res.	Seal	Trap	Tim/Mig.		Source	Res.	Seal	Trap	Tim/Mig.	
Lake Betty 1						✓	✓	-	✓	✖	✖						
Lanagan 1						✖	✓	✓	✖	✓	✖						
Ngalti 1	No wells intersect					✖	✓	✓	✖	✓	✓						
Lawford 1	Larapintine L2					✖	✓	✓	✓	✖	✖						
Olios 1	stratigraphy					✓	✖	✓	✖	✓	✖						
Selenops 1	Stratigraphic test - no targeted closure																
Atrax 1	Stratigraphic test - no targeted closure																
Bindi 1						✖	✓	✓	✓	✖	✖	✓	✖	✓	✓	✓	✖
Kilang Kilang 1						✖	✓	✓	✓	✓	✖	✓	✖	✓	✓	✓	✓

Table 9.1. Summary of exploratory tests within the project area, highlighting reasons for failure.

No wells within the project area drilled deep enough to intersect Larapintine L2 petroleum system stratigraphy (Ordovician – Silurian). All wells tested the Larapintine L3/L4, but Bindi 1 and Kilang Kilang 1 wells also tested the Gondwannan G1/G2 petroleum system.

9.2.1 *Lake Betty 1*

Lake Betty 1 was drilled to primarily test the Devonian Pillara and Ordovician Nita carbonates, and secondly to test the Carboniferous Laurel Formation, in an interpreted fault-bound 3-way structural closure defined on poor quality 2D seismic data (Figure 9.1). The well reached total depth in the Devonian Poulton Formation at 3145.8 mRT, but did not reach the Ordovician Nita carbonate. The Devonian Pillara Carbonate was absent because of normal faulting (Crank, 1972), such that the well did not test any of the primary objectives. Lake Betty 1 encountered a gas show in Laurel Formation sandstones; totalling 78 units of C1.

Geophysical logs confirm the presence of Laurel Formation sandstones and also the overlying Laurel Formation shales that suitably seal the reservoir. The Laurel Formation source rock at Lake Betty 1 has zones that are organically rich (1.16% to 3.29% TOC between 1660 – 2200 mRT), and modelling indicates that the source rock reaches the oil window (0.7 – 1.0 %Ro) in the Gregory Sub-basin during the Triassic; hence oil was expected, but a show of dry gas was observed.

Poor resolution of the controlling fault on the 2D seismic data, coupled with the uncertainty of the timing on the fault reactivation poses a serious question on the integrity of the structural closure. It is possible that the fault was reactivated during the late Triassic/early Jurassic Fitzroy compressional phase which post-dates the maturation of the Laurel Formation source rock. In conclusion, Lake Betty 1 may not have tested a valid structural closure.

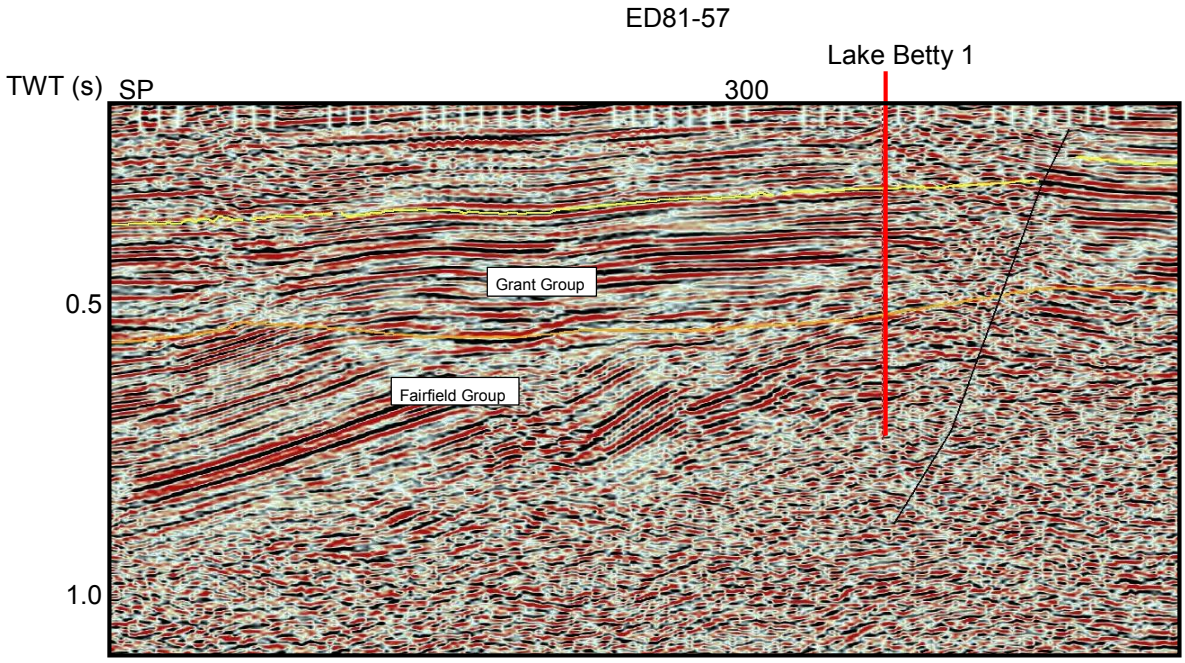

Figure 9.1. The Lake Betty 1 structure on 2D seismic.

The above analysis indicates that the reasons for Lake Betty 1 failure are;

- Integrity of the structural closure.
- Timing of the fault reactivation post-dating the thermal maturation of the Laurel source rock.
- The well failed to intersect the primary Devonian reservoir, and was not drilled deep enough for Ordovician stratigraphy.

9.2.2 *Lanagan 1*

Lanagan 1 drilled a seismically valid large horst related anticline in the (redefined) Gregory Sub-basin. The primary target was the Carboniferous Laurel Formation and Devonian Knobby Sandstone reservoirs. No hydrocarbon shows were observed other than background gas (maximum 10 units) during drilling. Lanagan 1 confirmed the presence of good quality reservoir rocks in the Knobby Sandstone and Laurel Formation. Geophysical logs (Figure 4.32) indicate that the Grant Group B member seal is present, though seismic (Figure 9.2) demonstrates that there may be

insufficient juxtaposition seal across faults allowing lateral leakage out of the Laurel Formation. Impermeable Laurel Formation microcrystalline limestones are assumed to be sufficient to cap the Knobby Sandstone reservoir unit.

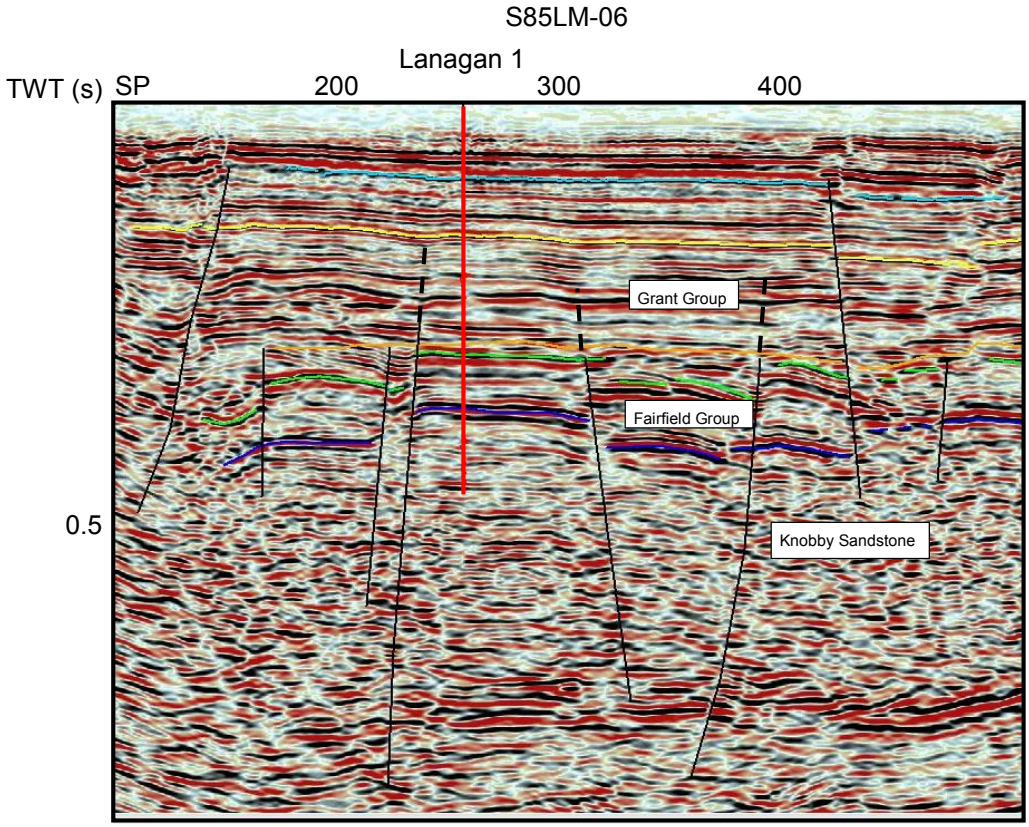

Figure 9.2. The Lanagan 1 structure on 2D seismic.

The Laurel Formation source rock is regionally organically lean (though increases in organic contents basinward) and thermally mature for oil in the Gregory Sub-basin (Table 8.10), thus migration from the Sub-basin is required, which is within achievable distances.

TWT structure on the Near Top Fairfield Group (Figure 6.15) confirms that Lanagan 1 is located in the footwall of a large listric fault. The gas show in the Laurel Formation is likely sourced from Devonian rocks (which are mature for gas generation). This indicates that there may be a migration problem at Lanagan 1. The

listric fault immediately south of Lanagan 1 might be an impermeable migration barrier causing hydrocarbons to migrate around the fault.

The above analysis indicates that the reasons for failure at Lanagan 1 are:

- Absence of seal to cap to Laurel Formation
- Preferential migration around an impermeable fault
- Regionally lean Laurel Formation source rocks.

9.2.3 *Ngalti 1*

Ngalti 1 was drilled to test a 3-way fault bound closure defined on 2D seismic data at the Knobby Sandstone level on the Balgo Terrace (Figure 9.3). No hydrocarbon shows were observed. The well confirmed the presence of good quality reservoir rocks in the Knobby Sandstone. The well intersected 271 metres of cryptocrystalline Laurel Formation, suggested by geophysical logs (Figure 4.25) to be tight. However, the juxtaposition fault seal required across the fault was likely porous Anderson Formation siliciclastics. Lack of lateral seal was a contributing factor to well failure.

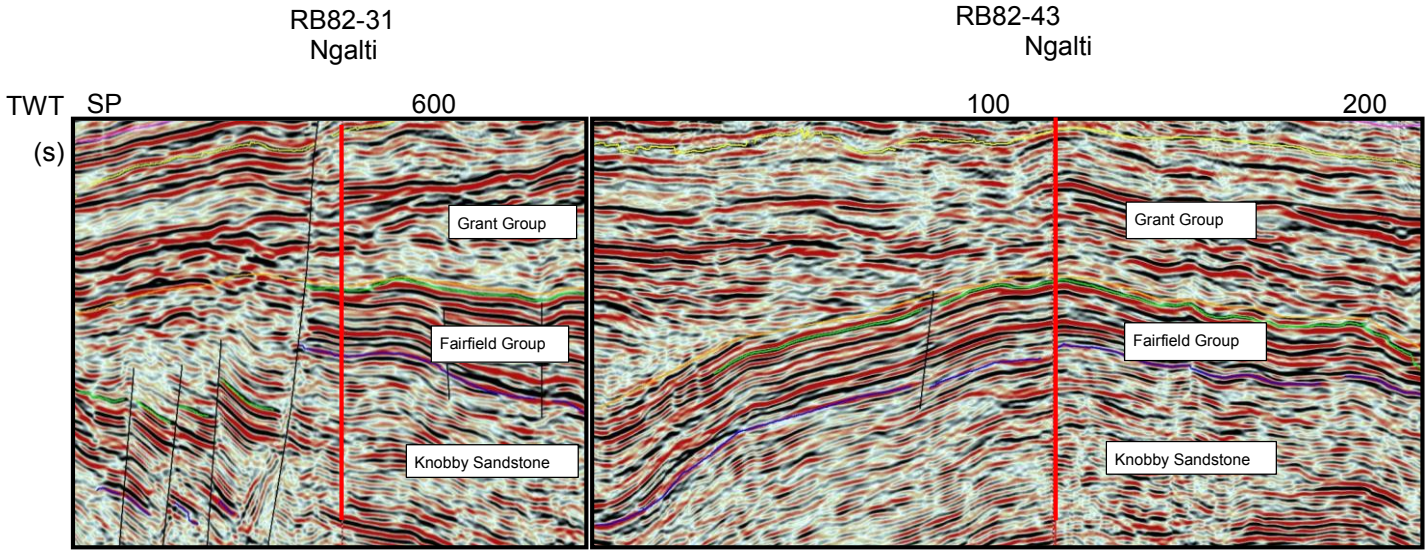

Figure 9.3. The Ngalti 1 structure on 2D seismic. Dip line on left, strike line image on right.

Source rock charge concerns the presence of the Gogo Formation in this portion of the study area, which is unknown. Given that no shows were observed; it seems that an absence of charge is a key reason for failure.

The above analysis indicates that the reasons for Ngalti 1 failure are:

- Absence of source rock charge;
- Failure to sufficiently acknowledge the presence of the porous Anderson Formation sandstones across the fault, thus an absence of lateral seal;

9.2.4 *Lawford 1*

Lawford 1 was drilled on a 4-way dip-closed anticline that was defined on a broad 2D seismic grid in the Gregory Sub-basin (Figure 9.4). The structure developed in the Carboniferous, but takes its present day form due to Triassic wrench faulting. The well confirmed good quality Carboniferous Laurel Formation and Anderson Formation reservoirs, and a thick preserved Anderson Formation intersection suggests the interbedded shales appropriately seal the underlying units. The paleogeographic location of the well (basinal setting) also points to higher shale content for Anderson Formation seal. No hydrocarbon shows were observed throughout drilling.

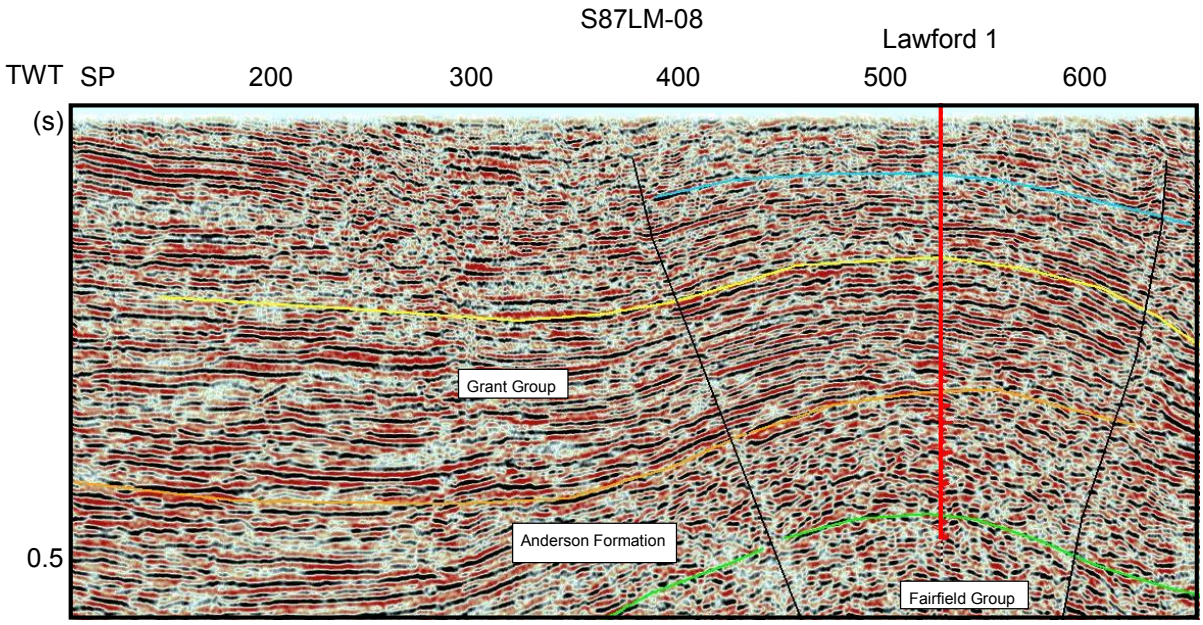

Figure 9.4. The Lawford 1 structure on 2D seismic.

The Anderson Formation and Laurel Formation are within the oil window and the Devonian Gogo Formation is within the dry gas window in the Gregory Sub-basin. Evidence of hydrocarbon generation was not observed by fluorescence or staining through the Laurel Formation and Anderson Formation, therefore a more likely scenario is that the source rocks are lean. Lawford 1 is located in a basinal position close to the hydrocarbon kitchen, thus migration of hydrocarbons should not be an issue.

The above analysis indicates that the reasons for failure at Lawford 1 are:

- Structural integrity because the closure is defined by a very broad 2D seismic grid.
- Timing of hydrocarbon migration could also be in doubt because, although the structure initially formed prior to the Carboniferous Meda Transpression, it was reactivated by the Triassic Fitzroy Movement potentially breaching the structure.

- Alternatively, the source rocks may be lean.

9.2.5 *Olios 1*

Olios 1 drilled a seismically-defined, fault bound 2-way horst block on the Betty Terrace thought to have developed during the Carboniferous, to test Devonian Carbonate reservoirs (Figure 9.5). Subtle disturbance in the overlying Grant Group and also small throws along the up-dip bounding fault indicate that Triassic episodes likely influenced the final geometry (potentially reactivating the sealing faults).

The well reached total depth in the Knobby Sandstone after no Devonian Carbonate reservoir was intersected. The well confirms the presence of good quality reservoir rocks in the Carboniferous Laurel Formation clastic section (sonic porosities in the 20% range, Figure 4.28), and confirms the Knobby Sandstone has excellent reservoir quality at this location (sonic porosities in the 10 – 20% range, Figure 4.23). Hydrocarbon shows were observed during drilling:

- Faint petroliferous odor and faint oil stain in the upper Laurel Formation;
- Gas shows over Laurel Carbonate member (1055 mRT to 1430 mRT); peak 113 units C1;
- Faint petroliferous odor and strong fluorescence in the Laurel Carbonate member; and
- Gas shows over the Knobby Sandstone reaching 577 units C1. Gas continued until the well reached total depth.

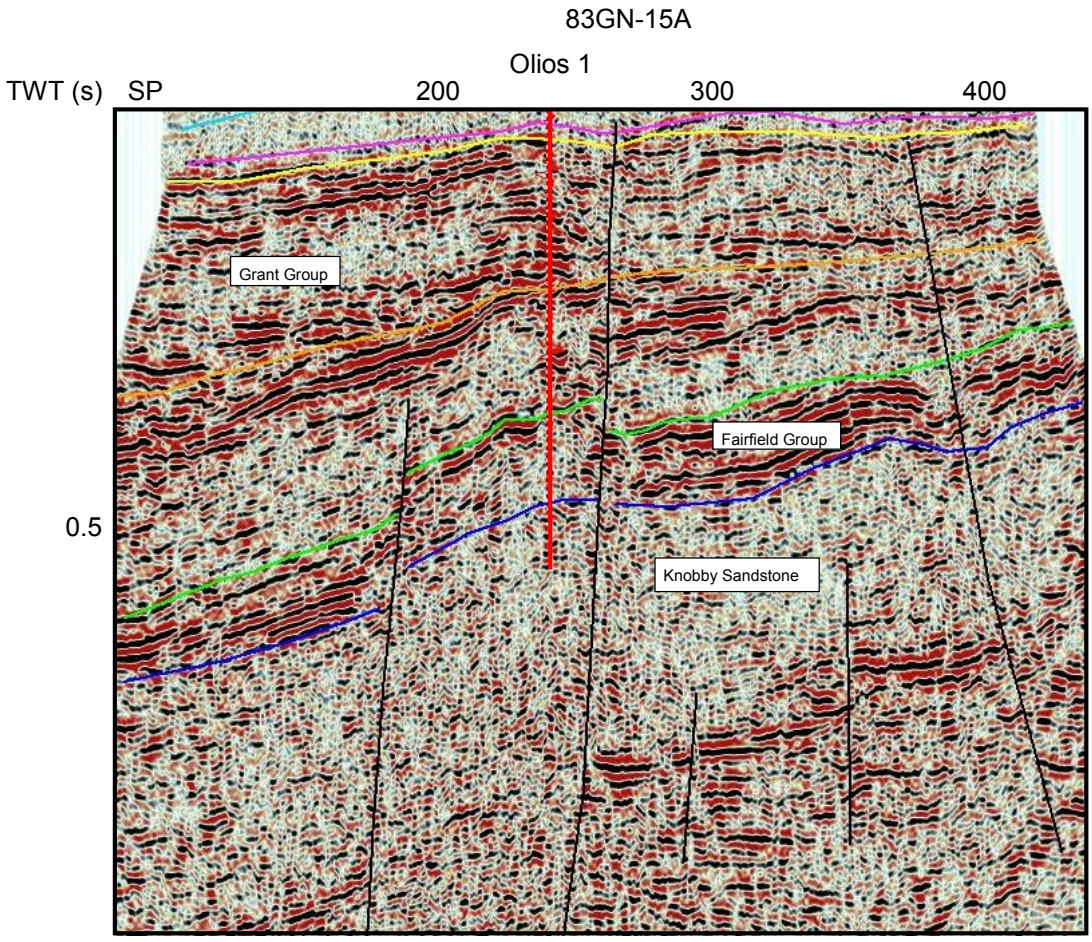

Figure 9.5. The Olios 1 structure on 2D seismic.

TWT structure on the Near Top Fairfield Group (Figure 5.16) indicates that Olios 1 is positioned between two large normal faults, potentially obstructing hydrocarbon migration from accumulating within the Olios 1 structure.

Olios 1 confirms the presence of the Laurel Formation carbonate reservoir and also confirms the absence of the lower Laurel Formation sealing shale – gas shows throughout the section appear continuous into the overlying Laurel Formation (Klappa, et al, 1984).

The Laurel Formation is in the early oil window at Olios 1 and within the main oil window in the Gregory Sub-basin, however the Laurel Formation is lean (less than

1% TOC at Olios 1). Oil shows noted in the upper Laurel Formation are likely derived from migrated hydrocarbons down-dip where the source rock is mature. The nature of the oil show (stain and fluorescence), the hydrocarbon product mix (oil and gas shows), along with limited degrees of staining, suggests that migration could be problematic, likely due to the fault down-dip of the structure acting as a barrier to migration.

Gas shows throughout the Laurel Formation and Knobby Sandstone were derived from a Devonian source rock, where modelling indicates that the Gogo Formation is mature for gas in the Gregory Sub-basin. The persistence of the show throughout the Laurel Formation and Knobby Sandstone is due to the absence of the Laurel Formation seal.

The above analysis indicates that the reasons for Olios 1 failure are:

- Migration difficulties regarding down-dip fault barrier;
- Migration around faults obscuring an accumulation;
- Absence of the Laurel Formation shale source rock.
- Similar to the other dry holes (e.g. Lawford 1 and Lake Betty 1), structural integrity is a risk for those structures reactivated during the Triassic Fitzroy movement.

9.2.6 *Bindi 1*

Bindi 1 was drilled into a subtle wrench related anticline defined on 2D seismic data in the Gregory Sub-basin. The well confirmed good quality sandstone reservoirs within the Poole Sandstone, Grant Group, and Anderson Formation (noting only 29.5 metres of the upper Laurel was intersected). Bindi 1 produced 3 poor oil shows and five dry gas shows:

- Patchy yellow fluorescence with instant cut and thick residual ring, between 934 – 949 mRT) in the Poole Sandstone; and

- Five small dry gas shows in Anderson Formation between 2350 mRT and 2450 mRT. The four shallowest were less than 2% C1, the deepest was 8% C1.

Seismic indicates that the Bindi 1 structure relies heavily on closure provided by juxtaposition of stratigraphy across the growth fault. Good reservoir potential within the Poole Sandstone, Grant Group, Anderson Formation and within parts of the Laurel Formation indicates that there are inherent risks in relying on these reservoir zones for good lateral seal, particularly because throw on the growth fault is small.

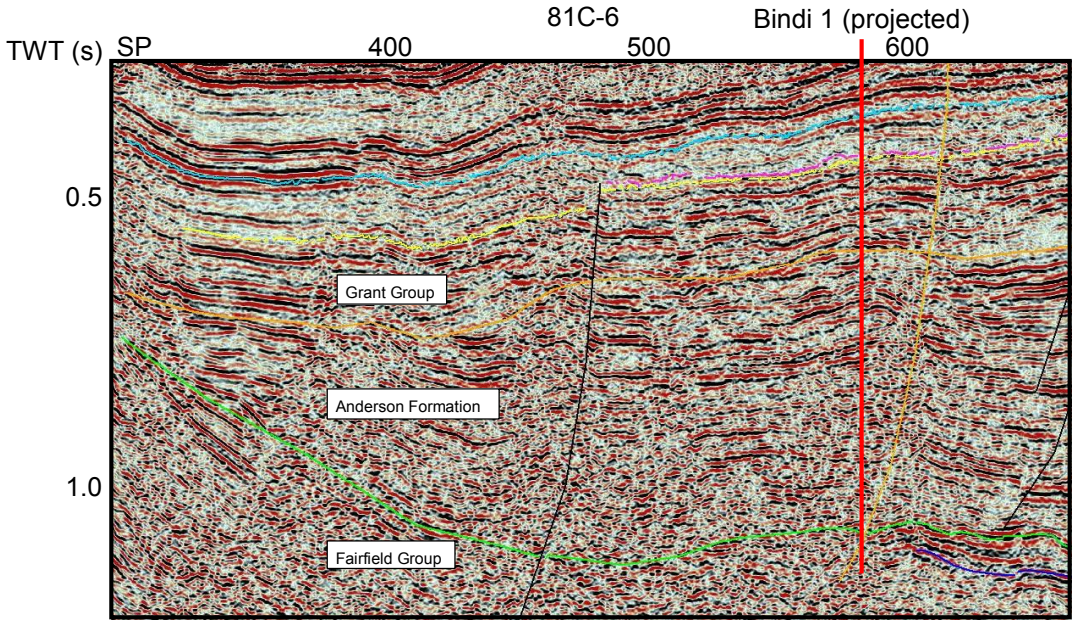

Figure 9.6. The Bindi 1 structure on 2D seismic. Bindi 1 well projected onto seismic as the well was drilled off the 81C-6 2D seismic line.

Although, geophysical logs at Bindi 1 indicate the presence of Anderson Formation lithologies with good sealing potential such as members A, C, E and G (high gamma ray blocky shales, Figure 4.29), juxtaposition of these seal rocks across the growth fault is high risk because growth fault throw is small and reservoir horizons are thick. A lack of lateral seal is also pertinent to other intersected horizons in the Grant Group B member and Laurel Formation.

The Noonkanbah Formation is immature across the project area, so the oil show in the Poole Sandstone has either migrated long distances from a Noonkanbah Formation source kitchen deeper in the Gregory Sub-basin (less likely), or the oil show demonstrates vertical migration from deeper source rocks. The Anderson Formation, though lean at Bindi 1 (Chapter 7.4.3) may generate hydrocarbons deeper in the Gregory Sub-basin, where the source rock is within the main oil window. Immature Permian source rocks explain why the shallow portion of the well failed.

The gas shows in the Anderson Formation are likely migrated hydrocarbons from the Devonian gas generative Gogo Formation within the Gregory Sub-basin. Lean source rocks indicate why the deeper portion of the well failed.

Interestingly, gas shows increase with depth in the lower Anderson Formation. The well reaches total depth in the upper-most shale of the Laurel Formation (thereby not penetrating any Laurel Formation reservoir zones). A gas charged Laurel Formation may exist below final TD of the Bindi 1 well. If this were the case, it would indicate the Laurel Formation seals are effective.

Timing is a potential cause for failure at Bindi 1.A fault-bound monocline existed at Bindi 1 prior to Triassic wrenching. The Carboniferous Gogo Formation generative phase potentially migrated through the Anderson Formation reservoirs at Bindi 1 in the absence of trap closure. This indicates that the gas at Bindi 1 is due to the Triassic generative phase from Devonian source rocks. Gas could be residual, but this option isn't preferred. Triassic aged traps occur at a similar time to the main Devonian generative phase, however a petroleum system elements diagram indicates that Triassic traps may have developed marginally late (Figure 9.14). Hydrocarbons generated in the Triassic may have migrated out and Triassic traps might have only caught the tail end of expulsion. If hydrocarbons did accumulate during the

Carboniferous generative phase, Triassic faulting might have caused leakage of hydrocarbons from the structure.

The above analysis indicates that the reasons for failure at Bindi 1 are:

- Immature Permian Source rocks;
- Lean Carboniferous Source rocks;
- Timing of the Bindi 1 anticline is potentially too late.
- Lack of lateral seal across the growth fault.

9.2.7 *Kilang Kilang 1*

Kilang Kilang 1 was drilled to test a large, four-way dip closed anticline defined on a broad 2D seismic in the Gregory Sub-basin to test the Larapintine L3 and L4, and Gondwannan G1 petroleum systems (Figure 9.7). Timing of the structure is related to wrench faulting during the Triassic (Smith, 1985a). The well confirmed the presence and reservoir quality of the Poole Sandstone and Grant Group. No shows were observed during the drilling of the well, with the exception of a 0.02% C1 gas show in the Laurel Formation.

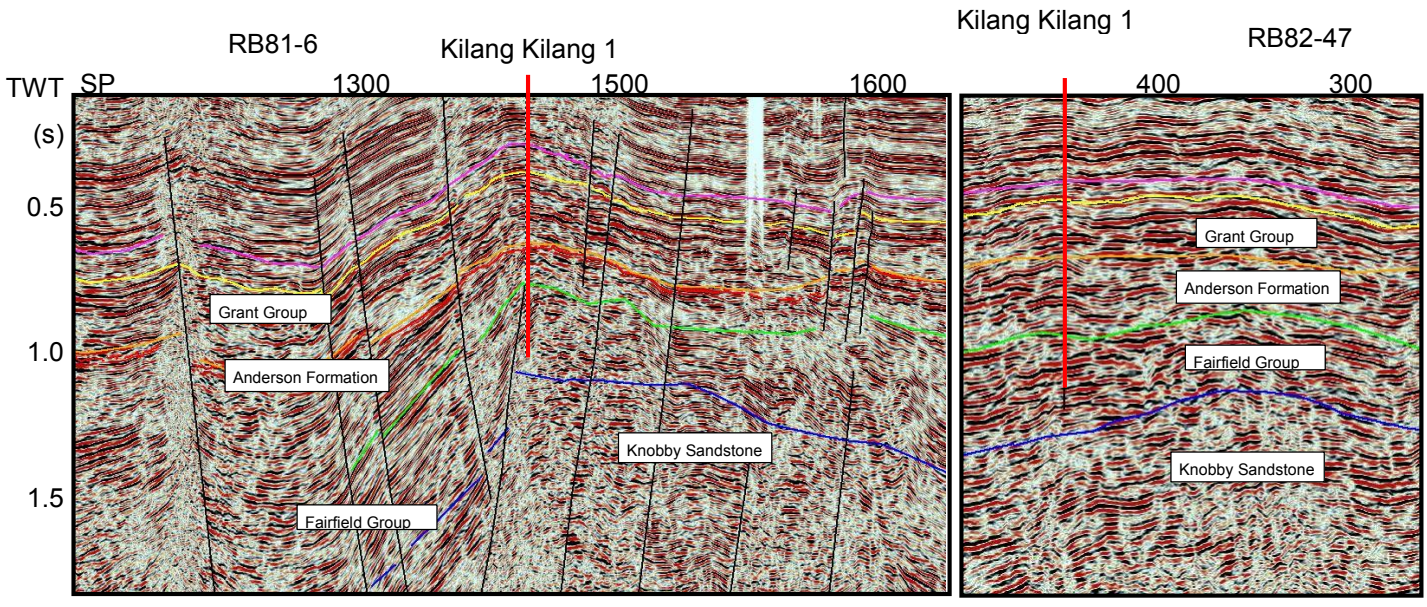

Figure 9.7. The Kilang Kilang 1 structure on 2D seismic. Dip line on left, Strike line on right.

Note that Kilang Kilang 1 was drilled down dip off the crestal position, demonstrated on the Siluro-Devonian isochron (Figure 6.16 and Figure 9.7). If source rocks are lean, though still generative to some extent, a small accumulation is still possible up dip from the well location. Interestingly, a 2D petroleum systems model (RB81-7, Figure 8.44), built to test the Kilang Kilang 1 crestal position, simulated that a small gas accumulation is present within the Poole Sandstone. The decision to drill off structure was perhaps intentional for commercial reasons (requiring a closure filled to the 1600 millisecond TWT contour level, for example), however the well is thus not a valid test of the structure.

The Noonkanbah Formation is correlated to this location, suitably sealing the Poole Sandstone reservoir. The intra-Grant Group seal (Grant B member) shows blocky shale packages at this location (Figure 4.32)

The Noonkanbah Formation is immature and does not generate hydrocarbons in the project area, which explains why the Poole Sandstone reservoir was dry. The Laurel Formation is mature for oil in the Gregory Sub-basin and generates during the Triassic, however TOC data indicates the Laurel Formation is lean (<0.37%) which explains the absence of charge.

The small dry gas show in the Laurel Formation suggests that a Devonian source rock provided the charge (sufficient maturity). Either Devonian source rocks at the Kilang Kilang 1 location are lean; lower sections of the Laurel Formation provide an adequate seal for Devonian reservoirs (the well terminated in the Laurel Formation thus Devonian accumulations remain untested); or trap timing possible occurs slightly late relative to Devonian expulsion (Figure 9.14).

The above analysis indicates that the reasons for failure at Kilang Kilang 1 are:

- Absence for source rock charge in the Poole Sandstone because the Noonkanbah Formation is immature;
- Absence for source rock charge in the Grant Group because the Laurel Formation is lean;
- Timing is potentially an issue, where trap formation in the Triassic is slightly too late to capture expulsion from mature Devonian source rocks;
- Kilang Kilang 1 is not a true test of the structure as the well did not test the crestal position.

9.3 Prospectivity within the Larapintine L2 Petroleum System (Ordovician – Silurian)

The Larapintine L2 petroleum system is the oldest petroleum system within the study area. Exploration prospectivity of the Larapintine L2 petroleum system within the study area is difficult to assess because of limited data. In light of this lack of exploration data, the L2 system must be considered high risk.

9.3.1 *Source Rocks*

As previously noted, there are no well tests of the Llanvirn (Early Ordovician) Goldwyer Formation or Late Ordovician Bongabinni Member of the Carribuddy Group which represent the candidate Ordovician source rocks.

Goldwyer Formation

The Goldwyer Formation comprises good average regional TOC (1.5%) and good pyrolysis yields (averaging 4.06 kg HC/ton S1 and 4.11 kg HC/ton S2). Ultimate genetic yield is good at 7.8 kg/ton. Van Krevalen diagrams indicate that the source rock is type II oil prone, supporting a marine origin for organic matter. Geochemical logs demonstrate good regional source rock coverage in the central Canning Basin. *G*.

prisca, a marine algae, was found to be widespread and represents marine origin throughout the formation (Chapter 7.4.7). The occurrence of *G. prisca* was found to be more regionally occurring than reported in literature; which is encouraging.

Petroleum systems modelling indicates that the Goldwyer Formation in the Gregory Sub-basin – the nearest province most likely to contain the organically rich marine source rock (and similarly the Bongabinni Member) – becomes mature for oil in the Early Silurian, gas mature in the Late Silurian, and over mature by the Late Devonian. Rapid subsidence along the Stansmore Fault is attributed to rapid burial and maturation. Modelling indicates complete kerogen conversion to petroleum (TR reaches 100% in the Early Mississippian). Generation and expulsion occur from the Silurian to the Mississippian, which indicates that Ordovician source rocks are available to charge reservoirs between 436 Ma – 350 Ma.

The main problem with the Goldwyer Formation is facies variability from areas of known source rock potential. Paleogeographic reconstructions (Figure 9.8) indicate that the Goldwyer Formation is unlikely to occur in marine form in the project area. Paleogeographic reconstructions indicate the source rock interval is likely to be dominated by a sandstone time equivalent, rather than marine shale facies. The marine environment may extend to distal portions of the Gregory Sub-basin, nearer the Barbwire Terrace. The interpretation proposed here indicates long distance migration would be required to transport petroleum from the Goldwyer Formation into reservoirs within the study area.

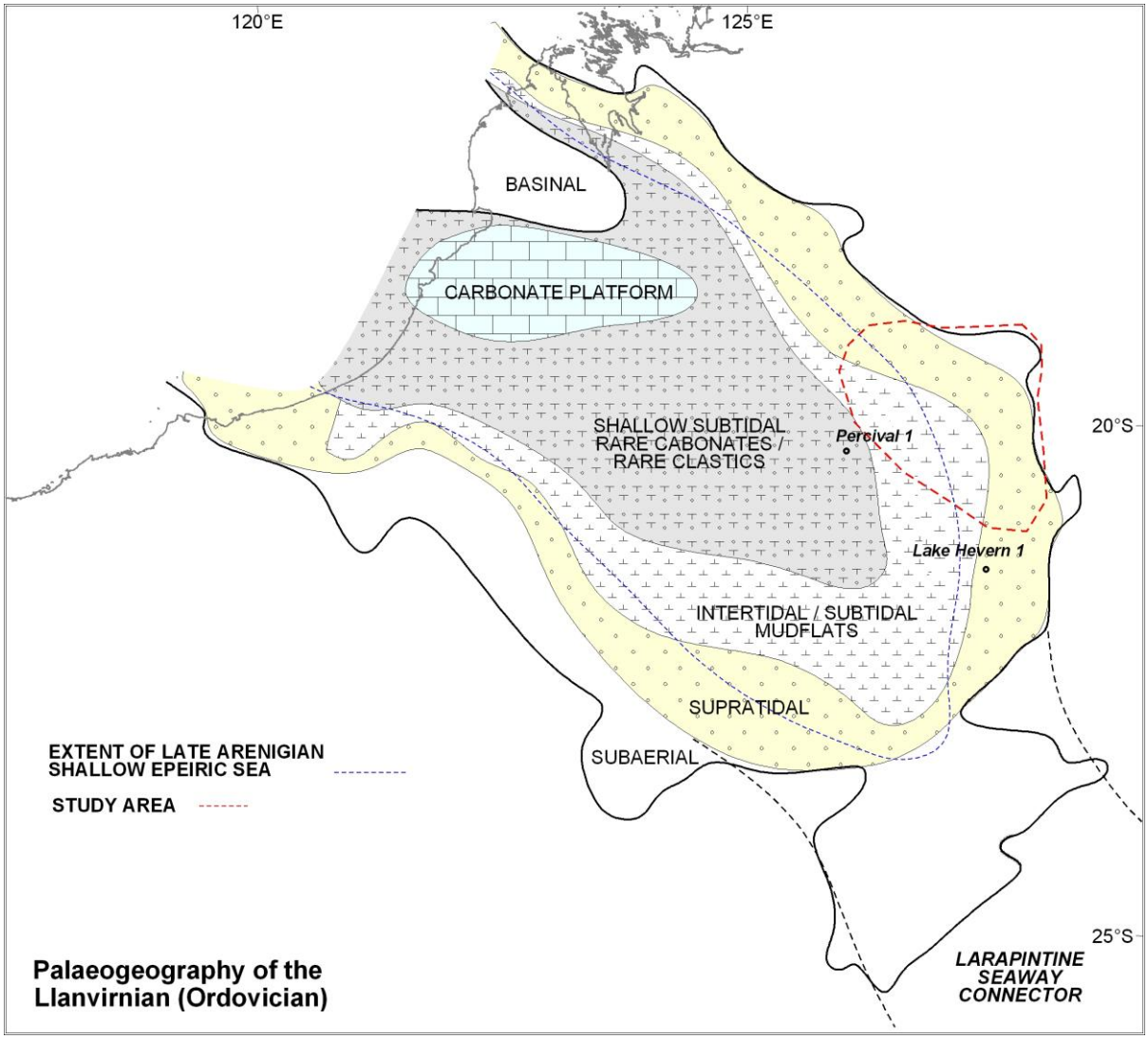

Figure 9.8. Palaeogeography of the Llanvirnian (Ordovician).

Bongabinni Member

The Bongabinni Member is organically rich and thermally mature for oil in the Admiral Bay Fault Zone (Chapter 7.4.6). Elsewhere however, geochemical data suggests the Member represents poor petroleum potential by TOC, and there are no Pyrolysis measurements to derive generative yields. The member is not discounted within the project area because there are no well tests.

Paleogeographic reconstructions of Ordovician to Silurian time (discussed within chapters 4.2 to 4.5) provide scope for the Bongabinni Member to exist with some marine influence, but risk is still pronounced because well intersections of the Bongabinni source rock are elusive near the study area to confirm organic richness of the source rock.

9.3.2 *Reservoir Rocks*

Reservoir rocks belonging to the Larapintine L2 petroleum system include the Ordovician Nita Formation carbonates or members of the Carribuddy Group (Figure 9.9)

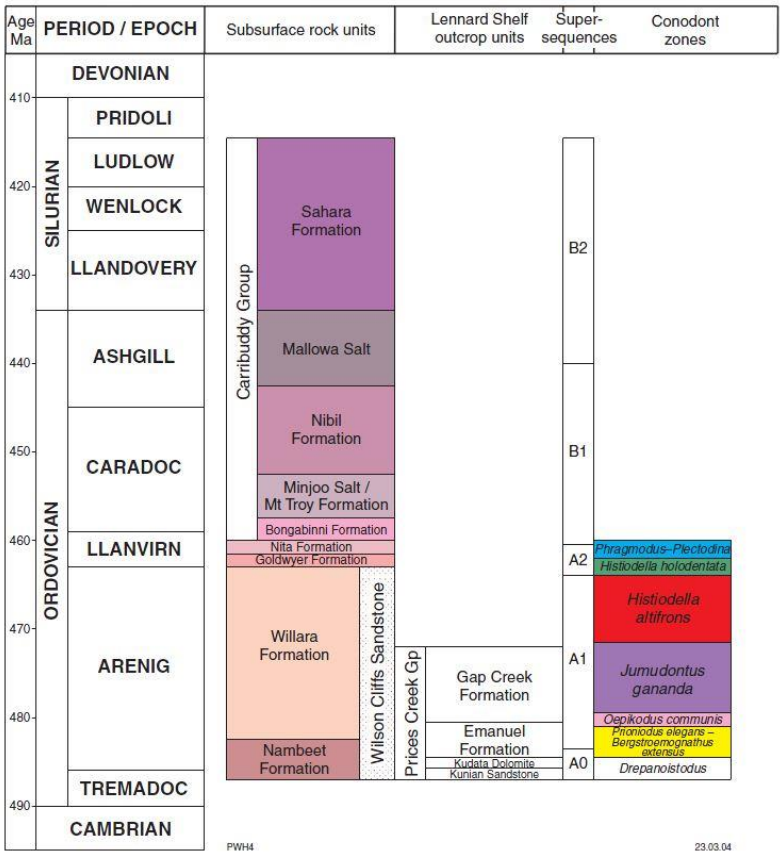

Figure 9.9. Stratigraphic column of Ordovician and Silurian aged rocks.

Reservoir property data for Ordovician rocks are scarce throughout the Canning Basin (Chapter 4.2). In the event that hydrocarbons sourced from the Goldwyer Formation are reservoired within the Goldwyer Formation (such as a self-sourcing unconventional play), the Goldwyer Formation shows reservoir porosity averaging 1.7% in WMC Unit 4 and 1.5% average in WMC Unit 3. Permeability is tight at 0.01 mD to 0.3 mD. The Nita Formation is a sucrosic dolomite, which if not diagenetically altered, can bear good reservoir properties. However, in the few well intersections in the Canning Basin, porosity measurements averaged 0.85% and permeability data is reported as nil.

Wireline log data and drill cuttings at Lake Havern 1 suggests that the likely reservoir is either a sandstone or carbonate equivalent of the Goldwyer Formation or

Carribuddy group. Sandstones would be preferable. If the Silurian Worral Formation Elsa member is present across the Gregory sub-basin, its channel or aeolian sand package also makes a favourable reservoir target.

Ordovician source rocks are still generative through to the Mississippian, which therefore makes it possible to charge Devonian aged reservoirs (of the L3 and L4 petroleum system) in traps developed early during the Carboniferous Meda Transpression. Early hydrocarbon emplacement is an important consideration because generation and migration during deposition of the Devonian reservoirs (for example the Knobby Sandstone) can lead to porosity preservation, as oil in pore space assists in impeding diagenesis (Bloch et. al., 2002).

The options for Devonian reservoirs in the project area include the Devonian polymict Conglomerate (averaging 10.3% porosity) or the Knobby Sandstone (averaging 20.6% porosity and 567 mD permeability). The Lennard River Group is present however no reservoir property data are available. Evidently, the fluvial Knobby Sandstone is the key candidate Devonian reservoir. Seismic interpretation indicates that the unit is regionally mappable and the Knobby Sandstone demonstrates excellent reservoir quality.

The availability of suitable reservoir rocks is not perceived as a problem for the Larapintine L2 petroleum system. Paleogeographic reconstructions (Figure 9.8) infer a favourable setting for reservoir development (nearby sand sedimentary source off the northeastern basin margin combined with progradational sand development), where several layers of stratigraphy appear suitable to harbour petroleum. Timing of key reservoir development is mostly related to the development of Carribuddy Group or Worral Formation sandstone packages between 452 Ma to 416 Ma, and the Devonian Knobby Sandstone between approximately 374 Ma to 359 Ma.

9.3.3 *Seals*

The sealing capacity of candidate sealing lithologies is difficult to quantify in the absence of complete laboratory data (such as Mercury Injection Capillary Pressures, MICP); so porosity, permeability, well logs and drill cuttings are used to make inferences. The Mallowa Salt of the Carribuddy Group would be ideal; however seismic interpretation does not infer its presence in the project area. The Nita Formation is potentially a better sealing unit with nil permeability. Shale within the Carribuddy Group (dolomitic claystone within the Nibil Member represented by a hot and blocky gamma ray log response) offers another alternative.

In the event that Ordovician source rocks charge the Knobby Sandstone, the seal would need to originate from the Carboniferous Laurel Formation. Although returned well cuttings from the formation indicate fine-grained siliciclastic constituents (siltstone and claystone), the Laurel Formation shale can be eroded under the Meda Transpression Unconformity, particularly in the footwall of the Stansmore and Mueller Faults. Paleogeographic reconstructions (Figure 9.13) indicate that the Laurel Formation shale (if preserved) is more likely found to the southwest of the project area in a basinal setting.

Timing of seal development is in relation to the deposition of the Nita Formation or Carribuddy Formation shales (461 Ma to 443 Ma, though timing of dolomite diagenesis is unknown), or a seal over the Devonian Knobby Sandstone (Laurel Formation shales) between 359 Ma to 345 Ma.

9.3.4 *Trap Development*

The timing of trap development for Ordovician hydrocarbons is likely to be around the Mississippian (360 Ma to 345 Ma), related to the Carboniferous Meda Transpression. RB81-1 (Figure 6.6) and RB81-7 (Figure 6.5) demonstrates that the Ordovician and Devonian sections are isopachus across the Billiluna Sub-basin, Balgo Terrace and Betty Terrace, and show thickening into the Gregory Sub-basin due to

syn-rifting in the Devonian. There are common thickness variations in the Fairfield Group and Anderson Formation, and truncation due to the Meda Transpression Unconformity. The Gregory Sub-basin RB81-7 pseudo well (Figure 9.10) illustrates continual subsidence until the Mississippian (330 Ma). Tilted fault blocks in the southwestern project area (RB82-28 modelled accumulations, Figure 8.46) likely occur between syn-rifting in the Devonian and prior to Carboniferous exhumation.

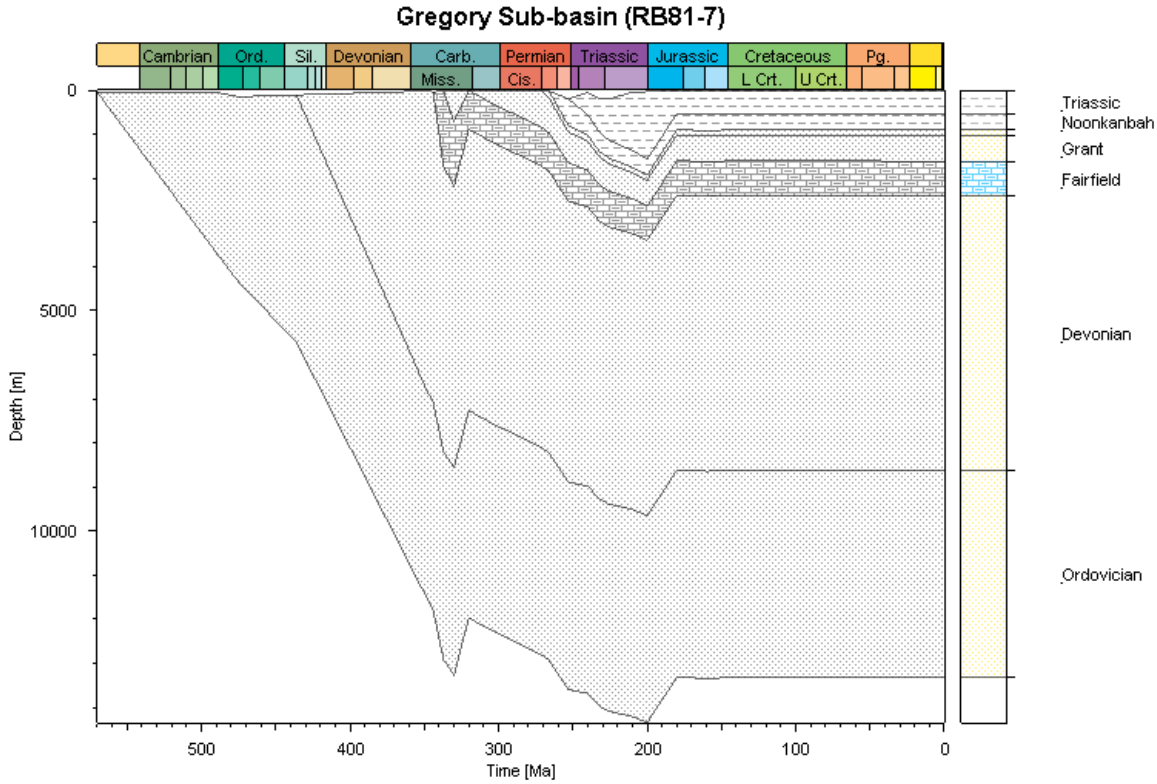

Figure 9.10. Burial history diagram of the RB81-7 Gregory Sub-basin pseudo well.

9.3.5 *Timing and Migration*

Ordovician sourced hydrocarbons are required to migrate to Devonian reservoirs. Although good reservoir potential exists within the project area, the migration distance is variable based on the proximity of the source rock. Long distance migration from kitchens near the Barbwire Terrace is feasible.

Timing can present a critical issue for the prospectivity involving the Larapintine L2 petroleum system (Figure 9.11). No seals are available to cap the Ordovician or Silurian reservoirs for a conventional play. This indicates that hydrocarbons that generated when the Ordovician source rocks passed through the oil window likely migrated out of the system. Ordovician source rocks would be required to be "self-sealing" (for example a shale gas play). No traps developed until the Late Devonian or Mississippian. Trap development likely occurred after the deposition of the Knobby Sandstone reservoir. Ordovician source rocks were generating gas hydrocarbon products at that time. Traps are available for filling over a 10 My period, between 360 Ma to 350 Ma.

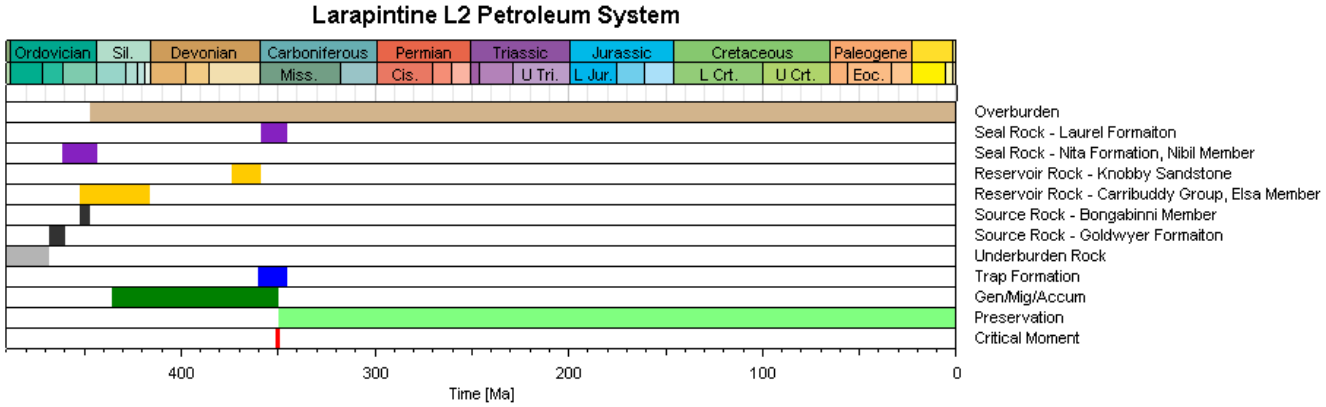

Figure 9.11. Petroleum system elements diagram for plays in the Larapintine L2 petroleum system.

9.3.6 *Play-type Targeting, Risks and Remarks*

Exploration prospectively concerning the Larapintine L2 petroleum system is considered high risk. The following are some play type targets, risks and remarks regarding future exploration.

- Unconventional shale gas plays within the hanging wall block of the Stansmore Fault are a suitable play-type, with the objective to intersect basinal-type Goldwyer Formation or Bongabinni Member shale facies,

- Conventional gas accumulations in Devonian reservoirs (for example the Knobby Sandstone) near or down-dip of the Stansmore Fault, maximizing hydrocarbon migration exposure from the Gregory Sub-basin. A target down-dip of the Stansmore Fault will maximize the chance of intersecting a fine-grained Laurel Formation seal (Figure 9.12).
- The Kilang Kilang 1 well location is an example of a suitable Larapintine L2 prospect. Unfortunately, the Kilang Kilang 1 well did not drill deep enough to test Devonian stratigraphy (Figure 9.7).
- Paleogeographic reconstructions indicate that the Goldwyer Formation is unlikely to be present in the study area as a marine shale source rock. A sandstone dominated time equivalent is the likely lithotype within the project area.
- In any case, the accumulation will be a gas hydrocarbon product.
- Devonian reservoirs were available for a relatively short time (374 Ma to 359 Ma) – towards the end of the Ordovician generative period, thus reducing the exposure time for which reservoirs may be charged.
- The Laurel Formation may be suitable as a seal because the formation represents fine-grained components, however the shale-rich lithostratigraphy may be restricted to basinal depocentres. Further, the Laurel Formation shales may be eroded under the Meda Transpression unconformity on terraces within the project area.
- Preservation of accumulated hydrocarbons is a risk because of basin activity in the Triassic. The Fitzroy Movement has been demonstrated to destroy trap integrity.

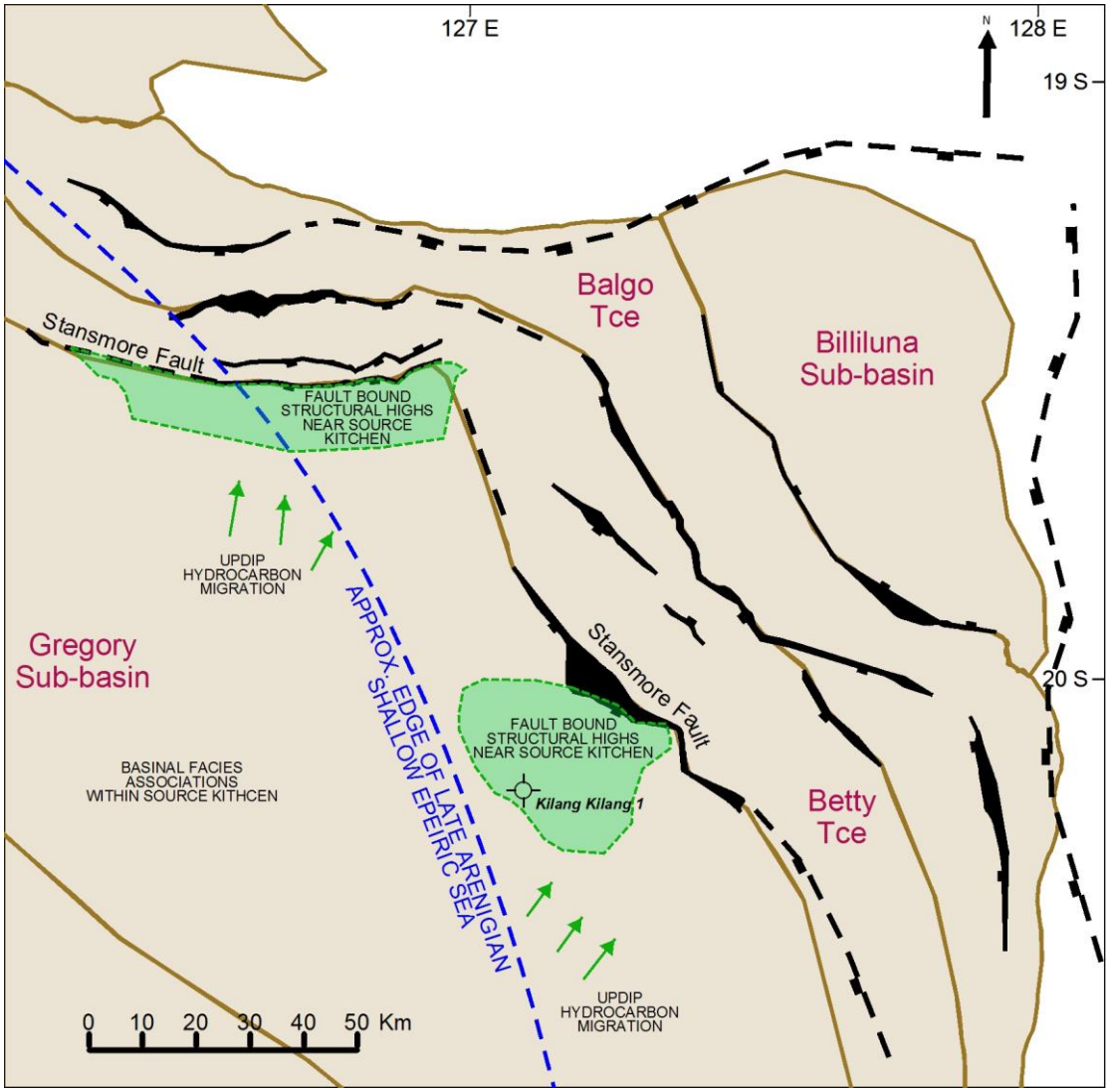

Figure 9.12. Play-type targets within the Larapintine L2 petroleum system.

9.3.7 *Key recommendations*

Some key recommendations to reduce exploration risk relating to the L2 petroleum system are:

- Undertake a study into suitable analogues to guide future exploration in the Goldwyer Formation and Bongabinni Member Shales.
- Obtain lab data to quantify sealing capacity of the Laurel Formation shales and the Nita Formation Carbonates,

- Obtain further porosity and permeability measurements for Carribuddy Group reservoirs to calibrate sonic derived porosity.

9.4 Prospectivity within the Larapintine L3 and L4 Petroleum Systems (Devonian – early Carboniferous)

The Larapintine L3 and L4 petroleum system hosts stratigraphy that has proven to contribute to hydrocarbon accumulations on the Lennard Shelf – a similar structural position to the study area (tables 2.1 and 2.2). There are more options available to explorers when targeting play types within the Larapintine L3 and L4 petroleum system, however exploration within this system is also considered to be high risk.

9.4.1 *Source Rocks*

There are three candidate source rocks within the L3 and L4 petroleum systems, each of which has demonstrated ability to produce hydrocarbons with varying generative potential; the Devonian Gogo Formation, the Early Carboniferous Laurel Formation, and the Carboniferous Anderson Formation.

Gogo Formation

The Devonian Gogo Formation, though attractive in description (a black micromicaceous shale, represented by mid to high ranging blocky gamma ray aggradational log patterns), has limited geochemical data to appraise it. TOC data indicates very low organic content (averaging 0.14% TOC) and poor generative potential (0.22 kg HC/ton S1, 0.26 kg HC/ton S2). Wulff (1987) advertises more encouraging results at 1.25% average TOC (and 0.18 kg HC/ton S1 and 2.4 kg HC/ton S2), which indicates fair to good generative potential.

The Gogo Formation is present within the project area at Selenops 1, confirming a localised occurrence. Paleogeographic settings were not reconstructed specifically for the source rock, however sedimentological interpretation (Chapter 4.5.5) indicates

that the formation represents a deeper water basinal environment that preceded deposition of the Knobby Sandstone (Figure 4.22; which illustrates the regressive phase succeeding Gogo Formation deposition). Seismic mapping indicates that the formation is present in the northwestern project area, and it is likely that the zone extends to the south into the project area-proper. The formation is believed to source the Blina Oil Field (Cadman, 1993; and Wulff, 1987).

Modelling indicates that the Gogo Formation is mature for oil within the project area. The source rock has higher maturity within the Gregory Sub-basin than terraced areas, where it enters the wet gas window by the Mississippian, and reaches the main oil window on terraced areas at a similar time. At maximum maturity (200 Ma) the Gregory Sub-basin sediments enter the dry gas window and the interval on the terraces reach the late oil window. The Billiluna Sub-basin remains in the main oil window at maximum maturity. Results indicate that the Gogo Formation is available to charge reservoirs across two expulsion periods; between 344 Ma to 330 Ma and between 255 Ma to 200 Ma.

Laurel Formation

The Early Carboniferous Laurel Formation (an interbedded siliciclastic package containing a regional limestone member) is organically lean (averaging 0.46%) and shows fair genetic potential (0.69 kg/ton genetic yield) within the study area, however organic content is noted to increase basinward, towards the Gregory Sub-basin (where TOC is ranked fair, 0.61%). Paleogeographic reconstructions (Figure 9.13) demonstrate that the source rock is interpreted to increase in shale content away from the limestone carbonate platform, in southwest and northwest directions. A key conclusion from geochemical analysis is that the Laurel Formation increases in organic contents down dip, in a basinal setting, thus hydrocarbon migration is required to charge shelfal reservoirs.

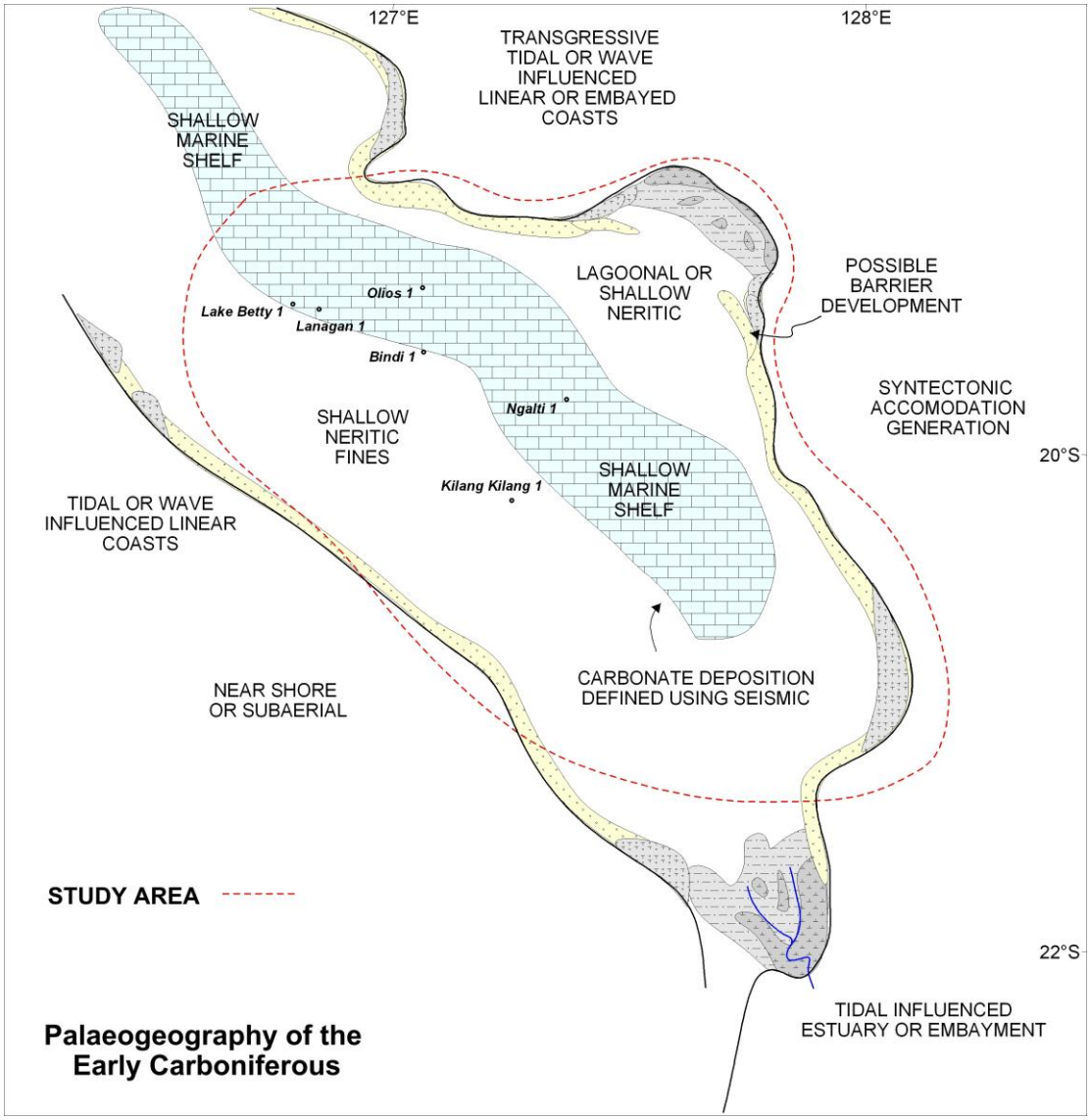

Figure 9.13. Palaeogeography of the early Carboniferous.

Modelling indicates that Laurel Formation is mature for oil in Gregory sub-basin by the Triassic (240 Ma). Sediments on the Betty Terrace and Balgo Terrace reach the early oil window at a similar time whilst the source rock in the Billiluna Sub-basin remains immature. Results indicate that the Laurel Formation is available to charge reservoirs between 220 Ma to 192 Ma.

Anderson Formation

The Middle Carboniferous Anderson Formation (a package of interbedded siliciclastics, divisible into 7 sub-units, where units C, E and G were investigated for source rock potential) is organically lean. Geochemical analysis indicates the source rock has low TOC (0.64%) and low genetic potential (averaging 0.32 kg HC/ton S1 and 1.74 kg HC/ton S2).

Modelling demonstrates that the Anderson Formation is mature for oil at peak maturity (200 Ma) in the Gregory Sub-basin, and within the early oil window on the Betty Terrace at a similar time. Transformation Ratios indicate that the source rock largely converts to petroleum in the central project depocentre (near Bindi 1), but kerogens elsewhere have low ratios of kerogen cracking to petroleum. Results indicate that the Anderson Formation is generative in the Gregory Sub-basin in the Triassic (between 235 Ma to 190 Ma). Expulsion is modelled to occur between 216 Ma to 192 Ma.

Petroleum systems modelling indicates that the central area depocentre (near Bindi 1) performs as a source kitchen, which improves the prospectivity of the surrounding terraces because lateral hydrocarbon migration is minimized. Plays that target oil in the central study area should ideally focus on trapping geometries closest to the central area depocentre in the first instance, or exploiting the preserved reservoir-and-seal couplets within the Anderson Formation that are preserved near Bindi 1.

In almost all cases, hydrocarbon accumulations attributed to the L3 and L4 petroleum system will be of an oil hydrocarbon product. The exception to this is the Gogo Formation, where a gas hydrocarbon product would be expected.

9.4.2 *Reservoir Rocks*

The candidate reservoir rocks within the Larapintine L3 and L4 petroleum system are likely the Devonian Conglomerate, Devonian Virgin Hills Formation, Devonian Knobby Sandstone, The Carboniferous Laurel Formation and the Carboniferous Anderson Formation.

The Devonian aged polymict conglomerate is a package of boulder, cobble and pebble clasts that represent alluvial fan apex deposits which likely trend into finer grained fan-toe sandstones further into the project area. The conglomerate demonstrates good quality reservoir potential within the project area. Sonic derived porosities indicate up to 10.9% at Atrax 1 and up to 7.7% porosity at Selenops 1.

The Devonian Virgin Hills Formation is a siliciclastic sequence deposited in a progradational near shore environment. Core data from Selenops 1 indicates good porosity, ranging 3.7% to 10.5%. Core data indicates 0.25 mD to 1.2 mD of permeability, which is tight.

The Late Devonian Knobby Sandstone is a key candidate reservoir within the Larapintine L3 and L4 petroleum system. Seismic interpretation indicates that the unit is regionally mappable. Core porosity data indicates that the Knobby Sandstone demonstrates excellent reservoir quality. Ngalti 1 indicates core porosity in the 10% to 20% range. The upper section averages 20.6% porosity. Permeability is excellent, averaging 567 mD.

The Carboniferous Laurel Formation also represents a favourable candidate reservoir. The Laurel Formation overlies the Knobby Sandstone and is regionally mappable on seismic data. The formation shows excellent reservoir characteristics – the upper section demonstrates 12.1% to 22% porosity and the lower siliciclastic zone demonstrates 16.7% - 19.8% porosity. The carbonate member has no reservoir

property data however its description as a fossiliferous limestone alludes to further reservoir potential.

The Carboniferous Anderson Formation is the youngest candidate reservoir within the Larapintine L3 and L4 petroleum system. The formation is a package of interbedded siliciclastics divisible into 7 sub-units. Units A, B, D, and F represent the candidate reservoir members, while units C, E and G show potential to act as sealing intervals (for example reservoir and seal couplets, in addition to the source rock potential described above). Reservoir quality is good; 6% to 11% porosity in unit A, 3% - 10% in unit B and unit D, and 3% - 11% porosity in unit F. Geophysical logs (Figure 4.29) illustrate the regionally correlatable character of the reservoir and seal pairs across the project area. The main problem with the Anderson Formation is that large sections are eroded by the Meda Transpression unconformity, discussed above.

The availability of suitable reservoir rocks is not deemed a problem for the Larapintine L3 and L4 petroleum system. Paleogeographic reconstructions infer a favourable setting for reservoir development throughout periods in the Devonian to Carboniferous, where candidate reservoir zones align with periods of progradational sediment deposition. Timing of key reservoir development is mostly related to the deposition of the Devonian Conglomerate approximately between 390 Ma – 380 Ma, the Knobby Sandstone between approximately 374 Ma – 359 Ma, the Laurel Formation between 359 Ma – 345 Ma, and the Anderson Formation between 345 Ma – 326 Ma.

9.4.3 *Seals*

Candidate seals are identified based on geophysical logs, porosity and permeability measurements, and drill cuttings. Seals within the L3 and L4 petroleum system includes the Devonian Bungle Gap Limestone, Shales in the Carboniferous Laurel Formation and sub-units C, E and G of the Carboniferous Anderson Formation.

The Devonian Bungle Gap Limestone is a thickly bedded arenaceous limestone that overlies the Devonian Conglomerate reservoir. It has secondary calcite and fracture fill, indicating impermeability. No laboratory data is available to validate the sealing potential. The interval is inferred to be regionally present within the Near Top Devonian seismic package, but is only confirmed in the northeastern project area at Atrax 1.

The Carboniferous Laurel Formation is mainly considered a candidate reservoir within the L3 and L4 petroleum system due to its good reservoir characteristics, although it contains interbedded shale lithologies that may provide seal coverage over the Devonian Knobby Sandstone. Reservoir property data (Table 4.3 and Figure 4.28) indicates that seal potential is minimal (ranging 12.1% to 22% sonic porosity), and the reliability of regional shale extent is probably limited, however will likely improve in a basinal setting.

Anderson Formation sub-units C, E and G are the youngest candidate seals at the top of the L3 and L4 petroleum system, providing coverage over the Laurel Formation reservoir. Unit C (a massively bedded siltstone and non-fissile claystone), unit E (a massively bedded claystone), and unit G (an interbedded claystone and sandstone sequence) appear suitably impermeable. Figure 4.29 and Figure 4.46 illustrate the regional correlation of the Anderson Formation sub-units and demonstrate zone potential as a package of reservoir and seal couplets. The persistent issue with the Anderson Formation (this time concerning its seal potential) is that large sections are eroded, and its ability to regionally seal the below reservoir units is limited to hanging wall blocks of large listric faults, or surrounding the Bindi 1 well (Figure 6.22).

Timing of seal availability relates to the deposition of the Bungle Gap Limestone (approximately 397 Ma – 391 Ma), Laurel Formation (349 Ma – 345 Ma) and Anderson Formation (345 Ma – 326 Ma).

9.4.4 *Trap Development*

Trap development for hydrocarbons generated in the Larapintine L3 and L4 petroleum system is similar to that of the L2 system; likely to be around the Mississippian (360 Ma to 345 Ma), related to the Carboniferous Meda Transpression. The Gregory Sub-basin RB81-7 pseudo well (Figure 9.10) illustrates continual subsidence until the Mississippian (330 Ma).

The timing of trap development is likely between the Late Devonian and immediately prior to Meda Transpression erosion. This indicates that the timing of initial trap development is relatively low risk as most Carboniferous and Devonian sediments reach optimal maturity in the Triassic (after traps are in place), however, the Triassic aged Fitzroy Movement created a structural overprint that imposes a significant threat to trap integrity of Carboniferous aged structures.

9.4.5 *Timing and Migration*

Hydrocarbons generated from the Anderson Formation are mature for oil in the Gregory Sub-basin and reach the early oil window at maximum maturity on terraced areas, indicating that hydrocarbons require long distance lateral migration from areas such as hanging wall blocks of the Stansmore Fault, or from the central area depocentre near Bindi 1.

Although Carboniferous sediments on the Betty Terrace and Balgo Terrace are within the oil window, long distance lateral migration is still a requirement because source rocks are organically lean within the project area.

Timing is considered favourable for the evolution of L3 and L4 petroleum system elements and processes. Figure 9.14 illustrates that in all cases; optimal maturity, generation and expulsion occur after reservoirs, seals and traps have developed.

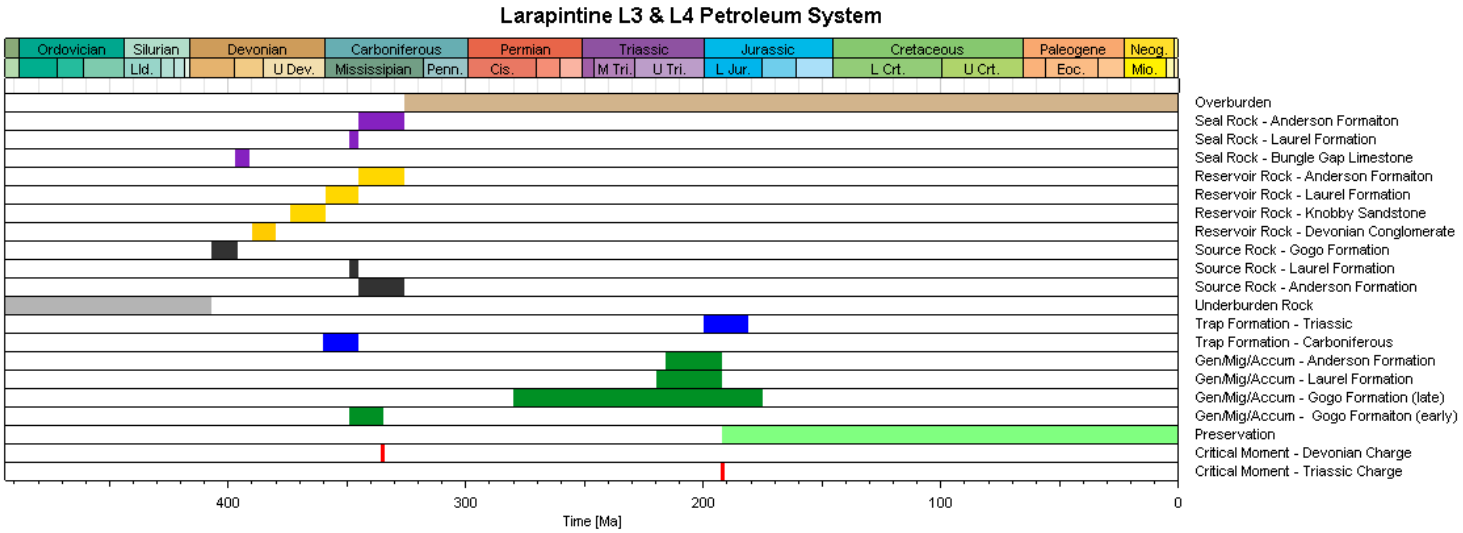

Figure 9.14. Petroleum system elements diagram for plays within the Larapintine L3 and L4 petroleum system.

A petroleum system element diagram (Figure 9.14) summaries that reservoirs and seals develop through the Devonian and Carboniferous. Trap development occurs during reservoir and seal development. No hydrocarbons have charged reservoirs at this time. The first period of charge (Devonian) occurs after all reservoirs are available, and occurs after traps have formed. The second (main) period of charge (Triassic) occurs after all reservoir, seal and traps develop.

9.4.6 *Simulated Accumulations – 2D Model RB82-28*

Figure 9.15 illustrates an accumulation analysis of 7 hypothetical oil accumulations in the Devonian Knobby Sandstone within a series of tilted fault blocks. This large apparent structure has not been tested by exploration drilling, and is the largest undrilled structure within the project area (Trap ‘A’, Figure 6.10). Although the hypothetical volume should not be taken as correct, the model demonstrates the favourable evolution of the Larapintine L3 and L4 petroleum system. The accumulations are simulated to be sealed by the Fairfield Group. Keep in mind that the interbedded shales are averaged (smoothed) in the model (Chapter 8.54), so further stages of vertical migration may be possible.

Migration vectors indicate liquid phase hydrocarbon flow. Vectors are relics rather than indicative of present day migration (note the Ordovician stratigraphy is not within the present day oil window!). Vectors indicate fluid escape along faults migrating into younger stratigraphy. Note that faulting in the Grant Group may continue shallower but is below seismic resolution to define. Triassic and younger regional events may facilitate trap breaches and hence hint at the inherent risk of leakage.

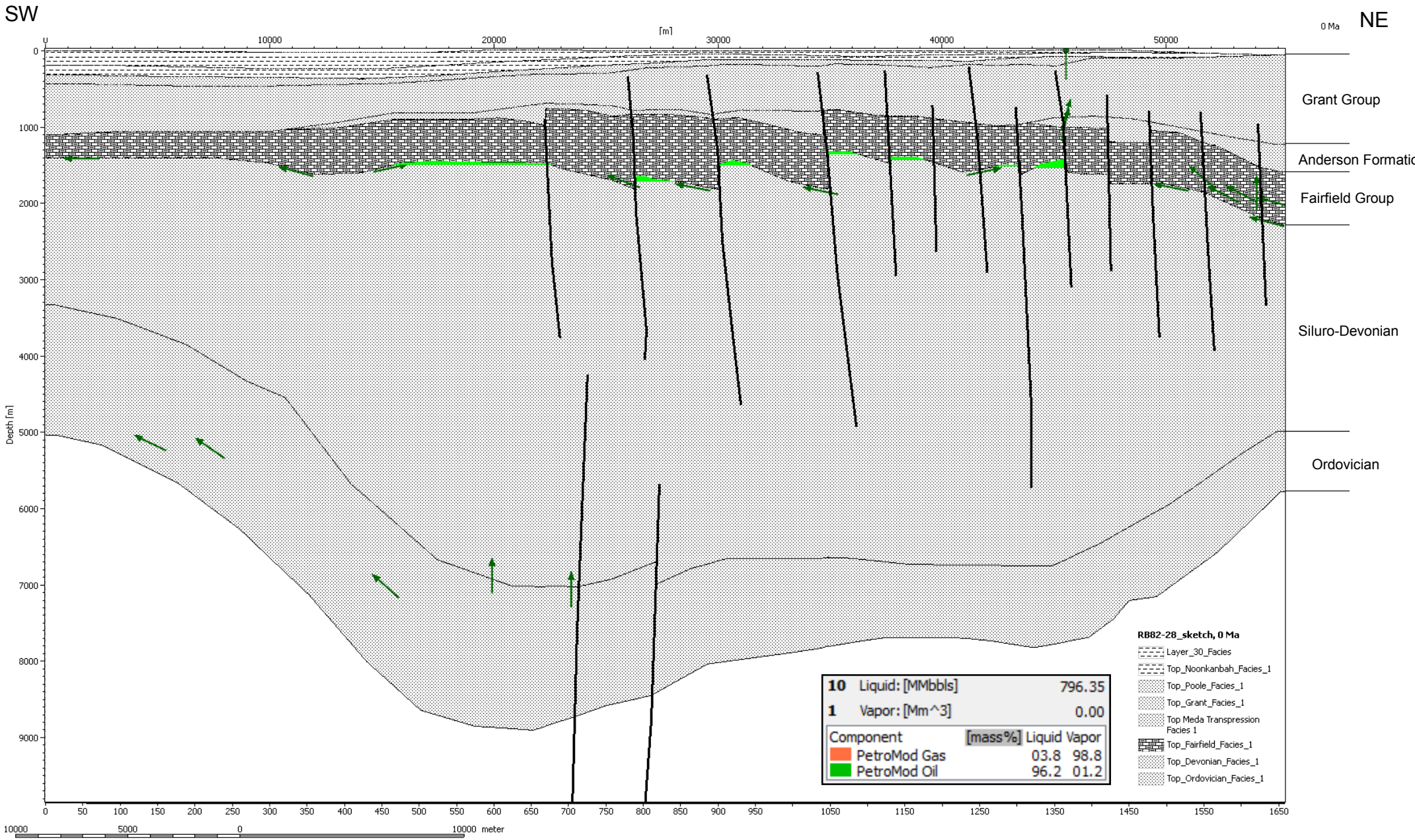

Figure 9.15. 2D model RB82-28 simulating eight large oil accumulations within the study area.

9.4.7 *Play-type Targeting, Risks and Remarks*

The Anderson Formation has been eroded from large portions of the project area, and thus its ability to fulfil the role of reservoir, seal and source rock is limited. Prospectivity within the Anderson Formation is restricted to hanging wall blocks of large listric faults (such as the Stansmore Fault) or in the central project area depocentre, near Bindi 1 – where modelling often indicates increased maturity of Devonian and Carboniferous source rocks (Table 8.10) due to deeper burial.

- Due to the interbedded nature of the Anderson Formation, and its characteristics as a generative source rock, porous reservoir rock, and zones of sealing potential; a play on the Anderson Formation could be self-generative and self-sealing where large proportions of the formation are preserved.
- Plays within the Laurel Formation should focus on areas within the hanging wall blocks of large listric faults to encourage preservation of the overlying seal, and also reduce the lateral migration distances required to charge reservoirs. A basinal setting will likely promote organic rich shale deposition.
- The Laurel Formation shales, although suitable as a seal, may be restricted to basinal depocentres. Further, the Laurel Formation shales may be eroded under the Meda Transpression unconformity on terraces within the project area.
- The Devonian Conglomerate is confirmed to exist as a suitable reservoir. Plays should target the fan-toe sandstone equivalent reservoirs towards the central basin depocentre (near Bindi 1). This will reduce lateral migration distances from a basinal Gogo Formation organic rich source rock.
- Considering the Anderson Formation and Laurel Formation play types (above), an unconventional basin-centered accumulation may be prospective in the central area depocentre (Figure 9.16). Further, an analogue play type may be present in the southeast project area in the hanging wall block of the Stansmore Fault, where a thicker preserved section of the Anderson Formation and Laurel Formation is anticipated.
- The largest structure within the project area (Trap A, Figure 6.10 and Figure 9.15) remains undrilled. The Knobby Sandstone is confirmed to exist at a suitable reservoir. Risk over this trap relates to hydrocarbon migration from organically rich source

rocks, and coverage by a Laurel Formation seal. The prospect warrants further investigation.

- Preservation of accumulated hydrocarbons is a risk. Basin activity in the Triassic may destroy trap integrity.
- Hydrocarbon leakage is a potential risk. The Fitzroy Movement is perceived as the greatest relative risk to trap integrity and hydrocarbon preservation. Any trap breaches would be likely at a similar time to hydrocarbon generation and migration, thus it's also possible that hydrocarbon charge continues after trap breach and therefore continual reservoir charge mitigates this risk.

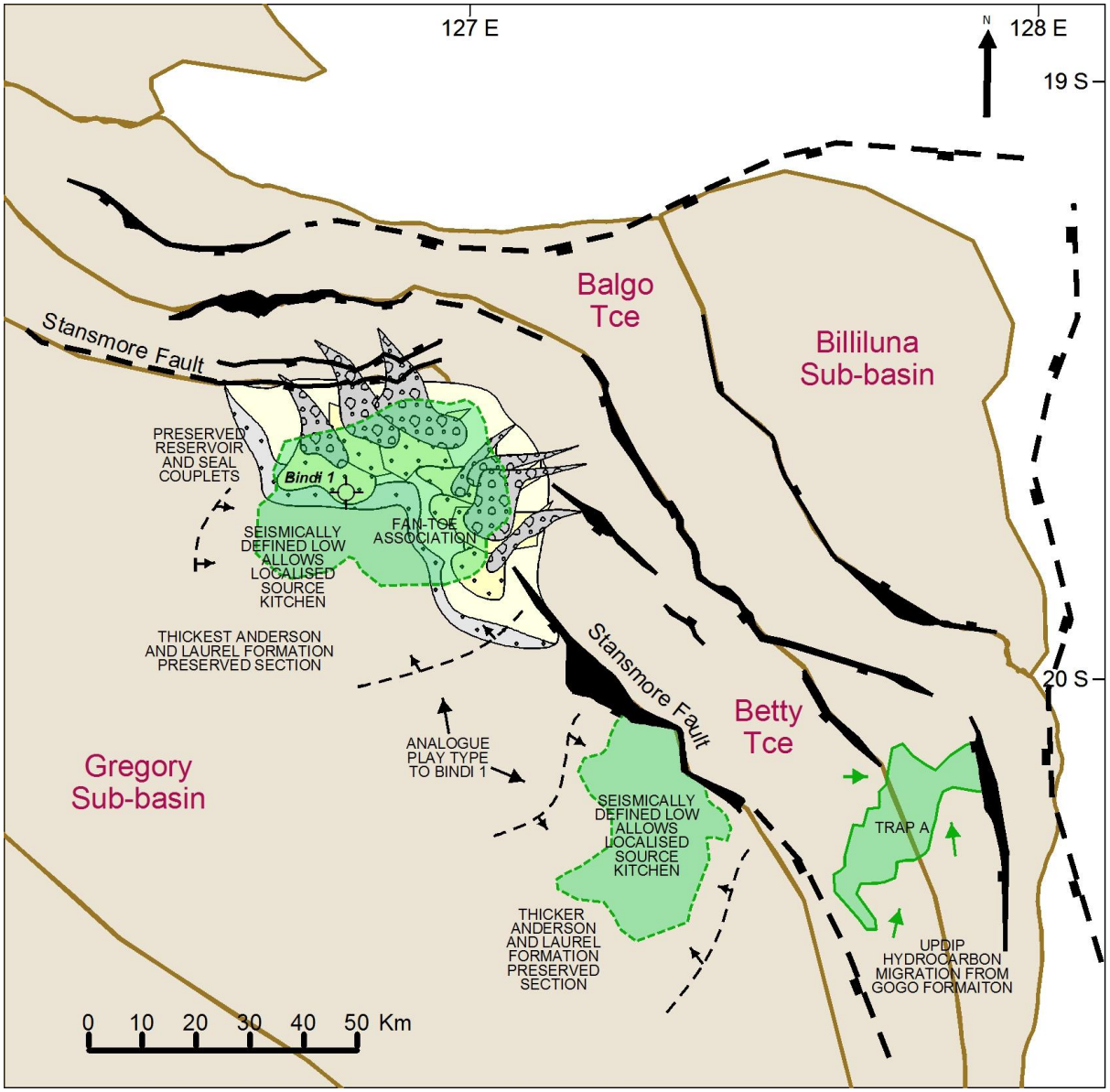

Figure 9.16. Play-type targets within the Larapintine L3 and L4 petroleum system.

9.4.8 *Key recommendations*

The key recommendations to reduce risk in exploration for L3 and L4 petroleum system related hydrocarbon plays are:

- Acquire vitrinite reflectance data from the Lake Betty 1 well location to calibrate 1D models. Similarly, undertake a sample in-fill program for vitrinite data across well locations in the study area. Some more VR would be useful at Ngalti 1 and Bindi 1;

- Acquire Apatite Fission Track Analysis (AFTA) at 2 to 3 well locations within the project area, for example at Bindi 1, Ngalti 1 and Olios 1, to assist in calibrating basin models and thermal histories. This will aid in a better understanding of the thermal maturity of the northeast Canning Basin, and will assist in reconciling exhumation estimated at White Hills 1 to the project area;
- Obtain porosity and permeability data to calibrate sonic derived porosity within the Laurel Formation;
- Perform a thorough depth conversion of the seismic interpretation to attain a better understanding of depth-structures;
- Enhance the fault interpretation across the seismic grid with attention to correlating smaller scale faults;
- Enhance the current 2D models by interpreting further seismic horizons to better reflect the lateral correlation of the Gogo Formation and Goldwyer Formation isopachs. This will provide a better assessment of accumulation analysis in the RB82-28 2D model.
- Enhance the current 2D models by exploiting the use of facies maps (including heat flow and TOC) to accommodate the lateral special variability in formations between wells. For example, TOC can be varied between wells indicated by percentage composition of shale lithologies. This will improve the conceptual accuracy of models.
- Undertake a study into a suitable analogue to guide future exploration.

9.5 Prospectivity within the Gondwannan G1 and G2 Petroleum System (late Carboniferous – Permian)

The Gondwannan G1 and G2 petroleum system is the shallowest system in the project area. Exploration prospectivity of the Gondwannan G2 petroleum system is considered to be high risk.

9.5.1 *Source Rocks*

The candidate source rock within the Gondwannan G1 and G2 petroleum system is the Noonkanbah Formation, however petroleum reservoired within the Grant Group has been

identified to have generated from the deeper Laurel Formation (Table 2.2) due to immaturity and low genetic potential of Noonkanbah Formation sediments.

Noonkanbah Formation

The Early Permian Noonkanbah Formation (a marginal marine to marine shale interbedded with siltstone) has good to very good organic contents (2.17% TOC regionally and 1.69% TOC in the project area). Despite favourable TOC, the formation shows poor genetic yields (0.11 kg HC/ton S1, 1.09 kg HC/ton S2). Kerogen typing shows that the formation is also likely inert – representing a type III to type IV kerogen.

Modelling indicates that the Noonkanbah Formation reaches peak maturity in the Late Triassic (200 Ma). The formation reaches the early oil window in the Gregory Sub-basin, though remains immature on the Betty Terrace, Balgo Terrace and Billiluna Sub-basin at peak maturity. The source rock shows very low transformation ratios well below the 50% threshold required for generation (showing a maximum 4% TR), thus it does produce petroleum to charge reservoirs within the project area, and migration is required from a deeper structural setting.

Laurel Formation

Although a member of the Larapintine L3 and L4 petroleum system, the effective source rock for plays in late Carboniferous to Permian stratigraphy is the Carboniferous Laurel Formation – a clastic and carbonate sequence. As discussed in above, the Laurel Formation is available to charge reservoirs between 220 Ma to 192 Ma. Vertical hydrocarbon migration through the Anderson Formation (where preserved) is required to charge Gondwannan G1 and G2 reservoirs.

9.5.2 *Reservoir Rocks*

The Late Carboniferous to Early Permian Grant Group (Grant Group members A and C), the Permian Poole Sandstone and Permian Liveringa Group are the candidate reservoir rocks of the G1 and G2 petroleum system.

The Late Carboniferous Grant Group member A (a medium to coarse grained sandstone) represents excellent reservoir quality, with 18.5% core porosity (Atrax 1) and 754 mD to 1015 mD permeability. Sonic derived porosities at Bindi 1, Kilang Kilang 1 and Olios 1 also demonstrate excellent reservoir quality, ranging 7 % up to 26%. Grant Group member C (an interbedded siliciclastic sequence) also displays excellent reservoir properties, showing an average sonic porosity of 13% at Bindi 1, up to 20% at Kilang Kilang 1 and up to 37% at Olios 1.

The Permian Poole Sandstone (a medium to coarse grained sandstone) deposited in a shallow marine to marginal marine paleogeographic environment (Figure 9.18) demonstrates excellent reservoir quality, with in excess of 20% sonic derived porosity across the project area (Table 4.7).

The Permian Liveringa Group Condren Sandstone (a coarse grained sandstone) and Lightjack Formation (an interbedded fine grained siliciclastic sequence) show good reservoir potential, however the upper Condren Sandstone is proposed as the main reservoir unit of the Liveringa Group, based on a cleaner gamma ray log relative to the Lightjack Formation. Sonic derived porosities at Kilang Kilang 1 show excellent reservoir characteristics, in excess of 21% porosity.

The availability of suitable reservoir rocks is not deemed problematic for the G1 and G2 petroleum system. Paleogeographic reconstructions infer a favourable setting for reservoir development throughout periods in the late Carboniferous to Permian, where candidate reservoir zones align with periods of low stand systems and progradational sediment

deposition (Figure 9.17 and Figure 9.18). Timing of key reservoir development is mostly related to the deposition of the Late Carboniferous Grant Group A member between 326 Ma to 303 Ma, the Grant Group C member between 299 Ma to 294 Ma, Poole Sandstone between approximately 294 Ma to 284 Ma, and the Liveringa Group between 265 Ma to 253 Ma.

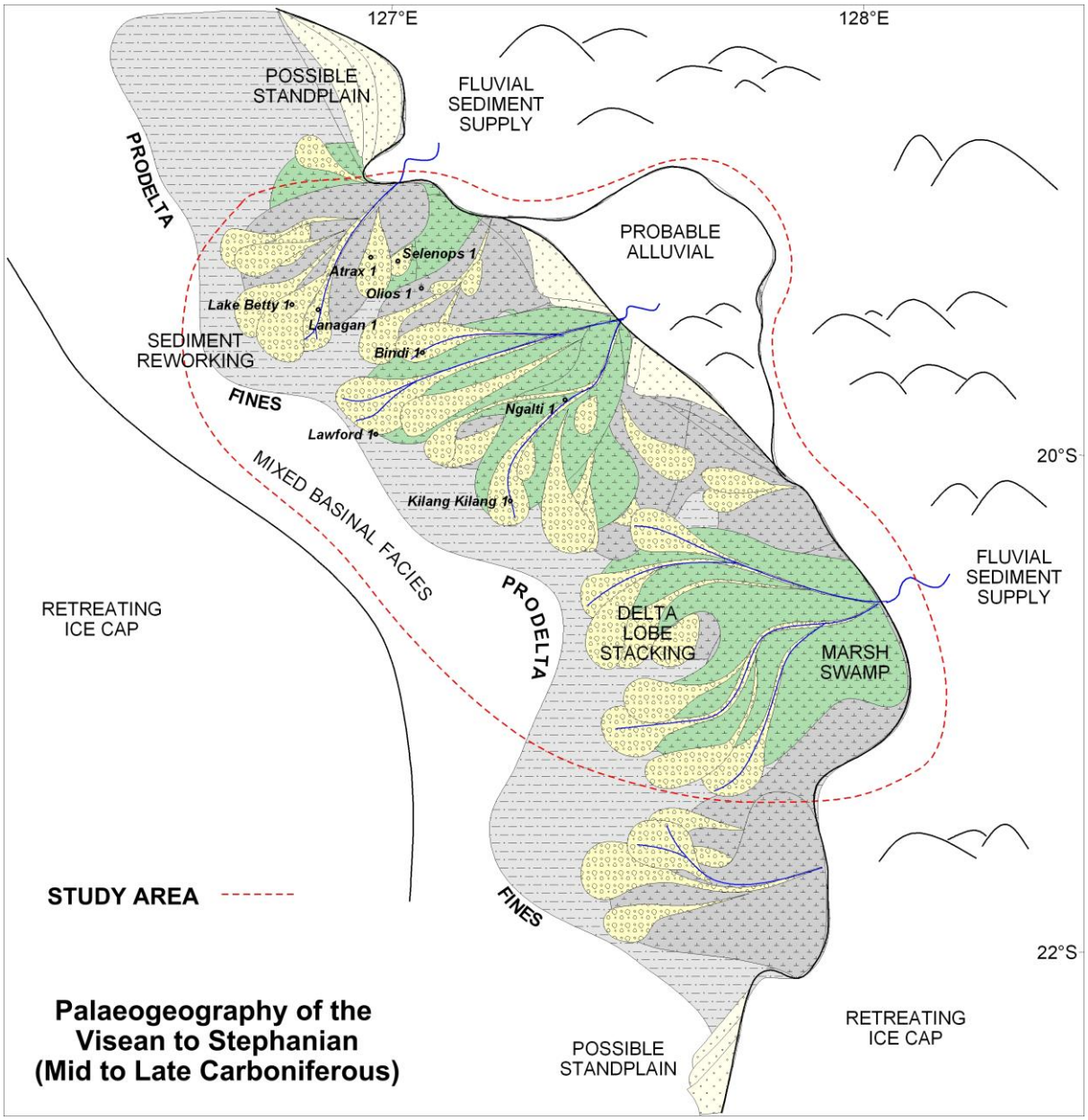

Figure 9.17. Palaeogeography of the mid to late Carboniferous.

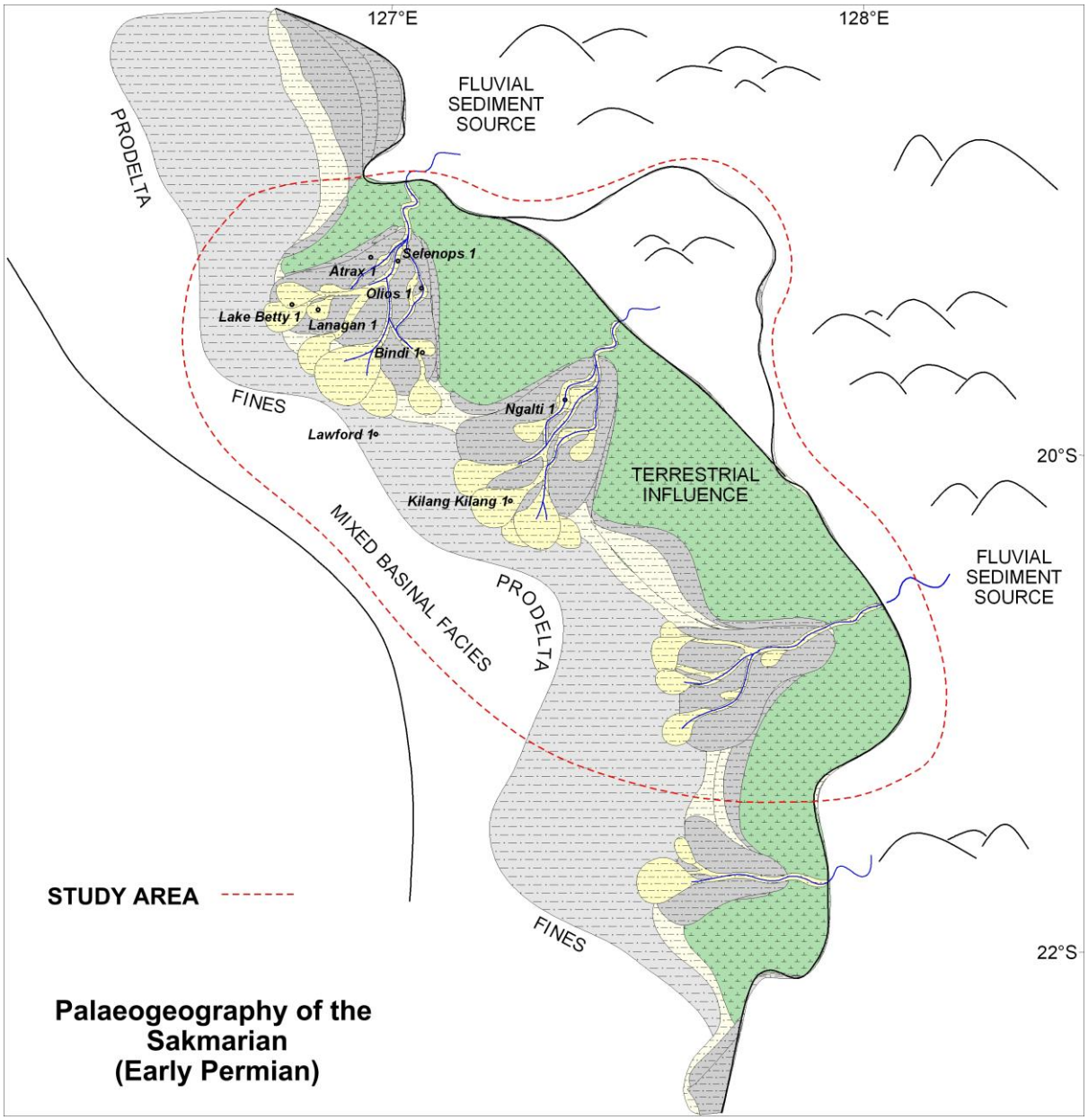

Figure 9.18. Palaeogeography of the early Permian.

9.5.3 *Seals*

Candidate seals within the G1 and G2 petroleum system includes the Late Carboniferous Grant Group B member and the Permian Noonkanbah Formation. The Triassic Blina Shale is

noted to occur at Bindi 1 and Lake Betty 1, however its regional extent is unknown. The Blina Shale may act as a potential seal within the project area.

The Late Carboniferous Grant Group B member (a fine grained siliciclastic interval) provides an 'intra-Grant Group seal'. Correlation of the B member across the study area (Figure 4.32, and figures 4.44 through 4.46) demonstrates that the seal is regional. Sonic derived porosity data indicates that the seal may be ineffective to hold back large hydrocarbon columns (sonic porosities up to 20% are observed at Kilang Kilang 1), however core calibrated data is not available. Based on the regional extent and lithological character, the Grant Group B member is considered capable to seal hydrocarbons.

The Permian Noonkanbah Formation is regionally extensive across the project area from well and seismic correlations. As per the Grant Group B member, core calibrated data is not available, however based on the regional extent and lithological character, the interval is considered capable to seal hydrocarbons.

Timing of seal availability relates to the deposition of the Late Carboniferous Grant Group B member (approximately 303 Ma to 299 Ma) and the Permian Noonkanbah Formation (284 Ma to 275 Ma).

9.5.4 *Trap Development*

Trap development for hydrocarbons generated in the Gondwannan G1 and G2 petroleum system is likely as a result of the Triassic Fitzroy Movement. Seismic evidence of structures that developed during the Triassic is limited. Shallow faulting is difficult to discern on seismic due to poor near-surface imaging. For example, the broad anticline on line RB81-7, (SP250, Figure 6.5) appears contiguous through most stratigraphy; the TWT surface on the regional Meda Transpression unconformity, Grant Group, Poole Sandstone, Noonkanbah Formation, and shallow reflection packages shows broad folding. The structure may have

initially developed in the Carboniferous but takes its present day geometry from the Triassic Fitzroy Movement (for example Lawford 1).

The RB82-28 pseudo well on the Betty Terrace (Figure 9.19) indicates uplift in the Triassic, which supports a regional structural episode at the time, supported by AFTA (Duddy et al, 2003), and indicates the timing of the Triassic Fitzroy Movement to occur between approximately 200 Ma to 181 Ma.

This indicates that trap development occurred at a similar time to sediments reaching maximum maturity in the project area.

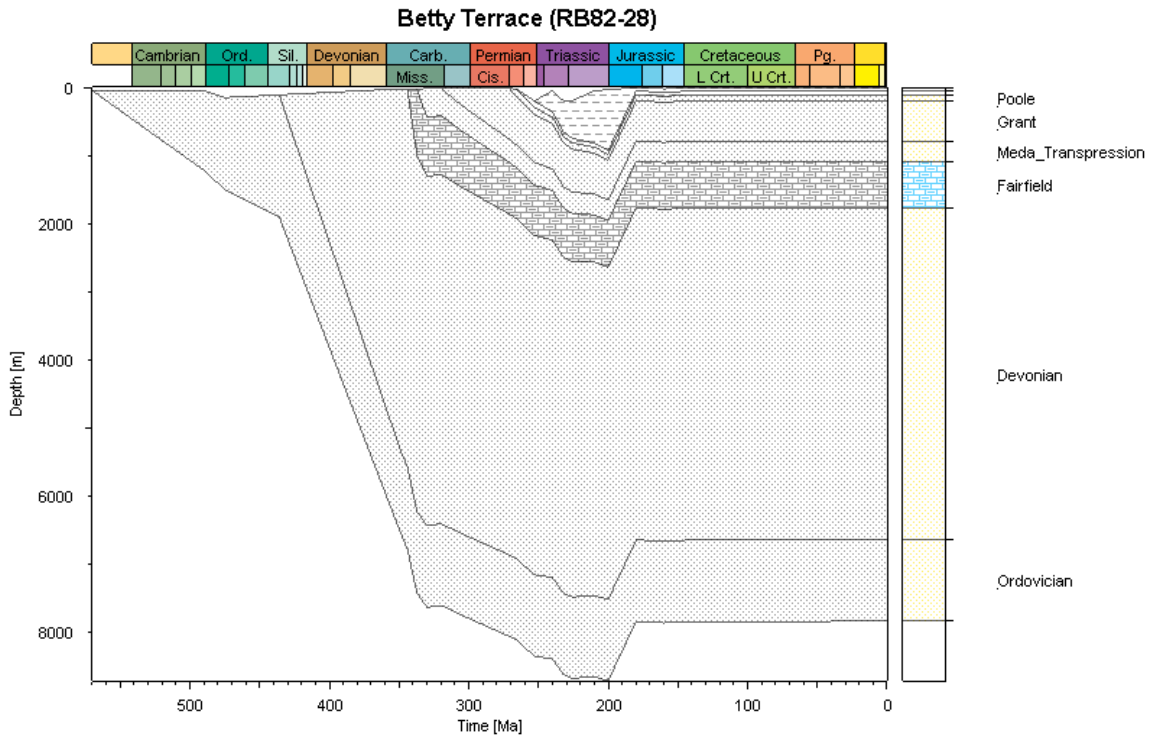

Figure 9.19. Burial history diagram of the RB82-28 Betty Terrace pseudo well.

9.5.5 *Timing and Migration*

The Noonkanbah Formation does not expel hydrocarbons because it is immature within the project area. Within the study area the Noonkanbah Formation contributes to the G1 and G2 petroleum system as a regional seal over the Poole Sandstone and Grant Group sediments. Hydrocarbons generated from the Laurel Formation are expected to migrate from areas of deeper burial and higher organic richness (i.e. the Gregory Sub-basin), as Permian sediments on the terraces are largely immature (or early oil mature at peak maturity).

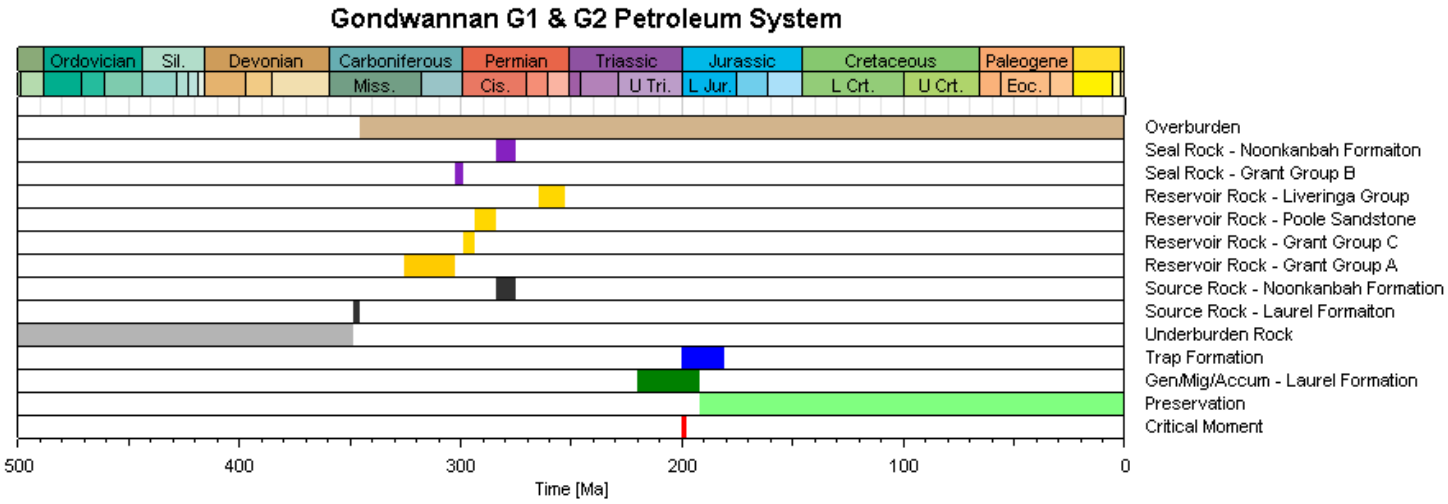

Figure 9.20. Critical moment diagram for plays within the Gondwannan G1 and G2 petroleum system.

Timing is potentially restrictive for accumulations within the G1 and G2 petroleum system. Figure 9.20 illustrates that reservoirs develop in the Late Carboniferous and Permian. Seals develop in the Late Carboniferous and Late Permian. Unless the Triassic Blina Shale is present, there is no seal for the Liveringa Group reservoir. Expulsion from the mature Laurel Formation occurs in the Triassic. Trap development occurs at the later stages of expulsion, with overlap across a narrow 8 My period between 200 Ma to 192 Ma.

9.5.6 *Play-type targeting, risks and remarks*

The Laurel Formation source rock matures to the oil window in the Gregory Sub-basin. Lateral migration is required to charge reservoirs. In any case, the accumulation will likely be

an oil hydrocarbon product, unless hydrocarbons from deeper systems migrate vertically to shallower targets at the G1 and G2 level.

Thermal maturity is a risk for the Gondwannan G1 and G2 petroleum system, with only the Laurel Formation maturing to the oil window, and only within the Gregory Sub-basin.

Hydrocarbon leakage is a potential risk. This would be due to more recent (Jurassic and Cretaceous) periods of basin activity, highlighted by Duddy et al (2003). Any reactivation on faults in the Jurassic is perceived as the greatest relative risk to trap integrity and hydrocarbon preservation in the G1 and G2 petroleum system.

Explorers should target migrated accumulations into late Triassic trapping configurations, within the Grant Group or Poole Sandstone (to intersect Grant Group B member or Noonkanbah Formation seal) on the Betty and Balgo Terraces. Traps should ideally be sought close to basinal positions (either near Bindi 1 or near the Gregory Sub-basin proper) to minimize migration distances (Figure 9.21), however a migration study is recommended to contemplate multi-phase hydrocarbon migration to traps nearer to the northeastern basin margin. The migration study should model geological history reconstructions to the late Triassic and consider any Jurassic reconfigurations.

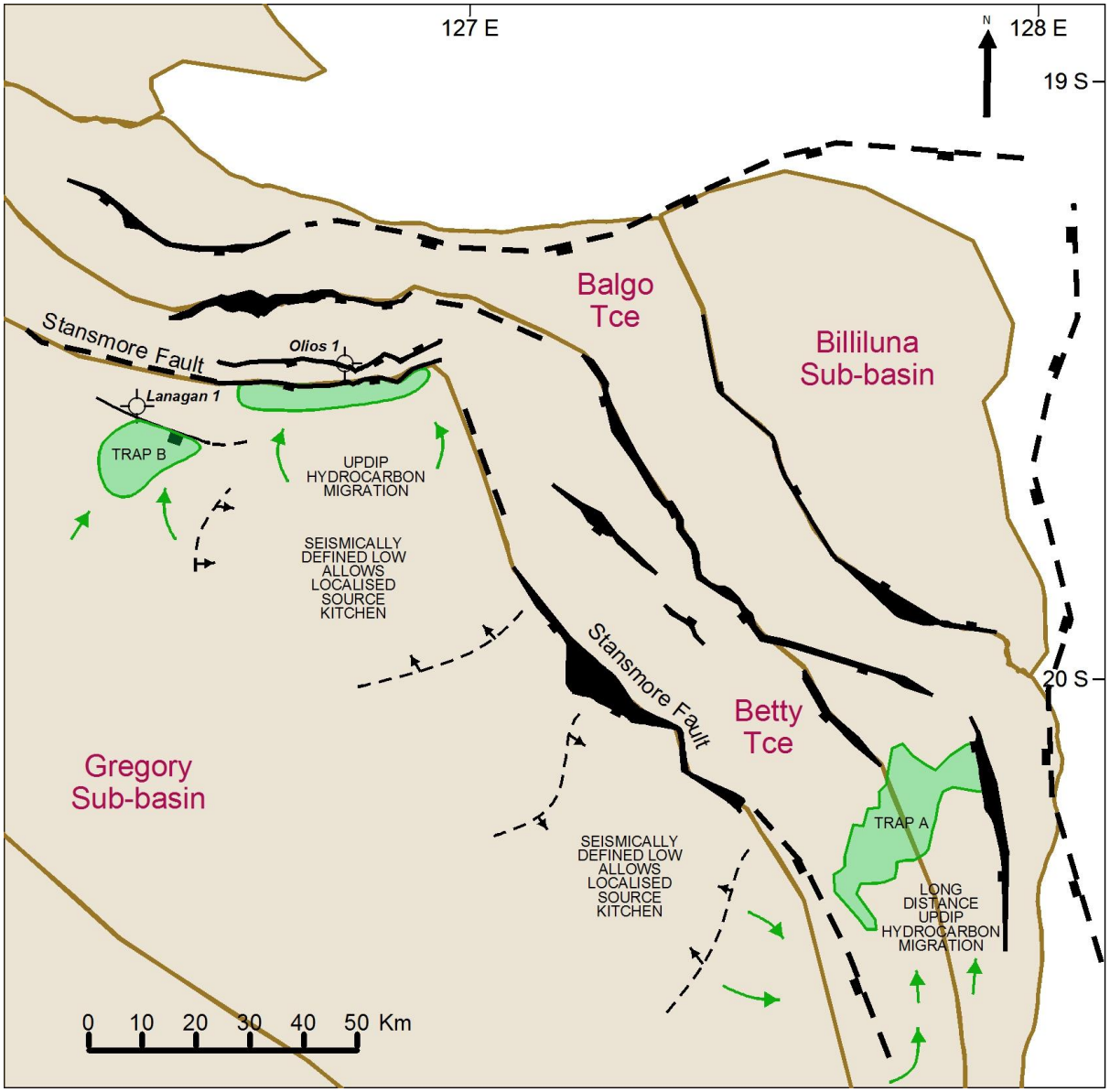

Figure 9.21. Play-type targets within the Gondwannan G1 and G2 petroleum system.

9.5.7 *Key Recommendations*

The key recommendations to reduce risk in exploration for G1 and G2 related hydrocarbon plays are:

- Similar to the L3 and L4 system; acquire vitrinite reflectance data from the Lake Betty 1 well location to calibrate 1D models. Similarly, undertake a sample in-fill program for vitrinite data across wells locations in the study area.
- Acquire Apatite Fission Track Analysis (AFTA) at 2 to 3 well locations within the project area to assist in calibrating basin models and thermal histories.

- Obtain porosity and permeability data to calibrate sonic derived porosity within the Grant Group and Poole Sandstone;
- Perform a thorough depth conversion of the seismic interpretation to attain a better understanding of depth-structures. This is particularly important for shallower stratigraphy as currently no significant structures appear in TWT, with the exception of the Kilang Kilang 1 structural closure (for example, the Near Top Poole Sandstone, Figure 6.13);
- Enhance the fault interpretation across the seismic grid with attention to correlating smaller scale faults in shallow stratigraphy;
- Enhance the current 2D models by exploiting the use of facies maps (including heat flow and TOC) to accommodate the lateral special variability in formations between wells. For example, TOC can be varied between wells indicated by percentage composition of shale lithologies. This will improve the conceptual accuracy of the models.

10. Conclusions and Recommendations

10.1 Conclusions

This study evaluated the petroleum systems on the Betty Terrace, Balgo Terrace and within the Billiluna Sub-basin in the northeast Canning Basin. The following conclusions can be drawn from this study:

Reservoir Rocks

1. Excellent reservoir conditions exist for the Devonian Knobby Sandstone and Permo-Carboniferous Grant Group (member A).
2. The Carboniferous Anderson Formation (units B, D, and F), the upper clastic zone of the Carboniferous Laurel Formation, the Grant Group (members B and C), and the Permian Poole Sandstone show excellent reservoir potential.
3. 2D Seismic indicates that there are numerous undrilled prospects within the project area.

Seal Rocks

4. There appears to be good sealing capacity in the lower Laurel Formation shales (indicated in the Lake Betty 1 well).
5. The Carboniferous Anderson Formation (units A, C, E, and G) show potential as intraformational seals (indicated in the Bindi 1 well).
6. The Permian Noonkanbah Formation represents good sealing potential. The formation signifies the maximum Permian transgression in the Canning Basin.

Source Rocks and Thermal Maturity

7. The Noonkanbah Formation is organically rich, but modelling indicates it is immature within the project area.
8. The Anderson Formation is organically lean, but modelling indicates it is mature for oil in the Gregory Sub-basin and immature on the terraced areas within the project area.

9. The Laurel Formation is organically lean on the Betty and Balgo Terraces, though appears more organically rich in basinal positions. Modelling indicates that the formation is mature for oil within the Gregory Sub-basin and early mature for oil on the terraced areas. Exploration at this level should focus on migrating hydrocarbons from basinal positions to shelfal reservoirs.
10. Modelling indicates that the Gogo Formation is mature for oil on terraced areas and mature for gas in the Gregory Sub-basin. Geochemical data indicates that the Gogo Formation has lean generative potential, however data is sparse.
11. The Bongabinni Member geochemical data suggests the member is a lean source rock but published literature advertises otherwise. Data is limited, so the source rock potential is not discounted at this stage. Modelling indicates that the Bongabinni Member is mature for gas on terraces and over mature in the Gregory Sub-basin.
12. The highly proclaimed organically rich Goldwyer Formation shales are unlikely to be present within the project area due to an unfavourable paleogeographic setting. The Goldwyer formation is likely to exist as a proximal sand-rich facies equivalent within the study area. The formation, should it be found in future to be present within the study area; is mature for gas on the terraced areas and over mature in the Gregory Sub-basin according to modelling undertaken in this project.
13. 1D and 2D modelling, supported by AFTA (Duddy et al., 2003), indicates sediments obtain maximum maturity in the Late Triassic (200 Ma).
14. Peak maturity is pushed forward from the Carboniferous to the Triassic. The Triassic generative phase gives some hope to hydrocarbon charge into Carboniferous and Triassic structures, thus enhancing the prospectivity.
15. 1D and 2D modelling indicates that all source rocks (except the Permian Noonkanbah Formation) appear to have generated hydrocarbons at some point within the Gregory Sub-basin and terraced areas.
16. 2D modelling indicates thermal maturity regionally increases in a southwest direction towards the Gregory Sub-basin, which is a source kitchen.
17. Seismic indicates the development of a central area depocentre surrounding the Bindi 1 well location. This is considered to be an extension of the Gregory Sub-basin source kitchen, thus improving prospectivity within the project area. Hydrocarbons generated in the Gregory Sub-basin therefore require less lateral migration than what was previously indicated by published literature.

18. The central area depocentre facilitates a slight a revision to the tectonic elements map, which allows for the Gregory Sub-basin source kitchen to extend northeast.
19. 2D modelling indicates favourable petroleum system evolution over a large undrilled structural closure in the southern project area, which warrants further investigation.

Prospectivity:

20. The Gondwannan G1 and G2 petroleum system is unlikely to be prospective within the project area. Prospectivity may exist where the Noonkanbah Formation can be found in a thermally mature setting. A migration study will enable consideration of accumulations resulting from multiple stage hydrocarbon migration to traps nearer the basin margin.
21. The Larapintine L3 and L4 petroleum system is proven to contain the most options for explorers in the study area. Prospectivity is enhanced by AFTA data (Duddy et al., 2013) and a thorough understanding of thermal maturity. Devonian and Carboniferous aged reservoirs are the most highly prospective. Exploration should focus on migrating petroleum from thermally mature areas to traps near the central area depocentre or on terraced positions near the Gregory Sub-basin. A Migration study should be undertaken to minimize risk.
22. The Larapintine L2 petroleum system is untested within the project area, but appears prospective. Perhaps, the simplest way to assess this petroleum system is to undertake a basic narrow-diameter core-hole drilling program to test Ordovician source rock organic richness where allowable within drillable depths. Prospectivity may exist within the Billiluna Sub-basin, which is currently untested.
23. The Billiluna Sub-basin has not been tested by exploration drilling, and there is little validation of subsurface stratigraphy in data at hand. A narrow-diameter drilling program within the Billiluna Sub-basin will confirm the nature of stratigraphy across the Billiluna horst block.

10.2 Recommendations:

The key recommendations that can be made after concluding this study are summarised as follows.

Lab Data Acquisition:

1. Obtain lab data (i.e. Mercury Injection Capillary Pressure, MICP) to quantify sealing capacity of the Laurel Formation shales and the Nita Formation Carbonates;
2. Obtain further porosity and permeability measurements for the Grant Group, Laurel Formation and Carribuddy Group reservoirs to calibrate sonic derived porosity;
3. Undertake a sample in-fill program for Vitrinite Reflectance data across well locations in the study area. More VR would be useful at Ngalti 1, Lake Betty 1 and Bindi 1;
4. Acquire Apatite Fission Track Analysis (AFTA) at 2 to 3 well locations within the project area; for example at Bindi 1, Ngalti 1 and Olios 1, to assist in calibrating basin models and thermal histories, and also further reconcile exhumation estimated at White Hills 1 to the project area.

Seismic Interpretation:

5. Perform a thorough depth conversion of the seismic interpretation to attain a better understanding of depth-structures. This is particularly important for shallower stratigraphy as currently no significant structures appear in TWT;
6. Enhance the fault interpretation across the seismic grid with attention to correlating smaller scale faults. This will aid in understanding hydrocarbon migration;
7. Ideally, reprocess the key internal loop tie lines (Figure 3.4) with the same reprocessing house to ensure correct phase and bulk shifts are applied.

Modelling:

8. Enhance the current 2D models by interpreting further seismic horizons to better reflect the lateral correlation of the Gogo Formation and Goldwyer Formation isopachs. This will provide a better assessment of accumulation analysis in the RB82-28 2D model.

9. Enhance the current 2D models by exploiting the use of facies maps (including heat flow and TOC) to accommodate the lateral variability in formations between wells. For example, TOC can be varied between wells by indicating a percentage composition of shale lithologies. This will improve the conceptual accuracy of the 2D models.

Drilling:

10. In the correct economic environment, drilling further exploratory wells are the key to understanding the petroleum systems in the northeastern Canning Basin. The largest apparent structure in the study area remains undrilled (Trap A, Figure 6.10). Petroleum systems modelling (RB82-28, Figure 8.46) indicates that Trap A has the potential to accumulate significant hydrocarbon volumes.

References

ABS (2006). National Regional Profile: Broome, Derby, Fitzroy. Retrieved 2011 28-November from Australian Bureau of Statistics.

Apak, S. N., & Backhouse, J., (1998). Redefinition of the Grant Group and Reinterpretation of the Permo-Carboniferous succession, Canning Basin. In Purcell, P. G., & Purcell, R. R., (Eds.), The Sedimentary Basins of Western Australia 2 (pp. 683-694). Petroleum Exploration Society of Australia; West Australian Basin Symposium, Perth, WA.

Australian Government Bureau of Meteorology (BOM), Temperature Records for Halls Creek WA, accessed 24th March 2015. www.bom.gov.au

Beardsmore, G. R., and Cull, J, P., (2001), Crustal Heat Flow. Cambridge University Press.

Beaumont, A. A., and Foster, N. H., (1999). Exploring for Oil and Gas Traps, American Association of Petroleum Geologists.

Bloch, S., Lander, R. H., and Bonnell, L., (2002). Anomalously high porosity and permeability in deeply buried sandstone reservoirs: Origin and predictability. *AAPG bulletin*, *86*(2), 301-328.

Bradshaw, M. T., Bradshaw, J., Murray, A. P., Needham, D. J., Spencer, L., Summons, R. E., Winn, S., (1994). Petroleum Systems in West Australia Basins. In P. G. Purcell, & R. R. Purcell (Eds.), The Sedimentary Basins of Western Australia. Proceedings, Western

Australian Basins Symposium, Perth, WA. (pp. 93-118). Geological Society Australia/Petroleum Exploration Society of Australia.

Brakel, A.T. and Totterdell, J. M., (1990). The Permian Paleogeography of Australia, BMR Record 1990/60, Geoscience Australia.

Brown, S.A., Boserio, I.M., Jackson, K.S., Spence, K.W., (1984). The Geological Evolution of the Canning Basin – Implications for Petroleum Exploration, in: Purcell, P.G., (Eds). Proceedings of the GSA/PESA Canning Basin Symposium, Perth.

Burrus, J., (1985). Thermal Modeling in Sedimentary Basins: 1st IFP Exploration Research Conference, Carcans, France

Burt, A., Champ, P., & Parks, A., (2002). Petroleum Prospectivity of the Eastern Canning Basin, WA. WA: Troy Ikoda (Department of Mineral and Petroleum Resources).

Buru Energy, (2015). Buru Energy's conventional oil discovery at Ungani. [ONLINE] Available at: http://www.buruenergy.com/canning-basin/oil/. [Accessed 19 November 15].

Cadman, S. J., Pain, L., Vuckovic, V., and le Poidevin, S. R., (1993). Bureau of Resource Sciences, Australian Petroleum Accumulations Report 9.

Carlsen, G. M., & Ghori, K. A., (2005). Canning Basin and Global Palaeozoic Petroleum Systems - A Review. APPEA Journal, 394-363.

Carr, A. D., 2000. Suppression and retardation of Vitrinite reflectance, part 1. Formation and significance for hydrocarbon generation: Journal of Petroleum Geology, v. 23, p. 313-343.

Casey, J. N., & Wells, A. T., (1960). Regional Geology of the North-East Canning Basin, Western Australia. Bureau of Mineral Resources Geology and Geophysics, 1960 (110), 147.

Cook, P. J. and Totterdell, J. M., (1990). The Ordovician Paleogeography of Australia, BMR Record 1990/60, Geoscience Australia.

Cookson, S and Jones, P, (2013a). Lawford 1 Deepening Well Completion Report (Basic and Interpretive), Geological Survey of Western Australia: New Standard Onshore Limited.

Cookson, S and Jones, P, (2013b). Lawford 1 Well Completion Report (Basic and Interpretive), Geological Survey of Western Australia: New Standard Onshore Limited.

Corcoran, D. V. and A. G. Doré (2005). A review of techniques for the estimation of magnitude and timing of exhumation in offshore basins. Earth-Science Reviews 72 (3–4). pp 129-168.

Crank, K, (1972). Lake Betty 1 Well Completion Report, Geological Survey of Western Australia: West Australian Petroleum Pty. Limited.

Dow, W. G., (1977). Kerogen studio and geological interpretations: Journal of Geochemical Exploration, v. 7, p. 79-99.

Duddy, I.R., Green, P.F., Gibson, H.J., and Hegarty, K.A., (2003). Regional paleo-thermal episodes in northern Australia. Timor Sea Petroleum Geoscience (Proceedings of the Timor Sea Symposium) 2003. pp 567-591.

Edwards, D. S., Summons, R. E., Kennard, J. M., Nicoll, R. S., Bradshaw, J., Bradshaw, M., Zumberge, J. E, (1997). Geochemical Characteristics of Palaeozoic Petroleum Systems in Northwestern Australia. APPEA Journal, 351-379.

Energy Information Administration, (2013). International Energy Outlook 2013. [Online] Available at: http://www.eia.gov/forecasts/aeo/pdf/0383(2013).pdf. [Access 30 November 2013].

Espitalie, J., Laporte, J. L., Madec, M., Marquis, F., Leplat, P., Paulet, J., and Boutefeu, A., (1977). Méthode rapide de caractérisation des roches mères de leur potentiel pétrolier et de leur degré d'évolution: Revue de'l Institut Français du Pétrole, v. 32, no. 1, p. 23-42.

France, R, (1984). Percival 1 Well Completion Report, Geological Survey of Western Australia: Western Mining Corporation Limited.

France, R and Scibiorski, J, (1984). Solanum 1 Well Completion Report, Geological Survey of Western Australia: Western Mining Corporation Limited.

Geological Survey of Western Australia (GSWA), (2013). Well Data from Regional Canning Basin Wells. WA Department of Mines and Petroleum. Available at: https://wapims.dmp.wa.gov.au/WAPIMS. [Access 20 January 2013].

Geoscience Australia (GA), (2015). Onshore Petroleum Project. Commonwealth of Australia. Available at: http://www.ga.gov.au/about/what-we-do/projects/energy/onshore-petroleum. [Accessed 7 July 2015].

Gorter J. D., (1978), Triassic Environments in the Canning Basin, Western Australia, BMR Journal of Australian Geology & Geophysics, 3 p 25-33

Goutorbe, B., Lucazeau, F. and Bonneville, A., 2008. Surface heat flow and the mantle contribution on the margins of Australia. Geochemistry Geophysics Geosystems, 9(5): Q05011.

Guppy, D. J., Lindner, A. W., Rattigan, J. H., & Casey, J. N, (1958). Geology of the Fitzroy Basin, WA. Bureau of Mineral Resources (36).

Haines, P. W., (2004). Depositional facies and regional correlations of the Ordovician Goldwyer and Nita Formations, Canning Basin, Western Australia, with implications for petroleum exploration: Geological Survey of Western Australia, Record 2004/7, 45p.

Haines, P. W., & Ghori, K. A., (2010). Geology and Petroleum Prospectivity of State Acreage Release Areas L10-6, L10-7, L10-8, L10-9 and L10-10, Canning Basin, Western Australia. Geological Survey of Western Australia, Record 2010/15.

Hantschel, T. and A. I. Kauerauf, (2009). Fundamentals of Basin and Petroleum Systems Modelling, Springer Berlin Heidelberg.

Irwin, G, (1998). Lake Havern 1 Well Completion Report, Geological Survey of Western Australia: Amity Oil NL.

Jacobson, T, (1984). The Role of Seismic in Play Type and Prospect Development: Eastern Canning Basin. In The Canning Basin WA: Proceedings GSA/PESA Canning Basin Symposium, Perth (pp. 121-134).

Kingdom, (v8.8. 2013). IHS. www.ihs.com

Klappa, C.F., Shelby, D.C., and Appleton, K.P., (1984). Olios 1 Well Completion Report, Geological Survey of Western Australia: Gulf Oil Australia PTY LTD.

Klappa, C.F., Shelby, D.C., Appleton, K.P., McCaskey, H.M., Hamill, G.S., (1985a). Atrax 1 Well Completion Report, Geological Survey of Western Australia: Gulf Oil Australia PTY LTD.

Klappa, C.F., Shelby, D.C., Appleton, K.P., McCaskey, H.M., Hamill, G.S., (1985b). Selenops 1 Well Completion Report, Geological Survey of Western Australia: Gulf Oil Australia PTY LTD.

Lehmann, P.R., and Haines, R.A., (1985). Bindi 1 Well Completion Report, Geological Survey of Western Australia: Santos Limited.

Makhous, M., and Galushkin, Y. I., (2005). Basin Analysis and Modelling of the Burial, Thermal and Maturation Histories in Sedimentary Basins, Editions TECHNIP France.

McKenzie, D., (1978). Some remarks on the development of Sedimentary Basins. Earth Planet Science Letters, 40, p 25-32.

Murchison, D. G., Pearson, J. A., Raymond, C., (1991). Anomalies in Vitrinite reflectance gradients: Bulletin De La Societe Geologique De France, v. 162, p. 183-191.

New Standard Onshore (NSO), (2008). Lanagan 1 Well Completion Report, Geological Survey of Western Australia: New Standard Onshore Limited.

Neumann, V., di Primo, R., Horsfield, B., (2008). Source Rock Distributions and Petroleum Fluid Bulk Compositional Predictions on the Vulcan Sub-Basin, Offshore Western Australia, Geoscience Australia report #GeoS420081201

Park, R.G., (1997). Foundations of Structural Geology. 3rd edition, Routledge, p 216

Peters, K. E., (1986). Guidelines for evaluating petroleum source rock using programmed pyrolysis. AAPG Bulletin 70: 318 - 329.

Peters, K.E. and Cassa, M.R., (1994). Applied Source Rock Geochemistry, in Magoon, L.B, and Dow, W.G. (ed.) The Petroleum System - From Source to Trap. : AAPG Memoir 60, pp. 93 - 120.

Peters, K. E., Walters, C.C., Moldowan, J.M., (2005). The Biomarker Guide: Biomarkers and isotopes in petroleum systems and Earth history, Cambridge University Press.

PetroMod, (v2014.1. 2014). Schlumberger.
www.software.slb.com/products/petromod/petromod-systems

Prayitno, W., Armon, J.W., & Haryono, S., (1992). The Implications of Basin Modelling for Exploration – Sunda Basin Case Study, Offshore South East Sumatra. Proceedings of Indonesian Petroleum Association. Twenty First Annual Convention.

Purcell, P. G., (1984). Canning Basin, Introduction. In The Canning Basin WA: Proceedings GSA/PESA Canning Basin Symposium, Perth (pp. 3-19). Geological Society of Australia.

Smith, G., (1984). The Tectonic Development of the Gregory Sub-Basin and Adjacent Areas, Northeastern Canning Basin. In The Canning Basin WA.: Proceedings GSA/PESA Canning Basin Symposium, Perth (pp. 109-120). Geological Society of Australia.

Smith, G., (1985a). Kilang Kilang 1 Well Completion Report, Geological Survey of Western Australia: Pontoon Oil and Minerals NL.

Smith, G., (1985b). Ngalti 1 Well Completion Report, Geological Survey of Western Australia: Pontoon Oil and Minerals NL.

Smith, T.E., Kelman, A.P., Nicoll, R.S., Laurie, J.R., Le Poidevin, S.R., (2013). Geoscience Australia's Basin Biozonation and Stratigraphy Chart Series. Basin Biozonation and Stratigraphy Chart Series. Geoscience Australia, Canberra.

Sweeney, J. J., and Burnham, A. K., (1990). Evaluation of a Simple Model of Vitrinite Reflectance Based on Chemical Kinetics. AAPG Bulletin, 74, p 1559–1570

Taylor, D. D., (1992). Blina Oilfield, Canning Basin, Case History. Exploration Geophysics (Abstract Only), 23, 467-480 (Available through: CSIRO Publishing). Retrieved 2012 January

Tissot, B. P., and Welte, D. H., (1984). Petroleum Formation and Occurrence, 2 ed.: New York, Springer-Verlag.

Waples, D., (2001). A New Model for Heat Flow in Extensional Basins: Radiogenic Heat, Asthenospheric Heat, and the McKenzie Model. Natural Resources Research 10 (3): 227-238.

Wulff, K., (1987). Source Rock Evaluation of the Eastern Canning Basin, Unpublished: Petroz Petroleum Australia.

Yeates, A. N., Gibson, D. L., Towner, R. R., Crowe, R. W., (1984). Regional Geology of the Onshore Canning Basin, WA. In P. G. Purcell, The Canning Basin, WA: Proceedings GSA/PESA Canning Basin Symposium, Perth (pp. 23-55). Geological Society of Australia.

Appendix A

Reservoir Property Data

Porosity and permeability measurements from open file well completion reports and a database constructed by the Geological Survey of Western Australia was utilised in this study. These data are included in this Appendix.

Formation	Well	Type	Depth (mRT)	Porosity %	Vert. Porosity %	Permeability mD	Vert. Permeability mD
Bungle Gap Limestone	Atrax 1	Sonic	603	6.5			
Bungle Gap Limestone	Atrax 1	Sonic	621	6.5			
Bungle Gap Limestone	Atrax 1	Core	627.2	2.7		0.1	
Bungle Gap Limestone	Atrax 1	Core	632.05	2.9		0.1	
Bungle Gap Limestone	Atrax 1	Core	640.9	4.2		0.1	
Bungle Gap Limestone	Atrax 1	Sonic	650.5	3.5			
Goldwyer Formation WMC 3	Percival 1	Core	2050.98	1.2			
Goldwyer Formation WMC 3	Percival 1	Core	2050.98	1.2			
Goldwyer Formation WMC 3	Percival 1	Core	2053.45	0.8		0.02	
Goldwyer Formation WMC 3	Percival 1	Core	2053.45	0.8		0.02	
Goldwyer Formation WMC 3	Percival 1	Core	2053.45	0.8		0.02	
Goldwyer Formation WMC 3	Percival 1	Core	2060.17	2.3			
Goldwyer Formation WMC 3	Percival 1	Core	2060.17	2.3			
Goldwyer Formation WMC 3	Percival 1	Core	2060.17	2.3			
Goldwyer Formation WMC 3	Percival 1	Core	2063.4	1.2		0.3	
Goldwyer Formation WMC 3	Percival 1	Core	2063.4	1.2		0.3	
Goldwyer Formation WMC 3	Percival 1	Core	2064.18	1.9			
Goldwyer Formation WMC 3	Percival 1	Core	2064.18	1.9			
Goldwyer Formation WMC 3	Percival 1	Core	2064.18	1.9			
Goldwyer Formation WMC 4	Percival 1	Core	2041.13	1.2			
Goldwyer Formation WMC 4	Percival 1	Core	2041.13	1.2			
Goldwyer Formation WMC 4	Percival 1	Core	2041.13	1.2			
Goldwyer Formation WMC 4	Percival 1	Core	2043.9	1.8			
Goldwyer Formation WMC 4	Percival 1	Core	2043.9	1.8			
Goldwyer Formation WMC 4	Percival 1	Core	2044.04	2			
Goldwyer Formation WMC 4	Percival 1	Core	2044.04	2			
Goldwyer Formation WMC 4	Percival 1	Core	2044.12	2.4		0.01	
Goldwyer Formation WMC 4	Percival 1	Core	2044.12	2.4		0.01	
Goldwyer Formation WMC 4	Percival 1	Core	2044.12	2.4		0.01	
Goldwyer Formation WMC 4	Percival 1	Core	2045.58	1.3			
Goldwyer Formation WMC 4	Percival 1	Core	2045.58	1.3			
Goldwyer Formation WMC 4	Percival 1	Core	2045.58	1.3			
Grant Group	Ngalti 1	Sonic	280	13-40			
Grant Group A	Atrax 1	Sonic	521	22			
Grant Group A	Atrax 1	Sonic	541.5	26.5			
Grant Group A	Atrax 1	Sonic	551	20.5			
Grant Group A	Atrax 1	Sonic	572	17			
Grant Group A	Atrax 1	Sonic	582	17			
Grant Group A	Atrax 1	Core	583.4	18		754	
Grant Group A	Atrax 1	Core	585.6	18.5		1015	
Grant Group A	Olios 1	Sonic	698.5	16.2			
Grant Group A	Olios 1	Sonic	727.5	23.6			
Grant Group A	Olios 1	Sonic	736	21.3			
Grant Group A	Olios 1	Sonic	769	23.9			
Grant Group A	Olios 1	Sonic	780	26			
Grant Group A	Olios 1	Sonic	784.5	22.8			
Grant Group A	Olios 1	Sonic	795	24.5			
Grant Group B	Atrax 1	Sonic	455	26			
Grant Group B	Selenops 1	Sonic	362.5	22			
Grant Group B	Selenops 1	Sonic	377.5	29			
Grant Group B	Selenops 1	Sonic	395	24			
Grant Group B	Selenops 1	Sonic	415	26			
Grant Group B	Selenops 1	Sonic	436	22			
Grant Group C	Olios 1	Sonic	310	31.5			
Grant Group C	Olios 1	Sonic	326	31			
Grant Group C	Olios 1	Sonic	350	27.5			
Grant Group C	Olios 1	Sonic	411	33.3			
Grant Group C	Olios 1	Sonic	426	36.7			
Grant Group C	Olios 1	Sonic	436.5	34.1			
Grant Group C	Olios 1	Sonic	448	34.9			
Grant Group C	Olios 1	Sonic	473	33.4			
Grant Group C	Olios 1	Sonic	492	30.7			
Grant Group C	Olios 1	Sonic	499.5	26.3			
Knobby Sandstone	Ngalti 1	Core	1067.1	20		238	
Knobby Sandstone	Ngalti 1	Core	1067.15				8.3
Knobby Sandstone	Ngalti 1	Core	1067.4	19.4		195	
Knobby Sandstone	Ngalti 1	Core	1067.7	22		386	
Knobby Sandstone	Ngalti 1	Core	1067.75				5.5
Knobby Sandstone	Ngalti 1	Core	1068	22.3		460	
Knobby Sandstone	Ngalti 1	Core	1068.3	19		476	
Knobby Sandstone	Ngalti 1	Core	1068.4				794
Knobby Sandstone	Ngalti 1	Core	1068.6	18.6		685	
Knobby Sandstone	Ngalti 1	Core	1068.9	18.9		326	
Knobby Sandstone	Ngalti 1	Core	1069.1				818
Knobby Sandstone	Ngalti 1	Core	1069.25	20.5		512	

Knobby Sandstone	Ngalti 1	Core	1069.6	22.3		870	
Knobby Sandstone	Ngalti 1	Core	1069.6				332
Knobby Sandstone	Ngalti 1	Core	1069.9	18.8		262	
Knobby Sandstone	Ngalti 1	Core	1070.2	22.7		870	
Knobby Sandstone	Ngalti 1	Core	1070.3				69
Knobby Sandstone	Ngalti 1	Core	1070.45	22.6		830	
Knobby Sandstone	Ngalti 1	Core	1070.7	22.3		527	
Knobby Sandstone	Ngalti 1	Core	1070.9				442
Knobby Sandstone	Ngalti 1	Core	1071.1	18.1		316	
Knobby Sandstone	Ngalti 1	Core	1071.4	22.6		668	
Knobby Sandstone	Ngalti 1	Core	1071.4				242
Knobby Sandstone	Ngalti 1	Core	1071.7	19.7		368	
Knobby Sandstone	Ngalti 1	Core	1072	22.9		979	
Knobby Sandstone	Ngalti 1	Core	1072.1				565
Knobby Sandstone	Ngalti 1	Core	1072.3	21.9		314	
Knobby Sandstone	Ngalti 1	Core	1072.56	22.6		589	
Knobby Sandstone	Ngalti 1	Core	1072.6				125
Knobby Sandstone	Ngalti 1	Core	1072.9	21.1		870	
Knobby Sandstone	Ngalti 1	Core	1073.2	19.4		356	
Knobby Sandstone	Ngalti 1	Core	1073.25				208
Knobby Sandstone	Ngalti 1	Core	1073.5	20.8		553	
Knobby Sandstone	Ngalti 1	Core	1073.76	22		721	
Knobby Sandstone	Ngalti 1	Core	1073.8				320
Knobby Sandstone	Ngalti 1	Core	1074.08	21		623	
Knobby Sandstone	Ngalti 1	Core	1074.3				309
Knobby Sandstone	Ngalti 1	Core	1074.4	17.5		397	
Knobby Sandstone	Ngalti 1	Core	1074.75	21		532	
Knobby Sandstone	Ngalti 1	Core	1075				527
Knobby Sandstone	Ngalti 1	Core	1075.1	20.6		623	
Knobby Sandstone	Ngalti 1	Core	1075.4	22.2		818	
Knobby Sandstone	Ngalti 1	Core	1075.6				668
Knobby Sandstone	Ngalti 1	Core	1075.7	20.5		630	
Knobby Sandstone	Ngalti 1	Core	1076	17.5		626	
Knobby Sandstone	Ngalti 1	Core	1077.1	19.9		731	
Knobby Sandstone	Ngalti 1	Core	1077.9	23.3		794	
Knobby Sandstone	Ngalti 1	Core	1077.9				637
Knobby Sandstone	Ngalti 1	Core	1779.1	11.8		2.82	
Knobby Sandstone	Ngalti 1	Core	1779.15				3.5
Knobby Sandstone	Ngalti 1	Core	1779.25	11.5		2.02	
Knobby Sandstone	Ngalti 1	Core	1779.45	10.3		0.89	
Knobby Sandstone	Ngalti 1	Core	1780.24	11.2			
Knobby Sandstone	Ngalti 1	Core	1780.5				1.4
Knobby Sandstone	Ngalti 1	Core	1780.55	12.1		21.5	
Knobby Sandstone	Ngalti 1	Core	1780.85	9.5		0.75	
Knobby Sandstone	Ngalti 1	Core	1781.2	10.3		0.68	
Knobby Sandstone	Ngalti 1	Core	1781.9	12.4		11.2	
Knobby Sandstone	Ngalti 1	Core	1782.17	12.2		22.6	
Knobby Sandstone	Ngalti 1	Core	1782.25				20.7
Knobby Sandstone	Ngalti 1	Core	1782.47	13.3		72	
Knobby Sandstone	Ngalti 1	Core	1782.77	12.1		55	
Knobby Sandstone	Ngalti 1	Core	1783.03	12.2		95	
Knobby Sandstone	Ngalti 1	Core	1783.38	11.6		76	
Knobby Sandstone	Ngalti 1	Core	1783.5				25.5
Knobby Sandstone	Ngalti 1	Core	1783.7	12.9		28.4	
Knobby Sandstone	Ngalti 1	Core	1784	12.5		19.7	
Knobby Sandstone	Ngalti 1	Core	1784.32	10.9		8.71	
Knobby Sandstone	Ngalti 1	Core	1784.6	11.8		24.9	
Knobby Sandstone	Ngalti 1	Core	1784.7				15.5
Knobby Sandstone	Ngalti 1	Core	1784.9	12.6		47.5	
Knobby Sandstone	Ngalti 1	Core	1785.2	12.2		36.1	
Knobby Sandstone	Ngalti 1	Core	1785.5	12.2		43.9	
Knobby Sandstone	Ngalti 1	Core	1786	12.1		37.7	
Knobby Sandstone	Ngalti 1	Core	1786				0.96
Knobby Sandstone	Ngalti 1	Core	1786.3	12.5		26	
Knobby Sandstone	Ngalti 1	Core	1786.6	13.1		96	
Knobby Sandstone	Ngalti 1	Core	1786.9	11.5		68	
Knobby Sandstone	Ngalti 1	Core	1787.2	12.2		31.5	
Knobby Sandstone	Ngalti 1	Core	1787.3				78
Knobby Sandstone	Ngalti 1	Core	1787.5	11.9		24.1	
Knobby Sandstone	Ngalti 1	Core	1787.8	12.2		63	
Knobby Sandstone	Ngalti 1	Core	1788.15	11.7		31.3	
Knobby Sandstone	Ngalti 1	Core	1788.45	12.5		74	
Knobby Sandstone	Ngalti 1	Core	1788.55				87
Knobby Sandstone	Ngalti 1	Core	1788.75	12.3		84	
Knobby Sandstone	Ngalti 1	Core	1789.05	12.1		94	
Knobby Sandstone	Ngalti 1	Core	1789.3	10.4		3.03	

Knobby Sandstone	Olios 1	Sonic	1561.5	14			
Knobby Sandstone	Olios 1	Sonic	1574	12.6			
Knobby Sandstone	Olios 1	Sonic	1589.5	18			
Knobby Sandstone	Olios 1	Sonic	1623	17.3			
Knobby Sandstone	Olios 1	Sonic	1657.8	15.7			
Knobby Sandstone	Olios 1	Sonic	1679.5	16.6			
Knobby Sandstone	Olios 1	Sonic	1715.5	12.6			
Knobby Sandstone	Olios 1	Sonic	1746	10.4			
Knobby Sandstone	Olios 1	Sonic	1776.7	16.6			
Knobby Sandstone	Olios 1	Sonic	1785.5	12.3			
Knobby Sandstone	Olios 1	Sonic	1813	13.3			
Knobby Sandstone	Olios 1	Sonic	1826.3	11.5			
Knobby Sandstone	Olios 1	Sonic	1845.5	13.3			
Knobby Sandstone	Olios 1	Sonic	1846.6	17.5			
Knobby Sandstone	Olios 1	Sonic	1859.7	6			
Knobby Sandstone	Olios 1	Sonic	1881.5	6			
Knobby Sandstone	Olios 1	Sonic	1899	12.5			
Knobby Sandstone	Olios 1	Sonic	1902	11.5			
Knobby Sandstone	Olios 1	Sonic	1926.5	12.1			
Laurel Formation	Olios 1	Sonic	926	22			
Laurel Formation	Olios 1	Sonic	930	21			
Laurel Formation	Olios 1	Sonic	938	22			
Laurel Formation	Olios 1	Sonic	955.2	19			
Laurel Formation	Olios 1	Sonic	964	15.8			
Laurel Formation	Olios 1	Sonic	967	19.7			
Laurel Formation	Olios 1	Sonic	969.5	20.7			
Laurel Formation	Olios 1	Sonic	981.2	21.6			
Laurel Formation	Olios 1	Sonic	983.2	14.1			
Laurel Formation	Olios 1	Sonic	986.5	20			
Laurel Formation	Olios 1	Sonic	993	19.3			
Laurel Formation	Olios 1	Sonic	995	20.5			
Laurel Formation	Olios 1	Sonic	1001.5	16.8			
Laurel Formation	Olios 1	Sonic	1011.5	20.5			
Laurel Formation	Olios 1	Sonic	1023	18.5			
Laurel Formation	Olios 1	Sonic	1037.5	19.3			
Laurel Formation	Olios 1	Sonic	1044	14.4			
Laurel Formation	Olios 1	Sonic	1055	17			
Laurel Formation	Olios 1	Sonic	1061.5	13.4			
Laurel Formation	Olios 1	Sonic	1069.8	12.1			
Laurel Formation	Olios 1	Sonic	1439	19.8			
Laurel Formation	Olios 1	Sonic	1450.5	18.7			
Laurel Formation	Olios 1	Sonic	1477.7	18			
Laurel Formation	Olios 1	Sonic	1498.8	19.3			
Laurel Formation	Olios 1	Sonic	1526.5	16.7			
Laurel Formation	Olios 1	Sonic	1542.5	17.8			
Laurel Formation	Olios 1	Sonic	1553.5	18.3			
Nita Formation	Percival 1	Core	2026.63	0.9			
Nita Formation	Percival 1	Core	2026.63	0.9			
Nita Formation	Percival 1	Core	2026.63	0.9			
Nita Formation	Percival 1	Core	2031.25	0.8			
Nita Formation	Percival 1	Core	2031.25	0.8			
Nita Formation	Percival 1	Core	2031.25	0.8			
Poole Sandstone	Ngalti 1	Sonic	179	29-40			
Unnamed Conglomerate	Atrax 1	Sonic	727	10			
Unnamed Conglomerate	Atrax 1	Core	778.2	9.6		0.8	
Unnamed Conglomerate	Atrax 1	Core	778.6	10.9		0.5	
Unnamed Conglomerate	Selenops 1	Sonic	935	5.5			
Unnamed Conglomerate	Selenops 1	Sonic	1000	15.5			
Unnamed Conglomerate	Selenops 1	Sonic	1028	0			
Unnamed Conglomerate	Selenops 1	Core	1075.65	4.7		0.01	
Unnamed Conglomerate	Selenops 1	Core	1079	5.5		0.01	
Unnamed Conglomerate	Selenops 1	Core	1081.3	7.7		0.01	
Unnamed Conglomerate	Selenops 1	Core	1083.4	4.5		0.01	
Unnamed Conglomerate	Selenops 1	Sonic	1086.5	14			
Unnamed Conglomerate	Selenops 1	Sonic	1118	2			
Unnamed Conglomerate	Selenops 1	Sonic	1182	18.5			
Unnamed Conglomerate	Selenops 1	Sonic	1190	7			
Unnamed Conglomerate	Selenops 1	Sonic	1202	7			
Virgin Hills Formation	Selenops 1	Sonic	472.5	9			
Virgin Hills Formation	Selenops 1	Core	476	3.7		0.25	
Virgin Hills Formation	Selenops 1	Core	479	10.5		0.64	
Virgin Hills Formation	Selenops 1	Core	482	7.5		0.43	
Virgin Hills Formation	Selenops 1	Core	485	4.4		1.2	
Virgin Hills Formation	Selenops 1	Core	488	8.4		0.34	
Virgin Hills Formation	Selenops 1	Core	491	9.9		0.25	

Appendix B

Synthetic Seismograms

Synthetic seismograms were generated for all wells in the study area, and tied to seismic lines prior to seismic interpretation. Images of all of these synthetics are included in this Appendix.

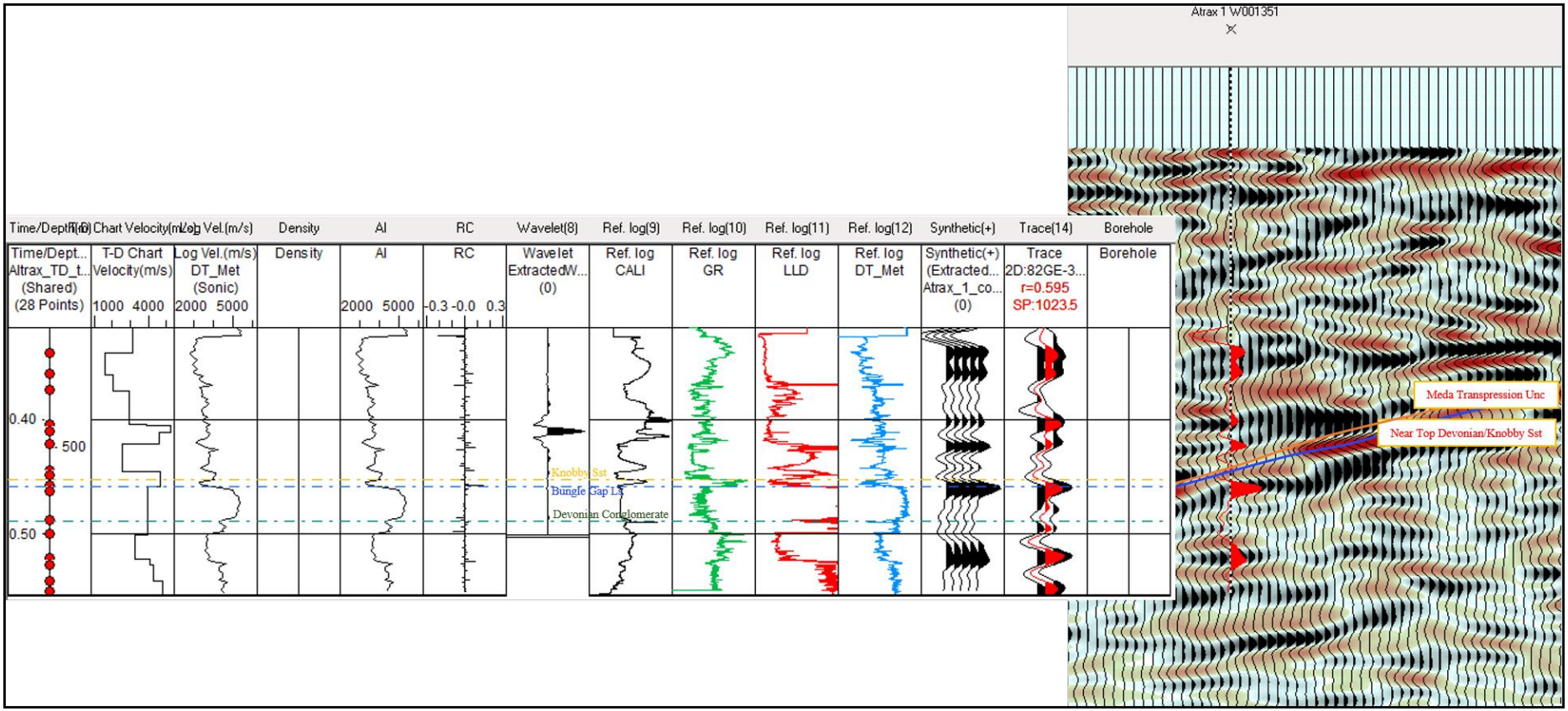

Atrax 1 synthetic seismogram (left), synthetic overlay on seismic (right).

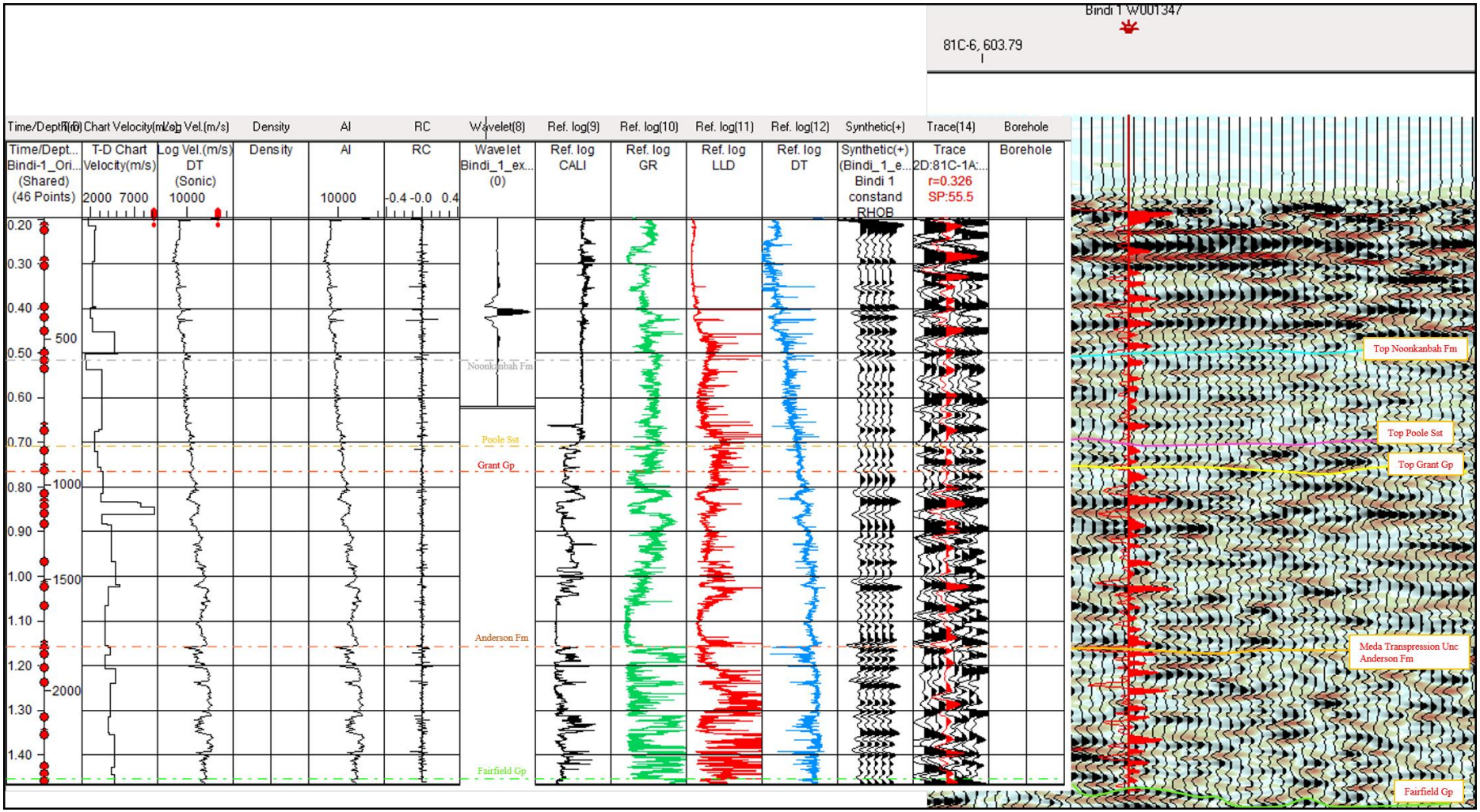

Bindi 1 synthetic seismogram (left), synthetic overlay on seismic (right).

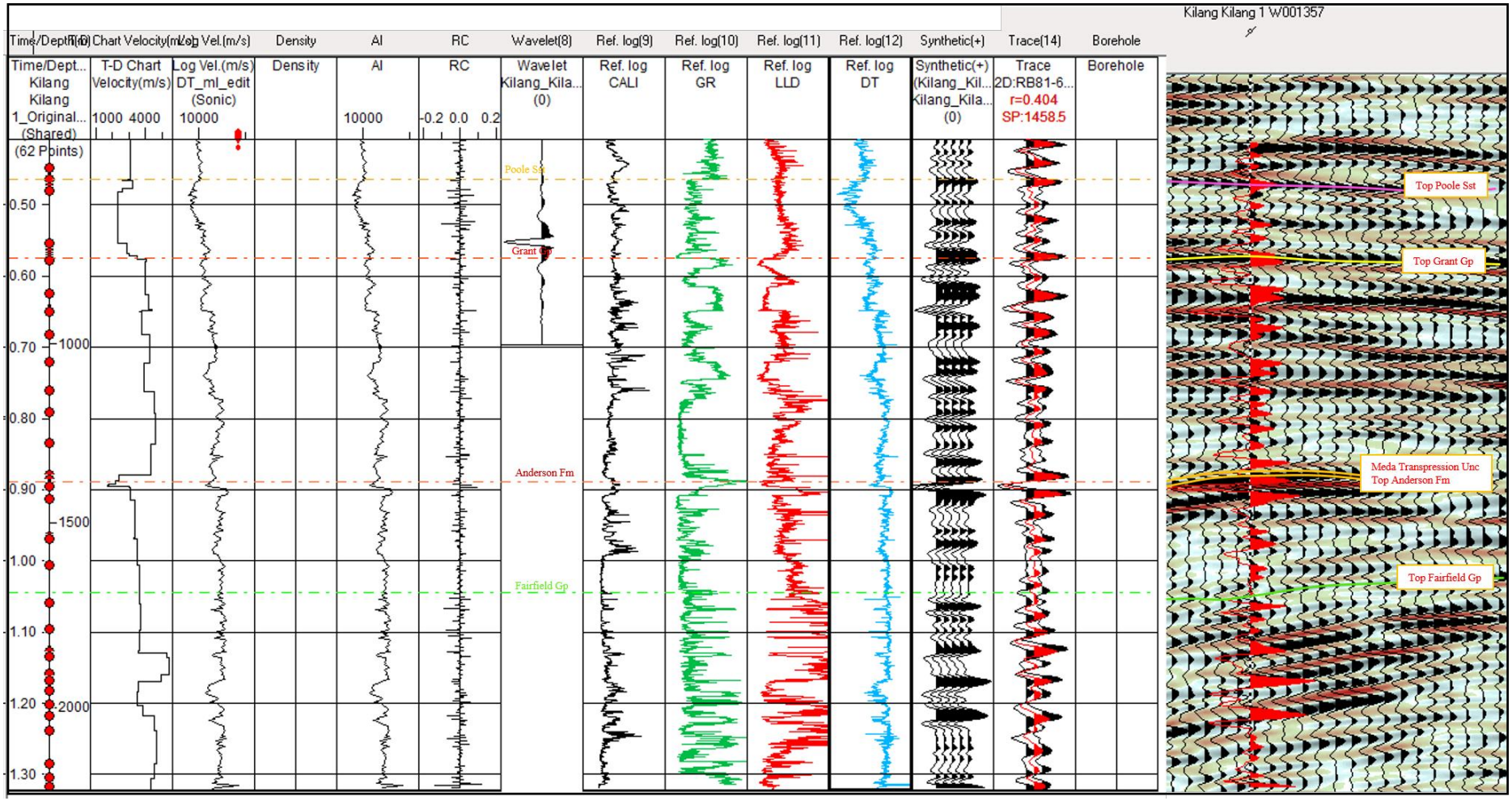

Kilang Kilang 1 synthetic seismogram (left), synthetic overlay on seismic (right).

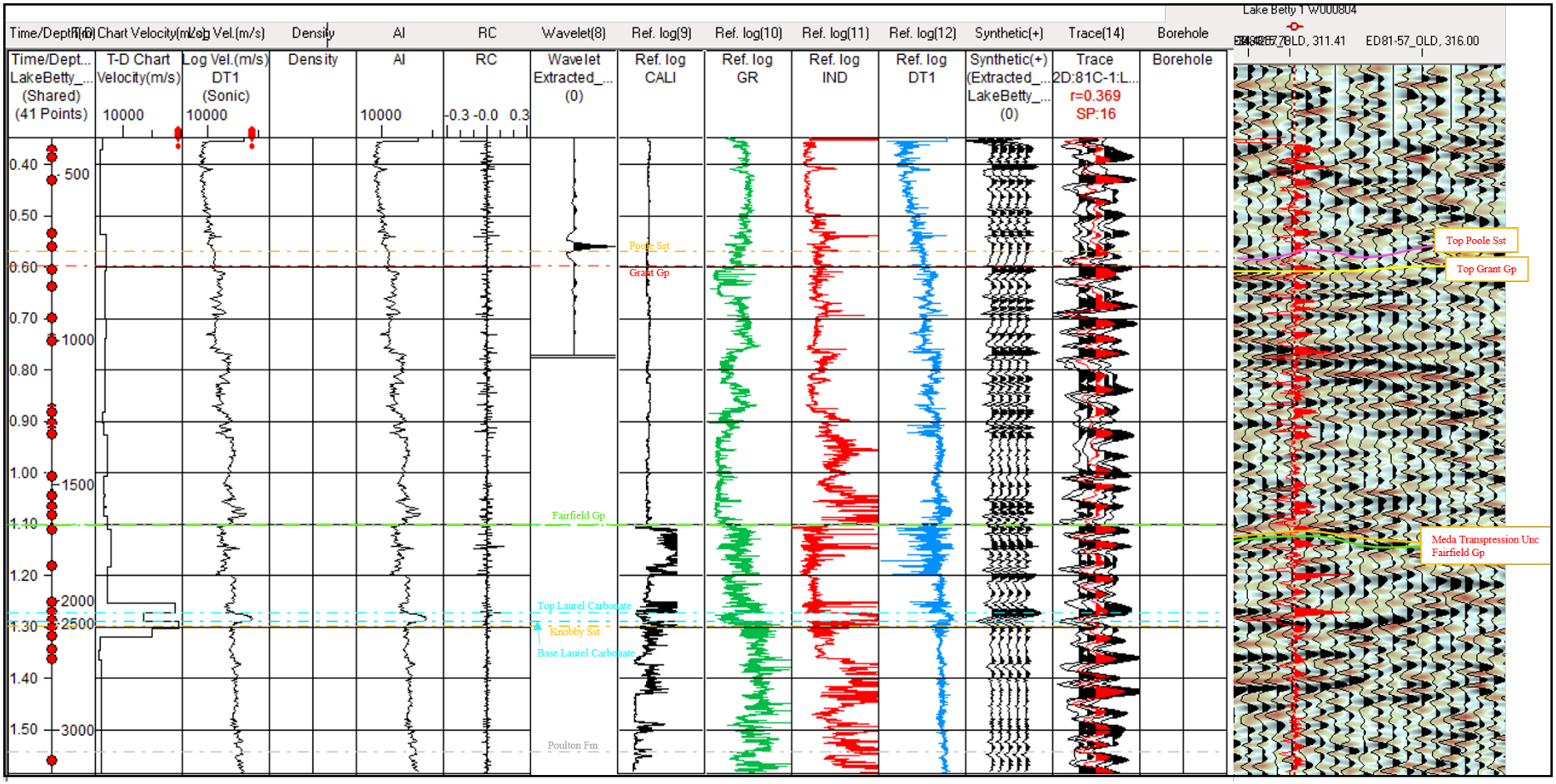

Lake Betty 1 synthetic seismogram (left), synthetic overlay on seismic (right).

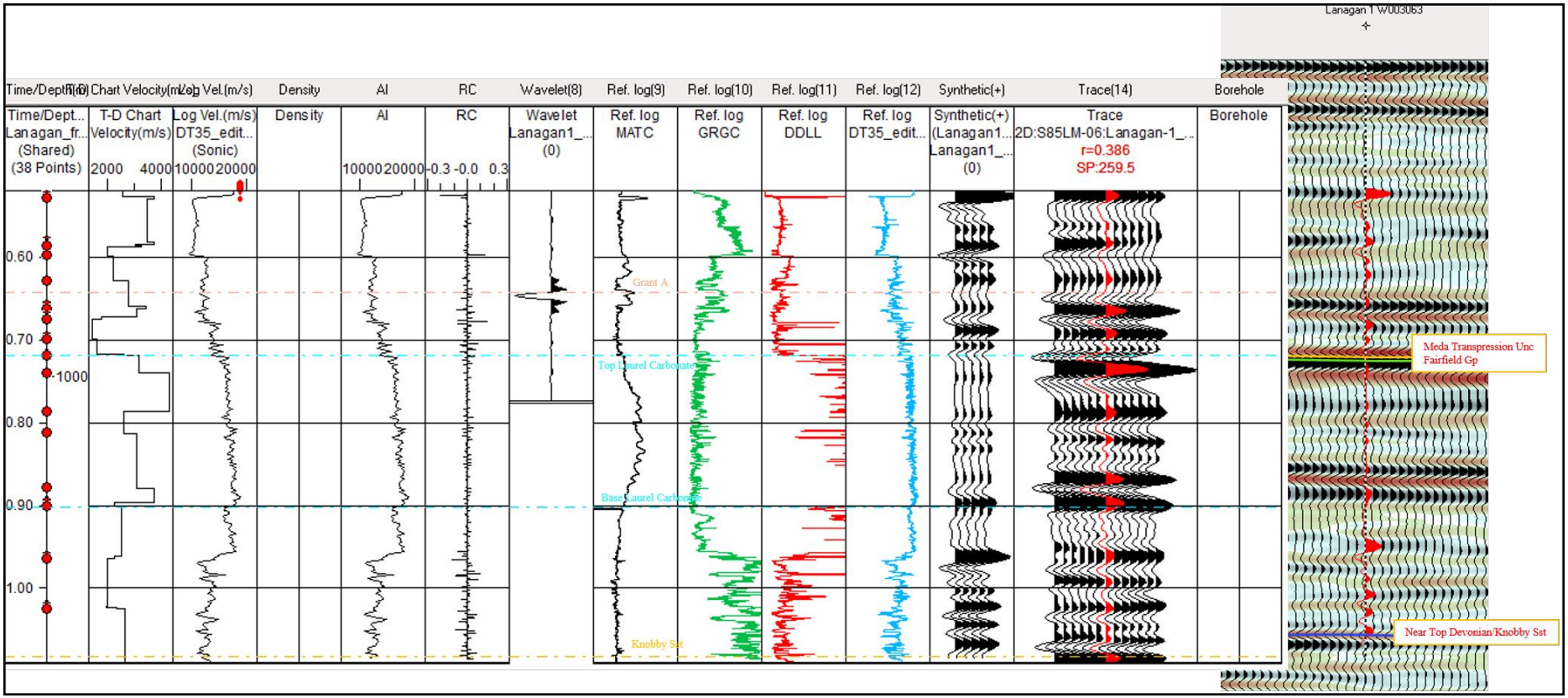

Lanagan 1 synthetic seismogram (left), synthetic overlay on seismic (right).

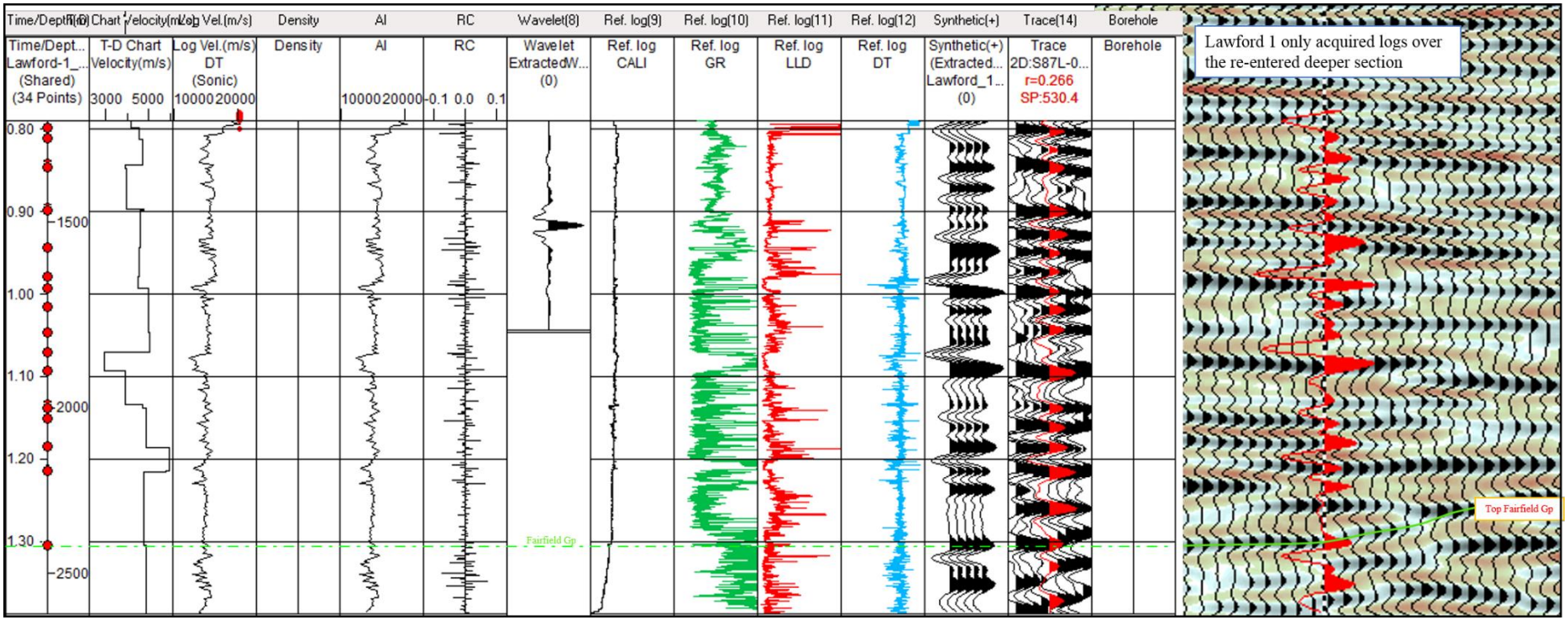

Lawford 1 synthetic seismogram (left), synthetic overlay on seismic (right).

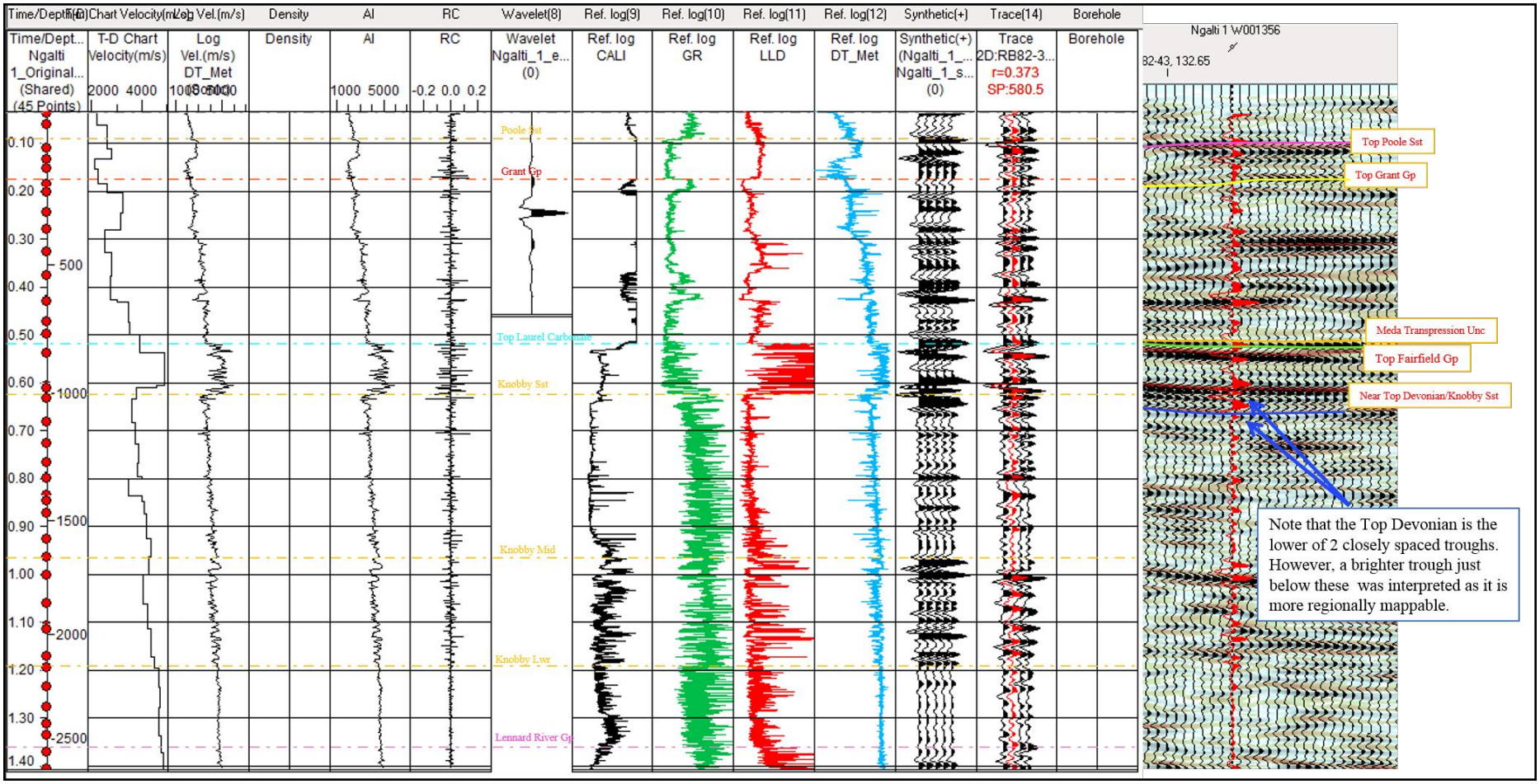

Ngalti 1 synthetic seismogram (left), synthetic overlay on seismic (right).

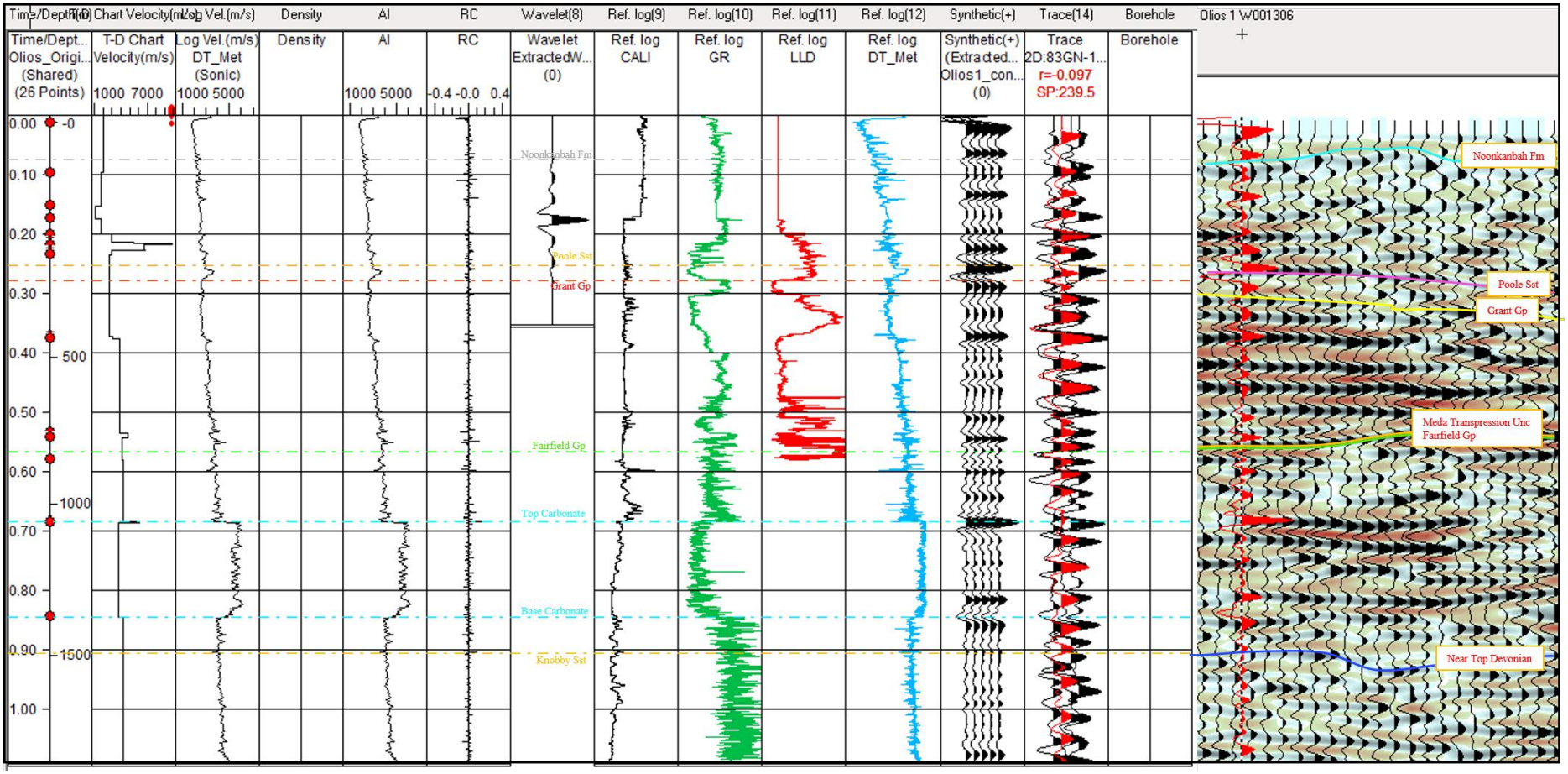

Olios 1 synthetic seismogram (left), synthetic overlay on seismic (right).

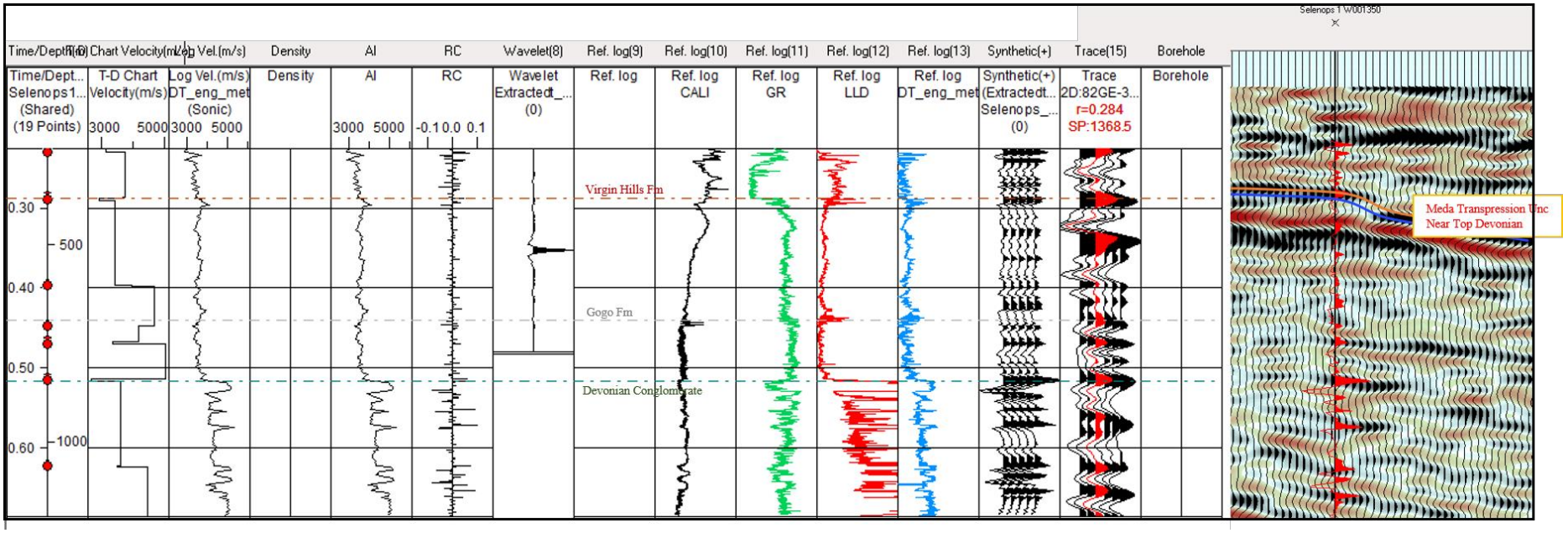

Selenops 1 synthetic seismogram (left), synthetic overlay on seismic (right).

Appendix C

Geochemical Data

Geochemical data from open file well completion reports and a database constructed by the Geological Survey of Western Australia was utilised in this study. These data are included in this Appendix.

Note, that colouring on these charts has the following meaning.

Legend	
	Data point from well within study area
	Zone contains *G. Prisca* algae

Noonkanbah Formation

Well	Depth (mRT)	TOC %	Tmax (°C)	S1 (kg/ton)	S2 (kg/ton)	S3 (kg/ton)	S1+S2	S2/S3	PI	PC	HI	OI
Atrax 1	30	0.83		0.02	0.06	1.35	0.08	0.0444	0.25	0.01	7.229	162.7
Atrax 1	45	1.95	431	0.02	0.44	1.48	0.46	0.2973	0.043	0.04	22.56	75.9
Atrax 1	60	1.4	436	0.01	0.24	1.01	0.25	0.2376	0.04	0.02	17.14	72.14
Atrax 1	75	1.66	433	0.01	0.34	0.97	0.35	0.3505	0.029	0.03	20.48	58.43
Atrax 1	90	1.61	431	0.03	0.35	0.61	0.38	0.5738	0.079	0.03	21.74	37.89
Atrax 1	105	1.15	428	0.02	0.71	2.99	0.73	0.2375	0.027	0.06	61.74	260
Auld 1	100	0.43										
Bindi 1	859.2	3.44	434	0.04	1.14	0.7	1.18	1.6286	0.03	0.09	33.14	20.35
Bindi 1	905.6	2.18	427	0.13	1.75	0.4	1.88	4.375	0.07	0.15	80.28	18.35
Booran 1	1000	3.13	434	0.5	1.41	0.52	1.91	2.7115	0.26	0.16	45.05	16.61
Booran 1	1086	2.97	430	0.85	1.29	0.44	2.14	2.9318	0.4	0.18	43.43	14.81
Booran 1	1160	4.81	435	0.59	4.46	0.39	5.05	11.436	0.12	0.42	92.72	8.108
Booran 1	1235	3.8	434	0.49	5.01	0.45	5.5	11.133	0.09	0.46	131.8	11.84
Canegrass 1	500.5	3.07	432	0.04	0.97	0.76	1.01	1.2763	0.04		31.6	24.76
Canegrass 1	500.5	3.07	432	0.04	0.97	0.76	1.01	1.2763	0.04	0.08	31.6	24.76
Canegrass 1	525	4.7	430	0.1	4.68	0.6	4.78	7.8	0.02		99.57	12.77
Canegrass 1	525	4.7	430	0.1	4.68	0.6	4.78	7.8	0.02	0.4	99.57	12.77
Canegrass 1	550	0.34										
Canegrass 1	550	0.34										
Contention Heights 1	106.68	2.05										
Crab Creek 1	706.5	1.91	432	0.05	0.9	0.42	0.95	2.1429	0.05	0.08	47.12	21.99
Curringa 1	806	3.55										
Cycas 1	339.2	4.91										
Cycas 1	425.6	9.37										
East Yeeda 1	780	1.16	428	0.03	0.63	1.75	0.66	0.36	0.05	0.05	54.31	150.9
East Yeeda 1	840	0.78	426	0.02	0.45	2.34	0.47	0.1923	0.04	0.04	57.69	300
East Yeeda 1	930	1.69	429	0.03	0.48	1.31	0.51	0.3664	0.06	0.04	28.4	77.51
East Yeeda 1	990	1.7	431	0.03	0.44	1.84	0.47	0.2391	0.06	0.04	25.88	108.2
East Yeeda 1	1010	1.98	431	0.03	0.64	1.02	0.67	0.6275	0.04	0.06	32.32	51.52
East Yeeda 1	1040	2.52	427	0.04	1.27	1.06	1.31	1.1981	0.03	0.11	50.4	42.06
East Yeeda 1	1070	3.38	425	0.09	3.01	1.34	3.1	2.2463	0.03	0.26	89.05	39.64
Hakea 1	549.1	2.33	434	0.07	1.34	0.19	1.41	7.0526	0.05	0.12	57.51	8.155
Hangover 1	465	0.63		0.02	0.11	0.23	0.13	0.4783	0.15		17.46	36.51
Hangover 1	485	1.17										
Hangover 1	510	1.97	432	0.03	0.57	0.51	0.6	1.1176	0.05		28.93	25.89
Hangover 1	510	1.62	430	0.03	0.37	0.24	0.4	1.5417			22.84	14.81
Hangover 1	535	1.88										
Hangover 1	560	1.02										
Hangover 1	580	1.63										
Hangover 1	595	2.13	436	0.04	0.4	0.42	0.44	0.9524	0.09		18.78	19.72
Hangover 1	613	2.61	438	0.05	0.55	0.67	0.6	0.8209	0.08		21.07	25.67
Hangover 1	615	2.06	434	0.03	0.48	0.29	0.51	1.6552	0.06		23.3	14.08
Hangover 1	660	1.87										
Hangover 1	680	2.12										
Hangover 1	695	2.05	435	0.03	0.4	0.1	0.43	4	0.07		19.51	4.878
Hangover 1	705	2.59										
Hangover 1	715	2.8										
Hangover 1	725	3.81	434	0.08	2.33	1.06	2.41	2.1981	0.04		61.15	27.82
Hangover 1	735	3.41	430	0.05	1.87	0.62	1.92	3.0161	0.03		54.84	18.18
Hangover 1	750	1.07									0	0
Hangover 1	756	2.51	430	0.07	1.46	0.75	1.53	1.9467	0.05		58.17	29.88
Hangover 1	760	2.71	433	0.06	1.92	0.93	1.98	2.0645	0.03		70.85	34.32
Jum Jum 1	1115	0.95		0.09	0.11	0.73	0.2	0.1507	0.45	0.02	11.58	76.84
Jum Jum 1	1150	0.62		0.59	0.04	0.54	0.63	0.0741	0.94	0.05	6.452	87.1
Jum Jum 1	1340	2.34	419	0.17	0.27	0.79	0.44	0.3418	0.39	0.04	11.54	33.76
Kambara 1	802.8	3.27	434	0.7	2.4	0.4	3.1	6	0.23		73.39	12.23
Kilang Kilang 1	330	1.55	428	0.02	0.46	0.4	0.48	1.15	0.04	0.04	29.68	25.81
Kilang Kilang 1	359	0.71	426	0.13	0.27	0.17	0.4	1.5882	0.33	0.03	38.03	23.94
Kilang Kilang 1	360	1.79	425	0.04	0.33	1.01	0.37	0.3267	0.11	0.03	18.44	56.42
Kilang Kilang 1	390	1.32		0.02	0.13	1.21	0.15	0.1074	0.13	0.01	9.848	91.67
Kilang Kilang 1	406.4	2.39	429	0.17	0.48	0.3	0.65	1.6	0.26	0.05	20.08	12.55
Kilang Kilang 1	420	1.39	433	0.04	0.2	1	0.24	0.2	0.17	0.02	14.39	71.94
Kilang Kilang 1	437.7	0.56		0.12	0.07	2.56	0.19	0.0273	0.63	0.02	12.5	457.1
Kilang Kilang 1	450	1.51	426	0.14	0.32	0.24	0.46	1.3333	0.3	0.04	21.19	15.89
Kilang Kilang 1	450	1.19		0.04	0.14	1.98	0.18	0.0707	0.22	0.01	11.76	166.4
Kilang Kilang 1	476	1.52	431	0.1	0.23	0.66	0.33	0.3485	0.3	0.03	15.13	43.42
Kilang Kilang 1	480	1.29		0.02	0.14	1.06	0.16	0.1321	0.13	0.01	10.85	82.17
Kilang Kilang 1	510	1.41	433	0.03	0.2	1.76	0.23	0.1136	0.13	0.03	14.18	124.8
Kilang Kilang 1	524	1.96	430	0.09	0.38	0.22	0.47	1.7273	0.19	0.04	19.39	11.22
Kilang Kilang 1	540	1.3	435	0.03	0.23	1.88	0.26	0.1223	0.12	0.02	17.69	144.6
Kilang Kilang 1	545	1.54	431	0.24	0.53	0.26	0.77	2.0385	0.31	0.06	34.42	16.88
Kilang Kilang 1	570	0.88	437	0.07	0.24	2.3	0.31	0.1043	0.23	0.03	27.27	261.4
Kilang Kilang 1	600	1.99	428	0.27	1.57	1.35	1.84	1.163	0.15	0.15	78.89	67.84
Kilang Kilang 1	610	2.48	430	0.13	0.7	0.33	0.83	2.1212	0.16	0.07	28.23	13.31
Kilang Kilang 1	630	2.62	429	0.1	3.77	0.11	3.87	34.273	0.03	0.32	143.9	4.198

Kilang Kilang 1	631	3.48	428	0.14	3.07	1.61	3.21	1.9068	0.04	0.27	88.22	46.26
Kilang Kilang 1	642.5	2.39	430	0.11	2.04	0.15	2.15	13.6	0.05	0.18	85.36	6.276
Kilang Kilang 1	660	2.63	429	0.09	3.33	0.24	3.42	13.875	0.03	0.28	126.6	9.125
Kora 1	940	3.85										
Kora 1	970	4.05										
Lake Betty 1	396.24	1.97	430	0.11	0.57	1.7	0.68	0.3353			28.93	86.29
Lake Betty 1	426.72	1.71	429	0.1	0.35	1.95	0.45	0.1795			20.47	114
Lake Betty 1	457.2	1.44	422	0.24	1.73	4.94	1.97	0.3502			120.1	343.1
Lake Betty 1	487.68	1.39		0.1	0.19	3.25	0.29	0.0585			13.67	233.8
Lake Betty 1	518.16	1.59	432	0.1	0.34	2.32	0.44	0.1466			21.38	145.9
Lake Betty 1	548.64	2.13	433	0.1	0.62	2.59	0.72	0.2394			29.11	121.6
Lake Betty 1	579.12	2.17	431	0.1	0.62	2.22	0.72	0.2793			28.57	102.3
Lake Betty 1	609.6	2.07	435	0.1	0.45	1.92	0.55	0.2344			21.74	92.75
Lake Betty 1	640.08	3.09	434	0.1	0.98	1.8	1.08	0.5444			31.72	58.25
Lake Betty 1	670.56	3.29	434	0.1	2.19	1.61	2.29	1.3602			66.57	48.94
Meda 1	595	2.2										
Mimosa 1	405	1.5										
Mimosa 1	510	2.2										
Minjin 1	750	2.38	427	0.08	1.28	0.39	1.36	3.2821	0.06	0.11	53.78	16.39
Minjin 1	766	2.41	424	0.06	0.72	0.51	0.78	1.4118	0.08	0.06	29.88	21.16
Moogana 1	995	1.44										
Moogana 1	1010	1.72										
Ngalti 1	120	1.04										
Ngalti 1	137.3	0.27										
Ngalti 1	150	0.34										
Ngalti 1	175.5	4	429	0.06	3.23	0.34	3.29	9.5	0.02	0.27	80.75	8.5
Olios 1	75	0.07										
Olios 1	105	1.45	432	0.04	0.31	0.76	0.35	0.4079	0.114	0.03	21.38	52.41
Olios 1	135	1.55	435	0.02	0.24	0.48	0.26	0.5	0.077	0.02	15.48	30.97
Olios 1	165	1.36	434	0.02	0.23	0.3	0.25	0.7667	0.08	0.02	16.91	22.06
Olios 1	195	1.58	434	0.01	0.31	0.27	0.32	1.1481	0.031	0.03	19.62	17.09
Olios 1	225	1.28	436	0.03	0.27	1.76	0.3	0.1534	0.1	0.02	21.09	137.5
Olios 1	225	1.39	432	0.02	0.33	1.56	0.35	0.2115	0.057	0.03	23.74	112.2
Olios 1	255	1.39	432	0.02	0.33	1.56	0.35	0.2115	0.057	0.03	23.74	112.2
Petaluma 1	295	3.05	430	0.1	2.64	1.96	2.74	1.3469	0.04	0.23	86.56	64.26
Petaluma 1	305	4.2	428	0.16	3.49	3.87	3.65	0.9018	0.04	0.3	83.1	92.14
Petaluma 1	330	1.61	429	0.05	0.54	2.18	0.59	0.2477	0.08	0.05	33.54	135.4
Petaluma 1	335	1.64	419	0.23	0.98	2.94	1.21	0.3333	0.19	0.1	59.76	179.3
Petaluma 1	350	2.09	430	0.1	0.61	1.86	0.71	0.328	0.14	0.06	29.19	89
Petaluma 1	355	1.94	425	0.2	1.39	1.7	1.59	0.8176	0.13	0.13	71.65	87.63
Petaluma 1	550	1.74	429	0.06	0.49	2.13	0.55	0.23	0.11	0.05	28.16	122.4
Petaluma 1	555	2.07	430	0.07	0.63	2.17	0.7	0.2903	0.1	0.06	30.43	104.8
Petaluma 1	670	3.58	430	0.14	2.79	2.27	2.93	1.2291	0.05	0.24	77.93	63.41
Petaluma 1	675	3.22	431	0.12	2.36	2.31	2.48	1.0216	0.05	0.21	73.29	71.74
Philydrum 1	512	4.65	428	0.19	5.04	1.1	5.23	4.5818	0.04	0.43	108.4	23.66
Puratte 1	1170	2.48										
Puratte 1	1245	1.96	431	0.03	0.43	1.09	0.46	0.3945	0.07		21.94	55.61
Puratte 1	1270	1.67	428	0.02	0.35	0.81	0.37	0.4321	0.05		20.96	48.5
Puratte 1	1290	1.81	430	0.04	0.36	1.09	0.4	0.3303	0.1		19.89	60.22
Puratte 1	1310	1.82	426	0.07	0.64	1.06	0.71	0.6038	0.1		35.16	58.24
Puratte 1	1330	2.2	431	0.05	0.69	1.29	0.74	0.5349	0.07		31.36	58.64
Puratte 1	1350	2.61	428	0.07	1.44	1.05	1.51	1.3714	0.05		55.17	40.23
Puratte 1	1365	3.18										
Puratte 1	1370	2.98	431	0.09	2.08	1.09	2.17	1.9083	0.04		69.8	36.58
Puratte 1	1390	2.34	430	0.05	1.58	1.23	1.63	1.2846	0.03		67.52	52.56
Puratte 1	1410	2.15	427	0.05	1.43	1.05	1.48	1.3619	0.03		66.51	48.84
Selenops 1	30	2.04	433	0.01	0.31	2.2	0.32	0.1409	0.03		15.2	107.8
Selenops 1	45	0.33										
Tappers Inlet 1	697.99	1.94		0.08	0.19	0.81	0.27	0.2346	0.3	0.02	9.794	41.75
Tappers Inlet 1	762	2.42	428	0.07	0.33	1	0.4	0.33	0.18	0.03	13.64	41.32
Tappers Inlet 1	822.96	2.77	430	0.07	0.46	1.04	0.53	0.4423	0.13	0.04	16.61	37.55
Tappers Inlet 1	908.3	2.77	431	0.1	0.77	1.01	0.87	0.7624	0.11	0.07	27.8	36.46
West Kora 1	900	3.7	423	0.16	0.85	0.28	1.01	3.0357	0.16	0.08	22.97	7.568
West Kora 1	975	2.38	423	0.16	1.36	0.17	1.52	8	0.11	0.12	57.14	7.143
West Philydrum 1	400	2.38	436	0.05	0.96	0.42	1.01	2.2857	0.05	0.08	40.34	17.65
Wilson Cliffs 1	347.5	2.48										

Anderson Formation

Well	Sub-unit	Depth (mRT)	TOC %	Tmax (°C)	S1 (kg/ton)	S2 (kg/ton)	S3 (kg/ton)	S1+S2	S2/S3	PI	PC	HI	OI
Bindi 1	Anderson G	1833.1	0.07					0					
Bindi 1	Anderson G	1897.1						0					
Bindi 1	Anderson G	1918.7	0.55	425	0.17	0.11	0.19	0.28	0.579	0.61	0.02	20	34.55
Bindi 1	Anderson E	1999.4						0					
Bindi 1	Anderson C	2176						0					
Bindi 1	Anderson C	2179						0					
Bindi 1	Anderson C	2224.9	0.09					0					
Bindi 1	Anderson A	2348.1	0.26					0					
Bindi 1	Anderson A	2373						0					
Bindi 1	Anderson A	2393	0.35	426	0.08	0.13	0.24	0.21	0.542	0.38	0.35	37.14	68.57
Bindi 1	Anderson A	2435.5						0					
Kilang Kilang 1	Anderson G	1460	0.17					0					
Kilang Kilang 1	Anderson F	1490	0.04					0					
Kilang Kilang 1	Anderson F	1512.2	0.14					0					
Kilang Kilang 1	Anderson E	1520	0.08					0					
Kilang Kilang 1	Anderson D	1550	0.08					0					
Kilang Kilang 1	Anderson D	1580	0.08					0					
Kilang Kilang 1	Anderson C	1610	0.06					0					
Kilang Kilang 1	Anderson B	1640	0.06					0					
Kilang Kilang 1	Anderson A	1670	0.04					0					
Kilang Kilang 1	Anderson A	1700	0.06					0					

Laurel Formation

Well	Tectonic Region	Depth (mRT)	TOC %	Tmax (°C)	S1 (kg/ton)	S2 (kg/ton)	S3 (kg/ton)	S1+S2	S2/S3	PI	PC	HI	OI
Aquanita 1	Lennard Shelf	1600	0.17										
Aquanita 1	Lennard Shelf	1605	0.48										
Aquanita 1	Lennard Shelf	1610	0.32										
Aquanita 1	Lennard Shelf	1615	0.26										
Aquanita 1	Lennard Shelf	1620	0.19										
Aquanita 1	Lennard Shelf	1625	0.16										
Aquanita 1	Lennard Shelf	1630	0.2										
Aquanita 1	Lennard Shelf	1635	0.36										
Aquanita 1	Lennard Shelf	1640	0.42										
Aquanita 1	Lennard Shelf	1645	0.36										
Aquanita 1	Lennard Shelf	1655	0.21										
Aquanita 1	Lennard Shelf	1665	0.3										
Aquanita 1	Lennard Shelf	1670	0.24										
Aquanita 1	Lennard Shelf	1680	0.3										
Aquanita 1	Lennard Shelf	1685	0.27										
Aquanita 1	Lennard Shelf	1690	0.34										
Aquanita 1	Lennard Shelf	1700	0.3										
Aquanita 1	Lennard Shelf	1705	0.24										
Bindi 1	Betty Terrace	2481.4	0.38										
Blackstone 1	Lennard Shelf	1532.2	1.79										
Blackstone 1	Lennard Shelf	1532.2	1.94										
Blackstone 1	Lennard Shelf	1536.2	0.2										
Blackstone 1	Lennard Shelf	1536.8	1.94										
Blackstone 1	Lennard Shelf	1536.8	2.08										
Blackstone 1	Lennard Shelf	1556	4.84	425	1.31	20.29	1.85	21.6		0.061		419.2	38.22
Blackstone 1	Lennard Shelf	1556	4.84	425	1.31	20.2	1.85	21.51		0.06		417.4	38.22
Blackstone 1	Lennard Shelf	1690.3	0.3										
Blackstone 1	Lennard Shelf	1819.3	0.1										
Blina 1	Lennard Shelf	1113.1	0.63										
Blina 1	Lennard Shelf	1122.6	0.42										
Blina 1	Lennard Shelf	1130	0.41										
Canegrass 1	Lennard Shelf	1304	1.17	436	0.1	1.28	0.06	1.38		0.07		109.4	5.128
Canegrass 1	Lennard Shelf	1304	1.17	436	0.1	1.28	0.06	1.38		0.07	0.11	109.4	5.128
Canegrass 1	Lennard Shelf	1400	0.51	432	0.09	0.57	0.16	0.66		0.14		111.8	31.37
Canegrass 1	Lennard Shelf	1400	0.51	432	0.09	0.57	0.16	0.66		0.14	0.05	111.8	31.37
Cow Bore 1	Jurgurra Terrace	1300	0.28										
Cow Bore 1	Jurgurra Terrace	1309	0.53	414	0.05	0.25	0.72	0.3		0.19	0.03	47.17	135.8
Cow Bore 1	Jurgurra Terrace	1320	0.49										
Cow Bore 1	Jurgurra Terrace	1340	0.7	427	0.03	0.21	0.67	0.24		0.13	0.02	30	95.71
Cow Bore 1	Jurgurra Terrace	1360	0.77	427	0.03	0.25	0.49	0.28		0.11	0.02	32.47	63.64
Cow Bore 1	Jurgurra Terrace	1380	0.64										
Cow Bore 1	Jurgurra Terrace	1400	0.52										
Cow Bore 1	Jurgurra Terrace	1408	0.42										
Cow Bore 1	Jurgurra Terrace	1411	0.42										
Cow Bore 1	Jurgurra Terrace	1420	0.42										
Cow Bore 1	Jurgurra Terrace	1440	0.48										
Cow Bore 1	Jurgurra Terrace	1450	0.46										
Cow Bore 1	Jurgurra Terrace	1460	0.44										
Cow Bore 1	Jurgurra Terrace	1470	0.56	427	0.02	0.25	0.26	0.27		0.07	0.02	44.64	46.43
Cow Bore 1	Jurgurra Terrace	1480	0.63										
Cow Bore 1	Jurgurra Terrace	1504	0.68	425	0.06	0.27	0.52	0.33		0.18	0.03	39.71	76.47
Cow Bore 1	Jurgurra Terrace	1510	0.59	428	0.03	0.26	0.18	0.29		0.1	2	44.07	30.51
Cow Bore 1	Jurgurra Terrace	1519	0.52										
Cow Bore 1	Jurgurra Terrace	1530	0.62										
Cow Bore 1	Jurgurra Terrace	1537	0.54										
Cow Bore 1	Jurgurra Terrace	1540	0.52										
Cow Bore 1	Jurgurra Terrace	1550	0.69										
Cow Bore 1	Jurgurra Terrace	1560	0.62	432	0.02	0.31	0.24	0.33		0.06	0.03	50	38.71
Cow Bore 1	Jurgurra Terrace	1570	0.64										
Cow Bore 1	Jurgurra Terrace	1580	0.72										
Cow Bore 1	Jurgurra Terrace	1590	0.68										
Cow Bore 1	Jurgurra Terrace	1600	0.73	427	0.06	0.32	0.51	0.38		0.16	0.03	43.84	69.86
Cow Bore 1	Jurgurra Terrace	1610	0.74										
Cow Bore 1	Jurgurra Terrace	1620	0.71	435	0.03	0.37	0.17	0.4		0.08	0.03	52.11	23.94
Cow Bore 1	Jurgurra Terrace	1630	0.71	435	0.04	0.47	0.13	0.51		0.08	0.04	66.2	18.31
Cow Bore 1	Jurgurra Terrace	1660	0.73										
Cow Bore 1	Jurgurra Terrace	1690	0.86										
Cow Bore 1	Jurgurra Terrace	1705	0.88	437	0.11	0.22	0.37	0.33		0.017	0.05	25	42.05
Cow Bore 1	Jurgurra Terrace	1710	0.77										
Cow Bore 1	Jurgurra Terrace	1730	0.81	438	0.12	0.35	0.48	0.47		0.26	0.04	43.21	59.26
Cow Bore 1	Jurgurra Terrace	1750	0.75										
Cow Bore 1	Jurgurra Terrace	1770	0.82	436	0.13	0.3	0.69	0.43		0.3	0.04	36.59	84.15
Cow Bore 1	Jurgurra Terrace	1790	0.95	397	0.46	0.69	0.97	1.15		0.4	0.1	72.63	102.1
Cow Bore 1	Jurgurra Terrace	1810			0.49	0.64		1.13		0.43			
Cow Bore 1	Jurgurra Terrace	1810	0.59										
Cow Bore 1	Jurgurra Terrace	1830	0.79		0.33	0.17	1.06	0.5		0.66	0.04	21.52	134.2
Cow Bore 1	Jurgurra Terrace	1850	0.24										
Cow Bore 1	Jurgurra Terrace	1870	0.34										
Cow Bore 1	Jurgurra Terrace	1890	0.09										
Cow Bore 1	Jurgurra Terrace	1910	0.21										
Cow Bore 1	Jurgurra Terrace	1930	0.27										
Cow Bore 1	Jurgurra Terrace	1950	0.46										
Cow Bore 1	Jurgurra Terrace	1970	0.36										
Cow Bore 1	Jurgurra Terrace	1990	0.46										
Cow Bore 1	Jurgurra Terrace	2110	0.8	438	0.15	0.32	0.22	0.47		0.32	0.04	40	27.5
Crab Creek 1	Broome Platform	1490	0.12										
Crab Creek 1	Broome Platform	1537	0.12										
Crab Creek 1	Broome Platform	1551.2	0.1										
Crimson Lake 1	Fitzroy Trough	1577	0.46										
Crimson Lake 1	Fitzroy Trough	1640	0.59	440	0.08	0.41	0.08	0.49		0.16		69.49	13.56
Crimson Lake 1	Fitzroy Trough	1676	0.83	436	0.16	1.22	0.27	1.38		0.12		147	32.53
Crimson Lake 1	Fitzroy Trough	1710	0.74	442	0.11	0.57	0.24	0.68		0.16		77.03	32.43

Crimson Lake 1	Fitzroy Trough	1783	0.51	439	0.1	0.39	0.15	0.49		0.2		76.47	29.41
Crimson Lake 1	Fitzroy Trough	1836	0.64	443	0.05	0.39	0.28	0.44		0.11		60.94	43.75
Crimson Lake 1	Fitzroy Trough	1962	0.3										
Curringa 1	Pender Terrace	1854.5	5.05										
Curringa 1	Pender Terrace	1865	2.57										
Curringa 1	Pender Terrace	1868.9	2.61										
Curringa 1	Pender Terrace	1871.04	5.81										
Curringa 1	Pender Terrace	1874.98	0.15										
Cycas 1	Fitzroy Trough	2816	0.14										
Cycas 1	Fitzroy Trough	2837.5	0.14										
Cycas 1	Fitzroy Trough	2897.5	0.14										
Cycas 1	Fitzroy Trough	2952.5	0.12										
Cycas 1	Fitzroy Trough	2987.5	0.12										
East Crab Creek 1	Broome Platform	1446	0.08										
East Yeeda 1	Fitzroy Trough	3040	0.22										
East Yeeda 1	Fitzroy Trough	3070	0.38										
East Yeeda 1	Fitzroy Trough	3085	0.32										
East Yeeda 1	Fitzroy Trough	3100	0.27										
East Yeeda 1	Fitzroy Trough	3115	0.22										
East Yeeda 1	Fitzroy Trough	3130	0.18										
East Yeeda 1	Fitzroy Trough	3145	0.13										
East Yeeda 1	Fitzroy Trough	3160	0.15										
East Yeeda 1	Fitzroy Trough	3175	0.26										
East Yeeda 1	Fitzroy Trough	3190	0.14										
East Yeeda 1	Fitzroy Trough	3205	0.24										
East Yeeda 1	Fitzroy Trough	3220	0.17										
East Yeeda 1	Fitzroy Trough	3235	0.23										
East Yeeda 1	Fitzroy Trough	3250	0.16										
East Yeeda 1	Fitzroy Trough	3265	0.22										
East Yeeda 1	Fitzroy Trough	3280	0.23										
East Yeeda 1	Fitzroy Trough	3295	0.2										
Ellendale 1	Fitzroy Trough	1550	0.19										
Ellendale 1	Fitzroy Trough	1570	0.84	486	0.17	1.19		1.36		0.12		141.7	
Ellendale 1	Fitzroy Trough	1590	0.44										
Ellendale 1	Fitzroy Trough	1610	0.57	487	0.09	0.57		0.66		0.14		100	
Ellendale 1	Fitzroy Trough	1630	0.48										
Ellendale 1	Fitzroy Trough	1650	0.64	493	0.13	0.78		0.91		0.35		121.9	
Ellendale 1	Fitzroy Trough	1670	0.42										
Ellendale 1	Fitzroy Trough	1690	1.3	530	0.43	2.53		2.96		0.14		194.6	
Ellendale 1	Fitzroy Trough	1690	0.73	439	0.22	0.59	0.25	0.81		0.27	0.07	80.82	34.25
Ellendale 1	Fitzroy Trough	1695	0.83	438	0.24	0.94	0.15	1.18		0.2	0.1	113.3	18.07
Ellendale 1	Fitzroy Trough	1710	0.73	473	0.18	1.29		1.47		0.12		176.7	
Ellendale 1	Fitzroy Trough	1730	0.78	512	0.21	1.22		1.43		0.15		156.4	
Fitzroy River 1	Fitzroy Trough	2080	0.09										
Fitzroy River 1	Fitzroy Trough	2100	0.12										
Fitzroy River 1	Fitzroy Trough	2120	0.21										
Fitzroy River 1	Fitzroy Trough	2140	0.17										
Fitzroy River 1	Fitzroy Trough	2160	0.62										
Fitzroy River 1	Fitzroy Trough	2180	0.5										
Fitzroy River 1	Fitzroy Trough	2200	0.16										
Fitzroy River 1	Fitzroy Trough	2220	0.18										
Fitzroy River 1	Fitzroy Trough	2240	0.17										
Fitzroy River 1	Fitzroy Trough	2260	0.16										
Fitzroy River 1	Fitzroy Trough	2280	0.18										
Fitzroy River 1	Fitzroy Trough	2300	0.06										
Fitzroy River 1	Fitzroy Trough	2320	0.19										
Fitzroy River 1	Fitzroy Trough	2340	0.2										
Fitzroy River 1	Fitzroy Trough	2360	0.15										
Fitzroy River 1	Fitzroy Trough	2380	0.25										
Fitzroy River 1	Fitzroy Trough	2400	0.18										
Fitzroy River 1	Fitzroy Trough	2420	0.19										
Fitzroy River 1	Fitzroy Trough	2440	0.34										
Fitzroy River 1	Fitzroy Trough	2460	0.31										
Fitzroy River 1	Fitzroy Trough	2480	0.33										
Fitzroy River 1	Fitzroy Trough	2500	0.13										
Fitzroy River 1	Fitzroy Trough	2520	0.18										
Fitzroy River 1	Fitzroy Trough	2540	0.32										
Fitzroy River 1	Fitzroy Trough	2560	0.44										
Fitzroy River 1	Fitzroy Trough	2580	0.23										
Fitzroy River 1	Fitzroy Trough	2600	0.36										
Fitzroy River 1	Fitzroy Trough	2620	0.43										
Fitzroy River 1	Fitzroy Trough	2640	0.55										
Fitzroy River 1	Fitzroy Trough	2660	0.53										
Fitzroy River 1	Fitzroy Trough	2680	0.36										
Fitzroy River 1	Fitzroy Trough	2700	0.38										
Fitzroy River 1	Fitzroy Trough	2720	0.48										
Fitzroy River 1	Fitzroy Trough	2740	0.33										
Fitzroy River 1	Fitzroy Trough	2760	0.31										
Fitzroy River 1	Fitzroy Trough	2780	0.45										
Fitzroy River 1	Fitzroy Trough	2800	0.39										
Fitzroy River 1	Fitzroy Trough	2820	0.49										
Fitzroy River 1	Fitzroy Trough	2840	0.44										
Fitzroy River 1	Fitzroy Trough	2860	0.43										
Fitzroy River 1	Fitzroy Trough	2880	0.5										
Fitzroy River 1	Fitzroy Trough	2900	0.53										
Fitzroy River 1	Fitzroy Trough	2920	0.57		0.02	0	0.35	0.02		1			61.4
Fitzroy River 1	Fitzroy Trough	2940	0.64										
Fitzroy River 1	Fitzroy Trough	2960	0.79										
Fitzroy River 1	Fitzroy Trough	2980	0.7		0.01	0	0.54	0.01		1		0	77.14
Fitzroy River 1	Fitzroy Trough	3000	0.4										
Fitzroy River 1	Fitzroy Trough	3020	0.56										
Fitzroy River 1	Fitzroy Trough	3040	0.74		0	0	0.3					0	40.54
Fitzroy River 1	Fitzroy Trough	3060	1.13										

Fitzroy River 1	Fitzroy Trough	3080	0.75										
Fitzroy River 1	Fitzroy Trough	3100	0.59		0.01	0.02	0.02	0.03		0.33		3.39	3.39
Fitzroy River 1	Fitzroy Trough	3120	0.98										
Hakea 1	Fitzroy Trough	1699	0.13										
Hakea 1	Fitzroy Trough	1703	0.17										
Janpam 1	Lennard Shelf	1450	0.19										
Janpam 1	Lennard Shelf	1460	0.15										
Janpam 1	Lennard Shelf	1470	0.16										
Janpam 1	Lennard Shelf	1485	0.22										
Janpam 1	Lennard Shelf	1500	0.27										
Janpam 1	Lennard Shelf	1515	0.48										
Janpam 1	Lennard Shelf	1530	0.33										
Janpam 1	Lennard Shelf	1535	0.4										
Jones Range 1	Gregory Sub-basin	1655	0.31										
Jones Range 1	Gregory Sub-basin	1675	0.25										
Jones Range 1	Gregory Sub-basin	1685	0.53										
Jones Range 1	Gregory Sub-basin	1700	0.36										
Jones Range 1	Gregory Sub-basin	1705	0.28										
Jones Range 1	Gregory Sub-basin	1735	0.36										
Jones Range 1	Gregory Sub-basin	1770	0.49										
Jones Range 1	Gregory Sub-basin	1780	0.37										
Jones Range 1	Gregory Sub-basin	1805	0.34										
Jones Range 1	Gregory Sub-basin	1815	0.5										
Jones Range 1	Gregory Sub-basin	1830	0.51										
Jones Range 1	Gregory Sub-basin	1830	0.51	444	0.27	0.29	0.03	0.56				56.86	5.882
Jones Range 1	Gregory Sub-basin	1835	0.2										
Jones Range 1	Gregory Sub-basin	1870	0.19										
Jones Range 1	Gregory Sub-basin	1895	0.18										
Jones Range 1	Gregory Sub-basin	1900	0.21										
Jones Range 1	Gregory Sub-basin	1905	0.17										
Jones Range 1	Gregory Sub-basin	1910	0.14										
Jones Range 1	Gregory Sub-basin	1910	0.13										
Jones Range 1	Gregory Sub-basin	1930	0.23										
Jones Range 1	Gregory Sub-basin	1945	0.12										
Jones Range 1	Gregory Sub-basin	1970	0.17										
Jones Range 1	Gregory Sub-basin	1990	0.17										
Jones Range 1	Gregory Sub-basin	2005	0.19										
Jones Range 1	Gregory Sub-basin	2030	0.3										
Jones Range 1	Gregory Sub-basin	2035	0.29										
Jones Range 1	Gregory Sub-basin	2040	0.31										
Jones Range 1	Gregory Sub-basin	2050	0.21										
Jones Range 1	Gregory Sub-basin	2060	0.3										
Jones Range 1	Gregory Sub-basin	2085	0.27										
Jones Range 1	Gregory Sub-basin	2090	0.26										
Jones Range 1	Gregory Sub-basin	2105	0.19										
Jones Range 1	Gregory Sub-basin	2120	0.21										
Jones Range 1	Gregory Sub-basin	2130	0.42										
Jones Range 1	Gregory Sub-basin	2140	0.28										
Jones Range 1	Gregory Sub-basin	2165	0.15										
Jones Range 1	Gregory Sub-basin	2255	0.48										
Jones Range 1	Gregory Sub-basin	2265	0.04										
Jones Range 1	Gregory Sub-basin	2285	0.05										
Jones Range 1	Gregory Sub-basin	2300	0.17										
Jones Range 1	Gregory Sub-basin	2305	0.1										
Jones Range 1	Gregory Sub-basin	2315	0.06										
Jones Range 1	Gregory Sub-basin	2340	0.06										
Jones Range 1	Gregory Sub-basin	2355	0.06										
Jones Range 1	Gregory Sub-basin	2385	0.07										
Justago 1	Lennard Shelf	215	0.17										
Justago 1	Lennard Shelf	385	0.1										
Kambara 1	Pender Terrace	1610	0.56			0.1	0.1	0.1				17.86	17.86
Kambara 1	Pender Terrace	1667.4	1.89	432	0.2	0.5	0.6	0.7		0.29		26.46	31.75
Kambara 1	Pender Terrace	1695.5	1.65	429	0.3	0.3	1.4	0.6		0.5		18.18	84.85
Kambara 1	Pender Terrace	1702	1.77	427	0.2	0.2	1	0.4		0.5		11.3	56.5
Kambara 1	Pender Terrace	1739.8	3.49	429	1.2	14.6	2.4	15.8		0.08		418.3	68.77
Kambara 1	Pender Terrace	1753.8	1.88	423	0.3	0.9	1.4	1.2		0.25		47.87	74.47
Kilang Kilang 1	Gregory Sub-basin	1730	0.11										
Kilang Kilang 1	Gregory Sub-basin	1757	0.19										
Kilang Kilang 1	Gregory Sub-basin	1760	0.07										
Kilang Kilang 1	Gregory Sub-basin	1790	0.1										
Kilang Kilang 1	Gregory Sub-basin	1820	0.07										
Kilang Kilang 1	Gregory Sub-basin	1850	0.12										
Kilang Kilang 1	Gregory Sub-basin	1880	0.09										
Kilang Kilang 1	Gregory Sub-basin	1882	0.31										
Kilang Kilang 1	Gregory Sub-basin	1910	0.06										
Kilang Kilang 1	Gregory Sub-basin	1940	0.07										
Kilang Kilang 1	Gregory Sub-basin	1970	0.07										
Kilang Kilang 1	Gregory Sub-basin	2000	0.11										
Kilang Kilang 1	Gregory Sub-basin	2010	0.15										
Kilang Kilang 1	Gregory Sub-basin	2030	0.07										
Kilang Kilang 1	Gregory Sub-basin	2060	0.13										
Kilang Kilang 1	Gregory Sub-basin	2090	0.08										
Kilang Kilang 1	Gregory Sub-basin	2120	0.12										
Kilang Kilang 1	Gregory Sub-basin	2136.9	0.08										
Kilang Kilang 1	Gregory Sub-basin	2150	0.14										
Kilang Kilang 1	Gregory Sub-basin	2180	0.08										
Kilang Kilang 1	Gregory Sub-basin	2210	0.12										
Kilang Kilang 1	Gregory Sub-basin	2240	0.08										
Kilang Kilang 1	Gregory Sub-basin	2260	0.13										
Kilang Kilang 1	Gregory Sub-basin	2270	0.12										
Kora 1	Fitzroy Trough	2300	1.29										
Kora 1	Fitzroy Trough	2305	2.94										
Kora 1	Fitzroy Trough	2335	0.33										

Kora 1	Fitzroy Trough	2348	1.01										
Kora 1	Fitzroy Trough	2360	0.57										
Kora 1	Fitzroy Trough	2365	0.39										
Kora 1	Fitzroy Trough	2395	0.56										
Kora 1	Fitzroy Trough	2397	0.49										
Kora 1	Fitzroy Trough	2425	0.46										
Kora 1	Fitzroy Trough	2459	0.53										
Kora 1	Fitzroy Trough	2474	0.36										
Kora 1	Fitzroy Trough	2485	0.61										
Kora 1	Fitzroy Trough	2515	0.82										
Kora 1	Fitzroy Trough	2517	0.73										
Kora 1	Fitzroy Trough	2525	0.56	445	0.15	0.59	0.94	0.74		0.2	0.06	105.4	167.9
Kora 1	Fitzroy Trough	2532.7	1.06										
Kora 1	Fitzroy Trough	2535	0.58	448	0.14	0.56	0.81	0.7		0.2	0.06	96.55	139.7
Kora 1	Fitzroy Trough	2542.5	1.01										
Kora 1	Fitzroy Trough	2545	0.7	448	0.18	0.75	0.72	0.93		0.19	0.06	107.1	102.9
Kora 1	Fitzroy Trough	2552.2	1.42										
Kora 1	Fitzroy Trough	2555	0.63	446	0.19	0.65	0.78	0.84		0.23	0.07	103.2	123.8
Lake Betty 1	Gregory Sub-basin	1660	1.73										
Lake Betty 1	Gregory Sub-basin	1700	1.59	432	0.1	0.34	2.32	0.44				21.38	145.9
Lake Betty 1	Gregory Sub-basin	1800	2.13	433	0.1	0.62	2.59	0.72				29.11	121.6
Lake Betty 1	Gregory Sub-basin	1859.28	1.98	449	0.2	1.64	0.93	1.84				82.83	46.97
Lake Betty 1	Gregory Sub-basin	1889.76	1.36	452	0.16	1.42	0.74	1.58				104.4	54.41
Lake Betty 1	Gregory Sub-basin	1900	2.17	431	0.1	0.62	2.22	0.72				28.57	102.3
Lake Betty 1	Gregory Sub-basin	1910	2.38										
Lake Betty 1	Gregory Sub-basin	1920.24	0.37										
Lake Betty 1	Gregory Sub-basin	1950.72	1.41	449	0.17	1.31	0.76	1.48				92.91	53.9
Lake Betty 1	Gregory Sub-basin	1981.2	1.16	447	0.15	0.91	0.65	1.06				78.45	56.03
Lake Betty 1	Gregory Sub-basin	2000	2.07	435	0.1	0.45	1.92	0.55				21.74	92.75
Lake Betty 1	Gregory Sub-basin	2011.68	2.08	453	0.14	1.54	0.41	1.68				74.04	19.71
Lake Betty 1	Gregory Sub-basin	2042.16	0.28										
Lake Betty 1	Gregory Sub-basin	2072.64	0.33										
Lake Betty 1	Gregory Sub-basin	2100	3.09	434	0.1	0.98	1.8	1.08				31.72	58.25
Lake Betty 1	Gregory Sub-basin	2103.12	0.22										
Lake Betty 1	Gregory Sub-basin	2133.6	0.44										
Lake Betty 1	Gregory Sub-basin	2164.08	0.76										
Lake Betty 1	Gregory Sub-basin	2194.56	0.82										
Lake Betty 1	Gregory Sub-basin	2200	3.29	434	0.1	2.19	1.61	2.29				66.57	48.94
Lake Betty 1	Gregory Sub-basin	2225.04	0.62										
Lake Betty 1	Gregory Sub-basin	2255.52	0.49										
Lake Betty 1	Gregory Sub-basin	2286	0.53										
Lake Betty 1	Gregory Sub-basin	2316.48	0.57										
Lake Betty 1	Gregory Sub-basin	2346.96	0.32										
Lake Betty 1	Gregory Sub-basin	2377.44	0.41										
Lake Betty 1	Gregory Sub-basin	2407.92	0.22										
Lake Betty 1	Gregory Sub-basin	2438.4	0.27										
Lake Betty 1	Gregory Sub-basin	2468.88	0.3										
Lake Betty 1	Gregory Sub-basin	2474.2	0.03										
Lake Betty 1	Gregory Sub-basin	2499.36	0.42										
Lake Betty 1	Gregory Sub-basin	2529.84	0.42										
Lake Betty 1	Gregory Sub-basin	2560.32	0.6										
Langoora 1	Lennard Shelf	1382	0.75	427	0.03	0.33	0.83	0.36		0.083		44	110.7
Langoora 1	Lennard Shelf	1491	0.85	427	0.2	0.87	0.47	1.07		0.187		102.4	55.29
Lloyd 1	Lennard Shelf	1765			0.03	0.15	0.74	0.18		0.17			
Lloyd 1	Lennard Shelf	1767.5		429	0.06	0.29	0.55	0.35		0.17			
Lloyd 1	Lennard Shelf	1770		430	0.05	0.22	0.39	0.27		0.19			
Lloyd 1	Lennard Shelf	1772.5			0.15	0.14	0.47	0.29		0.52			
Lloyd 1	Lennard Shelf	1775			0.16	0.12	0.44	0.28		0.57			
Lloyd 1	Lennard Shelf	1777.5			0.05	0.11	0.49	0.16		0.31			
Lloyd 1	Lennard Shelf	1780			0.06	0.16	0.52	0.22		0.27			
Lloyd 1	Lennard Shelf	1837.5			0.02	0.09	0.64	0.11		0.18			
Lloyd 1	Lennard Shelf	1840			0.02	0.07	0.45	0.09		0.22			
Lloyd 1	Lennard Shelf	1842.5			0.02	0.05	0.47	0.07		0.29			
Lloyd 1	Lennard Shelf	1845			0.04	0.08	0.47	0.12		0.33			
Lloyd 1	Lennard Shelf	1852.5			0.01	0.06	0.38	0.07		0.14			
Lloyd 1	Lennard Shelf	1855			0.07	0.11	0.33	0.18		0.39			
Lloyd 1	Lennard Shelf	1857.5			0.09	0.1	0.35	0.19		0.47			
Lloyd 1	Lennard Shelf	1860			0.06	0.09	0.49	0.15		0.4			
Lloyd 1	Lennard Shelf	1862.5			0.06	0.16	0.5	0.22		0.27			
Lloyd 1	Lennard Shelf	1865			0.04	0.11	0.5	0.15		0.27			
Lloyd 1	Lennard Shelf	1875			0.01	0.02	0.35	0.03		0.33			
Logue 1	Jurgurra Terrace	1368.103	0.13										
Logue 1	Jurgurra Terrace	1389.432	0.21										
Logue 1	Jurgurra Terrace	1398.573	0.14										
Logue 1	Jurgurra Terrace	1419.902	0.15										
Logue 1	Jurgurra Terrace	1429.043	0.1										
Logue 1	Jurgurra Terrace	1459.513	0.14										
Logue 1	Jurgurra Terrace	1527	0.25										
Mangaloo 1	Barbwire Terrace	930	0.49										
Mangaloo 1	Barbwire Terrace	950	0.22										
Mangaloo 1	Barbwire Terrace	970	0.34										
Mangaloo 1	Barbwire Terrace	1000	0.48										
Mangaloo 1	Barbwire Terrace	1007.5	0.66										
Mangaloo 1	Barbwire Terrace	1027.5	0.15										
Mangaloo 1	Barbwire Terrace	1047.5	0.16										
Mangaloo 1	Barbwire Terrace	1070	0.26										
Mangaloo 1	Barbwire Terrace	1080	1										
Mangaloo 1	Barbwire Terrace	1090	0.47										
Mangaloo 1	Barbwire Terrace	1110	0.19										
Mangaloo 1	Barbwire Terrace	1132.5	0.49										
Mangaloo 1	Barbwire Terrace	1150	0.3										
Mangaloo 1	Barbwire Terrace	1160	0.21										
Mangaloo 1	Barbwire Terrace	1230	0.37										

Mangaloo 1	Barbwire Terrace	1240	1.5										
Mangaloo 1	Barbwire Terrace	1250	1.5										
Mangaloo 1	Barbwire Terrace	1260	0.3										
Mangaloo 1	Barbwire Terrace	1270	0.48										
Mangaloo 1	Barbwire Terrace	1280	0.26										
Mangaloo 1	Barbwire Terrace	1340	0.11										
Mangaloo 1	Barbwire Terrace	1348.6	0.18										
Mangaloo 1	Barbwire Terrace	1350	0.16										
Mangaloo 1	Barbwire Terrace	1360	0.19										
Mangaloo 1	Barbwire Terrace	1370	0.1										
Mangaloo 1	Barbwire Terrace	1400	0.92										
Mangaloo 1	Barbwire Terrace	1410	0.39										
Mangaloo 1	Barbwire Terrace	1420	0.66										
Mangaloo 1	Barbwire Terrace	1440	0.19										
Mangaloo 1	Barbwire Terrace	1470	0.09										
Mangaloo 1	Barbwire Terrace	1615	0.11										
Mariana 1	Lennard Shelf	1175	1.04	423	0.05	0.38	0.5	0.43		0.12	0.04	36.54	48.08
Mariana 1	Lennard Shelf	1194.2	0.19										
Mariana 1	Lennard Shelf	1205	0.79	425	0.03	0.24	0.7	0.27		0.11	0.02	30.38	88.61
Mariana 1	Lennard Shelf	1270	0.51		0.04	0.14	0.8	0.18		0.22	0.01	27.45	156.9
Mariana 1	Lennard Shelf	1276	0.35										
Mariana 1	Lennard Shelf	1285	0.34										
Meda 1	Lennard Shelf	1542	0.2										
Meda 1	Lennard Shelf	1542.2	0.67										
Meda 1	Lennard Shelf	1556	0.46										
Meda 1	Lennard Shelf	1597.1	0.73										
Meda 1	Lennard Shelf	1665											
Meda 2	Lennard Shelf	1673	1.04	435	0.18	1.11	0.6	1.29		0.14		106.7	57.69
Meda 2	Lennard Shelf	1673	1.04	435	0.18	1.11	0.6	1.29		0.14		106.7	57.69
Meda 2	Lennard Shelf	1724	0.75	479	0.07	0.37	0.86	0.44		0.159		49.33	114.7
Meda 2	Lennard Shelf	1724	0.75	479	0.07	0.37	0.86	0.44		0.16		49.33	114.7
Mimosa 1	Lennard Shelf	1125	0.4										
Moogana 1	Pender Terrace	2030	2.17										
Mt Hardman 1	Fitzroy Trough	1999.4	0.68										
Mt Hardman 1	Fitzroy Trough	1999.4	0.68										
Mt Hardman 1	Fitzroy Trough	2008.6	0.64										
Mt Hardman 1	Fitzroy Trough	2017.7	0.62										
Mt Hardman 1	Fitzroy Trough	2026.9	0.69										
Mt Hardman 1	Fitzroy Trough	2036	0.65										
Mt Hardman 1	Fitzroy Trough	2045.2	0.68										
Mt Hardman 1	Fitzroy Trough	2054.3	0.66										
Mt Hardman 1	Fitzroy Trough	2063.5	0.97	436		1.73	1.45	1.73				178.4	149.5
Mt Hardman 1	Fitzroy Trough	2072.6	0.95										
Mt Hardman 1	Fitzroy Trough	2081.7	1.05	441		0.9	0.9	0.9				85.71	85.71
Mt Hardman 1	Fitzroy Trough	2090.9	1.11	441		0.4	1.2	0.4				36.04	108.1
Mt Hardman 1	Fitzroy Trough	2100	1.03	441		0.3	1.3	0.3				29.13	126.2
Mt Hardman 1	Fitzroy Trough	2109.2	1.22	446		0.7	1.6	0.7				57.38	131.1
Mt Hardman 1	Fitzroy Trough	2118.3	0.81	451		0.3	0.9	0.3				37.04	111.1
Mt Hardman 1	Fitzroy Trough	2127.5	0.72	441		0.2	0.9	0.2				27.78	125
Mt Hardman 1	Fitzroy Trough	2136.6	0.55	416		0.3	0.8	0.3				54.55	145.5
Mt Hardman 1	Fitzroy Trough	2145.7	0.48										
Mt Hardman 1	Fitzroy Trough	2154.9	0.32										
Mt Hardman 1	Fitzroy Trough	2164	0.41										
Mt Hardman 1	Fitzroy Trough	2173.2	0.42										
Mt Hardman 1	Fitzroy Trough	2182.3	0.37										
Mt Hardman 1	Fitzroy Trough	2191.5	0.47										
Mt Hardman 1	Fitzroy Trough	2200.6	0.53										
Mt Hardman 1	Fitzroy Trough	2209.8	0.57										
Mt Hardman 1	Fitzroy Trough	2218.9	0.37										
Mt Hardman 1	Fitzroy Trough	2228	0.54										
Mt Hardman 1	Fitzroy Trough	2237.2	0.4										
Mt Hardman 1	Fitzroy Trough	2246.3	0.38										
Mt Hardman 1	Fitzroy Trough	2255.5	0.37										
Mt Hardman 1	Fitzroy Trough	2264.6	0.58										
Mt Hardman 1	Fitzroy Trough	2273.8	0.49										
Mt Hardman 1	Fitzroy Trough	2282.9	0.63										
Mt Hardman 1	Fitzroy Trough	2292.1	0.36										
Mt Hardman 1	Fitzroy Trough	2301.2	0.54										
Nuytsia 1	Mowla Terrace	986.5	0.14										
Nuytsia 1	Mowla Terrace	988.7	0.06										
Nuytsia 1	Mowla Terrace	1011.7	0.13										
Olios 1	Balgo Terrace	825	0.18										
Olios 1	Balgo Terrace	840	0.34										
Olios 1	Balgo Terrace	855	0.55	432	0.11	0.42	0.39	0.53	1.07692	0.208	0.04	76.36	70.91
Olios 1	Balgo Terrace	870	0.19										
Olios 1	Balgo Terrace	885	0.09										
Olios 1	Balgo Terrace	900	0.14										
Olios 1	Balgo Terrace	915	0.25										
Olios 1	Balgo Terrace	930	0.2										
Olios 1	Balgo Terrace	945	0.86	422	2.52	2.08	0.76	4.6	2.73684	0.548	0.38	241.9	88.37
Olios 1	Balgo Terrace	960	0.39										
Olios 1	Balgo Terrace	975	0.13										
Olios 1	Balgo Terrace	990	0.19										
Olios 1	Balgo Terrace	1005	0.09										
Olios 1	Balgo Terrace	1020	0.12										
Olios 1	Balgo Terrace	1035	0.06										
Olios 1	Balgo Terrace	1050	0.1										
Olios 1	Balgo Terrace	1065	0.13										
Olios 1	Balgo Terrace	1080	0.09										
Olios 1	Balgo Terrace	1095	0.21										
Olios 1	Balgo Terrace	1110	0.19										
Olios 1	Balgo Terrace	1125	0.24										
Olios 1	Balgo Terrace	1140	0.22										

Olios 1	Balgo Terrace	1155	0.18										
Olios 1	Balgo Terrace	1170	0.19										
Olios 1	Balgo Terrace	1185	0.17										
Olios 1	Balgo Terrace	1200	0.19										
Olios 1	Balgo Terrace	1215	0.17										
Olios 1	Balgo Terrace	1230	0.15										
Olios 1	Balgo Terrace	1245	0.18										
Olios 1	Balgo Terrace	1260	0.14										
Olios 1	Balgo Terrace	1275	0.18										
Olios 1	Balgo Terrace	1290	0.3										
Olios 1	Balgo Terrace	1305	0.18										
Olios 1	Balgo Terrace	1320	0.18										
Olios 1	Balgo Terrace	1335	0.45										
Olios 1	Balgo Terrace	1350	0.31										
Olios 1	Balgo Terrace	1365	0.12										
Olios 1	Balgo Terrace	1380	0.13										
Olios 1	Balgo Terrace	1395	0.08										
Olios 1	Balgo Terrace	1410	0.13										
Olios 1	Balgo Terrace	1425	0.11										
Orange Pool 1	Lennard Shelf	888.1	0.48										
Orange Pool 1	Lennard Shelf	923.3	1.12										
Orange Pool 1	Lennard Shelf	971.3	0.7										
Orange Pool 1	Lennard Shelf	982.6	0.55										
Orange Pool 1	Lennard Shelf	1034.5	0.17										
Perindi 1	Pender Terrace	1773.6	0.21										
Philydrum 1	Fitzroy Trough	1450	0.37										
Puratte 1	Fitzroy Trough	2800	0.87										
Puratte 1	Fitzroy Trough	2830	0.88										
Puratte 1	Fitzroy Trough	2865	0.7										
Puratte 1	Fitzroy Trough	2895	0.6										
Puratte 1	Fitzroy Trough	2915	0.7										
Puratte 1	Fitzroy Trough	2940	0.76										
Puratte 1	Fitzroy Trough	2970	0.51										
St George Range 1	Fitzroy Trough	2902.6	0.5										
St George Range 1	Fitzroy Trough	2904.744	0.77		0.1	0.04	0.78	0.14			5.195	101.3	
St George Range 1	Fitzroy Trough	2935.224	0.7		0.09	0.05	0.51	0.14			7.143	72.86	
St George Range 1	Fitzroy Trough	2944.368	0.56										
St George Range 1	Fitzroy Trough	2950.464	0.53										
St George Range 1	Fitzroy Trough	2953.512	0.45										
St George Range 1	Fitzroy Trough	2959.608	0.4										
St George Range 1	Fitzroy Trough	2987.04	0.21										
St George Range 1	Fitzroy Trough	2993.136	0.19										
St George Range 1	Fitzroy Trough	2999.232	0.29										
St George Range 1	Fitzroy Trough	3002.5848	0.4										
St George Range 1	Fitzroy Trough	3011.424	0.34										
St George Range 1	Fitzroy Trough	3017.52	0.3										
St George Range 1	Fitzroy Trough	3032	2.61	489	0.05	0.47	0.45	0.52			18.01	17.24	
St George Range 1	Fitzroy Trough	3032	2.61	489	0.05	0.47	0.45	0.52			18.01	17.24	
St George Range 1	Fitzroy Trough	3032.76	0.33										
St George Range 1	Fitzroy Trough	3038.856	0.99	317	2.36	2.02	3.62	4.38			204	365.7	
St George Range 1	Fitzroy Trough	3066.288	0.51										
St George Range 1	Fitzroy Trough	3072.384	0.23										
St George Range 1	Fitzroy Trough	3078.48	0.3										
St George Range 1	Fitzroy Trough	3090.672	0.25										
St George Range 1	Fitzroy Trough	3099.816	0.32										
St George Range 1	Fitzroy Trough	3118.104	0.32										
St George Range 1	Fitzroy Trough	3124.5	0.2										
St George Range 1	Fitzroy Trough	3142.488	0.33										
St George Range 1	Fitzroy Trough	3148.584	0.31										
St George Range 1	Fitzroy Trough	3154.68	0.33										
St George Range 1	Fitzroy Trough	3160.776	0.36										
St George Range 1	Fitzroy Trough	3163.824	0.41										
St George Range 1	Fitzroy Trough	3185.16	0.24										
St George Range 1	Fitzroy Trough	3188.208	0.39										
St George Range 1	Fitzroy Trough	3191.256	0.35										
St George Range 1	Fitzroy Trough	3258.312	0.4										
St George Range 1	Fitzroy Trough	3261.36	0.29										
St George Range 1	Fitzroy Trough	3279.648	0.53										
St George Range 1	Fitzroy Trough	3300.984	0.38										
St George Range 1	Fitzroy Trough	3307.08	0.35										
St George Range 1	Fitzroy Trough	3328.416	0.52										
St George Range 1	Fitzroy Trough	3334.512	0.5										
St George Range 1	Fitzroy Trough	3349.752	0.3										
St George Range 1	Fitzroy Trough	3358.896	0.31										
St George Range 1	Fitzroy Trough	3371.088	0.3										
St George Range 1	Fitzroy Trough	3377.184	0.58										
St George Range 1	Fitzroy Trough	3383.28	0.55										
St George Range 1	Fitzroy Trough	3392.424	0.39										
St George Range 1	Fitzroy Trough	3398.52	0.47										
St George Range 1	Fitzroy Trough	3422.904	0.43										
St George Range 1	Fitzroy Trough	3425.952	0.55										
St George Range 1	Fitzroy Trough	3435.096	0.48										
St George Range 1	Fitzroy Trough	3442.1	0.1										
St George Range 1	Fitzroy Trough	3447.288	0.31										
St George Range 1	Fitzroy Trough	3453.384	0.41										
St George Range 1	Fitzroy Trough	3456.432	0.31										
St George Range 1	Fitzroy Trough	3462.528	0.27										
St George Range 1	Fitzroy Trough	3474	0.67	521	0.05	0.39	0.54	0.44			58.21	80.6	
St George Range 1	Fitzroy Trough	3474	0.67	521	0.05	0.39	0.54	0.44			58.21	80.6	
St George Range 1	Fitzroy Trough	3483.864	0.59										
St George Range 1	Fitzroy Trough	3489.96	0.62		0.12	0.17	0.39	0.29			27.42	62.9	
Sundown 1	Lennard Shelf	1805	0.33										
Sundown 1	Lennard Shelf	1815	0.27										

Sundown 1	Lennard Shelf	1855.5	0.52	432	0.24	0.43	1.1	0.67		0.36	0.06	82.69	211.5
Sundown 1	Lennard Shelf	1860	0.3										
Sundown 1	Lennard Shelf	1865	0.25										
Sundown 1	Lennard Shelf	1880	0.25										
Sundown 1	Lennard Shelf	1890	0.29										
Sundown 1	Lennard Shelf	1900	0.27										
Sundown 1	Lennard Shelf	1900.5	0.51	437	0.11	0.3	0.41	0.41		0.27	0.03	58.82	80.39
Sundown 1	Lennard Shelf	1935	0.28										
Sundown 1	Lennard Shelf	1950	0.27										
Sundown 1	Lennard Shelf	1955	0.22										
Sundown 1	Lennard Shelf	1965	0.26										
Sundown 1	Lennard Shelf	1968.1	0.58	441	0.16	0.46	0.29	0.62		0.26	0.05	79.31	50
Sundown 1	Lennard Shelf	1977.5	0.76	437	0.19	0.53	0.32	0.72		0.26	0.05	69.74	42.11
Sundown 1	Lennard Shelf	1980	0.25										
Valhalla 1 ST1	Fitzroy Trough	1985	0.16										
Valhalla 1 ST1	Fitzroy Trough	2005	0.21										
Valhalla 1 ST1	Fitzroy Trough	2035	0.37										
Valhalla 1 ST1	Fitzroy Trough	2045	0.3										
Valhalla 1 ST1	Fitzroy Trough	2070	0.34										
Valhalla 1 ST1	Fitzroy Trough	2085	0.34										
Valhalla 1 ST1	Fitzroy Trough	2100	0.4										
Valhalla 1 ST1	Fitzroy Trough	2150	0.27										
Valhalla 1 ST1	Fitzroy Trough	2170	0.42										
Valhalla 1 ST1	Fitzroy Trough	2185	0.33										
Valhalla 1 ST1	Fitzroy Trough	2220	0.44										
Valhalla 1 ST1	Fitzroy Trough	2235	0.28										
Valhalla 1 ST1	Fitzroy Trough	2285	0.37										
Valhalla 1 ST1	Fitzroy Trough	2320	0.49										
Valhalla 1 ST1	Fitzroy Trough	2335	0.62	441	0.16	0.49	1.96	0.65				79.03	316.1
Valhalla 1 ST1	Fitzroy Trough	2350	0.65	439	0.17	0.49	2.14	0.66				75.38	329.2
Valhalla 1 ST1	Fitzroy Trough	2390	0.55										
Valhalla 1 ST1	Fitzroy Trough	2440	0.8	442	0.21	0.61	1.51	0.82				76.25	188.8
Valhalla 1 ST1	Fitzroy Trough	2450	0.75	448	0.16	0.55	1.46	0.71				73.33	194.7
Valhalla 1 ST1	Fitzroy Trough	2500	0.88	442	0.26	0.61	1.36	0.87				69.32	154.5
Valhalla 1 ST1	Fitzroy Trough	2535	0.84	441	0.36	0.88	1.58	1.24				104.8	188.1
Valhalla 1 ST1	Fitzroy Trough	2545	1.33	439	0.58	1.19	1.53	1.77				89.47	115
Valhalla 1 ST1	Fitzroy Trough	2565	1.08	442	0.34	0.87	1.33	1.21				80.56	123.1
Valhalla 1 ST1	Fitzroy Trough	2620	0.83	445	0.24	0.53	1.47	0.77				63.86	177.1
Valhalla 1 ST1	Fitzroy Trough	2630	0.75	442	0.16	0.45	1.34	0.61				60	178.7
Valhalla 1 ST1	Fitzroy Trough	2640	0.9	441	0.19	0.49	1.57	0.68				54.44	174.4
Valhalla 1 ST1	Fitzroy Trough	2660	0.61	464	0.16	0.31	1.12	0.47				50.82	183.6
Valhalla 1 ST1	Fitzroy Trough	2670	0.77	452	0.15	0.33	1.17	0.48				42.86	151.9
Valhalla 1 ST1	Fitzroy Trough	2680	1.27	443	0.53	1.04	1.63	1.57				81.89	128.3
Valhalla 1 ST1	Fitzroy Trough	2690	0.6	465	0.14	0.35	0.92	0.49				58.33	153.3
Valhalla 1 ST1	Fitzroy Trough	2725	0.77	470	0.14	0.42	1.04	0.56				54.55	135.1
Valhalla 1 ST1	Fitzroy Trough	2740	0.72	464	0.13	0.4	0.89	0.53				55.56	123.6
Valhalla 1 ST1	Fitzroy Trough	2755	0.99	465	0.2	0.66	0.89	0.86				66.67	89.9
Valhalla 1 ST1	Fitzroy Trough	2815	0.56										
Valhalla 1 ST1	Fitzroy Trough	2860	0.75	418	0.15	0.47	1.43	0.62				62.67	190.7
Valhalla 1 ST1	Fitzroy Trough	2875	0.7	422	0.16	0.53	1.41	0.69				75.71	201.4
Valhalla 1 ST1	Fitzroy Trough	2890	0.48										
Valhalla 1 ST1	Fitzroy Trough	2930	0.54										
Valhalla 1 ST1	Fitzroy Trough	2945	0.54										
Valhalla 1 ST1	Fitzroy Trough	2960	0.62	426	0.11	0.31	1.31	0.42				50	211.3
Valhalla 1 ST1	Fitzroy Trough	2975	0.62	348	0.12	0.22	1.22	0.34				35.48	196.8
Valhalla 1 ST1	Fitzroy Trough	2985	0.64	366	0.11	0.26	1.16	0.37				40.63	181.3
Valhalla 1 ST1	Fitzroy Trough	3000	0.53										
Valhalla 1 ST1	Fitzroy Trough	3015	0.54										
Valhalla 1 ST1	Fitzroy Trough	3035	0.64		0.09	0.15	0.97	0.24				23.44	151.6
Valhalla 1 ST1	Fitzroy Trough	3045	0.5										
Valhalla 1 ST1	Fitzroy Trough	3095	0.63	366	0.13	0.22	0.51	0.35				34.92	80.95
Valhalla 1 ST1	Fitzroy Trough	3110	0.49										
Valhalla 1 ST1	Fitzroy Trough	3115	0.44										
Valhalla 1 ST1	Fitzroy Trough	3135	0.42										
Valhalla 1 ST1	Fitzroy Trough	3150	0.85	469	0.13	0.4	0.77	0.53				47.06	90.59
Valhalla 1 ST1	Fitzroy Trough	3160	0.53										
Valhalla 1 ST1	Fitzroy Trough	3180	0.54										
Valhalla 1 ST1	Fitzroy Trough	3195	0.62	447	0.09	0.26	0.92	0.35				41.94	148.4
Valhalla 1 ST1	Fitzroy Trough	3210	0.59										
Valhalla 1 ST1	Fitzroy Trough	3220	0.58										
Valhalla 1 ST1	Fitzroy Trough	3315	0.82	449	0.13	0.36	0.71	0.49				43.9	86.59
Valhalla 1 ST1	Fitzroy Trough	3325	0.81		0.09	0.19	0.57	0.28				23.46	70.37
Valhalla 1 ST1	Fitzroy Trough	3345	0.84		0.11	0.18	0.39	0.29				21.43	46.43
Valhalla 1 ST1	Fitzroy Trough	3360	0.63	455	0.12	0.24	0.48	0.36				38.1	76.19
Valhalla 1 ST1	Fitzroy Trough	3370	0.81	448	0.15	0.25	0.28	0.4				30.86	34.57
Valhalla 1 ST1	Fitzroy Trough	3385	0.87	457	0.16	0.39	0.33	0.55				44.83	37.93
Valhalla 1 ST1	Fitzroy Trough	3400	0.66	450	0.1	0.21	0.35	0.31				31.82	53.03
Valhalla 1 ST1	Fitzroy Trough	3410	0.64		0.08	0.19	0.34	0.27				29.69	53.13
West Kora 1	Fitzroy Trough	2263	1.98	430	0.11	0.24	0.16	0.35		0.31	0.02	12.12	8.081
West Kora 1	Fitzroy Trough	2279	0.71	434	0.09	0.21	0.16	0.3		0.3	0.02	29.58	22.54
West Kora 1	Fitzroy Trough	2290	1.74										
West Kora 1	Fitzroy Trough	2291	0.52		0.1	0.15	0.23	0.25		0.4	0.02	28.85	44.23
West Kora 1	Fitzroy Trough	2320	1.26										
West Kora 1	Fitzroy Trough	2367	0.31										
West Kora 1	Fitzroy Trough	2380	1.08										
West Kora 1	Fitzroy Trough	2387	0.3										
West Kora 1	Fitzroy Trough	2410	0.81										
West Kora 1	Fitzroy Trough	2435.9	0.63		0.07	0.08	0.25	0.15		0.47	0.01	12.7	39.68
West Kora 1	Fitzroy Trough	2440	0.7										
West Kora 1	Fitzroy Trough	2448	0.47										
West Kora 1	Fitzroy Trough	2470	0.58										
West Kora 1	Fitzroy Trough	2500	0.7										
West Kora 1	Fitzroy Trough	2530	0.64										

White Hills 1	Gregory Sub-basin	1090	0.25										
White Hills 1	Gregory Sub-basin	1100	0.17										
White Hills 1	Gregory Sub-basin	1105	0.43										
White Hills 1	Gregory Sub-basin	1110	0.33										
White Hills 1	Gregory Sub-basin	1120	0.4										
White Hills 1	Gregory Sub-basin	1130	0.35										
White Hills 1	Gregory Sub-basin	1140	0.67				0.29						43.28
White Hills 1	Gregory Sub-basin	1150	0.29										
White Hills 1	Gregory Sub-basin	1160	0.19										
White Hills 1	Gregory Sub-basin	1173	0.27										
White Hills 1	Gregory Sub-basin	1180	0.5				0.17						34
White Hills 1	Gregory Sub-basin	1190	0.46										
White Hills 1	Gregory Sub-basin	1200	0.27										
White Hills 1	Gregory Sub-basin	1210	0.23										
White Hills 1	Gregory Sub-basin	1220	0.36										
White Hills 1	Gregory Sub-basin	1230	0.3										
White Hills 1	Gregory Sub-basin	1239	0.29										
White Hills 1	Gregory Sub-basin	1240	0.63	438		0.21	0.19	0.21				33.33	30.16
White Hills 1	Gregory Sub-basin	1250	0.22										
White Hills 1	Gregory Sub-basin	1260	0.28										
White Hills 1	Gregory Sub-basin	1270	0.52				0.15						28.85
White Hills 1	Gregory Sub-basin	1280	0.88	438	0.23	0.47	0.18	0.7		0.33		53.41	20.45
White Hills 1	Gregory Sub-basin	1290	0.79	437	0.15	0.41	0.17	0.56		0.27		51.9	21.52
White Hills 1	Gregory Sub-basin	1300	0.37										
White Hills 1	Gregory Sub-basin	1310	0.29										
White Hills 1	Gregory Sub-basin	1320	0.37										
White Hills 1	Gregory Sub-basin	1330	0.5				0.07						14
White Hills 1	Gregory Sub-basin	1340	0.63	438	0.21	0.32	0.11	0.53		0.4		50.79	17.46
White Hills 1	Gregory Sub-basin	1350	0.62				0.13						20.97
White Hills 1	Gregory Sub-basin	1360	0.46										
White Hills 1	Gregory Sub-basin	1369	0.62	420	0.15	0.32	0.62	0.47		0.32		51.61	100
White Hills 1	Gregory Sub-basin	1370	0.79	438		0.31	0.16	0.31				39.24	20.25
White Hills 1	Gregory Sub-basin	1380	0.72	435		0.27	0.17	0.27				37.5	23.61
White Hills 1	Gregory Sub-basin	1390	0.46										
White Hills 1	Gregory Sub-basin	1400	0.54				0.13						24.07
White Hills 1	Gregory Sub-basin	1410	0.59	440		0.21	0.23	0.21				35.59	38.98
White Hills 1	Gregory Sub-basin	1414	0.38										
White Hills 1	Gregory Sub-basin	1420	0.51			0.15	0.15	0.15				29.41	29.41
White Hills 1	Gregory Sub-basin	1430	0.45										
White Hills 1	Gregory Sub-basin	1440	0.51				0.24						47.06
White Hills 1	Gregory Sub-basin	1450	0.45										
White Hills 1	Gregory Sub-basin	1460	0.59	447			0.18						30.51
White Hills 1	Gregory Sub-basin	1470	0.71	442		0.3	0.35	0.3				42.25	49.3
White Hills 1	Gregory Sub-basin	1480	0.74			0.15	0.21	0.15				20.27	28.38
White Hills 1	Gregory Sub-basin	1490	0.4										
White Hills 1	Gregory Sub-basin	1500	0.36										
White Hills 1	Gregory Sub-basin	1510	0.53				0.3						56.6
White Hills 1	Gregory Sub-basin	1516.4	0.84	433	0.13	0.54	0.83	0.67		0.19		64.29	98.81
White Hills 1	Gregory Sub-basin	1520	0.53	440	0.1	0.35	0.19	0.45		0.22		66.04	35.85
White Hills 1	Gregory Sub-basin	1530	0.43										
White Hills 1	Gregory Sub-basin	1540	0.47										
White Hills 1	Gregory Sub-basin	1550	0.65	449	0.16	0.48	0.13	0.64		0.25		73.85	20
White Hills 1	Gregory Sub-basin	1560	0.43										
White Hills 1	Gregory Sub-basin	1570	0.5		0.24	0.45	0.19	0.69		0.35		90	38
White Hills 1	Gregory Sub-basin	1580	0.66	448	0.15	0.45	0.16	0.6		0.25		68.18	24.24
White Hills 1	Gregory Sub-basin	1590	0.46										
White Hills 1	Gregory Sub-basin	1600	0.84	453	0.22	0.64	0.19	0.86		0.26		76.19	22.62
White Hills 1	Gregory Sub-basin	1610	0.7			0.19	0.28	0.19				27.14	40
White Hills 1	Gregory Sub-basin	1620	0.6		0.1	0.15	0.27	0.25		0.4		25	45
White Hills 1	Gregory Sub-basin	1621.7	0.45										
White Hills 1	Gregory Sub-basin	1630	0.55			0.13	0.21	0.13				23.64	38.18
White Hills 1	Gregory Sub-basin	1640	0.59			0.11	0.18	0.11				18.64	30.51
White Hills 1	Gregory Sub-basin	1650	0.65			0.17	0.2	0.17				26.15	30.77
White Hills 1	Gregory Sub-basin	1660	0.66			0.18	0.21	0.18				27.27	31.82
White Hills 1	Gregory Sub-basin	1670	0.61			0.1	0.17	0.1				16.39	27.87
White Hills 1	Gregory Sub-basin	1675.5	1.95	448	0.31	0.89	0.57	1.2		0.26		45.64	29.23
White Hills 1	Gregory Sub-basin	1680	0.7			0.15	0.24	0.15				21.43	34.29
White Hills 1	Gregory Sub-basin	1690	0.74			0.16	0.24	0.16				21.62	32.43
White Hills 1	Gregory Sub-basin	1692.5	0.57	445	0.12	0.27	0.39	0.39		0.31		47.37	68.42
White Hills 1	Gregory Sub-basin	1700	0.65			0.13	0.23	0.13				20	35.38
White Hills 1	Gregory Sub-basin	1710	0.48										
White Hills 1	Gregory Sub-basin	1720	0.47										
White Hills 1	Gregory Sub-basin	1730	0.57				0.1						17.54
White Hills 1	Gregory Sub-basin	1740	0.6				0.08						13.33
White Hills 1	Gregory Sub-basin	1750	0.71			0.11	0.17	0.11				15.49	23.94
White Hills 1	Gregory Sub-basin	1760	0.51				0.09						17.65
White Hills 1	Gregory Sub-basin	1770	0.64		0.12	0.18	0.08	0.3		0.4		28.13	12.5
White Hills 1	Gregory Sub-basin	1773	0.62		0.12	0.23	0.86	0.35		0.34		37.1	138.7
White Hills 1	Gregory Sub-basin	1780	0.78		0.1	0.18	0.18	0.28		0.36		23.08	23.08
White Hills 1	Gregory Sub-basin	1789.1	0.41										
White Hills 1	Gregory Sub-basin	1790	0.78			0.18	0.2	0.18				23.08	25.64
White Hills 1	Gregory Sub-basin	1800	0.64			0.18	0.21	0.18				28.13	32.81
White Hills 1	Gregory Sub-basin	1810	0.44										
White Hills 1	Gregory Sub-basin	1820	0.45										
White Hills 1	Gregory Sub-basin	1830	0.57		0.11	0.14	0.27	0.25		0.44		24.56	47.37
White Hills 1	Gregory Sub-basin	1840	0.51			0.18	0.2	0.18				35.29	39.22
White Hills 1	Gregory Sub-basin	1850	0.44										
White Hills 1	Gregory Sub-basin	1860	0.52		0	0.1	0.23	0.1		0.3		19.23	44.23
White Hills 1	Gregory Sub-basin	1860	0.65	460	0.13	0.3	0.74	0.43				46.15	113.8
White Hills 1	Gregory Sub-basin	1870	0.71			0.19	0.26	0.19				26.76	36.62
White Hills 1	Gregory Sub-basin	1876.5	1.43	446	0.37	1.05	0.4	1.42		0.26		73.43	27.97
White Hills 1	Gregory Sub-basin	1880	0.6	456	0.1	0.23	0.25	0.33		0.3		38.33	41.67
White Hills 1	Gregory Sub-basin	1890	0.72	458	0.1	0.29	0.24	0.39		0.26		40.28	33.33

White Hills 1	Gregory Sub-basin	1900	0.61			0.17	0.16	0.17				27.87	26.23
White Hills 1	Gregory Sub-basin	1910	0.55			0.13	0.22	0.13				23.64	40
White Hills 1	Gregory Sub-basin	1910.4	0.72	469	0.11	0.21	0.91	0.32		0.34		29.17	126.4
White Hills 1	Gregory Sub-basin	1920	0.6	447		0.38	0.16	0.38				63.33	26.67
White Hills 1	Gregory Sub-basin	1930	0.52				0.24						46.15
White Hills 1	Gregory Sub-basin	1938.8	1.06	425	0.12	0.32	0.68	0.44		0.27		30.19	64.15
White Hills 1	Gregory Sub-basin	1950	0.67		0.18	0.15	0.37	0.33		0.55		22.39	55.22
White Hills 1	Gregory Sub-basin	1958.3	0.98	431	0.31	0.58	1.27	0.89		0.35		59.18	129.6
White Hills 1	Gregory Sub-basin	1960	0.83		0.19	0.24	0.37	0.43		0.44		28.92	44.58
White Hills 1	Gregory Sub-basin	1970	0.99	454	0.23	0.39	0.39	0.62		0.37		39.39	39.39
White Hills 1	Gregory Sub-basin	1980	0.65			0.12	0.3	0.12				18.46	46.15
White Hills 1	Gregory Sub-basin	1990	1.11	463	0.17	0.42	0.35	0.59		0.29		37.84	31.53
White Hills 1	Gregory Sub-basin	2000	0.79		0.12	0.17	0.37	0.29		0.41		21.52	46.84
White Hills 1	Gregory Sub-basin	2010	0.76		0.12	0.16	0.2	0.28		0.43		21.05	26.32
White Hills 1	Gregory Sub-basin	2020	0.76			0.19	0.18	0.19				25	23.68
White Hills 1	Gregory Sub-basin	2029.9	0.87	482	0.12	0.35	0.62	0.47		0.26		40.23	71.26
White Hills 1	Gregory Sub-basin	2030	0.68			0.14	0.19	0.14				20.59	27.94
White Hills 1	Gregory Sub-basin	2040	0.87			0.16	0.33	0.16				18.39	37.93
White Hills 1	Gregory Sub-basin	2050	0.79			0.13	0.31	0.13				16.46	39.24
White Hills 1	Gregory Sub-basin	2060	1.17	465	0.2	0.35	0.45	0.55		0.36		29.91	38.46
White Hills 1	Gregory Sub-basin	2070	1.28	465	0.28	0.45	0.4	0.73		0.38		35.16	31.25
White Hills 1	Gregory Sub-basin	2080	1.2	468	0.22	0.42	0.39	0.64		0.34		35	32.5
White Hills 1	Gregory Sub-basin	2090	0.93		0.22	0.33	0.41	0.55		0.4		35.48	44.09
White Hills 1	Gregory Sub-basin	2100	0.83		0.14	0.21	0.3	0.35		0.4		25.3	36.14
White Hills 1	Gregory Sub-basin	2104.8	0.7	485	0.12	0.24	0.46	0.36		0.33		34.29	65.71
White Hills 1	Gregory Sub-basin	2110	0.65		0.16	0.21	0.31	0.37		0.43		32.31	47.69
Yarrada 1	Lennard Shelf	1798	0.64										
Yarrada 1	Lennard Shelf	1810.8	1.36										
Yarrada 1	Lennard Shelf	1836.5	0.45										
Yarrada 1	Lennard Shelf	1861.8	0.51										
Yarrada 1	Lennard Shelf	1891.7	0.45										
Yarrada 1	Lennard Shelf	1903	0.51										
Yarrada 1	Lennard Shelf	1925	0.46										
Yulleroo 1	Fitzroy Trough	690.07	0.12										
Yulleroo 1	Fitzroy Trough	828.9	0.13										
Yulleroo 1	Fitzroy Trough	2213.91	0.46										
Yulleroo 1	Fitzroy Trough	2235	0.5		0.01	0.05	0.83	0.06		0.17		10	166
Yulleroo 1	Fitzroy Trough	2321	2.49	436	0.35	0.67	0.39	1.02		0.34		26.91	15.66
Yulleroo 1	Fitzroy Trough	2519.63	0.5										
Yulleroo 1	Fitzroy Trough	2548	0.65	436	0.16	1.13	0.27	1.29		0.12		173.8	41.54
Yulleroo 1	Fitzroy Trough	2874.72	0.33										
Yulleroo 1	Fitzroy Trough	3027.73	0.43										
Yulleroo 1	Fitzroy Trough	3111.55	0.54	462	0.08	0.22	0.36	0.3		0.267		40.74	66.67
Yulleroo 1	Fitzroy Trough	3142	0.65	465	0.06	0.35	0.32	0.41		0.15		53.85	49.23
Yulleroo 1	Fitzroy Trough	3239	0.56	499	0.03	0.81	0.35	0.84		0.04		144.6	62.5
Yulleroo 1	Fitzroy Trough	3348.84	0.36										
Yulleroo 1	Fitzroy Trough	3381	0.52	494	0.04	0.39	0.3	0.43		0.09		75	57.69
Yulleroo 1	Fitzroy Trough	3490.26	0.63		0.14	0.19	0.35	0.33		0.424		30.16	55.56
Yulleroo 1	Fitzroy Trough	3524	0.64		0.07	0.11	0.35	0.18		0.39		17.19	54.69
Yulleroo 1	Fitzroy Trough	3583.53	0.96	471	0.11	0.29	0.31	0.4		0.275		30.21	32.29
Yulleroo 1	Fitzroy Trough	3658.21	2.18	448	0.69	0.83	0.4	1.52		0.454		38.07	18.35
Yulleroo 1	Fitzroy Trough	3694	2.48	449	0.64	0.61		1.25		0.51		24.6	
Yulleroo 1	Fitzroy Trough	3695	2.85	446	0.73	0.73		1.46		0.5		25.61	
Yulleroo 1	Fitzroy Trough	3696	4.4	449	0.75	1.06	0.56	1.81		0.41		24.09	12.73
Yulleroo 1	Fitzroy Trough	3830.73	0.32										

Gogo Formation

Well	Depth (mRT)	TOC %	Tmax (°C)	S1 (kg/ton)	S2 (kg/ton)	S3 (kg/ton)	S1+S2	S2/S3	PI	PC	HI	OI
Gap Creek 1	425	0.45	427	0.21	0.38	0.28	0.59		0.36		84.44	62.22
Gap Creek 1	500	0.15										
Kambara 1	2819.62	0.53	424	0.3	0.5	0.1	0.8		0.38		94.34	18.87
Kambara 1	2985	0.17	432	1.2	0.7	0.1	1.9		0.63		411.8	58.82
Kambara 1	3015	0.44	444	0.1	0.3	0.1	0.4		0.25		68.18	22.73
Kambara 1	3045	0.37	444	0.1	0.2	0.1	0.3		0.33		54.05	27.03
Kambara 1	3135	0.23				0.2						86.96
Matches Spring 1	1234	0.32	425	0.02	0.1		0.12		0.17		31.25	
Matches Spring 1	1234	0.32	425	0.02	0.1		0.12		0.167		31.25	
Matches Spring 1	1237	0.3	383	0.03	0.02	0.44	0.05		0.6		6.667	146.7
Matches Spring 1	1346	0.1	444	0.03	0.05	1.27	0.08		0.38		50	1270
Selenops 1	780	0.17										
Selenops 1	795	0.17										
Selenops 1	810	0.12										
Selenops 1	825	0.13										
Selenops 1	840	0.11										
Selenops 1	843	0.15										
Selenops 1	855	0.18										
Selenops 1	870	0.15										
Selenops 1	885	0.18										
Selenops 1	900	0.13										
Selenops 1	915	0.14										
C104		0.44	422	0.05	0.33		0.38				88	
C83		0.93	412									
I171		1.08	429	0.05	1.8		1.85				171	
I172		0.45	415	0.06	1.15		1.21				217	
P421		1.2	422	0.07	2.25		2.32				192	
P491		1.36	418	0.09	1.36		1.45				110	
P492		0.65	423	0.02	0.46		0.48				73	
P2181		0.76	422	0.05	1.62		1.67				219	
E151		1	429	0.02	0.34		0.36				36	
E152		2.08	410	0.14	4.4		4.54				218	
E201		1.32	416	1.08	7.02		8.1				613	
GSWA72335		1.89	428	0.05	2.83		2.88				149	
Eromophilia 1		1.49	428	0.14	1.96		2.1				131	
Eromophilia 1		3.1	427	0.16	5.06		5.22				163	
Eromophilia 1		1.08		0.36	3.03		3.39				280	

Bongabinni Member

Well/Hole ID	Top Depth (m)	TOC %	Tmax (°C)	S1 (kg/ton)	S2 (kg/ton)	S3 (kg/ton)	S1+S2	S2/S3	PI	PC	HI	OI
Frankenstein 1	1960	0.16										
Frankenstein 1	1980	0.16										
Frankenstein 1	2000	0.14										
Frankenstein 1	2015	0.2										
Frankenstein 1	2026.98	0.1										
Frankenstein 1	2033	0.12										
Frankenstein 1	2051	0.03										
Frankenstein 1	2069	0.08										
Frankenstein 1	2087	0.09										
Frankenstein 1	2100.55	0.17										
Frankenstein 1	2105	0.08										
Frankenstein 1	2121	0.32										
Frankenstein 1	2123	0.07										
Frankenstein 1	2141	0.1										
Frankenstein 1	2159	0.07										
Frankenstein 1	2166.73	0.15										
Frankenstein 1	2177	0.08										
Frankenstein 1	2186	0.07										
Frankenstein 1	2195	0.07										
Leo 1	1460	0.24										
Leo 1	1475	0.16										
Leo 1	1490	0.2										
Leo 1	1505	0.13										
Leo 1	1520	0.15										
Leo 1	1535	0.12										
Sally May 1	1521.2	0.08										
Sally May 1	1548.7	0.08										
Sally May 1	1564.1	0.2										

Goldwyer Formation

Well	Tectonic Region	Depth (mRT)	TOC %	Tmax (°C)	S1 (kg/ton)	S2 (kg/ton)	S3 (kg/ton)	S1+S2	S2/S3	PI	PC	HI	OI
Acacia 1	Barbwire Terrace	858.67	0.97										
Acacia 1	Barbwire Terrace	861.6	0.18										
Acacia 1	Barbwire Terrace	865.4	0.13										
Acacia 1	Barbwire Terrace	870	0.13										
Acacia 1	Barbwire Terrace	874	0.19										
Acacia 1	Barbwire Terrace	874.5	0.19										
Acacia 1	Barbwire Terrace	878.2	0.15										
Acacia 1	Barbwire Terrace	893.45	0.17										
Acacia 1	Barbwire Terrace	904.9	0.16										
Acacia 1	Barbwire Terrace	917.1	0.21										
Acacia 1	Barbwire Terrace	917.62	0.17										
Acacia 1	Barbwire Terrace	927.3	0.24										
Acacia 1	Barbwire Terrace	935	0.19										
Acacia 1	Barbwire Terrace	935	0.19										
Acacia 1	Barbwire Terrace	944.9	0.37										
Acacia 1	Barbwire Terrace	960.05	0.54										
Acacia 1	Barbwire Terrace	974	0.71	432	0.22	0.88	0.14	1.1		0.2		123.9	19.72
Acacia 1	Barbwire Terrace	978.82	0.76										
Acacia 1	Barbwire Terrace	987.19	0.74										
Acacia 1	Barbwire Terrace	993.2	1.92	438	0.49	6.24	0.88	6.73		0.073		325	45.83
Acacia 1	Barbwire Terrace	995	1.02	438	0.22	2.39	0.88	2.61		0.084		234.3	86.27
Acacia 1	Barbwire Terrace	995	1.24										
Acacia 1	Barbwire Terrace	1003.7	0.6										
Acacia 1	Barbwire Terrace	1009.95	0.97										
Acacia 1	Barbwire Terrace	1014	0.91	433	0.11	1.92	0.09	2.03		0.054		211	9.89
Acacia 1	Barbwire Terrace	1019.49	1.24										
Acacia 1	Barbwire Terrace	1019.5	1.01	438	0.19	2.06	0.65	2.25		0.084		204	64.36
Acacia 1	Barbwire Terrace	1026	0.73										
Acacia 1	Barbwire Terrace	1033	0.87	435	0.14	1.6	0.15	1.74		0.08		183.9	17.24
Acacia 1	Barbwire Terrace	1037.8	0.33										
Acacia 1	Barbwire Terrace	1037.8	1.3										
Acacia 1	Barbwire Terrace	1043	0.15										
Acacia 1	Barbwire Terrace	1048.2	0.2										
Anna Plains 1	Willara Sub-basin	1143	0.49										
Antares 1	Mowla Terrace	1255	0.18										
Antares 1	Mowla Terrace	1260.5	0.13										
Antares 1	Mowla Terrace	1278	0.13										
Antares 1	Mowla Terrace	1292	0.15										
Antares 1	Mowla Terrace	1295	0.11										
Aquila 1	Broome Platform	859	0.22										
Aquila 1	Broome Platform	893	0.23										
Aquila 1	Broome Platform	942	0.56	434	0.11	0.68	0.26	0.79		0.14		121.4	46.43
Aquila 1	Broome Platform	956	0.27										
Aquila 1	Broome Platform	976.5	0.25										
Aquila 1	Broome Platform	1020	0.22										
Aquila 1	Broome Platform	1020.5	0.3										
Aquila 1	Broome Platform	1030	0.28										
Aquila 1	Broome Platform	1040	0.36										
Aquila 1	Broome Platform	1050	0.81	436	0.39	1.24	0.33	1.63		0.24	0.14	153.1	40.74
Aquila 1	Broome Platform	1053	0.31										
Aquila 1	Broome Platform	1055	1.07	438	0.56	2.36	0.34	2.92		0.19	0.24	220.6	31.78
Aquila 1	Broome Platform	1060	1.39	438	0.87	3.66	0.34	4.53		0.19	0.38	263.3	24.46
Aquila 1	Broome Platform	1060	1.11	437	0.7	2.17	0.33	2.87		0.24	0.24	195.5	29.73
Aquila 1	Broome Platform	1060			0.65	0.63		1.28		0.51			
Aquila 1	Broome Platform	1065	1.55	439	1	3.89	0.35	4.89		0.2	0.41	251	22.58
Aquila 1	Broome Platform	1069.5	1.91	436	1.25	4.42	0.56	5.67		0.22		231.4	29.32
Aquila 1	Broome Platform	1070	1.52	438	0.89	4.05	0.32	4.94		0.18	0.41	266.4	21.05
Aquila 1	Broome Platform	1070	0.95	435	0.72	2.2	0.4	2.92		0.25	0.24	231.6	42.11
Aquila 1	Broome Platform	1080	0.74	435	0.44	1.23	0.36	1.67		0.26	0.14	166.2	48.65
Aquila 1	Broome Platform	1087.5	0.89	430	0.41	0.81	0.58	1.22		0.34		91.01	65.17
Aquila 1	Broome Platform	1090	0.83	435	0.55	1.5	0.45	2.05		0.27	0.17	180.7	54.22
Aquila 1	Broome Platform	1100	0.85	435	0.52	1.39	0.5	1.91		0.27	0.16	163.5	58.82
Aquila 1	Broome Platform	1110	1.23	436	1.02	2.55	0.38	3.57		0.29	0.3	207.3	30.89
Aquila 1	Broome Platform	1118.5	3.2	436	2.71	7.02	0.82	9.73		0.28		219.4	25.63
Aquila 1	Broome Platform	1120	1.46	431	1.51	3.1	0.51	4.61		0.33	0.38	212.3	34.93
Aquila 1	Broome Platform	1120			0.45	0.64		1.09		0.41			
Aquila 1	Broome Platform	1130	1.04	430	0.9	1.65	0.47	2.55		0.35	0.21	158.7	45.19
Aquila 1	Broome Platform	1140	1.16	426	1.21	2.38	0.56	3.59		0.34	0.3	205.2	48.28
Aquila 1	Broome Platform	1141	2.22	433	1.12	2.75	0.65	3.87		0.29		123.9	29.28
Aquila 1	Broome Platform	1150	1.18	429	1.09	1.92	0.71	3.01		0.36	0.25	162.7	60.17
Aquila 1	Broome Platform	1160	0.87	426	0.71	1.24	0.58	1.95		0.36	0.16	142.5	66.67
Aquila 1	Broome Platform	1164	0.77	432	0.31	0.67	0.42	0.98		0.32		87.01	54.55
Blackstone 1	Lennard Shelf	2621.3	0.22										
Blackstone 1	Lennard Shelf	2651.8	0.24										
Blackstone 1	Lennard Shelf	2674.3	0.14										
Blackstone 1	Lennard Shelf	2676.3	0.14										
Blackstone 1	Lennard Shelf	2676.9	0.14										
Blackstone 1	Lennard Shelf	2677.4	0.13										
Blackstone 1	Lennard Shelf	2677.5	0.12										
Blackstone 1	Lennard Shelf	2678.1	0.14										
Blackstone 1	Lennard Shelf	2678.7	0.13										
Blackstone 1	Lennard Shelf	2679.3	0.15										
Blackstone 1	Lennard Shelf	2680	0.14										
Blackstone 1	Lennard Shelf	2682.2	0.2										
Blackstone 1	Lennard Shelf	2712.7	0.22										
Blackstone 1	Lennard Shelf	2738.5	0.14										
Blackstone 1	Lennard Shelf	2740.6	0.06										
Blackstone 1	Lennard Shelf	2741.2	0.16										
Blackstone 1	Lennard Shelf	2741.2	0.16										
Blackstone 1	Lennard Shelf	2742	0.13										
Blackstone 1	Lennard Shelf	2743.2	0.24										
Blackstone 1	Lennard Shelf	2773.7	0.23										

Blackstone 1	Lennard Shelf	2804.2	0.24										
Blackstone 1	Lennard Shelf	2832.7	0.16										
Blackstone 1	Lennard Shelf	2833.1	0.17										
Blackstone 1	Lennard Shelf	2833.5	0.13										
Blackstone 1	Lennard Shelf	2833.9	0.18										
Blackstone 1	Lennard Shelf	2834.5	0.19										
Blackstone 1	Lennard Shelf	2834.6	0.23										
Blackstone 1	Lennard Shelf	2834.9	0.16										
Blackstone 1	Lennard Shelf	2835.7	0.17										
Blackstone 1	Lennard Shelf	2836.3	0.18										
Blackstone 1	Lennard Shelf	2836.9	0.08										
Blackstone 1	Lennard Shelf	2865.1	0.22										
Blackstone 1	Lennard Shelf	2895.6	0.24										
Blackstone 1	Lennard Shelf	2912.7	0.13										
Blackstone 1	Lennard Shelf	2913.3	0.11										
Blackstone 1	Lennard Shelf	2926.1	0.21										
Blackstone 1	Lennard Shelf	2956.6	0.22										
Blackstone 1	Lennard Shelf	2978.23	0.11										
Blackstone 1	Lennard Shelf	3008.8	0.1										
Blackstone 1	Lennard Shelf	3045	0.15										
Blackstone 1	Lennard Shelf	3045.6	0.23										
Blackstone 1	Lennard Shelf	3048.6					0						
Calamia 1	Willara Sub-basin	958	0.11										
Calamia 1	Willara Sub-basin	979.5	0.05										
Calamia 1	Willara Sub-basin	1002.5	0.2										
Calamia 1	Willara Sub-basin	1008	0.18										
Calamia 1	Willara Sub-basin	1027	0.44										
Calamia 1	Willara Sub-basin	1175.5	0.15										
Calamia 1	Willara Sub-basin	1218	0.2										
Calamia 1	Willara Sub-basin	1224.5	0.2										
Canopus 1	Mowla Terrace	1230	0.18										
Canopus 1	Mowla Terrace	1230	0.18										
Canopus 1	Mowla Terrace	1240	0.23										
Canopus 1	Mowla Terrace	1240	0.21										
Canopus 1	Mowla Terrace	1240	0.23										
Canopus 1	Mowla Terrace	1250	0.34										
Canopus 1	Mowla Terrace	1250	0.34										
Canopus 1	Mowla Terrace	1260	0.32										
Canopus 1	Mowla Terrace	1260	0.23										
Canopus 1	Mowla Terrace	1260	0.32										
Canopus 1	Mowla Terrace	1270	0.22										
Canopus 1	Mowla Terrace	1270	0.22										
Canopus 1	Mowla Terrace	1280	0.35										
Canopus 1	Mowla Terrace	1285	0.24										
Canopus 1	Mowla Terrace	1285	0.24										
Canopus 1	Mowla Terrace	1290	0.26										
Canopus 1	Mowla Terrace	1290	0.26										
Canopus 1	Mowla Terrace	1300	0.26										
Canopus 1	Mowla Terrace	1305	0.24										
Canopus 1	Mowla Terrace	1305	0.24										
Canopus 1	Mowla Terrace	1315	0.22										
Canopus 1	Mowla Terrace	1315	0.22										
Canopus 1	Mowla Terrace	1320	0.36										
Canopus 1	Mowla Terrace	1320	0.3										
Canopus 1	Mowla Terrace	1320	0.36										
Canopus 1	Mowla Terrace	1325	0.26										
Canopus 1	Mowla Terrace	1335	0.29										
Canopus 1	Mowla Terrace	1340	0.33										
Canopus 1	Mowla Terrace	1345	0.31										
Canopus 1	Mowla Terrace	1350	0.4										
Canopus 1	Mowla Terrace	1360	0.41										
Canopus 1	Mowla Terrace	1360	0.33										
Canopus 1	Mowla Terrace	1370	0.4										
Canopus 1	Mowla Terrace	1380	0.4										
Canopus 1	Mowla Terrace	1380	0.34										
Canopus 1	Mowla Terrace	1380	0.4										
Canopus 1	Mowla Terrace	1390	0.3										
Canopus 1	Mowla Terrace	1400	0.29										
Canopus 1	Mowla Terrace	1400	0.32										
Canopus 1	Mowla Terrace	1410	0.4										
Canopus 1	Mowla Terrace	1420	0.42										
Canopus 1	Mowla Terrace	1420	0.36										
Canopus 1	Mowla Terrace	1430	0.37										
Canopus 1	Mowla Terrace	1440	0.3										
Canopus 1	Mowla Terrace	1440	0.25										
Canopus 1	Mowla Terrace	1450	0.27										
Canopus 1	Mowla Terrace	1460	0.3										
Canopus 1	Mowla Terrace	1460	0.34										
Canopus 1	Mowla Terrace	1470	0.32										
Canopus 1	Mowla Terrace	1475	0.31										
Canopus 1	Mowla Terrace	1480	0.28										
Canopus 1	Mowla Terrace	1485	0.29										
Canopus 1	Mowla Terrace	1490	0.31										
Canopus 1	Mowla Terrace	1500	0.23										
Canopus 1	Mowla Terrace	1510	0.27										
Canopus 1	Mowla Terrace	1520	0.29										
Canopus 1	Mowla Terrace	1520	0.28										
Canopus 1	Mowla Terrace	1530	0.28										
Canopus 1	Mowla Terrace	1540	0.3										
Canopus 1	Mowla Terrace	1540	0.32										
Canopus 1	Mowla Terrace	1550	0.35										
Canopus 1	Mowla Terrace	1560	0.32										
Canopus 1	Mowla Terrace	1560	0.33										

Canopus 1	Mowla Terrace	1570	0.43										
Canopus 1	Mowla Terrace	1580	0.32										
Canopus 1	Mowla Terrace	1590	0.4										
Canopus 1	Mowla Terrace	1590	0.38										
Canopus 1	Mowla Terrace	1600	0.34										
Canopus 1	Mowla Terrace	1610	0.36										
Canopus 1	Mowla Terrace	1610	0.43										
Canopus 1	Mowla Terrace	1620	0.39										
Canopus 1	Mowla Terrace	1650	0.81	420	0.57	0.77	0.55	1.34		0.43	0.11	95.06	67.9
Canopus 1	Mowla Terrace	1670	1.16	425	0.89	1.01	0.64	1.9		0.47	0.16	87.07	55.17
Canopus 1	Mowla Terrace	1690	0.75	434	0.34	0.37	0.62	0.71		0.48	0.06	49.33	82.67
Canopus 1	Mowla Terrace	1695	1.4	430	0.6	1.09	0.29	1.69		0.36	0.14	77.86	20.71
Canopus 1	Mowla Terrace	1710	0.36										
Canopus 1	Mowla Terrace	1730	0.4										
Carina 1	Broome Platform	1560	0.36										
Carina 1	Broome Platform	1580	0.32										
Carina 1	Broome Platform	1600	0.5	419	0.49	0.71	0.73	1.2		0.41	0.1	142	146
Carina 1	Broome Platform	1620?	0.18										
Carina 1	Broome Platform	1640?	0.35										
Contention Heights 1	Ryan Shelf	1508.76	0.26										
Contention Heights 1	Ryan Shelf	1530.1	0.19										
Crystal Creek 1	Mowla Terrace	1818	0.19										
Crystal Creek 1	Mowla Terrace	1890	0.53	445	0.21	1.12	0.1	1.33		0.16	0.11	211.3	18.87
Crystal Creek 1	Mowla Terrace	1923.2	0.36										
Crystal Creek 1	Mowla Terrace	1940	0.61										
Crystal Creek 1	Mowla Terrace	1983	0.62	445	0.34	1.2	0.23	1.54		0.22	0.13	193.5	37.1
Crystal Creek 1	Mowla Terrace	2082.7	0.33										
Crystal Creek 1	Mowla Terrace	2117	0.17										
Crystal Creek 1	Mowla Terrace	2166.5	1.08	432	0.51	1.34	0.3	1.85		0.28	0.15	124.1	27.78
Crystal Creek 1	Mowla Terrace	2181	3.37	453	1.51	2.61	0.05	4.12		0.37	0.34	77.45	1.484
Crystal Creek 1	Mowla Terrace	2202.5	0.58	418	0.24	0.52	0.05	0.76		0.32	0.06	89.66	8.621
Crystal Creek 1	Mowla Terrace	2230.5	0.69	417	0.29	0.46	0.23	0.75		0.39	0.06	66.67	33.33
Crystal Creek 1	Mowla Terrace	2246.5	0.94	429	0.34	0.55	0.26	0.89		0.38	0.07	58.51	27.66
Cudalgarra 2	Willara Sub-basin	1413.53					0						
Cudalgarra 2	Willara Sub-basin	1462.16					0						
Cudalgarra 2	Willara Sub-basin	1469.7		301	0.02		1.39	0.02					
Cudalgarra 2	Willara Sub-basin	1471.33					0						
Cudalgarra 2	Willara Sub-basin	1477.55					0						
Cudalgarra 2	Willara Sub-basin	1480.7		249	0.04		1.97	0.04					
Darriwell 1	Willara Sub-basin	1575	0.16										
Darriwell 1	Willara Sub-basin	1575	0.19										
Darriwell 1	Willara Sub-basin	1576.5											
Darriwell 1	Willara Sub-basin	1588.5	0.13										
Dodonea 1	Barbwire Terrace	1537.8	3.6	441	1.11	23.56	0.4	24.61		0.04	2.05	652.8	11.11
Dodonea 1	Barbwire Terrace	1538.28	1.7	442	0.75	8.34	1.07	9.09		0.08	0.75	490.6	62.94
Dodonea 1	Barbwire Terrace	1538.43	2.2	438	0.8	13.3	1.49	14.1		0.06	1.18	604.5	67.73
Dodonea 1	Barbwire Terrace	1539.67	1.8	442	0.94	10.3	1.23	11.24		0.08	0.93	572.2	68.33
Dodonea 1	Barbwire Terrace	1539.98	2.1	441	0.81	12.8	1.49	13.61		0.06	1.13	609.5	70.95
Dodonea 1	Barbwire Terrace	1540.1	1.05	440	1.25	28.3	1.24	29.55		0.04	2.45	2695	118.1
Dodonea 1	Barbwire Terrace	1540.1	4.05	440	1.25	28.32		29.57		0.04		699.3	
Dodonea 1	Barbwire Terrace	1541.59	0.6	443	0.18	1.79	1.3	1.97		0.09	0.16	298.3	216.7
Dodonea 1	Barbwire Terrace	1541.95	0.83										
Dodonea 1	Barbwire Terrace	1542.31	0.87	444	0.26	2.64	0.86	2.9		0.09	0.24	303.4	98.85
Dodonea 1	Barbwire Terrace	1542.31	0.67										
Dodonea 1	Barbwire Terrace	1542.48	1.05	442	0.35	2.98	0.88	3.33		0.11	0.28	283.8	83.81
Dodonea 1	Barbwire Terrace	1542.95	0.83	443	0.24	2.22	1	2.46		0.1	0.2	267.5	120.5
Dodonea 1	Barbwire Terrace	1546.24	1.4					0					
Dodonea 1	Barbwire Terrace	1546.77	1.5					0					
Dodonea 1	Barbwire Terrace	1548.24	1.4	444	0.59	6.83	1.28	7.42		0.08	0.62	487.9	91.43
Dodonea 1	Barbwire Terrace	1548.77	1.5	443	0.62	7.07	1.82	7.69		0.08	0.64	471.3	121.3
Dodonea 1	Barbwire Terrace	1548.99	0.74	441	0.64	2.06	1.96	2.7		0.24	0.22	278.4	264.9
Edgar Range 1	Broome Platform	947.9	0.17										
Edgar Range 1	Broome Platform	948.6	0.15										
Edgar Range 1	Broome Platform	948.8	0.17										
Edgar Range 1	Broome Platform	949.1	0.19										
Edgar Range 1	Broome Platform	949.5	0.29										
Edgar Range 1	Broome Platform	950.4	0.29										
Edgar Range 1	Broome Platform	951	0.2										
Edgar Range 1	Broome Platform	978.4	0.24										
Edgar Range 1	Broome Platform	1012	0.25										
Edgar Range 1	Broome Platform	1039	0.19										
Edgar Range 1	Broome Platform	1042.7	0.29										
Edgar Range 1	Broome Platform	1043.6	0.36										
Edgar Range 1	Broome Platform	1044.2	0.26										
Edgar Range 1	Broome Platform	1044.9	0.4										
Edgar Range 1	Broome Platform	1045.2	0.42										
Edgar Range 1	Broome Platform	1048.5	0.26										
Edgar Range 1	Broome Platform	1048.5	0.32										
Edgar Range 1	Broome Platform	1080.5	0.23										
Edgar Range 1	Broome Platform	1136	0.27										
Edgar Range 1	Broome Platform	1144.5	0.33										
Edgar Range 1	Broome Platform	1188.7	0.16										
Edgar Range 1	Broome Platform	1188.9	0.12										
Edgar Range 1	Broome Platform	1189.6	0.16										
Edgar Range 1	Broome Platform	1190.5	1.1		0.1	0.2		0.3		0.33		18.18	
Edgar Range 1	Broome Platform	1191.2	0.68		0.6	0.9		1.5		0.4		132.4	
Edgar Range 1	Broome Platform	1214.6	0.34										
Edgar Range 1	Broome Platform	1264.9						0					
Edgar Range 1	Broome Platform	1271	1.68	435	1.19	2.2	0.68	3.39		0.35		131	40.48
Edgar Range 1	Broome Platform	1306.1	1.17	435	0.93	1.15	0.83	2.08		0.45		98.29	70.94
Edgar Range 1	Broome Platform	1313.6											
Edgar Range 1	Broome Platform	1348.8	0.65	425	0.49	0.49	0.82	0.98		0.5		75.38	126.2
Edgar Range 1	Broome Platform	1350	0.16										

Frankenstein 1	Anketell Shelf	2267	0.07										
Frankenstein 1	Anketell Shelf	2285	0.18										
Frankenstein 1	Anketell Shelf	2303	0.25										
Frankenstein 1	Anketell Shelf	2321	0.32										
Frankenstein 1	Anketell Shelf	2327.14	0.3										
Frankenstein 1	Anketell Shelf	2339	0.25										
Frankenstein 1	Anketell Shelf	2347.09	0.37										
Frankenstein 1	Anketell Shelf	2357	0.25										
Frankenstein 1	Anketell Shelf	2375	0.27										
Great Sandy 1	Willara Sub-basin	1535	0.16										
Great Sandy 1	Willara Sub-basin	1545	0.17										
Great Sandy 1	Willara Sub-basin	1555	0.19										
Great Sandy 1	Willara Sub-basin	1565	0.21										
Great Sandy 1	Willara Sub-basin	1575	0.18										
Great Sandy 1	Willara Sub-basin	1585	0.2										
Great Sandy 1	Willara Sub-basin	1595	0.19										
Great Sandy 1	Willara Sub-basin	1600	0.23										
Great Sandy 1	Willara Sub-basin	1605	0.24										
Great Sandy 1	Willara Sub-basin	1608	0.23										
Great Sandy 1	Willara Sub-basin	1608	0.23										
Great Sandy 1	Willara Sub-basin	1615	0.18										
Great Sandy 1	Willara Sub-basin	1615	0.19										
Great Sandy 1	Willara Sub-basin	1623	0.18										
Great Sandy 1	Willara Sub-basin	1623	0.18										
Great Sandy 1	Willara Sub-basin	1625	0.2										
Great Sandy 1	Willara Sub-basin	1635	0.23										
Great Sandy 1	Willara Sub-basin	1635	0.3										
Great Sandy 1	Willara Sub-basin	1640	0.23										
Great Sandy 1	Willara Sub-basin	1640	0.23										
Great Sandy 1	Willara Sub-basin	1645	0.25										
Great Sandy 1	Willara Sub-basin	1645	0.21										
Great Sandy 1	Willara Sub-basin	1653	0.25										
Great Sandy 1	Willara Sub-basin	1653	0.25										
Great Sandy 1	Willara Sub-basin	1655	0.2										
Great Sandy 1	Willara Sub-basin	1665	0.18										
Great Sandy 1	Willara Sub-basin	1668	0.18										
Great Sandy 1	Willara Sub-basin	1668	0.18										
Hedonia 1	Broome Platform	922			0.48	0.61		1.09		0.44			
Hedonia 1	Broome Platform	930	0.64	439	0.26	0.96	0.27	1.22		0.21	0.1	150	42.19
Hedonia 1	Broome Platform	935.4	0.6	430	0.3	0.69	0.33	0.99		0.3		115	55
Hedonia 1	Broome Platform	936.9			0.58	0.61		1.19		0.49			
Hedonia 1	Broome Platform	945	1.19	430	0.84	2.09	0.42	2.93		0.29		175.6	35.29
Hedonia 1	Broome Platform	960	2.07	435	1.72	4.28	0.41	6		0.29		206.8	19.81
Hedonia 1	Broome Platform	975	1.48	427	1.3	2.69	0.62	3.99		0.33		181.8	41.89
Hedonia 1	Broome Platform	976											
Hedonia 1	Broome Platform	990	1.19	435	0.91	1.93	0.26	2.84		0.32		162.2	21.85
Hedonia 1	Broome Platform	1005	1.19	427	0.95	1.69	0.37	2.64		0.36		142	31.09
Hedonia 1	Broome Platform	1020	0.84	430	0.49	0.95	0.3	1.44		0.34		113.1	35.71
Hedonia 1	Broome Platform	1020	0.99										
Hedonia 1	Broome Platform	1022.5	1	432	0.84	1.14	0.14	1.98		0.42		114	14
Hedonia 1	Broome Platform	1022.5	0.84										
Hedonia 1	Broome Platform	1046.7	0.99	428	0.58	0.86	0.62	1.44		0.4		86.87	62.63
Hilltop 1	Broome Platform	1052.5	2.1	433	1.68	4.74	0.25	6.42		0.26	0.53	225.7	11.9
Hilltop 1	Broome Platform	1079.1	1.45	438	1.1	2.37	0.31	3.47		0.32	0.29	163.4	21.38
Hilltop 1	Broome Platform	1098	2.5	432	2.29	4.51	0.34	6.8		0.34	0.56	180.4	13.6
Hilltop 1	Broome Platform	1128.1	1.3	438	0.92	1.42	0.28	2.34		0.39	0.19	109.2	21.54
Hilltop 1	Broome Platform	1170	0.8	447	0.42	0.54	0.31	0.96		0.44	0.08	67.5	38.75
Kidson 1	Kidson Sub-basin	4284.4	2.1		8	5.8	0	13.8		0.58		276.2	
Kidson 1	Kidson Sub-basin	4284.4			0.6	3.4		4					
Kidson 1	Kidson Sub-basin	4297.7	2.4		7.2	6.7	0	13.9		0.52		279.2	
Kidson 1	Kidson Sub-basin	4312.9	1.5		7.1	6.5	0	13.6		0.52		433.3	
Kidson 1	Kidson Sub-basin	4328.2	3		7.6	8.6	0	16.2		0.47		286.7	
Kidson 1	Kidson Sub-basin	4343.4	3.5		9.2	9.5	0	18.7		0.49		271.4	
Kidson 1	Kidson Sub-basin	4358.6	3.4		9.8	8.8	0	18.6		0.53		258.8	
Kidson 1	Kidson Sub-basin	4358.6			0.9	5.7		6.6					
Kidson 1	Kidson Sub-basin	4364.4	0.18										
Kidson 1	Kidson Sub-basin	4364.43	0.07										
Kidson 1	Kidson Sub-basin	4365	0.32										
Kidson 1	Kidson Sub-basin	4365	0.24										
Kidson 1	Kidson Sub-basin	4365.7	0.27										
Kidson 1	Kidson Sub-basin	4366	0.23										
Kidson 1	Kidson Sub-basin	4366.3	0.24										
Kidson 1	Kidson Sub-basin	4366.9	0.2										
Kidson 1	Kidson Sub-basin	4367.5	0.29										
Kidson 1	Kidson Sub-basin	4367.5	0.2										
Kidson 1	Kidson Sub-basin	4367.8	0.24										
Kidson 1	Kidson Sub-basin	4368.1	0.2										
Kidson 1	Kidson Sub-basin	4368.2	0.25										
Kidson 1	Kidson Sub-basin	4368.7	0.27										
Kidson 1	Kidson Sub-basin	4368.75					0						
Kidson 1	Kidson Sub-basin	4373.9	0.2										
Kidson 1	Kidson Sub-basin	4389.1	3.8		10.5	10	0	20.5		0.51		263.2	
Kidson 1	Kidson Sub-basin	4404.4	3		9.2	8.4	0	17.6		0.52		280	
Kunzea 1	Broome Platform	354.42	1.34	436	0.07	10.28		10.35		0.01		767.2	
Kunzea 1	Broome Platform	373.9	1.98	431	0.28	13.5	0.53	13.78		0.02		681.8	26.77
Kunzea 1	Broome Platform	379.95	4.8	434	0.65	41.45		42.1		0.02		863.5	
Kunzea 1	Broome Platform	390.18	1.84	437	0.16	12.5		12.66		0.01		679.3	
Kunzea 1	Broome Platform	390.5	1.69	427	0.19	10.48	0.67	10.67		0.018		620.1	39.64
Kunzea 1	Broome Platform	409.9	0.15										
Kunzea 1	Broome Platform	422.9	0.11										
Kunzea 1	Broome Platform	449.8	0.15										
Leo 1	Willara Sub-basin	1655	0.15										
Leo 1	Willara Sub-basin	1670	0.16										

Leo 1	Willara Sub-basin	1685	0.23										
Leo 1	Willara Sub-basin	1700	0.2										
Leo 1	Willara Sub-basin	1715	0.14										
Leo 1	Willara Sub-basin	1730	0.1										
Leo 1	Willara Sub-basin	1745	0.12										
Leo 1	Willara Sub-basin	1760	0.15										
Leo 1	Willara Sub-basin	1775	0.12										
Leo 1	Willara Sub-basin	1790	0.15										
Leo 1	Willara Sub-basin	1805	0.14										
Leo 1	Willara Sub-basin	1820	0.17										
Leo 1	Willara Sub-basin	1835	0.19										
Leo 1	Willara Sub-basin	1850	0.18										
Leo 1	Willara Sub-basin	1865	0.22										
Leo 1	Willara Sub-basin	1880	0.18										
Leo 1	Willara Sub-basin	1895	0.17										
Leo 1	Willara Sub-basin	1910	0.21										
Leo 1	Willara Sub-basin	1925	0.16										
Leo 1	Willara Sub-basin	1940	0.23										
Matches Spring 1	Mowla Terrace	2280	0.4										
Matches Spring 1	Mowla Terrace	2293.7	0.24										
Matches Spring 1	Mowla Terrace	2321.1	0.21										
Matches Spring 1	Mowla Terrace	2340.9	0.3										
Matches Spring 1	Mowla Terrace	2348.5	0.32										
Matches Spring 1	Mowla Terrace	2366.8	0.26										
Matches Spring 1	Mowla Terrace	2383.6	0.26										
Matches Spring 1	Mowla Terrace	2398.8	0.53	442	0.3	1.44	0.01	1.74		0.17		271.7	1.887
Matches Spring 1	Mowla Terrace	2404.9	1.52	443	2.3	9.56	0.49	11.86		0.19		628.9	32.24
Matches Spring 1	Mowla Terrace	2407.5			0.45	0.62		1.07		0.42			
Matches Spring 1	Mowla Terrace	2408	1.77	443	1.78	9.93	0.85	11.71		0.15		561	48.02
Matches Spring 1	Mowla Terrace	2408.8	3.7							1.3			
Matches Spring 1	Mowla Terrace	2409			0.52	0.64		1.16		0.45			
Matches Spring 1	Mowla Terrace	2409.9			0.45	0.62		1.07		0.42			
Matches Spring 1	Mowla Terrace	2430	1.88	443	1.18	5.1	0.64	6.28		0.19		271.3	34.04
Matches Spring 1	Mowla Terrace	2448.7	0.3										
Matches Spring 1	Mowla Terrace	2609.1	0.8										
Matches Spring 1	Mowla Terrace	2730.9											
Matches Spring 1	Mowla Terrace	2732.6	1.38	441	1.09	2.35	0.68	3.44		0.32		170.3	49.28
Matches Spring 1	Mowla Terrace	2733.9			0.21	0.47		0.68		0.31			
Matches Spring 1	Mowla Terrace	2750	0.16										
Matches Spring 1	Mowla Terrace	2753	0.14										
Matches Spring 1	Mowla Terrace	2754.3	0.3										
Matches Spring 1	Mowla Terrace	2754.8	0.62	430	0.78	0.91	0.4	1.69		0.46		146.8	64.52
Matches Spring 1	Mowla Terrace	2761.5	1.2							0.3			
Matches Spring 1	Mowla Terrace	2764.6	1.48	439	0.96	2.43	0.6	3.39		0.28		164.2	40.54
Matches Spring 1	Mowla Terrace	2769.1	2.11	441	1.3	3.21	0.83	4.51		0.29		152.1	39.34
Matches Spring 1	Mowla Terrace	2801.2	0.82	445	0.56	0.93	0.72	1.49		0.38		113.4	87.8
Matches Spring 1	Mowla Terrace	2811.8	0.34										
Matches Spring 1	Mowla Terrace	2833.8	0.6							0.1			
McLarty 1	Broome Platform	1685.5	1.9		7.4	3.1		10.5		0.7		163.2	
McLarty 1	Broome Platform	1688.59	1.22	391	11.91	2.69	1.91	14.6		0.82		220.5	156.6
McLarty 1	Broome Platform	1694.7	1.9		6.3	2.7		9		0.7		142.1	
McLarty 1	Broome Platform	1697.74	1.14	393	11.01	2.54	1.85	13.55		0.81		222.8	162.3
McLarty 1	Broome Platform	1703.8	2		6.6	3.4		10		0.66		170	
McLarty 1	Broome Platform	1706.88	0.93	419	10.14	2.99	1.84	13.13		0.77		321.5	197.8
McLarty 1	Broome Platform	1713	1.1		5	2.3		7.3		0.68		209.1	
McLarty 1	Broome Platform	1716.02	1.02	394	11.56	2.74	1.88	14.3		0.81		268.6	184.3
McLarty 1	Broome Platform	1722.1	1.6		5.8	2.5		8.3		0.7		156.3	
McLarty 1	Broome Platform	1725.17	1.13	408	13.01	3.09	1.86	16.1		0.81		273.5	164.6
McLarty 1	Broome Platform	1731.3	1.8		6.1	2.8		8.9		0.69		155.6	
McLarty 1	Broome Platform	1734.31	1.05	396	13.47	2.8	1.81	16.27		0.83		266.7	172.4
McLarty 1	Broome Platform	1740.4	2		6.3	2.9		9.2		0.68		145	
McLarty 1	Broome Platform	1743.46	1.03	400	11.38	2.48	1.75	13.86		0.82		240.8	169.9
McLarty 1	Broome Platform	1749.5	1.3		6.6	3.2		9.8		0.67		246.2	
McLarty 1	Broome Platform	1752.6	1.1	398	9.1	2.11	1.57	11.21		0.81		191.8	142.7
McLarty 1	Broome Platform	1757.88	0.1										
McLarty 1	Broome Platform	1757.93	0.1										
McLarty 1	Broome Platform	1758	0.1										
McLarty 1	Broome Platform	1758.09	0.31										
McLarty 1	Broome Platform	1758.1	0.1										
McLarty 1	Broome Platform	1758.2	0.2										
McLarty 1	Broome Platform	1758.4	0.2										
McLarty 1	Broome Platform	1758.6	0.1										
McLarty 1	Broome Platform	1758.7	0.38										
McLarty 1	Broome Platform	1758.8	0.2										
McLarty 1	Broome Platform	1759	0.11										
McLarty 1	Broome Platform	1759	0.1										
McLarty 1	Broome Platform	1759.1	0.2										
McLarty 1	Broome Platform	1759.3	0.2										
McLarty 1	Broome Platform	1759.5	0.1										
McLarty 1	Broome Platform	1759.6	0.22										
McLarty 1	Broome Platform	1759.6	0.2										
McLarty 1	Broome Platform	1759.8	0.2										
McLarty 1	Broome Platform	1759.9	0.2										
McLarty 1	Broome Platform	1760.1	0.2										
McLarty 1	Broome Platform	1760.2	0.1										
McLarty 1	Broome Platform	1760.4	0.2										
McLarty 1	Broome Platform	1760.5	0.3										
McLarty 1	Broome Platform	1761.74	1.1	388	11.63	2.66	1.04	14.29		0.81		241.8	94.55
McLarty 1	Broome Platform	1766.3	1.9		6.9	3.2		10.1		0.68		168.4	
McLarty 1	Broome Platform	1770.89	0.78	417	9.01	2.28	1.54	11.29		0.8		292.3	197.4
McLarty 1	Broome Platform	1780.03	0.6	424	9.56	2.76	1.34	12.32		0.78		460	223.3
McLarty 1	Broome Platform	1789.18	0.56	420	5.65	1.84	1.73	7.49		0.75		328.6	308.9
McLarty 1	Broome Platform	1798.32	0.53	395	4.98	1.39	1.77	6.37		0.78		262.3	334

McLarty 1	Broome Platform	1807.46	0.81	398	10.93	2.39	1.52	13.32		0.82	295.1	187.7
McLarty 1	Broome Platform	1816.61	1.14	427	13.93	3.59	1.64	17.52		0.8	314.9	143.9
McLarty 1	Broome Platform	1823.3	2.6		5.8	3.1		8.9		0.65	119.2	
McLarty 1	Broome Platform	1825.75	0.92	423	10.82	2.74	1.55	13.56		0.8	297.8	168.5
McLarty 1	Broome Platform	1834.9	0.93	429	10.27	3.37	1.43	13.64		0.75	362.4	153.8
McLarty 1	Broome Platform	1844.04	0.96	429	9.55	3.17	1.72	12.72		0.75	330.2	179.2
McLarty 1	Broome Platform	1853.18	0.83	434	7.1	2.29	0.88	9.39		0.76	275.9	106
McLarty 1	Broome Platform	1862.33	0.69	426	7.93	2.57	1.23	10.5		0.76	372.5	178.3
McLarty 1	Broome Platform	1871.47	1.05	427	9.65	2.49	1.46	12.14		0.79	237.1	139
McLarty 1	Broome Platform	1880.62	1.15	422	11.6	3.21	1.69	14.81		0.78	279.1	147
McLarty 1	Broome Platform	1883.7	2.4		0.1	0.1		0.2		0.5	4.167	
McLarty 1	Broome Platform	1891.28	2.2	427	15.98	5.7	1.32	21.68		0.74	259.1	60
McLarty 1	Broome Platform	1892.8	3.6		0.4	0.2		0.6		0.67	5.556	
McLarty 1	Broome Platform	1892.9	0.2									
McLarty 1	Broome Platform	1893	0.16									
McLarty 1	Broome Platform	1893	0.3									
McLarty 1	Broome Platform	1893.1	0.22									
McLarty 1	Broome Platform	1893.1	0.2									
McLarty 1	Broome Platform	1893.5	0.2									
McLarty 1	Broome Platform	1893.6	0.2									
McLarty 1	Broome Platform	1893.9	0.2									
McLarty 1	Broome Platform	1894	0.3									
McLarty 1	Broome Platform	1895.9	1.75	384	21.19	3.04	0.75	24.23		0.87	173.7	42.86
McLarty 1	Broome Platform	1897.38	1.82	384	15.01	3.88	0.58	18.89		0.79	213.2	31.87
McLarty 1	Broome Platform	1900.43	2.05	398	17.33	4.9	1.1	22.23		0.78	239	53.66
McLarty 1	Broome Platform	1901.95	2.4	429	18.21	4.77	1.52	22.98		0.79	198.8	63.33
McLarty 1	Broome Platform	1901.95	1.91	429	18.21	4.77	1.52	22.98		0.79	249.7	79.58
McLarty 1	Broome Platform	1903.48	2.5	430	20.46	6.16	1.54	26.62		0.77	246.4	61.6
McLarty 1	Broome Platform	1903.48	2.21	430	20.46	6.16	1.54	26.62		0.77	278.7	69.68
McLarty 1	Broome Platform	1905	1.66	422	13.51	3.51	1.6	17.02		0.79	211.4	96.39
McLarty 1	Broome Platform	1905	2.3		6	3.2		9.2		0.65	139.1	
McLarty 1	Broome Platform	1905	1.66	422	13.5	3.51	1.6	17.01		0.79	211.4	96.39
McLarty 1	Broome Platform	1914.14	1.89	422	14.72	3.66	1.63	18.38		0.8	193.7	86.24
McLarty 1	Broome Platform	1917.2	1.87	428	16.91	3.91	1.8	20.82		0.81	209.1	96.26
McLarty 1	Broome Platform	1923.29	1.85	427	14.86	3.6	1.64	18.46		0.8	194.6	88.65
McLarty 1	Broome Platform	1932.43	1.95	430	15.03	3.95	1.63	18.98		0.79	202.6	83.59
McLarty 1	Broome Platform	1941.58	1.41	430	11.93	3.47	1.49	15.4		0.77	246.1	105.7
McLarty 1	Broome Platform	1941.6	4.7		8.8	4.4		13.2		0.67	93.62	
McLarty 1	Broome Platform	1950.72	1.86	429	13.45	3.9	1.39	17.35		0.78	209.7	74.73
McLarty 1	Broome Platform	1959.86	1.56	416	12.94	3.34	1.48	16.28		0.79	214.1	94.87
McLarty 1	Broome Platform	1961.4	1.22	428	12.95	3.1	2.29	16.05		0.81	254.1	187.7
McLarty 1	Broome Platform	1961.4	1.4		7.3	3.1		10.4		0.7	221.4	
McLarty 1	Broome Platform	1969.01	2.2	428	3.06	4.48	1.69	7.54		0.41	203.6	76.82
McLarty 1	Broome Platform	1973.6	1.9	429	16.8	3.55	1.84	20.35		0.83	186.8	96.84
McLarty 1	Broome Platform	1978.15	2.2	419	17.08	4.37	1.62	21.45		0.8	198.6	73.64
McLarty 1	Broome Platform	1978.2	1.7		6.9	2.9		9.8		0.7	170.6	
McLarty 1	Broome Platform	1987.3	2.15	428	14.15	3.54	1.42	17.69		0.8	164.7	66.05
McLarty 1	Broome Platform	1996	0.22									
McLarty 1	Broome Platform	1996.4	2		2.7	3.3		6		0.45	165	
McLarty 1	Broome Platform	1996.44	3.1	429	19.12	4.64	1.5	23.76		0.8	149.7	48.39
McLarty 1	Broome Platform	1998	2.71	428	19.14	3.92	1.97	23.06		0.83	144.6	72.69
McLarty 1	Broome Platform	2002.2	3		1.4	1.4		2.8		0.5	46.67	
McLarty 1	Broome Platform	2002.4	1.8		1.6	1.3		2.9		0.55	72.22	
McLarty 1	Broome Platform	2002.5	1.6		2.6	3.3		5.9		0.44	206.3	
McLarty 1	Broome Platform	2002.7	2		2.8	3.5		6.3		0.44	175	
McLarty 1	Broome Platform	2002.8	3.1		2.8	3.2		6		0.47	103.2	
McLarty 1	Broome Platform	2002.9	2.48	433	3.43	2.65	0.73	6.08		0.56	106.9	29.44
McLarty 1	Broome Platform	2003	3.1		2.3	3		5.3		0.43	96.77	
McLarty 1	Broome Platform	2003.1	3		2.1	2.1		4.2		0.5	70	
McLarty 1	Broome Platform	2003.15	3.6	441	3.06	3.99	0.53	7.05		0.43	110.8	14.72
McLarty 1	Broome Platform	2003.3	2.5		2.2	3		5.2		0.42	120	
McLarty 1	Broome Platform	2003.5	2.2		2.5	2.9		5.4		0.46	131.8	
McLarty 1	Broome Platform	2003.6	2.3		2.8	3.7		6.5		0.43	160.9	
McLarty 1	Broome Platform	2003.8	2.3		3.1	4.6		7.7		0.4	200	
McLarty 1	Broome Platform	2003.9	2.6		1.8	2.1		3.9		0.46	80.77	
McLarty 1	Broome Platform	2004.1	3		6.6	2.6		9.2		0.72	86.67	
McLarty 1	Broome Platform	2005.58	2.35	432	17.06	4.06	1.21	21.12		0.81	172.8	51.49
McLarty 1	Broome Platform	2005.6	2.9		1.9	2.4		4.3		0.44	82.76	
McLarty 1	Broome Platform	2014.73	1.14	425	12.22	2.64	1.8	14.86		0.82	231.6	157.9
McLarty 1	Broome Platform	2017.7	1.7		6.5	2.7		9.2		0.71	158.8	
McLarty 1	Broome Platform	2023.87	0.93	424	12.4	2.29	1.83	14.69		0.84	246.2	196.8
McLarty 1	Broome Platform	2033.02	0.83	398	5.44	1.42	1.72	6.86		0.79	171.1	207.2
McLarty 1	Broome Platform	2036.1	4		9.9	4.5		14.4		0.69	112.5	
McLarty 1	Broome Platform	2042.16	0.78	425	7.43	1.93	1.6	9.36		0.79	247.4	205.1
McLarty 1	Broome Platform	2051.3	1.46	417	11.91	3.11	1.82	15.02		0.79	213	124.7
McLarty 1	Broome Platform	2060	0.25									
Munro 1	Willara Sub-basin	1606.3	0.24									
Munro 1	Willara Sub-basin	1612.39	0.26									
Munro 1	Willara Sub-basin	1618.5	0.18									
Munro 1	Willara Sub-basin	1621.54	0.28									
Munro 1	Willara Sub-basin	1630.68	0.21									
Munro 1	Willara Sub-basin	1636.8	0.15									
Munro 1	Willara Sub-basin	1639.82	0.2									
Munro 1	Willara Sub-basin	1648.97	0.23									
Munro 1	Willara Sub-basin	1652	0.7	345	0.01	0.04	0.7	0.05		0.2	5.714	100
Munro 1	Willara Sub-basin	1652	0.31									
Munro 1	Willara Sub-basin	1658.11	0.24									
Munro 1	Willara Sub-basin	1667.26	0.21									
Munro 1	Willara Sub-basin	1676.4	0.24									
Munro 1	Willara Sub-basin	1685.54	0.34									
Munro 1	Willara Sub-basin	1694.69	0.23									
Munro 1	Willara Sub-basin	1703.83	0.24									
Munro 1	Willara Sub-basin	1710	0.17									

Munro 1	Willara Sub-basin	1712.98	0.35										
Munro 1	Willara Sub-basin	1722.1	0.16										
Munro 1	Willara Sub-basin	1722.12	0.3										
Munro 1	Willara Sub-basin	1731.26	0.23										
Munro 1	Willara Sub-basin	1740.41	0.23										
Munro 1	Willara Sub-basin	1744.9	0.3										
Munro 1	Willara Sub-basin	1746.5	0.17										
Munro 1	Willara Sub-basin	1749.55	0.25										
Munro 1	Willara Sub-basin	1758.7	0.22										
Munro 1	Willara Sub-basin	1758.7	0.15										
Munro 1	Willara Sub-basin	1758.7	0.22										
Munro 1	Willara Sub-basin	1767.84	0.25										
Munro 1	Willara Sub-basin	1776.98	0.23										
Munro 1	Willara Sub-basin	1786.13	0.24										
Munro 1	Willara Sub-basin	1795.27	0.25										
Musca 1	Broome Platform	1510	0.17										
Musca 1	Broome Platform	1510	0.1										
Musca 1	Broome Platform	1520	0.24										
Musca 1	Broome Platform	1520	0.1										
Musca 1	Broome Platform	1520	0.14										
Musca 1	Broome Platform	1530	0.29										
Musca 1	Broome Platform	1530	0.14										
Musca 1	Broome Platform	1530	0.24										
Musca 1	Broome Platform	1535	0.24										
Musca 1	Broome Platform	1535	0.27										
Parda 1	Broome Platform	1277.1	0.18										
Parda 1	Broome Platform	1286.3	0.15										
Parda 1	Broome Platform	1292.3	0.22										
Parda 1	Broome Platform	1307.6	0.29										
Parda 1	Broome Platform	1310.7	0.18										
Parda 1	Broome Platform	1314.9	0.17										
Parda 1	Broome Platform	1315	0.27										
Parda 1	Broome Platform	1315.5	0.19										
Parda 1	Broome Platform	1316	0.3										
Parda 1	Broome Platform	1316.7	0.28										
Parda 1	Broome Platform	1316.8	0.22										
Parda 1	Broome Platform	1317.3	0.3										
Parda 1	Broome Platform	1322.8	0.24										
Parda 1	Broome Platform	1332	0.17										
Parda 1	Broome Platform	1338.1	0.26										
Parda 1	Broome Platform	1365.5	0.3										
Parda 1	Broome Platform	1380.7	0.23										
Parda 1	Broome Platform	1396	0.23										
Parda 1	Broome Platform	1411.2	0.28										
Parda 1	Broome Platform	1426.6	0.29										
Parda 1	Broome Platform	1441.7	0.25										
Parda 1	Broome Platform	1456.9	0.25										
Parda 1	Broome Platform	1472.2	0.25										
Parda 1	Broome Platform	1486.5	0.27										
Parda 1	Broome Platform	1486.5	0.3										
Parda 1	Broome Platform	1487.1	0.22										
Parda 1	Broome Platform	1487.7	0.28										
Parda 1	Broome Platform	1488.3	0.24										
Parda 1	Broome Platform	1488.9	0.06										
Patience 2	Kidson Sub-basin	2934	0.61	426	0.44	3.01	6.08	3.45		0.128		493.4	996.7
Patience 2	Kidson Sub-basin	2943	0.31										
Patience 2	Kidson Sub-basin	2958	0.26										
Patience 2	Kidson Sub-basin	2970	0.27										
Patience 2	Kidson Sub-basin	2985	0.32										
Patience 2	Kidson Sub-basin	3018	0.56	436	0.44	1.74	3.5	2.18		0.202		310.7	625
Patience 2	Kidson Sub-basin	3033	0.47										
Patience 2	Kidson Sub-basin	3057	0.37										
Patience 2	Kidson Sub-basin	3075	0.29										
Patience 2	Kidson Sub-basin	3114	0.49										
Patience 2	Kidson Sub-basin	3153	0.33										
Pegasus 1	Munro Arch	2347.5	0.2										
Pegasus 1	Munro Arch	2352.5	0.3										
Pegasus 1	Munro Arch	2357.5	0.2										
Pegasus 1	Munro Arch	2357.5	0.3										
Pegasus 1	Munro Arch	2360	0.2										
Pegasus 1	Munro Arch	2362.5	0.2										
Pegasus 1	Munro Arch	2365	0.2										
Pegasus 1	Munro Arch	2370	0.3										
Pegasus 1	Munro Arch	2375	0.3										
Pegasus 1	Munro Arch	2385	0.4										
Pegasus 1	Munro Arch	2390	0.2										
Pegasus 1	Munro Arch	2390	0.4										
Pegasus 1	Munro Arch	2392.5	0.4										
Pegasus 1	Munro Arch	2487.5	0.2										
Pegasus 1	Munro Arch	2605.5	0.3										
Percival 1	Barbwire Terrace	2038	0.19										
Percival 1	Barbwire Terrace	2038.6	0.12										
Percival 1	Barbwire Terrace	2042.25	0.66	446	0.29	0.7	0.08	0.99				106.1	12.12
Percival 1	Barbwire Terrace	2045.2	0.67	453	0.41	0.63	0.14	1.04				94.03	20.9
Percival 1	Barbwire Terrace	2049.51	1	448	0.44	0.89	0.07	1.33				89	7
Percival 1	Barbwire Terrace	2067.95	0.59	434	0.19	0.44	0.1	0.63			0.05	74.58	16.95
Percival 1	Barbwire Terrace	2147.5	0.13										
Percival 1	Barbwire Terrace	2152.5	0.25										
Percival 1	Barbwire Terrace	2165	0.31										
Percival 1	Barbwire Terrace	2172.5	0.27										
Percival 1	Barbwire Terrace	2177.5	0.16										
Percival 1	Barbwire Terrace	2180	0.21										
Pictor 1	Mowla Terrace	1070	0.18										

Pictor 1	Mowla Terrace	1160	0.31										
Pictor 1	Mowla Terrace	1250	0.22										
Pictor 1	Mowla Terrace	1340	0.21										
Pictor 1	Mowla Terrace	1355	0.2										
Pictor 1	Mowla Terrace	1370	0.2										
Pictor 1	Mowla Terrace	1385	0.2										
Pictor 1	Mowla Terrace	1400	0.32										
Pictor 1	Mowla Terrace	1430	0.83	429	0.58	0.51	0.56	1.09		0.53	0.09	61.45	67.47
Pictor 1	Mowla Terrace	1445	1.54	434	1.15	1.31	0.3	2.46		0.47	0.2	85.06	19.48
Pictor 1	Mowla Terrace	1460	0.92	435	0.52	0.54	0.24	1.06		0.49	0.09	58.7	26.09
Pictor 1	Mowla Terrace	1475	0.46										
Pictor 1	Mowla Terrace	1490	0.32										
Pictor 1	Mowla Terrace	1505	0.42										
Solanum 1	Barbwire Terrace	284.9	0.37										
Solanum 1	Barbwire Terrace	287.9	0.16										
Solanum 1	Barbwire Terrace	289.07	0.48										
Solanum 1	Barbwire Terrace	292.6	0.28										
Solanum 1	Barbwire Terrace	294.58	0.21										
Solanum 1	Barbwire Terrace	298.25	0.34										
Solanum 1	Barbwire Terrace	301.65	0.91	439	0.18	4.36	0.36	4.54		0.04		479.1	39.56
Solanum 1	Barbwire Terrace	302.8	0.42										
Solanum 1	Barbwire Terrace	303	0.44										
Solanum 1	Barbwire Terrace	303.24	0.95	440	0.21	5.14	0.45	5.35		0.04		541.1	47.37
Solanum 1	Barbwire Terrace	304.3	0.2										
Solanum 1	Barbwire Terrace	306.5	1.08	439	0.16	6.21	0.33	6.37		0.03		575	30.56
Solanum 1	Barbwire Terrace	308.2	1.31	438	0.34	7.99	0.29	8.33		0.04		609.9	22.14
Solanum 1	Barbwire Terrace	308.7	1.74	440	0.32	12.04	0.4	12.36		0.03		692	22.99
Solanum 1	Barbwire Terrace	309	2.44	438	0.48	19.31	0.32	19.79		0.02		791.4	13.11
Solanum 1	Barbwire Terrace	309.7	0.16										
Solanum 1	Barbwire Terrace	311.36	0.35										
Solanum 1	Barbwire Terrace	311.9	1.51	438	0.61	17.58	0.31	18.19		0.03		1164	20.53
Solanum 1	Barbwire Terrace	312.24	0.37										
Solanum 1	Barbwire Terrace	312.64	1.28	439	0.5	14.97	0.32	15.47		0.03		1170	25
Solanum 1	Barbwire Terrace	314.6	0.78	439	0.3	9.12	0.27	9.42		0.03		1169	34.62
Solanum 1	Barbwire Terrace	314.8	1.13	438	0.36	13.2	0.43	13.56		0.03		1168	38.05
Solanum 1	Barbwire Terrace	315.24	1.22	439	0.4	14.32	0.39	14.72		0.03		1174	31.97
Solanum 1	Barbwire Terrace	315.34	2.32	442	0.63	16.59		17.22		0.04		715.1	
Solanum 1	Barbwire Terrace	315.59	0.77	437	0.33	8.96	0.34	9.29		0.04		1164	44.16
Solanum 1	Barbwire Terrace	316.6	0.81	439	0.38	9.36	0.38	9.74		0.04		1156	46.91
Solanum 1	Barbwire Terrace	317.33	0.18										
Solanum 1	Barbwire Terrace	317.6	1	438	0.16	4.64	0.26	4.8		0.03		464	26
Solanum 1	Barbwire Terrace	318	1.55	439	0.26	7.66	0.23	7.92		0.03		494.2	14.84
Solanum 1	Barbwire Terrace	318.4	1.06	437	0.2	4.82	0.24	5.02		0.04		454.7	22.64
Solanum 1	Barbwire Terrace	319.1	1.25	436	0.23	5.96	0.13	6.19		0.04		476.8	10.4
Solanum 1	Barbwire Terrace	319.94	0.86	436	0.15	3.64	0.13	3.79		0.04		423.3	15.12
Solanum 1	Barbwire Terrace	320.42	0.55	436	0.07	1.88	0.33	1.95		0.04		341.8	60
Solanum 1	Barbwire Terrace	322.02	0.47										
Solanum 1	Barbwire Terrace	326.43	0.85	441	0.17	3.44		3.61		0.05		404.7	
Solanum 1	Barbwire Terrace	326.8	1.88	440	0.31	11.6	0.39	11.91		0.03		617	20.74
Solanum 1	Barbwire Terrace	329.8	0.25										
Solanum 1	Barbwire Terrace	346	0.16										
Solanum 1	Barbwire Terrace	346.39	0.13										
Solanum 1	Barbwire Terrace	361	0.13										
Solanum 1	Barbwire Terrace	397.63	0.26										
Solanum 1	Barbwire Terrace	401	0.18										
Solanum 1	Barbwire Terrace	406.1	0.14										
Solanum 1	Barbwire Terrace	407	0.18										
Solanum 1	Barbwire Terrace	449.1	0.12										
Solanum 1	Barbwire Terrace	471.2	0.23										
Solanum 1	Barbwire Terrace	484.05	0.74	435	3.5	1.49	0.37	4.99		0.7		201.4	50
Solanum 1	Barbwire Terrace	490.7	0.77	437	0.31	1.81	0.34	2.12		0.15		235.1	44.16
Solanum 1	Barbwire Terrace	498.4	0.71	434	0.26	1.13	0.43	1.39		0.19		159.2	60.56
Solanum 1	Barbwire Terrace	504.5	1.06	435	0.41	2.58	0.45	2.99		0.14		243.4	42.45
Solanum 1	Barbwire Terrace	515	1.16	435	0.42	2.57	0.37	2.99		0.14		221.6	31.9
Solanum 1	Barbwire Terrace	519.58	1.17	437	0.67	2.52		3.19		0.21		215.4	
Solanum 1	Barbwire Terrace	521.07	0.74	436	0.23	1.48	0.4	1.71		0.13		200	54.05
Solanum 1	Barbwire Terrace	523.3	1.15	436	0.39	2.35	0.29	2.74		0.14		204.3	25.22
Solanum 1	Barbwire Terrace	526	0.55	426	0.13	0.72	0.54	0.85		0.15		130.9	98.18
Solanum 1	Barbwire Terrace	526.2	1.34	433	0.48	2.82	0.3	3.3		0.15		210.4	22.39
Solanum 1	Barbwire Terrace	531.8	1.1	433	0.54	2.35	0.26	2.89		0.19		213.6	23.64
Solanum 1	Barbwire Terrace	532	1.09	434	0.45	2.13	0.3	2.58		0.17		195.4	27.52
Solanum 1	Barbwire Terrace	539	0.8	435	0.42	1.59	0.34	2.01		0.21		198.8	42.5
Solanum 1	Barbwire Terrace	543.4	0.59	431	0.21	0.91	0.22	1.12		0.19		154.2	37.29
Solanum 1	Barbwire Terrace	544.18	0.75	436	0.22	1.25	0.12	1.47		0.15		166.7	16
Solanum 1	Barbwire Terrace	549.3	0.63	434	0.17	0.85	0.18	1.02		0.17		134.9	28.57
Solanum 1	Barbwire Terrace	551.5	0.57	437	0.12	0.66	0.13	0.78		0.15		115.8	22.81
Solanum 1	Barbwire Terrace	552	0.6	436	0.2	0.83	0.1	1.03		0.19		138.3	16.67
Solanum 1	Barbwire Terrace	553.5	0.51	431	0.23	0.85	0.13	1.08		0.21		166.7	25.49
Solanum 1	Barbwire Terrace	556.04	0.22										
Solanum 1	Barbwire Terrace	557	0.79	432	0.23	0.99	0.19	1.22		0.19		125.3	24.05
Solanum 1	Barbwire Terrace	557.5	0.42										
Solanum 1	Barbwire Terrace	558.1	0.88	435	0.48	1.49	0.21	1.97		0.24		169.3	23.86
Solanum 1	Barbwire Terrace	559.7	0.65	433	0.34	0.96	0.24	1.3		0.26		147.7	36.92
Sunshine 1	Broome Platform	692	0.24										
Sunshine 1	Broome Platform	694	0.13										
Sunshine 1	Broome Platform	697	0.19										
Sunshine 1	Broome Platform	700	0.17										
Sunshine 1	Broome Platform	702	0.19										
Sunshine 1	Broome Platform	703	0.22										
Sunshine 1	Broome Platform	706	0.18										
Sunshine 1	Broome Platform	709	0.16										
Sunshine 1	Broome Platform	712	0.21										
Sunshine 1	Broome Platform	715	0.21										

Sunshine 1	Broome Platform	718	0.24										
Sunshine 1	Broome Platform	721	0.3										
Sunshine 1	Broome Platform	724	0.23										
Sunshine 1	Broome Platform	727	0.27										
Sunshine 1	Broome Platform	730	0.36										
Sunshine 1	Broome Platform	733	0.44										
Sunshine 1	Broome Platform	736	0.38										
Sunshine 1	Broome Platform	738	0.39										
Thangoo 1A	Kidson Sub-basin	869.3			0.42	0.66		1.08		0.39			
Thangoo 1A	Kidson Sub-basin	959.2			0.45	0.55		1		0.45			
Thangoo 1A	Kidson Sub-basin	959.52	2.57	441	1.43	5.88	0.63	7.31		0.2		228.8	24.51
Thangoo 1A	Kidson Sub-basin	961.05	3.4	443	1.86	7.86	1.03	9.72		0.19		231.2	30.29
Vela 1	Broome Platform	1860	0.1										
Vela 1	Broome Platform	1867	0.23										
Vela 1	Broome Platform	1870	0.14										
Vela 1	Broome Platform	1890	0.14										
Vela 1	Broome Platform	1900	0.14										
Vela 1	Broome Platform	1910	0.14										
Whistler 1	Broome Platform	835	0.11										
Whistler 1	Broome Platform	838	0.17										
Whistler 1	Broome Platform	839	0.23										
Whistler 1	Broome Platform	841	0.17										
Whistler 1	Broome Platform	844	0.16										
Whistler 1	Broome Platform	847	0.17										
Whistler 1	Broome Platform	850	0.23										
Whistler 1	Broome Platform	853	0.29										
Whistler 1	Broome Platform	853.4	0.23										
Whistler 1	Broome Platform	856	0.2										
Whistler 1	Broome Platform	859	0.28										
Whistler 1	Broome Platform	862	0.29										
Whistler 1	Broome Platform	865	0.51	440	0.14	1.5	0.67	1.64		0.09		294.1	131.4
Whistler 1	Broome Platform	867.8	0.63	438	0.31	1.99	0.19	2.3		0.13		315.9	30.16
Whistler 1	Broome Platform	868	0.38										
Whistler 1	Broome Platform	871	0.44										
Whistler 1	Broome Platform	874	0.37										
Whistler 1	Broome Platform	877	0.45										
Whistler 1	Broome Platform	880	0.42										
Whistler 1	Broome Platform	883	0.43										
Willara 1	Willara Sub-basin	1874.52	0.22										
Willara 1	Willara Sub-basin	1880.6	0.22										
Willara 1	Willara Sub-basin	1880.6	0.12										
Willara 1	Willara Sub-basin	1881.2	0.1										
Willara 1	Willara Sub-basin	1881.22	0.23										
Willara 1	Willara Sub-basin	1881.8	0.1										
Willara 1	Willara Sub-basin	1883.1	0.2										
Willara 1	Willara Sub-basin	1886.71	0.46										
Willara 1	Willara Sub-basin	1895.8	0.36										
Willara 1	Willara Sub-basin	1895.86	0.36										
Willara 1	Willara Sub-basin	1905	0.24										
Willara 1	Willara Sub-basin	1911.1	0.23										
Willara 1	Willara Sub-basin	1914.14	0.18										
Willara 1	Willara Sub-basin	1923.29	0.15										
Willara 1	Willara Sub-basin	1926.3	0.14										
Willara 1	Willara Sub-basin	1932.43	0.45										
Willara 1	Willara Sub-basin	1941.58	0.73	430	0.11	1.01	1.15	1.12		0.1		138.4	157.5
Willara 1	Willara Sub-basin	1941.6	0.13										
Willara 1	Willara Sub-basin	1950.72	0.26										
Willara 1	Willara Sub-basin	1953.8	0.15										
Willara 1	Willara Sub-basin	1956.8	0.27										
Willara 1	Willara Sub-basin	1959.86	0.19										
Willara 1	Willara Sub-basin	1966	0.14										
Willara 1	Willara Sub-basin	1969.01	0.23										
Willara 1	Willara Sub-basin	1972	0.16										
Willara 1	Willara Sub-basin	1978.15	0.2										
Willara 1	Willara Sub-basin	1981.2	0.19										
Willara 1	Willara Sub-basin	1987.3	0.2										
Willara 1	Willara Sub-basin	1996.44	0.24										
Willara 1	Willara Sub-basin	1999.5	0.14										
Willara 1	Willara Sub-basin	2005.58	0.21										
Willara 1	Willara Sub-basin	2014.73	0.25										
Willara 1	Willara Sub-basin	2014.8	0.16										
Willara 1	Willara Sub-basin	2023.87	0.2										
Willara 1	Willara Sub-basin	2026.9	0.13										
Willara 1	Willara Sub-basin	2033.02	0.2										
Willara 1	Willara Sub-basin	2042.16	0.19										
Willara 1	Willara Sub-basin	2042.2	0.2										
Willara 1	Willara Sub-basin	2051.3	0.24										
Willara 1	Willara Sub-basin	2060.45	0.25										
Willara 1	Willara Sub-basin	2069.59	0.26										
Willara 1	Willara Sub-basin	2072.6	0.17										
Willara 1	Willara Sub-basin	2078.74	0.23										
Willara 1	Willara Sub-basin	2082.7	0.2										
Willara 1	Willara Sub-basin	2083.3	0.11										
Willara 1	Willara Sub-basin	2084.5	0.24										
Willara 1	Willara Sub-basin	2085.1	0.1										
Willara 1	Willara Sub-basin	2085.7	0.3										
Willara 1	Willara Sub-basin	2085.7	0.03										
Willara 1	Willara Sub-basin	2086.4	0.02										
Willara 1	Willara Sub-basin	2087.88	0.22										
Willara 1	Willara Sub-basin	2097.02	0.26										
Willara 1	Willara Sub-basin	2103.1	0.2										
Willara 1	Willara Sub-basin	2106.17	0.22										
Willara 1	Willara Sub-basin	2115.31	0.27										

Willara 1	Willara Sub-basin	2124.46	0.25										
Willara 1	Willara Sub-basin	2133.6	0.21										
Willara 1	Willara Sub-basin	2133.6	0.2										
Willara 1	Willara Sub-basin	2142.74	0.32										
Willara 1	Willara Sub-basin	2151.89	0.22										
Willara 1	Willara Sub-basin	2161.03	0.25										
Willara 1	Willara Sub-basin	2164.1	0.2										
Willara 1	Willara Sub-basin	2170.18	0.26										
Willara 1	Willara Sub-basin	2179.32	0.24										
Willara 1	Willara Sub-basin	2188.46	0.37										
Willara 1	Willara Sub-basin	2194.6	0.3										
Willara 1	Willara Sub-basin	2197.61	0.47										
Willara 1	Willara Sub-basin	2206.75	0.4										
Willara 1	Willara Sub-basin	2215.9	0.31										
Willara 1	Willara Sub-basin	2225	0.2										
Willara 1	Willara Sub-basin	2225.04	0.55	236	0.19	0.07	0.52	0.26		0.73		12.73	94.55
Willara 1	Willara Sub-basin	2234.18	0.44										
Willara 1	Willara Sub-basin	2243.33	0.28										
Willara 1	Willara Sub-basin	2252.47	0.24										
Willara 1	Willara Sub-basin	2255.5	0.2										
Willara 1	Willara Sub-basin	2261.62	0.27										
Willara 1	Willara Sub-basin	2263.7	0.6		0.1	0.1	0	0.2		0.5		16.67	
Willara 1	Willara Sub-basin	2264.4	0.11										
Willara 1	Willara Sub-basin	2264.66	0.27										
Willara 1	Willara Sub-basin	2264.9	0.38										
Willara 1	Willara Sub-basin	2273.81	0.31										
Willara 1	Willara Sub-basin	2282.95	0.31										
Willara 1	Willara Sub-basin	2286	0.1										
Willara 1	Willara Sub-basin	2292.1	0.35										
Willara 1	Willara Sub-basin	2304.29	0.29										
Willara 1	Willara Sub-basin	2313.43	0.37										
Willara 1	Willara Sub-basin	2316.5	0.3										
Willara 1	Willara Sub-basin	2322.58	0.35										
Willara 1	Willara Sub-basin	2331.72	0.31										
Willara 1	Willara Sub-basin	2340.86	0.22										
Willara 1	Willara Sub-basin	2347	0.2										
Willara 1	Willara Sub-basin	2350.01	0.32										
Willara 1	Willara Sub-basin	2368.3	0.28										
Willara 1	Willara Sub-basin	2374.8	0.4										
Willara 1	Willara Sub-basin	2376.8	0.1										
Willara 1	Willara Sub-basin	2377.4	0.06										
Willara 1	Willara Sub-basin	2377.44	0.35										
Willara 1	Willara Sub-basin	2378	0.08										
Willara 1	Willara Sub-basin	2386.58	0.23										
Willara 1	Willara Sub-basin	2395.73	0.28										
Willara 1	Willara Sub-basin	2404.87	0.27										
Willara 1	Willara Sub-basin	2407.9	0.2										
Willara 1	Willara Sub-basin	2414.02	0.24										
Willara 1	Willara Sub-basin	2423.16	0.24										
Willara 1	Willara Sub-basin	2432.3	0.29										
Willara 1	Willara Sub-basin	2438.4	0.3										
Willara 1	Willara Sub-basin	2450.59	0.25										
Willara 1	Willara Sub-basin	2459.74	0.3										
Willara 1	Willara Sub-basin	2468.9	0.41										
Willara 1	Willara Sub-basin	2478.02	0.26										
Willara 1	Willara Sub-basin	2496.31	0.27										
Willara 1	Willara Sub-basin	2499.4	0.1										
Willara 1	Willara Sub-basin	2505.46	0.23										
Willara 1	Willara Sub-basin	2514.6	0.27										
Willara 1	Willara Sub-basin	2523.74	0.31										
Willara 1	Willara Sub-basin	2529.8	0.3										
Willara 1	Willara Sub-basin	2532.89	0.32										
Willara 1	Willara Sub-basin	2542.03	0.35										
Willara 1	Willara Sub-basin	2545.7	0.4										
Willara 1	Willara Sub-basin	2548.1	0.1										
Willara 1	Willara Sub-basin	2548.2					0						
Willara 1	Willara Sub-basin	2551.18	0.25										
Willara 1	Willara Sub-basin	2560.3	0.23										
Willara 1	Willara Sub-basin	2560.32	0.38										
Willara 1	Willara Sub-basin	2569.46	0.33										
Willara 1	Willara Sub-basin	2578.61	0.3										
Willara 1	Willara Sub-basin	2587.75	0.26										
Willara 1	Willara Sub-basin	2590.8	0.25										
Willara 1	Willara Sub-basin	2596.9	0.24										
Wilson Cliffs 1	Kidson Sub-basin	2679.2	0.09										
Wilson Cliffs 1	Kidson Sub-basin	2680	0.09										
Wilson Cliffs 1	Kidson Sub-basin	2680.7	0.19										
Wilson Cliffs 1	Kidson Sub-basin	2681	0.03										
Wilson Cliffs 1	Kidson Sub-basin	2682.1	0.09										
Wilson Cliffs 1	Kidson Sub-basin	2683.5	0.06										
Wilson Cliffs 1	Kidson Sub-basin	2685.3	0.42										
Wilson Cliffs 1	Kidson Sub-basin	2685.3	0.42										
Wilson Cliffs 1	Kidson Sub-basin	2712.72	0.64										
Wilson Cliffs 1	Kidson Sub-basin	2715.8	0.75		1.1	0.2	0	1.3		0.85		26.67	
Wilson Cliffs 1	Kidson Sub-basin	2734.1	0.42										
Wilson Cliffs 1	Kidson Sub-basin	2746.2	0.37										
Wilson Cliffs 1	Kidson Sub-basin	2770.7	0.46										
Wilson Cliffs 1	Kidson Sub-basin	2779.8	3.21	430	2.48	2.96	7.48	5.44		0.46		92.21	233
Wilson Cliffs 1	Kidson Sub-basin	2779.8	0.7		1.1	0.02		1.12				2.857	
Wilson Cliffs 1	Kidson Sub-basin	2780.5	0.4										
Wilson Cliffs 1	Kidson Sub-basin	2781	0.08										
Wilson Cliffs 1	Kidson Sub-basin	2782	0.22										
Wilson Cliffs 1	Kidson Sub-basin	2782.2	0.08										

Wilson Cliffs 1	Kidson Sub-basin	2783.4	0.09										
Wilson Cliffs 1	Kidson Sub-basin	2804.16	0.43										
Wilson Cliffs 1	Kidson Sub-basin	2807.2	0.35										
Wilson Cliffs 1	Kidson Sub-basin	2813.3	0.37										

Goldwyer Formation Geochemical Logs

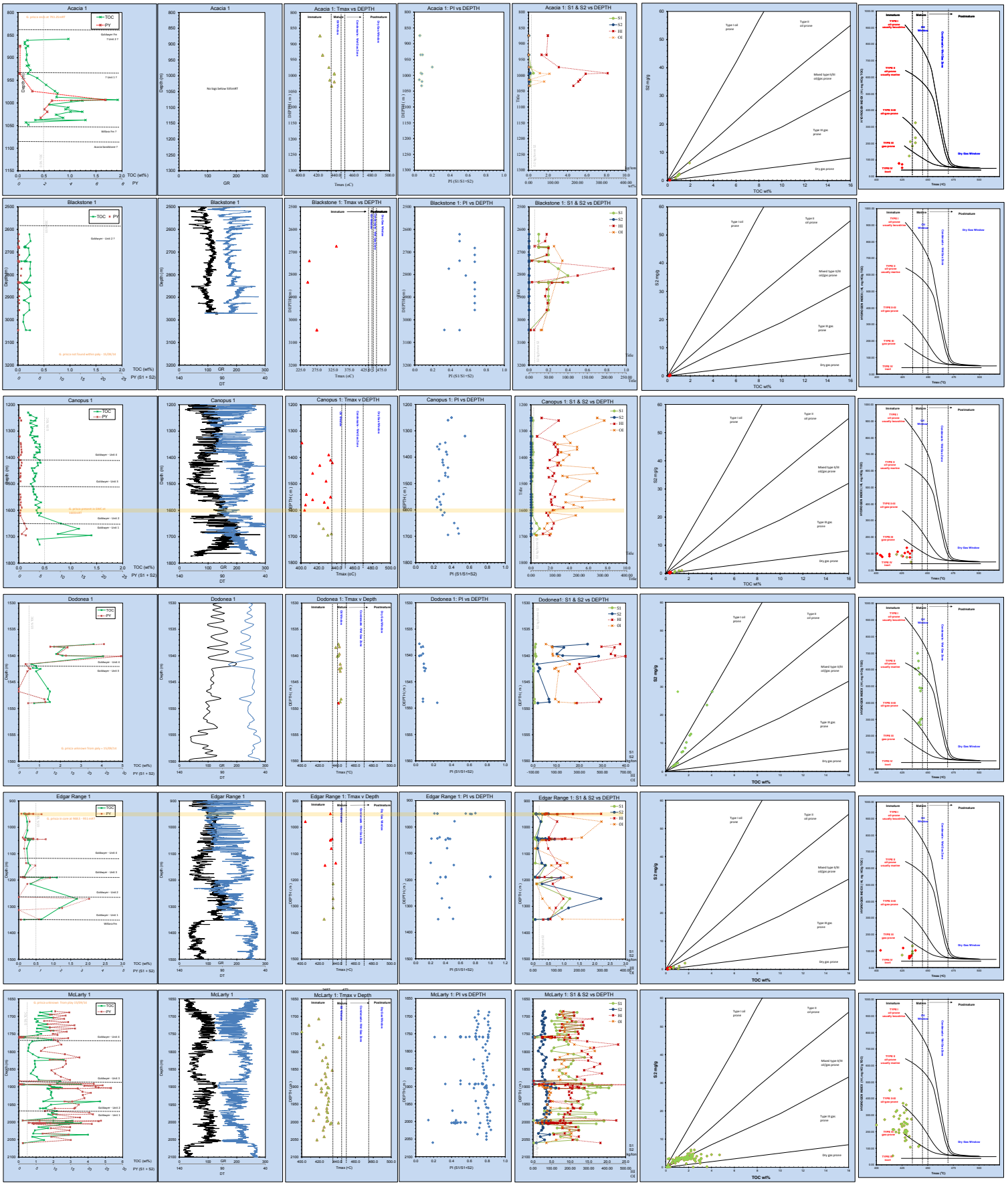

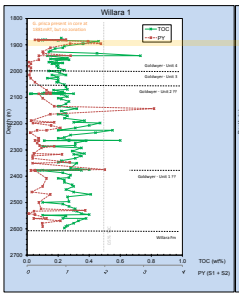
Willara 1
TOC
PY
Depth (ft)
TOC (wt%)
PY (S1 + S2)

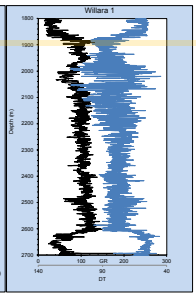
Willara 1
Depth (ft)
GR
DT

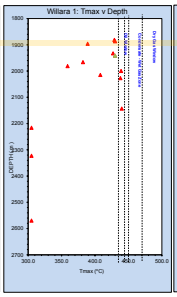
Willara 1: Tmax v Depth
Immature
Mature
Postmature
Tmax (°C)

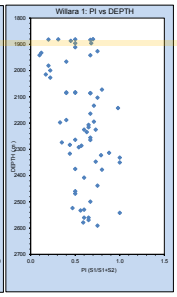
Willara 1: PI vs DEPTH
DEPTH (ft)
PI (S1/S1+S2)

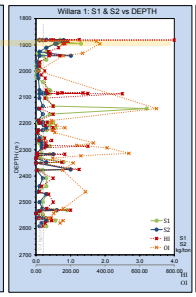
Willara 1: S1 & S2 vs DEPTH
S1
S2
HI
OI
DEPTH (ft)

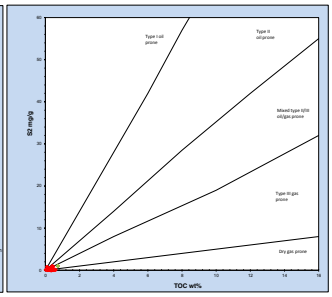
S2 mg/g
TOC wt%
Type I oil prone
Type II oil prone
Mixed type II/III oil/gas prone
Type III gas prone
Dry gas prone

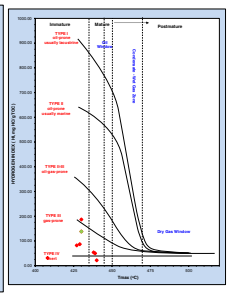
HYDROGEN INDEX (mg HC/g TOC)
Tmax (°C)
Immature
Mature
Postmature
Dry Gas Window

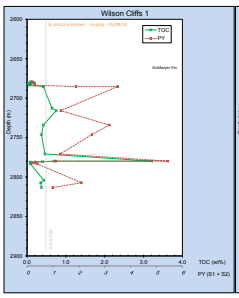
Wilson Cliffs 1
TOC
PY
Depth (ft)
TOC (wt%)
PY (S1 + S2)

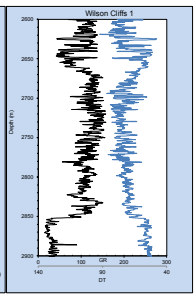
Wilson Cliffs 1
Depth (ft)
GR
DT

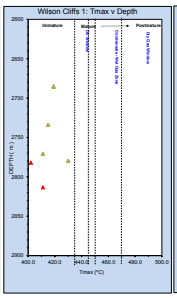
Wilson Cliffs 1: Tmax v Depth
Immature
Mature
Postmature
Tmax (°C)

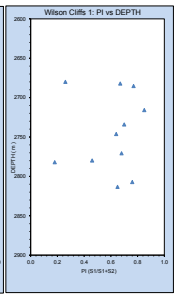
Wilson Cliffs 1: PI vs DEPTH
DEPTH (ft)
PI (S1/S1+S2)

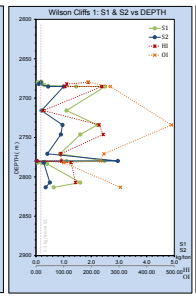
Wilson Cliffs 1: S1 & S2 vs DEPTH
S1
S2
HI
OI
DEPTH (ft)

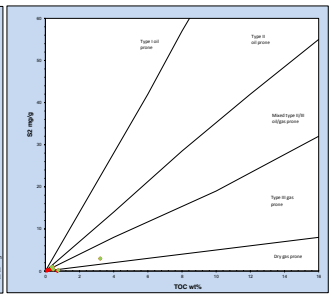
S2 mg/g
TOC wt%
Type I oil prone
Type II oil prone
Mixed type II/III oil/gas prone
Type III gas prone
Dry gas prone

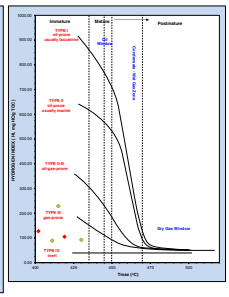
HYDROGEN INDEX (mg HC/g TOC)
Tmax (°C)
Immature
Mature
Postmature
Dry Gas Window

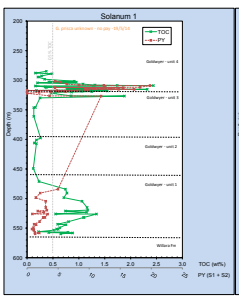
Solanum 1
TOC
PY
Depth (m)
TOC (wt%)
PY (S1 + S2)

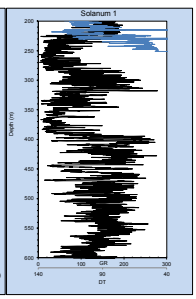
Solanum 1
Depth (m)
GR
DT

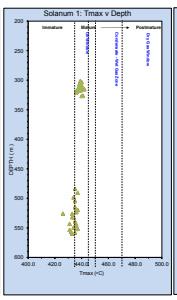
Solanum 1: Tmax v Depth
Immature
Mature
Postmature
Tmax (°C)

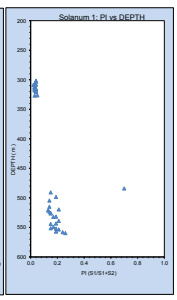
Solanum 1: PI vs DEPTH
DEPTH (m)
PI (S1/S1+S2)

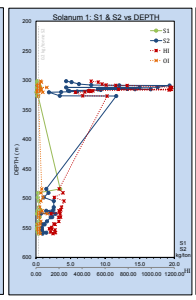
Solanum 1: S1 & S2 vs DEPTH
S1
S2
HI
OI
DEPTH (m)

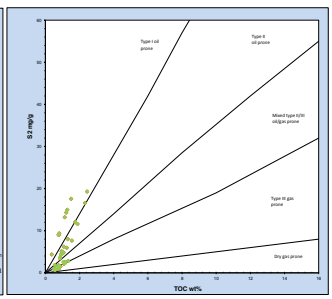
S2 mg/g
TOC wt%
Type I oil prone
Type II oil prone
Mixed type II/III oil/gas prone
Type III gas prone
Dry gas prone

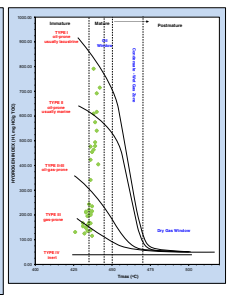
HYDROGEN INDEX (mg HC/g TOC)
Tmax (°C)
Immature
Mature
Postmature
Dry Gas Window

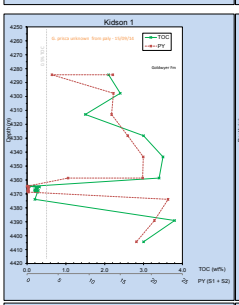
Kidson 1
TOC
PY
Depth (m)
TOC (wt%)
PY (S1 + S2)

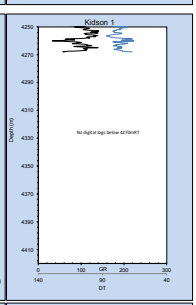
Kidson 1
No digital logs below 4270mMT
Depth (m)
GR
DT

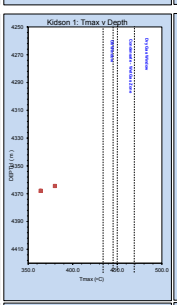
Kidson 1: Tmax v Depth
Immature
Mature
Postmature
Tmax (°C)

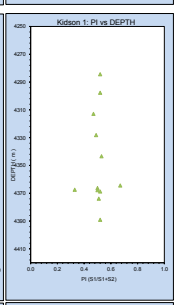
Kidson 1: PI vs DEPTH
DEPTH (m)
PI (S1/S1+S2)

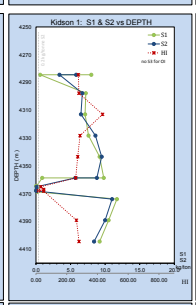
Kidson 1: S1 & S2 vs DEPTH
S1
S2
HI
OI
DEPTH (m)

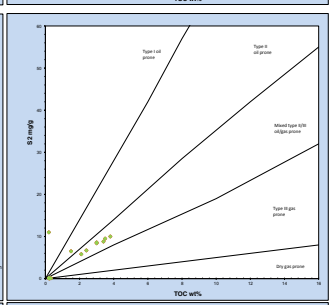
S2 mg/g
TOC wt%
Type I oil prone
Type II oil prone
Mixed type II/III oil/gas prone
Type III gas prone
Dry gas prone

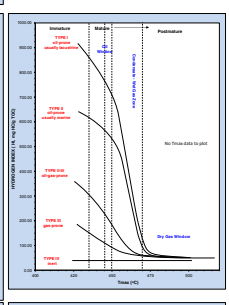
HYDROGEN INDEX (mg HC/g TOC)
Tmax (°C)
Immature
Mature
Postmature
Dry Gas Window

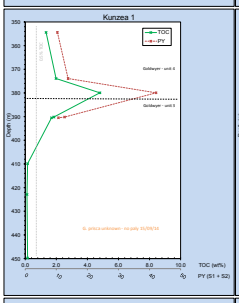
Kunzea 1
TOC
PY
Depth (m)
TOC (wt%)
PY (S1 + S2)

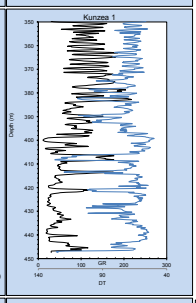
Kunzea 1
Depth (m)
GR
DT

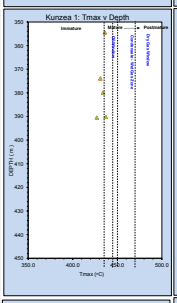
Kunzea 1: Tmax v Depth
Immature
Mature
Postmature
Tmax (°C)

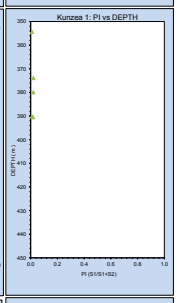
Kunzea 1: PI vs DEPTH
DEPTH (m)
PI (S1/S1+S2)

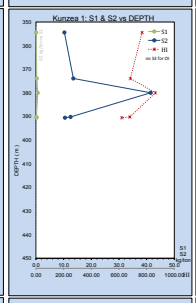
Kunzea 1: S1 & S2 vs DEPTH
S1
S2
HI
OI
DEPTH (m)

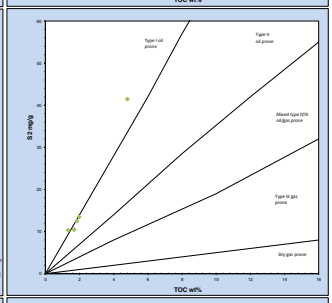
S2 mg/g
TOC wt%
Type I oil prone
Type II oil prone
Mixed type II/III oil/gas prone
Type III gas prone
Dry gas prone

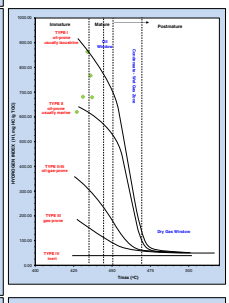
HYDROGEN INDEX (mg HC/g TOC)
Tmax (°C)
Immature
Mature
Postmature
Dry Gas Window

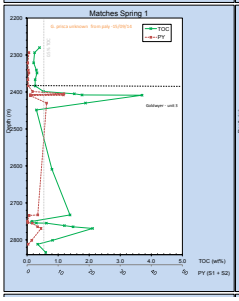
Matches Spring 1
TOC
PY
Depth (m)
TOC (wt%)
PY (S1 + S2)

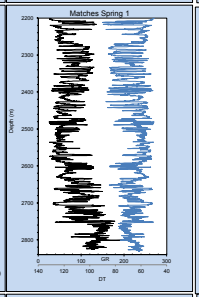
Matches Spring 1
Depth (m)
GR
DT

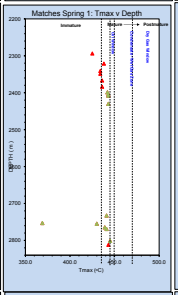
Matches Spring 1: Tmax v Depth
Immature
Mature
Postmature
Tmax (°C)

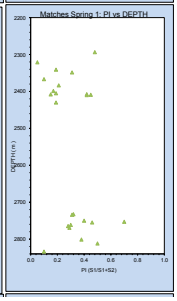
Matches Spring 1: PI vs DEPTH
DEPTH (m)
PI (S1/S1+S2)

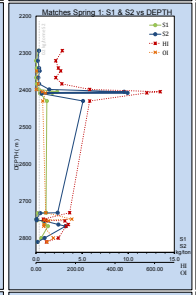
Matches Spring 1: S1 & S2 vs DEPTH
S1
S2
HI
OI
DEPTH (m)

S2 mg/g
TOC wt%
Type I oil prone
Type II oil prone
Mixed type II/III oil/gas prone
Type III gas prone
Dry gas prone

HYDROGEN INDEX (mg HC/g TOC)
Tmax (°C)
Immature
Mature
Postmature
Dry Gas Window

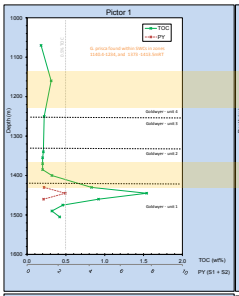
Pictor 1
TOC
PY
TOC (wt%)
PY (S1 + S2)

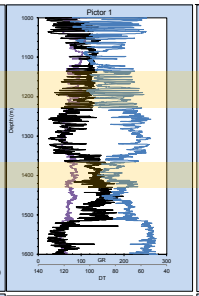
Pictor 1
GR
DT

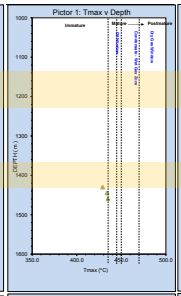
Pictor 1: Tmax v Depth
Immature
Mature
Postmature
Tmax (°C)

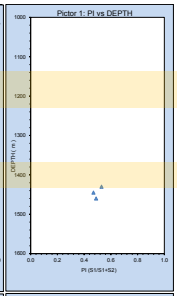
Pictor 1: PI vs DEPTH
PI (S1/S1+S2)

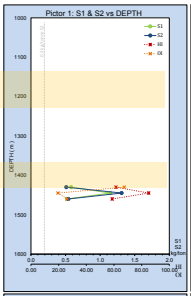
Pictor 1: S1 & S2 vs DEPTH
S1
S2
RI
OI

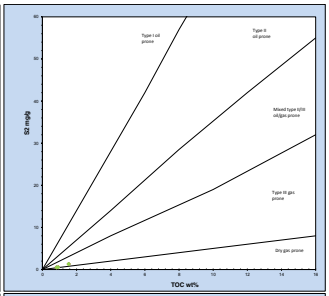
S2 mg/g
TOC wt%
Type I oil prone
Type II oil prone
Mixed type II/III oil/gas prone
Type III gas prone
Dry gas prone

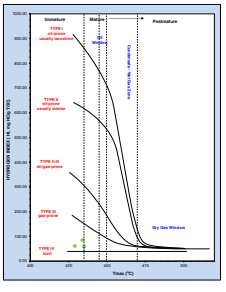
Immature
Mature
Postmature
Tmax (°C)
Dry Gas Window

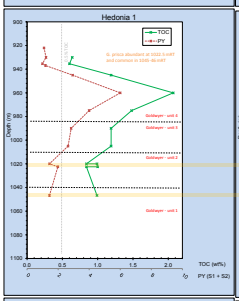
Hedonia 1
TOC
PY
TOC (wt%)
PY (S1 + S2)

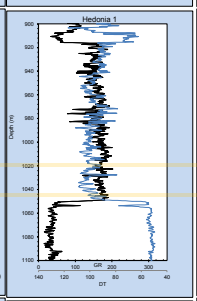
Hedonia 1
GR
DT

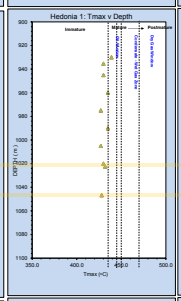
Hedonia 1: Tmax v Depth
Immature
Mature
Postmature
Tmax (°C)

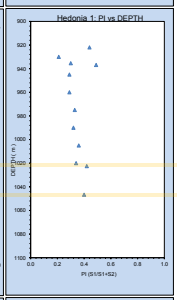
Hedonia 1: PI vs DEPTH
PI (S1/S1+S2)

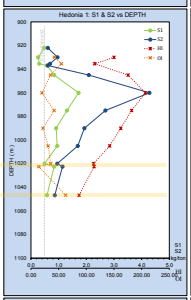
Hedonia 1: S1 & S2 vs DEPTH
S1
S2
RI
OI

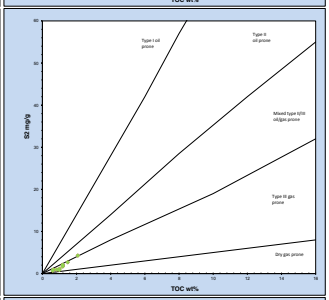
S2 mg/g
TOC wt%
Type I oil prone
Type II oil prone
Mixed type II/III oil/gas prone
Type III gas prone
Dry gas prone

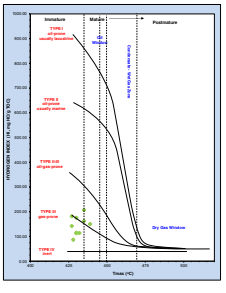
Immature
Mature
Postmature
Tmax (°C)
Dry Gas Window

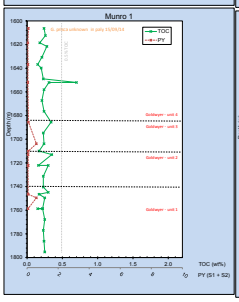
Munro 1
TOC
PY
TOC (wt%)
PY (S1 + S2)

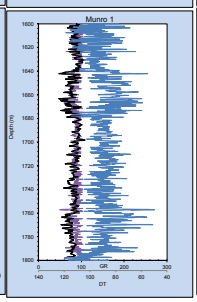
Munro 1
GR
DT

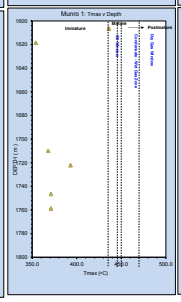
Munro 1: Tmax v Depth
Immature
Mature
Postmature
Tmax (°C)

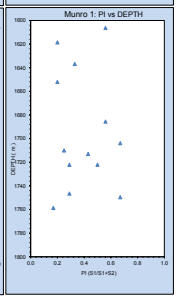
Munro 1: PI vs DEPTH
PI (S1/S1+S2)

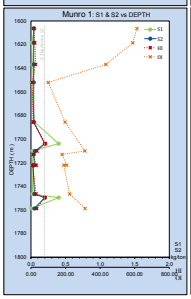
Munro 1: S1 & S2 vs DEPTH
S1
S2
RI
OI

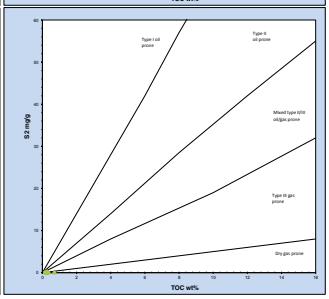
S2 mg/g
TOC wt%
Type I oil prone
Type II oil prone
Mixed type II/III oil/gas prone
Type III gas prone
Dry gas prone

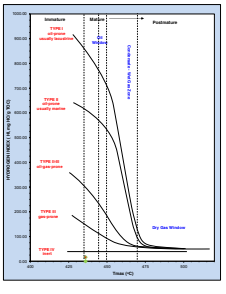
Immature
Mature
Postmature
Tmax (°C)
Dry Gas Window

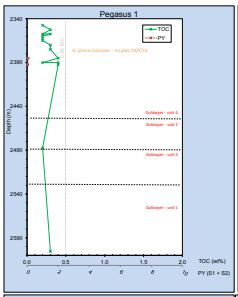
Pegasus 1
TOC
PY
TOC (wt%)
PY (S1 + S2)

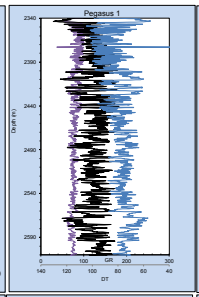
Pegasus 1
GR
DT

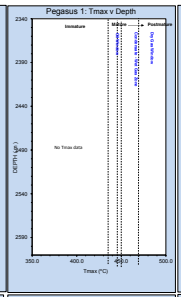
Pegasus 1: Tmax v Depth
Immature
Mature
Postmature
No Tmax data
Tmax (°C)

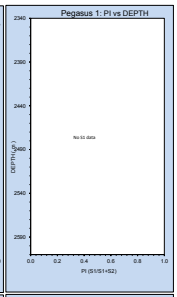
Pegasus 1: PI vs DEPTH
No S1 data
PI (S1/S1+S2)

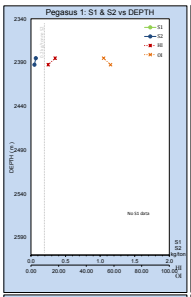
Pegasus 1: S1 & S2 vs DEPTH
No S1 data
S1
S2
RI
OI

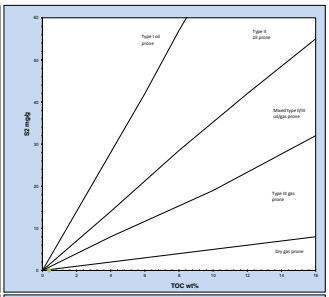
S2 mg/g
TOC wt%
Type I oil prone
Type II oil prone
Mixed type II/III oil/gas prone
Type III gas prone
Dry gas prone

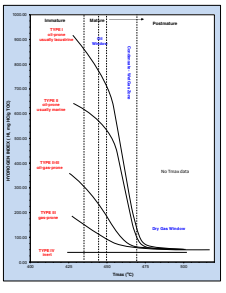
Immature
Mature
Postmature
No Tmax data
Tmax (°C)
Dry Gas Window

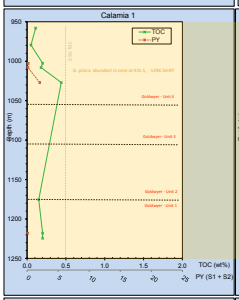
Calamia 1
TOC
PY
TOC (wt%)
PY (S1 + S2)

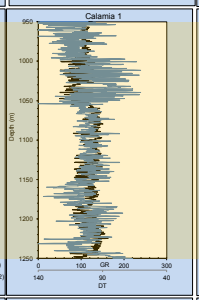
Calamia 1
GR
DT

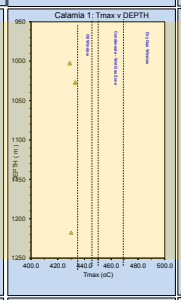
Calamia 1: Tmax v DEPTH
Tmax (oC)

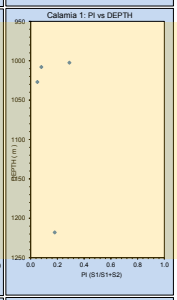
Calamia 1: PI vs DEPTH
PI (S1/S1+S2)

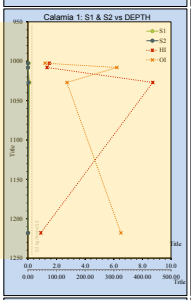
Calamia 1: S1 & S2 vs DEPTH

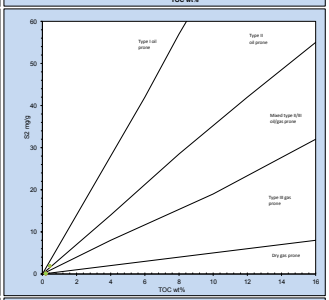
S2 mg/g
TOC wt%
Type I oil prone
Type II oil prone
Mixed type II/III oil/gas prone
Type III gas prone
Dry gas prone

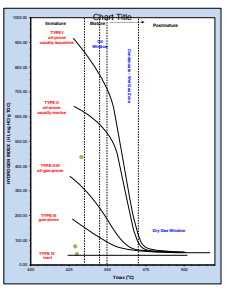
Chart Title
Immature
Mature
Postmature
Tmax (°C)

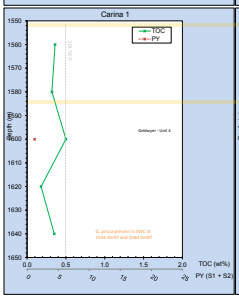
Carina 1
TOC
PY
TOC (wt%)
PY (S1 + S2)

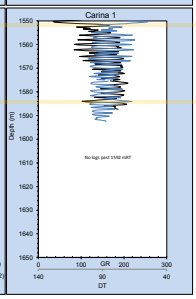
Carina 1
GR
DT

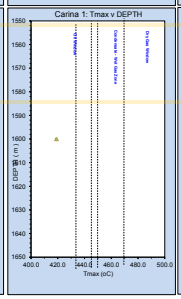
Carina 1: Tmax v DEPTH
Tmax (oC)

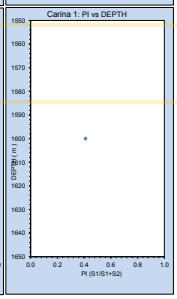
Carina 1: PI vs DEPTH
PI (S1/S1+S2)

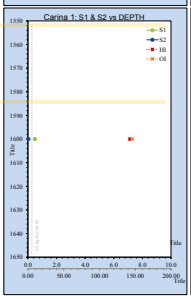
Carina 1: S1 & S2 vs DEPTH

S2 mg/g
TOC wt%
Type I oil prone
Type II oil prone
Mixed type II/III oil/gas prone
Type III gas prone
Dry gas prone

Immature
Mature
Postmature
Tmax (°C)
Dry Gas Window

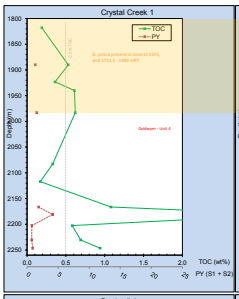
Crystal Creek 1
TOC
PY
Depth(m)
TOC (wt%)
PY (S1 + S2)

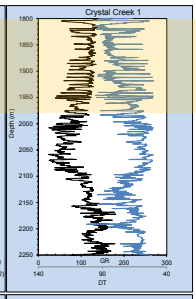
Crystal Creek 1
Depth (m)
GR
DT

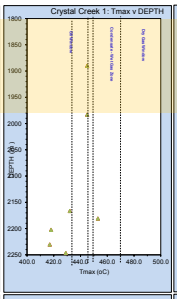
Crystal Creek 1: Tmax v DEPTH
Immature
Mature
Postmature
Tmax (oC)

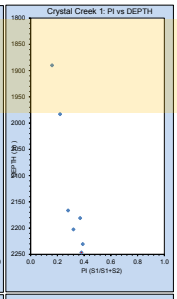
Crystal Creek 1: PI vs DEPTH
PI (S1/S1+S2)

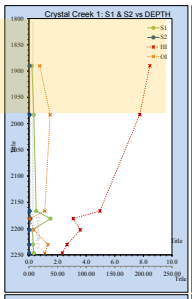
Crystal Creek 1: S1 & S2 vs DEPTH
S1
S2
III
OI

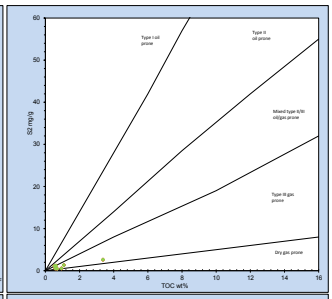
Type I oil prone
Type II oil prone
Mixed type II/III oil/gas prone
Type III gas prone
Dry gas prone
S2 mg/g
TOC wt%

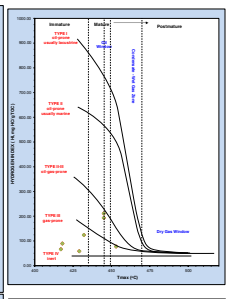
Immature
Mature
Postmature
TYPE I oil-prone usually lacustrine
TYPE II oil-prone usually marine
TYPE II/III oil/gas-prone
TYPE III gas-prone
TYPE IV inert
Dry Gas Window
Tmax (°C)

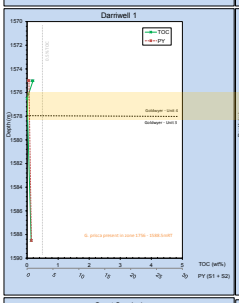
Darriwell 1
TOC
PY
Goldwyer - Unit 4
Goldwyer - Unit 3
Depth(m)
TOC (wt%)
PY (S1 + S2)

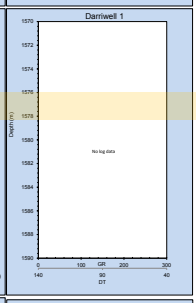
Darriwell 1
No log data
Depth (m)
GR
DT

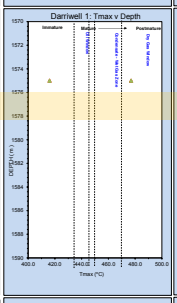
Darriwell 1: Tmax v Depth
Immature
Mature
Postmature
Tmax (°C)

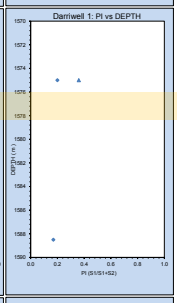
Darriwell 1: PI vs DEPTH
PI (S1/S1+S2)

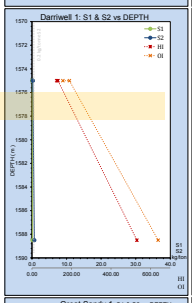
Darriwell 1: S1 & S2 vs DEPTH
S1
S2
III
OI

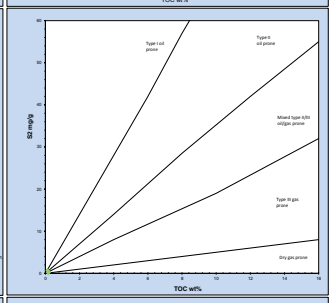
Type I oil prone
Type II oil prone
Mixed type II/III oil/gas prone
Type III gas prone
Dry gas prone
S2 mg/g
TOC wt%

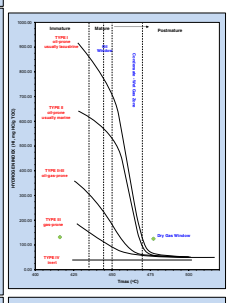
Immature
Mature
Postmature
TYPE I oil-prone usually lacustrine
TYPE II oil-prone usually marine
TYPE II/III oil/gas-prone
TYPE III gas-prone
TYPE IV inert
Dry Gas Window
Tmax (°C)

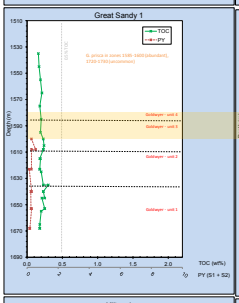
Great Sandy 1
TOC
PY
Goldwyer - unit 5
Goldwyer - unit 4
Goldwyer - unit 3
Goldwyer - unit 2
Depth(m)
TOC (wt%)
PY (S1 + S2)

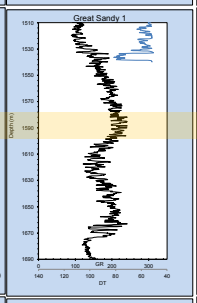
Great Sandy 1
Depth (m)
GR
DT

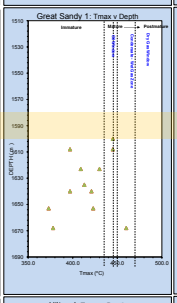
Great Sandy 1: Tmax v Depth
Immature
Mature
Postmature
Tmax (°C)

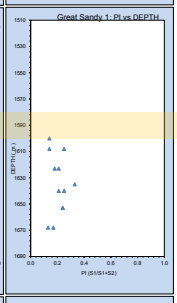
Great Sandy 1: PI vs DEPTH
PI (S1/S1+S2)

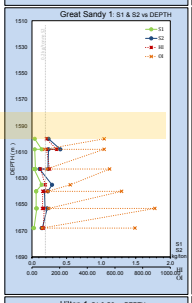
Great Sandy 1: S1 & S2 vs DEPTH
S1
S2
III
OI

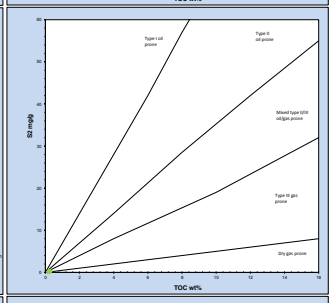
Type I oil prone
Type II oil prone
Mixed type II/III oil/gas prone
Type III gas prone
Dry gas prone
S2 mg/g
TOC wt%

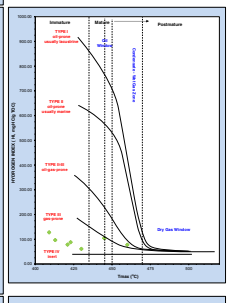
Immature
Mature
Postmature
TYPE I oil-prone usually lacustrine
TYPE II oil-prone usually marine
TYPE II/III oil/gas-prone
TYPE III gas-prone
TYPE IV inert
Dry Gas Window
Tmax (°C)

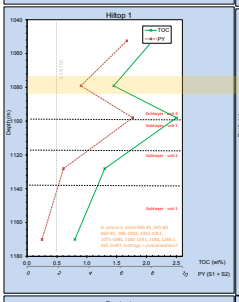
Hiltop 1
TOC
PY
Goldwyer - unit 5
Goldwyer - unit 4
Goldwyer - unit 3
Goldwyer - unit 2
Goldwyer - unit 1
Depth(m)
TOC (wt%)
PY (S1 + S2)

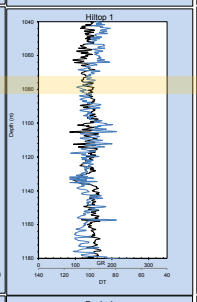
Hiltop 1
Depth (m)
GR
DT

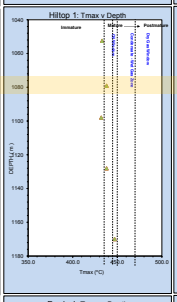
Hiltop 1: Tmax v Depth
Immature
Mature
Postmature
Tmax (°C)

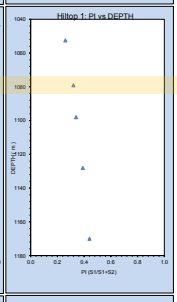
Hiltop 1: PI vs DEPTH
PI (S1/S1+S2)

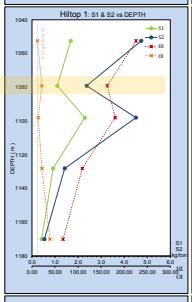
Hiltop 1: S1 & S2 vs DEPTH
S1
S2
III
OI

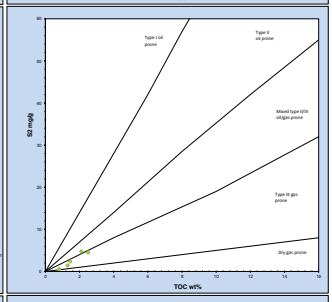
Type I oil prone
Type II oil prone
Mixed type II/III oil/gas prone
Type III gas prone
Dry gas prone
S2 mg/g
TOC wt%

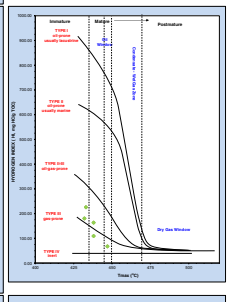
Immature
Mature
Postmature
TYPE I oil-prone usually lacustrine
TYPE II oil-prone usually marine
TYPE II/III oil/gas-prone
TYPE III gas-prone
TYPE IV inert
Dry Gas Window
Tmax (°C)

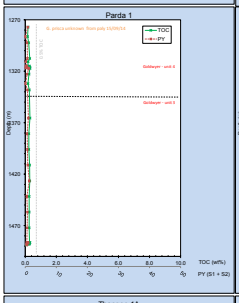
Parda 1
TOC
PY
Goldwyer - unit 6
Goldwyer - unit 5
Goldwyer - unit 4
Goldwyer - unit 3
Depth (m)
TOC (wt%)
PY (S1 + S2)

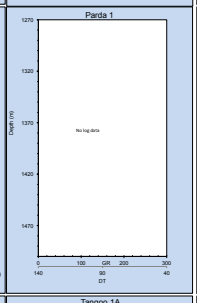
Parda 1
No log data
Depth (m)
GR
DT

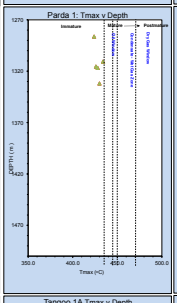
Parda 1: Tmax v Depth
Immature
Mature
Postmature
Tmax (°C)

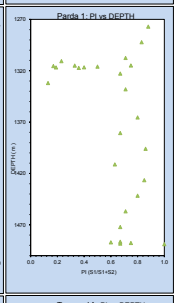
Parda 1: PI vs DEPTH
PI (S1/S1+S2)

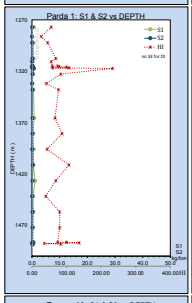
Parda 1: S1 & S2 vs DEPTH
S1
S2
III
no S3 for OI

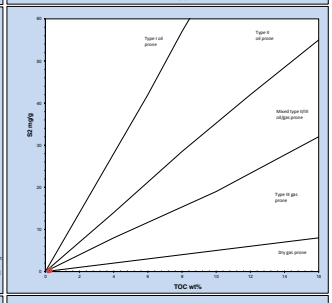
Type I oil prone
Type II oil prone
Mixed type II/III oil/gas prone
Type III gas prone
Dry gas prone
S2 mg/g
TOC wt%

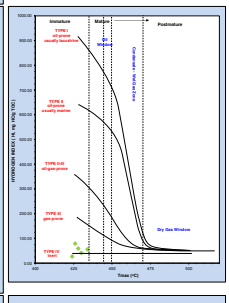
Immature
Mature
Postmature
TYPE I oil-prone usually lacustrine
TYPE II oil-prone usually marine
TYPE II/III oil/gas-prone
TYPE III gas-prone
TYPE IV inert
Dry Gas Window
Tmax (°C)

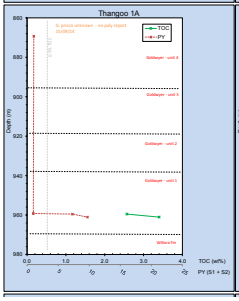
Thangoo 1A
TOC
PY
Goldwyer - unit 6
Goldwyer - unit 5
Goldwyer - unit 4
Goldwyer - unit 3
Depth (m)
TOC (wt%)
PY (S1 + S2)

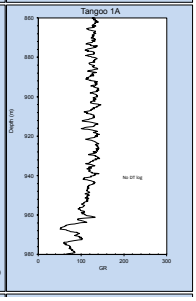
Tangoo 1A
No DT log
Depth (m)
GR

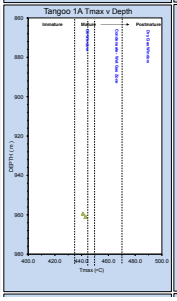
Tangoo 1A Tmax v Depth
Immature
Mature
Postmature
Tmax (°C)

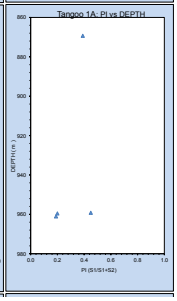
Tangoo 1A: PI vs DEPTH
PI (S1/S1+S2)

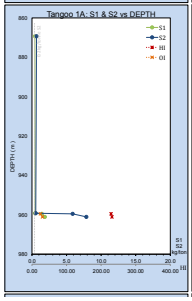
Tangoo 1A: S1 & S2 vs DEPTH
S1
S2
III
OI

Type I oil prone
Type II oil prone
Mixed type II/III oil/gas prone
Type III gas prone
Dry gas prone
S2 mg/g
TOC wt%

Immature
Mature
Postmature
TYPE I oil-prone usually lacustrine
TYPE II oil-prone usually marine
TYPE II/III oil/gas-prone
TYPE III gas-prone
TYPE IV inert
Dry Gas Window
Tmax (°C)

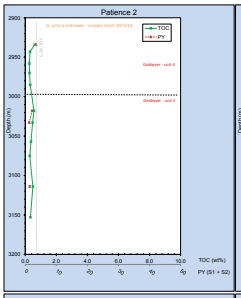

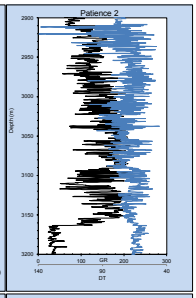

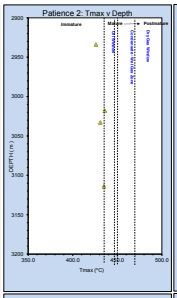

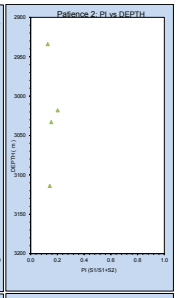

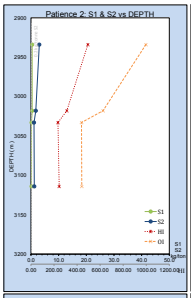

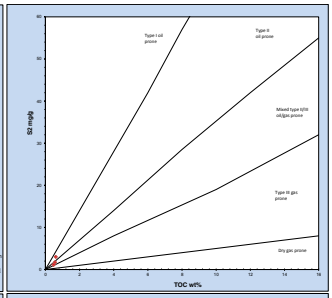

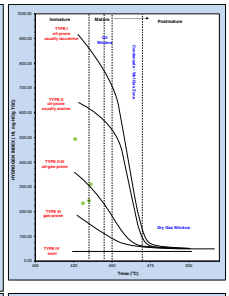

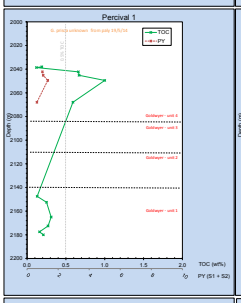

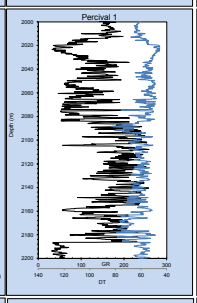

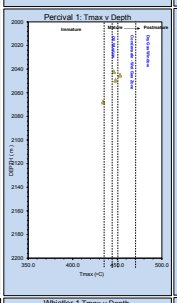

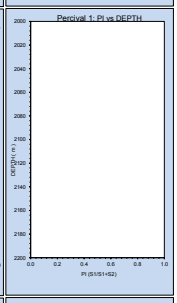

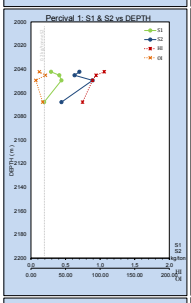

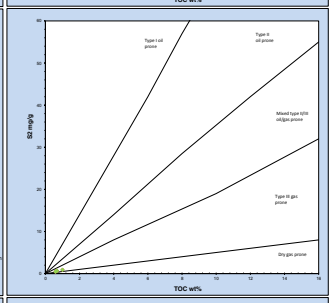

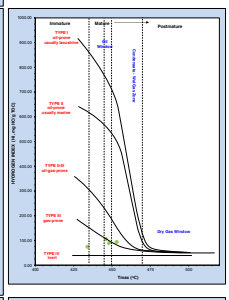

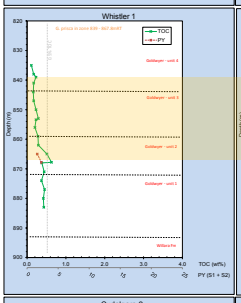

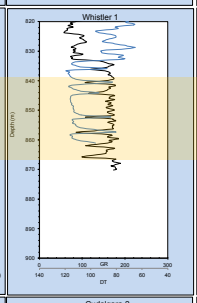

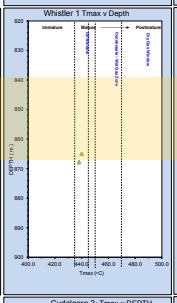

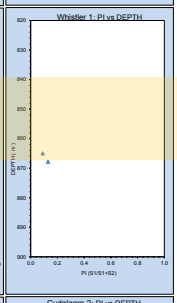

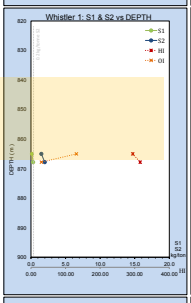

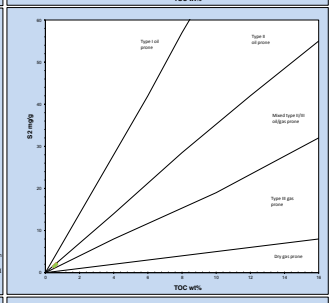

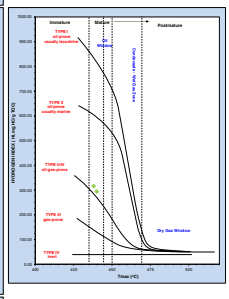

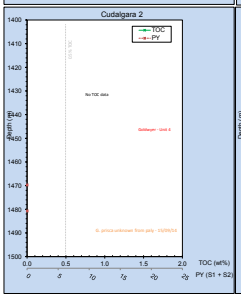

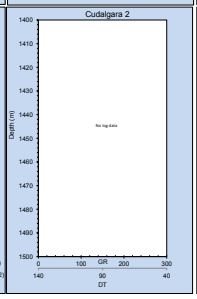

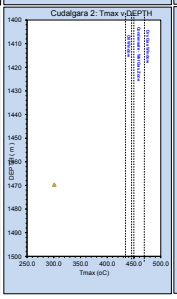

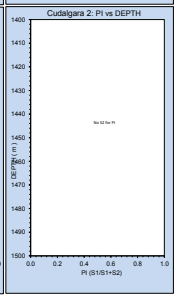

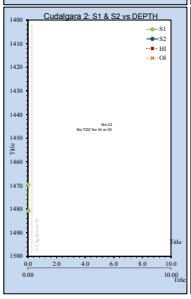

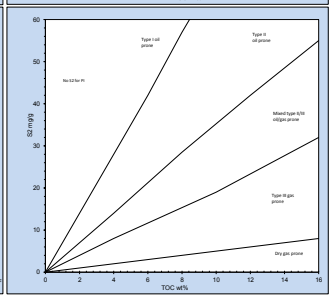

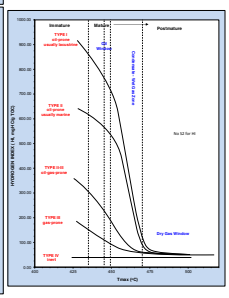

NOTES:

Green triangles = Tmax data from samples with TOC >0.5% and S2 >0.2 kg HC/ton
Red triangles = Tmax data from samples with low TOC <0.5% and low S2 <0.2 kg HC/ton
Orange bands = Occurance of G.prisca Ordovician algae

Appendix D

Thermal Maturity (Vitrinite Reflectance) Measurements

Vitrinite reflectance measurements from open file well completion reports and a database constructed by the Geological Survey of Western Australia was utilised in this study. These data are included in this Appendix.

Well	Depth (mRT)	Maceral	Type	Mean	Max	Min	No of Readings
Bindi 1	859.2	Vitrinite	SWC	0.51	1.28	0.7	20
Bindi 1	976	Vitrinite	SWC	0.56	0.48	0.32	34
Bindi 1	1065	Vitrinite	SWC	0.41	0.48	0.33	23
Bindi 1	1071	Vitrinite	SWC	0.56	0.76	0.42	18
Bindi 1	1235	Inertinite	SWC	1.3	1.54	1	
Bindi 1	1235	Vitrinite	SWC	0.56	0.64	0.48	10
Bindi 1	1248.5	Vitrinite	SWC	0.42	0.5	0.35	6
Bindi 1	1475.4	Vitrinite	SWC	0.45	0.53	0.38	4
Bindi 1	1918.7	Inertinite	SWC	1.4	1.76	1.02	25
Bindi 1	1918.7	Vitrinite	SWC				
Bindi 1	2481.4	Inertinite	SWC	1.52	2.16	1.1	17
Bindi 1	2481.4	Vitrinite	SWC				
Justago 1	250	Exinite	DC				
Justago 1	390	Exinite	DC				
Kilang Kilang 1	131.8	Exinite	SWC	0.57			1
Kilang Kilang 1	131.8	Inertinite	SWC	1.3	1.88	1	15
Kilang Kilang 1	131.8	Vitrinite	SWC				
Kilang Kilang 1	131.8	Exinite	SWC	0.57			1
Kilang Kilang 1	131.8	Inertinite	SWC	1.3	1.88	1	15
Kilang Kilang 1	131.8	Vitrinite	SWC				
Kilang Kilang 1	197.8	Inertinite	SWC	1.55	2.34	1.19	17
Kilang Kilang 1	197.8	Vitrinite	SWC	0.58			1
Kilang Kilang 1	229.3	Inertinite	SWC	1.35	2.5	0.74	14
Kilang Kilang 1	229.3	Vitrinite	SWC	0.53	0.62	0.47	8
Kilang Kilang 1	236.8	Inertinite	SWC	1.41	1.7	1.24	7
Kilang Kilang 1	236.8	Vitrinite	SWC				
Kilang Kilang 1	274	Exinite	SWC	0.3	0.41	0.21	3
Kilang Kilang 1	274	Inertinite	SWC	1.25	1.48	0.95	11
Kilang Kilang 1	274	Vitrinite	SWC	0.54	0.63	0.46	8
Kilang Kilang 1	294	Inertinite	SWC	1.41	2	0.96	14
Kilang Kilang 1	294	Vitrinite	SWC				
Kilang Kilang 1	338.7	Exinite	SWC	0.31			1
Kilang Kilang 1	338.7	Inertinite	SWC	1.38	2.26	0.94	16
Kilang Kilang 1	338.7	Vitrinite	SWC	0.7	0.8	0.58	11
Kilang Kilang 1	359	Exinite	SWC	0.3	0.35	0.25	5
Kilang Kilang 1	359	Inertinite	SWC	1.49	2.24	0.96	16
Kilang Kilang 1	358	Vitrinite	SWC	0.67	0.88	0.55	7
Kilang Kilang 1	406.4	Exinite	SWC	0.36	0.57	0.25	8
Kilang Kilang 1	406.4	Inertinite	SWC	1.34	1.79	1	20
Kilang Kilang 1	406.4	Vitrinite	SWC				
Kilang Kilang 1	437.7	Exinite	SWC	0.4	0.47	0.29	3
Kilang Kilang 1	437.7	Inertinite	SWC	1.63	2.68	1.1	12
Kilang Kilang 1	437.7	Vitrinite	SWC	0.63	0.74	0.52	4
Kilang Kilang 1	450	Exinite	SWC	0.34	0.44	0.29	4
Kilang Kilang 1	450	Inertinite	SWC	1.45	2.18	0.93	13
Kilang Kilang 1	450	Vitrinite	SWC	0.68	0.83	0.61	8
Kilang Kilang 1	476	Exinite	SWC	0.44	0.48	0.4	2
Kilang Kilang 1	476	Inertinite	SWC	1.47	1.86	1.11	15
Kilang Kilang 1	476	Vitrinite	SWC	0.77	0.8	0.75	3

Kilang Kilang 1	524	Exinite	SWC	0.42			
Kilang Kilang 1	524	Inertinite	SWC	1.47	2022	1.06	15
Kilang Kilang 1	524	Vitrinite	SWC	0.8	0.92	0.71	4
Kilang Kilang 1	545	Inertinite	SWC	1.61	2.02	1.28	12
Kilang Kilang 1	545	Vitrinite	SWC	0.82	0.89	0.71	6
Kilang Kilang 1	610	Exinite	SWC	0.34	0.43	0.25	4
Kilang Kilang 1	610	Inertinite	SWC	1.37	2.24	0.85	13
Kilang Kilang 1	610	Vitrinite	SWC	0.6	0.68	0.46	14
Kilang Kilang 1	631	Exinite	SWC	0.29	0.46	0.19	6
Kilang Kilang 1	631	Inertinite	SWC	1.47	2.54	0.77	10
Kilang Kilang 1	631	Vitrinite	SWC	0.59	0.67	0.47	14
Kilang Kilang 1	642.5	Exinite	SWC	0.28	0.43	0.2	4
Kilang Kilang 1	642.5	Inertinite	SWC	1.38	1.98	0.82	8
Kilang Kilang 1	642.5	Vitrinite	SWC	0.6	0.69	0.52	14
Kilang Kilang 1	807	Exinite	SWC	0.19			1
Kilang Kilang 1	807	Inertinite	SWC	1.45	2.36	0.84	15
Kilang Kilang 1	807	Vitrinite	SWC	0.59	0.65	0.54	5
Kilang Kilang 1	822	Exinite	SWC	0.32	0.33	0.31	2
Kilang Kilang 1	822	Inertinite	SWC	1.48	2.02	1.06	15
Kilang Kilang 1	822.1	Vitrinite	SWC	0.7	0.77	0.59	6
Kilang Kilang 1	889	Inertinite	SWC	1.28	1.75	0.96	15
Kilang Kilang 1	889	Vitrinite	SWC	0.73	0.77	0.68	8
Kilang Kilang 1	915	Inertinite	SWC	1.37	1.77	1.01	15
Kilang Kilang 1	915	Vitrinite	SWC	0.72	0.76	0.7	3
Kilang Kilang 1	935	Inertinite	SWC	1.46	1.88	1.18	15
Kilang Kilang 1	935	Vitrinite	SWC	0.75	0.87	0.45	10
Kilang Kilang 1	1000	Inertinite	SWC	1.44	1.78	1.1	15
Kilang Kilang 1	1000	Vitrinite	SWC	0.79	0.86	0.69	6
Kilang Kilang 1	1048	Inertinite	SWC	1.41	1.78	1.1	7
Kilang Kilang 1	1048	Vitrinite	SWC				
Kilang Kilang 1	1135	Inertinite	SWC	1.55	2.02	1.2	17
Kilang Kilang 1	1135	Vitrinite	SWC	0.69	0.85	0.53	14
Kilang Kilang 1	1185	Vitrinite	SWC				
Kilang Kilang 1	1453.6	Inertinite	SWC	1.59	1.92	1.22	9
Kilang Kilang 1	1453.6	Vitrinite	SWC	0.76	0.9	0.51	8
Kilang Kilang 1	1512.2	Vitrinite	SWC				
Kilang Kilang 1	1757.1	Inertinite	SWC	1.76	2.12	1.53	12
Kilang Kilang 1	1757.1	Vitrinite	SWC				
Kilang Kilang 1	1882	Inertinite	SWC	1.81	2.35	1.46	21
Kilang Kilang 1	1882	Vitrinite	SWC				
Kilang Kilang 1	2010	Inertinite	SWC	1.99	2.36	1.89	6
Kilang Kilang 1	2010	Vitrinite	SWC				
Kilang Kilang 1	2136.9	Vitrinite	SWC				
Kilang Kilang 1	2260	Vitrinite	SWC				
Ngalti 1	137.3	Inertinite	SWC	1.25	1.68	0.84	17
Ngalti 1	175.5	Bituminite	SWC	0.25	0.25	0.25	1
Ngalti 1	175.5	Vitrinite	SWC	0.42	0.66	0.26	7
Ngalti 1	299	Inertinite	SWC	1.3	1.3	1.3	1
Ngalti 1	299	Vitrinite	SWC	0.47	0.6	0.34	8
Ngalti 1	581.9	Inertinite	SWC	1.4	1.4	1.4	1

Ngalti 1	581.9	Vitrinite	SWC	0.43	0.81	0.31	19
Ngalti 1	631.5	Inertinite	SWC	0.97	1.54	0.74	1
Ngalti 1	631.5	Vitrinite	SWC	0.46	0.5	0.41	2
Ngalti 1	806.1	Inertinite	SWC	0.86	0.86	0.86	1
Ngalti 1	806.1	Vitrinite	SWC	0.37	0.48	0.26	16
Ngalti 1	812.6	Inertinite	SWC	1.24	1.24	1.24	1
Ngalti 1	812.6	Vitrinite	SWC	0.6	0.61	0.59	?2
Ngalti 1	817.6	Inertinite	SWC	1.91	2.08	1.64	3
Ngalti 1	1103.9	Inertinite	SWC	1.46	1.46	1.46	1
Ngalti 1	1103.9	Vitrinite	SWC	0.58	0.63	0.51	7
Ngalti 1	1467.8	Vitrinite	SWC				
Ngalti 1	1824	Vitrinite	SWC	0.67	0.67	0.67	1
Ngalti 1	1185	Inertinite	SWC	1.43	1.84	1.02	25
Ngalti 1	1355.5	Inertinite	SWC	1.42	1.92	1.02	12
Ngalti 1	1635	Inertinite	SWC	1.24	1.48	0.9	12
Ngalti 1	1774.4	Inertinite	SWC	1.16	1.16	1.16	1
Ngalti 1	1824	Inertinite	SWC	1.34	1.58	1.04	15
Ngalti 1	2119	Vitrinite	SWC				
Ngalti 1	1950.2	Inertinite	SWC	1.42	1.58	1.22	3
Ngalti 1	2157.3	Inertinite	SWC	1.52	1.86	1.08	4
Ngalti 1	2179	Inertinite	SWC	1.05			1
Ngalti 1	2265	Exinite	SWC	0.32	0.32	0.32	1
Ngalti 1	2265	Inertinite	SWC	1.23	1.7	0.99	5
Ngalti 1	2287	Inertinite	SWC	1.3	1.58	0.96	4
Ngalti 1	2325	Inertinite	SWC	1.57	2.08	1.23	4
Ngalti 1	2340.7	Inertinite	SWC	1.03	1.03	1.03	1
Ngalti 1	2379.7	Inertinite	SWC	1.36	1.36	1.36	1
Ngalti 1	2399	Inertinite	SWC	1.86	1.86	1.86	1
Ngalti 1	2430	Inertinite	SWC	1.46	1.46	1.46	1
Ngalti 1	2482.1	Inertinite	SWC	1.72	1.84	1.58	3
Ngalti 1	2541	Inertinite	SWC	1.51	2.1	1.05	
Ngalti 1	2598.1	Inertinite	SWC	1.7	2.72	1.18	20
Ngalti 1	2615.8	Inertinite	SWC	1.86	2.62	1.34	10
Ngalti 1	2630	Vitrinite	Cutt				
Ngalti 1	2629.4	Inertinite	SWC	1.69	1.69	1.69	1
Ngalti 1	2645.7	Inertinite	SWC	1.84	2.7	1.34	8
Ngalti 1	2663.3	Inertinite	SWC	1.73	2.24	1.21	10
Ngalti 1	2753	Inertinite	SWC	1.85	2.66	1.3	15
Ngalti 1	2753.28	Inertinite	SWC	2	2.72	1.36	11
Ngalti 1	2753.93	Exinite	SWC	0.5	0.58	0.48	5
Ngalti 1	2753.93	Inertinite	SWC	1.68	2.62	0.74	14
Ngalti 1	2754.6	Exinite	SWC	0.52	0.61	0.38	6
Ngalti 1	2754.6	Inertinite	SWC	1.46	2.6	0.91	10
Olios 1	220	Inertinite	SWC	1.04	1.41	0.72	10
Olios 1	220	Vitrinite	SWC	0.39	0.53	0.25	9
Olios 1	251.9	Inertinite	SWC	1.07	1.58	0.7	13
Olios 1	251.9	Vitrinite	SWC	0.46	0.52	0.38	15
Olios 1	269.1	Inertinite	SWC	1.08	1.58	0.74	9
Olios 1	269.1	Vitrinite	SWC	0.47	0.66	0.38	25
Olios 1	303.5	Inertinite	SWC	0.88	1.04	0.71	3

Olios 1	303.5	Vitrinite	SWC	0.52	0.66	0.38	19
Olios 1	375	Inertinite	SWC	1.34	1.34	1.34	2
Olios 1	375	Vitrinite	SWC	0.52	0.65	0.38	7
Olios 1	392	Inertinite	SWC	1.02	1.31	0.78	7
Olios 1	392	Vitrinite	SWC	0.53	0.6	0.41	6
Olios 1	501	Inertinite	SWC	1.21	1.81	0.97	4
Olios 1	501	Vitrinite	SWC	0.57	0.69	0.39	3
Olios 1	560	Inertinite	SWC	1.13	1.33	0.92	8
Olios 1	580	Vitrinite	SWC	0.54	0.68	0.38	13
Olios 1	577.9	Inertinite	SWC	1.24	1.4	0.98	4
Olios 1	557.9	Vitrinite	SWC	0.55	0.71	0.41	8
Olios 1	647	Inertinite	SWC	1.1	1.4	0.81	9
Olios 1	647	Vitrinite	SWC	0.58	0.7	0.43	12
Olios 1	688.1	Inertinite	SWC	1.01	1.19	0.87	3
Olios 1	688.1	Vitrinite	SWC	0.56	0.66	0.47	19
Olios 1	703	Inertinite	SWC	1.29	1.29	1.29	1
Olios 1	703	Vitrinite	SWC	0.52	0.62	0.42	5
Olios 1	733.1	Inertinite	SWC	1.35	1.74	0.96	6
Olios 1	733.1	Vitrinite	SWC	0.45	0.56	0.39	8
Olios 1	766.5	Inertinite	SWC	1.22	1.22	1.22	1
Olios 1	766.5	Vitrinite	SWC	0.51	0.64	0.4	6
Olios 1	810	Inertinite	SWC	1.55	2.18	1.04	5
Olios 1	810	Vitrinite	SWC	0.53	0.67	0.43	6
Olios 1	826.1	Inertinite	SWC	1.5	2.22	1	
Olios 1	826.1	Vitrinite	SWC	0.55	0.62	0.46	4
Olios 1	847.5	Vitrinite	SWC	0.55	0.73	0.43	20
Olios 1	871.1	Inertinite	SWC	1.25	1.42	1.08	2
Olios 1	871.1	Vitrinite	SWC	0.53	0.58	0.47	2
Olios 1	913	Inertinite	SWC	1.09	1.34	1	4
Olios 1	913	Vitrinite	SWC	0.64	0.71	0.49	8
Olios 1	985	Inertinite	SWC	1.23	1.88	0.82	12
Olios 1	985	Vitrinite	SWC	0.58	0.62	0.55	2
Olios 1	1114.75	Inertinite	SWC	1.05	1.36	0.87	5
Olios 1	1114.75	Vitrinite	SWC	0.64	0.74	0.5	25
Olios 1	1371.75	Vitrinite	SWC	0.62	0.62	0.62	1
Olios 1	1418	Vitrinite	SWC				
Olios 1	1434	Inertinite	SWC	1.52	1.84	1.4	2
Olios 1	1434	Vitrinite	SWC	0.62			1
Olios 1	1458	Inertinite	SWC	1.32	2	0.82	13
Olios 1	1458	Vitrinite	SWC	0.67	0.77	0.59	3
Olios 1	1512.5	Vitrinite	SWC				
Olios 1	1537.5	Inertinite	SWC	1.52	2.36	1.12	10
Olios 1	1537.5	Vitrinite	SWC	0.67	0.79	0.57	4
Olios 1	1571.5	Vitrinite	SWC				
Olios 1	1701	Vitrinite	SWC				
Olios 1	1759	Inertinite	SWC	1.81	1.92	1.04	9
Olios 1	1759	Vitrinite	SWC	0.66	0.66	0.66	1
Olios 1	1858.25	Vitrinite	SWC				
Olios 1	1890	Inertinite	SWC	1.54	1.64	1.3	4
Olios 1	1890	Vitrinite	SWC	0.79	0.79	0.79	1

Olios 1	1918	Vitrinite	SWC				

Appendix E

1D Petroleum Systems Models – Age Assignments

Age assignment inputs used within 1D petroleum systems models in this study are estimated from exploratory well locations, published literature and seismic interpretation. These inputs are summarised in this Appendix.

Header	Layer	Top (m)	Base (m)	Thickness (m)	Eroded (m)	Depo. start (Ma)	Depo. end (Ma)	Erosion start (Ma)	Erosion end (Ma)	Lithology	PSE	TOC (wt. %)	Kinetic	HI (mg HC/gTOC)
Explanation	*Name of formation in well-bore*	*Top depth of formation*	*Base of formation (auto populated)*	*Thickness of formation (auto populated)*	*Thickness of eroded sequence*	*Start date of formation deposition*	*End date of formation deposition*	*Start date of erosional period affecting formation*	*End date of erosional period affecting formation*	*Selection of lithology from library*	*Petroleum system element*	*Organic component (formation average)*	*Model to predict petroleum generative extent*	*Remaining generative capacity (formation average)*
Bindi 1	Miocene	0	0	0	50	38	15	15	0	Sandstone (typical)	Overburden Rock			
	Tertiary - Eocene	0	0	0	50	120	38	38	15	Sandstone (typical)	Overburden Rock			
	Cretaceous	0	0	0	300	175	135	135	120	Sandstone (typical)	Overburden Rock			
	Triassic	0	0	0	500	220	200	200	180	Triassic_Blina_Mylet_mix	Overburden Rock			
	Undiff. Qa	0	8.5	8.5	300	226	220	200	180	Sandstone (typical)	Overburden Rock			
	Blina Shale	8.5	228	219.5	200	232	226	200	180	Blina_sh_mix	Overburden Rock			
	Mylet Group	228	292.5	64.5	200	242.5	232	200	180	Mylet_gp_mix	Overburden Rock			
	Liveringa Group	292.5	629	336.5	200	253	242.5	200	180	Liveringa_Gp_mix	Overburden Rock			
	Noonkanbah Fm	629	910	281		266	253			Noonkanbah_sh_mix	Source Rock	2.2	Tissot_in_Waples(1992)_TII_Crack	36
	Poole Sandston	910	990	80		271	266			Poole_Sst_mix	Reservoir Rock	1.5		99.9
	Grant Group	990	1832	842		305	271			Grant_sst/sh_mix	Reservoir Rock	0.5		70
	Anderson Formation	1832	2457	625	250	337	322	322	305	Anderson_sst/slt_mix	Source Rock	0.9	Tissot_in_Waples(1992)_TII_Crack	48
	Laurel Formation	2457	2504	47		345	337			Laurel_fm_carb_mix	Source Rock	0.6	Tissot_in_Waples(1992)_TII_Crack	51

Header	Layer	Top (m)	Base (m)	Thickness (m)	Eroded (m)	Depo. start (Ma)	Depo. end (Ma)	Erosion start (Ma)	Erosion end (Ma)	Lithology	PSE	TOC (wt. %)	Kinetic	HI (mg HC/gTOC)
Explanation	*Name of formation in well-bore*	*Top depth of formation*	*Base of formation (auto populated)*	*Thickness of formation (auto populated)*	*Thickness of eroded sequence*	*Start date of formation deposition*	*End date of formation deposition*	*Start date of erosional period affecting formation*	*End date of erosional period affecting formation*	*Selection of lithology from library*	*Petroleum system element*	*Organic component (formation average)*	*Model to predict petroleum generative extent*	*Remaining generative capacity (formation average)*
Kilang Kilang 1	Miocene	0	0	0	50	38	15	15	0	Sandstone (typical)	Overburden Rock			
	Tertiary - Eocene	0	0	0	50	120	38	38	15	Sandstone (typical)	Overburden Rock			
	Cretaceous	0	0	0	200	175	135	135	120	Sandstone (typical)	Overburden Rock			
	Triassic	0	0	0	1100	220	200	200	180	Triassic_Blina_Mylet_mix	Overburden Rock			
	Undiff. Qa	0	15	15	300	242.5	220	200	180	Sandstone (typical)	Overburden Rock			
	Liveringa Group	15	354.5	339.5	100	253	242.5	200	180	Liveringa_Gp_mix	Overburden Rock			
	Noonkanbah Fm	354.5	660.5	306		266	253			Noonkanbah_sh_mix	Source Rock	2.2	Tissot_in_Waples(1992)_TII_Crack	36
	Poole Sandston	660.5	803.3	142.8		271	266			Poole_Sst_mix	Reservoir Rock	1.5		99.9
	Grant Group	803.3	1448	644.7		305	271			Grant_sst/sh_mix	Reservoir Rock	0.5		70
	Anderson Formation	1448	1717	269	250	337	322	322	305	Anderson_sst/slt_mix	Source Rock	0.9	Tissot_in_Waples(1992)_TII_Crack	48
	Laurel Formation	1717	2300	583		345	337			Laurel_fm_carb_mix	Source Rock	0.6	Tissot_in_Waples(1992)_TII_Crack	51

Header	Layer	Top (m)	Base (m)	Thickness (m)	Eroded (m)	Depo. start (Ma)	Depo. end (Ma)	Erosion start (Ma)	Erosion end (Ma)	Lithology	PSE	TOC (wt. %)	Kinetic	HI (mg HC/gTOC)
Explanation	*Name of formation in well-bore*	*Top depth of formation*	*Base of formation (auto populated)*	*Thickness of formation (auto populated)*	*Thickness of eroded sequence*	*Start date of formation deposition*	*End date of formation deposition*	*Start date of erosional period affecting formation*	*End date of erosional period affecting formation*	*Selection of lithology from library*	*Petroleum system element*	*Organic component (formation average)*	*Model to predict petroleum generative extent*	*Remaining generative capacity (formation average)*
Olios 1	Miocene	0	0	0	75	38	15	15	0	Sandstone (typical)	Overburden Rock			
	Tertiary - Eocene	0	0	0	75	120	38	38	15	Sandstone (typical)	Overburden Rock			
	Cretaceous	0	0	0	400	175	135	135	120	Sandstone (typical)	Overburden Rock			
	Triassic	0	0	0	850	225	200	200	180	Triassic_Blina_Mylet_mix	Overburden Rock			
	Undiff	0	0	0	300	242.5	225	200	180	Mylet_gp_mix	Overburden Rock			
	Liveringa Group	0	61	61	100	253	242.5	200	180	Liveringa_Gp_mix	Overburden Rock			
	Noonkanbah Fm	61	270.5	209.5		266	253			Noonkanbah_sh_mix	Source Rock	2.2	Tissot_in_Waples(1992)_TII_Crack	36
	Poole Sandston	270.5	306	35.5		271	266			Poole_Sst_mix	Reservoir Rock	1.5		99.9
	Grant Group	306	815	509		305	271			Grant_sst/sh_mix	Reservoir Rock	0.5		70
	Anderson Formation	815	815	0	250	337	322	322	305	Anderson_sst/slt_mix	Source Rock	0.9	Tissot_in_Waples(1992)_TII_Crack	48
	Laurel Formation	815	1131	316		342	337			Laurel_fm_carb_mix	Source Rock	0.6	Tissot_in_Waples(1992)_TII_Crack	51
	Laurel Basal Carbonate	1131	1431	300		344	342			Laurel_fm_carb_mix	Source Rock	0.6	Tissot_in_Waples(1992)_TII_Crack	51
	Yellow Drum Fm	1431	1468	37		345.5	344			Yellow_Drum_mix	Reservoir Rock			
	Gumhole Fm	1468	1560	92		347.5	345.5			Gumhole_mix	Overburden Rock			
	Knobby Sandstone	1560	1963	403		349	347.5			Knobby_sst_mix	Reservoir Rock			

Header	Layer	Top (m)	Base (m)	Thickness (m)	Eroded (m)	Depo. start (Ma)	Depo. end (Ma)	Erosion start (Ma)	Erosion end (Ma)	Lithology	PSE	TOC (wt. %)	Kinetic	HI (mg HC/gTOC)
Explanation	*Name of formation in well-bore*	*Top depth of formation*	*Base of formation (auto populated)*	*Thickness of formation (auto populated)*	*Thickness of eroded sequence*	*Start date of formation deposition*	*End date of formation deposition*	*Start date of erosional period affecting formation*	*End date of erosional period affecting formation*	*Selection of lithology from library*	*Petroleum system element*	*Organic component (formation average)*	*Model to predict petroleum generative extent*	*Remaining generative capacity (formation average)*
Ngalti 1	Miocene	0	0	0	100	38	15	15	0	Sandstone (typical)	Overburden Rock			
	Tertiary - Eocene	0	0	0	100	120	38	38	15	Sandstone (typical)	Overburden Rock			
	Cretaceous	0	0	0	350	175	135	135	120	Sandstone (typical)	Overburden Rock			
	Triassic	0	0	0	900	225	200	200	180	Triassic_Blina_Mylet_mix	Overburden Rock			
	Undiff	0	7	7	300	242.5	225	200	180	Mylet_gp_mix	Overburden Rock			
	Liveringa Group	7	112	105	100	253	242.5	200	180	Liveringa_Gp_mix	Overburden Rock			
	Noonkanbah Fm	112	178	66		266	253			Noonkanbah_sh_mix	Source Rock	2.2	Tissot_in_Waples(1992)_TII_Crack	36
	Poole Sandston	178	279	101		271	266			Poole_Sst_mix	Reservoir Rock	1.5		99.9
	Grant Group	279	796	517		305	271			Grant_sst/sh_mix	Reservoir Rock	0.5		70
	Anderson Formation	796	796	0	250	337	322	322	305	Anderson_sst/slt_mix	Source Rock	0.9	Tissot_in_Waples(1992)_TII_Crack	48
	Laurel Formation	796	1067	271		345	337			Laurel_fm_carb_mix	Source Rock	0.6	Tissot_in_Waples(1992)_TII_Crack	51
	Knobby Sandstone	1067	1705	638		349	345			Knobby_sst_mix	Reservoir Rock			
	Lennard River Group	1705	2757.8	1052.8		361	349			Bungle_Gap_mix	Reservoir Rock	0.5		

Header	Layer	Top (m)	Base (m)	Thickness (m)	Eroded (m)	Depo. start (Ma)	Depo. end (Ma)	Erosion start (Ma)	Erosion end (Ma)	Lithology	PSE	TOC (wt. %)	Kinetic	HI (mg HC/gTOC)
Explanation	*Name of formation in well-bore*	*Top depth of formation*	*Base of formation (auto populated)*	*Thickness of formation (auto populated)*	*Thickness of eroded sequence*	*Start date of formation deposition*	*End date of formation deposition*	*Start date of erosional period affecting formation*	*End date of erosional period affecting formation*	*Selection of lithology from library*	*Petroleum system element*	*Organic component (formation average)*	*Model to predict petroleum generative extent*	*Remaining generative capacity (formation average)*
Lake Betty 1	Miocene	0	0	0	150	38	15	15	0	Sandstone (typical)	Overburden Rock			
	Tertiary - Eocene	0	0	0	150	120	38	38	15	Sandstone (typical)	Overburden Rock			
	Cretaceous	0	0	0	550	175	135	135	120	Sandstone (typical)	Overburden Rock			
	Triassic	0	0	0	1050	220	200	200	180	Triassic_Blina_Mylet_mix	Overburden Rock			
	Undiff	0	0	0	200	242.4	220	200	180	Sandstone (typical)				
	Liveringa Group	0	378	378	300	253	242.5	200	180	Liveringa_Gp_mix	Overburden Rock			
	Noonkanbah Fm	378	678	300		266	253			Noonkanbah_sh_mix	Source Rock	2.2	Tissot_in_Waples(1992)_TII_Crack	36
	Poole Sandston	678	764	86		271	266			Poole_Sst_mix	Reservoir Rock	1.5		99.9
	Grant Group	764	1656	892		305	271			Grant_sst/sh_mix	Reservoir Rock	0.5		70
	Anderson Formation	1656	1656	0	250	337	322	322	305	Anderson_sst/slt_mix	Source Rock	0.9	Tissot_in_Waples(1992)_TII_Crack	48
	Laurel Formation	1656	2303	647		342	337			Laurel_fm_carb_mix	Source Rock	0.6	Tissot_in_Waples(1992)_TII_Crack	51
	Laurel Basal Carbonate	2303	2580	277		344	342			Laurel_fm_carb_mix	Source Rock	0.6	Tissot_in_Waples(1992)_TII_Crack	51
	Luluigui Fm	2580	3078	498		349	344			Bungle_Gap_mix	Reservoir Rock	0.5		
	Poulton Formation	3078	3146	68		373	366			Poulton_estimate_mix	Underburden Rock			